Fakultät für Maschinenwesen

Lehrstuhl für Flugsystemdynamik

Comparative Analysis of Adaptive Control Techniques for Improved Robust Performance

Dipl.-Ing. (Univ.) Thomas Bierling

Vollständiger Abdruck der von der Fakultät für Maschinenwesen
der Technischen Universität München
zur Erlangung des akademischen Grades eines
Doktor-Ingenieurs (Dr.-Ing.) genehmigten Dissertation.

Vorsitzender:	Univ.-Prof. Dr.-Ing. Mirko Hornung
Prüfer der Dissertation:	1. Univ.-Prof. Dr.-Ing. Florian Holzapfel
	2. Univ.-Prof. Dr.-Ing. habil. Boris Lohmann

Die Dissertation wurde am 09.10.2013 bei der Technischen Universität München eingereicht und durch die Fakultät für Maschinenwesen am 27.05.2014 angenommen.

Acknowledgments

At first I would like to thank Professor Florian Holzapfel who gave me the chance to write this thesis and supported me with his advice over the last four years. Secondly I want to thank my thesis committee members Professor Boris Lohmann and Professor Mirko Hornung.

Special thanks also go to Dr. Rudolf Maier. He made it possible to support this thesis financially under a contract between EADS Innovation Works and the Institute of Flight System Dynamics. Moreover his guidance, support, and many technical discussions greatly improved the quality and the pace of my work.

Regarding my research I would also like to thank my college Leonhard Höcht for the many, often controversial, discussions, and his help with challenging mathematical problems. This greatly improved my understanding and the quality of this thesis. Of course I also need to thank the rest of my co-workers for the great time at the Institute and the good cooperation. Especially I would like to mention Bernhard Baur, Farhana Chew, Markus Geiser, Miguel Leitao, Jakob Lenz, Maximillian Mühlegg, Florian Peter, Simon Schatz, Jian Wang, and Fubiao Zhang.

I would like to thank my extraordinary parents and my sister for supporting me in all possible ways.

Finally, I am also in debt to my friends and would like to thank them for accepting my frequent absence in stressful times.

Abstract

Adaptive control has the potential to improve control performance in presence of uncertainties or faults. In contrast to robust control techniques uncertain plant parameters are directly identified and compensated instead of trying to find a best compromise between performance and robustness. The thesis covers the theory of Model Reference Adaptive Control (MRAC) techniques which are well suited to flight control applications. Benefits and drawbacks are investigated in depth based on two benchmark problems: A linear short period approximation with an unknown pitch-up nonlinearity, and a full nonlinear aircraft model where the loss of a scheduling parameters due to a fault is considered.

At first recently suggested modifications of the basic MRAC approach are comprehensively analysed and assessed. During the investigation it was seen that MRAC with state feedback can reduce the robustness w.r.t. unmatched uncertainties in real application cases. In order to address this problem a modification is suggested in this thesis. Moreover an adaptation of reference model for a certain domain of matched uncertainties is suggested, which reduces the restrictiveness of the reference model and allows a certain set of response trajectories instead of only one. Additionally, $\mathcal{L}_1$ adaptive control, which gained enormous interest in the past years, was investigated. It is shown that $\mathcal{L}_1$ adaptive control and ordinary MRAC with the application of a hedging signal to reference model are extremely similar, and under certain conditions they are even mathematically equivalent. During the work the effects of different modifications are clearly pointed out, and by application of the novel extensions very good results could be achieved with MRAC. $\mathcal{L}_1$ piecewise constant control is also investigated. This approach is quite different, but leads to quite good results in particular for the pitch-up problem. It is a linear control approach, and hence, in difference to MRAC, linear assessment methods can be applied.

Secondly a full nonlinear, large transport aircraft model is used to investigate adaptive control techniques in order to compensate the loss of a scheduling parameter. Here the objective is to maintain good handling qualities over the complete envelope when the scheduling information is lost. In particular the longitudinal response and the loss of the calibrated airspeed are considered. The applied methods for the problem are $\mathcal{L}_1$ piecewise constant, MRAC, and an Extended Kalman Filter (EKF) to estimate the air speed directly. Though $\mathcal{L}_1$ piecewise constant can improve certain handling quality requirements it leads to a deterioration of others, and thus requires a trade-off. In

difference, for MRAC and the EKF very good results were achieved for all handling quality requirements, if enough excitation of the system is given.

Content

Nomenclature

Acronyms

ACFS	Advanced Concept Flight Simulator
CAP	Control Anticipation Parameter
CAT	Category
CG	Center of Gravity
DARPA	Defense Advanced Research Project Agency
DOB	Disturbance OBserver
EKF	Extended Kalman Filter
FAST	Full-Scale Advanced System Testbed
GM	Gain Margin
GTM	Generic Transport Model
HQ	Handling Qualities
IFCS	Intelligent Flight Control System Project
IRAC	Integrated Resilient Aircraft Control Project
IRS	Inertial Reference System
JDAM	Joint Direct Attack Munition
J-UCAS	Joint Unmanned Combat Air Systems Project
MIMO	Multiple-Input Multiple-Output
MMO	Maximum Operating Mach number
NN	Neural Network
MRAC	Model Reference Adaptive Control
PIO	Pilot Induced Oscillation
PM	Phase Margin
RESTORE	Project investing Reconfigurable Control for Tailless Fighter Aircraft

TDM	Time Delay Margin
TPR	Transient Peak Ratio
TRL	Technology Readiness Level
UCAV	Unmanned Combat Air Vehicle
VMO	Maximum operating speed

Greek Letters

α	Angle of attack
β	Sideslip angle
$\boldsymbol{\Gamma}/\gamma$	Update gain matrix/scalar
$\boldsymbol{\delta}$	Vector of control inputs
$\boldsymbol{\varepsilon}$	closed loop estimation error
$\boldsymbol{\varepsilon}$	Non parametric uncertainty
ζ	Rudder deflection
η	Elevator deflection
$\boldsymbol{\Lambda}/\lambda$	Control effectiveness matrix/scalar
λ	Eigenvalue
$\boldsymbol{\Xi}$	Dummy variable for robustness modification
$\boldsymbol{\Theta}/\boldsymbol{\theta}/\theta$	Adaptive controller parameter matrix/vector/scalar
ξ	Aileron deflection
ρ	Air density
σ	Gain for robustness modification
$\hat{\boldsymbol{\sigma}}$	Estimated disturbance
τ	Time interval
$\boldsymbol{\varphi}$	Nonlinear function
$\boldsymbol{\Omega}$	Compact convex set
$\boldsymbol{\omega}$	Angular velocity vector
$\boldsymbol{\omega}$	Regressor Vector
ω	Cut-off frequency of low pass filter

Latin Letters

$\mathbf{A}$	System matrix of a state space model
$\mathbf{B}/\mathbf{b}$	Input matrix/vector of a state space model
$\mathbf{C}/\ \mathbf{c}$	Output matrix/vector of state space model
C	Aerodynamic coefficient
$C(s)$	Lowpass filter transfer function
$\mathbf{D}/\mathbf{d}$	Feedthrough matrix/vector of a state space mode
$\mathbf{d}$	Disturbance
$\mathbf{e}$	Error
$\mathbf{F}/F$	Force vector/scalar
$\mathbf{f}$	Nonlinear function
$\mathbf{G}(s)/G(s)$	Transfer matrix/function
$\mathbf{I}$	Inertia tensor
$\mathbf{I}$	Identity matrix
J	Cost function
$\mathbf{K}, \mathbf{k}, k$	Static feedback/feedforward gain matrix/vector/scalar
l	Reference chord length
$\mathbf{M}/M$	Moment vector/scalar
$\mathbf{M}(s)$	Transfer matrix of the reference dynamics
M_α	Dimensionless moment derivative - Moment due to α
M_q	Dimensionless moment derivative - Moment due to q
M_η	Dimensionless moment derivative - Moment due to η
m	mass
n_Z	Load factor in direction of Z-axis of the body-fixed frame
$\mathbf{P}$	Solution matrix of the Lyapunov equation
$\mathbf{Q}$	Weighting matrix for the Lyapunov equation
q	Pitch rate
$\bar{q}$	Dynamic pressure
$\mathbf{R}$	Covariance matrix
$\mathbf{r}$	Reference command vector

S	Reference surface of the wing
s	Laplace variable
t	Time
$\mathbf{u}$	Control input vector
V	Speed – Euclidean norm of velocity
V	Lyapunov function candidate
$\mathbf{v}$	Velocity vector
$\mathbf{x}$	State vector
$\mathbf{y}$	Output vector
$\mathbf{z}$	State vector of the unmodeled dynamics
Z_α	Dimensionless force derivative - Force due to α
Z_q	Dimensionless force derivative - Force due to q
Z_η	Dimensionless force derivative - Force due to η

Subscripts

AD	Adaptive
act	Actuator
$aero$	Aerodynamic
BL	Baseline
C	Control
CAS	Calibrated Airspeed
CMD	Command
del	Delay
EST	Estimated
fil	Filter
For	Force
$grav$	Gravitational
I	Identification
ID	Ideal

INI	Initial condition
KF	Kalman Filter
M	Reference model
$MEAS$	Measured
Mom	Moment
ma	Matched
P	Plant
$prop$	Propulsive
ss	Steady state
TAS	True Airspeed
um	Unmatched

Superscripts

l	Left pseudoinverse
r	Right pseudoinverse
$*$	Ideal parameters
$+$	System dynamics extended by integrator

Notation

$\{\bullet\}_s$	Denotes that the term inside the brackets is transformed from the time domain to the Laplace domain
$\{\bullet\}_t$	Denotes that the term inside the brackets is transformed from the Laplace domain to the time domain
$(\mathbf{r}^{AB})_C$	Vector $\mathbf{r}$ from point A to point B denoted in the C-frame
$(\mathbf{v}^A)_B$	Is the velocity of the point A, denoted in the B-frame
$\left(\dot{\mathbf{v}}^{\mathrm{A}}\right)_B^C$	Is the time derivative of $(\mathbf{v}^A)_B$ taken in the C-frame
$\boldsymbol{\omega}^{AB}$	Is the angular velocity of the aircraft with respect to the A-frame
$\mathbf{T}_{BA}$	Is the transformation matrix from the A -frame to the B-frame

$\hat{\bullet}$	Estimated value
$\tilde{\bullet}$	Parameter error
$\bar{\bullet}$	Mean value

List of Tables

List of Figures

Chapter 1

Introduction

Current generation aircraft almost exclusively utilize flight control systems that are based on linear control theory. The reason for this is the large amount of experience together with mathematically proven concepts and methods for linear system analysis and controller design. More important, current certification requirements, like stability margins (MIL-DTL-9490E), are based on linear system theory. For such approaches, the nonlinear dynamics of the plant to be controlled is locally linearized around (quasi-) steady operating points based on a model of the real system. Then, the control design is performed for the linearized model. The so designed controller is capable of performing its task also for the nonlinear system if some conditions are met. The two most prominent ones are that 1.) the nonlinear system has to be operated close enough to the steady condition where the linearization was performed and that 2.) the structure and parameters of the model must be close enough to the real nonlinear system. Classical linear control only guarantees that the designed controller fulfills its task for the linear system and for the nonlinear system when operated directly in the linearization point, if the real dynamics matches the modeled dynamics. How far the model may be different from reality and how far the operating point may be left was up to heuristics and covered by robustness criteria stated in terms of gain and phase margin. These requirements were partially relaxed by the theories developed for so called robust control, where deviations between nominal and true dynamics could actively be specified in uncertainty models leading to control designs accounting for those deviations.

Adaptive control in contrast to robust control does not assume an interval for the unknown plant parameters but treats them as unknown and tries to either determine the parameters in order to compute suitable controller gains or to directly estimate appropriate control gains. As thus the controller gains are no longer constant but also changed dynamically and thus states of the system, the product of a controller gain and a measured process variable is a product of two states and as a consequence of this a nonlinear operation. Thus even the adaptive control of a first order, scalar linear plant leads to a nonlinear system, no longer covered by classical linear theories.

The attractiveness of adaptive control is that even in the case of uncertainties and failures a desired performance can be maintained. The increase in stability and the improvement of fault tolerance is a major selling point and makes the approach in particular interesting for flight control.

In the wide field of adaptive control the concept of Model Reference Adaptive Control (MRAC) gained significant attention and can be found in many standard text books on nonlinear adaptive control [1] [2] [3] [4] [5] [6]. Although the approach suffered from robustness problems, due to the large progress that was made during the last three decades the approach gained immense interest from the flight control community. Many examples have shown that adaptive control can be superior to robust control in the case of large uncertainties or failures. However, it is still controversially discussed because many problems have not been resolved yet.

In the scope of flight control the approach of adaptive control has been used for the control of systems with large uncertainties and nonlinearities and for control of aircraft in adverse conditions (damage, failure). In both cases the considered system is subject to large uncertainties, however, in the first case, uncertainties are usually smaller and adaptation can be slower. In difference, the case of damage constitutes a far off-nominal flight condition with a large number of effects that deteriorate the stability and controllability. This requires for fast adaptation and reconfiguration due to the large uncertainties that can render the system unstable. Furthermore, the loss of control effectiveness can require for automatically adjusting the control allocation to exploit control redundancy in order to preserve controllability. This might also include the use of control effectors that are usually not used for flight control, like spoilers or engine thrust. However, limited control authority and especially the use of slow actuators poses a difficult task due to time scale separation for different actuators, and these problems have still not been rigorously addressed.

Especially in recent years Model Reference Adaptive Control (MRAC) has gained enormous attention and popularity in the aerospace community. Successful flight test demonstrations, significant advances in the theoretical framework (especially with respect to stability and robustness), and the consensus to jointly define certification strategies and criteria for adaptive flight controllers are leading to an overwhelming multitude of new methods and approaches appearing in publications and conferences. As everybody represents the theories and applications in very different ways, they often seem to be far apart and different from each other although they are close together. The system model used for controller design is often subject to parameter uncertainties or the parameters of the system to be controlled might even change over time. These uncertainties or changes can lead to performance degradation or even instability for the controlled, closed loop system. Adaptive control offers an approach for online adaptation to maintain the desired controller performance in the presence of parameter uncertainties.

1.1 History in Adaptive Flight Control

The demanding control task arising for newly developed high performance aircraft in the beginning of 1950's fueled research efforts in the field of adaptive control. Because these aircraft operate at a wide range of speeds, altitudes and angles of attack where the parameter variations are large and nonlinearities become visible such that the classic, linear, fixed gain controller design posed a difficult challenge. Adaptive control was by definition seen as a solution to the problem: "A self-adaptive system will be defined as one which has the capability of changing its parameters through an internal process of measurement, evaluation, and adjustment to adjust to a changing environment, either external or internal to the vehicle control" [7]. Thus the main idea was to eliminate the need for gain scheduling by using an automatic adjustment algorithm for the controller parameters which provides consistent performance and handling qualities over the complete flight envelope.

The first adaptive flight tested adaptive control system was developed by Honeywell and based on a self-oscillating adaptive concept, where the gain is kept as high as possible [8] [9]. This concept was at first tested on an F-94C and an F-101A aircraft, and after further development the MH-96 control system was finally applied and tested on the X-15 experimental aircraft. The adaptive flight control system was successfully used on 64 flights and also obtained good pilot ratings [10] but a flight test in 1967 ended disastrous, whereat the Pilot was killed and the aircraft destroyed. The reason for the crash was partly attributed to instability in the adaptive control system [11]. After this incident the interest in adaptive control diminished and no adaptive flight controller was used on a manned aircraft for over 30 years. But in the last decades again attention has been directed towards adaptive flight control due to the advancement in nonlinear control theory and the development of robustness modifications, where especially the MRAC concept has gained interest. In [12] and [13] the X-15 flight test is theoretically revisited by simulation and it is shown that with a provably correct adaptive controller design, which is based on a rigorous mathematical frame work, the crash could have been prevented.

The Reconfigurable Control for Tailless Fighter Aircraft Project (RESTORE) was the next important project in adaptive flight control with the objective to increase survivability in the presence of unknown failures and damages [14]. The applied control law was based on dynamic inversion and augmented by a neural network-based nonlinear adaptive controller that relies on the MRAC principle. This approach was manly promoted by the research group of Prof. Calise at the Georgia Institute of Technology and it was able to exploit control surface redundancy in adverse conditions [15] [16] [17]. Next to piloted simulation the maturity of the control concept was also shown in two flight tests on the unmanned Boeing/Nasa X-36 1998, where also control surface failure were simulated during the test flights [18].

Together with the research group of Prof. Calise, Boeing also used the same MRAC based neural networks approach for its Joint Direct Attack Munition (JDAM). Here it could be demonstrated that adaptive control can reduce the dependency on accurate modeling and wind tunnel data and thus has the potential to save time and money. An adaptive autopilot was designed for use on different variants of JDAM (MK-84, BLU-109, MK-82), successfully flight tested, and finally Boeing even implemented this control technology into its production [19] [20] [21] [22].

Wise and Lavretsky also used the MRAC approach for the Boeing X-45 Unmanned Combat Air Vehicle (UCAV) and evaluated the performance in simulation studies [23] [24]. Moreover, $\mathcal{L}_1$ adaptive control was also tested on a simualation of the X-45, where actuator faiures have been investigated [25] [26].

The application of adaptive control concepts with the objective to improve fault tolerance was also investigated by the European Flight Mechanics Action Group FM-AG(16) form 2004 to 2008 under the auspices of the Group for Aeronautical Research and Technology in Europe (GARTEUR) [27]. Next to classic Fault Detection and Isolation (FDI) methods and reconfiguration based Fault Tolerant Control (FTC) also novel methods like adaptive control were addressed. Based on a Boeing 747 benchmark simulation model different adaptive approaches like MRAC and indemnification based adaptive control were evaluated. Some methods were also assessed in piloted simulation in the SIMONA research flight simulator at TU Delft [28].

In the Intelligent Flight Control System Project (IFCS) the objective was to develop a flight controller that can efficiently optimize aircraft performance in both normal and failure conditions [29]. Therefore neural network adaptive control was employed, where a highly-modified McDonnell-Douglas NF-15B Eagle was used. After Generation I flight tests were performed with a pre-trained neural network open loop controller that used an indirect estimation of aerodynamic parameters, in Generation II manned flight tests were successfully conducted with a closed loop direct adaptive neural network controller in 2005 [30]. For these flight tests the performance was evaluated for stabilator failure, and although improvements could be achieved by adaptation the control law also increased the pilot induced oscillation (PIO) tendency in some cases [31] [32]. The program ended in 2008.

In DARPA's (Defense Advanced Research Project Agency) Joint Unmanned Combat Air Systems program (J-UCAS) the objective is "to autonomously mitigate the effects of physical damage that could potentially occur in an air combat environment. They were looking for a technology that would provide a new option for surviving the effects of an adversary's attack, allowing the air vehicle to sustain flight and potentially continue its mission" [33]. Under contract Rockwell Collins (Athena) developed a flight control system with an inner loop MRAC controller. The FCS was tested on subscale, unmanned F/A-18 in June 2008, where it was shown that the system can even compensate for 60% wing loss and the adaptive controller could reestablish the

desired performance, such that the damaged aircraft was able to land autonomously [34].

Recently the Integrated Resilient Aircraft Control Project (IRAC) ended (2005-2010) where the purpose of the project was to provide on board resilience for ensuring safe flight in the presence of unforeseen, adverse conditions like faults or damage, with focus on current and next generation subsonic civil transport aircraft [35] [36]. The focus of IRAC was to investigate the applicability, evaluate, and compare different adaptive control methods. In the scope of the project different research groups applied their adaptive methods at first to a generic transport model (GTM) developed by NASA, which allowed high-fidelity simulation. Afterwards some methods were evaluated in pilot in the loop simulation on the Advanced Concept Flight Simulator (ACFS) [37] and investigated in flight tests on the NASA AirStar, a model-scale transport aircraft which is controlled by a pilot from a ground station [38]. This led to a large number of publications, where new problems were discovered and solutions for the former were presented [39] [40] [41] [42] [43] [44] [45] [46] [47] [48] [49] [50] [51] [52] [53] [54] [55] [56] [57] [58]. Within the project NASA also designed adaptive control laws for F/A-18A aircraft, which were at first evaluated in simulation [59] [60] [61]. Subsequently three MRAC laws were flight tested at NASA Dryden on a modified F/A-18A, the NASA Full-Scale Advanced System Testbed (FAST). During these flight test failure were simulated and handling qualities were evaluate for different maneuver based on Cooper-Harper ratings [62]. In general the funded research provided new inside and boosted the advance in adaptive control.

Although the early problems of adaptive control could be solved, many new developments emerged, and a huge amount of successful applications were published, however, for adaptive flight control some challenges remain [63]. Especially certification poses many open questions that still have to be addressed. For this purpose verification and validation metrics have to be developed which can be applied to show means of compliance. Therefore, at the moment one the main research directions is the development of metrics which can be used to guarantee robust stability and robust performance of adaptive flight control systems [64] [52] [65] [66] [67] [68]. In this prospect also the development of analysis and validation methods has received recent interest [69] [70] [71] [72] [73] [74] [75] [76].

1.2 Contribution

The thesis at hand is a method base work with focus on analyzing adaptive control architectures and investigating their applicability to flight control problems. Therefore the work aims at increasing the state of the art in adaptive control in general, as well as to raise the Technology Readiness Level (TRL) and establish requirements for commercial applicability and acceptance. Due to the complexity and limitation (e.g. plant has to be minimum phase) of output-feedback based MRAC, these methods

have only seldom been suggested for flight control and most publications focus on MRAC with assumed state-feedback, and this is also the approach chosen in this thesis. Some of the results presented within this work were already published by the author in [77] [78] [79].The scientific contribution of the thesis is given by the following points:

- In the available literature the authors often present the theory in a very different way such that they seem to be far apart and different from each other although they are close together. Likewise, many modifications may seem as something radically different representing completely new philosophies. Though they undoubtedly are of great value for both science and applications, they can still be assigned to various elements of the standard baseline MRAC architectures in many cases. The thesis tries to formulate the different MRAC approaches and modifications in a consistent manner and allocates the special characteristics of the respective method to the elements concerned in the standard MRAC architectures [77]. By presenting the different approaches in a unified manner, commonalities and links between various variants and modifications are particularly highlighted, and similarities and differences can be understood much easier. Furthermore, it becomes apparent that many different methods are no exclusive alternatives but may well be combined. So dependent on the task to be accomplished, different suitable elements from the growing field of MRAC can be selected in a target-oriented manner to pursue the respective control objective in the most efficient way. Elements to be addressed are baseline MRAC architectures, reference dynamics, structure of the adaptive elements and update laws.
- Based on a simple simulation model different methods are applied. However, the model is not overly simplified, as it contains higher order dynamics (e.g. actuators, structural filters) and time delay, which significantly limit the bandwidth. It gets obvious that these input dynamics can be a limiting factor for the achievable performance of the MRAC approach, but methods to prevent this performance reduction have already been suggested in literature, where the approach is referred to as “hedging”. One open problem for hedging was that no stability poof was available when it is applied to account for additional dynamic. During this work similarities of applying a hedging signal to the reference model, used in model reference adaptive control to account for dynamic constraints in the input channel, and $\mathcal{L}_1$ adaptive control have been discovered. In particular it is shown that in the case where the control effectiveness is known, both approaches are exactly the same, where the contribution of the $\mathcal{L}_1$ theory is the mathematically correct framework that provides a stability poof/condition which has not been available for the hedging approach [78]. Hence $\mathcal{L}_1$ adaptive control can be used to provide a stability proof for the modified reference model obtained by hedging. This also

means that the same performance guarantees as provided by $\mathcal{L}_1$ adaptive control hold.

- In difference to most publication, were only very particular uncertainties are considered, the robust performance w.r.t. all kinds of possible uncertainties is considered. Here it could be observed that standard direct MRAC approaches reduce the robust performance w.r.t. unmatched uncertainties in comparison to a baseline controller. Therefore a novel method is developed that additionally estimates the unmatched parameters and utilizes these estimates to adjust the reference model [79]. By means of this modification it is guaranteed that the reference trajectories remain achievable and thus the robust performance of the baseline controller can be reestablished. Note that within this work also an indirect MRAC approach is presented for MIMO (Multiple-Input Multiple-Output) systems, which automatically accounts for unmatched uncertainties. This is achieved by adjusting the identification model. To the authors best knowledge these approaches, designed to account for unmatched uncertainties, cannot be found in the MRAC literature.
  During the robustness analysis it was also observed that the robust performance w.r.t. certain matched uncertainties can deteriorate compared to a baseline controller. This could be attributed to the restrictiveness of the reference model, which “allows” only one reference trajectory. In difference the performance requirements allow a certain envelope for the response, which means that matched plant uncertainties can be tolerated to a certain extent. Therefore a solution is suggested, where the control signal is not augmented as long as the uncertainties are within a predefined set, and instead the reference model is adjusted to follow the plant [79].
- Finally the discussed control methods are applied to a full nonlinear model of a transport aircraft. Here the objective is to maintain good handling qualities over the complete flight envelope for the case when scheduling of the baseline controller is no longer possible due to the loss of the airspeed measurement. For this problem also the longitudinal response is considered. The applied control methods for the problem are $\mathcal{L}_1$ piecewise constant, direct MRAC. Results are also compared to an estimation of the airspeed by application of an Extended Kalman Filter (EKF).

1.3 Outline

The dissertation starts in Chapter 2 with a description of the simulations models that are used to evaluate the investigated adaptive control algorithms. Here also the problems are stated, which should be solved within this thesis by adaptive control.

In the subsequent Chapter 3 the requirements, which have to be satisfied, are defined. Particular interest is drawn to requirements for robust performance, as one of the main

claims of adaptive control is the improved performance w.r.t. parametric uncertainties. Hence, special focus is directed to the assessment of this property.

The basic concept and theory of MRAC with state feedback is explained in Chapter 4, where the fundamental difference of direct and indirect MRAC is pointed out and the parameter update laws and their stability properties are covered.

Following, different modifications of the reference model dynamics are discussed in Chapter 5. These modifications provide methods to account for certain issues that are not covered by the basic approaches in Chapter 4, like constraints in the input channel, or unmatched uncertainties.

5.2 shows the most basic robustness modifications, which were suggested in the standard literature on adaptive control, with the objective to guarantee robustness in the presence of non-parametric uncertainties.

A selection of update law modifications that should improve certain estimation properties like speed, transient characteristics, or long term learning are presented in 5.3.

The theory of $\mathcal{L}_1$ adaptive control is revisited in Chapter 6. Special interest is drawn to highlight the similarities of $\mathcal{L}_1$ adaptive control and the application of a hedging signal to the reference model. Furthermore the chapter also contains a section on $\mathcal{L}_1$ piecewise constant control, as it was suggested within the framework of $\mathcal{L}_1$ adaptive control. However, as it is pointed out, it is not an adaptive control approach.

While in the previous chapter a simple simulation model is used to assess the different methods and modifications, Chapter 7 contains the application of adaptive control to a full nonlinear model of a transport aircraft. For the particularly considered problem some selected adaptive control methods and an EKF are applied and evaluated.

Concluding this dissertation, Chapter 8 gives a summary of the thesis and provides a discussion and assessment of the methods that have been investigated. Moreover, future research directions are suggested.

Chapter 2

Model Description and Problem Formulation

In the scope of this thesis two different models will be used to investigate the capabilities of adaptive control. At first a simple short period model is used as a benchmark for the assessment of different adaptive control strategies. The aim is to improve the robust performance with respect to a nonlinear uncertainty in the pitch dynamics. Here the nonlinearity is dependent on the fast variables of the pitch dynamics, i. e. the angle of attack.

As second application example, some promising techniques are applied to a full nonlinear model of a transport aircraft. The problem considered here is the loss of the calibrated airspeed measurement, which is used as a scheduling parameter for the baseline controller. The augmenting adaptive control law should account for this loss by maintaining a homogenous response. As the air speed changes slowly compared to the short-period dynamics, in contrast to the previous problem, the augmenting control law has to adapt to slow changes of the dynamics.

2.1 Short Period Pitch-Up Model

2.1.1 Plant Dynamics

The following model is based on the linearized short period dynamics of a large transport aircraft and includes a nonlinear pitch-up. The linear approximation is valid for steady state horizontal flight condition with a true airspeed of $V_{TAS,trim} = 253.7\frac{m}{s}$. Pitch-up is a phenomenon where the pitch stiffness decreases with increasing angle of attack. As a result the assumed linear relation between angle of attack and pitching moment no longer holds. Due to the decreasing pitch-stiffness the system becomes less stable, which leads to a poor response for the pilot. This simple model is chosen for a first assessment of the capabilities of different adaptive control algorithms, with

the objective to improve the performance in the presence of the pitch-up phenomenon.

The system equations of the short-period dynamics with pitch-up nonlinearity are given by

$$\begin{aligned}\dot{\mathbf{x}}_P &= \mathbf{A}_P\mathbf{x}_P + \mathbf{b}_P\eta + \mathbf{f}(\mathbf{x}_P)\\ \mathbf{y}_P &= \mathbf{C}_P\mathbf{x}_P + \mathbf{d}_P\eta,\end{aligned} \tag{2.1}$$

where the states of the system are the angle of attack α in radians and the pith rate q in radians/second; the state vector is $\mathbf{x}_P = [\alpha \quad q]$. The elevator defection η is given in radians, and the outputs available for feedback are the load factor n_Z and the pitch rate q in radians/second, thus $\mathbf{y}_P = [n_Z \quad q]$. In detail Eq.(2.1) becomes

$$\begin{aligned}\begin{bmatrix}\dot{\alpha}\\ \dot{q}\end{bmatrix} &= \begin{bmatrix}Z_\alpha & 1+Z_q\\ M_\alpha & M_q\end{bmatrix}\begin{bmatrix}\alpha\\ q\end{bmatrix} + \begin{bmatrix}Z_\eta\\ M_\eta\end{bmatrix}\eta + \begin{bmatrix}0\\ f(\alpha)\end{bmatrix}\\ \begin{bmatrix}n_Z\\ q\end{bmatrix} &= \begin{bmatrix}-\frac{V_{TAS,trim}}{g}Z_\alpha & 0\\ 0 & 1\end{bmatrix}\begin{bmatrix}\alpha\\ q\end{bmatrix} + \begin{bmatrix}-\frac{V_{TAS,trim}}{g}Z_\eta\\ 0\end{bmatrix}\eta.\end{aligned} \tag{2.2}$$

The coefficients of the system matrix $\mathbf{A}_P$ and the input vector $\mathbf{b}_P$ are given in Table 2.1. Furthermore, $g = 9.81\frac{m}{s^2}$ and $V_{TAS,trim} = 253.7\frac{\mathrm{m}}{\mathrm{s}}$.

Z_α	Z_q	M_α	M_q	Z_η	M_η
-0.7040	0	-0.4839	-0.6538	-0.0248	-1.3505

Table 2.1: Coefficients of $\mathbf{A}_P$ and $\mathbf{b}_P$

With the parameters from Table 2.1 and by neglecting the nonlinearity $f(\alpha)$ the following transferfunctions for the outputs are obtained

$$\frac{n_Z(s)}{\eta(s)} = \frac{0.011\,s^2 + 0.001\,s - 0.43}{s^2 + 1.36\,s + 0.94} \tag{2.3}$$

$$\frac{q(s)}{\eta(s)} = \frac{-1.35\,s - 0.92}{s^2 + 1.36\,s + 0.94} \tag{2.4}$$

The pitch up nonlinearity $f(\alpha)$ is determined by

$$f(\alpha) = \begin{cases} 0 & \text{for } \alpha \cdot 180/\pi < 1{,}5deg \\ -2M_\alpha(\alpha \cdot 180/\pi - 1.5deg) & \text{for } \alpha \cdot 180/\pi \geq 1{,}5deg \end{cases} \tag{2.5}$$

and shown in Figure 2.1. This nonlinearity can also be interpreted as a break in the product $\widetilde{M}_\alpha(\alpha) \cdot \alpha$ which is shown in Figure 2.2.

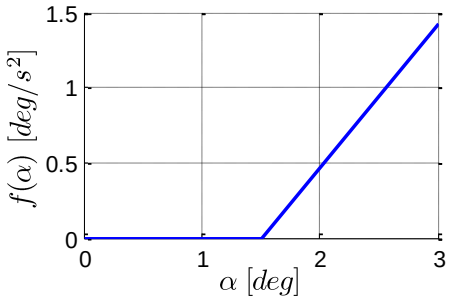

Figure 2.1: Pitch-up nonlinearity

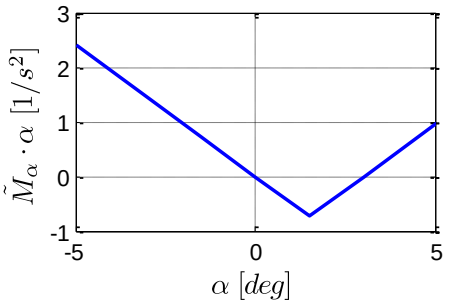

Figure 2.2: Pitch-up nonlinearity as nonlinearity in $M_\alpha\alpha$

The aircraft model furthermore contains an actuator model, a model for the computer delay, and a model for the dynamics of the structural filters as shown in Figure 2.3.

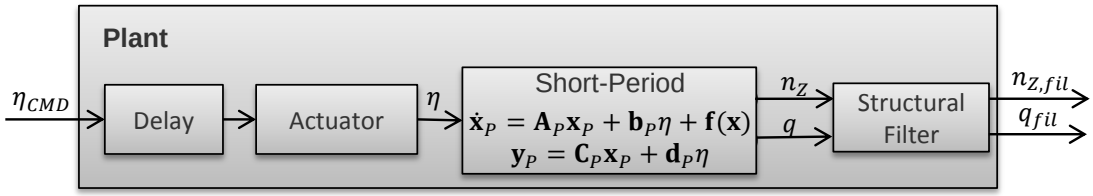

Figure 2.3: Short-period aircraft model with pitch-up nonlinearity

The actuator dynamics are given by a third order transfer function

$$G_{act}(s) = \frac{5.01s+19800}{s^3+81.41s^2+3564s+19800}, \tag{2.6}$$

where s is the Laplace variable.

The dynamics of the structural filters for the outputs n_Z and q are determined by the same second order transfer functions

$$G_{fil}(s) = \frac{1}{0.0063s^2+0.1125s+1}, \tag{2.7}$$

and the computer delay is modeled by

$$G_{del}(s) = \frac{5.208\cdot10^{-5}s^2-0.0125s+1}{5.208\cdot10^{-5}s^2+0.0125s+1}. \tag{2.8}$$

Including actuator, filters, and delay, the poles and zeros of the open-loop system, without nonlinearity, are shown in Table 2.2 and Figure 2.4.

By defining that the transfer functions of Eq.(2.6)-(2.8) have the following state-space representation

$$G_{(\cdot)}(s) = \left[\begin{array}{c|c} \mathbf{A}_{(\cdot)} & \mathbf{b}_{(\cdot)} \\ \hline \mathbf{c}_{(\cdot)}^T & d_{(\cdot)} \end{array}\right] \tag{2.9}$$

the complete open loop system can also be denoted as a state-space system:

$$\begin{bmatrix}\dot{\mathbf{x}}_{fil}\\ \dot{\mathbf{x}}_P\\ \dot{\mathbf{x}}_{act}\\ \dot{\mathbf{x}}_{del}\end{bmatrix}=\begin{bmatrix}\mathbf{A}_{fil} & \mathbf{b}_{fil}\mathbf{C}_P & \mathbf{b}_{fil}d_P\mathbf{c}_{act}^T & \mathbf{0}\\ \mathbf{0} & \mathbf{A}_P & \mathbf{B}_P\mathbf{c}_{act}^T & \mathbf{0}\\ \mathbf{0} & \mathbf{0} & \mathbf{A}_{act} & \mathbf{b}_{act}\mathbf{c}_{del}^T\\ \mathbf{0} & \mathbf{0} & \mathbf{0} & \mathbf{A}_{del}\end{bmatrix}\begin{bmatrix}\mathbf{x}_{fil}\\ \mathbf{x}_P\\ \mathbf{x}_{act}\\ \mathbf{x}_{del}\end{bmatrix}+\begin{bmatrix}\mathbf{0}\\ \mathbf{0}\\ \mathbf{b}_{act}d_{del}\\ \mathbf{b}_{act}\end{bmatrix}\eta_{CMD}+\begin{bmatrix}\mathbf{0}\\ \mathbf{f}(\mathbf{x})\\ \mathbf{0}\\ \mathbf{0}\end{bmatrix}$$

$$\mathbf{y}_{fil}=[\mathbf{C}_{fil}\quad\mathbf{0}\quad\mathbf{0}\quad\mathbf{0}]\begin{bmatrix}\mathbf{x}_{fil}\\ \mathbf{x}_P\\ \mathbf{x}_{act}\\ \mathbf{x}_{del}\end{bmatrix} \tag{2.10}$$

$$fil=filter, p=plant, act=actuator, del=delay$$

Within this thesis also a mixed notation of Laplace domain is used, where $\{\bullet\}_t$ denotes that the term inside the brackets is transformed from the Laplace domain to the time domain and in the following $\{\bullet\}_s$ denotes the reverse transformation. Using this notation the system in Eq.(2.10) can be written by

$$\begin{aligned}\dot{\mathbf{x}}_P(t)&=\mathbf{A}_P\mathbf{x}_P(t)+\mathbf{b}_P\{G_{act}(s)G_{del}(s)\eta_{CMD}(s)\}_t+\mathbf{f}(\mathbf{x}_P(t))\\ \mathbf{y}_P(t)&=\left\{G_{fil}(s)\{\mathbf{C}_P\mathbf{x}_P(t)+\mathbf{d}_P\{G_{act}(s)G_{del}(s)\eta_{CMD}(s)\}_t\}_s\right\}_t,\end{aligned} \tag{2.11}$$

In Appendix A a frequency anylysis of the linear plant dynamics is prvided. In particular, in Figure A.1 the bode plots of the plant transfer functions from the input η_{CMD} to the filtered outputs $n_{Z,fil}$ and q_{fil} are shown. Furthermore, for feedback of the filtered outputs $n_{Z,fil}$ and q_{fil} the root locus plots are shown in Figure A.2 and Figure A.3, and the Nichols plots are shown in Figure A.4 and Figure A.5.

	Poles	Damping	Frequency [rad/s]
Short period	$-0.7\pm0{,}7i$	0.70	0.97
Actuator	-6.4	1	6.42
	$-37\pm41i$	0.68	55.5
Filter n_Z	$-8.9\pm8.9i$	0.71	12.6
Filter q	$-8{,}9\pm8{,}9i$	0,71	12.6
Delay	$-120\pm69i$	0,87	139.0

Table 2.2: Poles of the plant

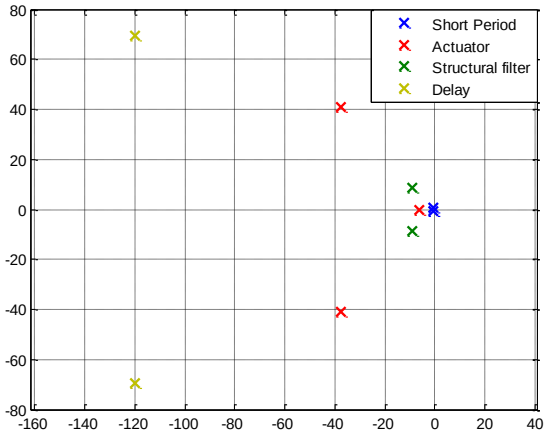

Figure 2.4: Open loop poles of the plant

2.1.2 Baseline Controller

For the nominal plant dynamics a baseline with proportional and integral feedback is provided as shown in figure Figure 2.5 and given by

$$\eta_{BL} = \mathbf{k}_y^T \mathbf{y}_P^+ + k_r n_{Z,CMD}, \tag{2.12}$$

where $n_{Z,CMD}$ is the load factor reference command and $\mathbf{y}_P^+ = [n_Z \quad q \quad e_I]^T$, with the integrated error $e_I = \int (n_{Z,CMD} - n_Z) dt$. Furthermore, $\mathbf{k}_y^T$ is the feedback gain vector and k_r is the feedforward gain. The representation of Figure 2.5 is used to highlight that the system is augmented by the additional integrator state. However, if the controller gains are scheduled, as it is normally done for the real aircraft, then the integral gain must be in front of the integrator.

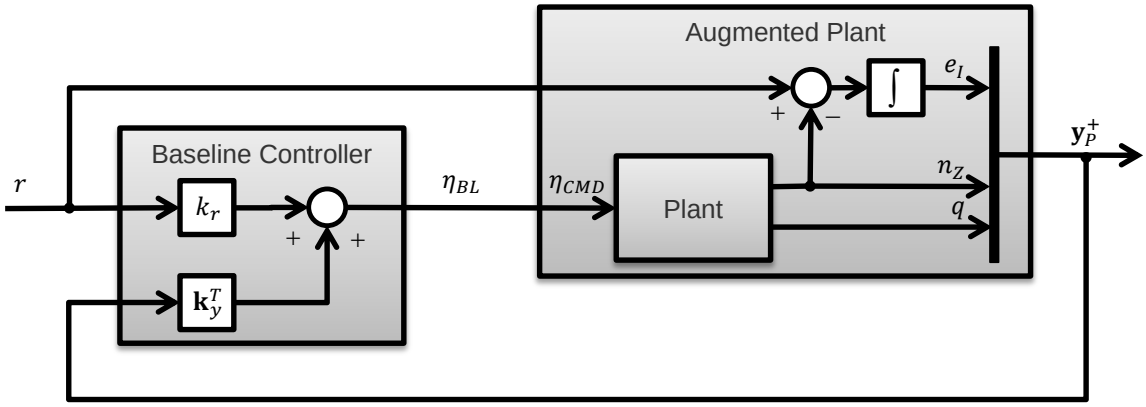

Figure 2.5: Baseline controller and plant

When the short period dynamics are augmented by the integrator it can be denoted by

$$\begin{aligned}\dot{\mathbf{x}}_P^+ &= \mathbf{A}_P^+\mathbf{x}_P^+ + \mathbf{b}_P^+\eta + \mathbf{b}_r^+ r + \mathbf{f}^+(\mathbf{x}_P)\\ \mathbf{y}_P^+ &= \mathbf{C}_P^+\mathbf{x}_P^+ + \mathbf{d}_P^+,\end{aligned} \tag{2.13}$$

where the states and the outputs of the system are augmented by the integrator state e_I, and hence the augmented state vector becomes $\mathbf{x}_P^+ = [\alpha \quad q \quad e_I]$. In detail the augmented open loop system can be denoted by

$$\begin{aligned}\begin{bmatrix}\dot{\alpha}\\ \dot{q}\\ \dot{e}_I\end{bmatrix} &= \begin{bmatrix} Z_\alpha & 1+Z_q & 0\\ M_\alpha & M_q & 0\\ \frac{V_{TAS,trim}}{g}Z_\alpha & 0 & 0\end{bmatrix}\begin{bmatrix}\alpha\\ q\\ e_I\end{bmatrix} + \begin{bmatrix}Z_\eta\\ M_\eta\\ 0\end{bmatrix}\eta + \begin{bmatrix}0\\ 0\\ 1\end{bmatrix}n_{Z,CMD} + \begin{bmatrix}0\\ f(\alpha)\\ 0\end{bmatrix}\\ \begin{bmatrix}n_Z\\ q\\ e_I\end{bmatrix} &= \begin{bmatrix} -\frac{V_{TAS,trim}}{g}Z_\alpha & 0 & 0\\ 0 & 1 & 0\\ 0 & 0 & 1\end{bmatrix}\begin{bmatrix}\alpha\\ q\\ e_I\end{bmatrix} + \begin{bmatrix} -\frac{V_{TAS,trim}}{g}Z_\eta\\ 0\\ 0\end{bmatrix}\eta.\end{aligned} \tag{2.14}$$

Applying the baseline control law of Eq.(2.12) to the reduced system in Eq.(2.14) (w/o actuator, delay, and structural filters) the poles given in Table 2.3 are obtained for the closed loop system.

	Poles	Damping	Frequency [rad/s]
Short period	$-0.7 \pm 0.7i$	0.71	0.99
Integrator	-1.0	1.0	1.0

Table 2.3: Poles of the reduced closed loop system

Including actuator, delay, and structural filters, the baseline control law places the eigenvalues of the closed loop nominal dynamics at the poles given in Table 2.4. And for the transfer function from the reference command r to the measured load factor also the zeros are given in Table 2.4.

Poles	Damping	Frequency [rad/s]	Zeros
$-0.71 \pm 0.69i$	0.71	0.99	-3919.81
-2.31 ± 0.52i	0.98	2.37	-0.0062
$-37.5 \pm 40.9i$	0.68	55.5	-0.0010
$-9.8 \pm 9.1i$	0.73	13.3	0.0061
$-8.9 \pm 8.9i$	0.71	12.6	$120 \pm 69i$
$-120 \pm 69i$	0.87	139	

Table 2.4: Poles and zeros of the transfer function from r to $n_{Z,fil}$ plant

Table 2.5 summarizes the robust stability metrics of the baseline controller. In particular the Gain Margin (GM), the Phase Margin (PM), and Time-Delay Margin (TDM) are calculated for the input channel. The GM is defined as the maximum gain, the PM is defined as the maximum phase delay, and the TDM is defined as the maximum amount of time-delay [64], which the system can sustain before instability occurs. All three margins are defined for the input channel. This metric is later used as a measure for robust stability of the adaptive systems.

GM	PM	TDM
15.7 dB (at 4.95 rad/sec)	70.4 deg (at 1.03 rad/sec)	1.19 sec (at 1.03 rad/sec)

Table 2.5: Gain, phase, and time-delay margin of baseline controller

The Bode plot of the open loop controlled plant, is shown in Figure 2.6, the Nichols plot is displayed in Figure 2.7 and the Nyquist plot is shown in Figure 2.8.

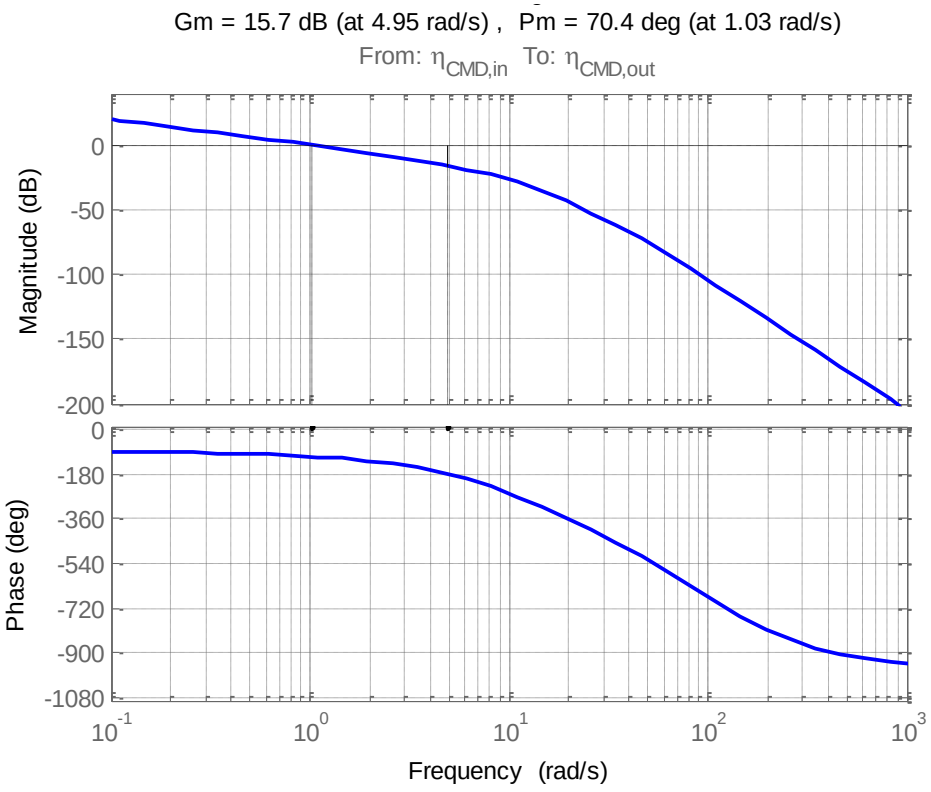

Figure 2.6: Bode plot of open loop controlled plant

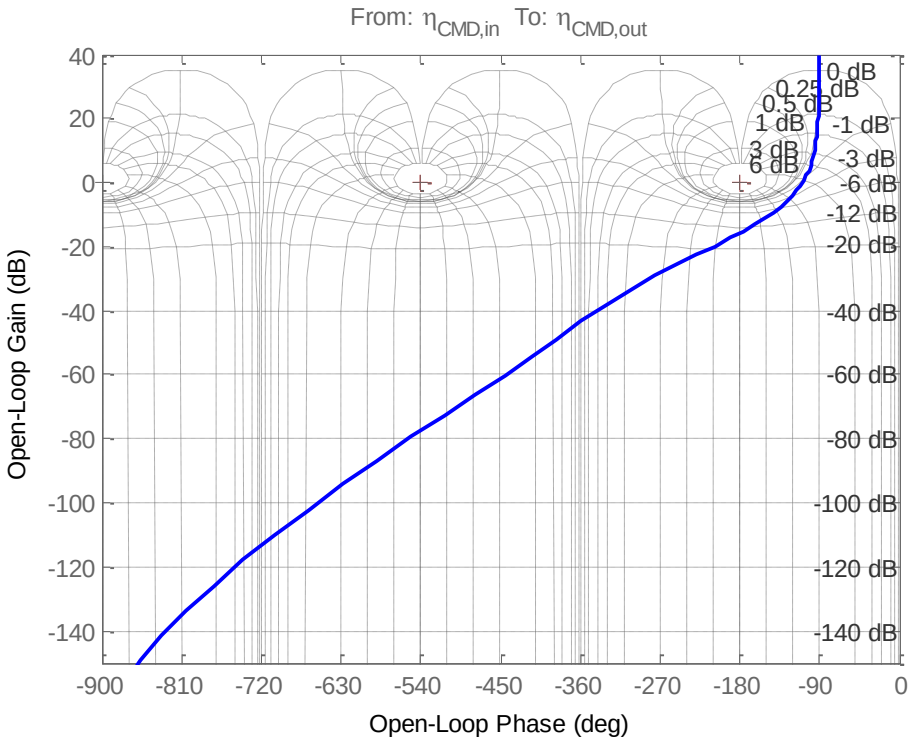

Figure 2.7: Nichols plot of open loop controlled plant

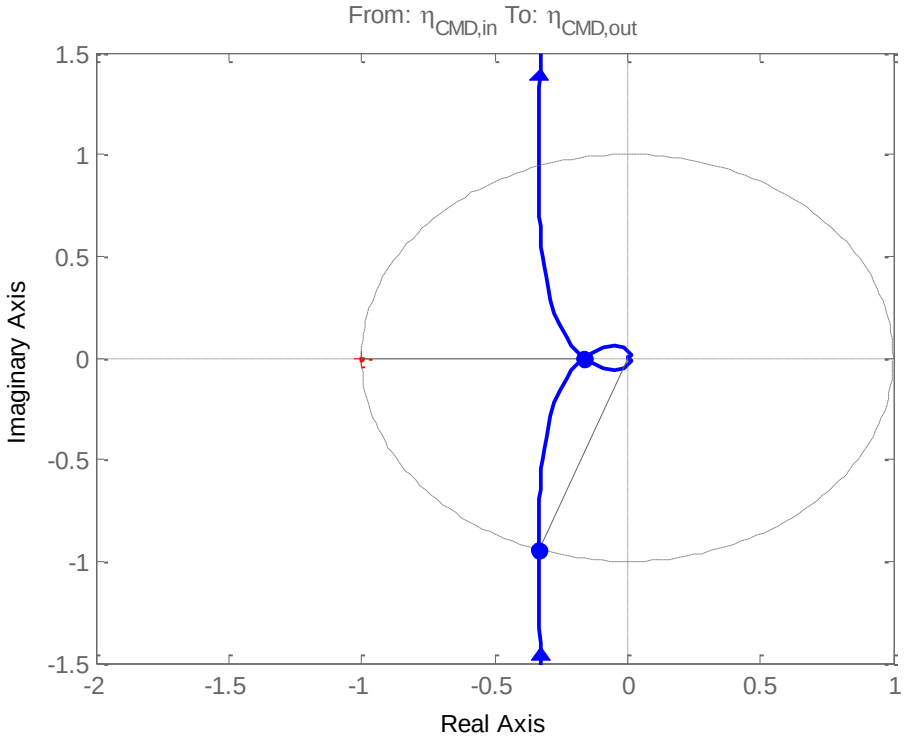

Figure 2.8: Nyquist plot of the open loop controlled plant

2.1.3 Problem formulation

For the nominal system, without nonlinearity, the closed-loop shows the desired response. However, in the presence of the nonlinearity the performance largely deteriorates with increasing load factor command (see Figure 2.10). This results from the destabilizing effect of the nonlinearity in higher α-regimes.

To obtain an ideal response in the presence of the nonlinearity, it would be necessary to cancel the nonlinearity with a feedback signal. Due to the fact that the nonlinearity is a function of the angle of attack this is not directly possible, as α is not an available feedback signal. However, for the considered case the relationship between α and n_Z is linear, and so, in close approximation, it can be assumed that $n_Z = \frac{V_{TAS,trim}}{g} Z_\alpha \cdot \alpha$, and thus $f(\alpha)$ can be transformed to $f^*(n_Z)$. That means the nonlinearity can be canceled in good approximation with the feedback signal $\eta_{nl}^* = -\frac{1}{M_\eta} f^*(n_Z)$. This is shown in Figure 2.9. In Figure 2.10 the response with the nonlinear feedback signal is shown in comparison to the system response with and without nonlinearity, in the presence of the baseline controller.

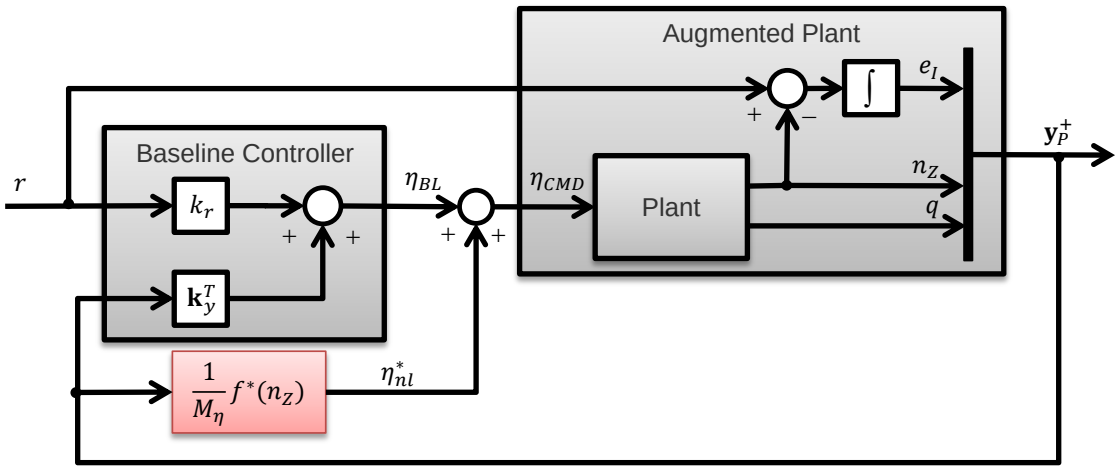

Figure 2.9: Closed loop with ideal, nonlinear feedback

It should be further noted, that the presence of actuators, filters and delay prohibits an exact cancelation of the nonlinearity. However, by using the feedback signal ν_{nl} a very good response can be achieved, and this response will be used as a benchmark for the assessment of the adaptive controllers. Obviously, the nonlinear feedback also leads to a new input signal, which in the following is assumed to be the ideal input benchmark, and it is shown in Figure 2.11 together with the actuator rate and acceleration.

Form the previous explanation the objective is to augment the baseline controller with an adaptive controller that solves the considered problem in a way that the response

should be as close to the ideal load factor trajectory as possible. Furthermore, the adaptive controllers should not only provide good performance for the considered uncertainty, but they should satisfy some general requirements for robust stability and performance, which are defined in Section 3.1. Based on the achievable performance and the defined requirements different approaches and modifications are compared.

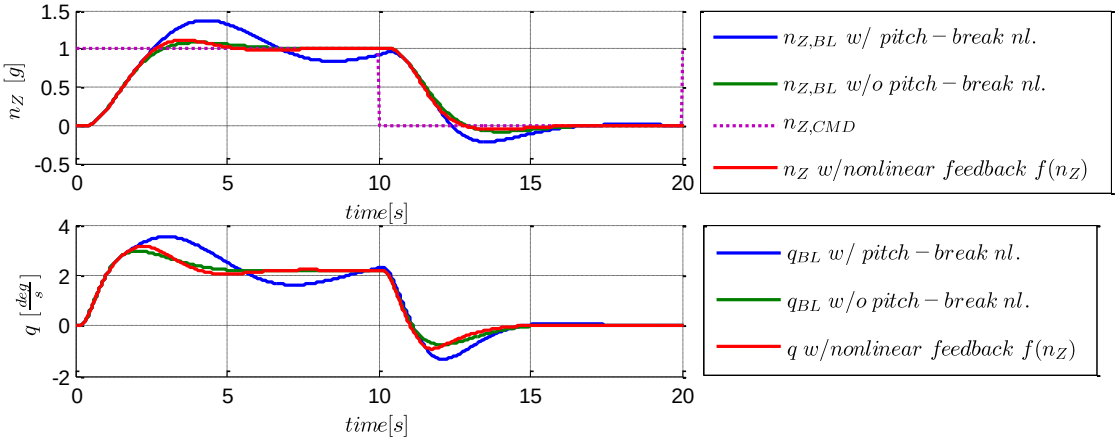

Figure 2.10: Plant response with baseline control law and nonlinear feedback

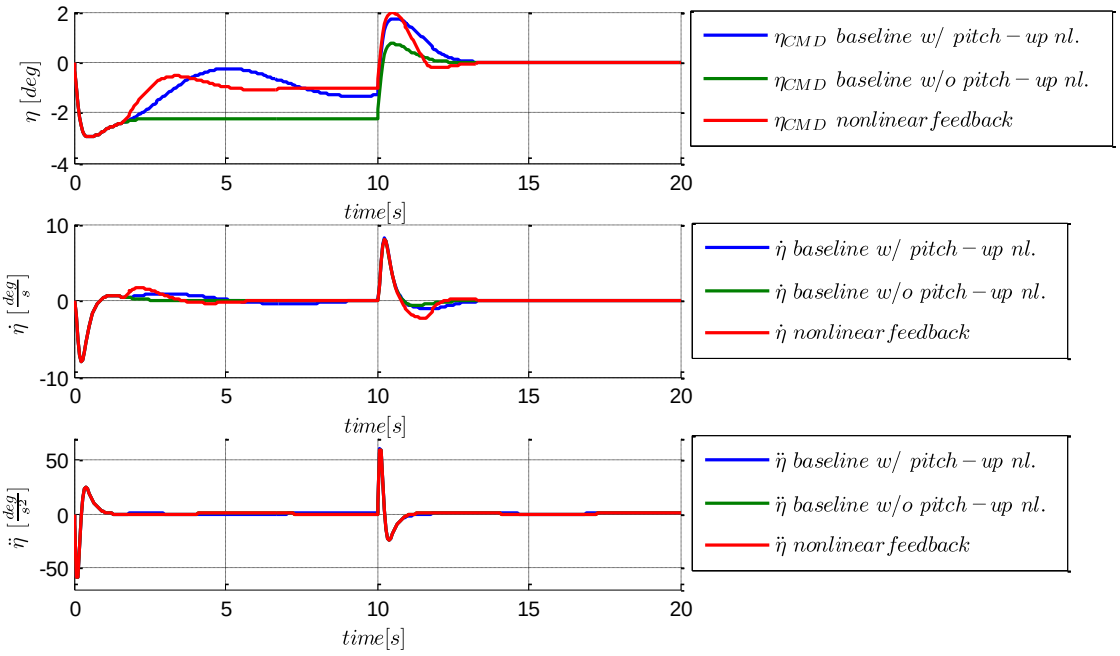

Figure 2.11: Control signal, rate, and acceleration of baseline control law and nonlinear feedback

2.2 Full Nonlinear Transport Aircraft Model

2.2.1 Plant Dynamics

In the following the model of a large transport aircraft is described. For this model the loss of scheduling parameters and the benefit of adaptive control will be investigated. As the main influence on the scheduled controller gains stems from the scheduling with the calibrated airspeed V_{CAS}, the evaluation also focuses on the loss of the V_{CAS} measurement for scheduling purpose.

In Table 2.6 the inputs to the model, which are available for control are summarized, with the abbreviations that are used in the course of this thesis. The important input variables are elevator deflection η_{CMD}, aileron deflection ξ_{CMD}, and rudder deflection ζ_{CMD}. Because the model provides auto thrust, the thrust lever is not considered as an input variable.

To give an idea of the flight envelope the feasible trim points for a horizontal wings-level flight are shown in Figure 2.12. Although the model allows to obtain trim points for Mach>1, these solutions are unrealistic and a reasonable upper bound for the Mach number can be assumed with $Ma_{max} = 0.86$ which is the MMO for the aircraft considered above 30000 feet. Below the maximum operating speed is not defined by the Mach number but by the speed: VMO=330kt. The speed and height limits which are enforced by protections are also shown in Figure 2.12 and defined by the black contour.

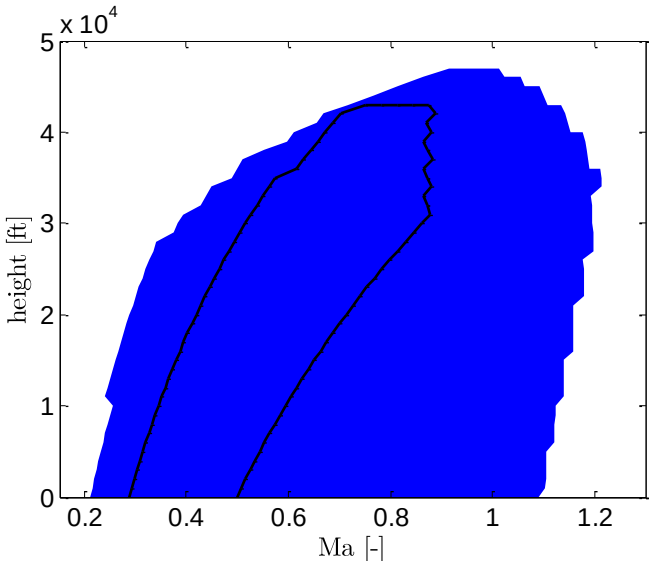

Figure 2.12: Flight envelope

2.2.1.1 Equations of Motion

In the following the equations of motions of the rigid body aircraft model are presented as they can be found in the standart literature [80] [81] [82].

2.2.1.1.1 Force Equations / Principle of Linear Momentum

The principle of linear momentum denoted in the body-fixed frame is given by

$$m\left(\dot{\mathbf{v}}_K^{\mathrm{G}}\right)_B^{EB} = (\mathbf{F}_{aero}^A)_B + \left(\mathbf{F}_{grav}^G\right)_B + \left(\mathbf{F}_{prop,l}^{E_l}\right)_B + \left(\mathbf{F}_{prop,r}^{E_r}\right)_B - (\boldsymbol{\omega}^{OB})_{\mathrm{B}} \times \left(\mathbf{v}_K^{\mathrm{G}}\right)_B^E, \quad (2.15)$$

where $\left(\mathbf{v}_K^G\right)_B^E$ is the kinematic velocity of the aircraft center of gravity G w.r.t. the Earth-Certered-Earth-Fixed frame (E-frame), denoted in the body-fixed frame (B-frame) and $\left(\dot{\mathbf{v}}_K^{\mathrm{G}}\right)_B^{EB}$ is the time derivative of $\left(\mathbf{v}_K^G\right)_B^E$ taken in the B-frame. Here a non-rotating flat earth is assumed. $(\boldsymbol{\omega}^{OB})_{\mathrm{B}}$ is the angular velocity of the aircraft with respect to the NED-frame (O -frame). The resulting force consist of an aerodynamic force $\mathbf{F}_{aero}^A$ the act on the the aerodynamic center A, the gravitational force $\mathbf{F}_{grav}^G$ that act on G, and two propulsive forces which are produce by the left $\left(\mathbf{F}_{prop,l}^{E_l}\right)_B$ and right $\left(\mathbf{F}_{prop,l}^{E_l}\right)_B$ engine, respectively. The propulsive act at the mounting point of the left and right engine, E_l and E_r, respectively. By denoting the forces in their respective frames we obtain

$$m\left(\dot{\mathbf{v}}_K^{\mathrm{G}}\right)_B^{EB} = \mathbf{T}_{BA}(\mathbf{F}_{aero}^A)_A + \mathbf{T}_{BO}\begin{bmatrix}0\\0\\mg\end{bmatrix}_{\mathrm{O}} + \begin{bmatrix}X_P\\0\\0\end{bmatrix}_{\mathrm{B}} - (\boldsymbol{\omega}^{OB})_{\mathrm{B}} \times \left(\mathbf{v}_K^G\right)_B^E. \quad (2.16)$$

$\mathbf{T}_{BA}$ is the transformation matrix from the aerodynamic frame (A -frame) to the B-frame, and $\mathbf{T}_{BO}$ from the O-frame to the B-frame. The aerodynamic force is defined by the lift, drag, and side-force coefficients:

$$(\mathbf{F}_{aero}^A)_A = [-L \quad Q \quad -D]^T = (\mathbf{C}_{For})_{\mathrm{A}} \cdot \bar{q}S = [-C_L \quad C_Q \quad -C_D]^T \cdot \bar{q}S \quad (2.17)$$

The dynamic pressure is denoted by $\bar{\mathrm{q}} = \frac{\rho \mathrm{V}_{TAS}^2}{2}$, S is the wing reference area, and the aerodynamic coefficients are provided in the Appendix A.

2.2.1.1.2 Moment Equations/ Principle of Angular Momentum

The principle of linear momentum denoted in the body-fixed frame is given by

$$(\mathbf{I}^G)_{BB}(\dot{\boldsymbol{\omega}}^{OB})_B^{\mathrm{B}} = (\mathbf{M}^G)_B - (\boldsymbol{\omega}^{OB})_B \times (\mathbf{I}^G)_{BB}(\boldsymbol{\omega}^{OB})_B, \quad (2.18)$$

where $(\mathbf{I}^G)_{BB}$ is the inertia tensor of the aircraft in the B-frame. The aerodynamic moment $\mathbf{M}_{aero}^A$ is not directly calculated at G, but at the aerodynamic center A. Therefore, for the resulting moment at the center of gravity the aerodynamic forces must be taken into account. Furthermore, the propulsive forces also produce a moment at the center of gravity, determined by the lever arm between G and the mounting point of the left and right engine, E_l and E_r, respectively.

$$(\mathbf{I}^G)_{BB}(\dot{\boldsymbol{\omega}}^{OB})_B^{\mathrm{B}} = (\mathbf{M}_{aero}^A)_B + (\mathbf{r}^{GA})_B \times (\mathbf{F}_{aero}^A)_B + (\mathbf{r}^{GE_l})_B \times \left(\mathbf{F}_{prop,l}^{E_l}\right)_B \quad (2.19)$$

$$+(\mathbf{r}^{GE_r})_B \times \left(\mathbf{F}_{prop,r}^{E_r}\right)_B - (\boldsymbol{\omega}^{OB})_B \times (\mathbf{I}^G)_{BB}(\boldsymbol{\omega}^{OB})_B$$

The aerodynamic moments are determined by the moment coefficients in the form

$$(\mathbf{M}_{aero}^A)_B = (\mathbf{C}_{Mom})_B \cdot \bar{q}Sl = [C_l \quad C_m \quad C_n]^T \cdot \bar{q}Sl, \tag{2.20}$$

where l is the reference chord length. The moment coefficients are divided into

$$(\mathbf{C}_{Mom})_B = \left(\mathbf{C}_{Mom,aero}\right)_B + \left(\mathbf{C}_{Mom,\omega}\right)_B \frac{l}{V_K}\boldsymbol{\omega}_B^{OB} + \left(\mathbf{C}_{Mom,\delta}\right)_B \boldsymbol{\delta}, \tag{2.21}$$

which are given in the Appendix A. $\boldsymbol{\delta}$ is the vector of control inputs.

2.2.1.2 Actuator Models

All actuators are modeled by first order lags as shown in Figure 2.13, where the time constants T are given in Table 2.6. Furthermore, the maximum and minimum rates are limited and the limits are also provided in Table 2.6.

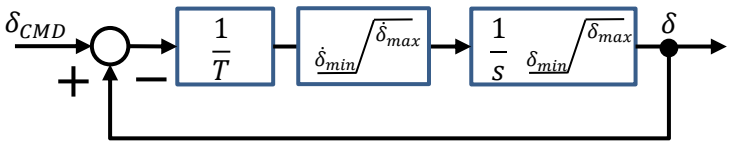

Figure 2.13: Actuator models

	Symbol	$\delta_{max}\ [deg]$	$\delta_{min}\ [deg]$	$\dot{\delta}_{max}\ \left[\frac{deg}{s}\right]$	$\dot{\delta}_{min}\ \left[\frac{deg}{s}\right]$	T
Aileron	ξ	30	−30	40	−40	0.15
Elevator	η	10	−25	40	−40	0.1
Rudder	ζ	30	−30	40	−40	0.15

Table 2.6: Parameters of the actuator model

2.2.2 Baseline Pitch Control Law

The inner loop longitudinal control law provides tracking for a commanded load factor. $n_{Z,CMD}$. As the measured load factor $n_{Z,IRS,MEAS}$ is given at the installation point of the Inertial Reference System (IRS) this measurement should track the command. The IRS is installed ahead of the center of gravity and near the cockpit. The elevator deflection is given by

$$\eta = -\eta_{FF} + \eta_{FB,Int} + \eta_{FB,n_z} + \eta_{FB,q} \tag{2.22}$$

η_{FF} is a feedforward signal determined by

$$\eta_{FF} = k_{FF}(V_{CAS,EST}) \cdot n_{Z,CMD} \tag{2.23}$$

where the gain $k_{FF}(V_{CAS,EST})$ is scheduled with the estimated calibrated airspeed $V_{CAS,EST}$, which is given in Eq.(2.28), and the gain change is shown in Figure 2.14.

$\eta_{FB,Int}$ provides integral error feedback of the form

$$\begin{aligned}\eta_{FB,Int} &= \int k_{e_I}(V_{CAS,EST}) \cdot [n_{Z,IRS,MEAS} - (n_{Z,CMD} - n_{Z,EQUI})] \cdot dt \\ &= \int k_{e_I}(V_{CAS,EST}) \cdot e_{n_z} \cdot dt.\end{aligned} \tag{2.24}$$

With $n_{Z,EQUI} = \frac{\cos(\Theta)}{\cos(\Phi)}$ being the necessary acceleration in direction of the z-axis of the b-frame to counteract the gravitational force. Here the integral gain $k_{e_I}(V_{CAS,EST})$ is only scheduled with the calibrated airspeed as displayed in Figure 2.15.

η_{FB,n_Z} provides feedback of the load factor

$$\eta_{FB,n_Z} = k_{n_Z}(V_{CAS,EST}) \cdot [n_{Z,IRS,MEAS} - \cos\Theta]. \tag{2.25}$$

The feedback gains for the load factor are scheduled with the calibrated airspeed $k_{n_Z}(V_{CAS,EST})$ as shown in Figure 2.17.

$\eta_{FB,q}$ provides feedback of the pitch rate, which is realized by means of a washout filter on Θ, whith a time constant of 0.05s. This washout filter provides a $\dot{\Theta}$, which is zero for a steady state turn where q takes a constant value.

$$\eta_{FB,q} = k_q(V_{CAS,EST}) \cdot G_{wo}(s) \cdot \Theta \tag{2.26}$$

where the washout filter is given by

$$G_{wo}(s) = \frac{Ts}{Ts+1}. \tag{2.27}$$

The feedback gain for the pitch rate is again only scheduled with the calibrated airspeed $k_q(V_{CAS,EST})$ and displayed in Figure 2.16

$V_{CAS,EST}$ is the estimated velocity given by

$$V_{CAS,EST}(s) = G_{PT1,2}(s) \cdot \left(V_{CAS,MEAS}(s) + 2a_V(s) * G_{PT1,5}(s)\frac{V_{CAS,MEAS}(s)}{V_{TAS,MEAS}(s)}\right) \tag{2.28}$$

Where a_V is the acceleration along the trajectory (in direction of the kinematic velocity). And $G_{PT1,2}(s)$ and $G_{PT1,5}(s)$ are stable first order lag transfer functions with time constants of 2 seconds and 5 seconds, respectively.

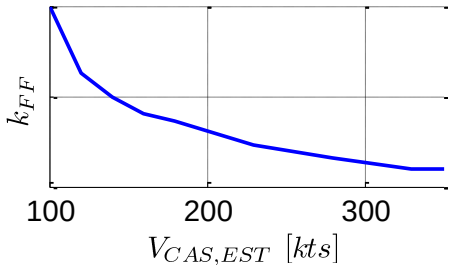

Figure 2.14: $k_{FF}(V_{CAS,EST})$

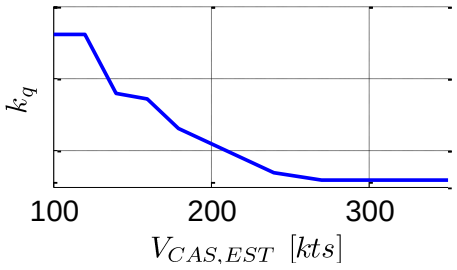

Figure 2.16: $K_q(V_{CAS,EST})$

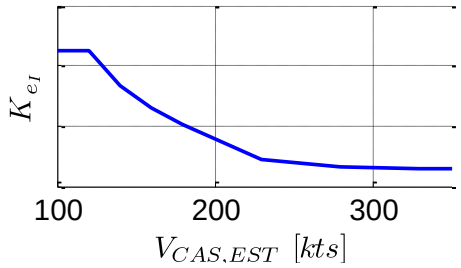

Figure 2.15: $k_{e_I}(V_{CAS,EST})$

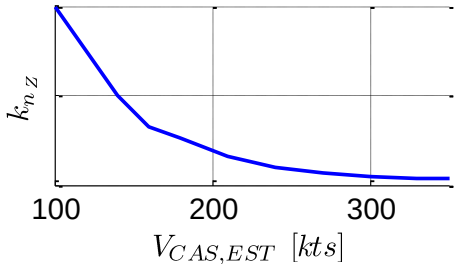

Figure 2.17: $K_{n_z}(V_{CAS,EST})$

2.2.3 Problem Formulation

As already mentioned the considered problem for the full nonlinear model is that the measurement of the calibrated airspeed is lost, and therefore the main parameter $V_{CAS,EST}$ cannot be used anymore to schedule the baseline control law. For the conventional control law, it follows, that the loss of measurement has to be detected and a robust set of controller gains must be chosen. Here it is considered that the gains of the baseline controller are fixed to the values that are obtained when the scheduling parameter $V_{CAS,EST}$ equals 320kts. This means, controller gains close to the boundary of the envelope are chosen. From Figure 2.14, Figure 2.15, Figure 2.16 and Figure 2.17 we can see that these gains are the smallest possible gains of the baseline controller. This is rather conservative and provides a more challenging task for the adaptive controller.

With the fixed robust set of gains the control law can only provide the desired performance in a certain region of the envelope, but if the airspeed deviates too much from this region the handling qualities of the aircraft will deteriorate. So the objective of the augmenting adaptive control law will be to maintain the desired performance and handling qualities as far as possible for the complete flight envelope. In this case the augmenting control law has to adjust to slowly changing parameters, as the dynamics change with the variation of airspeed, and the baseline controller does not account for this due to the loss of scheduling information.

In difference, for the pitch-up problem the augmenting control law has to adjust extremely fast to the nonlinearity which is dependent on the angle of attack, and hence it depends on a state that has a much faster dynamics than the calibrated airspeed.

Chapter 3

Requirements and Evaluation

As a manned aircraft is considered the handling qualities are of utmost importance. That means the control laws must not only provide robust stability, but robust performance is the key property of the control law to make the aircraft controllable for the pilot. The two most important specification documents for flying qualities are MIL-HDBK-1797A and MIL-F-8785C, and MIL-DTL-9490E "establishes general performance, design, development and quality assurance requirements for the flight control systems". Actually these specifications are for military aircraft, however they are also used as guidelines for civil aircraft certification.

To separate different levels of flying qualities the specification in MIL-F-8785C defines three different levels as shown in Table 3.1. These different levels of flying qualities are directly linked to pilot's opinion, and thus, to actually obtain a classification, flight tests need to be conducted to obtain and evaluate ratings from different pilots. The most prominent pilot opinion rating is the Cooper-Harper Rating and the different levels actually originate from this scale [83].

Level 1	Satisfactory	Flying qualities clearly adequate for the mission Flight Phase
Level 2	Acceptable	Flying qualities adequate to accomplish the mission Flight Phase, but some increase in pilot workload or degradation in mission effectiveness, or both, exists.
Level 3	Controllable	Flying qualities such that the airplane can be controlled safely, but pilot workload is excessive or mission effectiveness is inadequate, or both. Category A Flight Phases can be terminated safely, and Category B and C Flight Phases can be completed.

Table 3.1: Definition of handling quality levels according to MIL-F-8785C

According to MIL-F-8785C here a large and heavy transport aircraft corresponding to Class III is considered, where only nonterminal flight phases of category B (e.g. cruise, climb, loiter) are investigated. As the assessment of all handling quality requirements provided in the certification guidelines would be beyond the scope of this thesis, a set of reduced time domain requirements is chosen. Furthermore, many of the requirements are frequency domain requirements or defined for linear low order equivalent systems. These low order equivalent systems are derived from matching the frequency response of a linear higher order system to a system containing only the rigid body dynamics, in the frequency domain of interest. If a nonlinear control system is used a linear model approximation that is accurate enough over certain domain in the state space cannot always be obtained. Hence many of the criteria cannot be directly applied when a nonlinear control system is used. Especially during the transient phase, where the parameters are adjusted, the system dynamics can vary significantly due to the influence of the adaptive controller. Thus, frequency domain methods, like the one suggested in [84], where the frequency response is obtained experimentally from Bowditch-Lissajous curves, only provide meaningful results when it is guaranteed that the adaptation dynamics does not affect the rigid body dynamics. In the following the augmenting adaptive control laws are assessed by the chosen time domain criteria. Therefore the response w.r.t. a chosen set parametric uncertainties is evaluated, as explained in the following section. For adaptive control it is in general an open question what kind of performance metrics are feasible for the assessment. In [52] and [64] some general performance metrics for adaptive control are applied, where in the following some of them are used for the tuning of the controller parameters.

Even though robust performance is most important, the certification also requires a proof of robust stability. Because the stability results of adaptive control systems are all based on Lyapunov theory, with the attempt to prove global stability, complete knowledge of the system would be necessary to assess the robustness properties. As complete knowledge of the system dynamic is rarely available, it is more traceable to design a control system to satisfy certain robustness margins as in classic control theory. The most prominent certification criteria are gain and phase margin, for which MIL-DTL-9490E requires under normal conditions for each feedback channel 6dB and 45deg, respectively. Though the classic certification criteria, like gain and phase margin, do not guarantee stability in a mathematical exact sense, but rely on a vast amount of experience, they are valuable and traceable margins to account for system uncertainties. Since the adaptive system is inherently nonlinear, methods and metrics from classic linear control theory like gain and phase margin, Bode plots or Nyquist diagrams are not applicable, and reliable stability margins to assess the robustness of adaptive control systems in a unified and accepted framework are not available yet.

Although certification criteria for adaptive flight control systems are not available yet, first proposals are on the table. As mentioned above the concept of phase margin and

gain margin cannot be applied to the adaptive control system. Actually, the gain margin of the adaptive system is infinity because any gain in the plants input channel can be contributed to the matched uncertainties, and thus is compensated by the adaptive parameters [85] [64]. In difference, the phase margin does not even exist for adaptive systems due to the inherent nonlinearity. An approximate phase margin can only be calculated if the adaptive parameters have converged to a steady state value or if the adaptation is switched off and the adaptive parameters are frozen. This is why a time delay margin has been commonly suggested as a replacement for the phase margin [66] [86] [69] [73]. Though the time delay margin is a suitable robustness metric, the problem is that no analytic method, which can be used in a unified framework, is available for computing it. For example a method for estimating the time delay margin has been proposed in [66] by means of approximating the time delayed system with a Pade approximation. But the theoretically derived lower bounds are conservative compared to the time delay margins obtained in simulations. Furthermore, a method for the computation of the time delay margin via the Razumikhin Method has been proposed in [73]. Even good results for estimating the time delay margin could be achieved for scalar systems, the method has not been a applied to higher dimensional plants and is not ready to be used in a unified framework. So at the moment the best way to compute the time delay margin is by simulation, and this is the way it was computed in this thesis. In [65] an interesting assessment can be found, where the robustness of the adaptive system w.r.t. time delay margin and input gain variation is analyzed by Monte Carlo simulation and compared to the analytic results of a linear controller.

3.1 Requirements for the Short Period Model

3.1.1 Performance Metrics

According to the pitch-up problem stated in Section 2.1 the objective of the adaptive augmentation will be to improve the response to load factor commands in the presence of the nonlinearity. Therefore boundaries for the load factor step response are defined based on the following parameters: maximum overshoot, 80% rise time, 5% settling time, 1% settling time, t_1, t_2, and t_3 as shown in Figure 3.1. The 1% settling bound is used, to ensure that no significant limit cycle oscillations are caused by the nonlinear control system, although MIL-F-8785 is less restrictive on the requirement for sustained residual oscillations, as it only requires the amplitude of the load factor to be less than 0.05g in calm air for Level 1 and 2.

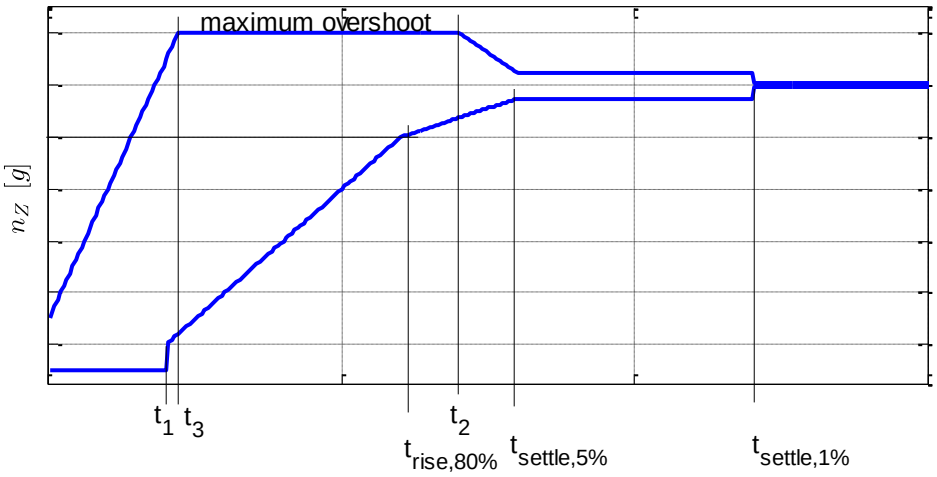

Figure 3.1: Definition of the load factor response boundaries

Based on these parameters three different boundaries are defined associated with three different levels of handling qualities (HQ). These boundaries are shown in Figure 3.2 and the associated parameters are given in Table 3.2.

Although the step response can be used to draw conclusions on the responsiveness of the control system, it should be noted that this kind of discontinuous input characteristics are not the only inputs issued by the pilot. This means the control law must be also tested in pilot in the loop simulation, and only by this it can be verified whether the results will really agree with pilot opinions [83]. It would be necessary to show that performance requirements are met for all expected input signals, but due to the lack of analytice performance bounds for nonlinear adaptive control systems this can be only shown by methods like Monte-Carlo-Simulation which is beyond the scope of this thesis.

HQ Level 1	HQ Level 2	HQ Level 3
Overshoot < 0.10	Overshoot < 0.20	Overshoot < 0.30
80% Rise time < 4s	80% Rise time < 6s	80% Rise time < 8s
5% Settling time < 6s	5% Settling time < 8s	5% Settling time < 10s
1% Settling time < 10s	1% Settling time < 12s	1% Settling time < 14s
t_1=2	t_1=2	t_1=2
t_2=5	t_2=7	t_2=9
t_3=2	t_3=2.2	t_3=2.4

Table 3.2: Parameters for the load factor response boundaries

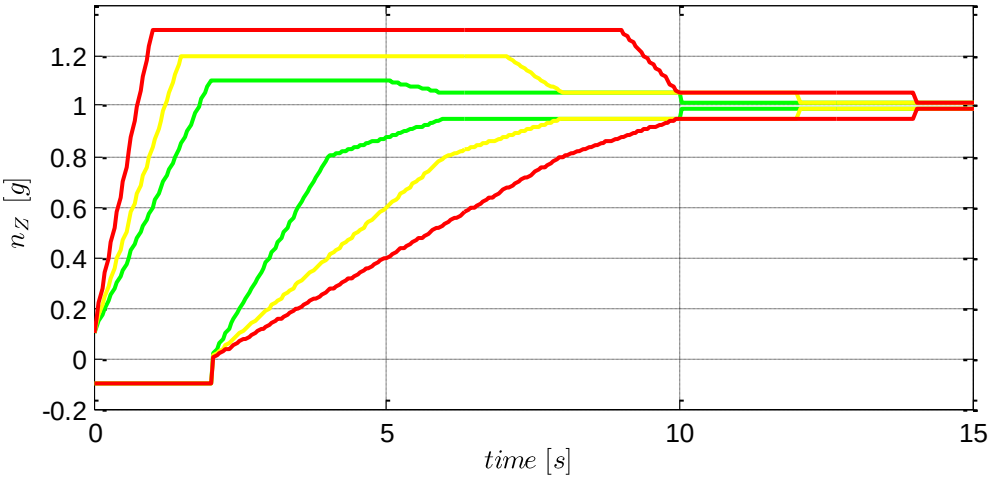

Figure 3.2: Load factor response boundaries for different HQ levels

3.1.2 Evaluation

The robust performance of the augmenting control laws will be evaluated based on step inputs together with the mentioned requirements for different kinds of uncertainties in the linear plant model of Eq.(2.1) without the pitch-up nonlinearity

$$\begin{aligned} \dot{\mathbf{x}}_P &= \mathbf{A}_P\mathbf{x}_P + \lambda \cdot \mathbf{b}_P\eta \\ \mathbf{y}_P &= \mathbf{C}_P\mathbf{x}_P + \lambda \cdot \mathbf{d}_P\eta, \end{aligned} \tag{3.1}$$

where λ is an assumed uncertainty in the control effectiveness. The results are compared to the performance of the baseline control law. In a first step the performance is evaluated over a grid of uncertainties in the coefficients determining the pitch stiffness M_α and the pitch damping M_q, which can be considered as matched or affine uncertainties, as the elevator predominantly produces a pitching moment and almost negligible lift force. The results for these kinds of uncertainties are shown in Figure 3.3, where the blue dot marks the nominal condition for which the controller is designed. Furthermore, the performance is evaluated for unmatched uncertainties in the coefficient Z_α, where the results for the baseline controller are shown in Figure 3.4. Finally the performance is assessed for uncertainties in the control effectiveness λ, which is equivalent to an uncertain gain in the input channel of the plant. The results of the baseline controller are shown in Figure 3.5.

As the baseline controller is linear, the evaluation is only performed for one input signal. Due to the nonlinearity of the adaptive control laws the evaluation will performed based on two step inputs with different magnitude: 1g command and 2g command. It should be noted that for adaptive controllers, this evaluation addresses the worst case, where uncertainties occur abruptly and the transient system response is considered.

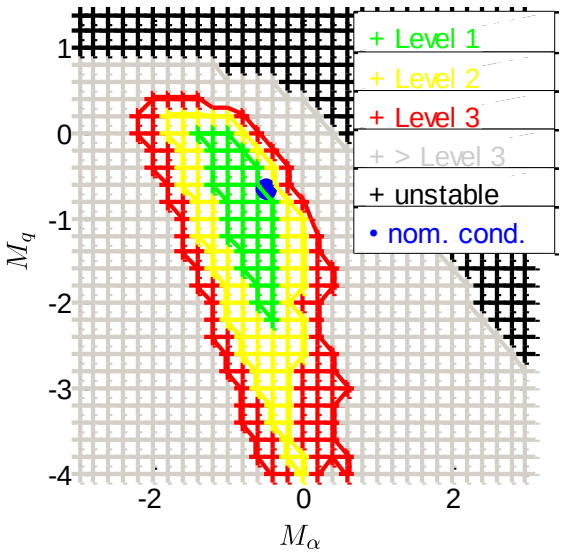

Figure 3.3: Robust performance of baseline controller for uncertain M_α and M_q

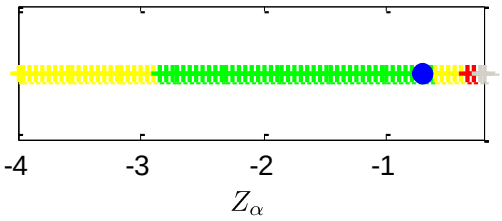

Figure 3.4: Robust performance of baseline controller for uncertain Z_α

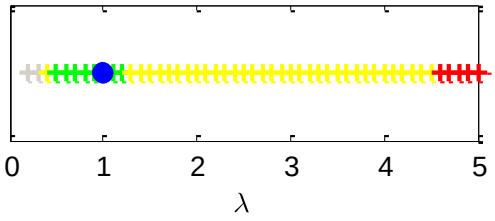

Figure 3.5: Robust performance of baseline controller for uncertain λ

3.2 Requirements for the Full Nonlinear Transport Aircraft

3.2.1 Performance Metrics

The following performance requirements roughly reflect the real response requirement for the type of considered aircraft which are used as design objectives for the baseline controller under nominal conditions.

3.2.1.1 Load factor step response

For the full nonlinear model a steady state load factor command cannot be followed by the plant for an arbitrary time. Therefore, only a reduced set of the metrics, which were defined in Section 3.1, is used and given in Table 3.3.

HQ Level 1	HQ Level 2	HQ Level 3
Overshoot < 0.10 80% Rise time < 4s	Overshoot < 0.20 80% Rise time < 6s	Overshoot < 0.30 80% Rise time < 8s

Table 3.3: HQ criteria for load factor response

3.2.1.2 Pitch rate response

The desired response of the pitch rate is determined based on the overshoot, and the assessment criteria is shown in Table 3.4

	HQ Level 1	HQ Level 2	HQ Level 3
Overshoot= $\frac{q_{peak}-q_{ss}}{q_{ss}}$	Overshoot < 0.3	Overshoot < 0.6	Overshoot < 1

Table 3.4: HQ criteria for pitch rate overshoot

3.2.1.3 Control Anticipation Parameter

The Control Anticipation Parameter (CAP) is usually defined for a second order (equivalent) system. It is an important handling quality parameter, as the pilot predicts the resulting steady-state load factor from the initial pitch rate acceleration. Thus CAP is defined by the pitch rate acceleration at $t = 0s$ divided by the resulting steady-state load factor

$$CAP = \frac{\dot{q}(0)}{n_{Z(\infty)}}. \tag{3.2}$$

For a second order equivalent system CAP can also be defined by $CAP = \omega_{0,SP}^2/(dn_Z/d\alpha)$, and thus it also provides a frequency specification. The denominator $(dn_Z/d\alpha)$ accounts for the effect of the zero T_{Θ_2} in the numerator of the pitch response.
However, as already mentioned CAP can only be calculated in this way for a second order (equivalent) system without time delay, as for example with actuator dynamics the initial $\dot{q}(0)$, following a step input, will always be zero. Therefore, in the following CAP is calculated from maximum pitch rate acceleration

$$CAP = \frac{\dot{q}_{max}}{n_Z(\infty)} \tag{3.3}$$

as it is mentioned in MIL-HDBK-1797A and shown in Figure 3.6.
Regions for CAP, which are associated with different Levels of flying qualities, are provided in MIL-HDBK-1797A and MIL-F-8785C. The specified values are shown together with the required damping in Table 3.5. However, the defined CAP regions for different levels are quite large, and CAP should not only be in the defined regions, but should be as homogenous as possible over the flight envelope.

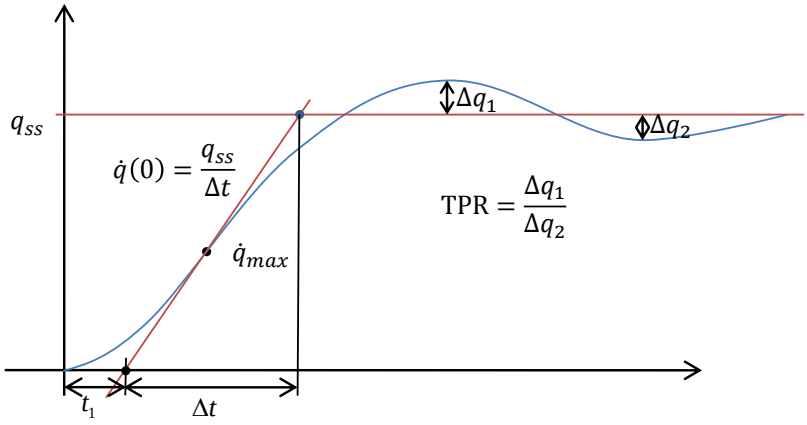

Figure 3.6: Control Anticipation Parameter and Transient Peak Ratio

The damping requirements, which are given for completeness in Table 3.5, can also be checked only for an equivalent low order system. Thus, in the following it is assumed that the damping requirements are covered by the response criteria's from Table 3.3, and in particular by the defined overshoot requirements.

	Level 1		Level 2		Level 3	
	Min	Max	Min	Max	Min	Max
Damping	0.3	2	0.2	2	0.15	-
CAP	0.085	3.6	0.038	10	0.038	-

Table 3.5: CAP requirements from MIL-HDBK-1797A for CAT B (nonterminal)

3.2.1.4 Transient peak ratio, rise time, effective time delay

According to MIL-HDBK-1797A the transient peak ratio, rise time parameter, and equivalent time delay are also defined for second order approximations of the pitch response. As they are time domain criteria they are also applicable to higher order systems as long as a "constant" pitch rate can be identified in the short term response. For calculating the parameters the following measurements, defined in MIL-HDBK-1797A and shown in Figure 3.6 are needed:

- q_{ss}: Steady state pitch rate
- $\dot{q}_{max}$: Maximum pitch rate acceleration
- t_1: Time difference from the instant of the step input to the time at the intersection of the maximum-slope tangent with the time axis.
- t_2: Time difference form the instant of the step input to the time corresponding to the intersection of the maximum-slope tangent with the steady-state line
- Δq_1: Maximum pitch rate minus steady state pitch rate
- Δq_2: Steady state pitch rate minus value at the first minimum

Equivalent time delay

Time delay and lag is in general critical in feedback control systems and for the pilot. Especially during tasks where precision and high bandwidth is required delay can largely deteriorate the pilot's performance or even lead to pilot induced oscillations. The equivalent time delay parameter should provide an indicator for the amount of time delay which the pilot experiences and how this delay impacts the flying qualities. The assessment criteria from MIL-HDBK-1797A are shown in Table 3.6.

Level	Equivalent time delay
1	$t_1 \leq 0.12$
2	$t_1 \leq 0.17$
3	$t_1 \leq 0.21$

Table 3.6: Equivalent time delay parameter

Transient peak ratio

The transient peak ratio (TPR) provides an indicator for the damping of the system as it is defined by the ratio of the first overshoot with respect to the following undershoot

$$TPR = \frac{\Delta q_1}{\Delta q_2}. \tag{3.4}$$

As the defined criteria for the load factor response also implicitly provides boundaries for the damping the TPR is somehow redundant for a system without direct lift control,

because feedback control does not modify the pitch rate response independently from the load factor response. In Table 3.7 the maximum TPR values for the different HQ Levels provided in MIL-HDBK-1797A are shown. To calculate the TPR, the steady state pitch rate must be known which is difficult to obtain for a nonlinear model. This is why the TPR is not used in the following assessment.

Level	$\Delta q_1 / \Delta q_2$
1	≤0.3
2	≤0.6
3	≤0.85

Table 3.7: Transient peak ratio parameter

Rise time parameter

The rise time parameter provides an indicator for the responsiveness of the system by calculating the time difference

$$\Delta t = t_2 - t_1 \tag{3.5}$$

and a conclusion on the handling quality level can be drawn from the data provided by MIL-HDBK-1797A which is shown in Table 3.8. It should be noted that the rise time parameter is redundant to CAP as shown in MIL-HDBK-1797A.

	CAT B Nonterminal Flight Phases		CAT C Terminal Flight Phases	
Level	$\min(\Delta t)$	$\max(\Delta t)$	$\min(\Delta t)$	$\max(\Delta t)$
1	$\frac{9}{V_{TAS}}$	$\frac{500}{V_{TAS}}$	$\frac{9}{V_{TAS}}$	$\frac{200}{V_{TAS}}$
2	$\frac{3.2}{V_{TAS}}$	$\frac{1600}{V_{TAS}}$	$\frac{3.2}{V_{TAS}}$	$\frac{645}{V_{TAS}}$

Table 3.8: Rise time parameter (with V_{TAS} in ft/s)

3.2.2 Evaluation

In the following two sections the handling quality criteria of the previous section are evaluated for the longitudinal response of the nonlinear model introduced in Section 2.2. The evaluation is performed over the flight envelope by using a grid in Mach and height. Starting from a wings leveled horizontal steady state flight condition the aircraft response to 0.1g step command is assessed.

In Section 3.2.2.1 the scheduled, nominal control law is investigated, and in Figure 3.7 one can see that the nominal control law provides Level 1 handling qualities over almost the complete envelope. In particular, Figure 3.7 shows the evaluation of the load factor response metrics from Section 3.2.1.1, the pitch rate response metrics from Section 3.2.1.2, the equivalent time delay from Section 3.2.1.4, the rise time parameter from Section 3.2.1.4, and the handling qualities for a combination of these metrics. Furthermore, also an evaluation of CAP is provided in Figure 3.7.

In Figure 3.8 and Figure 3.9 the load factor and the pitch rate response are plotted for a few selected points across the envelope. These points are also marked in the combined criteria in Figure 3.7. For a height of $30000ft$ the trajectories are additionally plotted in a magnified version in Figure 3.10 and Figure 3.11. Here the homogenous responses of the scheduled control law can be observed.

In the second Section 3.2.2.2 a loss of the calibrated airspeed V_{CAS} as scheduling parameter is considered. It is assumed that the airspeed measurement is lost at $V_{CAS} = 320\,kts$ and thus the controller gains are fixed for this airspeed. This gain setting is in the following referred to as non-scheduled. As already mentioned, normally a robust set of stored gains would be used which provide a good trade of between robust performance and robust stability. However, here controller gains close to the boundary of the envelope are chosen which is rather conservative and provides a more challenging task for the adaptive controller (these gains are the smallest possible gains of the baseline controller). From Figure 3.12 we can see that over a large envelope domain the handling qualities degrade to level two. This is mainly attributed to a slower rise time which results from the non-scheduled gains in combination with lower airspeeds. The increase rise time is also obvious in the load factor and the pitch rate response shown in Figure 3.13 and Figure 3.14, and in the magnified version for $h = 30000ft$ in Figure 3.15 and Figure 3.16.

3.2.2.1 Scheduled Control Law

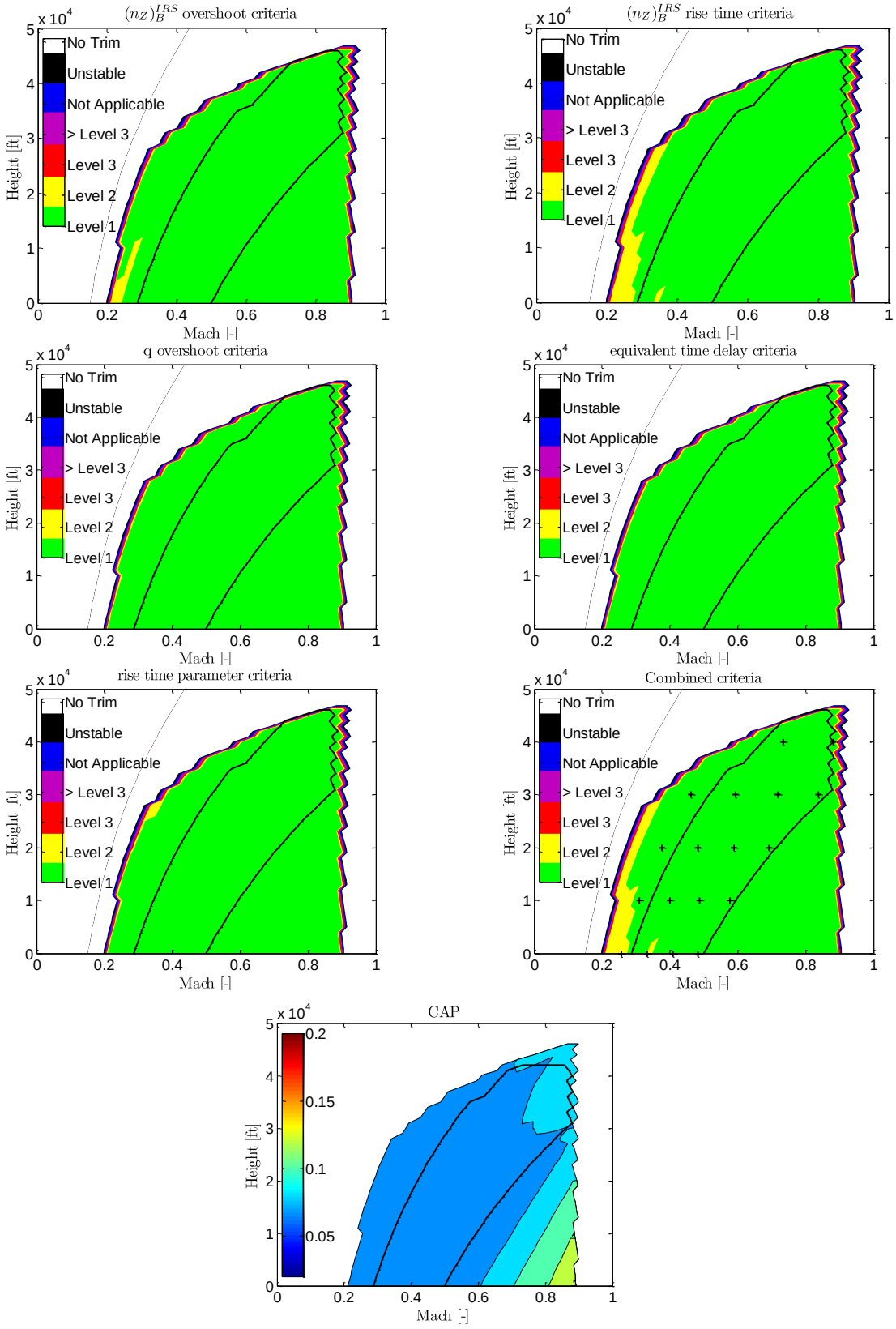

Figure 3.7: HQ assessment of the nominal, scheduled control law

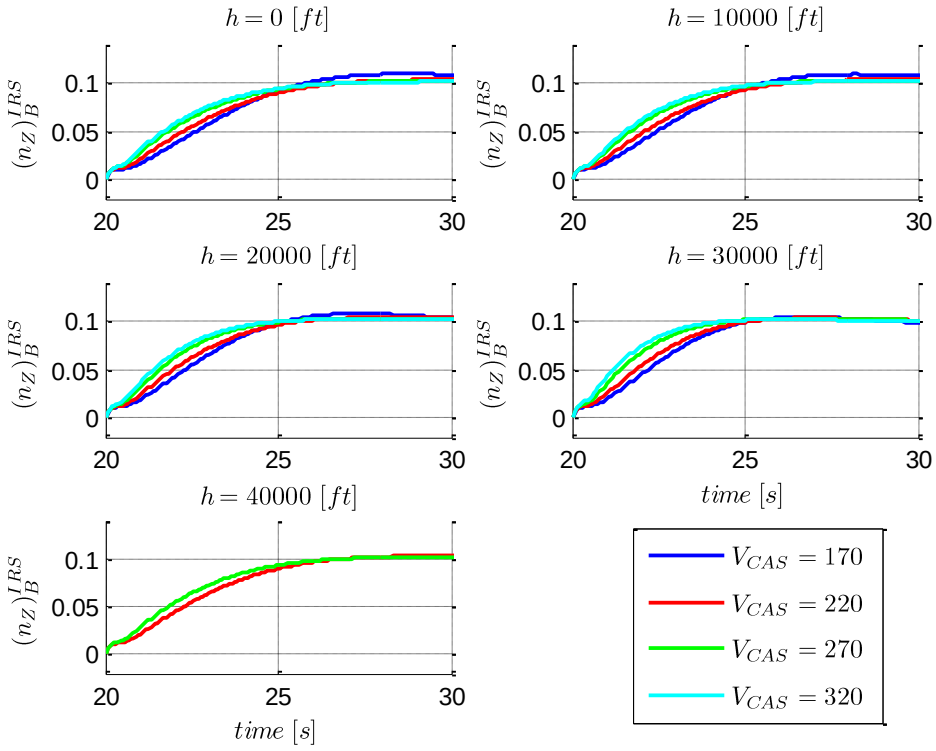

Figure 3.8: Load factor response of the scheduled control law at different envelope points

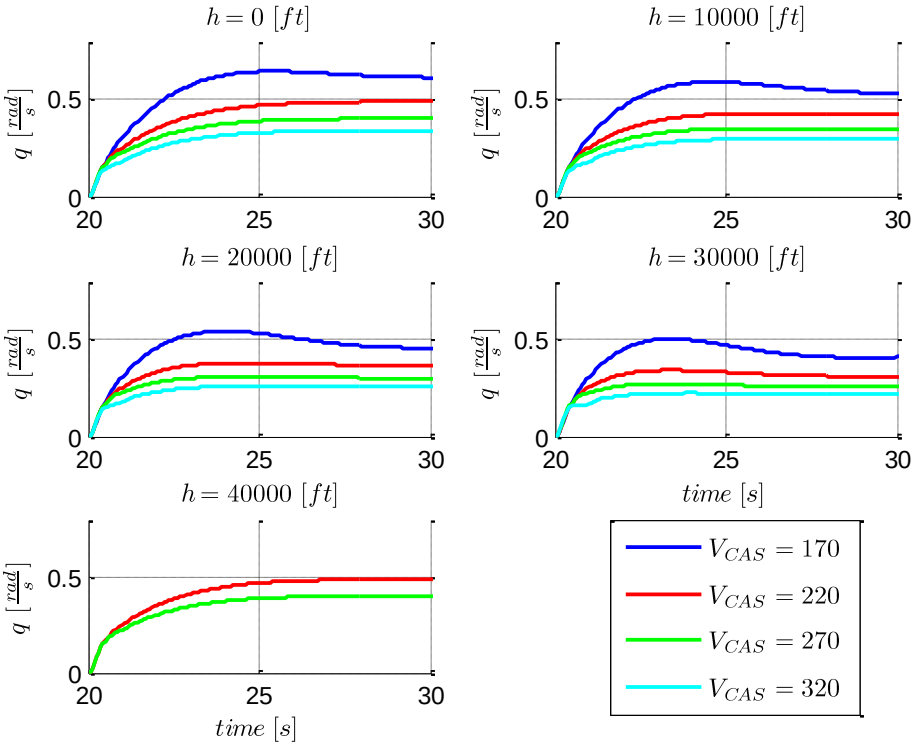

Figure 3.9: Pitch rate response of the scheduled control law at different envelope points

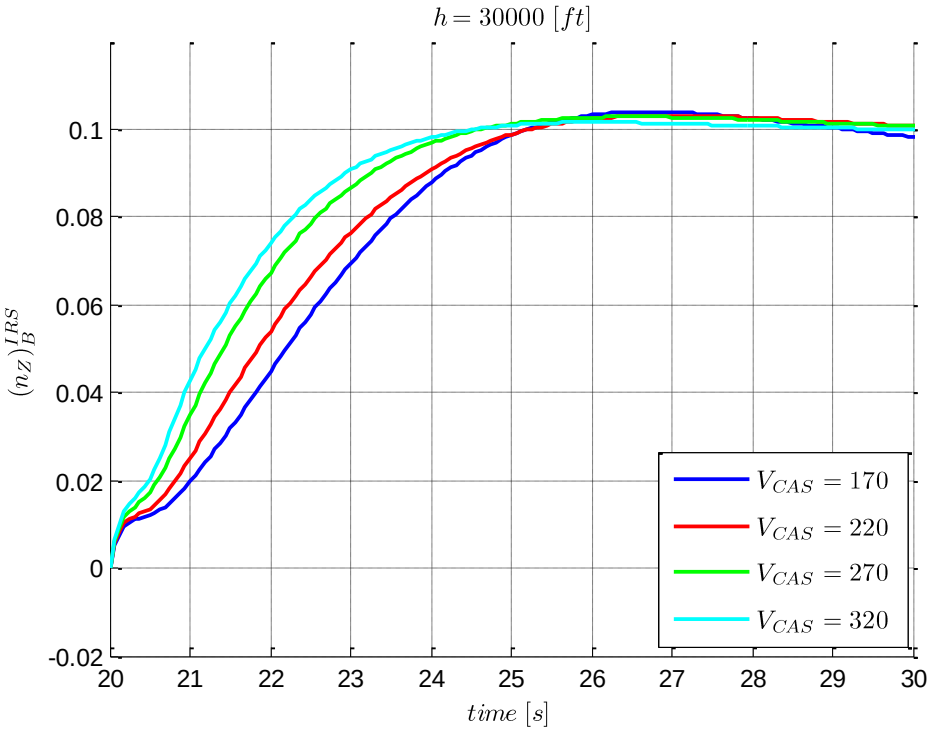

Figure 3.10: Load factor response of the scheduled control law at h=30000ft

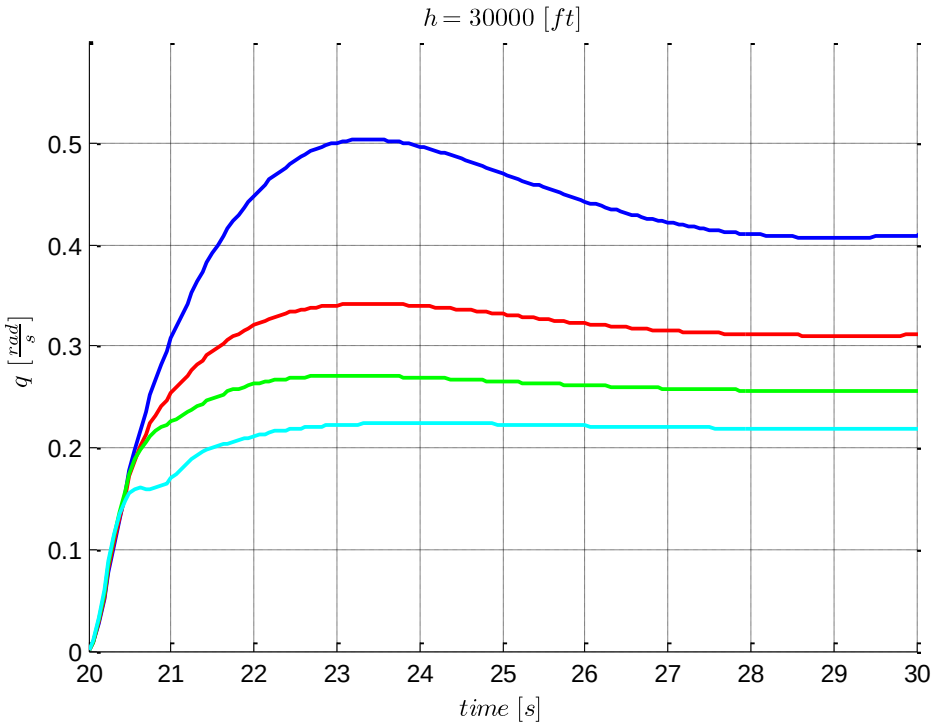

Figure 3.11: Pitch rate response of the scheduled control law at h=30000ft

3.2.2.2 Non-Scheduled Control Law

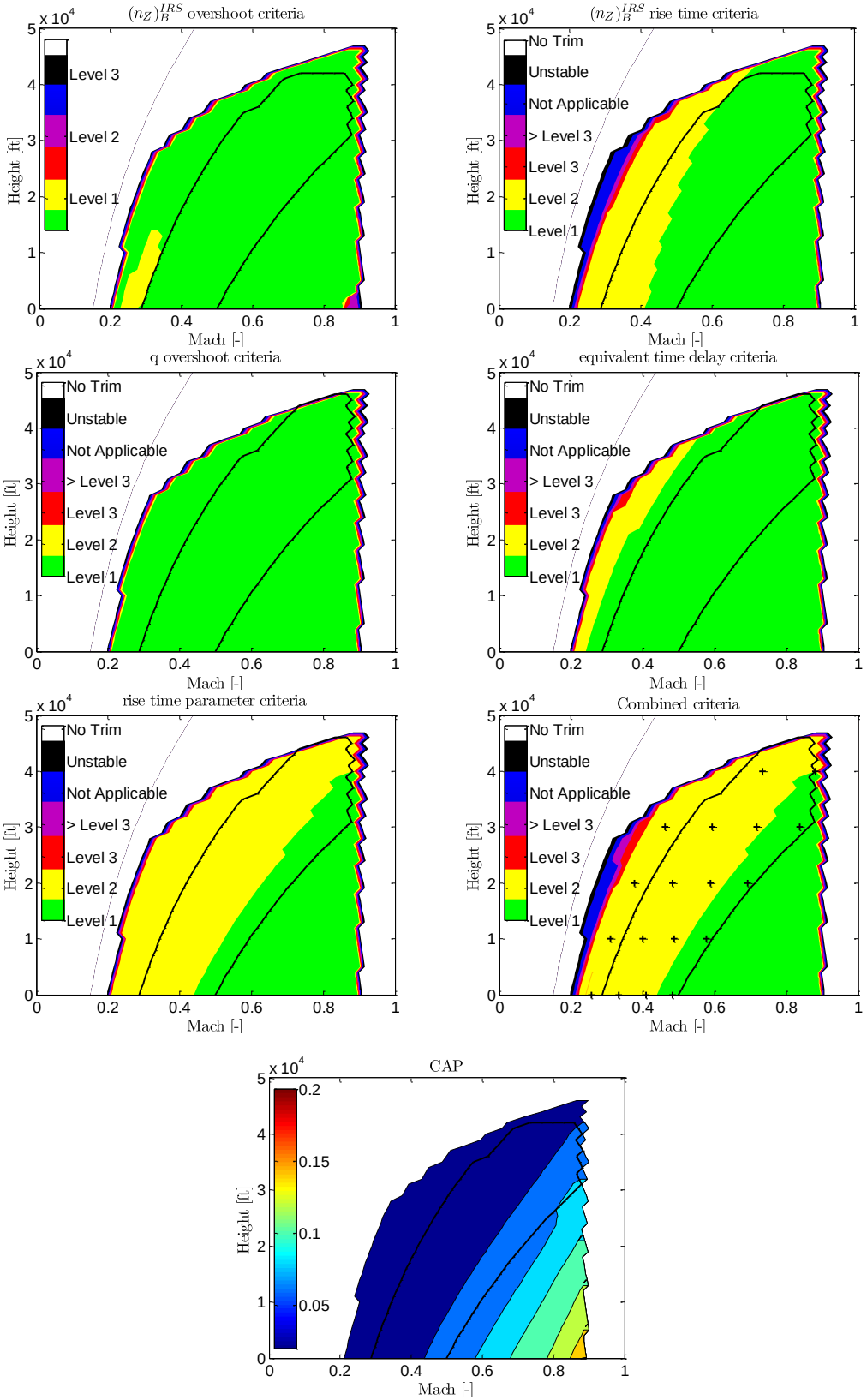

Figure 3.12: HQ assessment of the non-scheduled control law

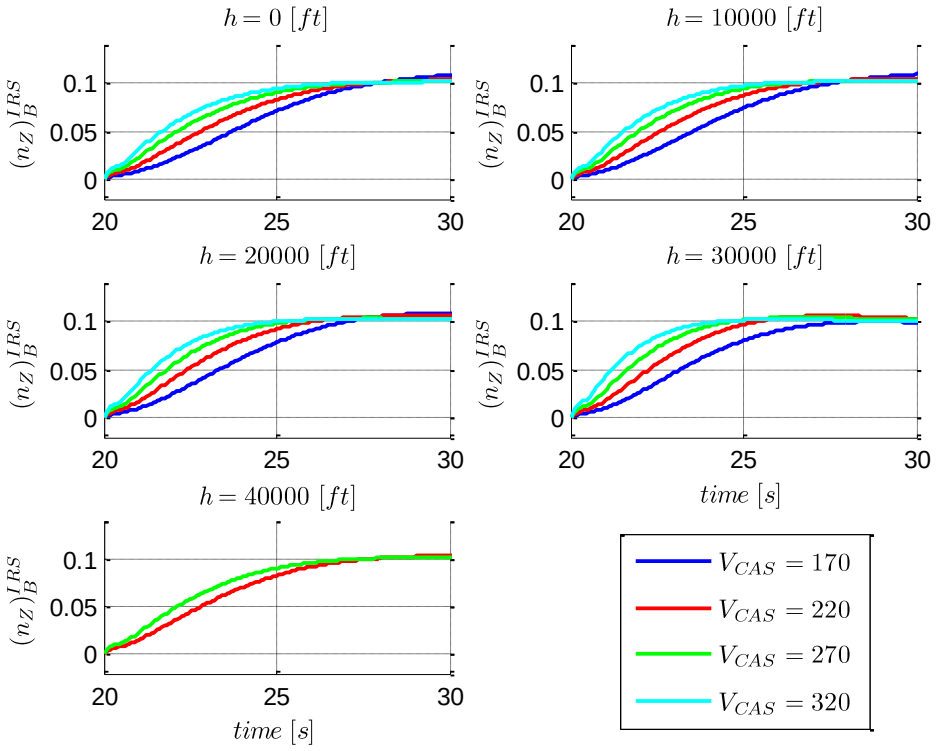

Figure 3.13: Load factor response of the non-scheduled control law at different envelope points

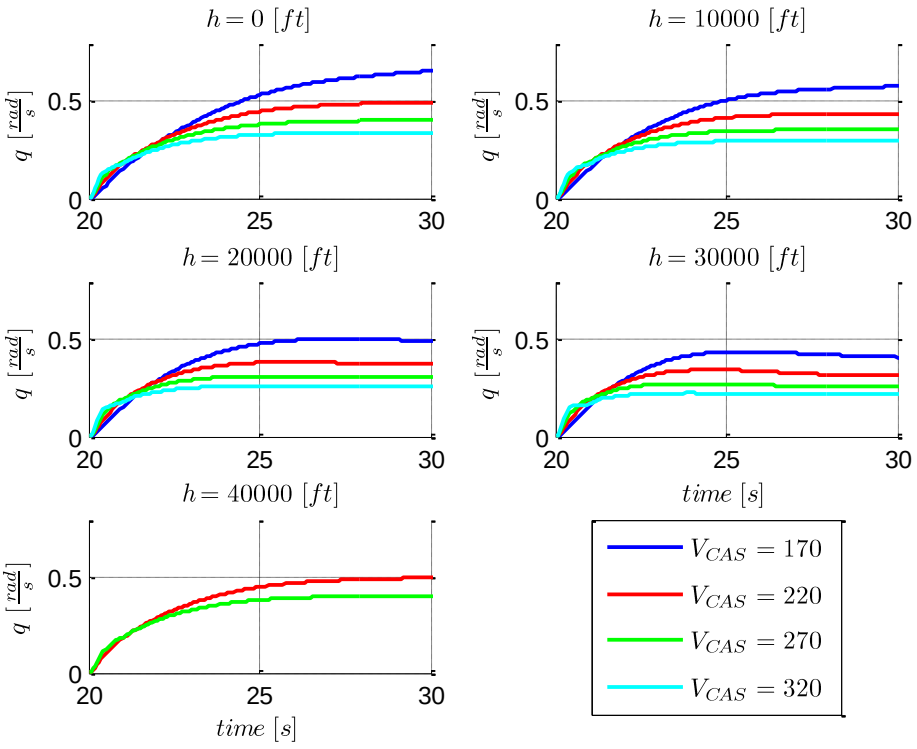

Figure 3.14: Pitch rate response of the non-scheduled control law at different envelope points

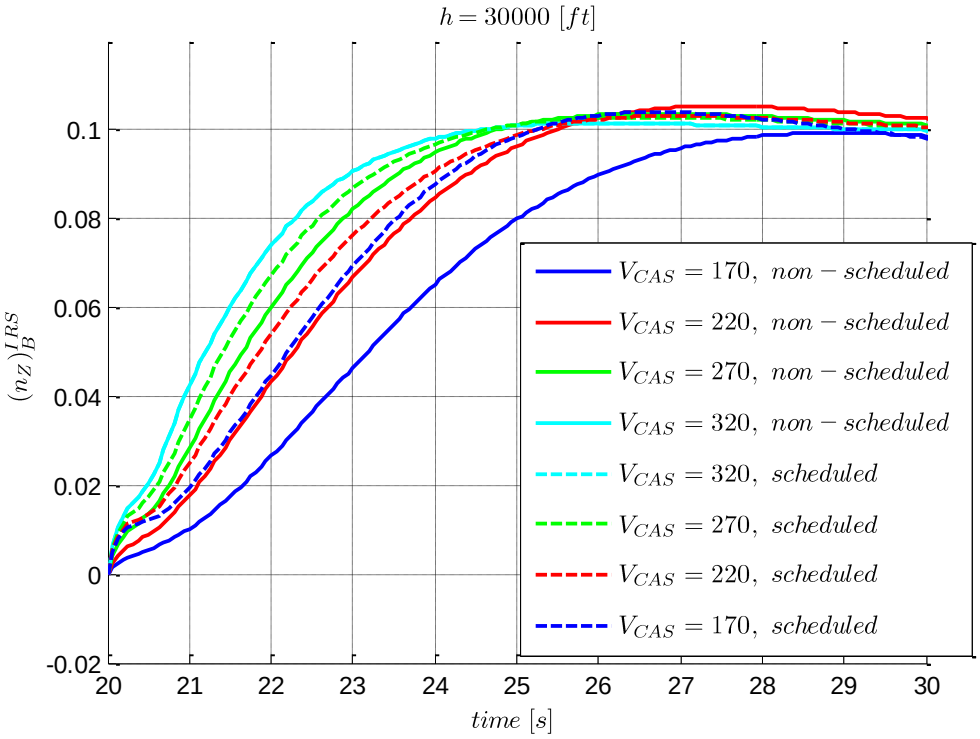

Figure 3.15: Load factor response of the non-scheduled control law at h=30000ft

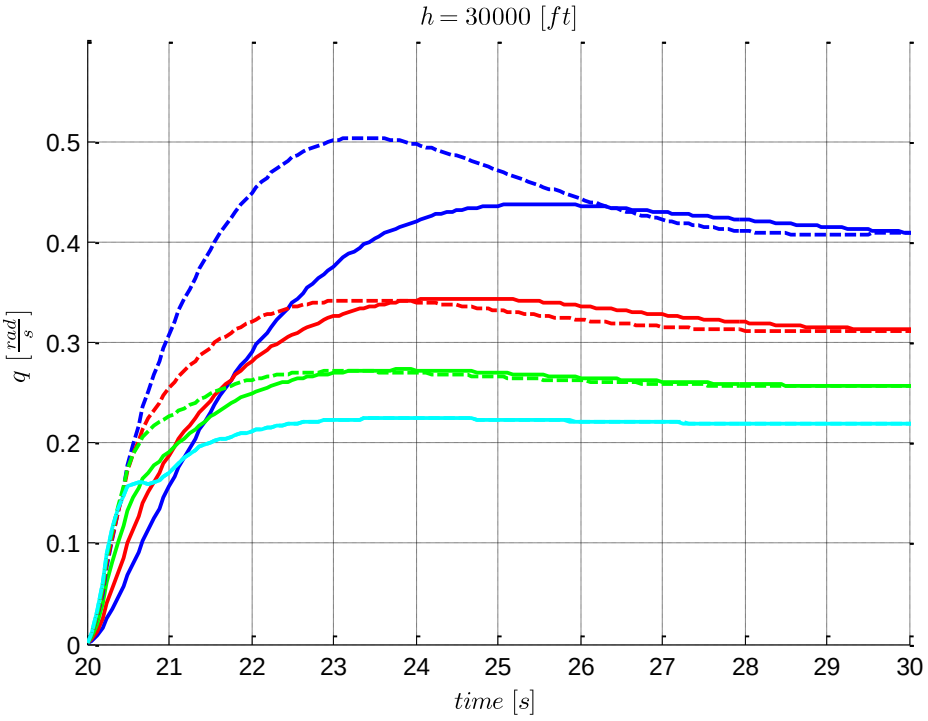

Figure 3.16: Pitch rate response of the non-scheduled control law at h=30000ft

Chapter 4

Basic Model Reference Adaptive Control Approaches

Adaptive control in contrast to robust control does not assume an interval for the unknown plant parameters but treats them as unknown and tries to either determine the parameters, to then compute suitable controller gains, or to directly estimate appropriate control gains. Therefore the controller gains are no longer constant but also change dynamically, and hence they become states of the system. The product of a controller gain and a measured process variable is a product of two states, and as a consequence of this a nonlinear operation. Thus, even the adaptive control of a first order, scalar linear plant leads to a nonlinear system, no longer covered by classical linear theories.

In particular in the MRAC approach the desired behavior is specified by a reference model, and measured system signals as well as the error between the plant output and the output of the reference model are used to update the parameters. The update equations are chosen in a way that the error is driven to zero and the transient response of the reference model is recovered by the plant.

In the case of state feedback the assumptions for the plant are less restrictive because the available system signals contain more information about the system dynamics, whereas for the case of output feedback dynamic compensators in the feedback and the feedforward path are necessary in the classical approach [1] [87].

In general two main MRAC approaches can be identified, *direct* and *indirect* MRAC as shown in Figure 4.2 and Figure 4.1. All other MRAC philosophies can be considered as extensions, modifications or combinations of these two architectures.

In the indirect case the plant is parameterized by the parameters $\widehat{\boldsymbol{\Theta}}_P^*$, these physical parameters are labeled by the “hat”, and they are estimated by the adaptation process. In the following the real parameters are denoted by an asterisk superscript (e.g. $\widehat{\boldsymbol{\Theta}}_P^*$) while the estimations have no superscript (e.g. $\widehat{\boldsymbol{\Theta}}_P(t)$). For the estimation an identification model is used, which has the same parameterization as the plant, and

the parameters $\widehat{\boldsymbol{\Theta}}_P(t)$ are updated in a way such that identification model follows the real plant. Based on these estimates the controller parameters $\boldsymbol{\Theta}_C(t)$ (controller gains) are calculated by an algebraic equation $\boldsymbol{\Theta}_C(t) = \varphi(\widehat{\boldsymbol{\Theta}}_P(t))$, where the control law $\mathbf{u}(t) = \mathbf{k}(\mathbf{y}_P(t), \mathbf{r}(t), \boldsymbol{\Theta}_C(t))$ has to be chosen such that the performance requirements would be satisfied if the ideal parameters $\widehat{\boldsymbol{\Theta}}_P^*$ were known.

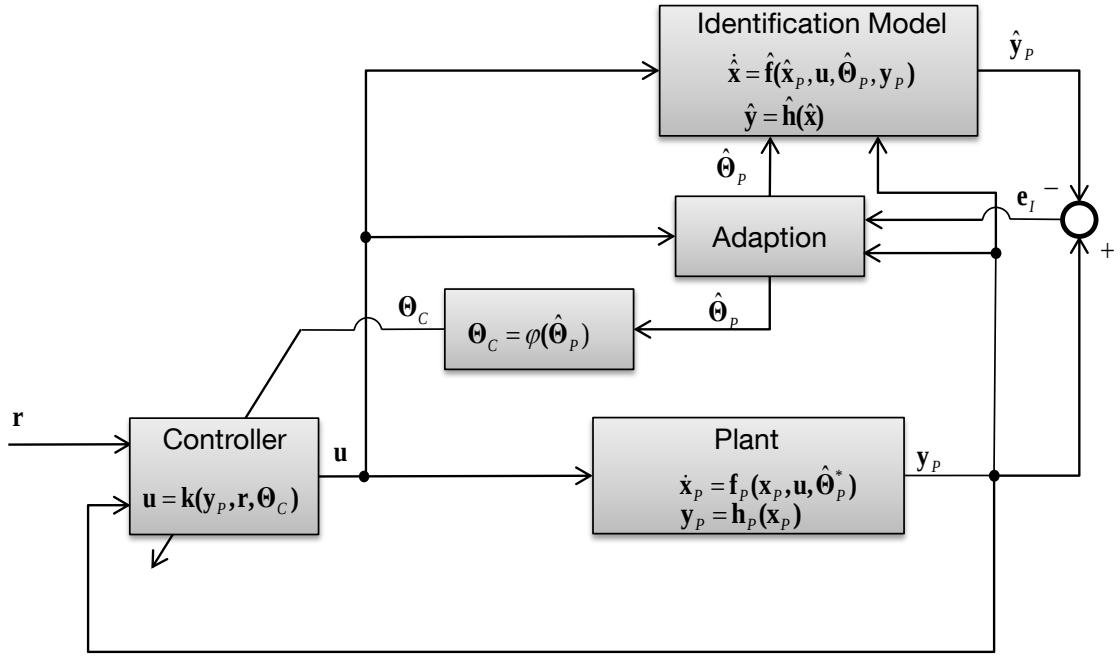

Figure 4.1: Indirect MRAC

For the direct approach only the controller is parameterized in terms of the unknown controller gains $\boldsymbol{\Theta}_C(t)$ which are directly estimated by the adaptation law. For the adaptation the error between the pant and a reference model, which specifies the desired performance, is used, and the gains are updated such that the plant follow the reference model. The parameterization can also be interpreted as a parameterization of the closed loop system, where the control law has to be chosen such that the closed loop plant satisfies the performance requirements for the "ideal" parameters $\boldsymbol{\Theta}_C^*$. Here "ideal" parameters refers to the set $\boldsymbol{\Theta}_C^*$ that leads to equal dynamics of the controlled plant and reference model. It has to be further assured that these ideal parameters exist, meaning that equality of the reference model and the pant must be achievable.

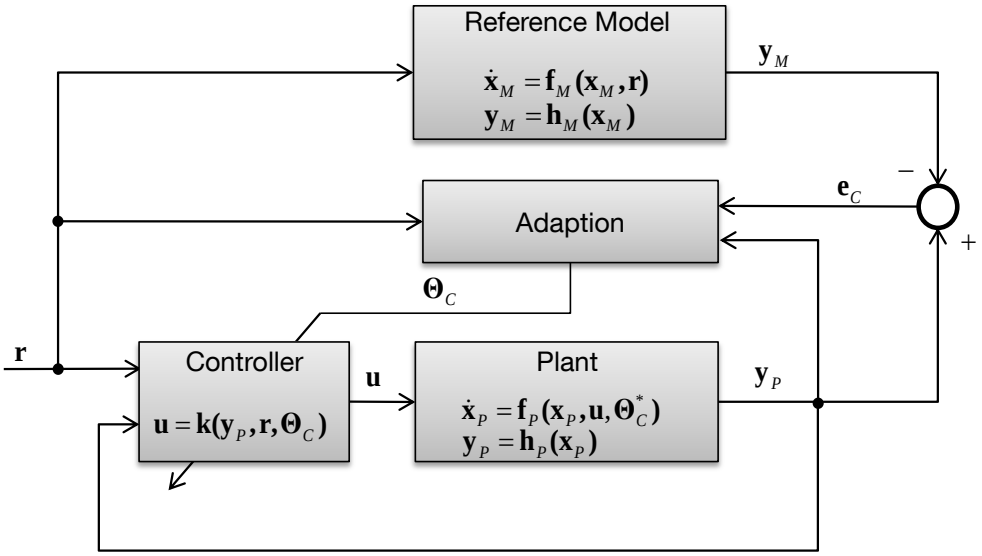

Figure 4.2: Direct MRAC

In both, direct and indirect schemes, if the design is based on the *certainty equivalence* approach, where the idea is that the parameters estimates $\boldsymbol{\Theta}_C(t)$ and $\widehat{\boldsymbol{\Theta}}_P(t)$, converge to their true values $\boldsymbol{\Theta}_C^*$ and $\widehat{\boldsymbol{\Theta}}_P^*$, respectively [2], the control objective can be met.

The two approaches are not necessarily equivalent, although in some cases it was shown that with the same amount of prior information about the plant the same results can be achieved [88].

For the state feedback approach it is considered that the whole state vector is fed back. This is not realistic, as in a real physical system not all system states are measurable and higher order dynamics are always present. However, if the part of the state vector that contains the dynamics within the bandwidth of interest can be measured and fed back, full state feedback can be assumed at first. In addition, as long as the dynamics of the neglected states are not strongly coupled within the frequency domain of interest, i.e. an adequate time scale separation w.r.t. the remaining states is given, robustness with respect to the neglected dynamics can be achieved by robustness modifications, which are discussed later. In this chapter the idealized case is considered, where asymptotic stability and convergence of the tracking error to zero can be proven.

The following presents the multitude of different approaches, that can be attributed to the field of MRAC, in a unified and transparent way, illustrates the different contributing elements, and highlights the alternative choices available. In short, the contributing elements are the plant to be controlled, the MRAC baseline philosophy, the parameterization of the adaptive component, the parameter update laws and the

reference model or identification model. To give an idea, the different features are addressed here in short:

Plant to be controlled / Plant transformations:

The plant to be controlled from the MRAC controller point of view does not necessarily have to be the unmodified physical plant. So if for example a conventional controller is built around the physical plant, the integrated system consisting of plant plus baseline controller would be the plant as seen by the MRAC controller. Even more, if the plant can be transformed by means of input-output linearization ("dynamic inversion") [89] [90], the combination of plant inverse and physical plant would be the plant as seen from the MRAC controller. To sum up, the MRAC theory covers certain classes of plants – predominantly linear systems with additional matched nonlinearities. In many cases, it is possible to transform the dynamics of the physical plant into a control task that fulfills the conditions to be met for the applicability of MRAC. The proper preparation or transformation of the plant for the application of MRAC is thus one element that already significantly affects the success of all subsequent steps. It also may be stated at this point that MRAC and dynamic inversion are in no way alternatives as often claimed – dynamic inversion is nothing else than a nonlinear state transformation of the plant in order to provide a close to linear input output dynamics. However, it should be noted that for this transformation, measurements of the states must be used, which are subject to availability, sensor uncertainties, and noise.

MRAC Baseline Philosophy:

As already mentioned the number of really fundamental MRAC structures is limited to two approaches. The first one is the direct approach, where controller parameters are adjusted based on the error between a reference model describing the desired dynamics and the closed-loop dynamics of the physical plant with the controller. The second one is the indirect approach, where the parameters of the plant are estimated by updating them based on the identification error between the measured plant outputs / states and those provided by the estimation model. The controller gains are then either directly computed from the estimated plant parameters, or updated based on them, by update differential equations.

Many other MRAC philosophies can be considered as extensions, modifications or combinations of those two basic architectures. Thus, composite or combined MRAC (CMARC) [91] [92] is a combination of both, Predictive MRAC (PMRAC) uses an additional state estimator [93] [94]. $\mathcal{L}_1$ adaptive control is another approach that has proven to bring significant progress and is definitely a very valuable and enabling achievement [95] [96] [97] [98] [99]. From its interpretation it may still be considered as a modification of MRAC control where the high frequency content is decoupled from the physical plant by means of a low pass filter to keep high frequency oscillations from the plant while retaining high learning rates. Furthermore, as already mentioned, in the course of this thesis the similarity of $\mathcal{L}_1$ adaptive control and the application of a

so called hedging signal is shown. Of course, the philosophy of $\mathcal{L}_1$ goes much further as it provides guaranteed transient performance and stability margins [100], but still it is encouraging to see that the concept may be interpreted that way as it still remains complementary to all the other elements and may arbitrarily be combined with them (reference dynamics, approximator structure, update laws, …)

Parameterization of the Adaptive Component:

The classical MRAC approach uses a linear combination of the unknown parameters and measured variables. However, the basic theory also covers that the adaptive control signal/estimated uncertainty may be given by linear combinations between the unknown parameters and arbitrary nonlinear functions computed from measurable system variables [1]. This for example allows to introduce physical insight on the structure of the uncertainties (e.g. of the aerodynamics of the system, inertia and coupling terms, etc.) into the adaptive system without even leaving the most basic MRAC theory. Beyond that, more complex approximator structures are widely used, e.g. radial basis functions or neural networks [101] [102]. A neural network with no hidden layer and a linear output is still within the basic MRAC framework. The successful extension to networks with hidden layers can be generalized as back-propagating parameter errors and may be accomplished using the chain rule, also for other structures than neural networks [103] [104]. Results where the problem may be even nonlinear in the unknown parameters were also presented [105] [106] [107], although they are not of general nature but limited to certain nonlinearities. Moreover, different approaches covering piecewise adaptation using constant or linear local values for the unknown parameters have gained recent attention [108].

Parameter Update Laws:

As far as the update laws are concerned, various aspects can be generalized. First, the type of update is of interest – do we consider single-point updates at every time instant or do we consider a hybrid update scheme, where updates to the parameters are performed slower than the actual control process [1]. In the following hybrid update laws are not considered. Second, do we include information over a longer period in the update process, e.g. by means of integrating or filtering the error measurements [4] [92], by approaches like the Q-modification [109] [110] [110] [111] or (concurrent learning) [112] [113] [114], where past data is used to update the parameters based on stored data points that have to be selected in an adequate way.

The next item concerning update laws addresses modifications to ensure stability and boundedness of parameters. Besides just clipping the values to a certain range or projection, classical approaches are the e- and σ-modification.

Finally, the basic philosophy behind the update law or parts of it and the resulting implementation may be very different and is often motivated by the source it originally stems from. As stability is the main objective, most of the time the laws are derived from Lyapunov function candidates. However, also gradient based approaches

stemming from optimization [2] [4] [92] [109], least square methods [1] [4] [115] [116], or Kalman filter based estimaion can be used. It becomes clear that using other alternatives than the original approach may offer multiple benefits without sacrificing the original boundary conditions like stability constraints. For example, a gradient based modification can offer better convergence and transient response, or the filter approach can increase the robustness properties due to a variable update gain for the robustness modification [117], along with the availability of statistical data to assess the quality and speed of adaptation [118] which is very beneficial in building confidence for certifying such systems.

It is important to realize that again these approaches may be well combined based on the control problem to be solved and they are in many ways no exclusive alternatives.

Reference and Identification Models:

The reference model and the reference dynamics to be selected offer many degrees of freedom. Whereas the original concept was to specify a linear transfer function matching the relative degree of the control problem, many extensions are available. Specifying a nonlinear reference dynamics including models of the known dynamic limitations of the plant provides much better control performance than the original approach [119] [120]. Here it is not only possible to account for the true dynamic order of the system and known hard and soft nonlinearities, but also to actively give priority to certain control objectives in the case of saturations [121] [122], or to account for the designers complete knowledge on the dynamics of the plant [123]. This may be either accomplished in an open loop feedforward manner, i.e. not affecting the stability of the system, but relying on pure assumptions, or by means of feedback of estimated responses into the reference models which is then affecting the stability of the reference dynamics but accounts for the actual performance of the system. The most prominent examples for an approach pursuing the latter concept are “training signal hedging” [124] [125] and “pseudo-control hedging” [126] [127].

Further, an error feedback to the reference model can be used to achieve an observer like approach, where the transient response can be improved by reducing the demand of the reference model [128] [129] [130].

As shown in this thesis the reference model can also be adjusted to account for unmatched uncertainties, by using their estimates to update the reference model such that the reference trajectories remain achievable for the plant.

In many publications and in many discussions, it appears that the different approaches concerning plant transformations, baseline MRAC structure, parameterization of the adaptive component, update laws and reference dynamics are considered as completely different, mutually excluding concepts and philosophies.

This is however not true, and depending on the problem to be addressed, most concepts can be arbitrarily combined to solve the problem in a satisfactory way.

4.1 Problem Formulation

In the following it is assumed that the plant is linear in the inputs and the input matrix $\mathbf{B}_\mathrm{P}$ is assumed to be known.

Let the considered nonlinear system dynamics be given by

$$\dot{\mathbf{x}}_P(t) = \mathbf{A}_P\mathbf{x}_P(t) + \mathbf{B}_P\boldsymbol{\Lambda}\mathbf{u}(t) + \mathbf{f}(\mathbf{x}_P(t)) + \mathbf{d}, \tag{4.1}$$

where $\mathbf{x}_P(t) \in \mathbb{R}^n$ is the state vector of the system, $\mathbf{u}(t) \in \mathbb{R}^m$ is the input to the system, $\mathbf{A}_P \in \mathbb{R}^{n\times n}$ is the unknown system matrix, $\mathbf{B}_P \in \mathbb{R}^{n\times m}$ is the known input matrix, $\boldsymbol{\Lambda} \in \mathbb{R}^{m\times m}$ is the diagonal, unknown control effectiveness matrix with known sign, $\mathbf{f}(\mathbf{x}_P(t)) \in \mathbb{R}^n$ is an unknown nonlinearity, and $\mathbf{d} \in \mathbb{R}^n$ is an unknown, constant disturbance. In the nominal case, without uncertainties, $\boldsymbol{\Lambda}$ is usually the identity matrix, and because the sign of $\boldsymbol{\Lambda}$ has to be known, without loss of generality, it is assumed that $\boldsymbol{\Lambda}$ is positive definite. It should be noted that in [1] an approach is presented where $\mathbf{B}_P$ is unknown, but it should be noted that this method cannot guarantee global stability.

The desired behavior for the system, which should be achieved by the controller, is usually specified by a linear reference model of the form

$$\dot{\mathbf{x}}_M(t) = \mathbf{A}_M\mathbf{x}_M(t) + \mathbf{B}_M\mathbf{r}(t), \tag{4.2}$$

where $\mathbf{x}_M(t) \in \mathbb{R}^n$ is the desired reference trajectory, $\mathbf{r}(t) \in \mathbb{R}^m$ is the reference command, $\mathbf{A}_M \in \mathbb{R}^{n\times n}$ is the desired, stable system matrix, and $\mathbf{B}_M \in \mathbb{R}^{n\times m}$ is the desired input matrix.

The following control law is chosen

$$\mathbf{u}(t) = \boldsymbol{\Theta}_x^T(t)\mathbf{x}_P(t) + \boldsymbol{\Theta}_\varphi^T(t)\boldsymbol{\varphi}(\mathbf{x}_P(t)) + \boldsymbol{\theta}_d(t) + \boldsymbol{\Theta}_r(t)\mathbf{r}. \tag{4.3}$$

The adaptive parameters are symbolized by $\boldsymbol{\Theta}(t)$ and they will be dynamically adjusted to compensate for the uncertainties in the system. To improve readability, time dependency is not explicitly denoted for most cases, i.e. the argument "(t)" is dropped. $\boldsymbol{\Theta}_x^T \in \mathbb{R}^{m\times n}$ is an unknown parameter to compensate a linear uncertainty in $\mathbf{A}_P$. $\boldsymbol{\Theta}_\varphi^T\,\boldsymbol{\varphi}(\mathbf{x}_P) \in \mathbb{R}^{m\times 1}$ is an unknown nonlinearity that can be linearly parameterized by $\boldsymbol{\Theta}_\varphi^T \in \mathbb{R}^{m\times k}$ and has a known structure $\boldsymbol{\varphi}(\mathbf{x}_P) \in \mathbb{R}^k$. $\boldsymbol{\theta}_d \in \mathbb{R}^m$ is an unknown parameter to compensate input disturbances, and $\boldsymbol{\Theta}_r \in \mathbb{R}^{mxm}$ is an unknown parameter to compensate the uncertainties in $\boldsymbol{\Lambda}$.

Without robustness modification the stability proof requires all uncertainties to be matched, that is, they have to be in the span of $\mathbf{B}_P$. This gets obvious by inserting the control law of Eq.(4.3) in the plant dynamics given by Eq.(4.1), and comparing the closed loop system to the reference model in Eq.(4.2). Hence, to achieve the desired

linear behavior the following matching conditions need to hold, where the ideal parameters, marked by the asterisk superscript, need to exist so that the equations can be satisfied:

$$\begin{aligned} \mathbf{A}_M &= \mathbf{A}_P + \mathbf{B}_P \boldsymbol{\Lambda} \boldsymbol{\Theta}_x^{*T} \\ \mathbf{B}_M &= \mathbf{B}_P \boldsymbol{\Lambda} \boldsymbol{\Theta}_r^{*} \\ \mathbf{f}(\mathbf{x}_P) &= -\mathbf{B}_P \boldsymbol{\Lambda} \boldsymbol{\Theta}_\varphi^{*T} \boldsymbol{\varphi}(\mathbf{x}_P) \\ \mathbf{d} &= -\mathbf{B}_P \boldsymbol{\Lambda} \boldsymbol{\theta}_d^{*} \end{aligned} \tag{4.4}$$

This is physically reasonable because the plant can in general not follow an arbitrary reference model, but the space of achievable reference models is limited by the available control authority ($\mathbf{B}_P$). From Eq.(4.5) it also follows, that in order to cancel the nonlinearity exactly its structure has to be known. Note that, the stability properties mentioned in this section only hold under these conditions.

Requiring the matching condition to hold is equal to assuming that the plant can be denoted by

$$\dot{\mathbf{x}}_\mathrm{P} = \mathbf{A}_M \mathbf{x}_P + \mathbf{B}_M \mathbf{r} + \mathbf{B}_P \boldsymbol{\Lambda} \left(\mathbf{u} - \boldsymbol{\Theta}_x^{*T} \mathbf{x}_P - \boldsymbol{\Theta}_\varphi^{*T} \boldsymbol{\varphi}(\mathbf{x}_P) - \boldsymbol{\theta}_d^{*} - \boldsymbol{\Theta}_r^{*} \mathbf{r} \right). \tag{4.5}$$

In the following, similar to [1] and [91] the two basic MRAC architectures are presented: Direct MRAC and Indirect MRAC. Here the indirect approach presented for the scalar case in [1] and [91] is extended to the more general state feed back case. Subsequently, a predictor based approach is shown which is also commonly used. The stability properties of the approaches are also discussed and in Appendix C.2 the stability definitions used in the scope of this thesis are given.

As shown for the scalar problem in [91], also Combined MRAC approaches, as a mixture between the direct and indirect approach, can be used, and the approach for state feedback was presented [77], but it is not revisited here. In the following the most basic update laws are derived from Lyapunov theory and the error models are dynamic. It must be noted that the term Combined MRAC is also sometimes used for update laws that contain a combination of the “normal” Lyapunov based update and an update based on parameter identification by means of an algebraic error equation (prediction-error-based estimation) [93]. The latter approach is discussed in 5.3.

4.2 Direct MRAC

For the direct MRAC approach only the controller is parameterized and the controller gains are directly updated based on the error signal between the desired reference model and the plant output as shown in Figure 4.3.

For this approach, let the control error be defined by

$$\mathbf{e}_C = \mathbf{x}_P - \mathbf{x}_M. \tag{4.6}$$

Thus, by subtracting Eq.(4.2) from Eq.(4.5) the following error dynamics are obtained

$$\begin{aligned}\dot{\mathbf{e}}_C &= \dot{\mathbf{x}}_P - \dot{\mathbf{x}}_M \\ &= \mathbf{A}_M\mathbf{x}_P + \mathbf{B}_M\mathbf{r} + \mathbf{B}_P\boldsymbol{\Lambda}\big(\mathbf{u} - \boldsymbol{\Theta}_x^{*\,T}\mathbf{x}_P - \boldsymbol{\Theta}_\varphi^{*\,T}\boldsymbol{\varphi}(\mathbf{x}_P) - \boldsymbol{\theta}_d^* - \boldsymbol{\Theta}_r^*\mathbf{r}\big) - \mathbf{A}_M\mathbf{x}_M - \mathbf{B}_M\mathbf{r} \\ &= \mathbf{A}_M(\mathbf{x}_P - \mathbf{x}_M) + \mathbf{B}_P\boldsymbol{\Lambda}\big(\mathbf{u} - \boldsymbol{\Theta}_x^{*\,T}\mathbf{x}_P - \boldsymbol{\Theta}_\varphi^{*\,T}\boldsymbol{\varphi}(\mathbf{x}_P) - \boldsymbol{\theta}_d^* - \boldsymbol{\Theta}_r^*\mathbf{r}\big).\end{aligned} \tag{4.7}$$

Inserting the control law from Eq.(4.3) into Eq.(4.7) yields

$$\begin{aligned}\dot{\mathbf{e}}_C &= \mathbf{A}_M\mathbf{e}_C + \mathbf{B}_P\boldsymbol{\Lambda}\left(\underbrace{\left(\boldsymbol{\Theta}_x^T - \boldsymbol{\Theta}_x^{*\,T}\right)}_{\tilde{\boldsymbol{\Theta}}_x^T}\mathbf{x}_P + \underbrace{\left(\boldsymbol{\Theta}_\varphi^T - \boldsymbol{\Theta}_\varphi^{*\,T}\right)}_{\tilde{\boldsymbol{\Theta}}_\varphi^T}\boldsymbol{\varphi}(\mathbf{x}_P) + \underbrace{\left(\boldsymbol{\theta}_d - \boldsymbol{\theta}_d^*\right)}_{\tilde{\boldsymbol{\Theta}}_d} + \underbrace{\left(\boldsymbol{\Theta}_r - \boldsymbol{\Theta}_r^*\right)}_{\tilde{\boldsymbol{\Theta}}_r}\mathbf{r}\right) \\ \dot{\mathbf{e}}_C &= \mathbf{A}_M\mathbf{e}_C + \mathbf{B}_P\boldsymbol{\Lambda}\underbrace{\begin{bmatrix}\tilde{\boldsymbol{\Theta}}_x^T & \tilde{\boldsymbol{\Theta}}_\varphi^T & \tilde{\boldsymbol{\Theta}}_d & \tilde{\boldsymbol{\Theta}}_r\end{bmatrix}}_{\tilde{\boldsymbol{\Theta}}_C^T}\underbrace{\begin{pmatrix}\mathbf{x}_P \\ \boldsymbol{\varphi}(\mathbf{x}_P) \\ 1 \\ \mathbf{r}\end{pmatrix}}_{\boldsymbol{\omega}_C},\end{aligned} \tag{4.8}$$

where "tilde" denotes the parameter error.

By choosing a Lyapunov function candidate of the form

$$\begin{aligned}\mathrm{V} = \frac{1}{2}\mathbf{e}_C^T\mathbf{P}\mathbf{e}_C + \frac{1}{2}\mathrm{Tr}\big[\tilde{\boldsymbol{\Theta}}_x^T\boldsymbol{\Gamma}_x^{-1}\tilde{\boldsymbol{\Theta}}_x\boldsymbol{\Lambda}\big] + \frac{1}{2}\mathrm{Tr}\big[\tilde{\boldsymbol{\Theta}}_\varphi^T\boldsymbol{\Gamma}_\varphi^{-1}\tilde{\boldsymbol{\Theta}}_\varphi\boldsymbol{\Lambda}\big] \\ + \frac{1}{2}\mathrm{Tr}\big[\gamma_d^{-1}\tilde{\boldsymbol{\theta}}_d\tilde{\boldsymbol{\theta}}_d^T\boldsymbol{\Lambda}\big] + \frac{1}{2}\mathrm{Tr}\big[\tilde{\boldsymbol{\Theta}}_r\boldsymbol{\Gamma}_r^{-1}\tilde{\boldsymbol{\Theta}}_r^T\boldsymbol{\Lambda}\big]\end{aligned} \tag{4.9}$$

the following update laws can be derived to render the time derivative of the Lyapunov function negative semi definite under the idealized assumptions [91] (see also Appendix D.1)

$$\begin{aligned}&\dot{\boldsymbol{\Theta}}_x = -\boldsymbol{\Gamma}_x\mathbf{x}_P\cdot\mathbf{e}_C^T\mathbf{P}\mathbf{B}_P \\ &\dot{\boldsymbol{\Theta}}_\varphi = \boldsymbol{\Gamma}_\varphi\boldsymbol{\varphi}(\mathbf{x}_P)\cdot\mathbf{e}_C^T\mathbf{P}\mathbf{B}_P \\ &\dot{\boldsymbol{\theta}}_d^T = -\gamma_{dd}\cdot\mathbf{e}_C^T\mathbf{P}\mathbf{B}_P \\ &\dot{\boldsymbol{\Theta}}_r^T = -\boldsymbol{\Gamma}_r\mathbf{r}\cdot\mathbf{e}_C^T\mathbf{P}\mathbf{B}_P\end{aligned} \quad\Leftrightarrow\quad \underbrace{\begin{bmatrix}\dot{\boldsymbol{\Theta}}_x \\ \dot{\boldsymbol{\Theta}}_\varphi \\ \dot{\boldsymbol{\theta}}_d^T \\ \dot{\boldsymbol{\Theta}}_r^T\end{bmatrix}}_{\dot{\boldsymbol{\Theta}}_C} = -\underbrace{\begin{bmatrix}\boldsymbol{\Gamma}_x & \mathbf{0} & \mathbf{0} & \mathbf{0} \\ \mathbf{0} & \boldsymbol{\Gamma}_\varphi & \mathbf{0} & \mathbf{0} \\ \mathbf{0} & \mathbf{0} & \gamma_{dd} & \mathbf{0} \\ \mathbf{0} & \mathbf{0} & \mathbf{0} & \boldsymbol{\Gamma}_r\end{bmatrix}}_{\boldsymbol{\Gamma}_C}\underbrace{\begin{pmatrix}\mathbf{x}_P \\ \boldsymbol{\varphi}(\mathbf{x}_P) \\ 1 \\ \mathbf{r}\end{pmatrix}}_{\boldsymbol{\omega}_C}\cdot\mathbf{e}_C^T\mathbf{P}\mathbf{B}_P. \tag{4.10}$$

$\mathbf{P} = \mathbf{P}^T \in \mathbb{R}^{n\times n}$ is the symmetric, positive definite solution of the Lyapunov equation

$$\mathbf{P}\mathbf{A}_M + \mathbf{A}_M^T\mathbf{P} = -\mathbf{Q} \tag{4.11}$$

with $\mathbf{Q} = \mathbf{Q}^T \in \mathbb{R}^{n\times n}$ being a symmetric, positive definite (design) matrix, that provides a weighting possibility for the system states. $\boldsymbol{\Gamma}_x \in \mathbb{R}^{n\times n}$, $\boldsymbol{\Gamma}_\varphi \in \mathbb{R}^{k\times k}$, $\gamma_{dd} \in \mathbb{R}$, and $\boldsymbol{\Gamma}_r \in \mathbb{R}^{m\times m}$ are symmetric positive definite design parameters that determine the adaption rate (speed of learning).

The control law of Eq.(4.3), the reference model of Eq.(4.2), and the update law given by Eq.(4.10) guarantee global stability ($\mathbf{x}_M$, $\mathbf{e}_C$, $\boldsymbol{\Theta}_C \in \mathcal{L}_\infty$) of the closed loop system, and Barbalat's Lemma guarantees that the error converges to zero [1]:

$$\lim_{t\to\infty}\mathbf{e}_C(t) = \mathbf{0} \tag{4.12}$$

I.e. $\mathbf{e}_C(t)$ is asymptotically stable, and the trajectory of the parameter errors $\tilde{\boldsymbol{\Theta}}_C(t)$ is stable, but not asymptotically stable. The stability proof is shown in the Appendix D.1.

Hence, it is in general not guaranteed that the parameters converge to their true values. However, this is necessary in order for the transient response of the controlled plant to exactly follow the reference model. Parameter convergence to the true values will only be guaranteed in the case of a persistently exciting reference input signal $\mathbf{r}$ [1] [4]. This means that the input signal has to contain sufficient different frequencies to excite all dynamic modes of the system, so that the output contains sufficient information about the system to identify the true parameters [131].

The closed loop structure of considered direct MRAC approach is shown in Figure 4.3.

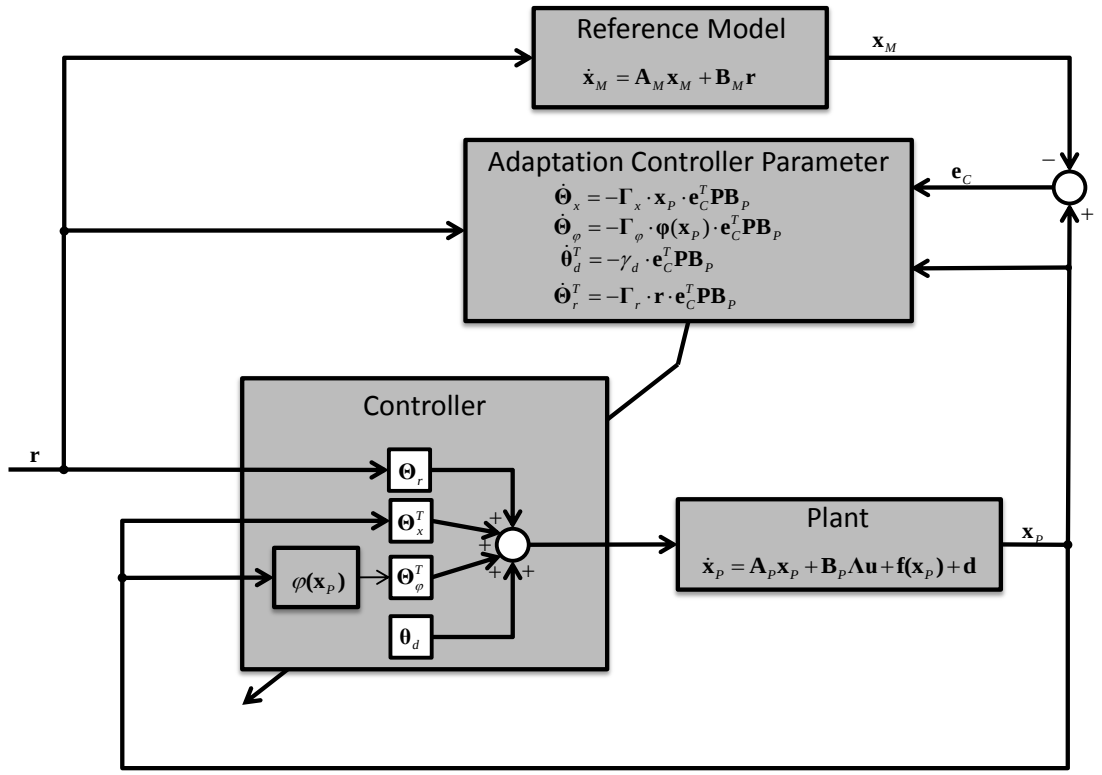

Figure 4.3: Direct MRAC with state feedback

4.3 Indirect MRAC

In contrast to the direct approach, indirect MRAC relies on identification of the plant parameters. The parameter estimation is based on an identification error between an identification model and the plant which is defined by

$$\mathbf{e}_I = \hat{\mathbf{x}}_P - \mathbf{x}_P. \tag{4.13}$$

With the dynamics of the identification model given by

$$\dot{\hat{\mathbf{x}}}_P = \mathbf{A}_M\hat{\mathbf{x}}_P + \left[\widehat{\mathbf{A}}_P - \mathbf{A}_M\right]\mathbf{x}_P + \mathbf{B}_P\widehat{\boldsymbol{\Lambda}}\mathbf{u} + \widehat{\boldsymbol{\Theta}}_f\boldsymbol{\varphi}(\mathbf{x}_P) + \hat{\mathbf{d}}, \tag{4.14}$$

where $\widehat{\mathbf{A}}_P \in \mathbb{R}^{n\times n}$ is an estimate of the unknown system matrix, $\widehat{\boldsymbol{\Lambda}} \in \mathbb{R}^{m\times m}$ is an estimate of the unknown control effectiveness matrix, $\widehat{\boldsymbol{\Theta}}_f\boldsymbol{\varphi}(\mathbf{x}_P) \in \mathbb{R}^{n\times k}$ is an estimate of unknown nonlinearity, and $\hat{\mathbf{d}}$ is an estimate of the constant disturbance.

Assume that the nonlinearity in the plant can be linearly parameterized by $\mathbf{f}(\mathbf{x}_P) = \boldsymbol{\Theta}_f^*\boldsymbol{\varphi}(\mathbf{x}_P)$, then the plant dynamics of Eq. (4.1) can be denoted by

$$\dot{\mathbf{x}}_P = \mathbf{A}_P\mathbf{x}_P + \mathbf{B}_P\boldsymbol{\Lambda}\mathbf{u} + \widehat{\boldsymbol{\Theta}}_f^*\boldsymbol{\varphi}(\mathbf{x}_P) + \mathbf{d}. \tag{4.15}$$

It should be mentioned that for pure parameter identification based on $\mathbf{e}_I$ the matching condition (see Eq.(4.4)) is not required to hold. However, the matching condition must still be satisfied to achieve the control objective and make the plant follow the reference model.

By subtracting Eq.(4.15) from Eq.(4.14) we obtain the following identification error dynamics

$$\begin{aligned}\dot{\mathbf{e}}_I &= \mathbf{A}_M\underbrace{(\hat{\mathbf{x}}_P - \mathbf{x}_P)}_{\mathbf{e}_I} + \underbrace{\left[\widehat{\mathbf{A}}_P - \mathbf{A}_P\right]}_{\tilde{\mathbf{A}}_P}\mathbf{x}_P + \underbrace{\left(\widehat{\boldsymbol{\Theta}}_f - \widehat{\boldsymbol{\Theta}}_f^*\right)}_{\tilde{\boldsymbol{\Theta}}_f}\boldsymbol{\varphi}(\mathbf{x}_P) + \underbrace{\hat{\mathbf{d}} - \mathbf{d}}_{\tilde{\mathbf{d}}} + \mathbf{B}_P\underbrace{\left(\widehat{\boldsymbol{\Lambda}} - \boldsymbol{\Lambda}\right)}_{\tilde{\boldsymbol{\Lambda}}}\mathbf{u} \\ &= \mathbf{A}_M\mathbf{e}_I + \underbrace{\left[\tilde{\mathbf{A}}_P \quad \tilde{\boldsymbol{\Theta}}_f \quad \tilde{\mathbf{d}} \quad \mathbf{B}_P\tilde{\boldsymbol{\Lambda}}\right]}_{\tilde{\boldsymbol{\Theta}}_I}\underbrace{\begin{pmatrix}\mathbf{x}_P\\ \boldsymbol{\varphi}(\mathbf{x}_P)\\ 1\\ \mathbf{u}\end{pmatrix}}_{\boldsymbol{\omega}_I}.\end{aligned} \tag{4.16}$$

Using Lyapunov analysis, stable update laws for the plant parameters can be derived. Based on the estimated plant parameters the controller gains for the control law of Eq.(4.3) can either be calculated or updated by additional differential equations. The update requires the same amount of prior information as in the direct case, whereat for calculation of the controller gains a bound on $\widehat{\boldsymbol{\Lambda}}$ has to be realized to ensure that the inverse exists.

4.3.1 Calculation of Controller Gains

In Figure 4.4 indirect MRAC with calculation of the controller gains is shown and in the following the update laws for this approach are given.

Choosing the Lyapunov function candidate

$$\mathrm{V} = \frac{1}{2}\mathbf{e}_I^T\mathbf{P}\mathbf{e}_I + \frac{1}{2}\mathrm{Tr}\left[\tilde{\mathbf{A}}_P\boldsymbol{\Gamma}_A^{-1}\tilde{\mathbf{A}}_P^T\right] + \frac{1}{2}\mathrm{Tr}\left[\tilde{\boldsymbol{\Lambda}}\boldsymbol{\Gamma}_\Lambda^{-1}\tilde{\boldsymbol{\Lambda}}^T\right] + \frac{1}{2}\mathrm{Tr}\left[\tilde{\boldsymbol{\Theta}}_f\boldsymbol{\Gamma}_f^{-1}\tilde{\boldsymbol{\Theta}}_f^T\right] + \frac{1}{2}\mathrm{Tr}\left[\gamma_d^{-1}\tilde{\mathbf{d}}\tilde{\mathbf{d}}^T\right], \tag{4.17}$$

it can be verified that for the error dynamics of Eq.(4.16) the following adaptation laws make the time derivative of the Lyapunov function negative semi definite

$$\begin{aligned}\dot{\tilde{\mathbf{A}}}_P^T &= -\boldsymbol{\Gamma}_A \mathbf{x}_P \cdot \mathbf{e}_I^T \mathbf{P} \\ \dot{\tilde{\boldsymbol{\Lambda}}}^T &= -\boldsymbol{\Gamma}_\Lambda \mathbf{u} \cdot \mathbf{e}_I^T \mathbf{P} \mathbf{B}_P \\ \dot{\tilde{\boldsymbol{\Theta}}}_f^T &= -\boldsymbol{\Gamma}_f \boldsymbol{\varphi}(\mathbf{x}_P) \cdot \mathbf{e}_I^T \mathbf{P} \\ \dot{\tilde{\mathbf{d}}}^T &= -\gamma_d \mathbf{e}_I^T \mathbf{P}\end{aligned} \quad \Leftrightarrow \quad \begin{aligned}\dot{\hat{\mathbf{A}}}_P^T &= -\boldsymbol{\Gamma}_A \mathbf{x}_P \cdot \mathbf{e}_I^T \mathbf{P} \\ \dot{\hat{\boldsymbol{\Lambda}}}^T &= -\boldsymbol{\Gamma}_\Lambda \mathbf{u} \cdot \mathbf{e}_I^T \mathbf{P} \mathbf{B}_P \\ \dot{\hat{\boldsymbol{\Theta}}}_f^T &= -\boldsymbol{\Gamma}_f \boldsymbol{\varphi}(\mathbf{x}_P) \cdot \mathbf{e}_I^T \mathbf{P} \\ \dot{\hat{\mathbf{d}}}^T &= -\gamma_d \mathbf{e}_I^T \mathbf{P}\end{aligned} \quad . \tag{4.18}$$

Hence stable parameter estimation is guaranteed ($\mathbf{e}_I$, $\widehat{\mathbf{A}}_P$, $\widehat{\boldsymbol{\Lambda}}$, $\widehat{\boldsymbol{\Theta}}_f$, and $\hat{\mathbf{d}} \in \mathcal{L}_\infty$).

To actually control the plant in a desired behavior choose the control law

$$\mathbf{u} = \left(\mathbf{B}_P \widehat{\boldsymbol{\Lambda}}\right)^{-1} \left[-\left[\widehat{\mathbf{A}}_P - \mathbf{A}_M\right] \mathbf{x}_P - \widehat{\boldsymbol{\Theta}}_f \boldsymbol{\varphi}(\mathbf{x}_P) - \hat{\mathbf{d}} + \mathbf{B}_M \mathbf{r} \right]. \tag{4.19}$$

It is obvious that for this control law the inverse of $\mathbf{B}_P \widehat{\boldsymbol{\Lambda}}$ has to exist. This is similar to the requirement that the uncertainties have to be in the span of $\mathbf{B}_P$ as it was required in the direct case, because for the existence of the inverse, $\mathbf{B}_P$ has to be $\in \mathbb{R}^{n \times n}$, and thus has to span the complete state space. Inserting the control law of Eq.(4.19) in the identification model of Eq.(4.14) we immediately obtain

$$\dot{\hat{\mathbf{x}}}_P = \mathbf{A}_M \hat{\mathbf{x}}_P + \mathbf{B}_M \, \mathbf{r}. \tag{4.20}$$

Choosing $\hat{\mathbf{x}}_P(t_0) = \mathbf{x}_M(t_0)$, it follows that $\hat{\mathbf{x}}_P(t) = \mathbf{x}_M(t) \; \forall \, t \geq t_0$, and hence the predictor dynamics are equal to the dynamics of the reference model. This also means that for a stable reference model $\hat{\mathbf{x}}_P$ is bounded.

If $rank(\mathbf{B}_P) < n$ the left pseudo inverse $\mathbf{B}_P^l = (\mathbf{B}_P^T \mathbf{B}_P)^{-1} \mathbf{B}_P^T$ can be used instead of $\mathbf{B}_P^{-1}$. Additionally, it must be guaranteed that the estimation $\widehat{\boldsymbol{\Lambda}}$ is well conditioned and non singular, what can be assured by the projection operator. These requirements are more restrictive and require more knowledge than in the direct case, but in the next section it is shown that this problem can be circumvented by using additional update laws for the controller parameters.

Note that if $rank(\mathbf{B}_P) < n$ and the pseudo inverse $\mathbf{B}_P^l$ is used, then inserting the control law of Eq.(4.19) in the identification model of Eq.(4.14) does not result in the stable system given in Eq.(4.20). But rather the identification dynamics which is not in the span $\mathbf{B}_P$ is adjusted, because the term $\left[\widehat{\mathbf{A}}_P - \mathbf{A}_M\right] \mathbf{x}_P$ in Eq.(4.14) is not completely canceled. This means the estimated unmatched uncertainties are used to adjust the dynamics of the identification model in a way that it follows the plant. As we will see later this can be advantageous for the robustness w.r.t. unmatched uncertainties. In Section 5.1.4 it is shown how this relaxation of the matching condition can also be achieved for the direct and the predictor based approach, where also a stability proof is given. With the modification in Section 5.1.4 the predictor based approach basically collapses to the indirect approach, and thus a stability proof is omitted for the indirect approach as it would be essentially similar to the proof given in Section 5.1.4.2.

Previously it was mentioned that in the indirect approach the controller gains are usually derived from an algebraic equation, which depends on the estimated plant

parameters. In the current case the algebraic equation is given by Eq.(4.19), what can be easily seen by rewriting the control law:

$$\mathbf{u} = \left[\underbrace{-\left(\mathbf{B}_P\widehat{\mathbf{\Lambda}}\right)^{-1}\left[\widehat{\mathbf{A}}_P - \mathbf{A}_M\right]}_{\widehat{\mathbf{\Theta}}_x^T}\mathbf{x}_P \underbrace{-\left(\mathbf{B}_P\widehat{\mathbf{\Lambda}}\right)^{-1}\widehat{\mathbf{\Theta}}_f}_{\widehat{\mathbf{\Theta}}_\varphi^T}\boldsymbol{\varphi}(\mathbf{x}_P) \underbrace{-\left(\mathbf{B}_P\widehat{\mathbf{\Lambda}}\right)^{-1}\hat{\mathbf{d}}}_{\boldsymbol{\theta}_d} + \underbrace{\left(\mathbf{B}_P\widehat{\mathbf{\Lambda}}\right)^{-1}\mathbf{B}_M}_{\mathbf{\Theta}_r}\mathbf{r} \right] \tag{4.21}$$

$$\mathbf{u} = \mathbf{\Theta}_x^T\mathbf{x}_P + \mathbf{\Theta}_\varphi^T\,\boldsymbol{\varphi}(\mathbf{x}_P) + \boldsymbol{\theta}_d + \mathbf{\Theta}_r\,\mathbf{r}$$

This is similar to the controller in the direct case. However, as mentioned the controller gains $\mathbf{\Theta}_x^T$, $\mathbf{\Theta}_\varphi^T$, θ_d, and $\mathbf{\Theta}_r$ are not directly derived from the adaptation laws but from algebraic equations, and hence their existence is only guaranteed if the matching condition holds:

$$\begin{aligned}
\mathbf{\Theta}_x^T &= -\left(\mathbf{B}_P\widehat{\mathbf{\Lambda}}\right)^{-1}\left[\widehat{\mathbf{A}}_P - \mathbf{A}_M\right] \\
\mathbf{\Theta}_\varphi^T &= -\left(\mathbf{B}_P\widehat{\mathbf{\Lambda}}\right)^{-1}\widehat{\mathbf{\Theta}}_f \\
\boldsymbol{\theta}_d &= -\left(\mathbf{B}_P\widehat{\mathbf{\Lambda}}\right)^{-1}\hat{\mathbf{d}} \\
\mathbf{\Theta}_r &= \left(\mathbf{B}_P\widehat{\mathbf{\Lambda}}\right)^{-1}\mathbf{B}_M
\end{aligned} \quad . \tag{4.22}$$

As $\hat{\mathbf{x}}_P$ and as $\mathbf{e}_I$ are bounded, $\mathbf{x}_P = \hat{\mathbf{x}}_P + \mathbf{e}_I$ is bounded. Furthermore, by application of Barbalat's Lemma [1] it can be show that

$$\lim_{t\to\infty}\mathbf{e}_I\,(t) = \lim_{t\to\infty}(\hat{\mathbf{x}}_P - \mathbf{x}_P) = \lim_{t\to\infty}(\mathbf{x}_M - \mathbf{x}_P) = \mathbf{0}.$$

Inserting the control law in the identification model leads to the dynamics of the reference model. Thus $\mathbf{e}_I$ is equal to the error between the reference dynamics and the plant, and it converges to zero. This is also shown in the stability proof in the Appendix D.2.1.

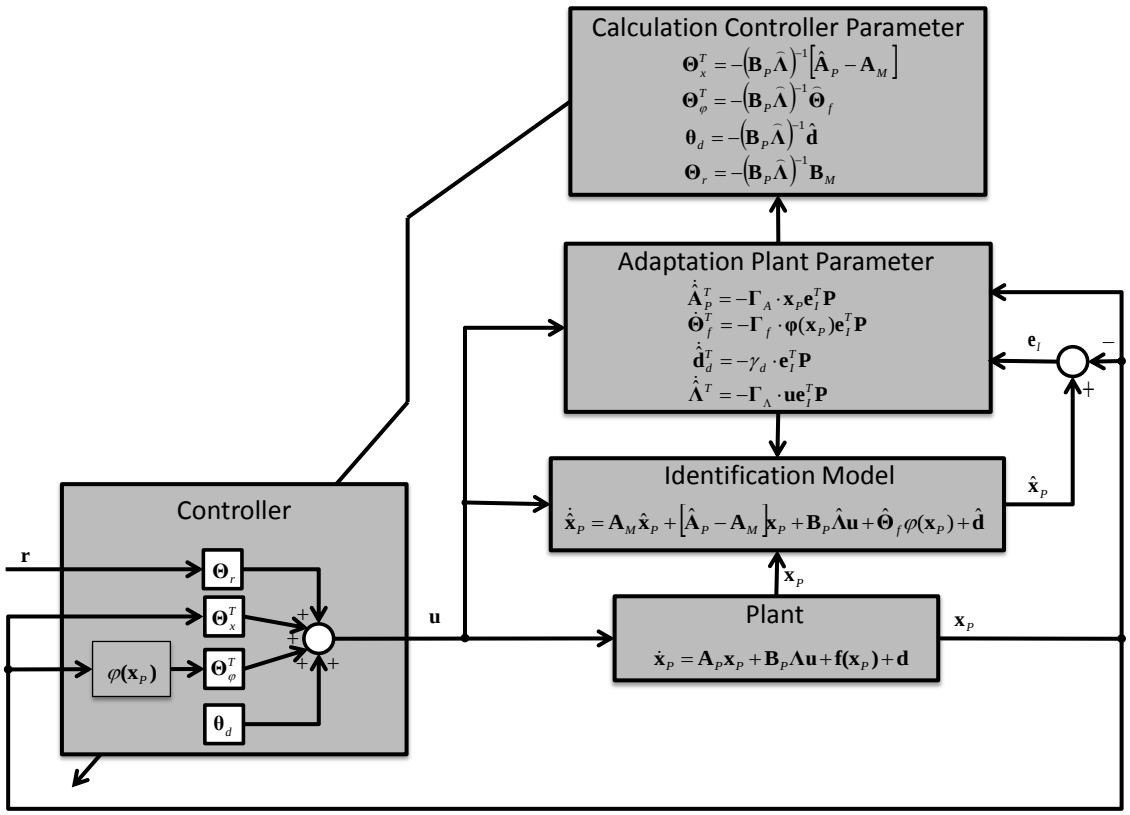

Figure 4.4: Indirect MRAC with controller gain calculation and state feedback

4.3.2 Update of Controller Gains

In Figure 4.5 indirect MRAC with update the controller gains is shown.

The control law is again given by

$$\mathbf{u} = \boldsymbol{\Theta}_x^T\mathbf{x}_P + \boldsymbol{\Theta}_\varphi^T\,\boldsymbol{\varphi}(\mathbf{x}_P) + \boldsymbol{\theta}_d + \boldsymbol{\Theta}_r\,\mathbf{r}, \tag{4.23}$$

However, in difference to Eq.(4.21) the controller gains are not directly calculated from the estimated plant parameters but updated from additional differential equations. In the following the update laws for this approach are given.

Using an appropriate Lyapunov function candidate of the form

$$\begin{aligned} \mathrm{V} = \frac{1}{2}\mathbf{e}_I^T\mathbf{P}\mathbf{e}_I + \frac{1}{2}\mathrm{Tr}\left[\tilde{\boldsymbol{\Theta}}_x^T\boldsymbol{\Gamma}_x^{-1}\tilde{\boldsymbol{\Theta}}_x\boldsymbol{\Lambda}\right] + \frac{1}{2}\mathrm{Tr}\left[\tilde{\boldsymbol{\Theta}}_\varphi^T\boldsymbol{\Gamma}_\varphi^{-1}\tilde{\boldsymbol{\Theta}}_\varphi\boldsymbol{\Lambda}\right] + \frac{1}{2}\mathrm{Tr}\left[\gamma_{dd}^{-1}\tilde{\boldsymbol{\theta}}_d\tilde{\boldsymbol{\theta}}_d^T\boldsymbol{\Lambda}\right] + \frac{1}{2}\mathrm{Tr}\left[\tilde{\boldsymbol{\Theta}}_r\boldsymbol{\Gamma}_r^{-1}\tilde{\boldsymbol{\Theta}}_r^T\boldsymbol{\Lambda}\right] \\ + \frac{1}{2}\mathrm{Tr}\left[\tilde{\mathbf{A}}_P\boldsymbol{\Gamma}_A^{-1}\tilde{\mathbf{A}}_P^T\right] + \frac{1}{2}\mathrm{Tr}\left[\tilde{\boldsymbol{\Theta}}_f\boldsymbol{\Gamma}_f^{-1}\tilde{\boldsymbol{\Theta}}_f^T\right]\frac{1}{2}\mathrm{Tr}\left[\gamma_{di}^{-1}\tilde{\mathbf{d}}\tilde{\mathbf{d}}^T\right] + \frac{1}{2}\mathrm{Tr}\left[\tilde{\boldsymbol{\Lambda}}\boldsymbol{\Gamma}_\Lambda^{-1}\tilde{\boldsymbol{\Lambda}}^T\right], \end{aligned} \tag{4.24}$$

it can be verified that the following update laws render the time derivative of the Lyapunov function negative semi definite [1] [91] under the ideal assumptions. This means, the matching condition again needs to hold.

For the update laws the definition of the additional errors $\boldsymbol{\varepsilon}_x$, $\boldsymbol{\varepsilon}_\varphi$, $\boldsymbol{\varepsilon}_d$ and $\boldsymbol{\varepsilon}_r$ is necessary. Based on the matching condition and the knowledge that it is desired that $\widehat{\mathbf{A}}_P + \mathbf{B}_P\widehat{\boldsymbol{\Lambda}}\boldsymbol{\Theta}_x^T$ converges to $\mathbf{A}_M$, $\mathbf{B}_P\widehat{\boldsymbol{\Lambda}}\boldsymbol{\Theta}_\varphi^T$ converges to $-\widehat{\boldsymbol{\Theta}}_f$, $\mathbf{B}_P\widehat{\boldsymbol{\Lambda}}\boldsymbol{\theta}_d$ converges to $-\mathbf{d}$, and $\mathbf{B}_P\widehat{\boldsymbol{\Lambda}}\boldsymbol{\Theta}_r$ converges to $\mathbf{B}_M$ (see Eq. (4.4)) the additional closed loop estimation errors (matching errors) are defined:

$$\begin{aligned}\boldsymbol{\varepsilon}_x &= \left[\widehat{\mathbf{A}}_P + \mathbf{B}_P\widehat{\boldsymbol{\Lambda}}\boldsymbol{\Theta}_x^T - \mathbf{A}_M\right]\\ \boldsymbol{\varepsilon}_\varphi &= \left[\mathbf{B}_P\widehat{\boldsymbol{\Lambda}}\boldsymbol{\Theta}_\varphi^T + \widehat{\boldsymbol{\Theta}}_f\right]\\ \boldsymbol{\varepsilon}_d &= \left[\mathbf{B}_P\widehat{\boldsymbol{\Lambda}}\boldsymbol{\theta}_d + \hat{\mathbf{d}}\right]\\ \boldsymbol{\varepsilon}_r &= \left[\mathbf{B}_P\widehat{\boldsymbol{\Lambda}}\boldsymbol{\Theta}_r - \mathbf{B}_M\right]\end{aligned} \tag{4.25}$$

With the update laws for the plant parameters given by

$$\begin{aligned}\dot{\widehat{\mathbf{A}}}_P^T &= -\boldsymbol{\Gamma}_A(\mathbf{x}_P\mathbf{e}_I^T\mathbf{P} + \gamma_\varepsilon\boldsymbol{\varepsilon}_x^T)\\ \dot{\widehat{\boldsymbol{\Theta}}}_f^T &= -\boldsymbol{\Gamma}_f\left(\boldsymbol{\varphi}(\mathbf{x}_P)\mathbf{e}_I^T\mathbf{P} + \gamma_\varepsilon\boldsymbol{\varepsilon}_\varphi^T\right)\\ \dot{\hat{\mathbf{d}}}^T &= -\gamma_{di}\left(\mathbf{e}_I^T\mathbf{P} + \gamma_\varepsilon\boldsymbol{\varepsilon}_d^T\right)\\ \dot{\widehat{\boldsymbol{\Lambda}}}^T &= -\boldsymbol{\Gamma}_\Lambda\left(\mathbf{u}\mathbf{e}_I^T\mathbf{P} + \gamma_\varepsilon\left[\boldsymbol{\Theta}_x^T\boldsymbol{\varepsilon}_x^T + \boldsymbol{\Theta}_\varphi^T\boldsymbol{\varepsilon}_\varphi^T + \boldsymbol{\theta}_d\boldsymbol{\varepsilon}_d^T + \boldsymbol{\Theta}_r\boldsymbol{\varepsilon}_r^T\right]\right)\mathbf{B}_P,\end{aligned} \tag{4.26}$$

where $\boldsymbol{\Gamma}_A \in \mathbb{R}^{n\times n}$, $\boldsymbol{\Gamma}_f \in \mathbb{R}^{k\times k}$, $\gamma_{di} \in \mathbb{R}$ and $\boldsymbol{\Gamma}_\Lambda \in \mathbb{R}^{m\times m}$ are symmetric positive definite design parameters that determine the adaption rate, and $\gamma_\varepsilon \in \mathbb{R}$ provides a weighting for the additional errors $\boldsymbol{\varepsilon}$ in the adaptation law.

Together with the update laws for the controller parameters given by

$$\begin{aligned}\dot{\boldsymbol{\Theta}}_x &= -\boldsymbol{\Gamma}_x\gamma_\varepsilon\boldsymbol{\varepsilon}_x^T\,\mathbf{B}_P\\ \dot{\boldsymbol{\Theta}}_\varphi &= -\boldsymbol{\Gamma}_\varphi\gamma_\varepsilon\boldsymbol{\varepsilon}_\varphi^T\mathbf{B}_P\\ \dot{\boldsymbol{\theta}}_d^T &= -\gamma_d\gamma_\varepsilon\boldsymbol{\varepsilon}_d^T\mathbf{B}_P\\ \dot{\boldsymbol{\Theta}}_r^T &= -\boldsymbol{\Gamma}_r\gamma_\varepsilon\boldsymbol{\varepsilon}_r^T\mathbf{B}_P\end{aligned} \tag{4.27}$$

the identification error and the parameters are globally stable ($\mathbf{e}_I$, $\boldsymbol{\Theta}_x^T$, $\boldsymbol{\Theta}_\varphi^T$, $\boldsymbol{\theta}_d$, $\boldsymbol{\Theta}_r$, $\widehat{\mathbf{A}}_P$, $\widehat{\boldsymbol{\Theta}}_f$, $\hat{\mathbf{d}}$ and $\widehat{\boldsymbol{\Lambda}} \in \mathcal{L}_\infty$). By application of Barbalat's Lemma it can be shown that $\mathbf{e}_I$, $\boldsymbol{\varepsilon}_x$, $\boldsymbol{\varepsilon}_\varphi$, $\boldsymbol{\varepsilon}_d$ and $\boldsymbol{\varepsilon}_r$ converge to zero asymptotically. From this, and by inserting the control law Eq.(4.3) in the estimator dynamics Eq.(4.14), it directly follows that the estimator dynamics converge to the dynamics of the reference model, and because $\mathbf{e}_I$ converges to zero it holds that

$$\lim_{t\to\infty}\left(\mathbf{x}_P(t) - \mathbf{x}_M(t)\right) = \mathbf{0}. \tag{4.28}$$

The stability proof is shown in the Appendix D.2.2.

In most cases the indirect approach leads to a larger number of adaptive parameters than the direct approach because the complete system dynamics is estimated. Due to this the convergence speed in the indirect case is usually slower. However, the update of the controller parameter has a low pass character and it could be observed that better transient response can be achieved compared to direct MRAC.

It should be noted that the terminology is often not used in a rigorous way. As mentioned in [91] the presented approach could also be interpreted as a combined approach because the estimation errors $\boldsymbol{\varepsilon}$ are used in the update law for the plant parameters as well as in the update law for the controller parameters.

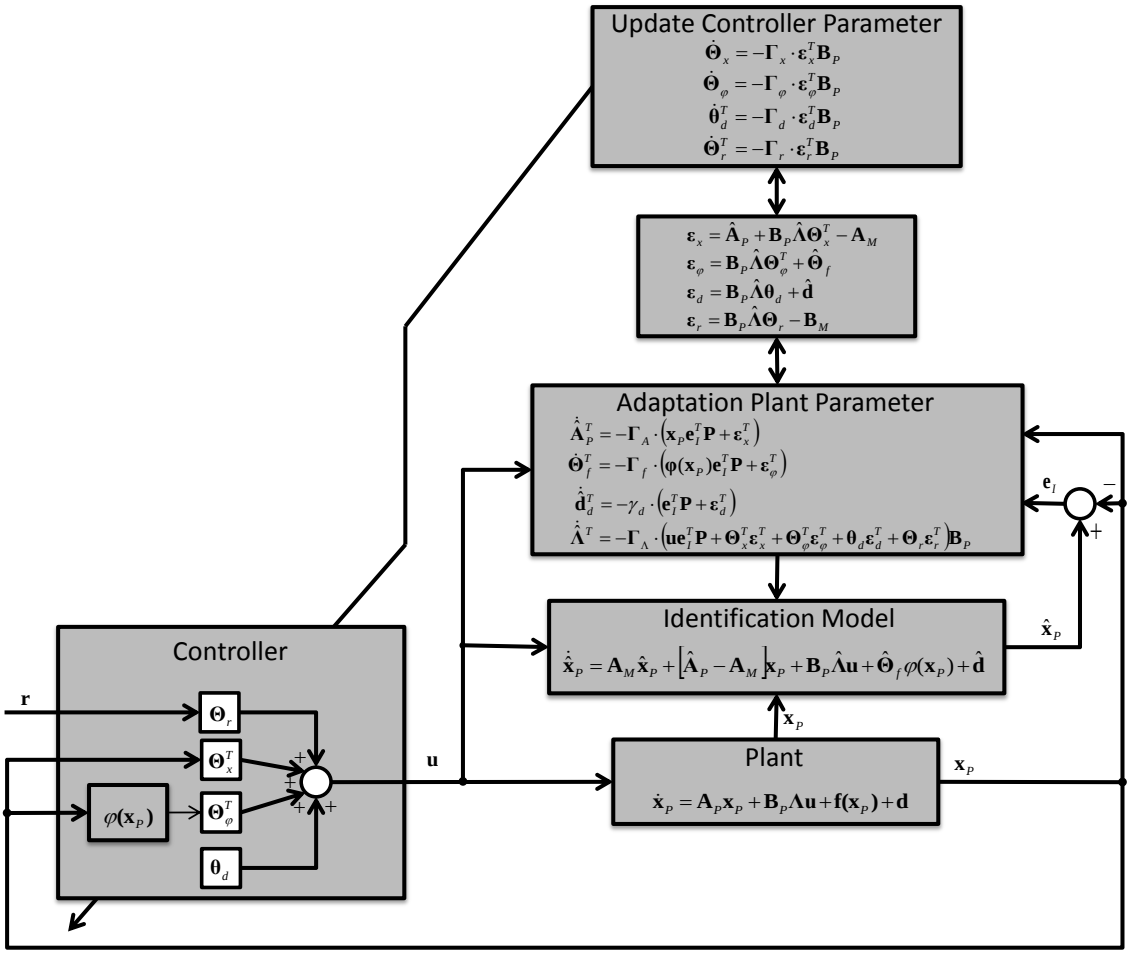

Figure 4.5: Indirect MRAC with controller gain update and state feedback

4.4 Predictor based MRAC

This structure is also commonly used in adaptive control, as for example for the $\mathcal{L}_1$ architecture presented in [23] or the Q-modification presented in [109] [110] [111]. The term predictor based MRAC is used here because instead of a reference model a state predictor is used. Actually the approach can also be interpreted as an indirect approach, where the plant uncertainties are a-priori parameterized in an input affine way. This means only matched plant uncertainties are estimated.

Therefore, the parameterized system dynamics form Eq.(4.5) can be reparameterized in the following way

$$\dot{\mathbf{x}}_P = \mathbf{A}_M\mathbf{x}_P + \mathbf{B}_P\left(\boldsymbol{\Lambda}\mathbf{u} - \underbrace{\boldsymbol{\Lambda}\boldsymbol{\Theta}_x^{*\,T}}_{\widehat{\boldsymbol{\Theta}}_x^{*\,T}}\mathbf{x}_P - \underbrace{\boldsymbol{\Lambda}\boldsymbol{\Theta}_\varphi^{*\,T}}_{\widehat{\boldsymbol{\Theta}}_\varphi^{*\,T}}\boldsymbol{\varphi}(\mathbf{x}_P) - \underbrace{\boldsymbol{\Lambda}\boldsymbol{\theta}_d^*}_{\widehat{\boldsymbol{\theta}}_d^*}\right)$$

$$\dot{\mathbf{x}}_P = \mathbf{A}_M\mathbf{x}_P + \mathbf{B}_P\left(\boldsymbol{\Lambda}\mathbf{u} - \widehat{\boldsymbol{\Theta}}_x^{*\,T}\mathbf{x}_P - \widehat{\boldsymbol{\Theta}}_\varphi^{*\,T}\boldsymbol{\varphi}(\mathbf{x}_P) - \widehat{\boldsymbol{\theta}}_d^*\right). \tag{4.29}$$

A state predictor is defined in the form of

$$\dot{\hat{\mathbf{x}}}_P = \mathbf{A}_M\hat{\mathbf{x}}_P + \mathbf{B}_P\left(\widehat{\boldsymbol{\Lambda}}\mathbf{u} - \widehat{\boldsymbol{\Theta}}_x^T\mathbf{x}_P - \widehat{\boldsymbol{\Theta}}_\varphi^T\boldsymbol{\varphi}(\mathbf{x}_P) - \widehat{\boldsymbol{\theta}}_d\right). \tag{4.30}$$

This state predictor is very similar to the identification model of the indirect approach, with the difference stemming from the input affine parameterization. To see this, assume a matched parameterization for the identification model of Eq.(4.14) which results in Eq.(4.30)

$$\dot{\hat{\mathbf{x}}}_P = \mathbf{A}_M\hat{\mathbf{x}}_P + \underbrace{\left[\widehat{\mathbf{A}}_P - \mathbf{A}_M\right]}_{\mathbf{B}_P\widehat{\boldsymbol{\Theta}}_x^T}\mathbf{x}_P + \mathbf{B}_P\widehat{\boldsymbol{\Lambda}}\mathbf{u} + \underbrace{\widehat{\boldsymbol{\Theta}}_f\boldsymbol{\varphi}(\mathbf{x}_P)}_{\mathbf{B}_P\widehat{\boldsymbol{\Theta}}_\varphi^T} + \underbrace{\hat{\mathbf{d}}}_{\mathbf{B}_P\widehat{\boldsymbol{\theta}}_d}. \tag{4.31}$$

As the approach is very similar to the indirect approach we also can apply the two previously discussed methods to obtain the controller gains.

To highlight the idea, considering a simplified problem with $\boldsymbol{\Lambda} = \mathbf{I}$, $\widehat{\boldsymbol{\Theta}}_\varphi^{*\,T} = \mathbf{0}$, $\widehat{\boldsymbol{\theta}}_d^* = \mathbf{0}$. The philosophy is to identify the difference between the true plant dynamics given by $\mathbf{A}_P = \mathbf{A}_M - \mathbf{B}_P\widehat{\boldsymbol{\Theta}}_x^{*\,T}\mathbf{x}_P$ and the assumed plant behavior characterized by $\mathbf{A}_M$. This difference $\mathbf{B}_P\widehat{\boldsymbol{\Theta}}_x^{*\,T}$ can also be interpreted as a $\Delta\mathbf{u}$ and we can choose the input $\mathbf{u}$ to chancel this mismatch, as shown in Figure 4.6. Of course, for implementation the real difference $\widehat{\boldsymbol{\Theta}}_x^{*\,T}$ cannot be used and the estimation $\widehat{\boldsymbol{\Theta}}_x^T$ must be applied instead.

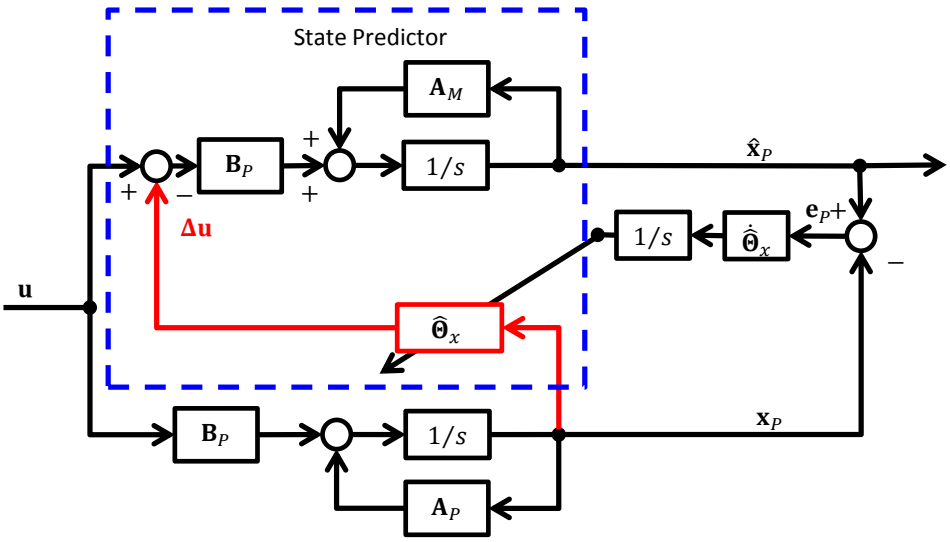

Figure 4.6: Philosophy of predictor based MRAC

4.4.1 Calculation of Controller Gains

A similar control law as in Eq.(4.19) can be chosen, which reflects the attempt to cancel the uncertainties in the plant dynamics

$$\mathbf{u} = \widehat{\boldsymbol{\Lambda}}^{-1}\left[\widehat{\boldsymbol{\Theta}}_x^T\mathbf{x}_P + \widehat{\boldsymbol{\Theta}}_\varphi^T\boldsymbol{\varphi}(\mathbf{x}_P) + \widehat{\boldsymbol{\theta}}_d + \mathbf{K}_r\,\mathbf{r}\right], \tag{4.32}$$

with the static feedforward gain $\mathbf{K}_r \in \mathbb{R}^{m\times m}$. Due to the use of the inverse $\widehat{\boldsymbol{\Lambda}}^{-1}$, the control effectiveness $\widehat{\boldsymbol{\Lambda}}$ has to be bounded in a way that it cannot become singular. This actually requires again more knowledge than the direct structure, however as the sign of $\boldsymbol{\Lambda}$ has to be known the required bound on $\widehat{\boldsymbol{\Lambda}}$ is reasonable. A benefit of the approach compared to direct MRAC is that the plant is parameterized linearly in the unknown parameters (see Eq.(4.29)).

Of course the control law of Eq.(4.32) can be implemented directly as shown in Figure 4.7, but equally one can also calculate the controller gains used in the control law of the direct approach given by Eq.(4.3). Therefore it is obvious by comparing Eq.(4.3) and Eq.(4.32) that the following algebraic equations have to apply

$$\begin{aligned}
\boldsymbol{\Theta}_x^T &= \widehat{\boldsymbol{\Lambda}}^{-1}\widehat{\boldsymbol{\Theta}}_x^T \\
\boldsymbol{\Theta}_\varphi^T &= \widehat{\boldsymbol{\Lambda}}^{-1}\widehat{\boldsymbol{\Theta}}_\varphi^T \\
\boldsymbol{\Theta}_d &= \widehat{\boldsymbol{\Lambda}}^{-1}\widehat{\boldsymbol{\theta}}_d \\
\boldsymbol{\Theta}_r &= \widehat{\boldsymbol{\Lambda}}^{-1}\mathbf{K}_r.
\end{aligned} \tag{4.33}$$

Inserting the control law of Eq. (4.32) in the predictor dynamics yields

$$\dot{\hat{\mathbf{x}}}_P = \mathbf{A}_M\hat{\mathbf{x}}_P + \mathbf{B}_P\mathbf{K}_r\mathbf{r}. \tag{4.34}$$

Hence, $\mathbf{K}_r$ has to be chosen such that $\mathbf{B}_M = \mathbf{B}_P\mathbf{K}_r$ in order to make the predictor dynamics equal to the reference model. By choosing $\hat{\mathbf{x}}_P(t_0) = \mathbf{x}_M(t_0)$ it follows that $\hat{\mathbf{x}}_P(t) = \mathbf{x}_M(t)\ \forall\ t \geq t_0$, and hence, the predictor dynamics are equal to the dynamics of the reference model.

Defining the error as the difference between the predictor states and the states of the plant

$$\mathbf{e}_P = \hat{\mathbf{x}}_P - \mathbf{x}_P \tag{4.35}$$

we obtain the error dynamics in the form

$$\begin{aligned}
\dot{\mathbf{e}}_P &= \mathbf{A}_M\underbrace{\left(\mathbf{x}_P - \hat{\mathbf{x}}_P\right)}_{\mathbf{e}_P} + \mathbf{B}_P\left(\underbrace{\left(\widehat{\boldsymbol{\Theta}}_x^{*\,T} - \widehat{\boldsymbol{\Theta}}_x^T\right)}_{\tilde{\widehat{\boldsymbol{\Theta}}}_x^T}\mathbf{x}_P + \underbrace{\left(\widehat{\boldsymbol{\Theta}}_\varphi^{*\,T} - \widehat{\boldsymbol{\Theta}}_\varphi^T\right)}_{\tilde{\widehat{\boldsymbol{\Theta}}}_\varphi^T}\boldsymbol{\varphi}(\mathbf{x}_P) + \underbrace{\left(\widehat{\boldsymbol{\theta}}_d^* - \widehat{\boldsymbol{\theta}}_d\right)}_{\tilde{\widehat{\boldsymbol{\theta}}}_d} + \underbrace{\left(\widehat{\boldsymbol{\Lambda}} - \boldsymbol{\Lambda}\right)}_{\tilde{\boldsymbol{\Lambda}}}\mathbf{u}\right) \\
&= \mathbf{A}_M\mathbf{e}_P + \mathbf{B}_P\underbrace{\left[\tilde{\widehat{\boldsymbol{\Theta}}}_x^T \quad \tilde{\widehat{\boldsymbol{\Theta}}}_\varphi^T \quad \tilde{\widehat{\boldsymbol{\theta}}}_d \quad \tilde{\boldsymbol{\Lambda}}\right]}_{\tilde{\widehat{\boldsymbol{\theta}}}_P^T}\underbrace{\begin{pmatrix}\mathbf{x}_P\\ \boldsymbol{\varphi}(\mathbf{x}_P)\\ 1\\ \mathbf{u}\end{pmatrix}}_{\boldsymbol{\omega}_P}.
\end{aligned} \tag{4.36}$$

With this error dynamics and the Lyapunov function candidate

$$\mathrm{V} = \frac{1}{2}\mathbf{e}_P^T\mathbf{P}\mathbf{e}_P + \frac{1}{2}\mathrm{Tr}\left[\tilde{\hat{\boldsymbol{\Theta}}}_x^T\boldsymbol{\Gamma}_x^{-1}\tilde{\hat{\boldsymbol{\Theta}}}_x\right] + \frac{1}{2}\mathrm{Tr}\left[\tilde{\hat{\boldsymbol{\Theta}}}_\varphi^T\boldsymbol{\Gamma}_\varphi^{-1}\tilde{\hat{\boldsymbol{\Theta}}}_\varphi\right] + \frac{1}{2}\mathrm{Tr}\left[\gamma_{dd}^{-1}\tilde{\hat{\boldsymbol{\theta}}}_d\tilde{\hat{\boldsymbol{\theta}}}_d^T\right] + \frac{1}{2}\mathrm{Tr}\left[\tilde{\boldsymbol{\Lambda}}\boldsymbol{\Gamma}_\Lambda^{-1}\tilde{\boldsymbol{\Lambda}}^T\right] \tag{4.37}$$

the following update laws can be derived

$$\begin{aligned}
\dot{\hat{\boldsymbol{\Theta}}}_x &= \boldsymbol{\Gamma}_x\mathbf{x}_P\cdot\mathbf{e}_P^T\mathbf{P}\mathbf{B}_P \\
\dot{\hat{\boldsymbol{\Theta}}}_\varphi &= \boldsymbol{\Gamma}_\varphi\boldsymbol{\varphi}(\mathbf{x}_P)\cdot\mathbf{e}_P^T\mathbf{P}\mathbf{B}_P \\
\dot{\hat{\boldsymbol{\theta}}}_d^T &= \gamma_{dd}\cdot\mathbf{e}_P^T\mathbf{P}\mathbf{B}_P \\
\dot{\hat{\boldsymbol{\Lambda}}}^T &= -\boldsymbol{\Gamma}_\Lambda\mathbf{u}\cdot\mathbf{e}_P^T\mathbf{P}\mathbf{B}_P
\end{aligned} \quad\Leftrightarrow\quad \underbrace{\begin{bmatrix}\dot{\hat{\boldsymbol{\Theta}}}_x\\ \dot{\hat{\boldsymbol{\Theta}}}_\varphi\\ \dot{\hat{\boldsymbol{\theta}}}_d^T\\ \dot{\hat{\boldsymbol{\Lambda}}}^T\end{bmatrix}}_{\dot{\hat{\boldsymbol{\Theta}}}_P} = \underbrace{\begin{bmatrix}\boldsymbol{\Gamma}_x & \mathbf{0} & \mathbf{0} & \mathbf{0}\\ \mathbf{0} & \boldsymbol{\Gamma}_\varphi & \mathbf{0} & \mathbf{0}\\ \mathbf{0} & \mathbf{0} & \gamma_{dd} & \mathbf{0}\\ \mathbf{0} & \mathbf{0} & \mathbf{0} & -\boldsymbol{\Gamma}_\Lambda\end{bmatrix}}_{\boldsymbol{\Gamma}_P}\underbrace{\begin{pmatrix}\mathbf{x}_P\\ \boldsymbol{\varphi}(\mathbf{x}_P)\\ 1\\ \mathbf{u}\end{pmatrix}}_{\boldsymbol{\omega}_P}\cdot\mathbf{e}_P^T\mathbf{P}\mathbf{B}_P. \tag{4.38}$$

Again, the update laws render the time derivative of the Lyapunov function in Eq.(4.37) negative semi definite and it follows that the control law in Eq.(4.32) and the update laws in Eq.(4.38) guarantee stability. Barbalat's Lemma in turn guarantees that the error $\mathbf{e}_P$ converges to zero asymptotically.

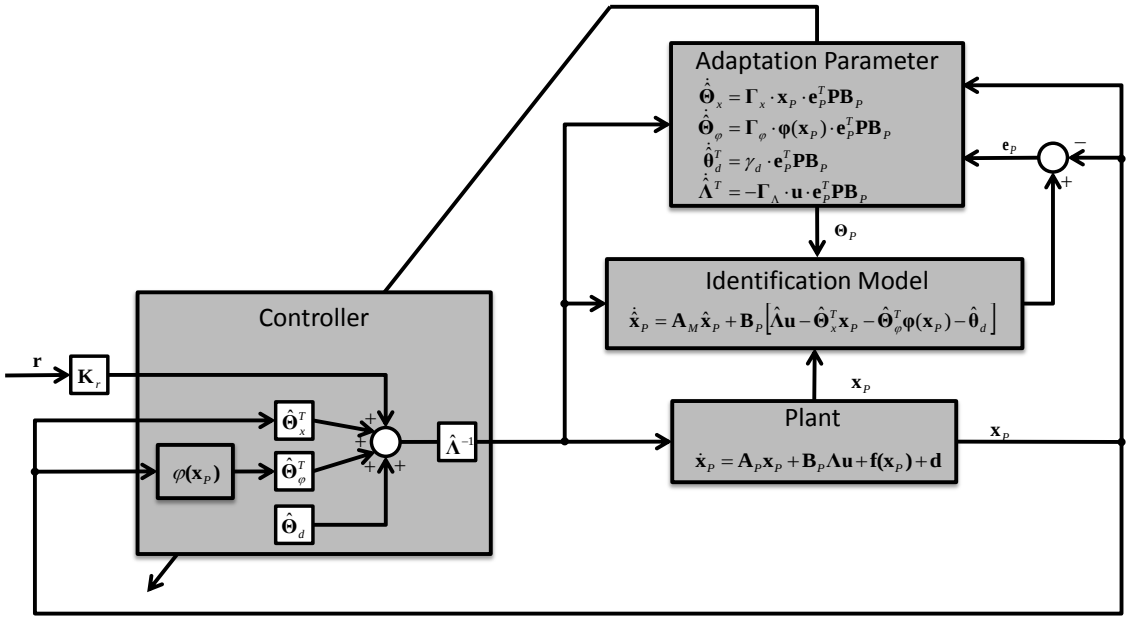

Figure 4.7: Predictor based MRAC with state feedback

4.4.2 Update of Controller Gains

The approach is almost the same as in Section 4.3.2. Hence we can choose a similar Lyapunov function candidate:

$$\begin{aligned}\mathrm{V} = \frac{1}{2}\mathbf{e}_P^T\mathbf{P}\mathbf{e}_P + \frac{1}{2}\mathrm{Tr}\left[\tilde{\boldsymbol{\Theta}}_x^T\boldsymbol{\Gamma}_x^{-1}\tilde{\boldsymbol{\Theta}}_x\boldsymbol{\Lambda}\right] + \frac{1}{2}\mathrm{Tr}\left[\tilde{\boldsymbol{\Theta}}_\varphi^T\boldsymbol{\Gamma}_\varphi^{-1}\tilde{\boldsymbol{\Theta}}_\varphi\boldsymbol{\Lambda}\right] + \frac{1}{2}\mathrm{Tr}\left[\gamma_{dd}^{-1}\tilde{\boldsymbol{\theta}}_d\tilde{\boldsymbol{\theta}}_d^T\boldsymbol{\Lambda}\right] + \frac{1}{2}\mathrm{Tr}\left[\tilde{\boldsymbol{\Theta}}_r\boldsymbol{\Gamma}_r^{-1}\tilde{\boldsymbol{\Theta}}_r^T\boldsymbol{\Lambda}\right] \\ + \frac{1}{2}\mathrm{Tr}\left[\tilde{\hat{\boldsymbol{\Theta}}}_x\boldsymbol{\Gamma}_A^{-1}\tilde{\hat{\boldsymbol{\Theta}}}_P^T\right] + \frac{1}{2}\mathrm{Tr}\left[\tilde{\hat{\boldsymbol{\Theta}}}_f\boldsymbol{\Gamma}_f^{-1}\tilde{\hat{\boldsymbol{\Theta}}}_f^T\right]\frac{1}{2}\mathrm{Tr}\left[\gamma_{di}^{-1}\tilde{\hat{\boldsymbol{\theta}}}_a\tilde{\hat{\boldsymbol{\theta}}}_a^T\right] + \frac{1}{2}\mathrm{Tr}\left[\tilde{\boldsymbol{\Lambda}}\boldsymbol{\Gamma}_\Lambda^{-1}\tilde{\boldsymbol{\Lambda}}^T\right]\end{aligned} \tag{4.39}$$

Again the definition of the additional closed loop estimation errors $\boldsymbol{\varepsilon}_x$, $\boldsymbol{\varepsilon}_\varphi$, $\boldsymbol{\varepsilon}_d$ and $\boldsymbol{\varepsilon}_r$ is necessary. Based on the matching condition and the knowledge that it is desired that

$\widehat{\boldsymbol{\Lambda}}\boldsymbol{\Theta}_x^T$ converges to $\widehat{\boldsymbol{\Theta}}_x^T$, $\widehat{\boldsymbol{\Lambda}}\boldsymbol{\Theta}_\varphi^T$ converges to $\widehat{\boldsymbol{\Theta}}_\varphi^T$, $\widehat{\boldsymbol{\Lambda}}\boldsymbol{\theta}_d$ converges to $\widehat{\boldsymbol{\theta}}_d$, and $\widehat{\boldsymbol{\Lambda}}\boldsymbol{\Theta}_r$ converges to $\mathbf{K_r}$ (see Eq. (4.22)) the additional closed loop estimation errors are:

$$\begin{aligned}\boldsymbol{\varepsilon}_x &= \left[\widehat{\boldsymbol{\Lambda}}\boldsymbol{\Theta}_x^T - \widehat{\boldsymbol{\Theta}}_x^T\right]\\ \boldsymbol{\varepsilon}_\varphi &= \left[\widehat{\boldsymbol{\Lambda}}\boldsymbol{\Theta}_\varphi^T - \widehat{\boldsymbol{\Theta}}_\varphi^T\right]\\ \boldsymbol{\varepsilon}_d &= \left[\widehat{\boldsymbol{\Lambda}}\boldsymbol{\theta}_d - \widehat{\boldsymbol{\theta}}_d\right]\\ \boldsymbol{\varepsilon}_r &= \left[\widehat{\boldsymbol{\Lambda}}\boldsymbol{\Theta}_r - \mathbf{K_r}\right].\end{aligned} \tag{4.40}$$

With the update laws for the plant parameters given by

$$\begin{aligned}\dot{\widehat{\boldsymbol{\Theta}}}_x &= \widehat{\boldsymbol{\Gamma}}_x(\mathbf{x}_P\mathbf{e}_P^T\mathbf{P}\mathbf{B}_P + \gamma_\varepsilon\boldsymbol{\varepsilon}_x^T)\\ \dot{\widehat{\boldsymbol{\Theta}}}_\varphi &= \widehat{\boldsymbol{\Gamma}}_\varphi\left(\boldsymbol{\varphi}(\mathbf{x}_P)\mathbf{e}_P^T\mathbf{P}\mathbf{B}_P + \gamma_\varepsilon\boldsymbol{\varepsilon}_\varphi^T\right)\\ \dot{\widehat{\boldsymbol{\Theta}}}_d^T &= \hat{\gamma}_{dd}\left(\mathbf{e}_l^T\mathbf{P}\mathbf{B}_P + \gamma_\varepsilon\boldsymbol{\varepsilon}_d^T\right)\\ \dot{\widehat{\boldsymbol{\Lambda}}}^T &= -\boldsymbol{\Gamma}_\Lambda\left(\mathbf{u}\mathbf{e}_P^T\mathbf{P}\mathbf{B}_P + \gamma_\varepsilon\left[\boldsymbol{\Theta}_x^T\boldsymbol{\varepsilon}_x^T + \boldsymbol{\Theta}_\varphi^T\boldsymbol{\varepsilon}_\varphi^T + \boldsymbol{\theta}_d\boldsymbol{\varepsilon}_d^T + \boldsymbol{\Theta}_r\boldsymbol{\varepsilon}_r^T\right]\right),\end{aligned} \tag{4.41}$$

where $\widehat{\boldsymbol{\Gamma}}_x \in \mathbb{R}^{n\times n}$, $\widehat{\boldsymbol{\Gamma}}_\varphi \in \mathbb{R}^{k\times k}$, $\hat{\gamma}_{dd} \in \mathbb{R}$ and $\boldsymbol{\Gamma}_\Lambda \in \mathbb{R}^{m\times m}$ are symmetric positive definite design parameters that determine the adaption rate, and $\gamma_\varepsilon \in \mathbb{R}$ provides a weighting for the additional errors $\boldsymbol{\varepsilon}$ in the adaptation law.

With the update laws for the controller parameters given by

$$\begin{aligned}\dot{\boldsymbol{\Theta}}_x &= -\boldsymbol{\Gamma}_x\gamma_\varepsilon\boldsymbol{\varepsilon}_x^T\\ \dot{\boldsymbol{\Theta}}_\varphi &= -\boldsymbol{\Gamma}_\varphi\gamma_\varepsilon\boldsymbol{\varepsilon}_\varphi^T\\ \dot{\boldsymbol{\theta}}_d^T &= -\gamma_d\gamma_\varepsilon\boldsymbol{\varepsilon}_d^T\\ \dot{\boldsymbol{\Theta}}_r^T &= -\boldsymbol{\Gamma}_r\gamma_\varepsilon\boldsymbol{\varepsilon}_r^T,\end{aligned} \tag{4.42}$$

it can be verified (is the same way as for the indirect approach) that these update laws render the time derivative of the Lyapunov function negative semi definite [1] [91] under the idealized assumptions, meaning the matching condition again needs to hold. Hence, the closed loop system is globally stable. By application of Barbalat's Lemma it can be shown that $\mathbf{e}_P$, $\boldsymbol{\varepsilon}_x$, $\boldsymbol{\varepsilon}_\varphi$, $\boldsymbol{\varepsilon}_d$ and $\boldsymbol{\varepsilon}_r$ converge to zero asymptotically. From this, and by inserting the control law Eq.(4.3) in the predictor dynamics of Eq.(4.30) it directly follows that the estimator dynamics converge to the dynamics of the reference model [1]. Furthermore, as $\mathbf{e}_P$ converges to zero it holds that

$$\lim_{t\to\infty}\left(\mathbf{x}_P(t) - \mathbf{x}_M(t)\right) = \mathbf{0}. \tag{4.43}$$

Here the low pass character of the controller parameter update can easily be seen by inserting the closed loop estimation errors of Eq.(4.40) in the update law of Eq.(4.42), what leads to

$$\begin{aligned}\dot{\boldsymbol{\Theta}}_x &= -\boldsymbol{\Gamma}_x\gamma_\varepsilon\left[\widehat{\boldsymbol{\Lambda}}\boldsymbol{\Theta}_x^T - \widehat{\boldsymbol{\Theta}}_x^T\right]^T\\ \dot{\boldsymbol{\Theta}}_\varphi &= -\boldsymbol{\Gamma}_\varphi\gamma_\varepsilon\left[\widehat{\boldsymbol{\Lambda}}\boldsymbol{\Theta}_\varphi^T - \widehat{\boldsymbol{\Theta}}_\varphi^T\right]^T\\ \dot{\boldsymbol{\theta}}_d^T &= -\gamma_d\gamma_\varepsilon\left[\widehat{\boldsymbol{\Lambda}}\boldsymbol{\theta}_d - \widehat{\boldsymbol{\theta}}_d\right]^T\\ \dot{\boldsymbol{\Theta}}_r^T &= -\boldsymbol{\Gamma}_r\gamma_\varepsilon\left[\widehat{\boldsymbol{\Lambda}}\boldsymbol{\Theta}_r - \mathbf{K_r}\right]^T\end{aligned} \tag{4.44}$$

4.5 Short Period Example

The direct MRAC approach is applied in the following to the problem introduced in Section 2.1. Based on the example some of the problems of the adaptive control theory presented above are illustrated, which are not only present in the direct case but also for the indirect approach.

The baseline control law of Eq.(2.12) is augmented with an adaptive controller as shown in Figure 4.8. Thus the elevator input is given by

$$\eta_{CMD} = \eta_{BL} + \eta_{AD}. \tag{4.45}$$

The adaptive controller is chosen to employ the same structure as the baseline control law. Hence only a linear regressor vector is used, and the adaptive feedback is provided by

$$\eta_{AD} = \boldsymbol{\theta}_y^T \mathbf{y}_P^+ = [\theta_{n_Z} \quad \theta_{\mathrm{q}} \quad \theta_{\mathrm{e_I}}][n_Z \quad q \quad e_I]^T. \tag{4.46}$$

From the problem formulation it is clear that using a linear regressor violates the basic theory, because there can be no constant parameters which satisfy the matching condition for the nonlinear pitch-up uncertainty. When the angle of attack is smaller than 1.5 degree the pitch break is not visible and thus the adaptive parameters need to be zero. For angles of attack larger than 1.5 degree the adaptive gains would need to compensate for the change of sign in the pitch stiffness which is caused by the pitch-up nonlinearity. This problem could be solved by a linear parameterization of the nonlinearity and this would be theoretically possible. However, the onset of the pitch-up is in reality not exactly known, and therefore using this knowledge in the controller design will provide purely theoretical results. Another approch would be a nonlinear regressor vector that provides a set of basis functions which allows the approximation of a broad class of nonlinearities. This approach is dicussed in Section 4.6. Furthermore, instead of the states $\mathbf{x}_P$ the outputs $\mathbf{y}_P$ are used, and thus the objective is that $\mathbf{y}_P^+$ tracks the reference trajectory $\mathbf{y}_M^+$, which is obtained by implementing the desired reference model. This is no problem, if the output matrix $\mathbf{C}_P^+$ has full rank and the direct feedthrough $\mathbf{d}_P$ from the input to the output is zero. In this case a state transformation from $\mathbf{x}_P^+$ to $\mathbf{y}_P^+$ can be achived by $\mathbf{C}_P^+$, such that the transformed system is given by

$$\dot{\mathbf{y}}_P^+ = \mathbf{C}_P^+ \mathbf{A}_P^+ \mathbf{C}_P^{+^{-1}} \mathbf{y}_P^+ + \mathbf{C}_P^+ \mathbf{b}_P^+ \eta + \mathbf{C}_P^+ \mathbf{b}_r^+ r \tag{4.47}$$

with

$$\begin{aligned} \mathbf{A}_{P,n_Z}^+ &= \mathbf{C}_P^+ \mathbf{A}_P^+ \mathbf{C}_P^{+^{-1}} \\ \mathbf{b}_{P,n_Z}^+ &= \mathbf{C}_P^+ \mathbf{b}_P^+. \end{aligned} \tag{4.48}$$

Although the feedthrough is small, the second condition ($\mathbf{d}_P = 0$) is not satisfied for the current example as can be seen in Eq.(2.2). Clearly, effects like these limit the speed of adaptation, however, as the effect is very small it is treated as a disturbance here.

The error for adaptation is given by

$$\mathbf{e}_C = \mathbf{y}_M^+ - \mathbf{y}_P^+. \tag{4.49}$$

For the reference model, the closed loop plant with baseline controller, including actuator dynamics, delay, and sensor dynamics, but without the pitch-up nonlinearity, is used. This means the reference model is given by the base line control law of Eq.(2.12), the augmented plant dynamics of Eq.(2.13), the actuator dynamics in Eq.(2.6), the delay in Eq.(2.8), and the filter dynamics in Eq.(2.7):

$$\begin{aligned} \dot{\mathbf{x}}_M^+ &= \mathbf{A}_P^+ \mathbf{x}_M^+ + \mathbf{b}_P^+ \eta_M + \mathbf{b}_r^+ r \\ \mathbf{y}_M^+ &= \mathbf{C}_P^+ \mathbf{x}_M^+ + \mathbf{d}_P^+ \eta_M \\ \eta_M &= G_{act}(s) G_{del}(s) G_{fil}(s) \left(\mathbf{k}_y^T \mathbf{y}_M^+ + k_r r \right) \end{aligned} \tag{4.50}$$

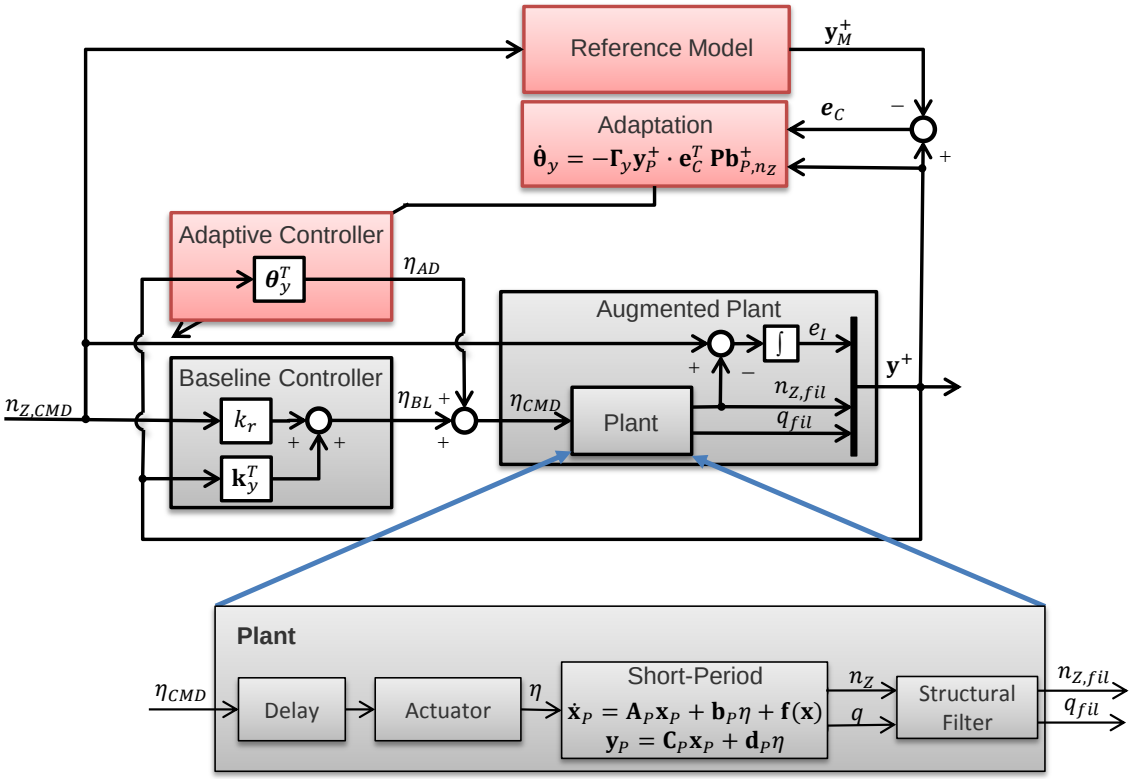

Figure 4.8: Augmentation with direct MRAC controller

Further prerequisities from the theory presented above are already violated by the simple example. On the one hand the matching condition can not be satisfied exacly with the linear parameterization of the adaptive control law due to the nonlinear uncertainty in the moment dynamics. In addition an elevator deflection does not only produce a moment but also a small change in the lifting force. Evenso the matching condintion does not hold exactly for the considered problem it still holds in good

approximtion as the coefficient Z_η is small compared to M_η. On the other hand the assumtion of full state feedback is not satisfied due to the additional dynamics of actuators, structural filters and delay. This also causes noncompliance with the matching condition as can be seen in Eq.(2.12). However, the main problem results from the time delay that is introduced due to the additional dynamics, and this will also become obvious from the simulation results.

According to Eq.(4.10) the following update law for the controller parameters is used

$$\dot{\boldsymbol{\theta}}_y = -\boldsymbol{\Gamma}_y \mathbf{y}_P^+ \cdot \mathbf{e}_C^T \mathbf{P} \mathbf{b}_{P,n_Z}^+. \tag{4.51}$$

The adaptive controller is composed of Eq.(4.46)-(4.51).

The parameters of the adaptive controller are tuned with the genetic algorithm provided by Matlab©, based on the command signal shown in Figure 4.9. For the first step input of 2g the pitch-up nonlinearity will be visible and here the adaptive control law should improve the performance. In difference, for the second reference command of 0.5g the system will remain in an angle of attack region, where it behaves linear, what means that the adaptive controller should have no impact on the performance provided by the baseline controller.

For tuning the ideal response signals $n_{Z,ID}$, and the ideal control signal η_{ID} are used, which are obtained from the ideal cancelation of the nonlinearity by feedback (see Section 2.1.3).

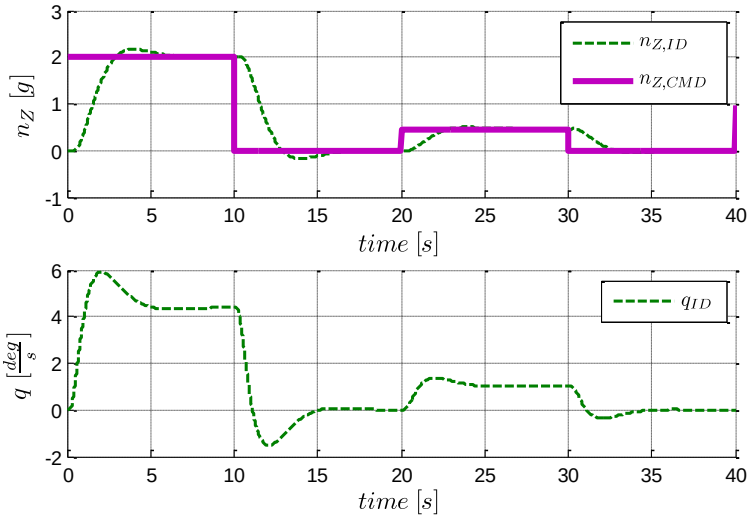

Figure 4.9: Command signal and ideal response for the tuning process

The cost function for the tuning is based on a combination of the performance metrics suggested in [64]. As these performance metrics use signal norms they have to be evaluated by simulation. A short introduction to norms and the notation used in this thesis is given in Appendix C.1.

In particular the cost function is given by

$$J = M_1 + M_2 + 2M_3, \tag{4.52}$$

where M_1 is the $\mathcal{L}_\infty$ norm of the tracking error, and hence, a measure for the overshoot of the adaptive response relative to the ideal response

$$M_1 = \frac{\|n_Z(t) - n_{Z,ID}(t)\|_{\mathcal{L}_\infty}}{\|n_{Z,ID}(t)\|_{\mathcal{L}_\infty}} = \frac{\max_{t\in[0,t_f]}\|n_Z(t) - n_{Z,ID}(t)\|_\infty}{\max_{t\in[0,t_f]}\|n_{Z,ID}(t)\|_\infty}. \tag{4.53}$$

M_2 is the $\mathcal{L}_2$ norm of the tracking error, and hence, a measure for the oscillations in the adaptive response relative to the ideal response

$$M_2 = \frac{\|n_Z(t) - n_{Z,ID}(t)\|_{\mathcal{L}_2}}{\|n_{Z,ID}(t)\|_{\mathcal{L}_2}} = \frac{\sqrt{\int_0^{t_f}\|n_Z(t) - n_{Z,ID}(t)\|_2^2 dt}}{\sqrt{\int_0^{t_f}\|n_{Z,ID}(t)\|_2^2 dt}}, \tag{4.54}$$

and M_3 is the $\mathcal{L}_2$ norm of the difference between the ideal control signal and the adaptive control signal, and thus a measurement for the oscillations in the adaptive control signal relative to the ideal control signal

$$M_3 = \frac{\|\eta(t) - \eta_{ID}(t)\|_{\mathcal{L}_2}}{\|\eta_{ID}(t)\|_{\mathcal{L}_2}} = \frac{\sqrt{\int_0^{t_f}\|\eta(t) - \eta_{ID}(t)\|_2^2 dt}}{\sqrt{\int_0^{t_f}\|\eta_{ID}(t)\|_2^2 dt}}. \tag{4.55}$$

The tuning minimizes the defined cost function to $J = 0.835$ and yields the following learning rate for the adaptive controller:

$$\Gamma_y = \begin{bmatrix} 0.061 & 0 & 0 \\ 0 & 0.139 & 0 \\ 0 & 0 & 0.037 \end{bmatrix}$$

It is already evident that the tuning results in small gains for the adaptive controller, and the reasons therefore are the already mentioned violations of the theory, where especially the additional dynamics and time delays constitute the main problem.

In Figure 4.10 the load factor and pitch rate response with the adaptive controller (subscript AD) and the response of the reference model (subscript M) is shown in comparison to the response with only the base-line controller (subscript BL). The related tracking error is shown in Figure 4.11, the elevator deflection, rate, and acceleration is given in Figure 4.12, and the adaptive parameters are shown in Figure 4.13. It is evident that for the first step the adaptive controller largely reduces the overshoot resulting from the destabilizing pitch-up by increasing mainly the pitch damping Θ_q (see Figure 4.13).

In Figure 4.14 – Figure 4.19 the robust performance of the adaptive controller is evaluated for a 1g and a 2g step command based on the requirements defined in Section 3.1. It is obvious that even though the adaptive controller can improve the performance in presence of the pitch-up it largely reduces the overall robustness in terms of performance. Furthermore, it is obvious that due to the nonlinearity of the

adaptive controller the results for the 1g and the 2g command are different, and hence the linear scaling is lost. This is also reflected by the time delay margin, where the values, obtained by simulation, are 0.55s for the 1g command and 0.27s for 2g command.

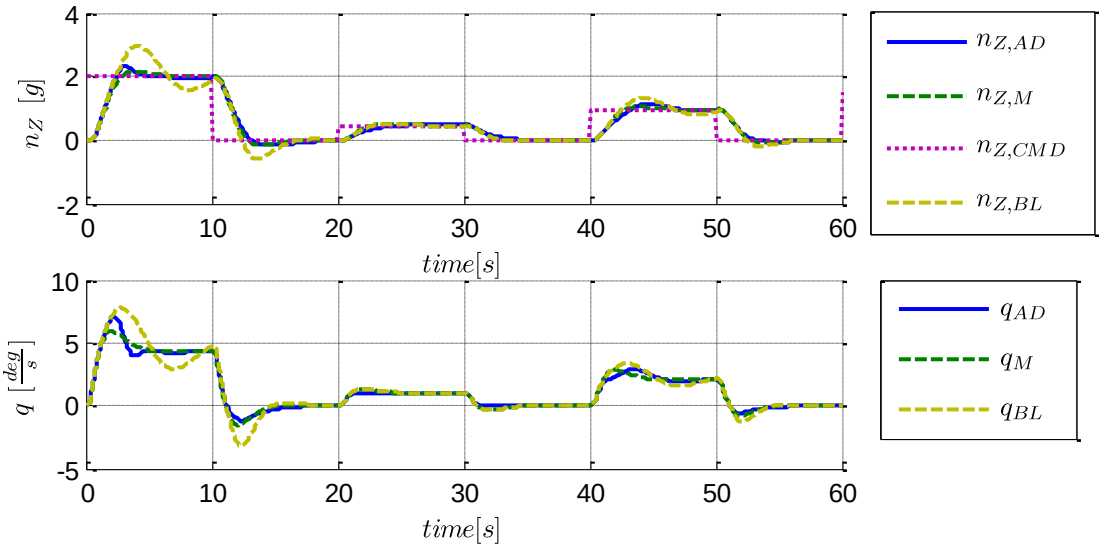

Figure 4.10: Load factor and pitch rate response

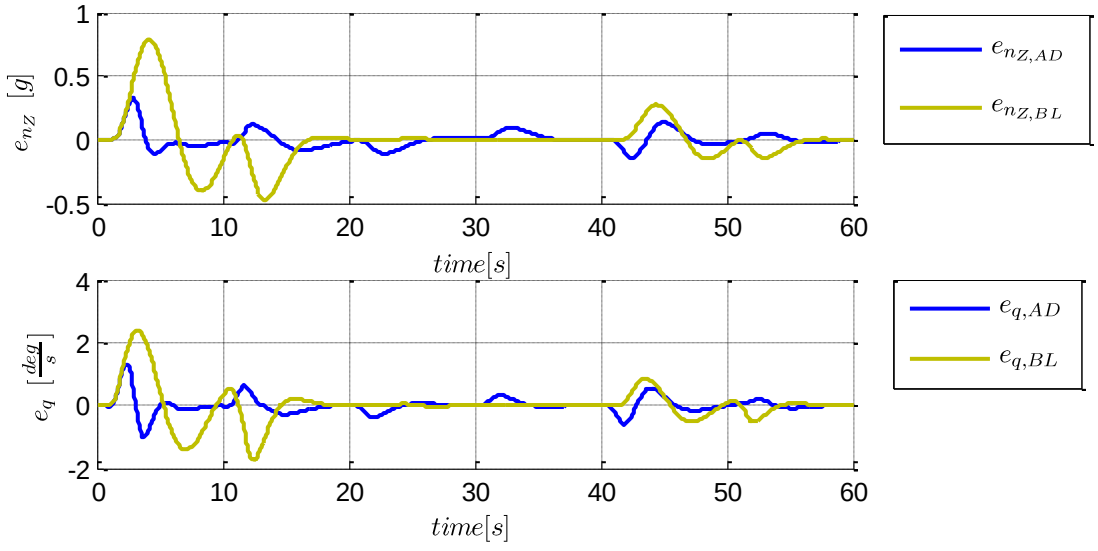

Figure 4.11: Error in load factor and pitch rate response

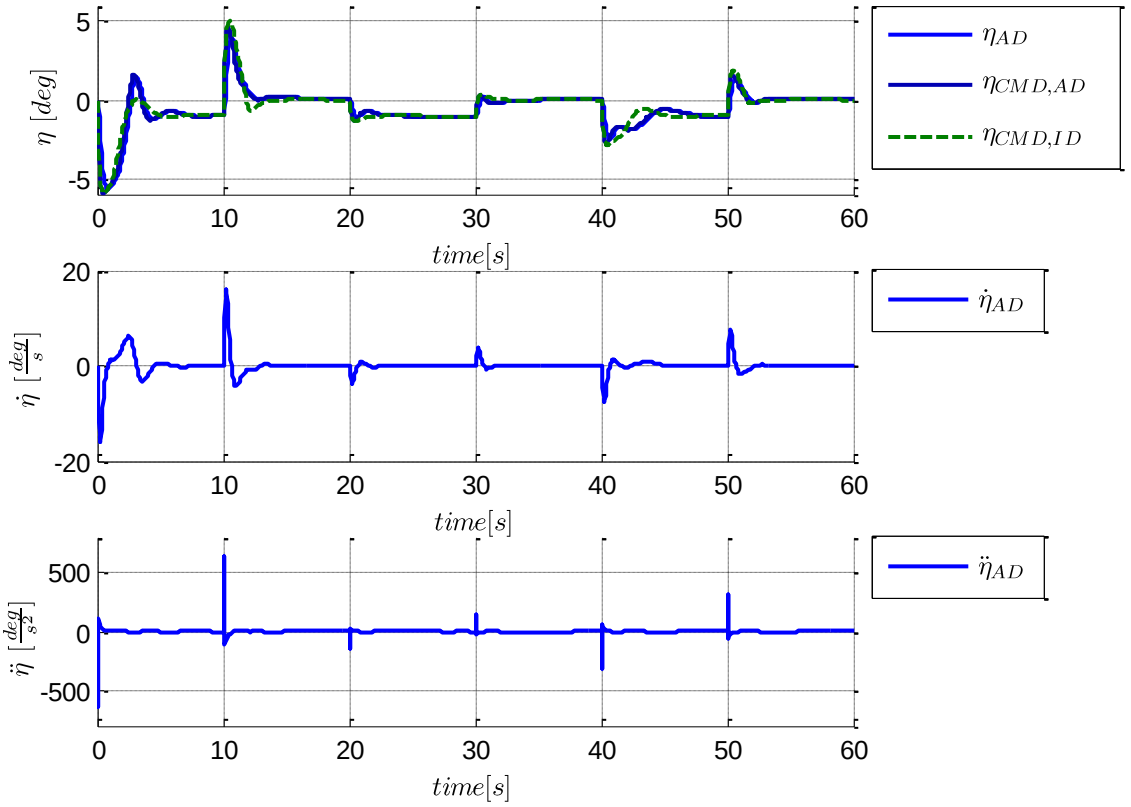

Figure 4.12: Elevator deflection, rate, and acceleration

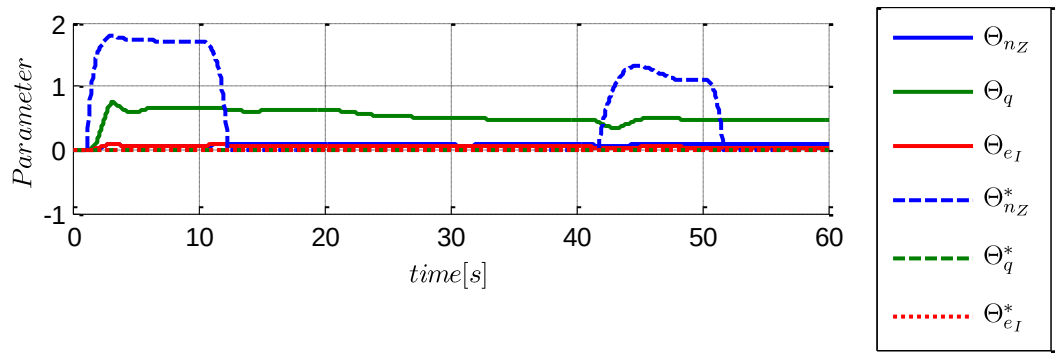

Figure 4.13: Adaptive controller parameters

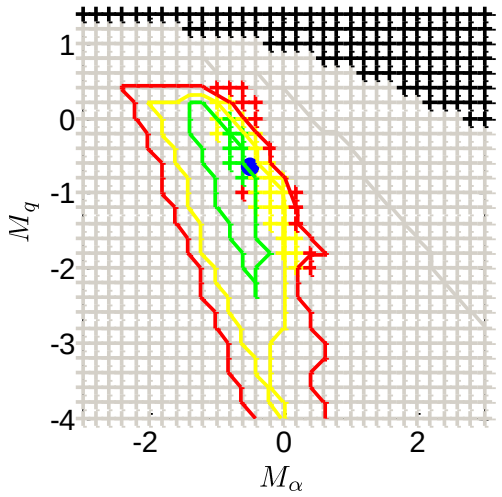

Figure 4.14: Robust perfomance w.r.t. M_α and M_q; $n_{z,CMD}$=1

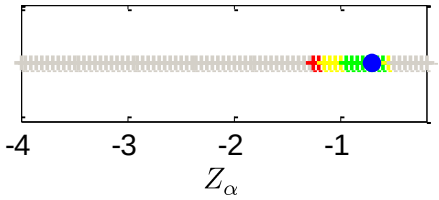

Figure 4.15: Robust perfomance w.r.t. Z_α; $n_{z,CMD}$=1

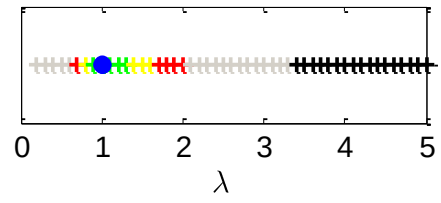

Figure 4.16: Robust perfomance w.r.t. λ $n_{z,CMD}$=1

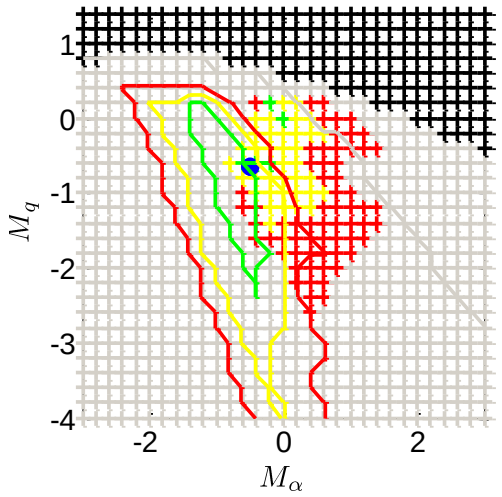

Figure 4.17: Robust performance w.r.t. M_α and M_q; $n_{z,CMD}$=2

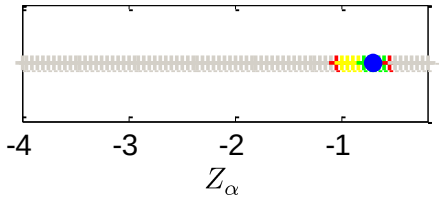

Figure 4.18: Robust perfomance w.r.t. Z_α; $n_{z,CMD}$=2

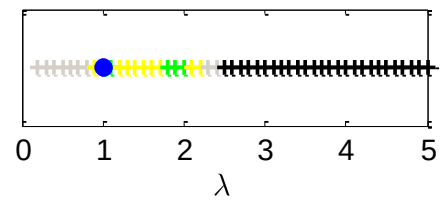

Figure 4.19: Robust perfomance w.r.t. λ $n_{z,CMD}$=2

The loss of robustness can be easily explained. To achieve a fast compensation of the nonlinearity a large adaptive gain is required, however a large integral gain hurts the robustness in the presence of the actuator, delay and filter dynamics. In particular for the error dynamics the additional dynamics spoils the error dynamics. To see this let us assume that there is no nonlinearity in the plant, so that by exploiting the linear properties, the structural filter can equivalently be applied in the input channel, instead of the output channel, as shown in Figure 4.20.

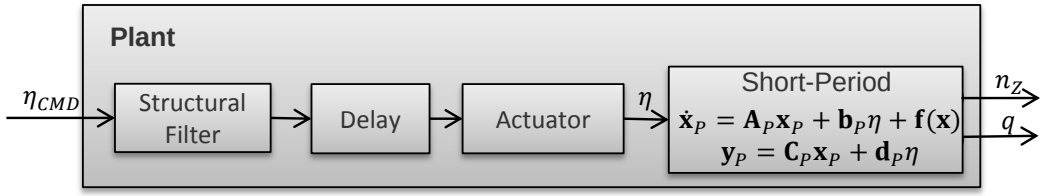

Figure 4.20: Plant withe structural filter in the input channel

The only difference is, that now also the feed-forward signal is passed through the filter dynamics. However, this also makes sense because then also the reference command cannot excite the structural modes. It is in general very common in flight control to apply the structural filters in the input channel. Note, the equality only holds with the linear assumptions. Thus, according to Figure 4.20. and Eq.(2.13), and by defining $G(s) = G_{fil}(s)G_{del}(s)G_{act}(s)$ the augmented plant dynamics can equivalently be denoted by

$$\dot{\mathbf{x}}_P^+ = \mathbf{A}_P^+\mathbf{x}_P^+ + \mathbf{b}_P^+\{G(s)\cdot\eta_{CMD}(s)\}_\mathrm{t} + \mathbf{b}_r^+ r. \tag{4.56}$$

Here the notation introduced in Section 2.1.1 is used.

Using the control law from Eq.(2.12) and Eq.(4.45), and assuming that there is an affine uncertainty in $\mathbf{A}_P$, such that the matching condition holds, gives

$$\begin{aligned}\dot{\mathbf{x}}_P^+ &= \mathbf{A}_P^+\mathbf{x}_P^+ + \mathbf{b}_P^+\left\{G(s)\cdot\left(\mathbf{k}_y^T\mathbf{y}_P^+(s) + k_r r(s)\right)\right\}_\mathrm{t} + \mathbf{b}_r^+ r + \mathbf{b}_P^+\left\{G(s)\cdot\eta_{AD}(s) - \boldsymbol{\theta}_x^{*T}\mathbf{x}_P(s)\right\}_\mathrm{t}\\ \mathbf{y}_P^+ &= \mathbf{C}_P^+\mathbf{x}_P^+ + \mathbf{d}_P^+\eta.\end{aligned} \tag{4.57}$$

The reference model, as specified before, is given by the closed loop plant without nonlinearity

$$\begin{aligned}\dot{\mathbf{x}}_M^+ &= \mathbf{A}_P^+\mathbf{x}_M^+ + \mathbf{b}_P^+\left\{G(s)\cdot\left(\mathbf{k}_y^T\mathbf{y}_M^+(s) + k_r r(s)\right)\right\}_\mathrm{t} + \mathbf{b}_r^+ r\\ \mathbf{y}_M^+ &= \mathbf{C}_P^+\mathbf{x}_M^+ + \mathbf{d}_P^+\eta.\end{aligned} \tag{4.58}$$

Because the error used for adaptation is defined based on the outputs, the system dynamic needs to be transformed using the output matrix, and it must be assumed that $\mathbf{d}_P^+ = \mathbf{0}$. Applied to Eq.(4.57) yields

$$\begin{aligned}\dot{\mathbf{y}}_P^+ = \mathbf{C}_P^+\mathbf{A}_P^+\mathbf{C}_P^{+-1}\mathbf{y}_P^+ + \mathbf{C}_P^+\mathbf{b}_P^+\left\{G(s)\cdot\left(\mathbf{k}_y^T\mathbf{y}_P^+(s)+k_r r(s)\right)\right\}_t + \mathbf{C}_P^+\mathbf{b}_r^+ r \\ + \mathbf{C}_P^+\mathbf{b}_P^+\left\{G(s)\cdot\eta_{AD}(s) - \boldsymbol{\theta}_x^{*T}\mathbf{C}_P^{+-1}\mathbf{y}_P^{*+}(s)\right\}_t\end{aligned} \tag{4.59}$$

And transformation of Eq.(4.58) gives

$$\dot{\mathbf{y}}_M^+ = \mathbf{C}_P^+\mathbf{A}_P^+\mathbf{C}_P^{+-1}\mathbf{y}_M^+ + \mathbf{C}_P^+\mathbf{b}_P^+\left\{\boldsymbol{G}(s)\cdot\left(\mathbf{k}_y^T\mathbf{y}_M^+(\boldsymbol{s})+k_r r(s)\right)\right\}_t + \mathbf{C}_P^+\mathbf{b}_r^+ r \tag{4.60}$$

Thus with the adaptive control law from Eq.(4.46) and the error defined in Eq.(4.49) we obtain for the error dynamics

$$\dot{\mathbf{e}}_C = \underbrace{\mathbf{A}_{P,n_Z}^+\mathbf{e}_C + \mathbf{b}_{P,n_Z}^+\left\{G(s)\cdot\mathbf{k}_y^T\mathbf{y}_P^+(s)\right\}_t}_{Desired\ dynamics} + \mathbf{b}_{P,n_Z}^+\left\{G(s)\cdot\left\{\boldsymbol{\theta}_y^T(t)\mathbf{y}_P^+(t)\right\}_s - \boldsymbol{\theta}_y^{*T}\mathbf{y}_P^+(s)\right\}_t. \tag{4.61}$$

Here it gets obvious that the additional dynamics $G(s)$ spoils the error dynamics, as this dynamics makes it impossible to cancel the uncertainty $\boldsymbol{\theta}_y^{*T}\mathbf{y}_P$ in transients. This means during transients, where the dynamics of $G(s)$ has not decayed yet, the adaptive law will try to adjust to this dynamics, and this is the reason that large adaptive gains cause instability. Adding and subtracting $\mathbf{b}_{P,n_Z}^+\eta_{AD}$ the error dynamics can also be denoted by

$$\begin{aligned}\dot{\mathbf{e}}_C = \mathbf{A}_{P,n_Z}^+\mathbf{e}_C + \mathbf{b}_{P,n_Z}^+\left\{G(s)\cdot\mathbf{k}_y^T\mathbf{y}_P^+(s)\right\}_t + \mathbf{b}_{P,n_Z}^+\left(\boldsymbol{\theta}_y^T - \boldsymbol{\theta}_y^{*T}\right)\mathbf{y}_P^+ \\ + \mathbf{b}_{P,n_Z}^+\underbrace{\left\{(G(s)-1)\cdot\eta_{AD}(s)\right\}_t}_{\boldsymbol{Undesired\ control\ deficiency}},\end{aligned} \tag{4.62}$$

where the control deficiency disturbs the error dynamics during transients. In Section 5.1.1 a modification of the reference model is discussed that allows to resolve the problem by accounting for the additional dynamics in the input channel.

4.6 Nonlinear Regressor

4.6.1 Structurally Known Nonlinearity

As we have seen in Chapter 4 the basic theory of MRAC also covers nonlinear uncertainties. I.e. nonlinear uncertainties can be adapted and canceled out if they can be parameterized in a linear way (linear combination between unknown parameters and known arbitrary nonlinear functions computed from measurable system variables), are within the span of the input matrix (matched), and are structurally known. This allows the introduction of physical insight on the structure of the plant without leaving the most basic theory (e.g. the aerodynamics of the system, inertia and coupling terms etc.).

4.6.2 Linear in the Parameters Neural Network

The assumption on the structural knowledge of the nonlinearity can be relaxed by providing a set of basis functions which can approximate a large class of nonlinear

functions. This set of basis functions is then contained in the regressor vector $\boldsymbol{\varphi}(\mathbf{x}_P)$. The concept of using a set of basis functions to approximate a nonlinear mapping is often referred to as Neural Network (NN) [132], where for adaptive flight control mainly Single Hidden Layer (SHL) Feedforward Neural Networks (FNN) are used. However, the term neural network might be misleading as in the considered case the approach has nothing to do with artificial intelligence, but only has the purpose to approximate a nonlinear function.

For a linear-in-the-parameters feedforward neural network the nonlinear term retains the same form as in the case considered above:

$$\bar{\mathbf{f}}(\mathbf{x}_P) = \boldsymbol{\Theta}_{\varphi}^{T}\boldsymbol{\varphi}(\mathbf{x}_P) \tag{4.63}$$

In the neural network terminology it is said, that in this case only the output layer weights are adapted. This concept is often used in conjunction with radial basis functions, but in general a large number of different basis functions is available for the nonlinear regressor (e.g. constant, linear, radial, B-splines, sigma-pi etc. [133] [104] [134] [135]). Here the distribution of the basis function over state space $\mathbb{R}^n$ has to be predetermined.

In general NNs can provide a universal approximation property, but to approximate any nonlinearity arbitrarily close, an infinite number of basis functions is necessary, leading to an infinite number of adaptive parameters. As for any practical case the number of basis functions is limited, it arises the question: how many basis functions are necessary, and how do they have to be distributed to allow a sufficiently close approximation of the system nonlinearities? Furthermore, from the limited number of basis functions it follows that in reality only a close approximation can be achieved and thus, a residual nonlinearity will always remain. It should be mentioned that this already causes problems in the stability proof and requires for robustness modifications.

On the one hand, NNs can approximate a large class of nonlinear functions and, hence, provide larger flexibility and require less knowledge about the plant, compared to case when structural knowledge on the involved nonlinearities is assumed. On the other hand, the approach also leads to reduced traceability due to the increased number of adaptive parameters.

4.6.3 Nonlinear in the Parameters Neural Network

The concept on NNs can also be extended to additional adaptation of the input layer weights of the neural network. This type is also referred to as single hidden layer feed-forward neural networks, where the approximation of the nonlinearity is nonlinear in the unknown parameters. The approach can be denoted by

$$\bar{\mathbf{f}}(\mathbf{x}_P) = \boldsymbol{\Theta}_{\varphi}^T \boldsymbol{\varphi}\left(\underbrace{\mathbf{V}^T \underbrace{\begin{bmatrix} 1 \\ \mathbf{x}_P \end{bmatrix}}_{\bar{\mathbf{x}}}}_{\mathbf{z}}\right), \tag{4.64}$$

where $\mathbf{V}^T$ is the matrix of input layer weights, for which an additional update law can be derived by backpropagation [126] [136] to obtain

$$\begin{aligned} \dot{\boldsymbol{\Theta}}_{\varphi} &= -\boldsymbol{\Gamma}_{\varphi}(\boldsymbol{\varphi}(\mathbf{z}) - \boldsymbol{\varphi}'(\mathbf{z})\mathbf{V}\bar{\mathbf{x}})\mathbf{e}^T\mathbf{P}\mathbf{B}_P \\ \dot{\mathbf{V}} &= -\boldsymbol{\Gamma}_V \bar{\mathbf{x}}\mathbf{e}^T\mathbf{P}\mathbf{B}_P\boldsymbol{\Theta}_{\varphi}^T\boldsymbol{\varphi}'(\mathbf{z}). \end{aligned} \tag{4.65}$$

For this approach the distribution of the basis functions has not to be predetermined, but is also adjusted dynamically through the update of the input layer weights V. Here most commonly sigmoid- and tanh- basis functions (activation functions) are used.

On the one hand this approach provides even more flexibility, but on the other hand this again largely reduces the physical traceability. By just using a large number of basis functions, less knowledge about the system is used and one tries to solve the problem by brute force. As mentioned, a large number of basis functions decreases the traceability of the approach, and due to the increased complexity it gets difficult to validate the correctness of adaptation (especially online). In general it seems to be more promising to employ structural knowledge about the system and try to use physical insight to parameterize the nonlinearities of the system. Usually this can lead to large reduction in the number of parameters.

4.7 Short Period Example

In the following example nonlinear regressors are used for the problem stated in Section 2.1. Clearly this approach does not solve the problem of additional dynamics in the input channel, which was encountered in Section 4.4. In the following the application of nonlinear regressors is shown to highlight the general idea and show how the approach can be used for a real problem. Thus, no improvement can be expected w.r.t. robust performance and so the robustness evaluation is omitted here.

Instead of using $\eta_{AD} = \boldsymbol{\theta}_y^T \mathbf{y}_P^+$ as in Section 4.4, the adaptive control signal is given by

$$\eta_{AD} = \boldsymbol{\theta}_{\varphi}^T \boldsymbol{\varphi}(\mathbf{y}_P), \tag{4.66}$$

where $\boldsymbol{\varphi}(\mathbf{y}_P)$ is the nonlinear regressor. For the considered problem, it would be desirable to cancel the nonlinearity $f(\alpha)$ with the nonlinear feedback $\boldsymbol{\theta}_{\varphi}^T \boldsymbol{\varphi}(\mathbf{y}_P)$ by adjusting $\boldsymbol{\theta}_{\varphi}^T$. The problem is that α is not an available feedback signal. However, as already mentioned, for the considered case n_Z is almost proportional to α, and hence, it can be assumed that the nonlinearity $f(\alpha)$ can be closely approximated by $f^+(n_Z)$, and therefore a regressor $\boldsymbol{\varphi}(n_Z)$ is used in the following. In contrast to the previous example, if a parameterization $\boldsymbol{\theta}_{\varphi}^T \boldsymbol{\varphi}(n_Z)$ is used that allows to approximate the

nonlinearity sufficiently close, then there exist constant (static), ideal parameters that cancel the pitch-up nonlinearity by feedback and provide the desired performance.

4.7.1 Structurally Known Nonlinearity

Even though, in the problem formulation it is not assumed that the structure of the nonlinearity is known, the simplest approach that can be made would be obtained if this knowledge is available. This means the parameterization of the nonlinearity could be obtained from Eq.(2.5) and given by

$$\theta_\varphi \varphi(\mathbf{y}_P) = \theta_\varphi \varphi(n_Z) = \begin{cases} 0 & n_Z < 0.477g \\ -\theta_\varphi \cdot 2\left(\frac{n_Z}{0.318} - 1{,}5deg\right) & n_Z \geq 0.477g \end{cases}. \tag{4.67}$$

Hence, only the slope has to be adjusted by θ_φ. Here the unrealistic assumption is used, that the onset of the pitch-up, in terms of the angle α or n_Z, respectively, is exactly known.

To adjust Θ_φ the update law from Eq.(4.10) is used

$$\dot{\theta}_\varphi^T = \gamma_\varphi \varphi(n_Z) \cdot \mathbf{e}_C^T \mathbf{P} \mathbf{b}_{P,n_Z}^+. \tag{4.68}$$

The tuning based on Section 4.4 minimizes the cost function to $J = 1.328$ and yields the following learning rate for the adaptive controller: $\gamma_\varphi = 0.54$.

In Figure 4.21 - Figure 4.25 the simulation results for this case are shown. In comparison to the results obtained in Section 4.4 the response to the first step command now shows a larger overshoot. This is due to the fact that previously the pitch-rate was an available feedback signal for the adaptive controller, where now only the load factor is available. Even though, the nonlinear regressor used now is tailored to the problem and a static approximation of the nonlinearity can be achieved, the results appear to be worse at first glance. However, it has to be noted that the response will improve over time, because if the input is exciting the system further the approximation of the nonlinearity improves. Furthermore, the adaptive controller cannot deteriorate the performance of the nominal control systems in the region where the nonlinearity has no impact on the system dynamics.

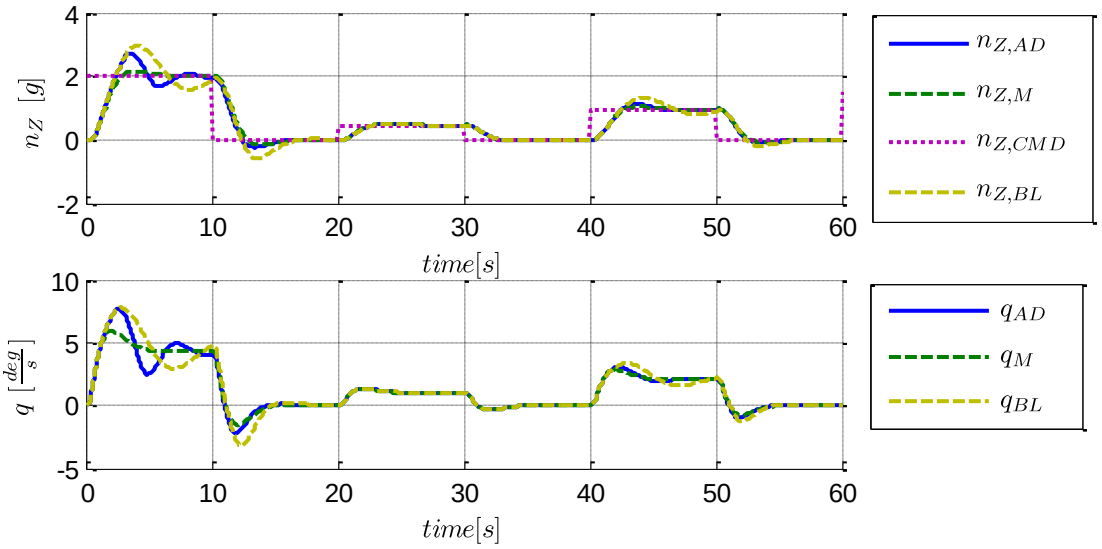

Figure 4.21: Load factor and pitch rate response

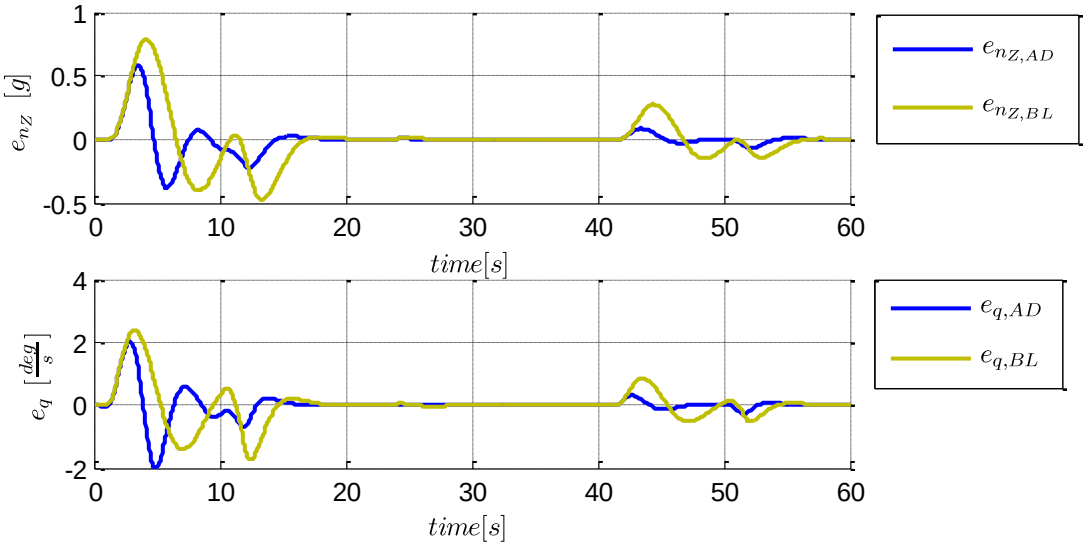

Figure 4.22: Error in load factor and pitch rate response

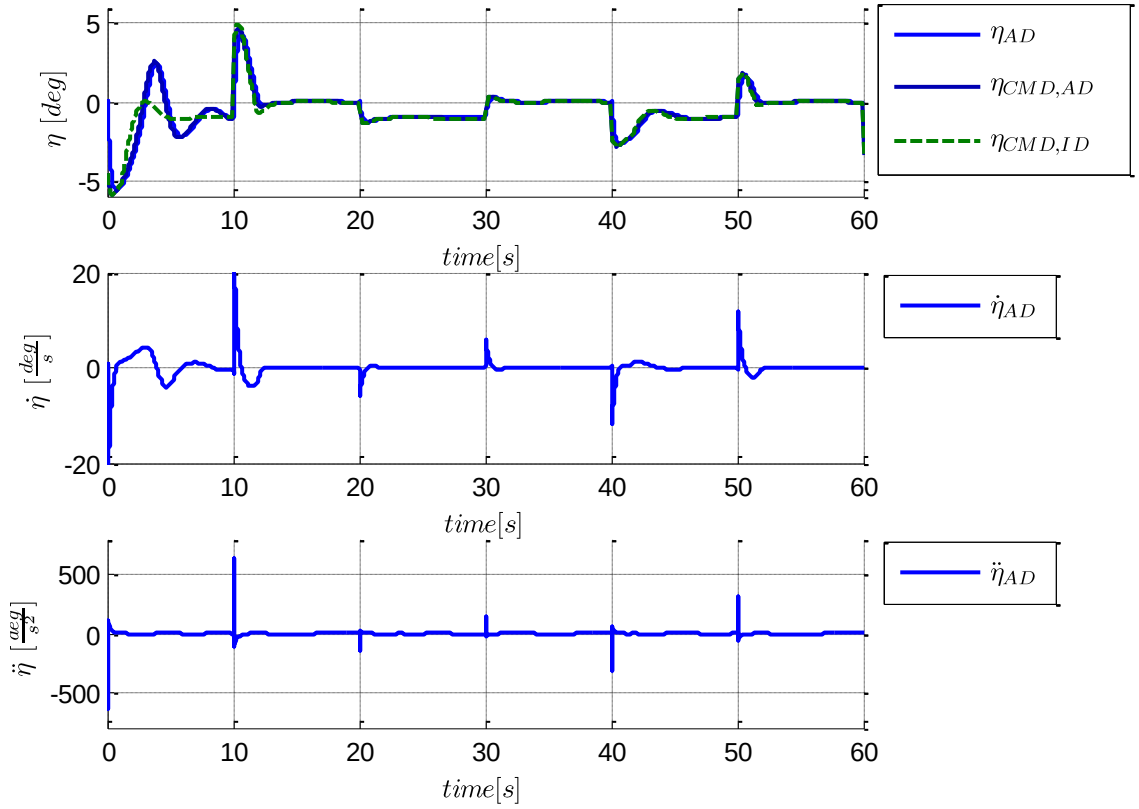

Figure 4.23: Elevator deflection, rate, and acceleration

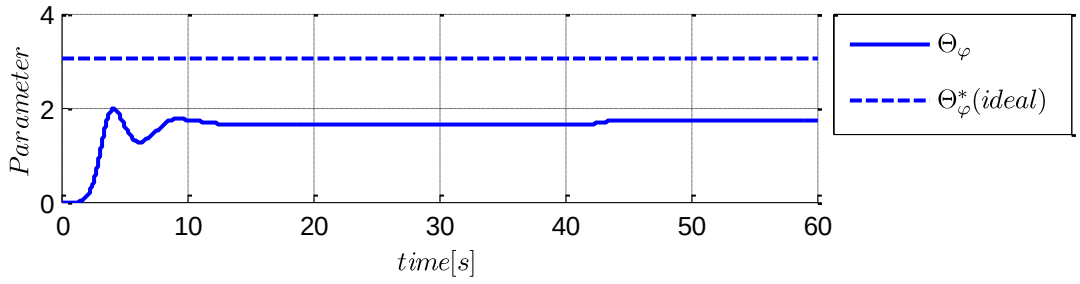

Figure 4.24: Adaptive controller parameters

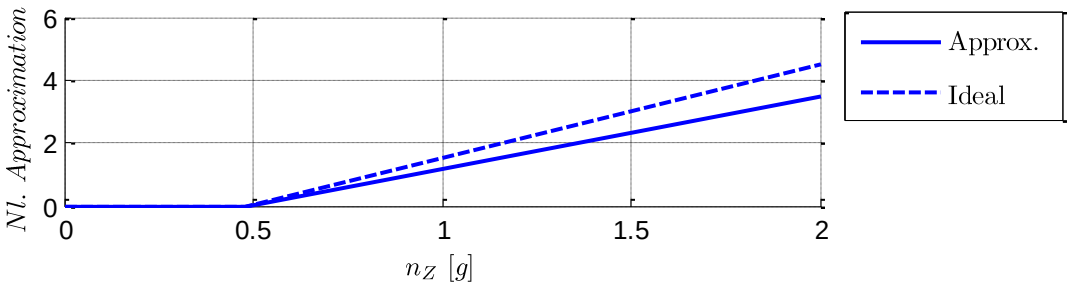

Figure 4.25: Approximation of the nonlinearity after 60 seconds

4.7.2 Linear in the Parameters Neural Network

In the following two examples are shown, where no structural knowledge on the nonlinearity is assumed. This is achieved by providing a set of basis functions that allows the approximation of a large class of nonlinear functions.

4.7.2.1 Radial Basis Functions

To approximate $f^+(n_z)$ with $\boldsymbol{\theta}_\varphi^T \boldsymbol{\varphi}(n_Z)$ a set of radial basis functions is used for $\boldsymbol{\varphi}(n_Z)$. Here 16 radial basis functions are uniformly distributed over the domain $0 \leq n_z \leq 3g$ as it is shown in Figure 4.26. The nonlinear regressor vector is given by

$$\boldsymbol{\varphi}(n_Z) = [\varphi_1(n_Z), \cdots, \varphi_k(n_Z), \cdots, \varphi_{16}(n_Z)], \tag{4.69}$$

where each radial basis function is defined by

$$\varphi_k(n_Z) = e^{-\frac{(n_Z - C_k)^2}{2\sigma^2}}. \tag{4.70}$$

C_k are the uniformly distributed centers on the domain $D = \{n_Z | 0 \leq n_z \leq 3\}$, and it is chosen $\sigma = 0.14$.

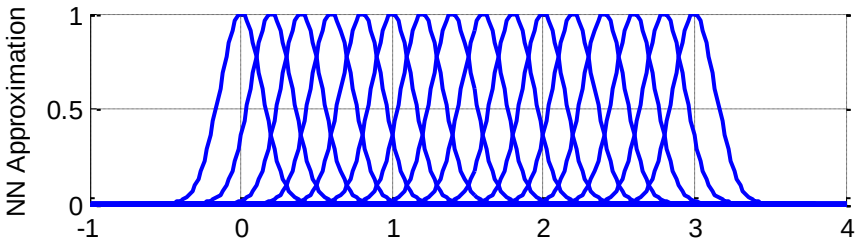

Figure 4.26: Distribution of radial basis functions

Again, the update law from Eq.(4.10) is used

$$\dot{\boldsymbol{\theta}}_\varphi = \gamma_\varphi \boldsymbol{\varphi}(n_Z) \cdot \mathbf{e}_C^T \mathbf{P} \mathbf{b}_P^+. \tag{4.71}$$

The tuning based on Section 4.4 minimizes the defined cost function to $J = 1.365$ and yields the following learning rate for the adaptive controller: $\gamma_\varphi = 1.90$

In Figure 4.27 - Figure 4.31 the simulation results are shown, and it can be seen, that for the first step, almost no improvement in comparison to the baseline controller can be achieved. Moreover, due to the large number of parameters the convergence is even slower than in the previous example. This can be seen in Figure 4.31, where it is shown that, for the given input, only a poor approximation of the nonlinearity is obtained after 60s.

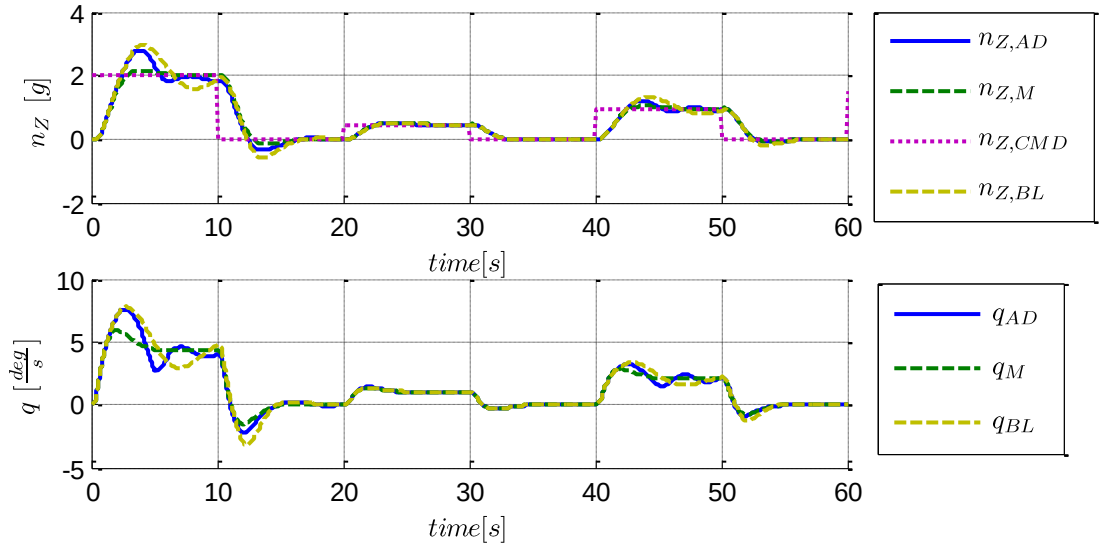

Figure 4.27: Load factor and pitch rate response

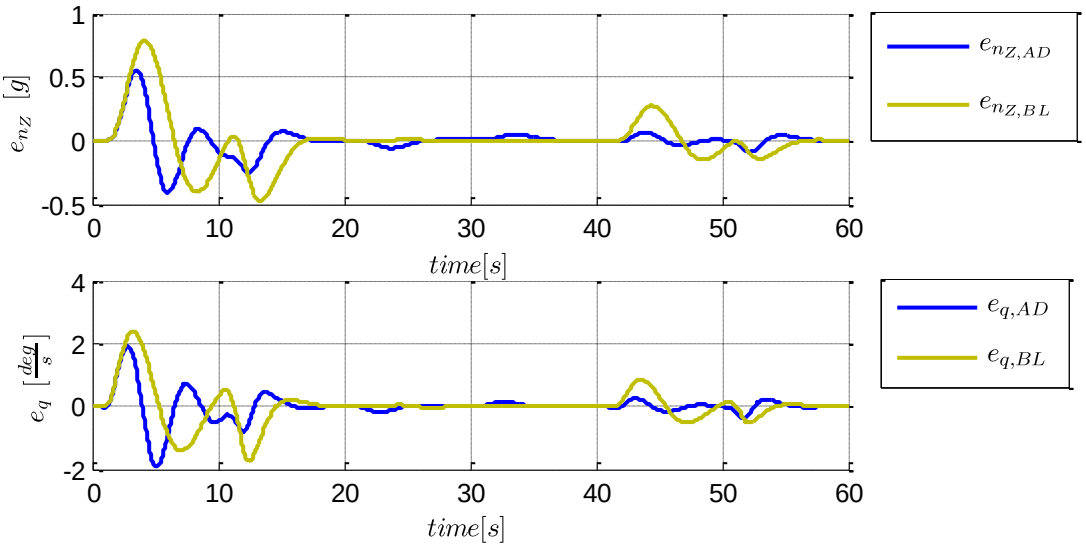

Figure 4.28: Error in load factor and pitch rate response

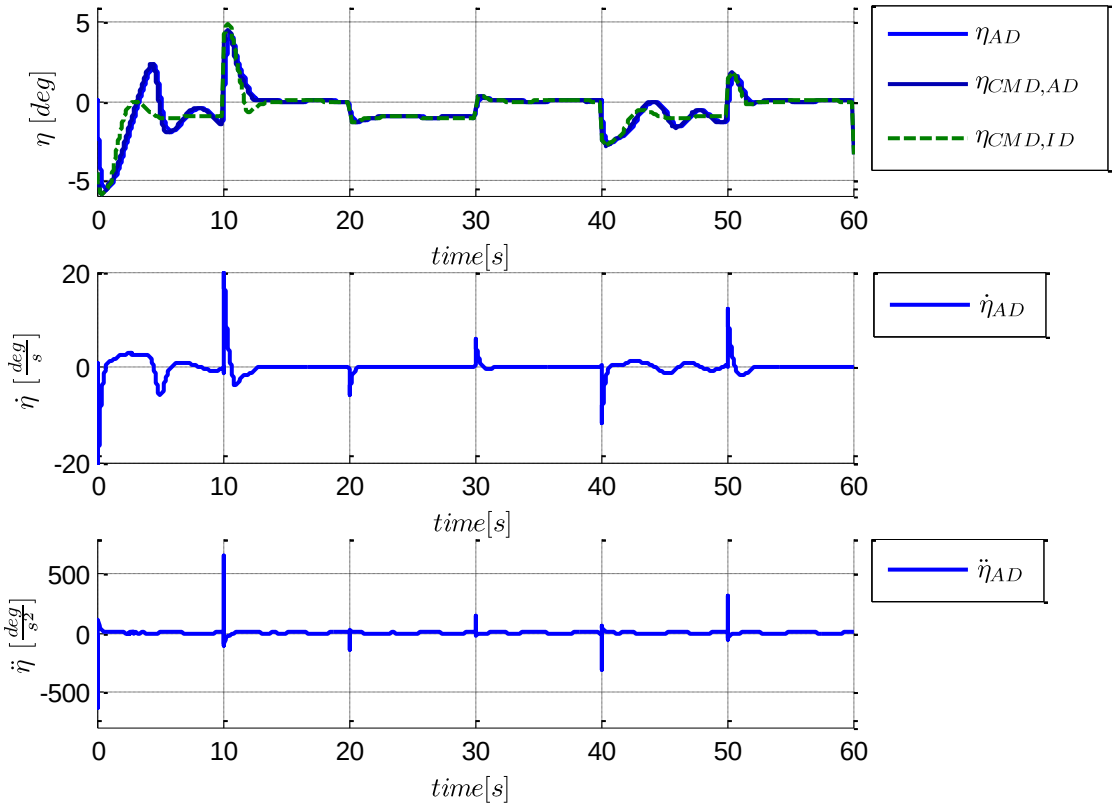

Figure 4.29: Elevator deflection, rate, and acceleration

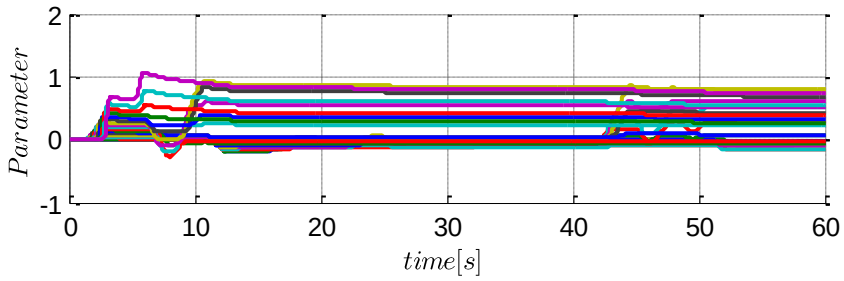

Figure 4.30: Adaptive controller parameters

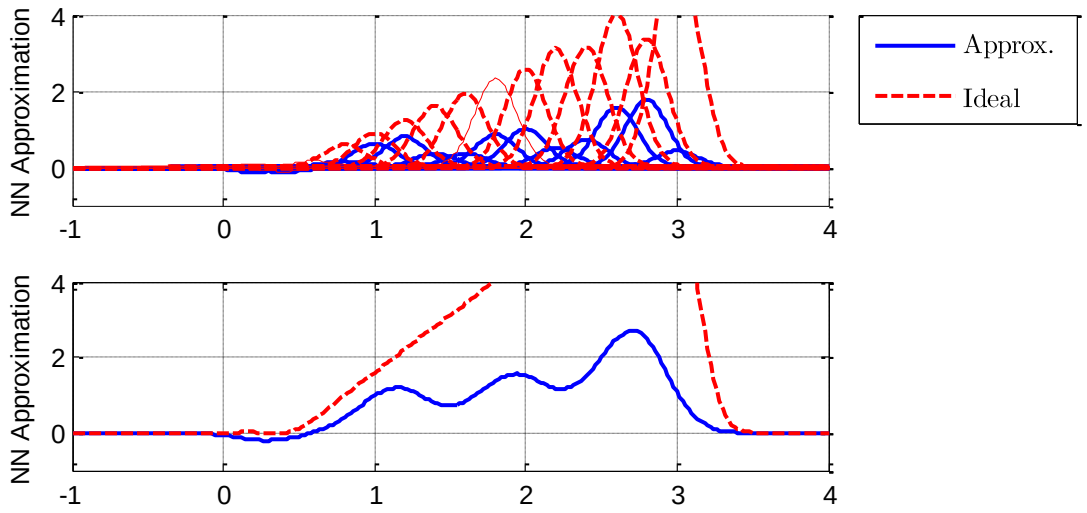

Figure 4.31: Approximation of the nonlinearity after 60 seconds

4.7.2.2 Sigmoid Basis Functions

In contrast to the previous paragraph only different basis functions are used. To approximate $f^+(n_z)$ with $\boldsymbol{\theta}_{\varphi}^T \boldsymbol{\varphi}(n_Z)$ a set of sigmoid basis functions is used for $\boldsymbol{\varphi}(n_Z)$. In the following 26 sigmoid basis functions are uniformly distributed over the domain $0 \leq n_z \leq 2.5g$

$$\boldsymbol{\varphi}(n_Z) = [\varphi_1(n_Z), \cdots, \varphi_k(n_Z), \cdots, \varphi_{26}(n_Z)], \tag{4.72}$$

where each sigmoid basis function is defined by

$$\varphi_k(n_Z) = \frac{1}{1+e^{\sigma(n_Z - C_k)}}. \tag{4.73}$$

C_k are the uniformly distributed centers on the domain $D = \{n_Z | 0 \leq n_z \leq 2.5\}$, and it is chosen $\sigma = 20$.

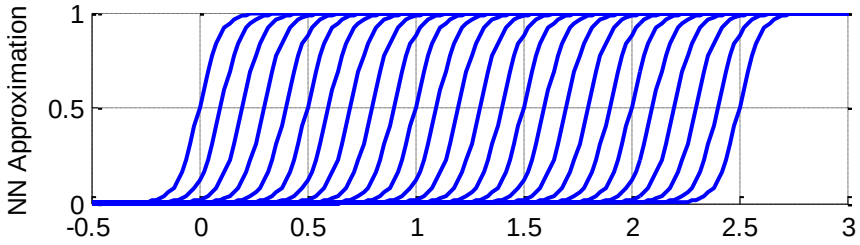

Figure 4.32: Distribution of sigmoid basis functions

Using the update law from Eq.(4.71), the tuning based on Section 4.4 minimizes the defined cost function to $J = 1.286$ and yields the following learning rate for the adaptive controller: $\gamma_\varphi = 0.087$.

From the simulation results in Figure 4.33 - Figure 4.37 it is obvious that the sigmoid basis functions are better suited for the considered problem than the radial basis functions, as a faster and more accurate approximation is achieved. This becomes also obvious from Figure 4.38 and Figure 4.39, where a longer simulation is considered. However, it has to be mentioned that the quasi local support of the radial basis functions can be an advantage, as their influence is restricted to a local domain.

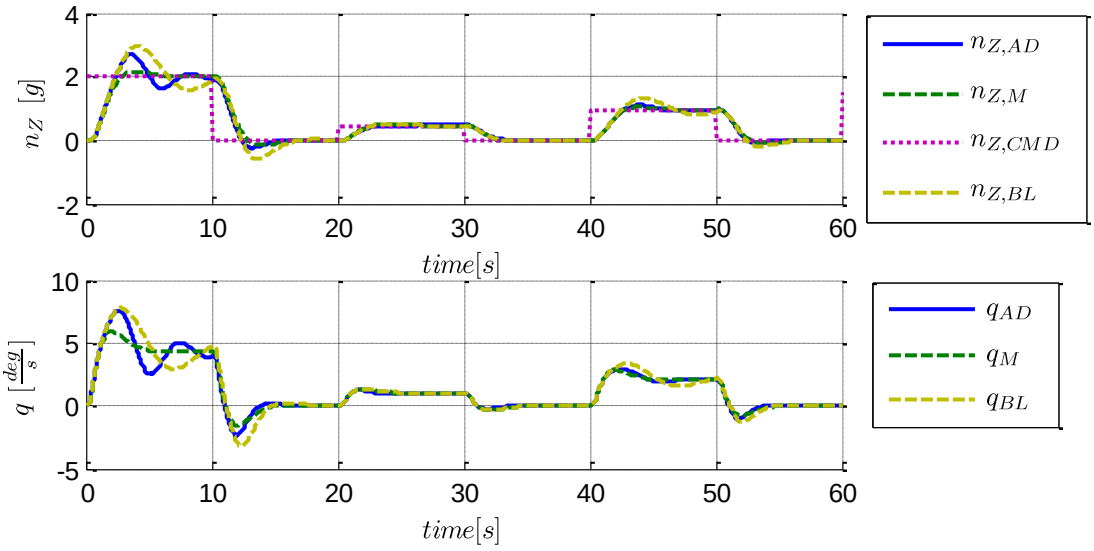

Figure 4.33: Load factor and pitch rate response

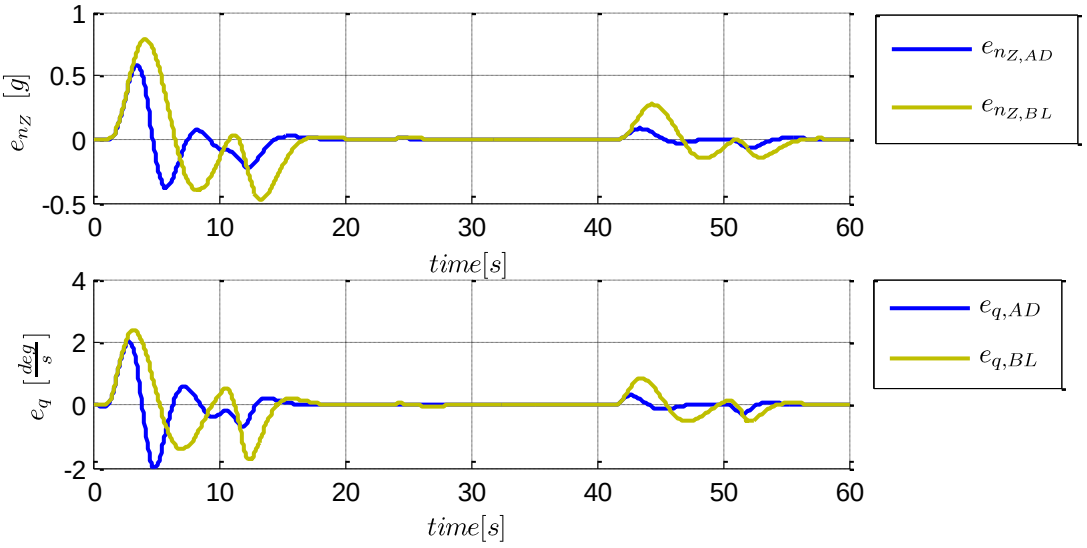

Figure 4.34: Error in load factor and pitch rate response

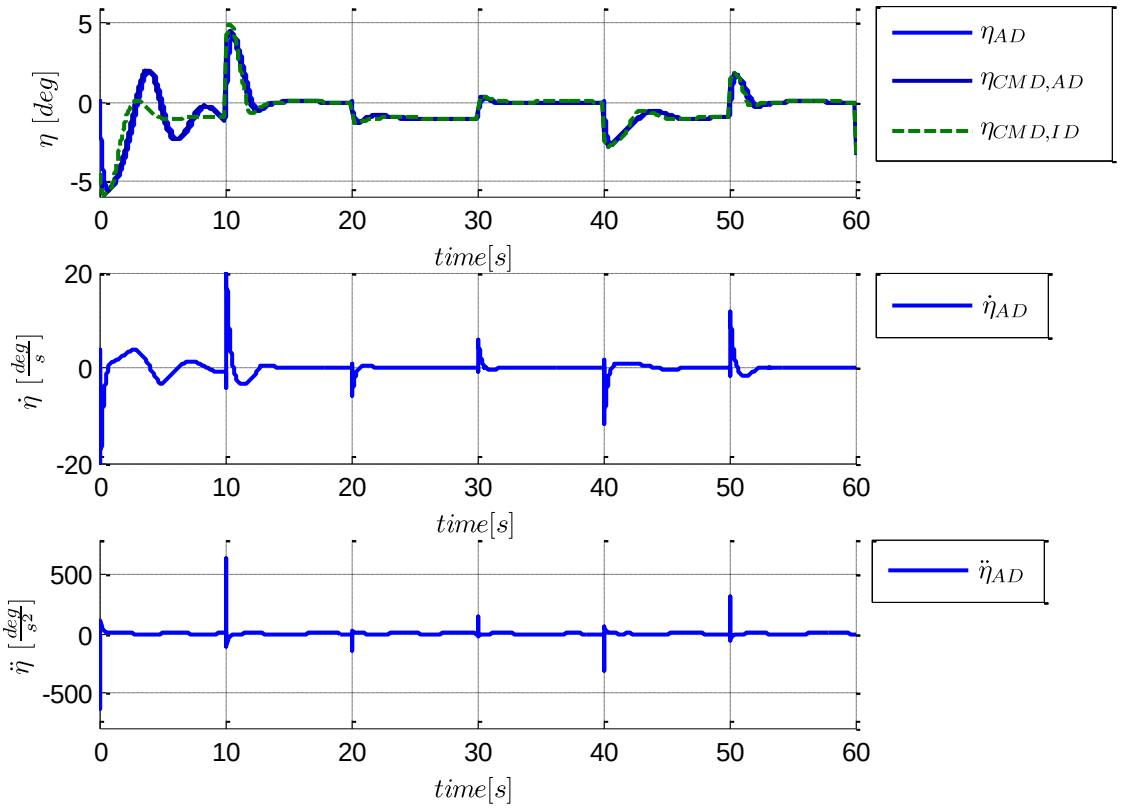

Figure 4.35: Elevator deflection, rate, and acceleration

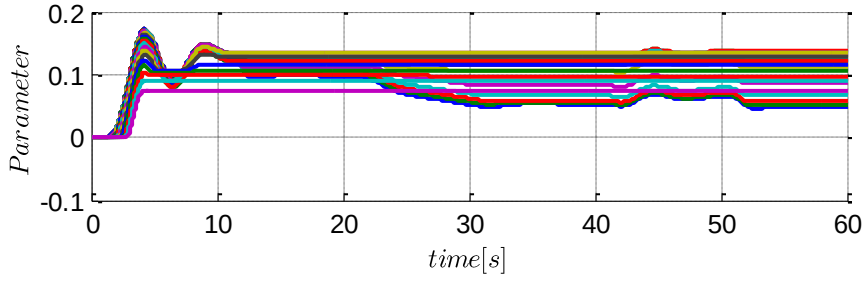

Figure 4.36: Adaptive controller parameters

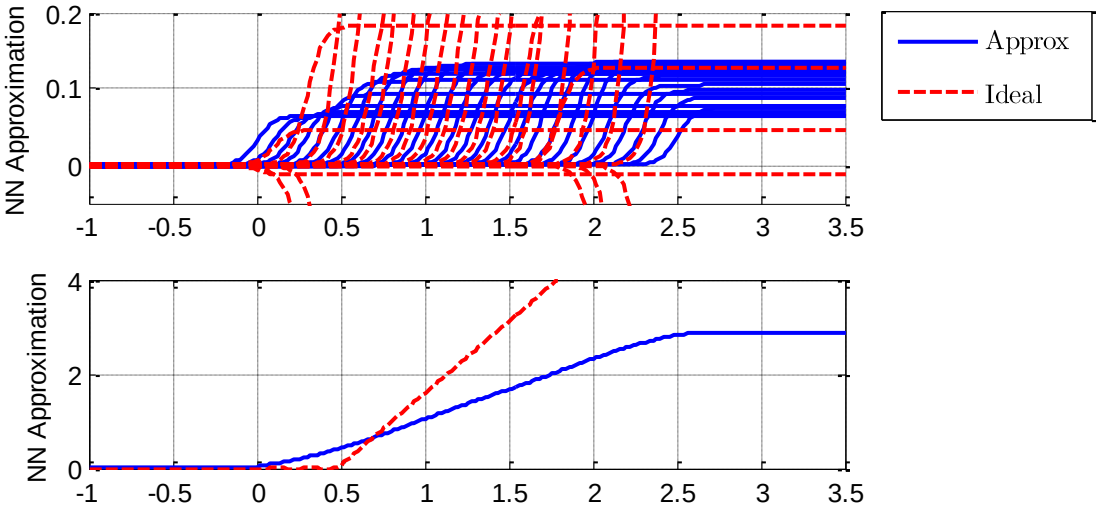

Figure 4.37: Approximation of the nonlinearity after 60 seconds

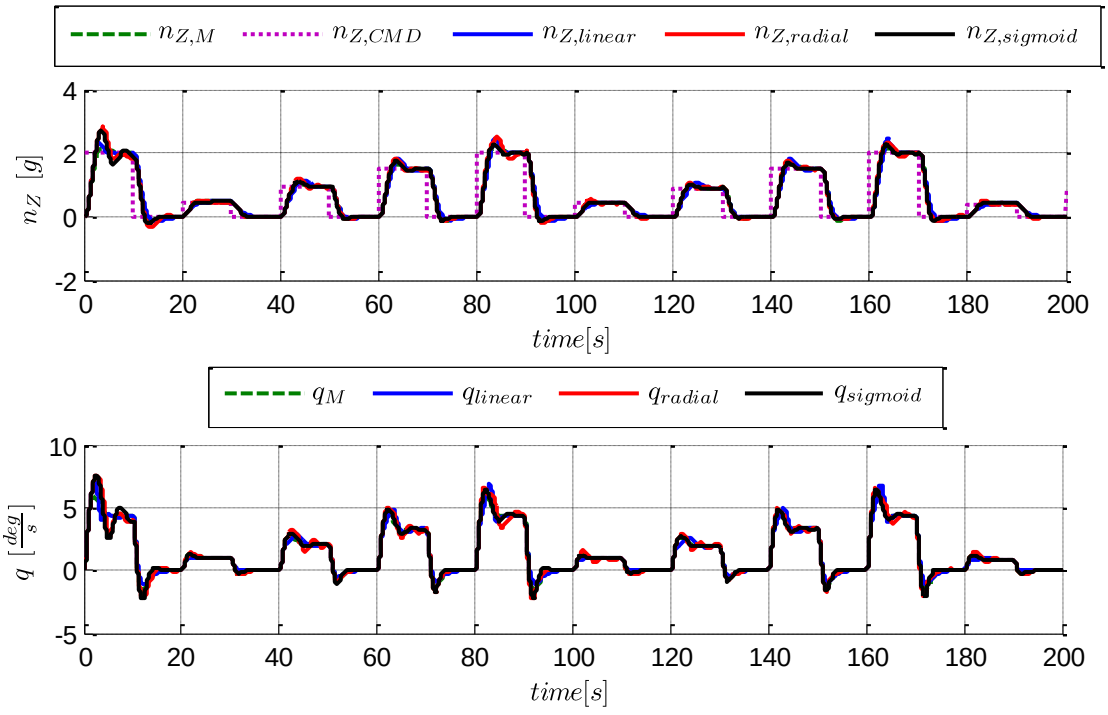

Figure 4.38: Load factor and pitch rate response

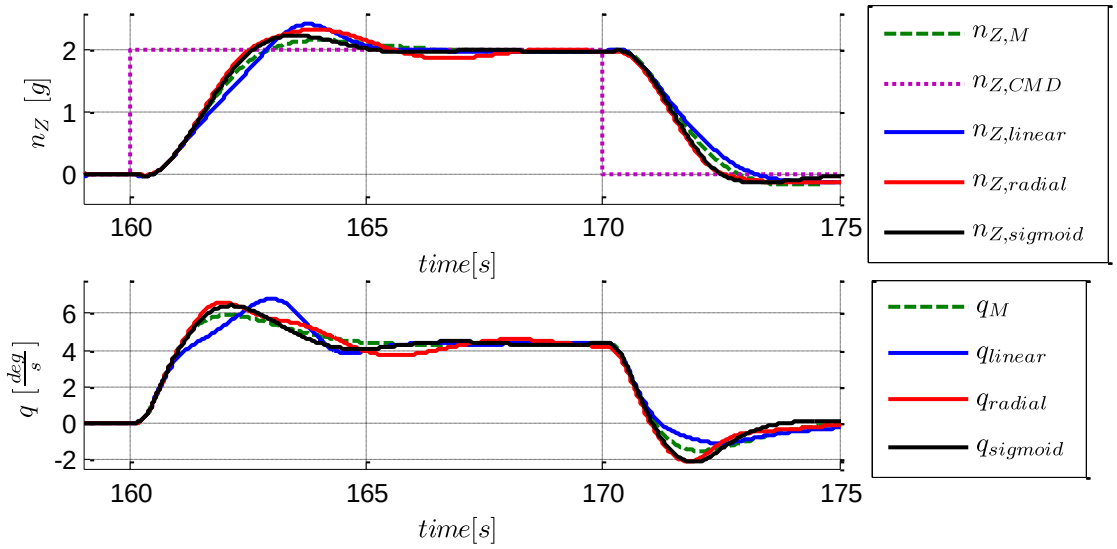

Figure 4.39: Magnified section of load factor and pitch rate response form Figure 4.38

Chapter 5

Modifications

5.1 Reference Model Modifications

In this chapter different modifications of the reference model are presented. In general the idea behind these modifications is an adjustment of the reference model such that the reference trajectories remain achievable by the plant. In Section 4.4 it was for example shown that in the presence of additional dynamics in the input channel an exact match between reference trajectories and plant is not possible. For this problem the concept of hedging was suggested in the adaptive control literature and is presented in the following. Additionally, two novel modifications of the reference model are presented. The suggested modifications adjust the reference model with the objective to allow a larger set of reference trajectories to exist. This is less restrictive, and therefore the reference trajectories remain achievable by the plant. The first modification allows to relax the restrictiveness w.r.t. matched uncertainties, and the second accounts for unmatched uncertainties. Finally, an error feedback modification is presented which was commonly suggested in literature.

5.1.1 Hedging

Actuator limits pose hard nonlinearities in the input channel of a system. These limits arise from physical constraints and are necessary to avoid damages of the system or deterioration of the process dynamics (e. g. flow separation). However, these limits also limit the available control energy at the system input and consequently the state space where the system is controllable is limited as well. Furthermore, actuator saturation especially poses difficulties for MRAC-type controllers as it violates some of the basic assumptions. For example, when all inputs saturate the plant is open loop and the control effectiveness reduces to zero. This means, the sign of control effectiveness is indefinite and the uncertainties are not matched anymore. In the previous chapters actuator limitations have been neglected, but if the reference model does not account for actuator saturation this directly means that the real plant cannot

follow the reference model for every command that is issued. As the linear reference model assumes unlimited control energy, whereas for the plant this is not available. In the case of saturation an error, which cannot be compensated, will result from the error dynamics, and as the parameters are adjusted based on integration of this error they will increase as long as the input saturates. Obviously this does not make any sense. If the reference trajectory is not achievable due to limited control authority then increasing the gains will not help either. A simple solution would be to switch of adaptation when actuator saturation occurs, however this switching can lead to limit cycle oscillations.

To overcome this problem the use of a hedging signal, which modifies the error dynamics, was already suggested in [137]. In the adaptive control literature the word hedging is in general used to refer to a modification of certain signals with the objective to “hide” certain input characteristics of the plant from the error dynamics. This means either the error signals are augmented directly, or indirectly by a modification of the reference dynamics. As mentioned, the approach was originally suggested to account for saturations and the first stability proof for SISO systems was given in [124], and further developed for MIMO systems can be found in [138] and [139]. In [140] the problem of rate saturation was considered, where also a stability proof is provided. Approaches wich are based on the same principle are also suggested in [141], [142], and [143]. Furthermore, it was suggested to use the approach in order to account for dynamic constraints in the input channel [126].

In the following, at first the problem of hard input saturations is discussed and second additional dynamics in the input channel (e.g. actuators) are covered.

5.1.1.1 Hedging for Actuator Saturation

5.1.1.1.1 *Direct MRAC with Actuator Saturation*

In the following the approach suggested in [124] and [125] is considered, where the error dynamics is adjusted such that the effect of actuator saturation on the error dynamics is removed. This can also be interpreted as a modification of the reference model in a way that its dynamics become achievable by the plant. This means, that during saturation the gains and the reference model are adjusted such that the reference model follows the plant. It is also an important question whether the control effectiveness $\mathbf{\Lambda}$ is known or not. If the control effectiveness is unknown an additional estimation of the control effectiveness is required for the hedging signal, and this problem is discussed in the following. If the control effectiveness is known the approach remains the same, but the estimation of the control effectiveness can be omitted.

Let’s consider the direct case where the plant without actuator saturation is assumed to be given by

$$\dot{\mathbf{x}}_P = \mathbf{A}_M\mathbf{x}_P + \mathbf{B}_M\mathbf{r} + \mathbf{B}_P\boldsymbol{\Lambda}\left(\mathbf{u} - \boldsymbol{\Theta}_x^{*\,T}\mathbf{x}_P - \boldsymbol{\Theta}_r^*\mathbf{r}\right). \tag{5.1}$$

For simplicity nonlinear and constant uncertainties are omitted, but an extension is easily possible. Adding a saturation nonlinearity in the input channel of Eq.(5.1) yields

$$\dot{\mathbf{x}}_P = \mathbf{A}_M\mathbf{x}_P + \mathbf{B}_M\mathbf{r} + \mathbf{B}_P\boldsymbol{\Lambda}\left(\mathbf{f}_s(\mathbf{u}) - \boldsymbol{\Theta}_x^{*\,T}\mathbf{x}_P - \boldsymbol{\Theta}_r^*\mathbf{r}\right), \tag{5.2}$$

where $\mathbf{f}_s(\mathbf{u})$ is the saturation nonlinearity

$$\mathbf{f}_s(\mathbf{u}) = \begin{cases} \mathbf{u} & \text{if } \mathbf{u}_{min} < \mathbf{u} < \mathbf{u}_{max} \\ \mathbf{u}_{max} & \text{if } \mathbf{u} > \mathbf{u}_{max} \\ \mathbf{u}_{min} & \text{otherwise} \end{cases}. \tag{5.3}$$

Denoting the control deficiency by

$$\boldsymbol{\Delta}\mathbf{u} = \mathbf{f}_s(\mathbf{u}) - \mathbf{u}, \tag{5.4}$$

we can write the plant dynamics by

$$\dot{\mathbf{x}}_P = \mathbf{A}_M\mathbf{x}_P + \mathbf{B}_M\mathbf{r} + \mathbf{B}_P\boldsymbol{\Lambda}\left(\mathbf{u} + \boldsymbol{\Delta}\mathbf{u} - \boldsymbol{\Theta}_x^{*\,T}\mathbf{x}_P - \boldsymbol{\Theta}_r^*\mathbf{r}\right). \tag{5.5}$$

Again, we consider a linear reference model given by

$$\dot{\mathbf{x}}_M = \mathbf{A}_M\mathbf{x}_M + \mathbf{B}_M\mathbf{r}, \tag{5.6}$$

and choose the same control law as before

$$\mathbf{u} = \boldsymbol{\Theta}_x^T\mathbf{x}_P + \boldsymbol{\Theta}_r\mathbf{r} \tag{5.7}$$

If we insert the control law of Eq.(5.7) in the plant in Eq.(5.5) and build the error dynamics w.r.t. Eq.(5.6) we obtain

$$\dot{\mathbf{e}}_C = \mathbf{A}_M\mathbf{e}_C + \mathbf{B}_P\boldsymbol{\Lambda}\left(\widetilde{\boldsymbol{\Theta}}_x^T\mathbf{x}_P + \widetilde{\boldsymbol{\Theta}}_r\mathbf{r}\right) + \mathbf{B}_P\boldsymbol{\Lambda}\,\boldsymbol{\Delta}\mathbf{u} \tag{5.8}$$

From Eq.(5.8) it can be seen, that despite the undesirable term $\mathbf{B}_P\boldsymbol{\Lambda}\,\boldsymbol{\Delta}\mathbf{u}$, the error dynamics is the same as previously. To remove the effect due to actuator saturation from the error dynamics we can define a differential equation of the form

$$\Delta\dot{\mathbf{e}}_C = \mathbf{A}_M\Delta\mathbf{e}_C + \mathbf{B}_P\widehat{\boldsymbol{\Lambda}}\,\boldsymbol{\Delta}\mathbf{u}, \tag{5.9}$$

where $\widehat{\boldsymbol{\Lambda}}$ is an additional parameter that will be adapted (remember: $\boldsymbol{\Lambda}$ is unknown). To remove the undesirable term $\mathbf{B}_P\boldsymbol{\Lambda}\,\boldsymbol{\Delta}\mathbf{u}$ we can build the new error $\mathbf{e}_U = \mathbf{e}_C - \Delta\mathbf{e}_C$, and obtain a new error dynamics of the form

$$\begin{aligned} \dot{\mathbf{e}}_U &= \mathbf{A}_M\mathbf{e}_U + \mathbf{B}_P\boldsymbol{\Lambda}\left(\widetilde{\boldsymbol{\Theta}}_x^T\mathbf{x}_P + \widetilde{\boldsymbol{\Theta}}_r\mathbf{r}\right) + \mathbf{B}_P\underbrace{\left(\boldsymbol{\Lambda} - \widehat{\boldsymbol{\Lambda}}\right)}_{\widetilde{\boldsymbol{\Lambda}}}\boldsymbol{\Delta}\mathbf{u} \\ \dot{\mathbf{e}}_U &= \mathbf{A}_M\mathbf{e}_U + \mathbf{B}_P\boldsymbol{\Lambda}\left(\widetilde{\boldsymbol{\Theta}}_x^T\mathbf{x}_P + \widetilde{\boldsymbol{\Theta}}_r\mathbf{r}\right) + \mathbf{B}_P\widetilde{\boldsymbol{\Lambda}}\boldsymbol{\Delta}\mathbf{u}. \end{aligned} \tag{5.10}$$

Appropriate adaptation laws can be derived by choosing the following Lyapunov function candidate

$$\mathrm{V} = \tfrac{1}{2}\mathbf{e}_U^T\mathbf{P}\mathbf{e}_U + \tfrac{1}{2}\mathrm{Tr}\left[\widetilde{\boldsymbol{\Theta}}_x^T\boldsymbol{\Gamma}_x^{-1}\widetilde{\boldsymbol{\Theta}}_x\boldsymbol{\Lambda}\right] + \tfrac{1}{2}\mathrm{Tr}\left[\widetilde{\boldsymbol{\Theta}}_r\boldsymbol{\Gamma}_r^{-1}\widetilde{\boldsymbol{\Theta}}_r^T\boldsymbol{\Lambda}\right] + \tfrac{1}{2}\mathrm{Tr}\left[\widetilde{\boldsymbol{\Lambda}}\boldsymbol{\Gamma}_\Lambda^{-1}\widetilde{\boldsymbol{\Lambda}}^T\right], \tag{5.11}$$

where the time derivative is given by

$$\dot{\mathrm{V}} = \frac{1}{2}\mathbf{e}_U^T \underbrace{\left(\mathbf{P}\mathbf{A}_M + \mathbf{A}_M^T\mathbf{P}\right)}_{-\mathbf{Q}} \mathbf{e}_U + \mathbf{e}_U^T\mathbf{P}\mathbf{B}_P\boldsymbol{\Lambda}\left(\widetilde{\boldsymbol{\Theta}}_x^T\mathbf{x}_P + \widetilde{\boldsymbol{\Theta}}_r\mathbf{r}\right) + \mathbf{e}_U^T\mathbf{P}\mathbf{B}_P\widetilde{\boldsymbol{\Lambda}}\boldsymbol{\Delta}\mathbf{u}$$
$$+\mathrm{Tr}\left[\widetilde{\boldsymbol{\Theta}}_x^T\boldsymbol{\Gamma}_x^{-1}\dot{\widetilde{\boldsymbol{\Theta}}}_x\boldsymbol{\Lambda}\right] + \mathrm{Tr}\left[\widetilde{\boldsymbol{\Theta}}_r\boldsymbol{\Gamma}_r^{-1}\dot{\widetilde{\boldsymbol{\Theta}}}_r^T\boldsymbol{\Lambda}\right] + \mathrm{Tr}\left[\widetilde{\boldsymbol{\Lambda}}\boldsymbol{\Gamma}_\Lambda^{-1}\dot{\widetilde{\boldsymbol{\Lambda}}}^T\right]. \tag{5.12}$$

Applying the trace identity $\mathbf{a}^T\mathbf{b} = \mathrm{Tr}[\mathbf{b}\mathbf{a}^T]$ we can rewrite the following terms

$$\begin{aligned}\dot{\mathrm{V}} = &-\frac{1}{2}\mathbf{e}_U^T\mathbf{Q}\mathbf{e}_U \\ &+\mathrm{Tr}\left[\widetilde{\boldsymbol{\Theta}}_x^T\left(\boldsymbol{\Gamma}_x^{-1}\dot{\widetilde{\boldsymbol{\Theta}}}_x + \mathbf{x}_P\cdot\mathbf{e}_U^T\mathbf{P}\mathbf{B}_P\right)\boldsymbol{\Lambda}\right] \\ &+\mathrm{Tr}\left[\widetilde{\boldsymbol{\Theta}}_r\left(\boldsymbol{\Gamma}_r^{-1}\dot{\widetilde{\boldsymbol{\Theta}}}_r^T + \mathbf{r}\cdot\mathbf{e}_U^T\mathbf{P}\mathbf{B}_P\right)\boldsymbol{\Lambda}\right] \\ &+\mathrm{Tr}\left[\widetilde{\boldsymbol{\Lambda}}\left(\boldsymbol{\Gamma}_\Lambda^{-1}\dot{\widetilde{\boldsymbol{\Lambda}}}^T + \boldsymbol{\Delta}\mathbf{u}\cdot\mathbf{e}_U^T\mathbf{P}\mathbf{B}_P\right)\right]\end{aligned} \tag{5.13}$$

From Eq.(5.13) it is clear that with the following update laws

$$\begin{aligned}\dot{\widetilde{\boldsymbol{\Theta}}}_x &= -\boldsymbol{\Gamma}_x\mathbf{x}_P\cdot\mathbf{e}_U^T\mathbf{P}\mathbf{B}_P \\ \dot{\widetilde{\boldsymbol{\Theta}}}_r^T &= -\boldsymbol{\Gamma}_r\mathbf{r}\cdot\mathbf{e}_U^T\mathbf{P}\mathbf{B}_P \\ \dot{\widetilde{\boldsymbol{\Lambda}}}^T &= -\boldsymbol{\Gamma}_\Lambda\boldsymbol{\Delta}\mathbf{u}\cdot\mathbf{e}_U^T\mathbf{P}\mathbf{B}_P\end{aligned} \quad\Leftrightarrow\quad \begin{aligned}\dot{\boldsymbol{\Theta}}_x &= -\boldsymbol{\Gamma}_x\mathbf{x}_P\cdot\mathbf{e}_U^T\mathbf{P}\mathbf{B}_P \\ \dot{\boldsymbol{\Theta}}_r^T &= -\boldsymbol{\Gamma}_r\mathbf{r}\cdot\mathbf{e}_U^T\mathbf{P}\mathbf{B}_P \\ \dot{\boldsymbol{\Lambda}}^T &= \boldsymbol{\Gamma}_\Lambda\boldsymbol{\Delta}\mathbf{u}\cdot\mathbf{e}_U^T\mathbf{P}\mathbf{B}_P\end{aligned} \tag{5.14}$$

the time derivative of the Lyapunov function becomes negative semi definite:

$$\dot{\mathrm{V}} = -\tfrac{1}{2}\mathbf{e}_U^T\mathbf{Q}\mathbf{e}_U. \tag{5.15}$$

Thus boundedness of the states can be followed ($\mathbf{e}_U, \widetilde{\boldsymbol{\Theta}}_x, \widetilde{\boldsymbol{\Theta}}_r, \widetilde{\boldsymbol{\Lambda}} \in \mathcal{L}_\infty$).

However, this does not guarantee stability, because of the additionally introduced dynamics in Eq.(5.9), the additional state $\Delta\mathbf{e}_C$ is not guaranteed to be bounded. This gets more obvious if we modify the reference model directly instead of introducing the additional dynamics of Eq.(5.9):

$$\dot{\mathbf{x}}_{M,h} = \mathbf{A}_M\mathbf{x}_{M,h} + \mathbf{B}_M\mathbf{r} + \mathbf{B}_P\widehat{\boldsymbol{\Lambda}}\,\boldsymbol{\Delta}\mathbf{u}. \tag{5.16}$$

This is equal to introducing Eq.(5.9), and it is obvious that this modification can also be interpreted as a modification of the reference input in case of actuator saturation. Furthermore, it is obvious that the states of the reference model $\mathbf{x}_M$ are not inherently bounded, as it was the case without modification. Thus, even though Eq.(5.15) guarantees boundedness of $\mathbf{e}_U = \mathbf{x}_P - \mathbf{x}_M - \Delta\mathbf{e}_C = \mathbf{x}_P - \mathbf{x}_{M,h}$ it does not guarantee boundedness of $\mathbf{x}_P$ and $\mathbf{x}_{M,h}$, as they could diverge at the same rate.

In case the plant is inherently stable, overall stability of the closed loop can still be guaranteed, because due to the boundedness of the input $\mathbf{f}_s(\mathbf{u})$, the plant states $\mathbf{x}_P$ are bounded.

For unstable plants, it is obvious that with limited control energy the tracking problem cannot be solved globally. That is, it needs to be ensured that the domain in the state space where the plant can be stabilized is not left. This is equivalent to restricting the reference command $\mathbf{r}$ such that the former is satisfied. However, in the case of

uncertain systems this is difficult and only feasible as long as the uncertainties are small. On the contrary, if uncertainties in the system are small there is no purpose for adaptive control. To guarantee stability when the uncertainties are large, the reference command $\mathbf{r}$ has to be restricted in a conservative way (even for the nominal case), which is often inacceptable [144]. However, fixed-gain controllers suffer from the same problem.

For unstable plants, conditions for the initial condition $\mathbf{x}_0$ and the maximum reference command $\mathbf{r}_{\max}$, that guarantee local stability, can in general only be derived when no nonlinearities are considered. These conditions are extremely conservative for higher order plants and MIMO systems due to the applied matrix norms, and result in requirements for the reference command $\mathbf{r}_{\max}$ that are extremely small or even cannot be satisfied [144]. Even though the approach might also work when the derived condition $\mathbf{r}_{\max}$ is not satisfied, stability is not guaranteed in rigorous mathematical sense.

5.1.1.1.2 *Indirect and Predictor Based MRAC with Actuator Saturation*

For the indirect and the predictor based approach, actuator saturation can be accounted for in a similar way. In both cases it is sufficient to use the constrained input signal in the identification/predictor dynamics. Due to the similarity, in the following, the approach is only outlined for predictor based MRAC from Section 4.4.

Omitting nonlinear and constant uncertainties, and including actuator saturation the plant form Eq.(4.29) becomes

$$\dot{\mathbf{x}}_P = \mathbf{A}_M \mathbf{x}_P + \mathbf{B}_P \left(\boldsymbol{\Lambda} \mathbf{f}_s(\mathbf{u}) - \widehat{\boldsymbol{\Theta}}_x^{*\,T} \mathbf{x}_P \right). \tag{5.17}$$

And similar to Eq.(4.32) the control law is given by

$$\mathbf{u} = \widehat{\boldsymbol{\Lambda}}^{-1} \left[\widehat{\boldsymbol{\Theta}}_x^T \mathbf{x}_P + \mathbf{K}_r \, \mathbf{r} \right]. \tag{5.18}$$

In difference to the predictor given in Eq.(4.30) we now account for the control deficiency and obtain

$$\dot{\hat{\mathbf{x}}}_P = \mathbf{A}_M \hat{\mathbf{x}}_P + \mathbf{B}_P \left(\widehat{\boldsymbol{\Lambda}} \mathbf{f}_s(\mathbf{u}) - \widehat{\boldsymbol{\Theta}}_x^T \mathbf{x}_P \right). \tag{5.19}$$

It can be easily verified that this is equal to applying a hedging signal in the following form

$$\dot{\hat{\mathbf{x}}}_P = \mathbf{A}_M \hat{\mathbf{x}}_P + \mathbf{B}_P \left(\widehat{\boldsymbol{\Lambda}} \mathbf{u} - \widehat{\boldsymbol{\Theta}}_x^T \mathbf{x}_P \right) + \mathbf{B}_P \widehat{\boldsymbol{\Lambda}} \, \boldsymbol{\Delta} \mathbf{u}. \tag{5.20}$$

Thus, for the error dynamics we get form Eq.(5.17) and Eq.(5.19)

$$\dot{\mathbf{e}}_P = \mathbf{A}_M \mathbf{e}_P + \mathbf{B}_P \left(\widetilde{\boldsymbol{\Theta}}_x^T \mathbf{x}_P + \widetilde{\boldsymbol{\Lambda}} \mathbf{f}_s(\mathbf{u}) \right) \tag{5.21}$$

Using a Lyapunov function on the basis of Eq.(4.37) the update laws can be derived to take the form

$$\begin{aligned}\dot{\hat{\boldsymbol{\Theta}}}_x &= -\boldsymbol{\Gamma}_x \mathbf{x}_P \cdot \mathbf{e}_P^T \mathbf{P} \mathbf{B}_P \\ \dot{\hat{\boldsymbol{\Lambda}}}^T &= \boldsymbol{\Gamma}_\Lambda \mathbf{f}_s(\mathbf{u}) \cdot \mathbf{e}_P^T \mathbf{P} \mathbf{B}_P\end{aligned} \tag{5.22}$$

Comparing the update laws in Eq.(5.22) with the update laws from the direct approach in Eq.(5.14) it becomes obvious, that for the same problem, the direct approach leads to a larger number of adaptive parameter. With hedging, direct MRAC requires the estimation of the feedforward gain and the control effectiveness, where for the predictor based approach only the control effectiveness must be estimated. From this point of view the predictor based approach seems to be favorable.

5.1.1.2 Hedging for Input Dynamics

Additional dynamics in the input channel, e.g. actuator dynamics, are often neglected for the controller design. However, this is only feasible if the frequency-scale separation between pant and actuation dynamics is large enough, i.e. the actuation system has to be much faster and decay sufficiently fast in comparison to the plant dynamics. Neglecting the additional input dynamics for an adaptive controller also results in a perturbation of the error dynamics during transients. In the simulation example in Section 4.4 this was already pointed out. This perturbation is similar to the saturation effect shown in Eq.(5.8) as it also results from a control deficiency. In the following the problem is considered that additional dynamics (e.g. actuator or structural filter dynamics) are present in the input channel of the plant, and it is assumed that they can be represented by a stable, strictly-proper, linear low pass filter $\mathbf{C}(s)$ with DC gain of 1, where s is the Laplace variable. Hence, the system input is

$$\mathbf{u}(s) = \mathbf{C}(s)\mathbf{u}_{CMD}(s), \tag{5.23}$$

and $\mathbf{u}_{CMD}$ is the commanded input. These input constraints are present in any real system due to actuator dynamics. Especially in aircraft control it is state of the art to further limit the bandwidth of the input channel by introducing structural filters to avoid an excitation of the structural modes.

If we insert the control law Eq.(5.7) in the pant Eq.(5.1) with the input dynamics of Eq.(5.23) and build the error dynamics we obtain Eq.(5.8)

$$\dot{\mathbf{e}}_C = \mathbf{A}_M \mathbf{e}_C + \mathbf{B}_P \boldsymbol{\Lambda}\left(\widetilde{\boldsymbol{\Theta}}_x^T \mathbf{x}_P + \widetilde{\boldsymbol{\Theta}}_r \mathbf{r}\right) + \mathbf{B}_P \widetilde{\boldsymbol{\Lambda}} \boldsymbol{\Delta}\mathbf{u}, \tag{5.24}$$

where the control deficiency $\boldsymbol{\Delta}\mathbf{u}$ is now given by $\boldsymbol{\Delta}\mathbf{u}(s) = (\mathbf{C}(s) - 1)\mathbf{u}_{CMD}(s)$.

From this it directly follows, that for the case, where we do not only have to consider input magnitude saturation, but additional dynamics in the input channel, the problem can also be addressed by hedging and the modified reference model is given by

$$\dot{\mathbf{x}}_M = \mathbf{A}_M \mathbf{x}_M + \mathbf{B}_M \mathbf{r} + \mathbf{B}_P \boldsymbol{\Delta}\mathbf{u}. \tag{5.25}$$

The general concept is shown for a linear single input system with known input gain in Figure 5.1, where it is assumed that the actuator position is measurable and the deficiency can be calculated form the difference between commanded and measured

actuator deflection. In case of no available measurement an actuator model can be used, which must provide a good approximation of the actuator dynamics. From the difference between the model and the real actuator a small disturbance on the error dynamics will remain, but the impact will still be smaller than in case of neglected dynamics.

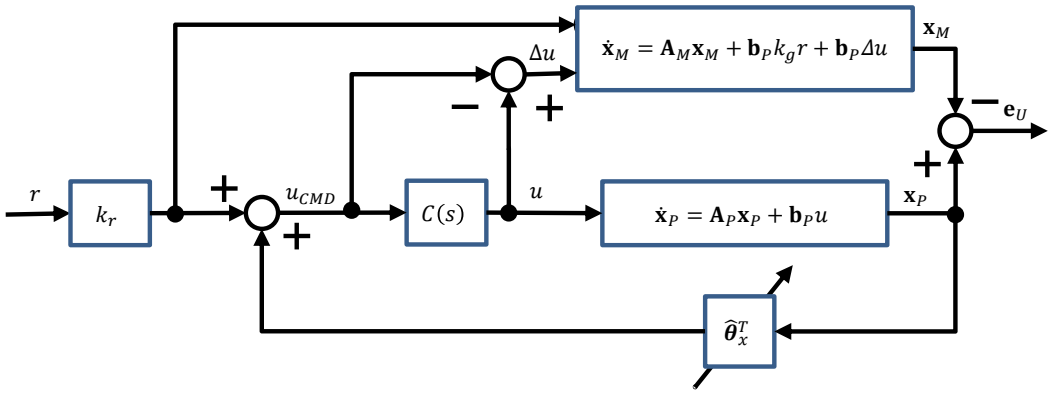

Figure 5.1: Architecture of direct MRAC with hedging

In difference to the saturation problem, no stability proof is available. However, in Chapter 6 it is shown that for the case of known input gain matrix $\boldsymbol{\Lambda}$ the application of a hedging signal can be equivalently realized by an $\mathcal{L}_1$ adaptive controller, and hence, the stability concepts of $\mathcal{L}_1$ adaptive control are applicable. Due to the equivalence this also directly recommends the use of an $\mathcal{L}_1$ adaptive controller as the frame work already provides a closed theory. Moreover, for the case of unknown input gain matrix $\boldsymbol{\Lambda}$ it will become obvious that the concept of $\mathcal{L}_1$ adaptive control is very similar to hedging.

5.1.2 Short Period Example

The benchmark problem from Section 2.1 is used again and hedging is applied to account for the dynamic constraints in the input channel. To also account for the dynamics of the structural filters, these are implemented in the input channel as shown in Figure 4.20.

The predictor based approach is applied in the following, as it leads to a reduced number of adaptive parameters compared to the direct approach. The reason for this is that only the control effectiveness is estimated, but not the feedforward gain. The control law is given by

$$\eta_{CMD} = \frac{1}{\hat{\lambda}}(\eta_{BL} + \eta_{AD}), \tag{5.26}$$

where η_{BL} is given by Eq.(2.12) and

$$\eta_{AD} = \hat{\boldsymbol{\theta}}_y^T \mathbf{y}_P^+ = \begin{bmatrix} \hat{\theta}_{n_Z} & \hat{\theta}_q & \hat{\theta}_{e_I} \end{bmatrix} [n_Z \quad q \quad e_I]^T. \tag{5.27}$$

Uncertainties in the dynamics of the integral error e_I have not to be expected, and hence, for the predictor based approach uncertainties in $\hat{\theta}_{e_I}$ are not expected. Therefore $\hat{\theta}_{e_I}$ is not adapted, what is realized by setting the respective value in $\boldsymbol{\Gamma}_y$ to zero. As $\hat{\lambda}$ must be bounded away form zero, $\hat{\lambda}$ is constrained to $\hat{\lambda} \in [0.3,3]$ by projection (see Section 5.2.2).

Furthermore, the predictor is now modified by hedging the control deficiency as shown in Eq.(5.16). The control deficiency $\Delta\eta$ is calculated from the actuator and sensor dynamics and from the time delay given by Eq.(2.6)-(2.8). This means it is assumed that a perfect model of the dynamics in input channel is available. Equivalently, we could of course use a measurement of the control deficiency. According to Eq.(5.20) the linear predictor is defined, where by inserting the control law of Eq.(5.26) the predictor results in the reference model. Hence, the desired performance is specified by a linear reference model, given by the augmented plant dynamics of Eq.(2.13) without pitch-up nonlinearity, the base line control law of Eq.(2.12), and the hedging signal

$$\begin{aligned} \dot{\hat{\mathbf{x}}}_P^+ &= \mathbf{A}_P^+ \hat{\mathbf{x}}_P^+ + \mathbf{b}_P^+ \eta_M + \mathbf{b}_r^+ r + \mathbf{b}_P^+ \hat{\lambda}\, \Delta\eta \\ \hat{\mathbf{y}}_P^+ &= \mathbf{C}_P^+ \hat{\mathbf{x}}_P^+ + \mathbf{d}_P^+ \eta_M \\ \eta_M &= \mathbf{k}_y^T \hat{\mathbf{y}}_P^+ + k_r r, \end{aligned} \tag{5.28}$$

where

$$\Delta\eta(s) = (G_{act}(s) G_{fil}(s) G_{del}(s) - 1) \cdot \eta_{CMD}(s), \tag{5.29}$$

From Eq.(4.10) the following update laws for the controller parameters are used

$$\begin{aligned} \dot{\hat{\boldsymbol{\theta}}}_y &= \boldsymbol{\Gamma}_y \mathbf{y}_P^+ \cdot \mathbf{e}_P^T \mathbf{P} \mathbf{b}_{P,n_Z}^+ \\ \dot{\hat{\lambda}} &= -\Gamma_\Lambda \eta \cdot \mathbf{e}_P^T \mathbf{P} \mathbf{b}_{P,n_Z}^+ \end{aligned} \tag{5.30}$$

The adaptive controller is assembled by Eq.(5.26)-Eq.(5.30).

From the genetic algorithm (see Section 4.4) the controller parameters in Table 5.1 are obtained and the cost function yields $J = 0.217$. From the adaptive gains it is obvious that the hedging allows much larger values, and thus much faster adaptation is achieved. The fast adaptation is also apparent from the low value of the cost function and the good tracking of the reference response shown in Figure 5.2, and the tracking error in Figure 5.3. Furthermore, a fast adjustment of the parameters is observed (see Figure 5.5) without any oscillations in the input channel (see Figure 5.4).

$\boldsymbol{\Gamma}_y$	Γ_Λ
$\begin{bmatrix} 315.3 & 0 & 0 \\ 0 & 25.5 & 0 \\ 0 & 0 & 0 \end{bmatrix}$	3.1

Table 5.1: Controller parameters

Considering robust stability, the time delay margin is shown in Table 5.2, and it can be seen that it is highly reduced in comparison to the baseline controller. However, a reduction has to be expected as it is a well know trade off in adaptive control [66] [73] [145].

	1g CMD	2g CMD
TDM	0.08	0.01

Table 5.2: Time delay margins

In Figure 5.6 - Figure 5.11 the robust performance is evaluated for a 1g, and a 2g command, respectively. It can be concluded from Figure 5.6 that the robustness w.r.t. matched uncertainties is improved and a good transient response is achieved by the adaptive augmentation for a 1g command. In difference for the 2g command the robustness in the case of increased plant stability is reduced by the adaptive controller as shown in Figure 5.9. This nonlinear behavior is objectionable and it would be preferable to attain a linear performance w.r.t. the command signal. In general - also for the 1g command - the domains where certain levels of performance are achieved change in comparison to the baseline controller, and especially for increased pitch damping the adaptive controller shows worse performance. The reason for this is that the adaptive controller tries to drive the response of the plant exactly to the reference trajectory. This means, in the case of increased pitch damping the response might get slower but can still be within the level 1 boundary. However the adaptive controller will try to accelerate the response by reducing that damping gain. Without additional dynamics in the input channel (e.g. actuator) this works and the desired response can be matched perfectly. In presence of the input-channel-dynamics a cancelation of the pitch damping uncertainty is still possible and the hedging provides a feasible trajectory of the reference model, but it leads to an increased overshoot due to the reaction deficit caused by the additional dynamics. A solution for this problem is suggested in the next section. The robustness w.r.t. unmatched uncertainties is shown in Figure 5.7 and Figure 5.10 and it can be seen, that compared to the baseline controller it is reduced in an intolerable manner. In the following section also an approach to account for the unmatched uncertainties, by modification of the reference model, is suggested. Comparing the robustness w.r.t. uncertainties in the input gain to

the baseline controller it is obvious from Figure 5.8 and Figure 5.10 that the robustness w.r.t. increased input gain can be reduced by the adaptive augmentation.

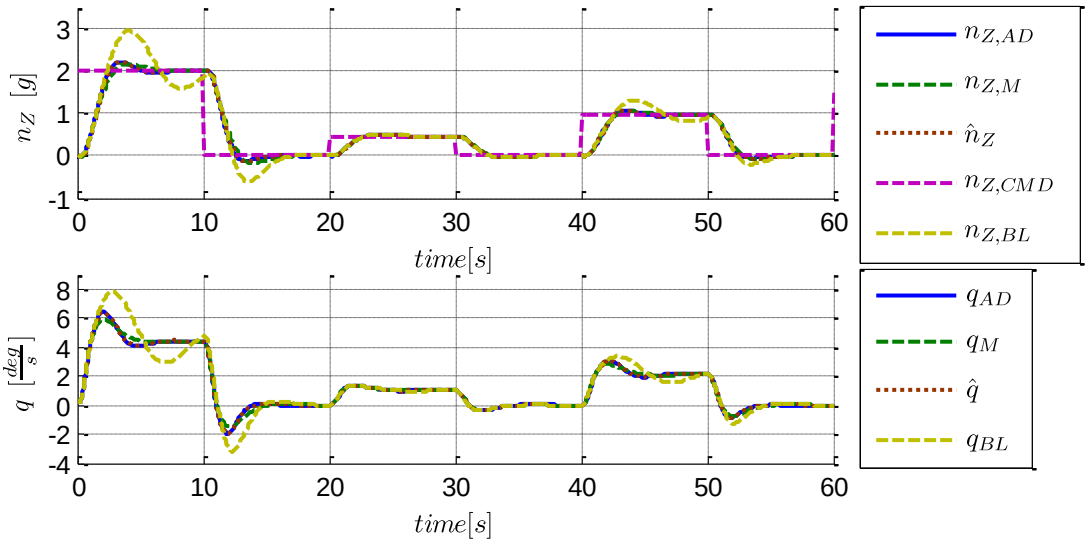

Figure 5.2: Load factor and pitch rate response

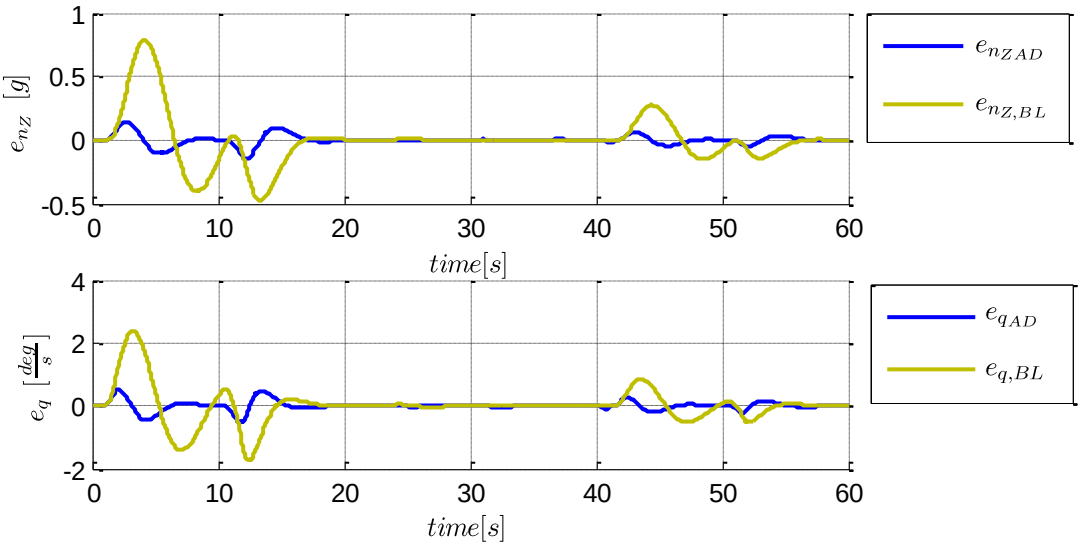

Figure 5.3: Error in load factor and pitch rate response

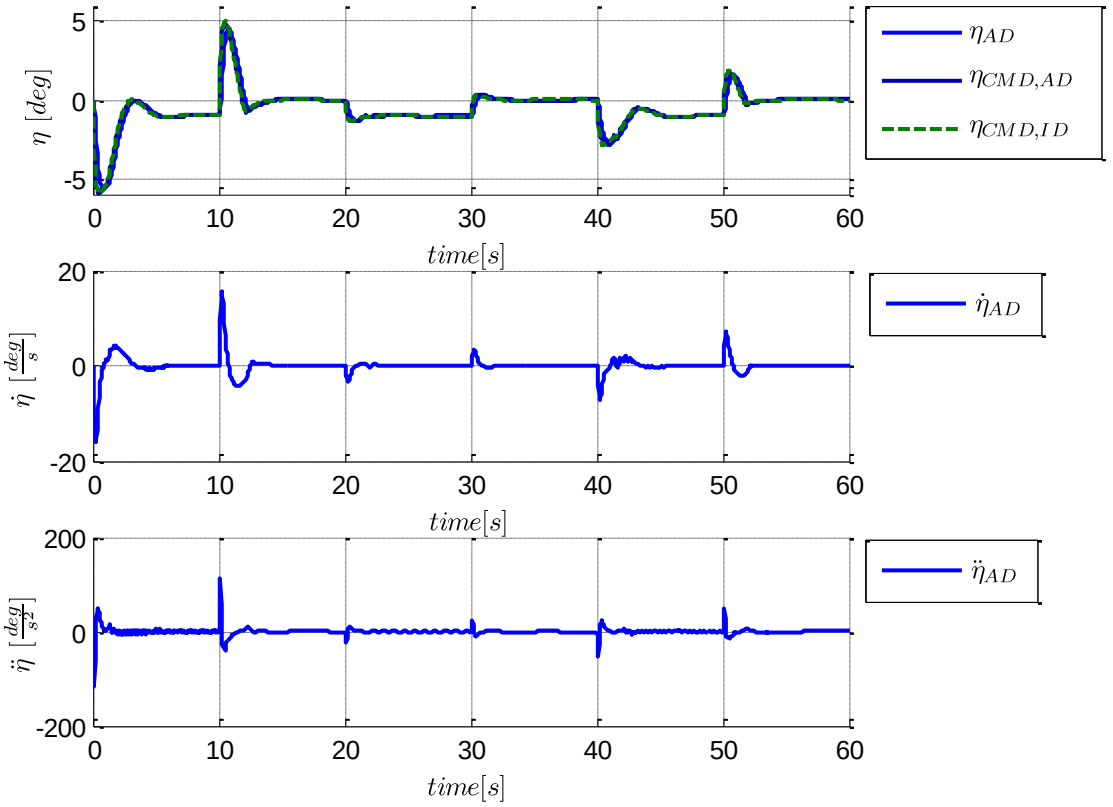

Figure 5.4: Elevator deflection and rate

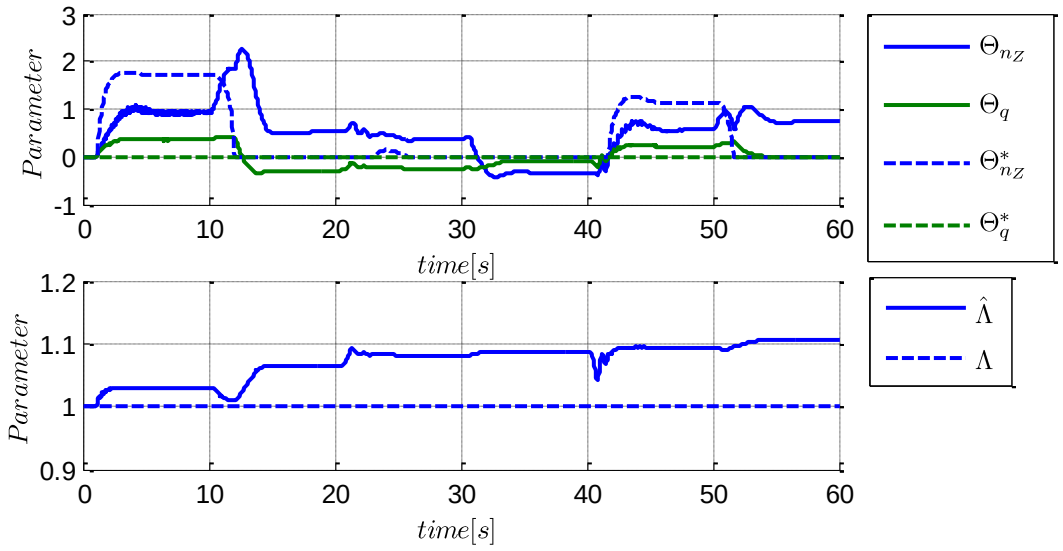

Figure 5.5: Adaptive controller parameters

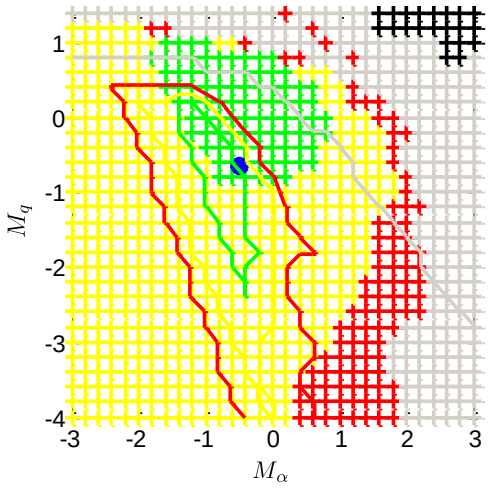

Figure 5.6: Robust perfomance w.r.t. M_α and M_q; $n_{z,CMD}$=1

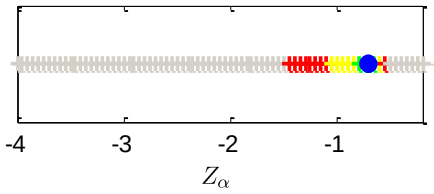

Figure 5.7: Robust perfomance w.r.t. Z_α; $n_{z,CMD}$=1

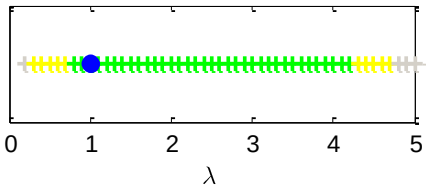

Figure 5.8: Robust perfomance w.r.t. λ $n_{z,CMD}$=1

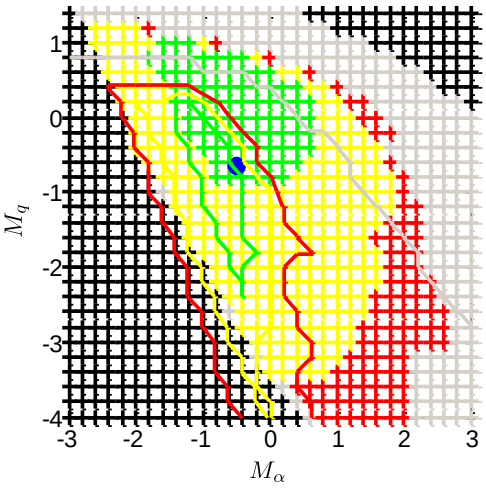

Figure 5.9: Robust perfomance w.r.t. M_α and M_q; $n_{z,CMD}$=2

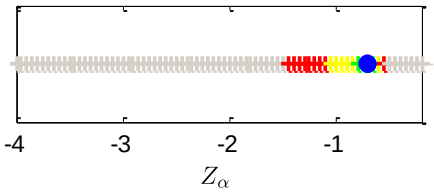

Figure 5.10: Robust perfomance w.r.t. Z_α; $n_{z,CMD}$=2

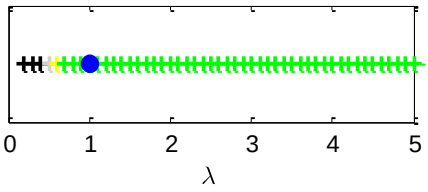

Figure 5.11: Robust perfomance w.r.t. λ $n_{z,CMD}$=2

5.1.3 Matched Uncertainties

From the previous simulation results two problems could be identified. At first it could be observed that the response w.r.t. certain matched uncertainties can deteriorate compared to the baseline controller. The reason for this lies in the restrictive reference model, which "allows" only one trajectory for each state. However, from the performance requirements a certain envelope for the response can be specified. This means there exists a set of reference models, where all models within this set provide adequate performance. Vice versa this means that there exists a set of matched plant uncertainties, and as long as the plant uncertainties are within this set no augmentation of the control is required, because even in presence of the uncertainties the performance is still adequate. For simplicity, again no nonlinear and constant uncertainties are considered. The suggested modification is shown for direct MRAC and predictor based MRAC in the following.

5.1.3.1 Direct MRAC

The plant dynamics is assumed to be given by

$$\dot{\mathbf{x}}_P = \mathbf{A}_M \mathbf{x}_P + \mathbf{B}_M \mathbf{r} + \mathbf{B}_P \boldsymbol{\Lambda}\left(\mathbf{u} - \boldsymbol{\Theta}_x^{*\,T} \mathbf{x}_P - \boldsymbol{\Theta}_r^* \mathbf{r}\right), \tag{5.31}$$

where nonlinear and constant uncertainties are omitted. In the following it is considered that there is a set of matched uncertainties for which the plant dynamics show acceptable performance. Let this set of uncertainties be defined by a hypercube with the limits $\boldsymbol{\Theta}_{x,M,max}^*$ and $\boldsymbol{\Theta}_{x,M,min}^*$. Hence, if the uncertainties are within the hypercube the feedback gain must not be adjusted.

Therefore, it is suggested to modify the adaptive control signal in a way that it only provides a contribution if the estimated parameters $\boldsymbol{\Theta}_x$ are outside the hypercube:

$$\mathbf{u} = \left(\boldsymbol{\Theta}_x^T - \Delta\boldsymbol{\Theta}_{x,M}^T\right)\mathbf{x}_P + \boldsymbol{\Theta}_r \mathbf{r}, \tag{5.32}$$

where the signal $\Delta\boldsymbol{\Theta}_{x,M}$ is a limited version of $\boldsymbol{\Theta}_x$ which is restricted to the hypercube

$$\Delta\boldsymbol{\Theta}_{x,M} = \begin{cases} \boldsymbol{\Theta}_x & for \quad \boldsymbol{\Theta}_{x,M,min}^* \leq \boldsymbol{\Theta}_x \leq \boldsymbol{\Theta}_{x,M,max}^* \\ \boldsymbol{\Theta}_{x,M,max}^* & for \quad \boldsymbol{\Theta}_x > \boldsymbol{\Theta}_{x,M,max}^* \\ \boldsymbol{\Theta}_{x,M,min}^* & for \quad \boldsymbol{\Theta}_x < \boldsymbol{\Theta}_{x,M,min}^* \end{cases}. \tag{5.33}$$

As we are not trying to cancel plant uncertainties within the hypercube we also need to modify the reference model, because the adaptive control law is still trying to drive the error to zero. To make this possible in the region were $\boldsymbol{\Theta}_x$ is within the hypercube we adjust the reference model in this domain instead of the control signal such that

$$\dot{\mathbf{x}}_M = \mathbf{A}_M \mathbf{x}_M + \mathbf{B}_M\, \mathbf{r} - \mathbf{B}_P \widehat{\boldsymbol{\Lambda}} \Delta\boldsymbol{\Theta}_{x,M}^T \mathbf{x}_P. \tag{5.34}$$

Using the definition of the control error $\mathbf{e}_C$ from Eq.(4.6) we can rewrite

$$\dot{\mathbf{x}}_M = \left(\mathbf{A}_M - \mathbf{B}_P \widehat{\boldsymbol{\Lambda}} \Delta\boldsymbol{\Theta}_{x,M}^T\right)\mathbf{x}_M + \mathbf{B}_M\, \mathbf{r} - \mathbf{B}_P \widehat{\boldsymbol{\Lambda}} \Delta\boldsymbol{\Theta}_{x,M}^T \mathbf{e}_C. \tag{5.35}$$

For stability proof we can build the error dynamics from Eq.(5.31), Eq.(5.32), and Eq.(5.34)

$$\begin{aligned}\dot{\mathbf{e}}_C &= \mathbf{A}_M\mathbf{e}_C+\mathbf{B}_P\boldsymbol{\Lambda}\left(\left(\boldsymbol{\Theta}_x^T-\Delta\boldsymbol{\Theta}_{x,M}^T\right)\mathbf{x}_P+\boldsymbol{\Theta}_r\mathbf{r}-{\boldsymbol{\Theta}_x^*}^T\mathbf{x}_P-\boldsymbol{\Theta}_r^*\mathbf{r}\right)+\mathbf{B}_P\widehat{\boldsymbol{\Lambda}}\Delta\boldsymbol{\Theta}_{x,M}^T\mathbf{x}_P \\ &= \mathbf{A}_M\mathbf{e}_C+\mathbf{B}_P\boldsymbol{\Lambda}\left(\widetilde{\boldsymbol{\Theta}}_x^T\mathbf{x}_P+\widetilde{\boldsymbol{\Theta}}_r\mathbf{r}\right)-\mathbf{B}_P\widetilde{\boldsymbol{\Lambda}}\Delta\boldsymbol{\Theta}_{x,M}^T\mathbf{x}_P.\end{aligned} \tag{5.36}$$

Again it can be seen that $\mathbf{A}_M$ must be Hurwitz. Furthermore, the additional term $\mathbf{B}_P\widetilde{\boldsymbol{\Lambda}}\Delta\boldsymbol{\Theta}_{x,M}^T\mathbf{x}_P$ requires the estimation of $\widehat{\boldsymbol{\Lambda}}$ and to derive adaptation laws which guarantee stability the Lyapunov function candidate from Eq.(5.11) can be used

$$\mathrm{V}=\tfrac{1}{2}\mathbf{e}_C^T\mathbf{P}\mathbf{e}_C+\tfrac{1}{2}\mathrm{Tr}\left[\widetilde{\boldsymbol{\Theta}}_x^T\boldsymbol{\Gamma}_x^{-1}\widetilde{\boldsymbol{\Theta}}_x\boldsymbol{\Lambda}\right]+\tfrac{1}{2}\mathrm{Tr}\left[\widetilde{\boldsymbol{\Theta}}_r\boldsymbol{\Gamma}_r^{-1}\widetilde{\boldsymbol{\Theta}}_r^T\boldsymbol{\Lambda}\right]+\tfrac{1}{2}\mathrm{Tr}\left[\widetilde{\boldsymbol{\Lambda}}\boldsymbol{\Gamma}_\Lambda^{-1}\widetilde{\boldsymbol{\Lambda}}^T\right], \tag{5.37}$$

The time derivative of Eq.(5.37) is given by

$$\begin{aligned}\dot{\mathrm{V}} = &-\frac{1}{2}\mathbf{e}_C^T\mathbf{Q}\mathbf{e}_C \\ &+\mathrm{Tr}\left[\widetilde{\boldsymbol{\Theta}}_x^T\left(\boldsymbol{\Gamma}_x^{-1}\dot{\widetilde{\boldsymbol{\Theta}}}_x+\mathbf{x}_P\cdot\mathbf{e}_C^T\mathbf{P}\mathbf{B}_P\right)\boldsymbol{\Lambda}\right] \\ &+\mathrm{Tr}\left[\widetilde{\boldsymbol{\Theta}}_r\left(\boldsymbol{\Gamma}_r^{-1}\dot{\widetilde{\boldsymbol{\Theta}}}_r^T+\mathbf{r}\cdot\mathbf{e}_C^T\mathbf{P}\mathbf{B}_P\right)\boldsymbol{\Lambda}\right] \\ &+\mathrm{Tr}\left[\widetilde{\boldsymbol{\Lambda}}\left(\boldsymbol{\Gamma}_\Lambda^{-1}\dot{\widetilde{\boldsymbol{\Lambda}}}^T-\Delta\boldsymbol{\Theta}_{x,M}\mathbf{x}_P\cdot\mathbf{e}_C^T\mathbf{P}\mathbf{B}_P\right)\right]\end{aligned} \tag{5.38}$$

From Eq.(5.38) it follows that with the update laws

$$\begin{aligned}\dot{\widetilde{\boldsymbol{\Theta}}}_x &= -\boldsymbol{\Gamma}_x\mathbf{x}_P\cdot\mathbf{e}_C^T\mathbf{P}\mathbf{B}_P \\ \dot{\widetilde{\boldsymbol{\Theta}}}_r^T &= -\boldsymbol{\Gamma}_r\mathbf{r}\cdot\mathbf{e}_C^T\mathbf{P}\mathbf{B}_P \\ \dot{\widetilde{\boldsymbol{\Lambda}}}^T &= \boldsymbol{\Gamma}_\Lambda\Delta\boldsymbol{\Theta}_{x,M}^T\mathbf{x}_P\cdot\mathbf{e}_C^T\mathbf{P}\mathbf{B}_P\end{aligned} \quad\Leftrightarrow\quad \begin{aligned}\dot{\boldsymbol{\Theta}}_x &= -\boldsymbol{\Gamma}_x\mathbf{x}_P\cdot\mathbf{e}_C^T\mathbf{P}\mathbf{B}_P \\ \dot{\boldsymbol{\Theta}}_r^T &= -\boldsymbol{\Gamma}_r\mathbf{r}\cdot\mathbf{e}_C^T\mathbf{P}\mathbf{B}_P \\ \dot{\widehat{\boldsymbol{\Lambda}}}^T &= -\boldsymbol{\Gamma}_\Lambda\Delta\boldsymbol{\Theta}_{x,M}^T\mathbf{x}_P\cdot\mathbf{e}_C^T\mathbf{P}\mathbf{B}_P\end{aligned} \tag{5.39}$$

the time derivative of the Lyapunov function becomes negative semi definite, and hence $\mathbf{e}_C$, $\widetilde{\boldsymbol{\Theta}}_x^T$, $\widetilde{\boldsymbol{\Theta}}_r$, and $\widetilde{\boldsymbol{\Lambda}}$ are bounded. Obviously it must be guaranteed that for all possible constant values of $\widehat{\boldsymbol{\Lambda}}$ and $\Delta\boldsymbol{\Theta}_{x,M}$, the reference model is stable. This means $\left(\mathbf{A}_M-\mathbf{B}_P\widehat{\boldsymbol{\Lambda}}\Delta\boldsymbol{\Theta}_{x,M}^T\right)$ must be Hurwitz. But for stability considerations, note that the adjustment of the reference model leads to a Linear Time Varying (LTV) system, with $\mathbf{A}_M^*(t)=\left(\mathbf{A}_M-\mathbf{B}_P\widehat{\boldsymbol{\Lambda}}\Delta\boldsymbol{\Theta}_{x,M}^T\right)$. This means stability of the reference model can not be guaranteed by the eigenvalues of $\mathbf{A}_M^*(t)$ [89]. A sufficient condition for stability of the reference model can for example be given when there exists a symmetric, positive definite $\mathbf{P}=\mathbf{P}^T\in\mathbb{R}^{n\times n}$ such that the Lyapunov equation

$$\mathbf{P}\mathbf{A}_M^*(t)+{\mathbf{A}_M^*}^T(t)\mathbf{P}=-\mathbf{Q}(t) \tag{5.40}$$

yields a symmetric, positive definite solution $\mathbf{Q}(t)=\mathbf{Q}^T(t)\in\mathbb{R}^{n\times n}$ for all $\mathbf{A}_M^*(t)$. However this condition is only sufficient and not necessary. It can also be argued that as long as the uncertainties are within the hypercube only the reference model is adjusted and no adaptive feedback is issued to the plant. Furthermore, as long as the real uncertainties are within the hypercube the plant is stable, as the hypercube defines the set of desired trajectories, which all should be stable. Hence for this case stability is guaranteed. In the case where the uncertainties lie outside the hypercube and they lead to an unstable plant, also the estimated parameters must eventually

leave the hypercube and in this moment the reference model becomes a stable LTI system.

The fact that the estimations of $\widehat{\mathbf{\Lambda}}$ and $\Delta\boldsymbol{\Theta}_{x,M}^{T}$ appear as product makes it difficult to guarantee that $\left(\mathbf{A}_M - \mathbf{B}_P\widehat{\mathbf{\Lambda}}\Delta\boldsymbol{\Theta}_{x,M}^{T}\right)$ provides the desired performance. Furthermore it also requires the boundedness of $\widehat{\mathbf{\Lambda}}$ to certain limits. Thus it would be beneficial if $\widehat{\mathbf{\Lambda}}$ would not appear, and as we will see in the next section, this is the case for predictor based MRAC.

5.1.3.2 Predictor Based MRAC

Nonlinear and constant uncertainties are not considered in the following and according to Eq.(4.29) the plant dynamics is given by

$$\dot{\mathbf{x}}_P = \mathbf{A}_M\mathbf{x}_P + \mathbf{B}_P\left(\mathbf{\Lambda}\mathbf{u} - \widehat{\boldsymbol{\Theta}}_x^{*\,T}\mathbf{x}_P\right). \tag{5.41}$$

Again it is assumed that for a set of uncertainties, within a hypercube defined by the limits $\widehat{\boldsymbol{\Theta}}_{x,M,max}^{*}$ and $\widehat{\boldsymbol{\Theta}}_{x,M,min}^{*}$, the plant shows adequate performance. Hence no adjustment of the feedback gains is necessary within the hypercube. This is achieved by adjusting the control law of Eq.(4.32) to

$$\mathbf{u} = \widehat{\mathbf{\Lambda}}^{-1}\left[\left(\widehat{\boldsymbol{\Theta}}_x^{T} - \Delta\widehat{\boldsymbol{\Theta}}_{x,M}^{T}\right)\mathbf{x}_P + \mathbf{K}_r\,\mathbf{r}\right]. \tag{5.42}$$

The signal $\Delta\widehat{\boldsymbol{\Theta}}_{x,M}$ is a limited version of $\widehat{\boldsymbol{\Theta}}_x$ which is restricted to the hypercube

$$\Delta\widehat{\boldsymbol{\Theta}}_{x,M} = \begin{cases} \widehat{\boldsymbol{\Theta}}_x & for \quad \widehat{\boldsymbol{\Theta}}_{x,M,min}^{*} \le \widehat{\boldsymbol{\Theta}}_x \le \widehat{\boldsymbol{\Theta}}_{x,M,max}^{*} \\ \widehat{\boldsymbol{\Theta}}_{x,M,max}^{*} & for \quad \widehat{\boldsymbol{\Theta}}_x > \widehat{\boldsymbol{\Theta}}_{x,M,max}^{*} \\ \widehat{\boldsymbol{\Theta}}_{x,M,min}^{*} & for \quad \widehat{\boldsymbol{\Theta}}_x < \widehat{\boldsymbol{\Theta}}_{x,M,min}^{*} \end{cases}. \tag{5.43}$$

As long as the estimation $\widehat{\boldsymbol{\Theta}}_x$ is within the hypercube the predictor from Eq.(4.30) should follow the plant dynamic, and for this no modification is necessary:

$$\dot{\hat{\mathbf{x}}}_P = \mathbf{A}_M\hat{\mathbf{x}}_P + \mathbf{B}_P\left(\widehat{\mathbf{\Lambda}}\mathbf{u} - \widehat{\boldsymbol{\Theta}}_x^{T}\mathbf{x}_P\right). \tag{5.44}$$

Inserting the control law from Eq.(5.42) in the predictor of Eq.(5.44) gives

$$\dot{\hat{\mathbf{x}}}_P = \mathbf{A}_M\hat{\mathbf{x}}_P + \mathbf{B}_M\,\mathbf{r} - \mathbf{B}_P\Delta\widehat{\boldsymbol{\Theta}}_{x,M}^{T}\mathbf{x}_P. \tag{5.45}$$

In comparison to the direct approach in the previous Section 5.1.3.1 the additional term $\mathbf{B}_P\Delta\widehat{\boldsymbol{\Theta}}_{x,M}^{T}\mathbf{x}_P$ does not contain the estimation of $\widehat{\mathbf{\Lambda}}$. This makes it easier to guarantee that all models in the set $\left(\mathbf{A}_M - \mathbf{B}_P\Delta\widehat{\boldsymbol{\Theta}}_{x,M}^{T}\right)$ provide the desired performance as only reasonable bounds for $\widehat{\boldsymbol{\Theta}}_{x,M,max}^{*}$ and $\widehat{\boldsymbol{\Theta}}_{x,M,min}^{*}$ must be chosen.

Building the error dynamics from Eq.(5.41) and Eq.(5.44) yields

$$\dot{\mathbf{e}}_P = \mathbf{A}_M\mathbf{e}_P + \mathbf{B}_P\left(\widetilde{\boldsymbol{\Theta}}_x^{T}\mathbf{x}_P + \widetilde{\mathbf{\Lambda}}\mathbf{u}\right) \tag{5.46}$$

This is a simplified version of the error dynamics from Section 4.4.1. Thus, the stability properties derived in Section 4.4.1 also hold, if the respective update laws (Eq.(4.38)) are applied.

5.1.4 Unmatched Uncertainties

The previously presented MRAC approaches all require the matching condition to hold. However, a real system might also have uncertainties that are not affine with respect to the available inputs, e. g. an aircraft that does not possess any controls to produce direct lift but the dependence of lift on the system states contains uncertainties. From the previous simulation example we could also see that the applied adaptive control approach could lead to reduced robustness with respect to unmatched uncertainties. Since the applied approach is explicitly designed with the assumption of a matching condition this is not surprising, especially when we consider the update law, which tries to reduce the error between the states of the reference model and the plant to zero. However, in the case of unmatched uncertainties it is obvious that it is not possible for the complete error vector to converge to zero, as not all states of the system can be controlled independently. Thus, not all state reference trajectories, generated by the reference model, can be followed simultaneously. A similar problem occurs in the presence of actuator dynamics. In this case the matching condition is a-priori not satisfied, because during transients all uncertainties in the plant become unmatched and only with sufficiently fast decaying actuator dynamics the assumptions can "approximately" be satisfied. To account for the deficiency due to actuator dynamics it was suggested in [44] to additionally estimate the system dynamics and modify the reference model with this estimation so that exact matching can be achieved. In the following a similar approach is used, however the focus will be to account for unmatched uncertainties due to limited control authority, rather than due to actuator dynamics. It should be noted that the following modification is only necessary for the direct approach and the predictor based approach. For the indirect approach, if $rank(\mathbf{B}_P) < n$ the identification model is automatically adjusted based on the estimation of the unmatched uncertainties (see Eq.(4.14)).

For the sake of simplicity in the following only linear uncertainties are considered. By taking into account additional unmatched uncertainties $\widehat{\boldsymbol{\Theta}}_{x,um}^{*}$, the plant dynamics from Eq.(4.5) can be extended to

$$\dot{\mathbf{x}}_P = \mathbf{A}_M \mathbf{x}_\mathrm{P} + \mathbf{B}_M \mathbf{r} + \mathbf{B}_P \boldsymbol{\Lambda}\left(\mathbf{u} - \boldsymbol{\Theta}_x^{*T} \mathbf{x}_P - \boldsymbol{\Theta}_r^{*} \mathbf{r}\right) - \mathbf{B}_{P,um} \widehat{\boldsymbol{\Theta}}_{x,um}^{*T} \mathbf{x}_\mathrm{P}, \tag{5.47}$$

where $\mathbf{B}_{P,um} \in \boldsymbol{R}^{n\times(n-m)}$ spans the null space of $\mathbf{B}_P^T$, this means it holds that $\mathbf{B}_P^T \mathbf{B}_{P,um} = \mathbf{0}$. This also means $\mathbf{B}_{P,um}$ defines an input matrix that is orthogonal to $\mathbf{B}_P$ and the concatenation spans the complete state space: $rank[\mathbf{B}_P, \mathbf{B}_{P,um}] = n$. If the plant dynamics are denote in a suitable way for the predictor based approach, according to Eq.(4.29) they can be given by

$$\dot{\mathbf{x}}_P = \mathbf{A}_M \mathbf{x}_P + \mathbf{B}_P\left(\boldsymbol{\Lambda}\mathbf{u} - \widehat{\boldsymbol{\Theta}}_x^{*T} \mathbf{x}_P\right) - \mathbf{B}_{P,um} \widehat{\boldsymbol{\Theta}}_{x,um}^{*T} \mathbf{x}_\mathrm{P}. \tag{5.48}$$

5.1.4.1 Direct MRAC

To account for the deficiency due to the unmatched uncertainties a similar term, which utilizes an estimation of the uncertainties $\widehat{\boldsymbol{\Theta}}_{x,um}$, is added to the dynamics of the reference model, similar to the hedging introduced in the previous section:

$$\dot{\mathbf{x}}_M = \mathbf{A}_M\mathbf{x}_M + \mathbf{B}_M\mathbf{r} - \mathbf{B}_{P,um}\widehat{\boldsymbol{\Theta}}_{x,um}^T\mathbf{x}_P \tag{5.49}$$

Using the definition of the control error $\mathbf{e}_C$ from Eq.(4.6) we can rewrite

$$\dot{\mathbf{x}}_M = \left(\mathbf{A}_M - \mathbf{B}_{P,um}\widehat{\boldsymbol{\Theta}}_{x,um}^T\right)\mathbf{x}_M + \mathbf{B}_M\mathbf{r} - \mathbf{B}_{P,um}\widehat{\boldsymbol{\Theta}}_{x,um}^T\mathbf{e}_C \tag{5.50}$$

The idea is to adjust the reference model by $\mathbf{B}_{P,um}\widehat{\boldsymbol{\Theta}}_{x,um}^T\mathbf{x}_P$ such that it follows the plant dynamics in the presence of unmatched uncertainties. Due to the adjustment of the reference model it becomes a LTV system $\mathbf{A}_M^*(t) = \mathbf{A}_M - \mathbf{B}_{P,um}\widehat{\boldsymbol{\Theta}}_{x,um}^T$ and stability cannot be guaranteed by the location of the eigenvalues [89]. Although this does not guarantee stability it must be obviously satisfied that $\left(\mathbf{A}_M - \mathbf{B}_{P,um}\widehat{\boldsymbol{\Theta}}_{x,um}^T\right)$ is Hurwitz, and this can be ensured by constraining $\widehat{\boldsymbol{\Theta}}_{x,um}^T$ to a convex set (can be achieved by projection). Note, that limiting $\boldsymbol{\Theta}_{x,um}^T$ to a set where $\mathbf{A}_M^*(t)$ is Hurwitz makes sense, as the real uncertainties $\boldsymbol{\Theta}_{x,um}^{*T}$ should also lie in this set. A sufficient condition for stability of the reference model in Eq.(5.50) can for example be given when there exists a symmetric, positive definite $\mathbf{P} = \mathbf{P}^T \in \mathbb{R}^{n\times n}$ such that the Lyapunov equation

$$\mathbf{P}\mathbf{A}_M^*(t) + \mathbf{A}_M^{*T}(t)\mathbf{P} = -\mathbf{Q}(t) \tag{5.51}$$

yields a symmetric, positive definite solution $\mathbf{Q}(t) = \mathbf{Q}^T(t) \in \mathbb{R}^{n\times n}$ for all $\mathbf{A}_M^*(t)$. However this condition is only sufficient and not necessary. In the case when $\mathbf{A}_M^*(t)$ changes with a dynamics that is much slower than the dynamics of $\mathbf{A}_M$ stability can also be guaranteed from a time scale separation argument.

From Eq.(5.47) and (5.52) the following error dynamics results

$$\begin{aligned}\dot{\mathbf{e}}_C &= \mathbf{A}_M\mathbf{e}_C + \mathbf{B}_P\boldsymbol{\Lambda}\left(\widetilde{\boldsymbol{\Theta}}_x^T\mathbf{x}_P + \widetilde{\boldsymbol{\Theta}}_r\mathbf{r}\right) + \mathbf{B}_{P,um}\left(\widehat{\boldsymbol{\Theta}}_{x,um}^T\mathbf{x}_P - \widehat{\boldsymbol{\Theta}}_{x,um}^{*T}\mathbf{x}_P\right)\\ &= \mathbf{A}_M\mathbf{e}_C + \mathbf{B}_P\boldsymbol{\Lambda}\left(\widetilde{\boldsymbol{\Theta}}_x^T\mathbf{x}_P + \widetilde{\boldsymbol{\Theta}}_r\mathbf{r}\right) + \mathbf{B}_{P,um}\widetilde{\widehat{\boldsymbol{\Theta}}}_{x,um}^T\mathbf{x}_P\end{aligned} \tag{5.52}$$

By choosing a Lyapunov function candidate of the form

$$\mathrm{V} = \frac{1}{2}\mathbf{e}_C^T\mathbf{P}\mathbf{e}_C + \frac{1}{2}\mathrm{Tr}\left[\widetilde{\boldsymbol{\Theta}}_x^T\boldsymbol{\Gamma}_x^{-1}\widetilde{\boldsymbol{\Theta}}_x\boldsymbol{\Lambda}\right] + \frac{1}{2}\mathrm{Tr}\left[\widetilde{\boldsymbol{\Theta}}_r\boldsymbol{\Gamma}_r^{-1}\widetilde{\boldsymbol{\Theta}}_r^T\boldsymbol{\Lambda}\right] + \frac{1}{2}\mathrm{Tr}\left[\widetilde{\widehat{\boldsymbol{\Theta}}}_{x,um}^T\boldsymbol{\Gamma}_{x,um}^{-1}\widetilde{\widehat{\boldsymbol{\Theta}}}_{x,um}\right] \tag{5.53}$$

the following update law for $\widehat{\boldsymbol{\Theta}}_{x,um}$ can be derived to render the time derivative of the Lyapunov function negative semi definite

$$\dot{\widehat{\boldsymbol{\Theta}}}_{x,um} = -\boldsymbol{\Gamma}_{x,um}\mathbf{x}_P \cdot \mathbf{e}_C^T\mathbf{P}\mathbf{B}_{P,um} \tag{5.54}$$

Following from the Lyapunov analysis stability of $\mathbf{e}_C$, $\widetilde{\boldsymbol{\Theta}}_x$, $\widetilde{\boldsymbol{\Theta}}_r$, and $\widetilde{\widehat{\boldsymbol{\Theta}}}_{x,um}$ is also guaranteed.

With the suggested approach the reference model is adjusted such that it follows the plant in the presence of unmatched uncertainties. On the one side the restrictive matching condition is removed as the reference model remains achievable, but on the

other hand the response of the reference model might be changed in a way such that it does not satisfy the desired specifications. In particular, if the desired behavior is specified in terms of the poles, the desired pole location given by the original reference model is not maintained in the presence of the feedback $\mathbf{B}_{P,um}\widehat{\mathbf{\Theta}}_{x,um}^{T}\mathbf{x}_P$.

Therefore, for a single input system, an additional feedback $\mathbf{b}_P \cdot \mathbf{k}(\widehat{\mathbf{\Theta}}_{x,um}) \cdot \mathbf{x}_P$ can be applied to the reference model based on the estimated unmatched uncertainty that maintains the desired pole location.

$$\dot{\mathbf{x}}_M = \mathbf{A}_M\mathbf{x}_M + \mathbf{b}_M\mathbf{r} - \mathbf{B}_{P,um}\widehat{\mathbf{\Theta}}_{x,um}^{T}\mathbf{x}_P + \mathbf{b}_P\mathbf{k}(\widehat{\mathbf{\Theta}}_{x,um})\,\mathbf{x}_P \tag{5.55}$$

For a single input system $\mathbf{k}(\widehat{\mathbf{\Theta}}_{x,um})$ can be determined as an analytic function of $\widehat{\mathbf{\Theta}}_{x,um}$, which is derived from standard pole placement.

5.1.4.2 Predictor Based MRAC

For the predictor based MRAC the approach is very similar to the direct case of the prior section. Thus the predictor dynamics is adjusted by the estimated unmatched uncertainties

$$\dot{\hat{\mathbf{x}}}_P = \mathbf{A}_M\hat{\mathbf{x}}_P + \mathbf{B}_P\left(\widehat{\mathbf{\Lambda}}\mathbf{u} - \widehat{\mathbf{\Theta}}_x^{T}\mathbf{x}_P\right) - \mathbf{B}_{P,um}\widehat{\mathbf{\Theta}}_{x,um}^{T}\mathbf{x}_P. \tag{5.56}$$

where the additional term $\mathbf{B}_{P,um}\widehat{\mathbf{\Theta}}_{x,um}^{T}\mathbf{x}_P$ is the same as in Eq.(5.48).

The error dynamics obtained from Eq.(5.48) and Eq.(4.55) is given by

$$\dot{\mathbf{e}}_P = \mathbf{A}_M\mathbf{e}_P + \mathbf{B}_P\left(\widetilde{\widehat{\mathbf{\Theta}}}_x^{T}\mathbf{x}_P + \widetilde{\mathbf{\Lambda}}\mathbf{u}\right) + \mathbf{B}_{P,um}\widetilde{\widehat{\mathbf{\Theta}}}_{x,um}^{T}\mathbf{x}_P \tag{5.57}$$

Choosing the Lyapunov function candidate

$$\mathrm{V} = \frac{1}{2}\mathbf{e}_P^{T}\mathbf{P}\mathbf{e}_P + \frac{1}{2}\mathrm{Tr}\left[\widetilde{\widehat{\mathbf{\Theta}}}_x^{T}\mathbf{\Gamma}_x^{-\mathbf{1}}\widetilde{\widehat{\mathbf{\Theta}}}_x\right] + \frac{1}{2}\mathrm{Tr}\left[\widetilde{\mathbf{\Lambda}}\mathbf{\Gamma}_\Lambda^{-\mathbf{1}}\widetilde{\mathbf{\Lambda}}^{T}\right] + \frac{1}{2}\mathrm{Tr}\left[\widetilde{\widehat{\mathbf{\Theta}}}_{x,um}^{T}\mathbf{\Gamma}_{x,um}^{-\mathbf{1}}\widetilde{\widehat{\mathbf{\Theta}}}_{x,um}\right], \tag{5.58}$$

leads to the same adaptation law for $\widetilde{\widehat{\mathbf{\Theta}}}_{x,um}$ as it was given in Eq.(5.54)

$$\dot{\widehat{\mathbf{\Theta}}}_{x,um} = -\mathbf{\Gamma}_{x,um}\mathbf{x}_P \cdot \mathbf{e}_P^{T}\mathbf{P}\mathbf{B}_{P,um} \tag{5.59}$$

5.1.5 Short Period Example

In the following the adaptive control approach from Section 5.1.2 is used and additionally the suggested modifications from Section 5.1.3 and Section 5.1.4 are applied.

For a set of matched uncertainties the baseline controller still provides level 1 performance, and therefore, according to Section 5.1.3, the adaptive control law is adjusted such that within the hypercube defined by $\widehat{\boldsymbol{\theta}}_{y,M,max}^{*T} = [0 \quad 0 \quad 0]$ and $\widehat{\boldsymbol{\theta}}_{y,M,min}^{*T} = [-0.5 \quad -1.2 \quad 0]$ no adaptive feedback is generated. This is achieved by modification of the adaptive control law of Eq.(5.27) according to Eq.(5.42)

$$\eta_{AD} = \widehat{\boldsymbol{\theta}}_y^{T}\mathbf{y}_P^{+} - \Delta\widehat{\boldsymbol{\theta}}_{y,M}^{T}\mathbf{y}_P^{+}, \tag{5.60}$$

where $\Delta\widehat{\boldsymbol{\theta}}_{y,M}$ is defined on the basis of Eq.(5.43):

$$\Delta\widehat{\boldsymbol{\theta}}_{y,M} = \begin{cases} \widehat{\boldsymbol{\theta}}_y & for \quad \widehat{\boldsymbol{\theta}}^*_{y,M,min} \leq \widehat{\boldsymbol{\theta}}_y \leq \widehat{\boldsymbol{\theta}}^*_{y,M,max} \\ \widehat{\boldsymbol{\theta}}^*_{y,M,max} & for \quad \widehat{\boldsymbol{\theta}}_y < \widehat{\boldsymbol{\theta}}^*_{y,M,max} \\ \widehat{\boldsymbol{\theta}}^*_{y,M,min} & for \quad \widehat{\boldsymbol{\theta}}_y > \widehat{\boldsymbol{\theta}}^*_{y,M,min} \end{cases}. \tag{5.61}$$

From Eq.(5.45) it follows that that an additional term is added to the predictor dynamics when the adaptive control law is inserted in the predictor dynamic. Thus, with the control law in Eq.(5.60) the predictor of Eq.(5.28) is modified to

$$\begin{aligned} \dot{\hat{\mathbf{x}}}_P^+ &= \mathbf{A}_P^+\hat{\mathbf{x}}_P^+ + \mathbf{b}_P^+\eta_M + \mathbf{b}_r^+ r + \mathbf{b}_P^+\hat{\lambda}\,\Delta\eta - \mathbf{b}_P^+\Delta\widehat{\boldsymbol{\theta}}_{y,M}^T\mathbf{y}_P^+ \\ \hat{\mathbf{y}}_P^+ &= \mathbf{C}_P^+\hat{\mathbf{x}}_P^+ + \mathbf{d}_P^+\eta_M \\ \eta_M &= \mathbf{k}_y^T\hat{\mathbf{y}}_P^+ + k_r r, \end{aligned} \tag{5.62}$$

To account for unmatched uncertainties, in the dynamics of the angle of attack, they are estimated according to Eq.(5.54)

$$\dot{\hat{\boldsymbol{\theta}}}_{y,um} = -\boldsymbol{\Gamma}_{y,um}\mathbf{y}_P^+ \cdot \mathbf{e}_P^T\mathbf{P}\mathbf{b}_{P,n_Z,um}^+, \tag{5.63}$$

and the reference model/predictor is adjusted based on Eq.(5.42). The unmatched input direction $\mathbf{b}_{P,n_Z,um}^+ = \begin{bmatrix}\mathbf{b}_{P,n_Z,um} \\ 0\end{bmatrix}$ is only determined by $\mathbf{b}_{P,n_Z,um}$, which is the nullspace of $\mathbf{b}_{P,n_Z}$ instead of $\mathbf{b}_{P,n_Z}^+$, as unmatched uncertainties in the dynamics of the integral error are not possible. To guarantee stability when the estimated unmatched parameters are fed back to the predictor, they are bounded by projection (see Section 5.2.2) with the minimum $\boldsymbol{\theta}_{y,um,min}^T = [-5.7 \quad -0.3 \quad 0]$ and the maximum $\boldsymbol{\theta}_{y,um,max}^T = [1.3 \quad 0.3 \quad 0]$.

Similar to the previous section a hedging signal is used so that the predictor model is given by

$$\begin{aligned} \dot{\hat{\mathbf{x}}}_P^+ &= \mathbf{A}_P^+\hat{\mathbf{x}}_P^+ + \mathbf{b}_P^+\eta_M + \mathbf{b}_r^+ r + \mathbf{b}_P^+\,\hat{\lambda}\,\Delta\eta - \mathbf{b}_P^+\Delta\widehat{\boldsymbol{\theta}}_{y,M}^T\mathbf{y}_P^+ - \mathbf{b}_{P,um}^+\widehat{\boldsymbol{\theta}}_{y,um}^T\mathbf{y}_P^+ \\ \hat{\mathbf{y}}_P^+ &= \mathbf{C}_P^+\hat{\mathbf{x}}_P^+ + \mathbf{d}_P^+\eta_M \\ u_M &= \mathbf{k}_y^T\hat{\mathbf{y}}_P^+ + k_r r \end{aligned} \tag{5.64}$$

The adaptive controller is assembled by Eq.(5.26), Eq.(5.60), Eq.(5.61), Eq.(5.64), Eq.(5.29), Eq.(5.30), and Eq.(5.63).

For the tuning, the approach from the previous example (see Section 5.1.2) was extended in order to maintain the robust performance of the baseline controller w.r.t. matched and unmatched uncertainties. Therefore certain constraints were added in the form that the system response w.r.t. a 1g command input has to satisfy level 1 HQ in the presence of the selected uncertainties. For the matched uncertainties the four point of Table 5.3 are considered, and for the unmatched uncertainties the two points in Table 5.4 are used. Furthermore, a constraint on the uncertainties in the control effectives that need to be tolerated is used. This constraint requires that for a 1g

command input the response satisfies level 2 HQ in the presence of the uncertainties given in Table 5.5.

	1	2	3	4
M_α	-1	-0.4	-0.4	-1.2
M_q	-0.6	-0.6	-2	0

Table 5.3: Matched uncertainties for parameter tuning

	1	2
Z_α	-3.5	-0.45

Table 5.4: Unmatched uncertainties for parameter tuning

	1	2
λ	0.4	3.5

Table 5.5: Input gain uncertainties for parameter tuning

From the genetic algorithm the controller parameters in Table 5.6 are obtained and the cost function yields $J = 0.174$. Considering performance and robustness, the following results shown in Table 5.7 and Figure 5.12 - Figure 5.21 are very similar to the previous section. However with the adaptation of the reference model, the robustness of the baseline controller w.r.t. unmatched uncertainties can be maintained. Hence, it seems that the proposed adaptive controller sufficiently solves the pitch-up problem. It must be noted that this improved robustness w.r.t. matched uncertainties has to be bought by a robustness reduction w.r.t. time delay (see Table 5.7). Additionally, also the robust performance w.r.t. input gain uncertainty is slightly reduced (see Figure 5.21).

$\boldsymbol{\Gamma}_y$	Γ_Λ	$\boldsymbol{\Gamma}_{y,um}$
$\begin{bmatrix} 333.0 & 0 & 0 \\ 0 & 25.9 & 0 \\ 0 & 0 & 0 \end{bmatrix}$	0.9	$\begin{bmatrix} 40.3 & 0 & 0 \\ 0 & 12.7 & 0 \\ 0 & 0 & 0 \end{bmatrix}$

Table 5.6: Controller parameter

	1g CMD	2g CMD
TDM	0.09	0.01

Table 5.7: Time delay margins

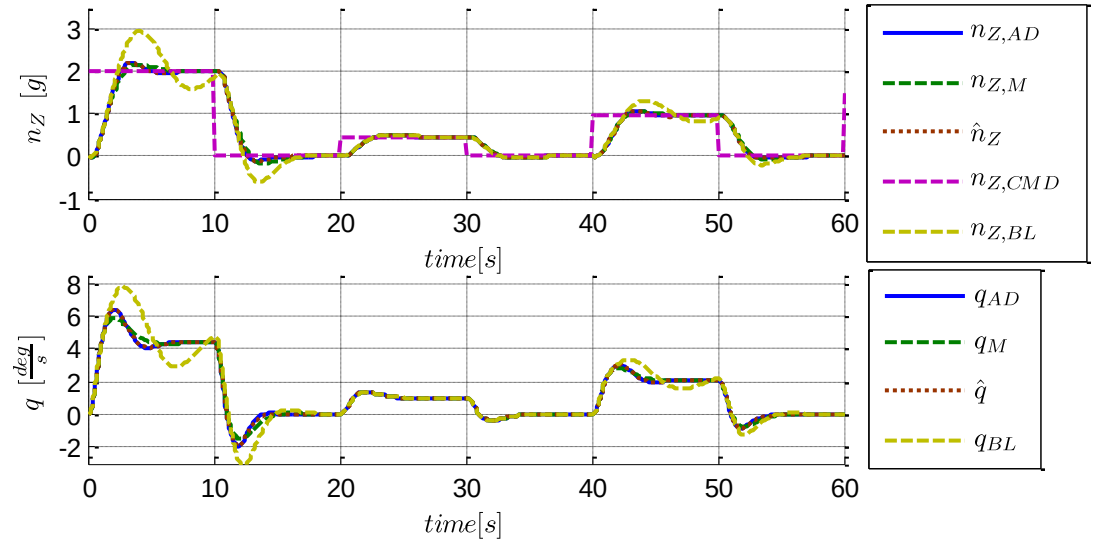

Figure 5.12: Load factor and pitch rate response

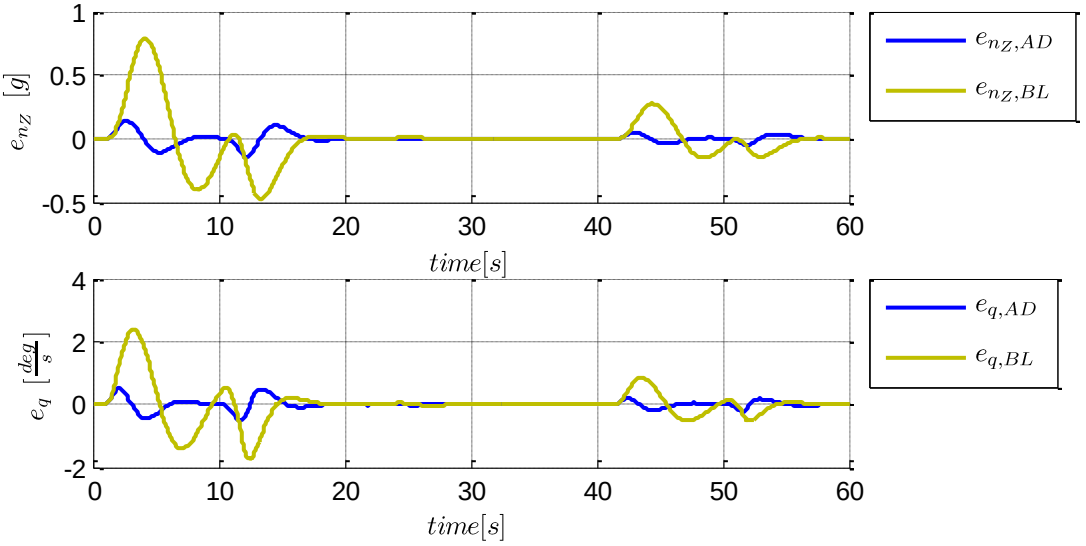

Figure 5.13: Error in load factor and pitch rate response

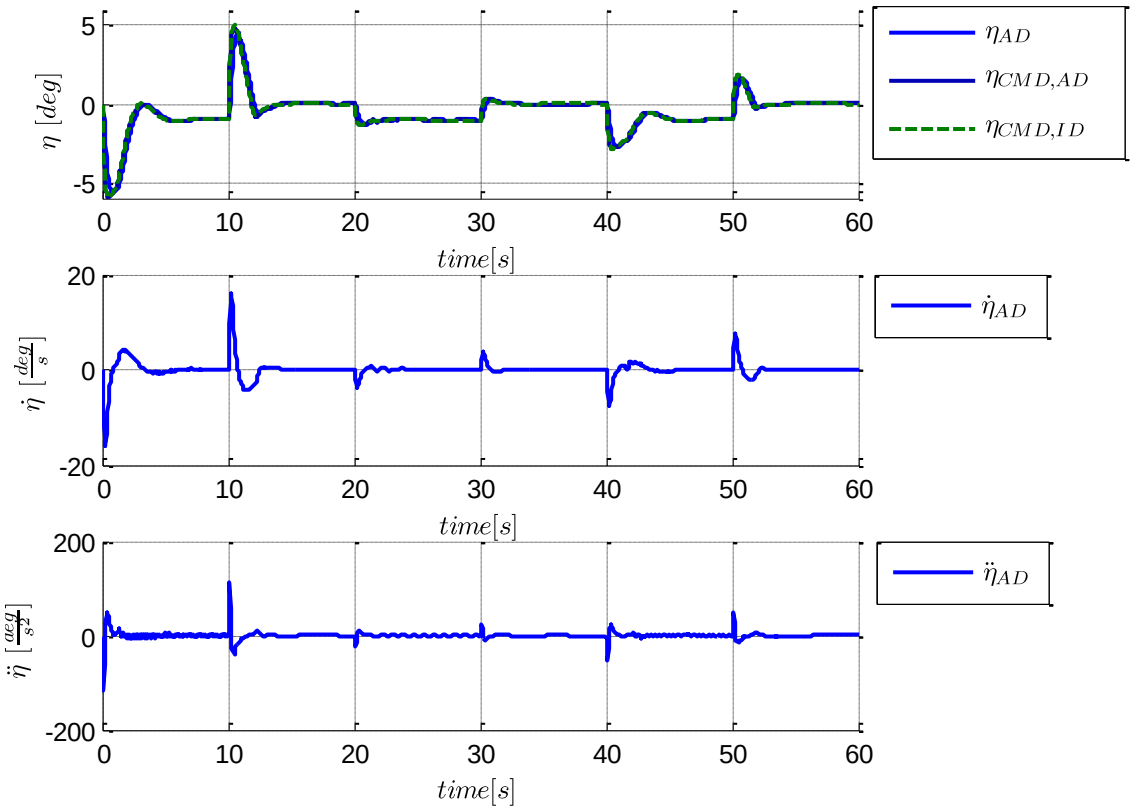

Figure 5.14: Elevator deflection and rate

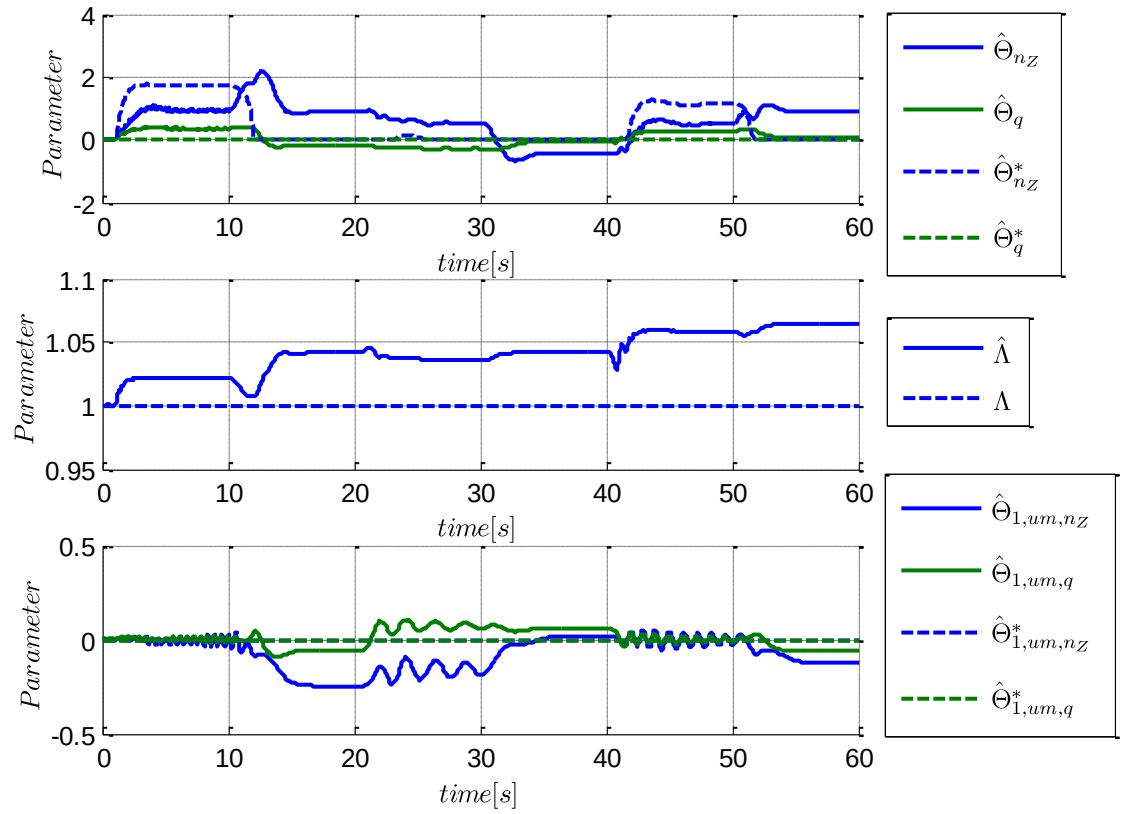

Figure 5.15: Adaptive controller parameters

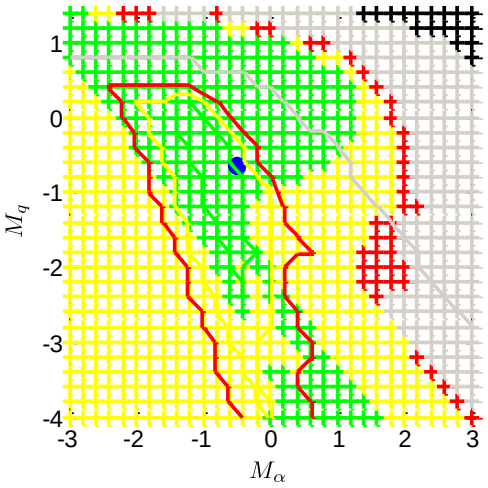

Figure 5.16: Robust perfomance w.r.t. M_α and M_q; $n_{Z,CMD}$=1

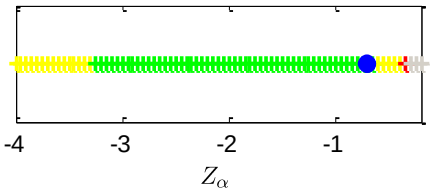

Figure 5.17: Robust perfomance w.r.t. Z_α; $n_{Z,CMD}$=1

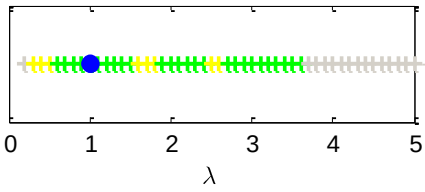

Figure 5.18: Robust perfomance w.r.t. λ $n_{Z,CMD}$=1

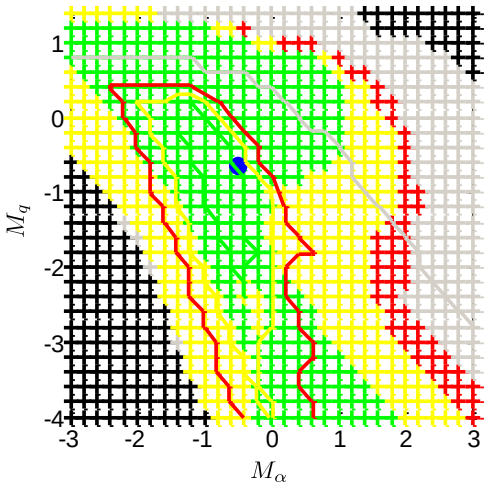

Figure 5.19: Robust perfomance w.r.t. M_α and M_q; $n_{Z,CMD}$=2

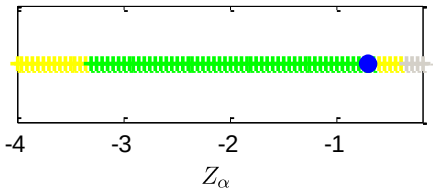

Figure 5.20: Robust perfomance w.r.t. Z_α; $n_{Z,CMD}$=2

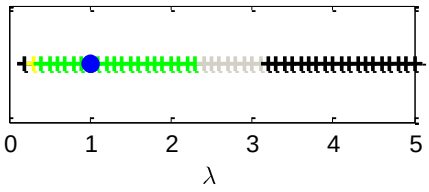

Figure 5.21: Robust perfomance w.r.t. λ $n_{Z,CMD}$=2

5.1.6 Error Feedback

The feedback of an error signal to the reference model was already suggested in [128], and lately the approach was revisited and the properties were further investigated in [129], [146], [147], [130], and [148]. Here the approach is motivated by the fact that for large uncertainties the initial error between reference model and plant can be large. As this error is used for the adaptation process it in turn leads to fast changes in the adaptive parameters, and thus also in the control signal. This means the large error can result in a very aggressive adaptation, which leads to oscillations in the input signal or even instability if the bandwidth of the input channel is restricted by actuator dynamics. To reduce the error during transients, the error can be fed back to the reference model in the form

$$\dot{\mathbf{x}}_M = \mathbf{A}_M\mathbf{x}_M + \mathbf{B}_M\mathbf{r} + \mathbf{L}(\mathbf{x}_P - \mathbf{x}_M), \tag{5.65}$$

where $\mathbf{L} \in \mathbb{R}^{\boldsymbol{n}}$ is a positive definite matrix, such that $\mathbf{A}_M - \mathbf{L}$ is Hurwitz. From Eq.(5.65) we can see that the reference model with error feedback has the form of a Luenberger observer, as it was interpreted in [130]. For large errors, during the transients the reference model is driven towards the plant dynamics, and thus the error signal is reduced. Furthermore, take for simplification $\mathbf{L} = k_e\mathbf{I}$ than with Eq.(4.2) the following error dynamics follows

$$\dot{\mathbf{e}}_C = (\mathbf{A}_M - k_e\mathbf{I})\mathbf{e}_C + \mathbf{B}_P\boldsymbol{\Lambda}\tilde{\boldsymbol{\Theta}}_C^T\boldsymbol{\omega}_C \tag{5.66}$$

For this error dynamics it is obvious that the error feedback shifts the eigenvalues further to left half-plane, and thus leads to a faster error dynamics. This also means that it does not affect the stability proof.

5.1.7 Short Period Example

5.1.7.1 Predictor Based MRAC with Parameter Calculation

Here the additional error feedback suggested in the Section 5.1.6 is applied to the adaptive controller of Section 5.1.6. Hence, only the reference model changes due to the added error feedback. From Eq.(5.64) we obtain

$$\begin{aligned}\dot{\hat{\mathbf{x}}}_P^+ &= \mathbf{A}_P^+\hat{\mathbf{x}}_P^+ + \mathbf{b}_P^+\eta_M + \mathbf{b}_r^+ r + \mathbf{b}_P^+\,\hat{\lambda}\,\Delta\eta - \mathbf{b}_P^+\Delta\hat{\boldsymbol{\theta}}_{y,M}^T\mathbf{y}_P^+ - \mathbf{b}_{P,um}^+\hat{\boldsymbol{\theta}}_{y,um}^T\mathbf{y}_P^+ - k_e\mathbf{e}_P \\ \hat{\mathbf{y}}_P^+ &= \mathbf{C}_P^+\hat{\mathbf{x}}_P^+ + \mathbf{d}_P^+\eta_M \\ \eta_M &= \mathbf{k}_y^T\hat{\mathbf{y}}_P^+ + k_r r,\end{aligned} \tag{5.67}$$

where instead of the matrix $\mathbf{L}$ from Eq.(5.65) a scalar parameter $k_e \geq 0$ is introduced for the error feedback.

The adaptive controller is assembled by Eq.(5.26), Eq.(5.60), Eq.(5.61), Eq.(5.67), Eq.(5.29), Eq.(5.30), and Eq.(5.63).

For the tuning the approach from Section 4.4 with the constraints form Section 5.1.5 is used. Additional a constraint is added, which requires a guaranteed time delay margin of 0.3 seconds for a step command with $n_{Z,CMD} = 1g$.

From the genetic algorithm the controller parameters in Table 5.8 are obtained and the cost function yields $J = 0.193$. The results of the robustness and performance evaluation are shown in Table 5.9 and Figure 5.23 - Figure 5.32, respectively. From the response in presence of the pitch-up nonlinearity (see Figure 5.23-Figure 5.26) it can be concluded that the adaptive controller improves the response. Moreover, it can be seen that, as demanded by the constraints, the error feedback leads to a much better time delay margin (compare Table 5.9 with Table 5.7). Compared to the results from Section 5.1.7.1, also a more homogenous performance for different inputs is achieved w.r.t. matched uncertainties (see Figure 5.27 and Figure 5.30) and w.r.t. uncertainties in the input gain (see Figure 5.29 and Figure 5.32). Although a reduction of the time delay margin has to be accepted the results lead to the conclusion that the adaptive controller solves the pitch-up problem and clearly improves the performance w.r.t. parametric uncertainties. In Figure 5.33 - Figure 5.38 the system responses for the uncertainties considered in Figure 5.27-Figure 5.32 are shown, but only points are plotted where the response satisfies at least level 3 HQ.

$\boldsymbol{\Gamma}_y$	Γ_Λ	$\boldsymbol{\Gamma}_{y,um}$	k_e
$\begin{bmatrix} 272.5 & 0 & 0 \\ 0 & 21.7 & 0 \\ 0 & 0 & 0 \end{bmatrix}$	1.9	$\begin{bmatrix} 30.8 & 0 & 0 \\ 0 & 7.3 & 0 \\ 0 & 0 & 0 \end{bmatrix}$	12.6

Table 5.8: Controller parameter

	1g CMD	2g CMD
TDM	0.31s	0.28s

Table 5.9: Time delay margins

Additionally the performance improvement over time is addressed by considering an input signal consisting of three consecutive steps as shown in Figure 5.22. For the third step of this input signal the performance is evaluated and shown in Figure 5.39 - Figure 5.41, and it is obvious that with additional excitation the performance improves even further over time. This can be also concluded from the associated system responses shown in Figure 5.42 - Figure 5.44, where the improvement over time can be clearly seen.

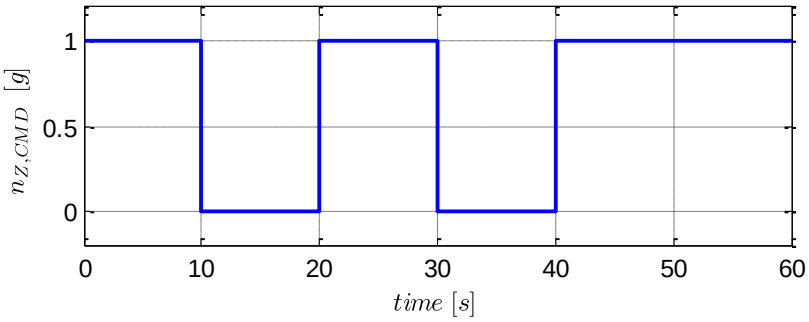

Figure 5.22: Three step input signal

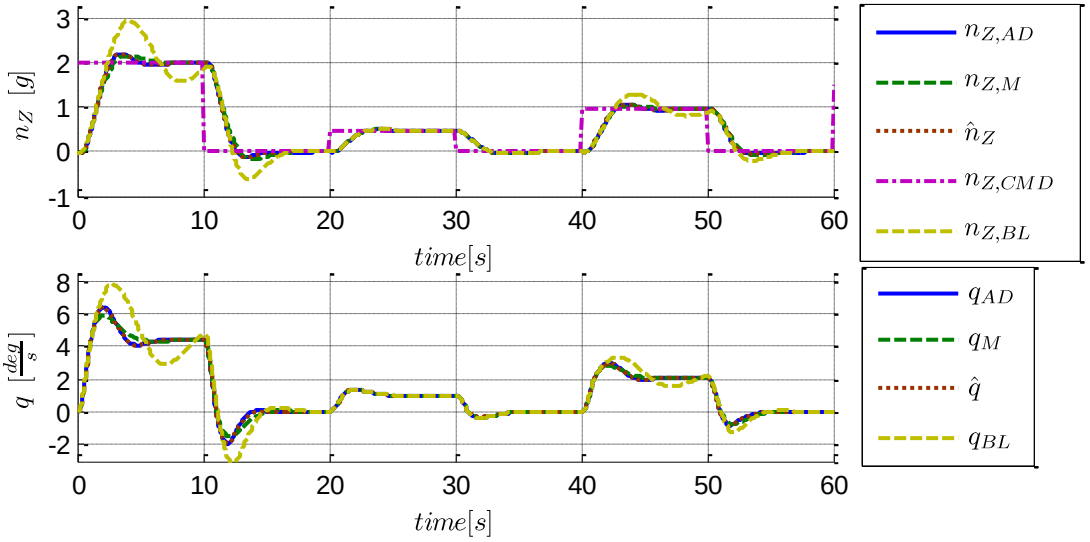

Figure 5.23: Load factor and pitch rate response

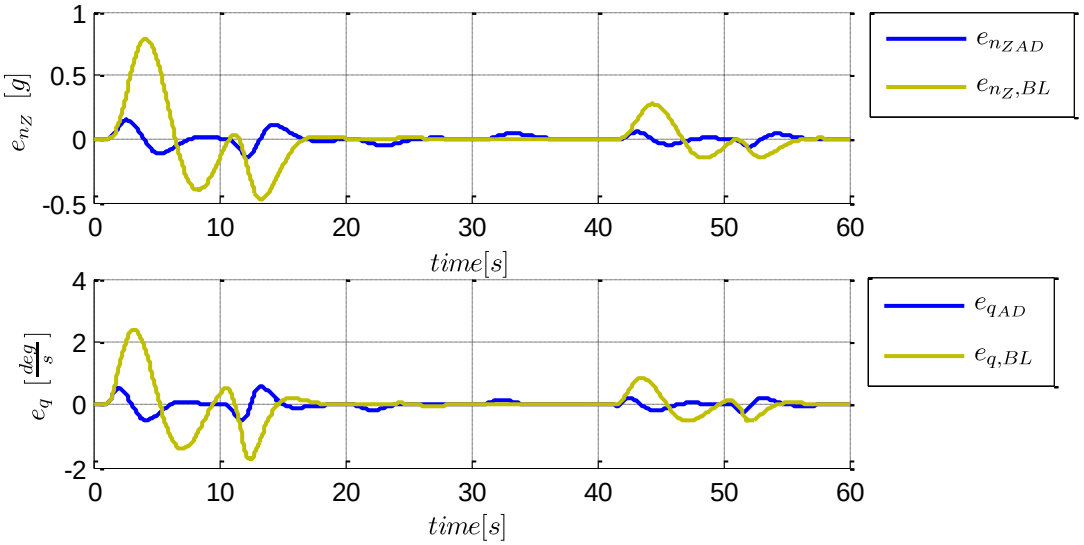

Figure 5.24: Error in load factor and pitch rate response

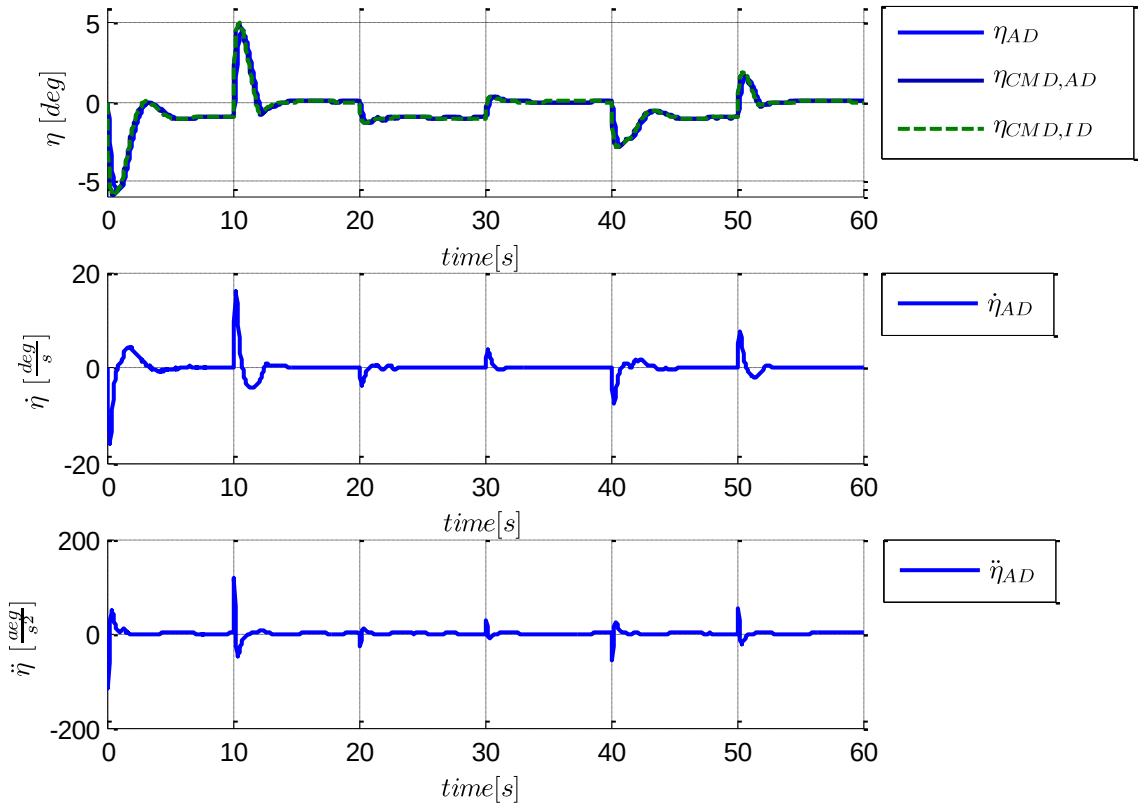

Figure 5.25: Elevator deflection and rate

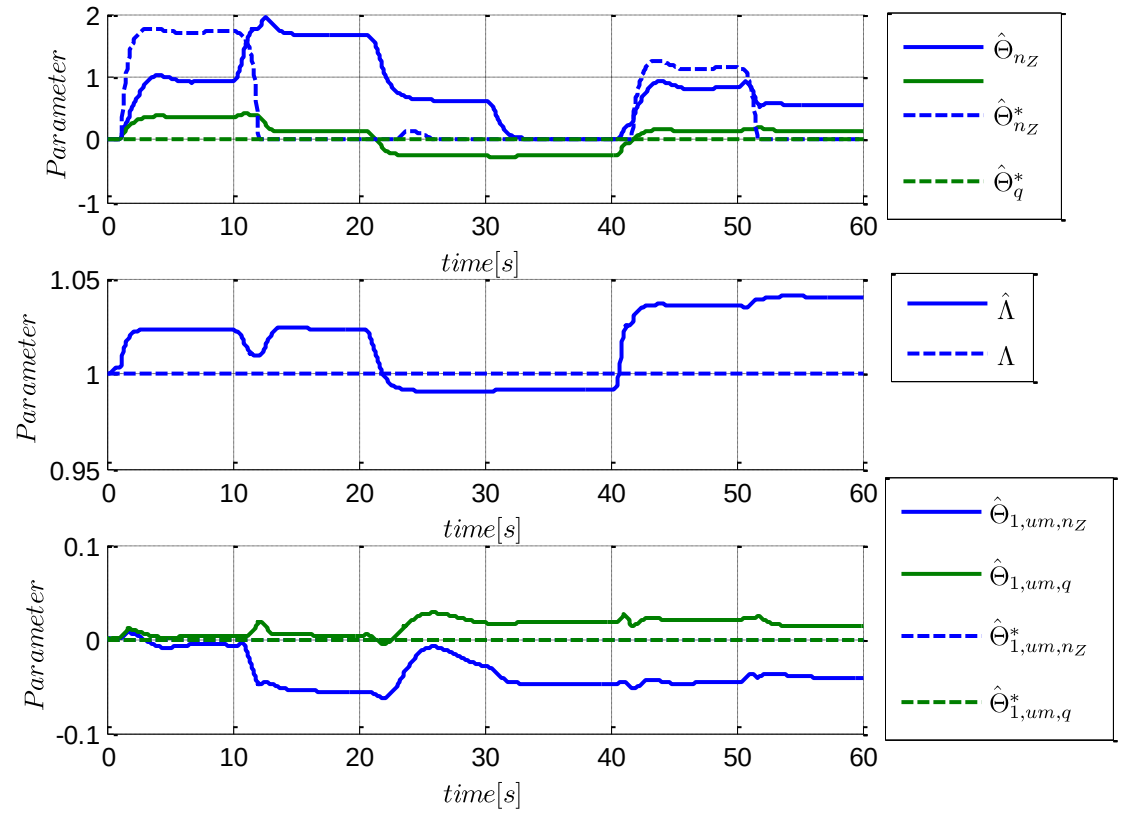

Figure 5.26: Adaptive controller parameters

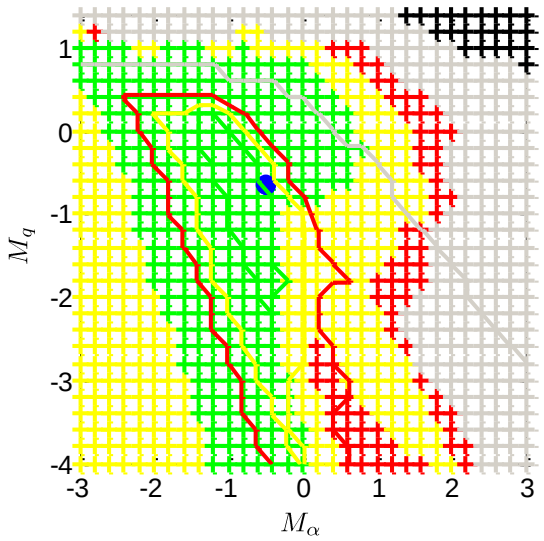

Figure 5.27: Robust perfomance w.r.t. M_α and M_q; $n_{z,CMD}$=1

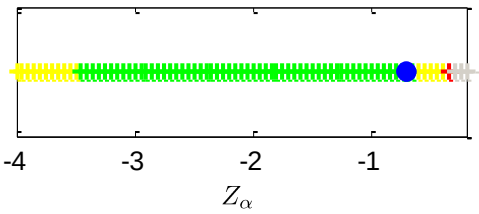

Figure 5.28: Robust perfomance w.r.t. Z_α; $n_{z,CMD}$=1

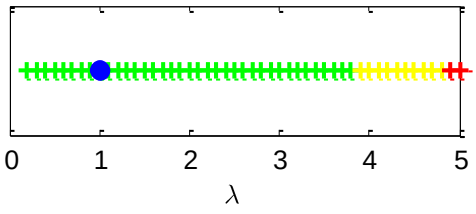

Figure 5.29: Robust perfomance w.r.t. λ $n_{z,CMD}$=1

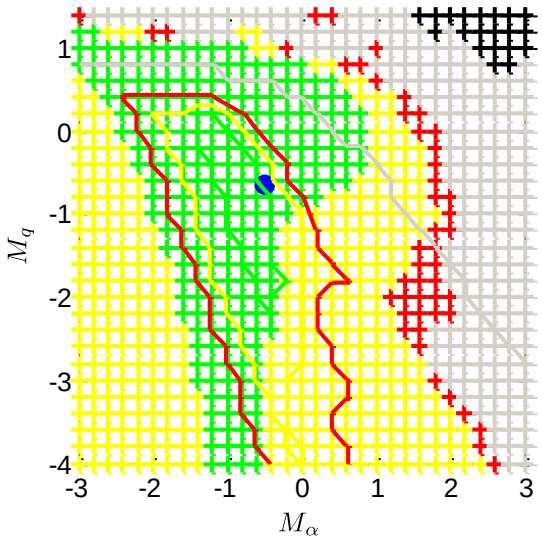

Figure 5.30: Robust perfomance w.r.t. M_α and M_q; $n_{z,CMD}$=2

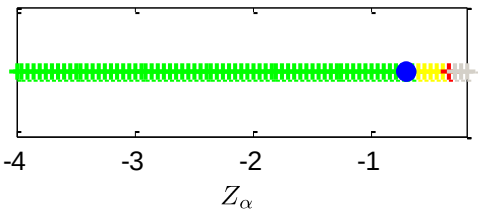

Figure 5.31: Robust perfomance w.r.t. Z_α; $n_{z,CMD}$=2

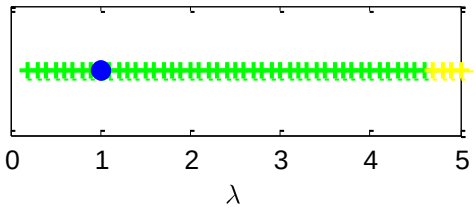

Figure 5.32: Robust perfomance w.r.t. λ $n_{z,CMD}$=2

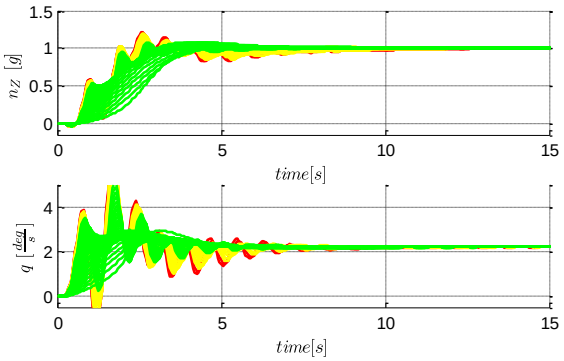

Figure 5.33: Response w.r.t. uncertain M_α and M_q; $n_{z,CMD}$=1

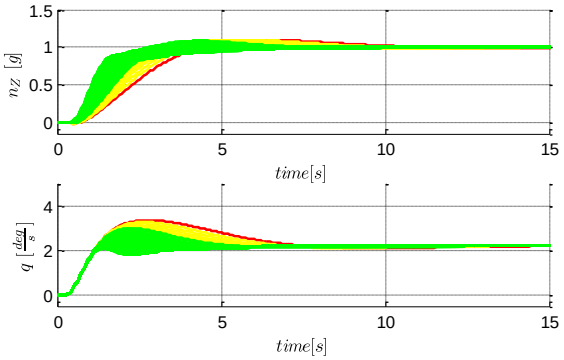

Figure 5.34: Response w.r.t. uncertain Z_α; $n_{z,CMD}$=1

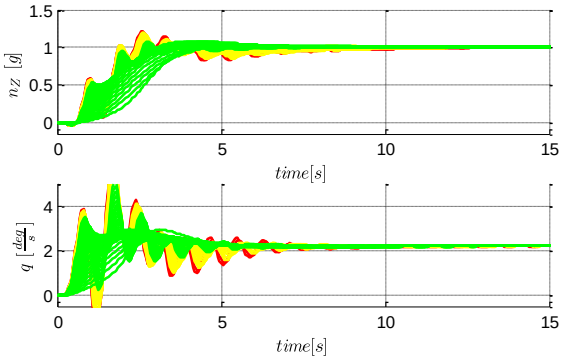

Figure 5.35: Response w.r.t. uncertain λ $n_{z,CMD}$=1

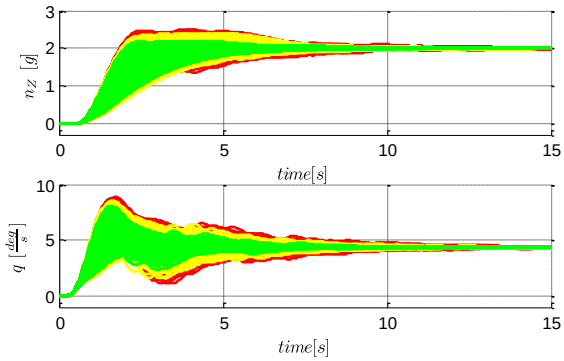

Figure 5.36: Response w.r.t. uncertain M_α and M_q; $n_{z,CMD}$=2

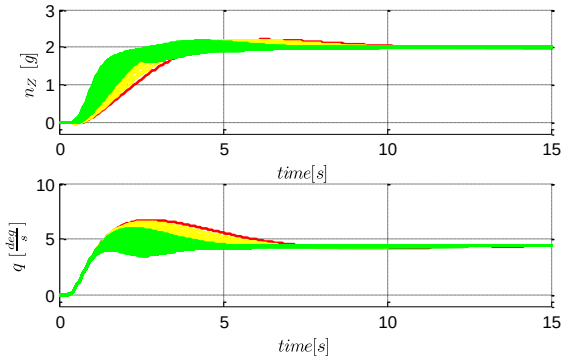

Figure 5.37: Response w.r.t. uncertain Z_α; $n_{z,CMD}$=2

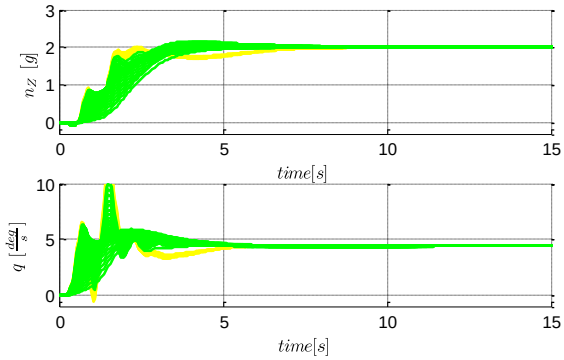

Figure 5.38: Response w.r.t. uncertain λ $n_{z,CMD}$=2

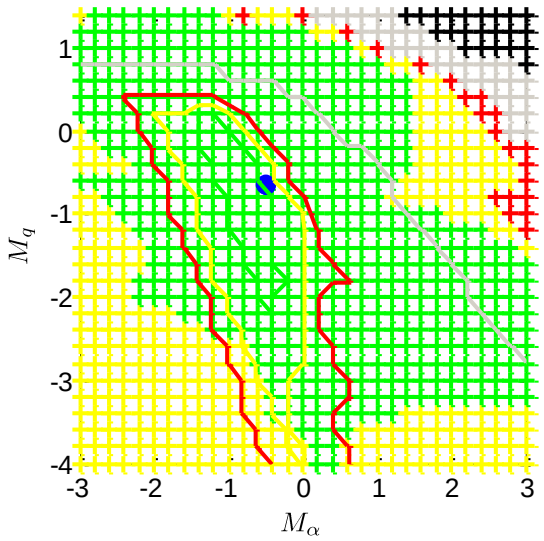

Figure 5.39: Robust perfomance w.r.t. M_α and M_q; $n_{z,CMD}$=1, 3rd step

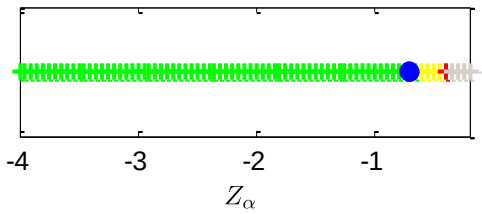

Figure 5.40: Robust perfomance w.r.t. Z_α; $n_{z,CMD}$=1, 3rd step

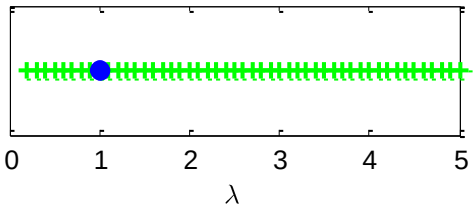

Figure 5.41: Robust perfomance w.r.t. λ $n_{z,CMD}$=1, 3rd step

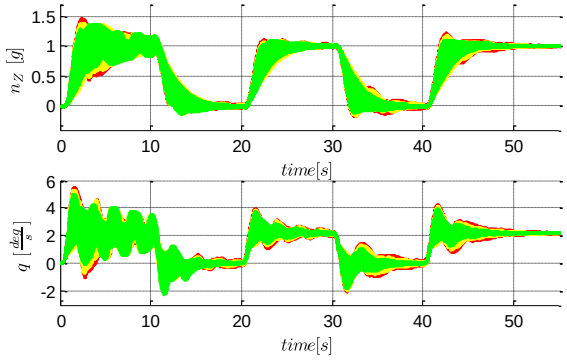

Figure 5.42: Response w.r.t. uncertain M_α and M_q; $n_{z,CMD}$=1, 3rd step

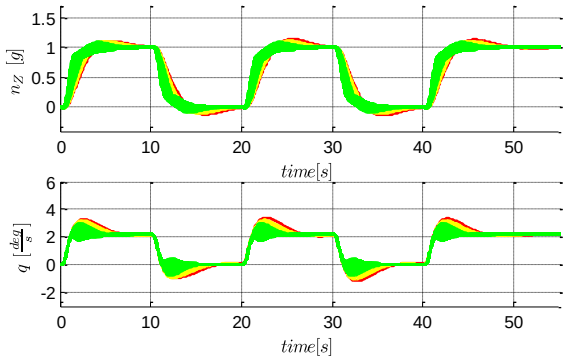

Figure 5.43: Response w.r.t. uncertain Z_α; $n_{z,CMD}$=1, 3rd step

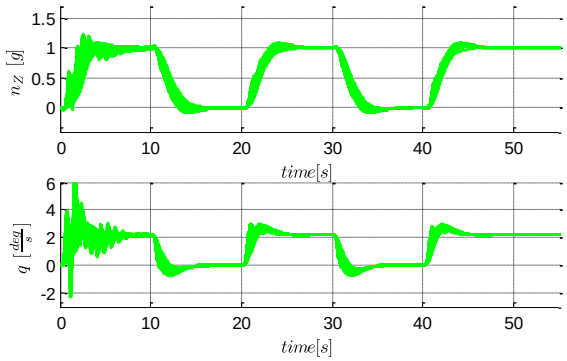

Figure 5.44: Response w.r.t. uncertain λ $n_{z,CMD}$=1, 3rd step

5.1.7.2 Indirect MRAC with Parameter Update

As mentioned, the predictor based approach with calculation of the controller gains, as it was implemented in the previous Section 5.1.7.1, is equivalent to the indirect approach with calculation of the controller gains. For comparison, in this section, the indirect approach with update of the controller gains according to Section 4.3.2 is applied.

The control law is given by

$$\eta_{CMD} = \eta_{BL} + \eta_{AD}, \tag{5.68}$$

where $\eta_{BL}$is given by Eq.(2.12) and

$$\eta_{AD} = \boldsymbol{\theta}_y^T \mathbf{y}_P^+ + \theta_r n_{Z,CMD} = [\theta_{n_Z} \quad \theta_q \quad \theta_{e_I}][n_Z \quad q \quad e_I]^T + \theta_r n_{Z,CMD}. \tag{5.69}$$

The controller parameters $\boldsymbol{\theta}_y^T$ and θ_r are updated from the estimated plant parameters according to Eq.(4.27)

$$\begin{aligned} \dot{\boldsymbol{\theta}}_y &= -\gamma_y \gamma_\varepsilon \boldsymbol{\varepsilon}_y^T \, \mathbf{b}_{P,n_Z}^+ \\ \dot{\theta}_r &= -\gamma_r \gamma_\varepsilon \boldsymbol{\varepsilon}_r^T \mathbf{b}_{P,n_Z}^+, \end{aligned} \tag{5.70}$$

and the plant parameters are estimated similar to Eq.(4.26)

$$\begin{aligned} \dot{\hat{\mathbf{A}}}_{P,n_Z}^{+T} &= -\boldsymbol{\Gamma}_A \left(\mathbf{y}_P \mathbf{e}_I^T \mathbf{P} + \gamma_\varepsilon \boldsymbol{\varepsilon}_y^T \right) \\ \dot{\hat{\lambda}} &= -\boldsymbol{\Gamma}_\lambda \left(\eta \mathbf{e}_I^T \mathbf{P} + \gamma_\varepsilon \left[\boldsymbol{\theta}_y^T \boldsymbol{\varepsilon}_y^T + \theta_r \boldsymbol{\varepsilon}_r^T \right] \right) \mathbf{b}_{P,n_Z}^+ \end{aligned}, \tag{5.71}$$

Because $\mathbf{y}_P^+$ is used instead of $\mathbf{x}_P^+$ not the original system matrix $\mathbf{A}_P^+$ is estimated, but the transformed version $\mathbf{A}_{P,n_Z}^+ = \mathbf{C}_P^+ \mathbf{A}_P^+ \mathbf{C}_P^{+^{-1}}$ describing the dynamics in the $\mathbf{y}_P^+$ state space. To provide the same parameter freedom as in Section 5.1.7.1, where the unmatched and matched uncertainties are estimated with different learning rates, the rows of the system matrix $\dot{\hat{\mathbf{A}}}_{P,n_Z}^+ = \begin{bmatrix} \dot{\hat{\mathbf{a}}}_{P,n_Z,1}^{+T} \\ \dot{\hat{\mathbf{a}}}_{P,n_Z,2}^{+T} \\ \dot{\hat{\mathbf{a}}}_{P,n_Z,3}^{+T} \end{bmatrix}$ are estimated separately. Furthermore, as no uncertainties are expected in the integral dynamics, the last row of $\hat{\mathbf{A}}_{P,n_Z}^+$ is not updated:

$$\begin{aligned} \dot{\hat{\mathbf{a}}}_{P,n_Z,1}^{+T} &= -\boldsymbol{\Gamma}_{A,1} \left(\mathrm{y}_{P,1} \mathbf{e}_I^T \mathbf{P} + \gamma_\varepsilon \boldsymbol{\varepsilon}_{y,1}^T \right) \\ \dot{\hat{\mathbf{a}}}_{P,n_Z,2}^{+T} &= -\boldsymbol{\Gamma}_{A,2} \left(\mathrm{y}_{P,2} \mathbf{e}_I^T \mathbf{P} + \gamma_\varepsilon \boldsymbol{\varepsilon}_{y,2}^T \right) \\ \dot{\hat{\mathbf{a}}}_{P,n_Z,3}^{+T} &= \mathbf{0} \\ \dot{\hat{\lambda}} &= -\boldsymbol{\Gamma}_\lambda \left(\eta \mathbf{e}_I^T \mathbf{P} + \gamma_\varepsilon \left[\boldsymbol{\theta}_y^T \boldsymbol{\varepsilon}_y^T + \theta_r \boldsymbol{\varepsilon}_r^T \right] \right) \mathbf{b}_{P,n_Z}^+. \end{aligned} \tag{5.72}$$

The closed loop estimation errors are defined by (see Eq.(4.25)):

$$\begin{aligned} \boldsymbol{\varepsilon}_x &= \left[\hat{\mathbf{A}}_{P,n_Z}^+ + \mathbf{b}_{P,n_Z}^+ \hat{\lambda} \boldsymbol{\theta}_y^T - \mathbf{A}_{M,n_Z}^+ \right] \\ \boldsymbol{\varepsilon}_r &= \left[\mathbf{b}_{P,n_Z}^+ \hat{\lambda} \theta_r - \mathbf{b}_{M,n_Z}^+ \right] \end{aligned} \tag{5.73}$$

To allow certain matched uncertainties, as it was suggested in 5.1.3 the closed loop estimation error $\boldsymbol{\varepsilon}_x$ is adjusted to

$$\begin{aligned}\boldsymbol{\varepsilon}_x &= \left[\widehat{\mathbf{A}}^{+}_{P,n_Z} - (\boldsymbol{\Delta}\widehat{\mathbf{A}}^{+}_{P,n_Z} - \widehat{\mathbf{A}}^{+}_{P,n_Z}(0)) + \mathbf{b}^{+}_{P}\hat{\lambda}\boldsymbol{\theta}^{T}_{y} - \mathbf{A}^{+}_{M,n_Z}\right] \\ \boldsymbol{\varepsilon}_r &= \left[\mathbf{b}^{+}_{P,n_Z}\hat{\lambda}\theta_r - \mathbf{b}^{+}_{M,n_Z}\right]\end{aligned}. \tag{5.74}$$

where $\widehat{\mathbf{A}}^{+}_{P,n_Z}(0)$ is the initial condition of $\widehat{\mathbf{A}}^{+}_{P,n_Z}$, and $\boldsymbol{\Delta}\widehat{\mathbf{A}}^{+}_{P,n_Z}$ is limited version of $\widehat{\mathbf{A}}^{+}_{P,n_Z}$

$$\boldsymbol{\Delta}\widehat{\mathbf{A}}^{+}_{P,n_Z} = \begin{cases} \widehat{\mathbf{A}}^{+}_{P,n_Z} & for \quad \mathbf{A}_{P,n_Z,min} \le \widehat{\mathbf{A}}^{+}_{P,n_Z} \le \mathbf{A}_{P,n_Z,max} \\ \mathbf{A}^{+}_{P,n_Z,max} & for \quad \widehat{\mathbf{A}}^{+}_{P,n_Z} < \mathbf{A}^{+}_{P,n_Z,max} \\ \mathbf{A}^{+}_{P,n_Z,min} & for \quad \widehat{\mathbf{A}}^{+}_{P,n_Z} > \mathbf{A}^{+}_{P,n_Z,min} \end{cases}$$

The limits for $\boldsymbol{\Delta}\widehat{\mathbf{A}}^{+}_{P,n_Z}$ are given by

$$\mathbf{A}^{+}_{P,n_Z,min} = \begin{bmatrix} -0.70 & 0.32 & 0 \\ -2.19 & -2.27 & 0 \\ -1 & 0 & 0 \end{bmatrix} \quad \mathbf{A}^{+}_{P,n_Z,max} = \begin{bmatrix} -0.70 & 0.32 & 0 \\ -1.52 & -0.64 & 0 \\ -1 & 0 & 0 \end{bmatrix}. \tag{5.75}$$

Applying hedging and error feedback to the identification model from Eq.(4.14) we obtain

$$\dot{\hat{\mathbf{x}}}^{+}_{P} = \mathbf{A}_P\hat{\mathbf{x}}^{+}_{P} + \mathbf{C}^{+^{-1}}_{P}\left[\widehat{\mathbf{A}}^{+}_{P,n_Z} - \mathbf{A}^{+}_{M,n_Z} + \mathbf{b}^{+}_{P,n_Z}\mathbf{k}^{T}_{y}\right]\mathbf{y}^{+}_{P} + \mathbf{b}^{+}_{P}\eta_{CMD} + \mathbf{b}^{+}_{r}r + \mathbf{b}^{+}_{P}\hat{\lambda}\,\Delta\eta - k_e\mathbf{e}_I \tag{5.76}$$

The complete adaptive controller is given by Eq.(5.69), Eq.(5.70), Eq.(5.72), Eq.(5.74), and Eq.(5.76).

The controller parameters given in Table 5.10 are obtained from the same tuning algorithm and the same constraints, that were used in the previous Section 5.1.7.1. These parameters yield an objective value of $J = 0.231$.

Numeric values for the time delay margin are provided in Table 5.11.

γ_y	γ_r	$\boldsymbol{\Gamma}_y$	$\boldsymbol{\Gamma}_{y,um}$	Γ_Λ	γ_ε	k_e
415.0	253.7	$\begin{bmatrix} 184.1 & 0 & 0 \\ 0 & 14.3 & 0 \\ 0 & 0 & 0 \end{bmatrix}$	$\begin{bmatrix} 267.4 & 0 & 0 \\ 0 & 57.9 & 0 \\ 0 & 0 & 28.3 \end{bmatrix}$	1.27	0.68	23.6

Table 5.10: Controller parameter

	1g CMD	2g CMD
TDM	0.32s	0.27s

Table 5.11: Time delay margins

From Figure 5.45 - Figure 5.48 it is obvious that the approach solves the pitch-up problem and good performance is achieved. However, from the robust performance assessment in Figure 5.49 - Figure 5.54 it has to be concluded that for the considered problem an update of the controller gains cannot achieve an improvement compared

to the direct calculation of the controller gains which was applied in form of the predictor based approach in the previous Section 5.1.7.1(compare Figure 5.27 - Figure 5.32). The reason therefore can be assigned to the additional update of the controller parameters. This introduces a low pass filter effect, and thus large uncertainties cannot be compensates as fast as with direct calculation of the controller gains. Furthermore, the inverse of the control effectiveness is not used directly in the control law, and due to this a larger number of parameters need to be estimated and updated.

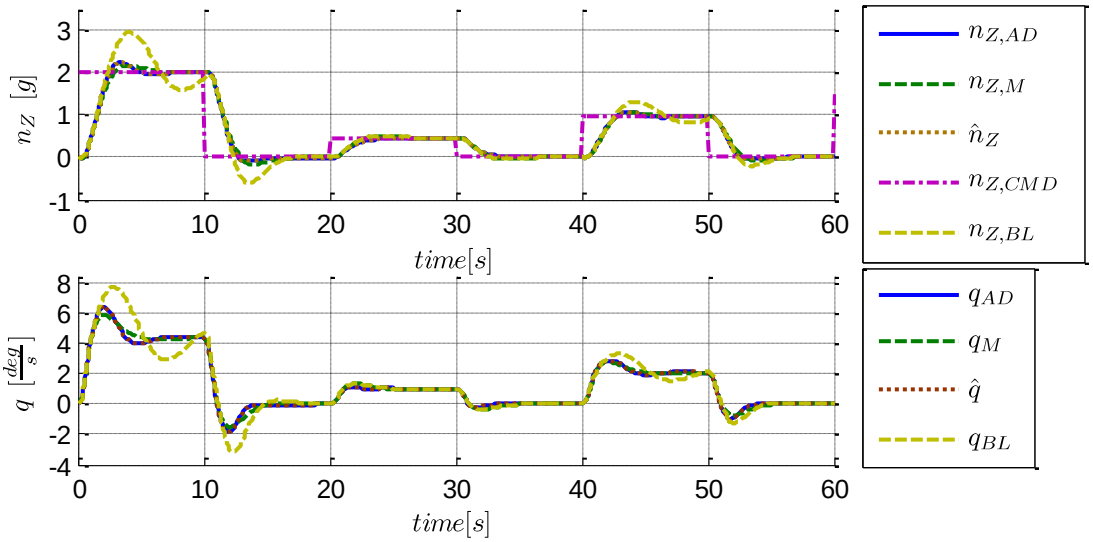

Figure 5.45: Load factor and pitch rate response

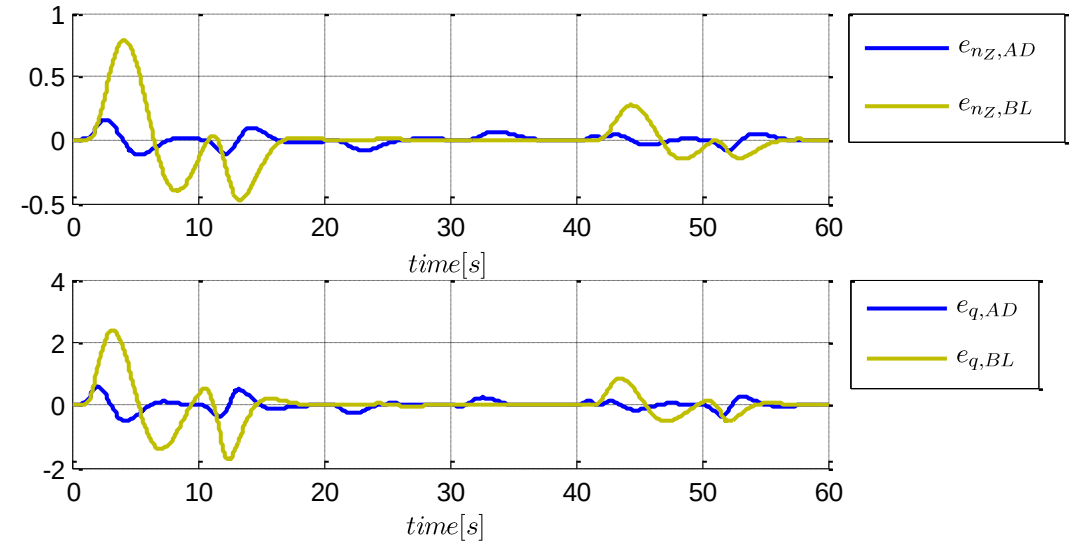

Figure 5.46: Error in load factor and pitch rate response

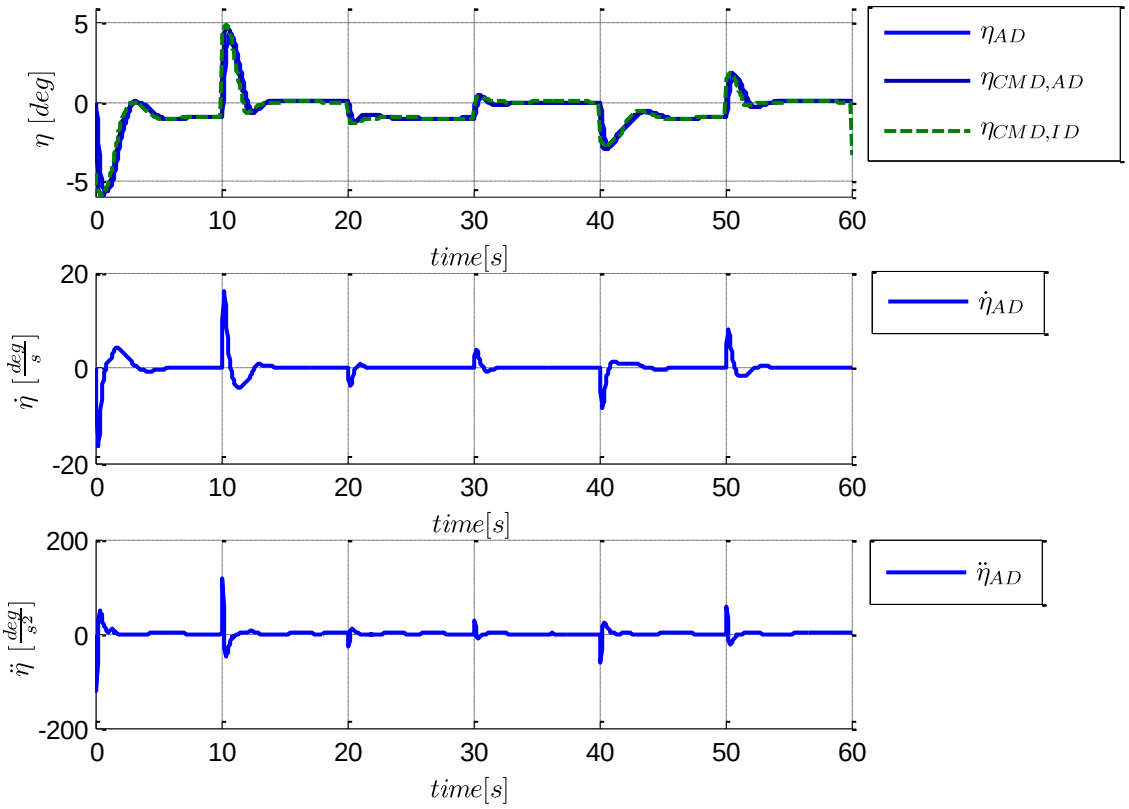

Figure 5.47: Elevator deflection and rate

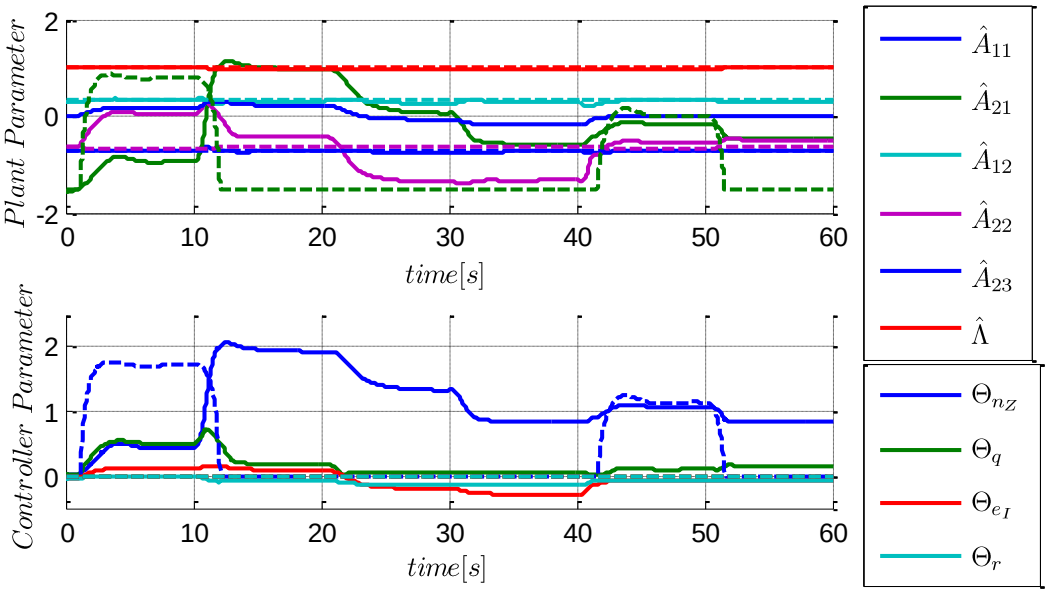

Figure 5.48: Adaptive controller parameters

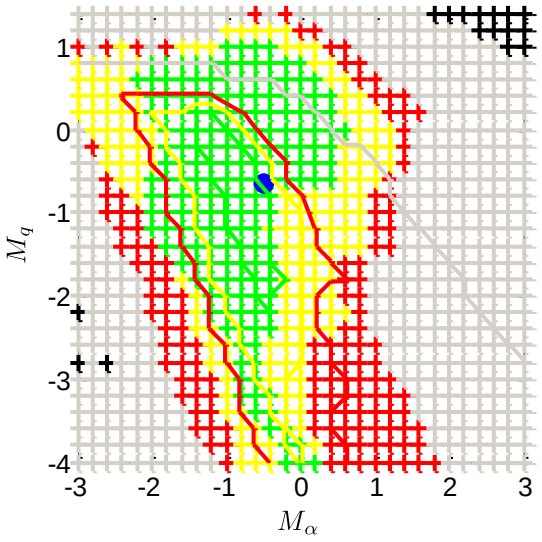

Figure 5.49: Robust perfomance w.r.t. M_α and M_q; $n_{Z,CMD}$=1

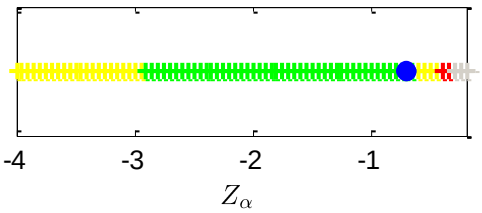

Figure 5.50: Robust perfomance w.r.t. Z_α; $n_{Z,CMD}$=1

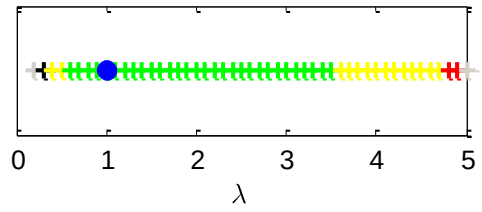

Figure 5.51: Robust perfomance w.r.t. λ $n_{Z,CMD}$=1

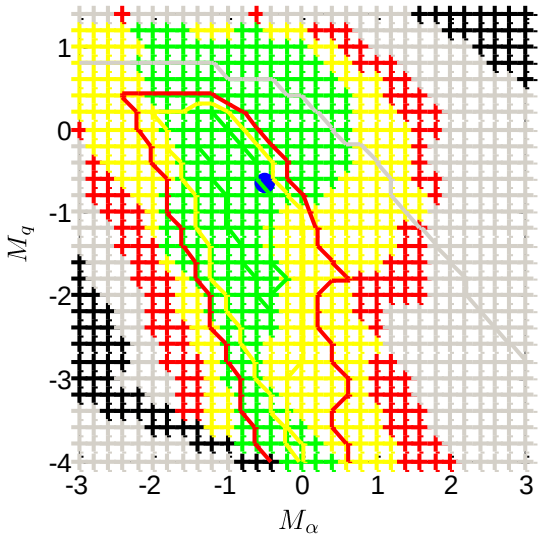

Figure 5.52: Robust perfomance w.r.t. M_α and M_q; $n_{Z,CMD}$=2

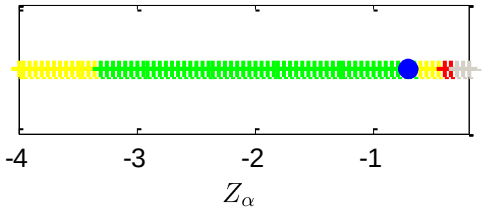

Figure 5.53: Robust perfomance w.r.t. Z_α; $n_{Z,CMD}$=2

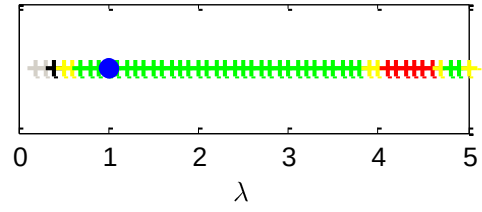

Figure 5.54: Robust perfomance w.r.t. λ $n_{Z,CMD}$=2

5.2 Robustness Modifications

In the previous chapters it was assumed that the complete state vector can be fed back and that all uncertainties are structurally known, and can be linearly parameterized. Only under these assumptions the uncertainties can be compensated exactly and global stability is guaranteed. However, the prerequisites are unreasonable for real physical systems because nonparametric uncertainties like time varying disturbances (e.g. turbulence), unmodeled dynamics (e.g. actuators, structural dynamics), sensor noise, numerical errors, and delays will always be present [4]. It is well known that MRAC suffers from robustness problems in the presence of these nonparametric uncertainties [149] [150] [151]. The reason therefore can be directly seen from the time derivative of the Lyapunov function which contains a sign indefinite term in the presence of unmatched and nonparametric uncertainties.

Taking the plant dynamics of Eq.(4.5) and introducing an unmatched, nonparametric uncertainty $\boldsymbol{\varepsilon}(\mathbf{x},\mathbf{u},t)$ leads to

$$\dot{\mathbf{x}}_P = \mathbf{A}_M\mathbf{x}_P + \mathbf{B}_M\mathbf{r} + \mathbf{B}_P\boldsymbol{\Lambda}\left(\mathbf{u} - \boldsymbol{\Theta}_C^{*T}\boldsymbol{\omega}_C\right) + \boldsymbol{\varepsilon}(\mathbf{x},\mathbf{u},t) \tag{5.77}$$

Using, for example, the direct MRAC approach (Eq.(4.2), Eq.(4.3) and Eq.(4.10)) and the Lyapunov candidate of Eq.(4.9), a sign indefinite term remains in the time derivative

$$\dot{\mathrm{V}} = -\frac{1}{2}\mathbf{e}_C^T\mathbf{Q}\mathbf{e}_C + \mathbf{e}_C^T\mathbf{P}\,\boldsymbol{\varepsilon}(\mathbf{x},\mathbf{u},t) \tag{5.78}$$

From this it directly follows that neither boundedness of the parameter errors $\widetilde{\boldsymbol{\Theta}}_C$, nor convergence of $\mathbf{e}_C$ to zero is guaranteed. Hence, to guarantee stability the boundedness of the adaptive parameters must be ensured.

To establish boundedness for the adaptive parameters $\boldsymbol{\Theta}_C$, different robustness modifications have been suggested, where the most important ones are shortly presented in the following. These are: Dead Zone, Parameter Projection, σ-modification, e-modification, and Optimal-modification. Where the last three modifications add damping to the adaptation law.

In general, these modifications are no exclusive methods but can be arbitrarily combined. For more detailed information the reader is referred to [1] [2] [4]. Further robustifying modification that have been recently suggested, but are not taken into account in the following, are a Kalman filter based modification [117], a loop recovery method [152], and the K-modification [153].

5.2.1 Dead Zone

The approach relies on a known bound on the nonparametric uncertainties $\|\boldsymbol{\varepsilon}(\mathbf{x},\mathbf{u},t)\|_2 < \varepsilon_{max}$. If this bound is known then a region where the time derivative of

the Lyapunov function candidate $\dot{V}$ is guaranteed to be negative can be derived from Eq.(5.78) and is given by

$$\|\mathbf{e}_C\|_2 > \frac{2\lambda_{max}(\mathbf{P})\varepsilon_{max}}{\lambda_{min}(\mathbf{Q})} = e_{max}, \tag{5.79}$$

where $\lambda_{max}(\cdot)$ and $\lambda_{min}(\cdot)$ is the maximum and minimum eigenvalue, respectively.

The method is simply based on the idea to switch the adaptation off when $\|\mathbf{e}_C\|_2 \leq e_{max}$, where the transition can be implemented in a discontinuous or a continuous way [88] [2]. This means, adaptation is only enforced as long as it is guaranteed that $\dot{V} < 0$. From the assumed bound on $\boldsymbol{\varepsilon}(\mathbf{x}, \mathbf{u}, t)$ it is clear that the modification requires system knowledge in order to be applied appropriately, and the upper bound ε_{max} has to be a chosen conservative. The more conservative this bound is, the larger the error will remain. Furthermore, even when $\boldsymbol{\varepsilon}(\mathbf{x}, \mathbf{u}, t) = \mathbf{0}$ the error might not converge to zero as time goes to infinity.

5.2.2 Parameter Projection

The simple idea behind parameter projection is to establish a bound on the adaptive parameters and constrain them to a convex set. Thus, boundedness is guaranteed and stability can directly be followed, if the set to which the parameters are constrained contains the ideal parameters. However, bounding does not solve the problem of parameter drift. Thus, for a real system, meaningful boundaries have to be known, which can be derived from the expected uncertainties in the system.

The bounding must not be established in a hard, discontinuous way, and the projection operator offers a method based on gradient projection that allows for a smooth transition and assures that the time course of the parameters is $\in C^1$ [2] [154].

5.2.3 σ-Modification

The σ-modification was originally suggested in [155] and is comprised of an additional term in the adaptation law which introduces general damping. Taking for example the adaptation law from Eq.(4.10) and introducing the σ-modification, leads to

$$\dot{\boldsymbol{\Theta}}_C = -\boldsymbol{\Gamma}_C \boldsymbol{\omega}_C \cdot \mathbf{e}_C^T \mathbf{P} \mathbf{B}_P - \boldsymbol{\Gamma}_C \sigma \boldsymbol{\Theta}_C. \tag{5.80}$$

From Lyapunov analysis it follows that there exist positive constants k_1 and k_2 such that $\dot{V} < 0$ outside a compact set defined by $\mathrm{D} = \{(\mathbf{e}_C, \widetilde{\boldsymbol{\Theta}}_C) \,|\, \|\mathbf{e}_C\|_2 \leq \mathrm{k}_1,\ \|\widetilde{\boldsymbol{\Theta}}_C\|_{\mathrm{F}} \leq \mathrm{k}_2\}$, where subscript F denotes the Frobenius norm (see Appendix C.1). From this it follows that the trajectories of $\mathbf{e}_C(t)$ and $\widetilde{\boldsymbol{\Theta}}_C(t)$ converge to this compact set, and hence $\mathbf{e}_C(\mathrm{t})$ and $\widetilde{\boldsymbol{\Theta}}_C(\mathrm{t})$ are bounded [1]. The size of the compact set is determined by the design parameter σ, which is the gain of the modification term.

The drawback is, that the parameter error will not converge to zero even when $\boldsymbol{\varepsilon}(\mathbf{x}, \mathbf{u}, t) = \mathbf{0}$ and the reference input is persistently exciting.

Furthermore, the introduced modification term acts as a forgetting factor on the adaptive parameters. As long as the error is small it is dominating the adaptation law. Hence, it makes the adaptive parameters converge to zero, although these are not the correct parameters to follow an arbitrary reference command. This problem mainly occurs if the reference command is constant during longer periods of time.

From the above equations it would follow that no knowledge about the system is required and stability is always guaranteed for an arbitrary gain σ. This is however not true for a real system with actuator and bandwidth constraints. The parameter σ determines the region to which the parameters are confined, and thus it cannot be arbitrary small because this would allow arbitrary large parameter drifts. So the design problem is how to choose σ to guarantee a certain amount of robustness for the adaptive system, but no general solution is available for that.

5.2.4 e-Modification

The e-modification was suggested in [156] and is quite similar to the σ-modification, with the difference that the damping term is proportional to the norm of the error. If exemplarily the update law of Eq.(4.10) is used again, the modified update law is given by

$$\dot{\boldsymbol{\Theta}}_C = -\boldsymbol{\Gamma}_C \boldsymbol{\omega}_C \cdot \mathbf{e}_C^T \mathbf{P} \mathbf{B}_P - \boldsymbol{\Gamma}_C \sigma \|\mathbf{e}_C\|_2 \boldsymbol{\Theta}_C. \tag{5.81}$$

The motivation for this modification is to reduce the effect of the forgetting factor when the error goes to zero and the system is not excited. It follows that $\dot{V} < 0$ outside a compact set defined by

$$D = \left\{ \left(\mathbf{e}, \tilde{\boldsymbol{\theta}}_C\right) \middle| \left(\frac{1}{2} \lambda_{\min}(\mathbf{Q}) \|\mathbf{e}_C\|_2 - \lambda_{\max}(\mathbf{P}) \|\boldsymbol{\varepsilon}(\mathbf{x}, \mathbf{u}, t)\|_2 + \sigma \left\|\tilde{\boldsymbol{\Theta}}_C\right\|_F^2 - \sigma \|\boldsymbol{\Theta}_C^*\|_F^2 \right) \leq 0 \right\}.$$

From this it can be concluded that the trajectories of $\mathbf{e}_C(t)$ and $\tilde{\boldsymbol{\Theta}}(t)$ converge to this compact set [1]. Thus, $\mathbf{e}_C(t)$ and $\tilde{\boldsymbol{\Theta}}_C(t)$ are bounded. With this modification and when $\boldsymbol{\varepsilon}(\mathbf{x}, \mathbf{u}, t) = \mathbf{0}$ the origin is an equilibrium point of the closed loop system if the input is sufficiently excited. Hence, in difference to the σ-modification the error $\mathbf{e}_C(t)$ can converge to and remain zero. Moreover, the parameters can converge to their ideal values.

However, the problem of choosing the design parameter σ still remains an issue. It should be noted that in [117] a Kalman filter based approach was suggested for the e-modification, where the gain for the e-modification term is adjusted dynamically and it is claimed that significant improvement could be achieved.

5.2.5 Optimal-Modification

This modification was recently proposed in [157], where the update laws are derived from solving the optimal control problem for minimizing the $\mathcal{L}_2$ norm of the tracking error. The additional term that is occurring in the adaptation law also introduces

damping, but in difference to the σ-modification and e-modification the damping is proportional to the amount of persistent excitation of the system

$$\dot{\boldsymbol{\Theta}}_C = -\boldsymbol{\Gamma}_C \boldsymbol{\omega}_C \cdot \mathbf{e}_C^T \mathbf{P} \mathbf{B}_P + \boldsymbol{\Gamma}_C \sigma \cdot \boldsymbol{\omega}_C \boldsymbol{\omega}_C^T \cdot \boldsymbol{\Theta}_C {\mathbf{B}_P}^T \mathbf{P} \mathbf{A}_M^{-1} \mathbf{B}_P. \tag{5.82}$$

Due to the term $\boldsymbol{\omega}_C \boldsymbol{\omega}_C^T$ the damping is proportional to the excitation of the system and the ${\mathbf{B}_P}^T \mathbf{P} \mathbf{A}_M^{-1} \mathbf{B}_P$ is constant and necessary for the stability proof [157].

The modified adaptive law guarantees that $\dot{V} < 0$ outside a compact set given by

$$D = \left\{ \left(\mathbf{e}, \widetilde{\boldsymbol{\Theta}}_C \boldsymbol{\omega}_C \right) \middle| \, \|\mathbf{e}_C\|_2 \leq \mathrm{k}_1, \left\| \widetilde{\boldsymbol{\Theta}}_C \boldsymbol{\omega}_C \right\|_2 \leq \mathrm{k}_2 \right\},$$

where $\mathrm{k}_1 \text{ and } \mathrm{k}_2$ are positive constants. This means, it is only guaranteed that the product $\widetilde{\boldsymbol{\Theta}}_C \boldsymbol{\omega}_C$ is bounded, but not the boundedness of $\widetilde{\boldsymbol{\Theta}}_C$. Or, boundedness of $\widetilde{\boldsymbol{\Theta}}_C$ is only guaranteed when the system is persistently excited. It was seen that with the Optimal-modification fast adaptation can be achieved while oscillations, resulting from high adaptation gain, are largely reduced [157].

5.2.6 Short Period Example

To assess the different robustness modifications the benchmark problem from Section 2.1 is used again with the predictor based adaptive controller from Section 5.1.7.1. Because sensor noise is not present in the considered problem the dead-zone is not evaluated in the following. Only σ- , e-, and optimal modification are applied to the update laws used in Section 5.1.7.1, which are given by Eq.(5.30) and Eq.(5.63). However, the modifications are only applied to the update laws of the parameters which are used for control, because the estimation of the unmatched parameters only affects the reference model, and by projection it is guaranteed that this cannot cause instability. Thus the update laws are given by

$$\begin{aligned} \dot{\widehat{\boldsymbol{\theta}}}_y &= \boldsymbol{\Gamma}_y \left(\mathbf{y}_P^+ \cdot \mathbf{e}_P^T \mathbf{P} \mathbf{b}_{P,n_Z}^+ - \sigma \boldsymbol{\Xi}_\theta \right) \\ \dot{\hat{\lambda}} &= -\Gamma_\Lambda \left(\eta \cdot \mathbf{e}_P^T \mathbf{P} \mathbf{b}_{P,n_Z}^+ + \sigma \boldsymbol{\Xi}_\Lambda \right) \end{aligned} \tag{5.83}$$

$$\dot{\widehat{\boldsymbol{\theta}}}_{y,um} = -\boldsymbol{\Gamma}_{y,um} \mathbf{y}_P \cdot \mathbf{e}_P^T \mathbf{P} \mathbf{b}_{P,um}^+ \tag{5.84}$$

where Ξ_θ and Ξ_Λ are defined in Table 5.12 for the respective modifications.

	σ-Mod.	e-Mod.	Optimal-Mod.
$\boldsymbol{\Xi}_\theta$	$\widehat{\boldsymbol{\theta}}_y$	$\|\mathbf{e}_P\|_2 \widehat{\boldsymbol{\theta}}_y$	$-\mathbf{x}_P \mathbf{x}_P^T \cdot \widehat{\boldsymbol{\theta}}_y \cdot \mathbf{b}_{P,n_Z}^{+T} \mathbf{P} \mathbf{A}_M^{-1} \mathbf{b}_{P,n_Z}^+$
$\boldsymbol{\Xi}_\Lambda$	$\hat{\lambda}$	$\|\mathbf{e}_P\|_2 \hat{\lambda}$	$-\eta^2 \cdot \hat{\lambda} \cdot \mathbf{b}_{P,n_Z}^{+T} \mathbf{P} \mathbf{A}_M^{-1} \mathbf{b}_{P,n_Z}^+$

Table 5.12: Modification terms for σ-, e-, and optimal modification

In the following the different modifications are evaluated for certain values of the parameter σ, which are given in Table 5.13. Note that the remaining parameters of the adaptive controller have not been retuned, and the parameters from Table 5.8 are used.

	σ-mod.	e-mod.	optimal-mod.
σ	0.05	1	0.1

Table 5.13: Simulation parameters for robustness modifications

In Table 5.14 the values for the time delay margin are given. It can be seen that for all modification the time delay margin increases with increasing σ. The evaluation results, regarding robust performance, for the different robustness modifications are shown in the following subsections. As expected, the results show that all robustness modification deteriorate the performance. Especially the σ-modification leads to an aggravation, which can be seen in Figure 5.55 - Figure 5.60 . The performance in presence of the matched uncertainties becomes strongly discontinuous and is even worse than the baseline controller, while the improvement on the time delay margin is only small. In difference the e-modification (Figure 5.61 - Figure 5.66) and the optimal modification (Figure 5.67 - Figure 5.72) still show good performance and provide a better time delay margin. In particular the results indicate that the optimal modification yields the best trade-off between robustness and performance. It should be noted that better results might be possible if different parameters σ are used on each adaptation law and if a retuning of all parameter is applied.

	σ-mod.	e-mod.	optimal-mod.
TDM: 1g CMD	0.37	0.39	0.39
TDM: 2g CMD	0.31	0.35	0.39

Table 5.14: Time delay margins for different robustness modifications

5.2.6.1 σ-Modification

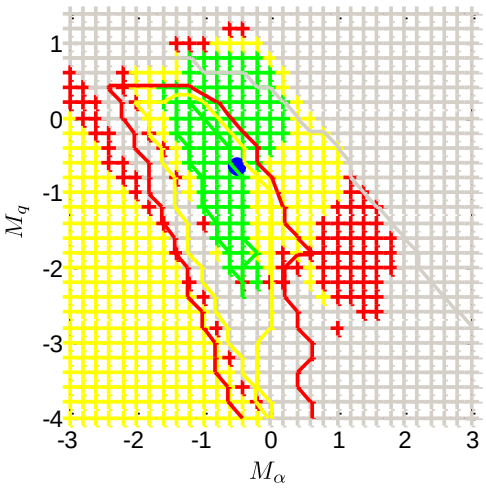

Figure 5.55: Robust perfomance w.r.t. M_α and M_q; $n_{z,CMD}$=1

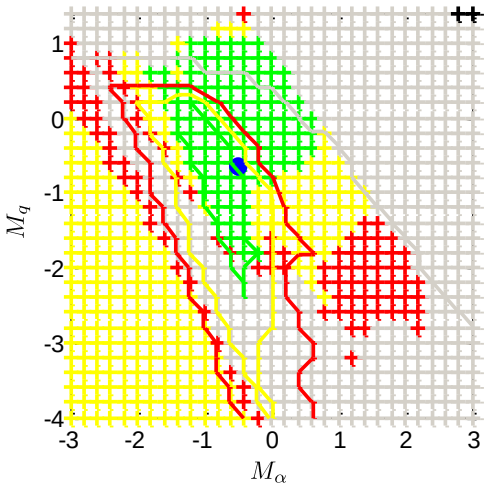

Figure 5.58: Robust perfomance w.r.t. M_α and M_q; $n_{z,CMD}$=2

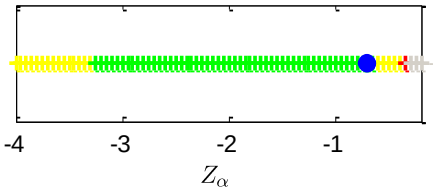

Figure 5.56: Robust perfomance w.r.t. Z_α; $n_{z,CMD}$=1

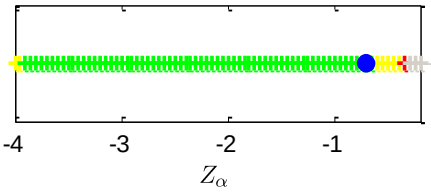

Figure 5.59: Robust perfomance w.r.t. Z_α; $n_{z,CMD}$=2

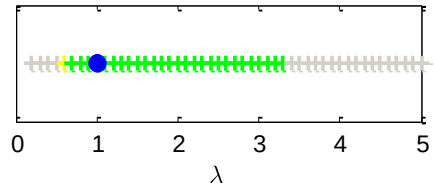

Figure 5.57: Robust perfomance w.r.t. λ $n_{z,CMD}$=1

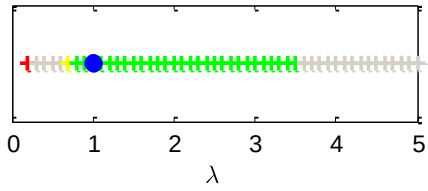

Figure 5.60: Robust perfomance w.r.t. λ $n_{z,CMD}$=2

5.2.6.2 e-Modification

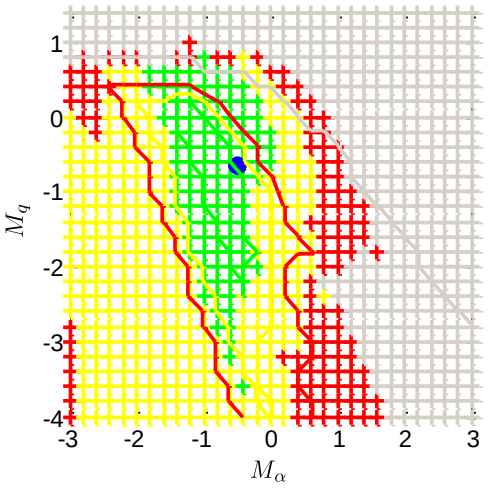

Figure 5.61: Robust perfomance w.r.t. M_α and M_q; $n_{z,CMD}$=1

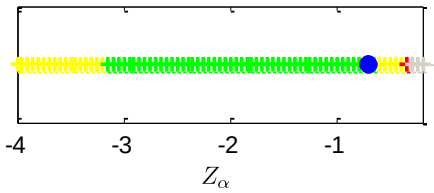

Figure 5.62: Robust perfomance w.r.t. Z_α; $n_{z,CMD}$=1

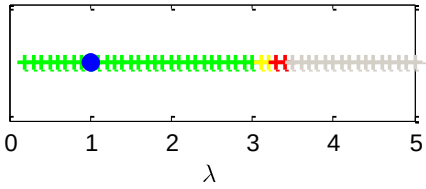

Figure 5.63: Robust perfomance w.r.t. λ $n_{z,CMD}$=1

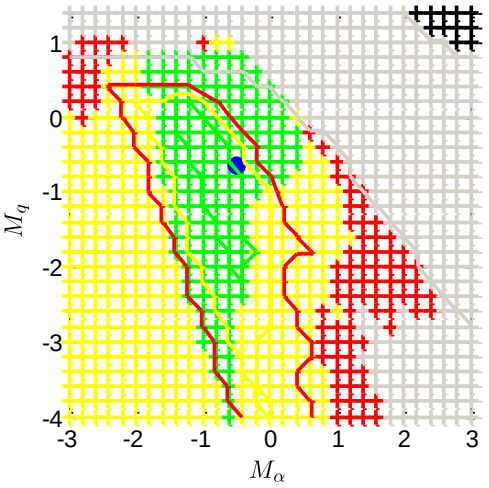

Figure 5.64: Robust perfomance w.r.t. M_α and M_q; $n_{z,CMD}$=2

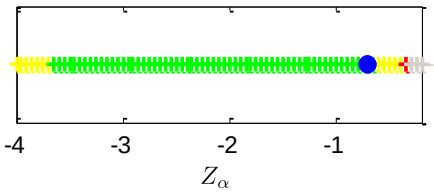

Figure 5.65: Robust perfomance w.r.t. Z_α; $n_{z,CMD}$=2

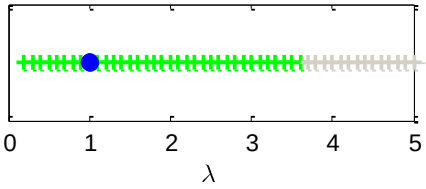

Figure 5.66: Robust perfomance w.r.t. λ $n_{z,CMD}$=2

5.2.6.3 Optimal-Modification

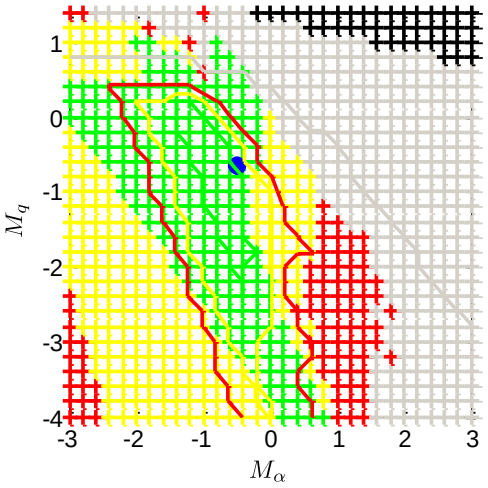

Figure 5.67: Robust perfomance w.r.t. M_α and M_q; $n_{Z,CMD}$=1

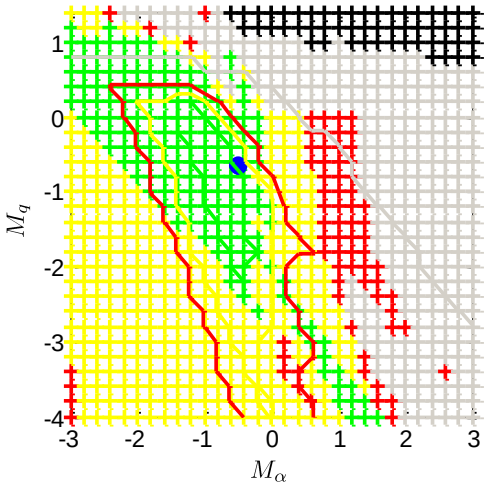

Figure 5.70: Robust perfomance w.r.t. M_α and M_q; $n_{Z,CMD}$=2

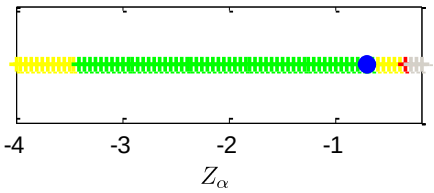

Figure 5.68: Robust perfomance w.r.t. Z_α; $n_{Z,CMD}$=1

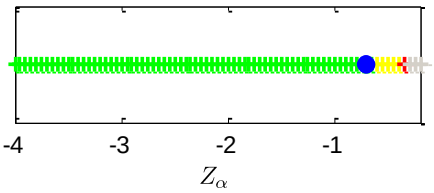

Figure 5.71: Robust perfomance w.r.t. Z_α; $n_{Z,CMD}$=2

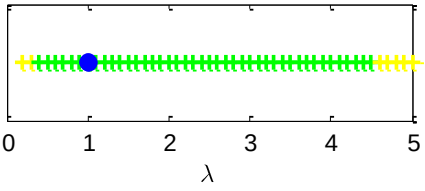

Figure 5.69: Robust perfomance w.r.t. λ $n_{Z,CMD}$=1

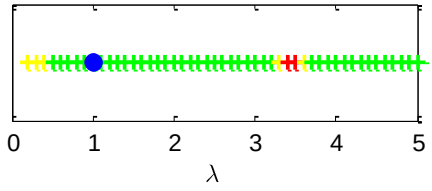

Figure 5.72: Robust perfomance w.r.t. λ $n_{Z,CMD}$=2

5.3 Update Law Modifications

In difference to the robustness modifications the following modifications are mainly introduced to increase the speed of parameter convergence while maintaining a desired transient response. The modifications rely on additional parameter identification based on an algebraic error equation, and are also referred to as Composite, Combined or Hybrid MRAC. Here the additional error model is algebraic and not dynamic as in the standard direct and indirect approach. The algebraic error equations/models are directly derived from the plant dynamics.

Regarding Chapter 4, there arise two different problems depending on the plant parameterization and the resulting error dynamics. This means the applicability of different approaches is depending on weather the plant parameterization is bilinear in the unknown parameters like in the direct case, or if it is linear in the unknown parameters as it is in the indirect or the predictor based approach.

For the direct approach the following plant parameterization is used (see Eq.(4.5))

$$\begin{aligned}\dot{\mathbf{x}}_P &= \mathbf{A}_M\mathbf{x}_P + \mathbf{B}_M\mathbf{r} + \mathbf{B}_P\boldsymbol{\Lambda}\left(\mathbf{u} - \boldsymbol{\Theta}_x^{*\,T}\mathbf{x}_P - \boldsymbol{\Theta}_\varphi^{*\,T}\boldsymbol{\varphi}(\mathbf{x}_P) - \boldsymbol{\theta}_d^* - \boldsymbol{\Theta}_r^*\mathbf{r}\right)\\ &= \mathbf{A}_M\mathbf{x}_P + \mathbf{B}_M\mathbf{r} + \mathbf{B}_P\boldsymbol{\Lambda}\left(\mathbf{u} - \boldsymbol{\Theta}_C^{*\,T}\boldsymbol{\omega}_C\right)\end{aligned} \tag{5.85}$$

with $\boldsymbol{\Theta}_C^* = \left[\boldsymbol{\Theta}_x^{*\,T} \quad \boldsymbol{\Theta}_\varphi^{*\,T} \quad \boldsymbol{\theta}_d^* \quad \boldsymbol{\Theta}_r^*\right]$ and $\boldsymbol{\omega}_C = [\mathbf{x}_P^T \quad \boldsymbol{\varphi}(\mathbf{x}_P)^T \quad 1 \quad \mathbf{r}^T]^T$. It is obvious that the parameterization is bilinear in the unknown parameters due to the product $\boldsymbol{\Lambda}\boldsymbol{\Theta}_C^*$.

In difference, in the indirect and predictor based approach the parameterization is linear. Taking the predictor based approach for example, the parameterized plant is given by (see Eq.(4.29))

$$\begin{aligned}\dot{\mathbf{x}}_P &= \mathbf{A}_M\mathbf{x}_P + \mathbf{B}_P\left(\boldsymbol{\Lambda}\mathbf{u} - \widehat{\boldsymbol{\Theta}}_x^{*\,T}\mathbf{x}_P - \widehat{\boldsymbol{\Theta}}_\varphi^{*\,T}\boldsymbol{\varphi}(\mathbf{x}_P) - \widehat{\boldsymbol{\theta}}_d^*\right)\\ &= \mathbf{A}_M\mathbf{x}_P + \mathbf{B}_P\widehat{\boldsymbol{\Theta}}_P^*\boldsymbol{\omega}_P,\end{aligned} \tag{5.86}$$

with $\widehat{\boldsymbol{\Theta}}_P^* = \left[\widehat{\boldsymbol{\Theta}}_{\boldsymbol{x}}^{*\,T} \quad \widehat{\boldsymbol{\Theta}}_{\boldsymbol{\varphi}}^{*\,T} \quad \widehat{\boldsymbol{\theta}}_{\boldsymbol{d}}^* \quad \boldsymbol{\Lambda}\right]$ and $\boldsymbol{\omega}_P = [\mathbf{x}_P^T \quad \boldsymbol{\varphi}(\mathbf{x}_P)^T \quad 1 \quad \mathbf{u}^T]^T$.

If the state derivatives $\dot{\mathbf{x}}_P$ are available Eq.(5.85) and Eq.(5.86) directly provide algebraic equations that have to be satisfied by the unknown parameters. By defining

$$\boldsymbol{\upsilon} = \dot{\mathbf{x}}_P - \mathbf{A}_M\mathbf{x}_P, \tag{5.87}$$

Eq.(5.86) can for example be rewritten by

$$\boldsymbol{\upsilon} = \mathbf{B}_P\widehat{\boldsymbol{\Theta}}_P^{*\,T}\boldsymbol{\omega}_P. \tag{5.88}$$

With $\boldsymbol{\upsilon}$ available from measurement, this poses a standard problem of parameter estimation, where gradient algorithms or least square estimation is directly applicable. In the following, at first gradient based modifications are discussed for bilinear parametric models and linear parametric models, respectively. For simplicity the subsequently discussed approaches are only shown for linear parametric models.

The state derivatives are usually not available and simple numeric differentiation schemes can result in amplification of sensor noise. However, better methods have

been suggested to approximate them from the state measurements (e.g. fixed point smoothing [113] [158] or approximation from spline interpolation [115]). In difference, the approaches suggested in [109] [110] [111] [159] [4] [92] do not directly estimate the state derivatives. Instead similar algebraic equations as above are derived from integration of the plant dynamics over a fixed time window or filtered plant dynamics, respectively. However, the purpose of these approaches is basically also to obtain smooth derivatives through averaging over a time window or filtering, respectively.

In the following, these two methods for obtaining an algebraic constraint for the parameters, by means of integration or filtering are considered. The Q-modification, that relies on integration of the plant dynamics and is referred to *Integral Approach* in the following, was introduced in [109] [110] [111] [159]. In [4] [92] approaches were presented that use the filtered system signals, and thus are referred to as *Filtered Approach* in the following.

Integral Approach:

In the following at first the integral version is considered, which is at first applied to the bilinear parameterized plant. Therefore, integrate the system dynamics of Eq.(5.85) over a moving time window $[t_d, t]$, $t > 0$, where $t_d \widehat{=} \max(0, t - \tau_d)$, and $\tau_d > 0$ is a design parameter that determines the length of the integration window

$$\int_{t_d}^{t} \dot{\mathbf{x}}_P \, \mathrm{ds} = \int_{t_d}^{t} \left(\mathbf{A}_M \mathbf{x}_P + \mathbf{B}_M \mathbf{r} + \mathbf{B}_P \boldsymbol{\Lambda} \left(\mathbf{u} - \boldsymbol{\Theta}_C^{*T} \boldsymbol{\omega}_C \right) \right) \mathrm{ds}. \tag{5.89}$$

Actually, under the idealized assumptions the integration could also be carried out over the complete time interval $[0, t]$. However, when non-parametric uncertainties are present, that cannot be compensated by the control architecture, they will also enter in an integrated form. Hence, the time window is usually chosen small.

Eq.(5.89) can also be denoted by

$$\mathbf{x}_P(t) - \mathbf{x}_P(t - \tau_d) - \mathbf{A}_M \int_{t_d}^{t} \mathbf{x}_P \, \mathrm{ds} - \mathbf{B}_M \int_{t_d}^{t} \mathbf{r} \, \mathrm{ds} = \mathbf{B}_P \boldsymbol{\Lambda} \left(\int_{t_d}^{t} \mathbf{u} \, \mathrm{ds} - \boldsymbol{\Theta}_C^{*T} \int_{t_d}^{t} \boldsymbol{\omega}_C \, \mathrm{ds} \right). \tag{5.90}$$

By defining

$$\bar{\boldsymbol{\upsilon}} = -\left(\mathbf{x}_P(t) - \mathbf{x}_P(t - \tau_d) - \mathbf{A}_M \int_{t_d}^{t} \mathbf{x}_P \, \mathrm{ds} - \mathbf{B}_M \int_{t_d}^{t} \mathbf{r} \, \mathrm{ds} \right) \tag{5.91}$$

$$\bar{\mathbf{u}} = \int_{t_d}^{t} \mathbf{u} \, \mathrm{ds} \tag{5.92}$$

$$\bar{\boldsymbol{\omega}}_C = \int_{t_d}^{t} \boldsymbol{\omega}_C \, \mathrm{ds}, \tag{5.93}$$

we obtain

$$\bar{\boldsymbol{\upsilon}} = \mathbf{B}_P \boldsymbol{\Lambda} \left(\boldsymbol{\Theta}_C^{*T} \bar{\boldsymbol{\omega}}_C - \bar{\mathbf{u}} \right). \tag{5.94}$$

Hence, the true parameters have to satisfy this algebraic equation which is bilinear in the unknown parameters.

Using the estimated parameters $\boldsymbol{\Theta}_C$ and $\widehat{\boldsymbol{\Lambda}}$, an error can be defined in the form

$$\bar{\mathbf{e}}_C\left(\boldsymbol{\Theta}_C, \widehat{\boldsymbol{\Lambda}}\right) = \mathbf{B}_P\widehat{\boldsymbol{\Lambda}}(\boldsymbol{\Theta}_C^T\,\bar{\boldsymbol{\omega}}_C - \bar{\mathbf{u}}) - \mathbf{B}_P\boldsymbol{\Lambda}\left(\boldsymbol{\Theta}_C^{*\,T}\,\bar{\boldsymbol{\omega}}_C - \bar{\mathbf{u}}\right) = \mathbf{B}_P\widehat{\boldsymbol{\Lambda}}(\boldsymbol{\Theta}_C^T\,\bar{\boldsymbol{\omega}}_C - \bar{\mathbf{u}}) - \bar{\boldsymbol{\upsilon}}. \tag{5.95}$$

If the same approach, of integrating the plant dynamics is used for the linear parameterized plant of Eq.(5.86), instead of Eq.(5.91) we obtain the algebraic constraint

$$\bar{\boldsymbol{\upsilon}} = \mathbf{B}_P\widehat{\boldsymbol{\Theta}}_P^{*\,T}\,\bar{\boldsymbol{\omega}}_P, \tag{5.96}$$

which is linear in the unknown parameters. From this, also an error depending on the estimated parameters, can be defined

$$\bar{\mathbf{e}}_P\left(\widehat{\boldsymbol{\Theta}}_P\right) = \mathbf{B}_P\widehat{\boldsymbol{\Theta}}_P^T\,\bar{\boldsymbol{\omega}}_P - \mathbf{B}_P\widehat{\boldsymbol{\Theta}}_P^{*\,T}\bar{\boldsymbol{\omega}}_P = \mathbf{B}_P\widehat{\boldsymbol{\Theta}}_P^T\bar{\boldsymbol{\omega}}_P - \bar{\boldsymbol{\upsilon}}. \tag{5.97}$$

Filtered Approach:

Instead of integrating the plant dynamics they can be filtered with a stable, proper filter. In the following, for simplicity a first order lag filter is considered with the transfer function $C(s) = \frac{\lambda_F}{s+\lambda_F}$, where $\lambda_F > 0$ is the inverse time constant of the filter. This design parameter is similar to the integration window length τ_d. Applying this filter to both sides of the system dynamics of Eq.(5.85) yields

$$\underbrace{\frac{\lambda_F}{s+\lambda_F}\dot{\mathbf{x}}_P}_{\dot{\bar{\mathbf{x}}}_P} = \frac{\lambda_F}{s+\lambda_F}\left(\mathbf{A}_M\mathbf{x}_P + \mathbf{B}_M\mathbf{r} + \mathbf{B}_P\boldsymbol{\Lambda}\left(\mathbf{u} - \boldsymbol{\Theta}_C^{*\,T}\boldsymbol{\omega}_C\right)\right). \tag{5.98}$$

By defining $\dot{\bar{\mathbf{x}}}_P(s) = \frac{\lambda_F}{s+\lambda_F}\dot{\mathbf{x}}_P(s)$ and noticing that $\dot{\bar{\mathbf{x}}}_P(t) = \lambda_F(\mathbf{x}_P(t) - \bar{\mathbf{x}}_P(t))$ we can rewrite

$$\lambda_F(\mathbf{x}_P - \bar{\mathbf{x}}_P) - \mathbf{A}_M\underbrace{\frac{\lambda_F}{s+\lambda_F}\mathbf{x}_P}_{\bar{\mathbf{x}}_P} - \mathbf{B}_M\underbrace{\frac{\lambda_F}{s+\lambda_F}\mathbf{r}}_{\bar{\mathbf{r}}} = \mathbf{B}_P\boldsymbol{\Lambda}\left(\underbrace{\frac{\lambda_F}{s+\lambda_F}\mathbf{u}}_{\bar{\mathbf{u}}} - \boldsymbol{\Theta}_C^{*\,T}\underbrace{\frac{\lambda_F}{s+\lambda_F}\boldsymbol{\omega}_C}_{\bar{\boldsymbol{\omega}}_C}\right). \tag{5.99}$$

Similar to the previous approach we can define

$$\bar{\boldsymbol{\upsilon}} = -(\lambda_F(\mathbf{x}_P - \bar{\mathbf{x}}_P) - \mathbf{A}_M\bar{\mathbf{x}}_P - \mathbf{B}_M\bar{\mathbf{r}}) \tag{5.100}$$

Thus, a similar algebraic equation as in the previous section is obtained (compare Eq.(5.94)), which has to be satisfied by the true parameters

$$\bar{\boldsymbol{\upsilon}} = \mathbf{B}_P\boldsymbol{\Lambda}\left(\boldsymbol{\Theta}_C^{*\,T}\bar{\boldsymbol{\omega}}_C - \bar{\mathbf{u}}\right). \tag{5.101}$$

And again an algebraic error model can be defined in the form

$$\bar{\mathbf{e}}_C(\boldsymbol{\Theta}_C, \boldsymbol{\Lambda}) = \mathbf{B}_P\widehat{\boldsymbol{\Lambda}}(\boldsymbol{\Theta}_C^T\bar{\boldsymbol{\omega}}_C - \bar{\mathbf{u}}) - \mathbf{B}_P\boldsymbol{\Lambda}\left(\boldsymbol{\Theta}_C^{*\,T}\bar{\boldsymbol{\omega}}_C - \bar{\mathbf{u}}\right) = \mathbf{B}_P\widehat{\boldsymbol{\Lambda}}(\boldsymbol{\Theta}_C^T\bar{\boldsymbol{\omega}}_C - \bar{\mathbf{u}}) - \bar{\boldsymbol{\upsilon}}. \tag{5.102}$$

5.3.1 Gradient Based Modifications

In the previous section it was shown how an algebraic error model for parameter identification can be obtained by filtering or integrating the plant dynamics. In the following two gradient based update law modifications are considered. The Q-modification, which relies on integration of the plant dynamics, was introduced in Refs. [109] [110] [111] [159] for the predictor based MRAC structure with a linear error model. And in [64] an approach was presented that uses the filtered system signals and is applicable to the bilinear error model. However, the approaches are similar as they use an additional error in from of an algebraic equation that is dependent on the estimated parameters, and this algebraic constraint is minimized by applying the gradient method.

5.3.1.1 Bilinear Error Model:

The bilinear nature of the error model in the direct case results from the assumed parameterization of the plant Eq.(5.85) and the control law Eq.(4.3).

Based on the error defined in Eq.(5.95) the cost functional

$$J\left(\boldsymbol{\Theta}_C^T, \widehat{\boldsymbol{\Lambda}}\right) = \frac{1}{2}\bar{\mathbf{e}}_C^{\mathrm{T}}\bar{\mathbf{e}}_C = \frac{1}{2}\left[\mathbf{B}_{\mathrm{P}}\widehat{\boldsymbol{\Lambda}}(\boldsymbol{\Theta}_C^T\bar{\boldsymbol{\omega}}_C - \bar{\mathbf{u}}) - \bar{\mathbf{v}}\right]^T\left[\mathbf{B}_{\mathrm{P}}\widehat{\boldsymbol{\Lambda}}(\boldsymbol{\Theta}_C^T\bar{\boldsymbol{\omega}}_C - \bar{\mathbf{u}}) - \bar{\mathbf{v}}\right], \tag{5.103}$$

is defined, and by application of the gradient method (see [4] [92]) with respect to the unknown parameters $\boldsymbol{\Theta}_C^T$ and $\widehat{\boldsymbol{\Lambda}}$. Calculating the gradients for $J\left(\boldsymbol{\Theta}_C^T, \widehat{\boldsymbol{\Lambda}}\right)$ gives

$$\begin{aligned}\frac{\partial J\left(\boldsymbol{\Theta}_C^T, \widehat{\boldsymbol{\Lambda}}\right)}{\partial \boldsymbol{\Theta}_C^T} &= \bar{\boldsymbol{\omega}}_C\left[\mathbf{B}_P\widehat{\boldsymbol{\Lambda}}(\boldsymbol{\Theta}_C^T\bar{\boldsymbol{\omega}}_C - \bar{\mathbf{u}}) - \bar{\mathbf{v}}\right]^T\mathbf{B}_P\widehat{\boldsymbol{\Lambda}} = \bar{\boldsymbol{\omega}}_C\bar{\mathbf{e}}_C^T\mathbf{B}_P \\ \frac{\partial J\left(\boldsymbol{\Theta}_C^T, \widehat{\boldsymbol{\Lambda}}\right)}{\partial \widehat{\boldsymbol{\Lambda}}} &= (\boldsymbol{\Theta}_C^T\bar{\boldsymbol{\omega}}_C - \bar{\mathbf{u}})\left[\mathbf{B}_P\widehat{\boldsymbol{\Lambda}}(\boldsymbol{\Theta}_C^T\bar{\boldsymbol{\omega}}_C - \bar{\mathbf{u}}) - \bar{\mathbf{v}}\right]^T\mathbf{B}_P = (\boldsymbol{\Theta}_C^T\bar{\boldsymbol{\omega}}_C - \bar{\mathbf{u}})\bar{\mathbf{e}}_C^T\mathbf{B}_P.\end{aligned} \tag{5.104}$$

and the following update laws can be used

$$\begin{aligned}\dot{\boldsymbol{\Theta}}_C &= -\boldsymbol{\Gamma}_C\frac{\partial J\left(\boldsymbol{\Theta}_C^T, \widehat{\boldsymbol{\Lambda}}\right)}{\partial \boldsymbol{\Theta}_C^T}\widehat{\boldsymbol{\Lambda}}^{-1} = -\boldsymbol{\Gamma}_C\bar{\boldsymbol{\omega}}_C\bar{\mathbf{e}}_C^T\mathbf{B}_P \\ \dot{\widehat{\boldsymbol{\Lambda}}}^T &= -\boldsymbol{\Gamma}_\Lambda\frac{\partial J\left(\boldsymbol{\Theta}_C^T, \widehat{\boldsymbol{\Lambda}}\right)}{\partial \widehat{\boldsymbol{\Lambda}}} = \boldsymbol{\Gamma}_\Lambda(\boldsymbol{\Theta}_C^T\bar{\boldsymbol{\omega}}_C - \bar{\mathbf{u}})\bar{\mathbf{e}}_C^T\mathbf{B}_P.\end{aligned} \tag{5.105}$$

Now the standard update law from Eq.(4.10) can be altered by the additional term for the update of $\boldsymbol{\Theta}_C$ and the estimation of the control effectiveness $\widehat{\boldsymbol{\Lambda}}$ from Eq.(5.105) to obtain

$$\begin{aligned}\dot{\boldsymbol{\Theta}}_C &= -\boldsymbol{\Gamma}_C(\boldsymbol{\omega}_C\mathbf{e}_C^T\mathbf{P} + \gamma_C\bar{\boldsymbol{\omega}}_C\bar{\mathbf{e}}_C^T)\mathbf{B}_P \\ \dot{\widehat{\boldsymbol{\Lambda}}}^T &= \boldsymbol{\Gamma}_\Lambda\gamma_C(\boldsymbol{\Theta}_C^T\bar{\boldsymbol{\omega}}_C - \bar{\mathbf{u}})\bar{\mathbf{e}}_C^T\mathbf{B}_P,\end{aligned} \tag{5.106}$$

where an additional weighting factor γ_C for the term derived from gradient minimization can be introduced.

As shown in [92], these update laws guarantee global asymptotic stability of the closed loop error dynamics. In Appendix D only the stability proof for the linear error

model (see next section) is shown, but due to similarity the transfer to the bilinear error model is easy.

The errors $\mathbf{e}_C$ and $\bar{\mathbf{e}}_C$ converge to zero asymptotically. This can be shown with the Lyapunov function candidate:

$$V = \frac{1}{2}\mathbf{e}_C^T\mathbf{P}\mathbf{e}_C + \frac{1}{2}\mathrm{Tr}\left[\widetilde{\boldsymbol{\Theta}}_C^T\boldsymbol{\Gamma}_C^{-1}\widetilde{\boldsymbol{\Theta}}_C\boldsymbol{\Lambda}\right] + \frac{1}{2}\mathrm{Tr}\left[\widetilde{\boldsymbol{\Lambda}}\boldsymbol{\Gamma}_\Lambda^{-1}\widetilde{\boldsymbol{\Lambda}}^T\right]. \tag{5.107}$$

The simple Lyapunov based update law in Eq.(4.10), is subject to a rank one limitation because the term $\boldsymbol{\omega}_C\mathbf{e}_C^T$ results in a rank one matrix, and thus the update of $\boldsymbol{\Theta}_C^T$ is limited to this direction. In difference the additional term in Eq.(5.105) helps to overcome this limitation as $\bar{\boldsymbol{\omega}}_C$ is the integrated or filtered version of $\boldsymbol{\omega}_C$ that contains information from a previous time interval in averaged from, and has not necessarily the same direction as $\boldsymbol{\omega}_C$. Hence, it is likely that $\boldsymbol{\omega}_C\mathbf{e}_C^T\mathbf{P}$ and $\bar{\boldsymbol{\omega}}_C\bar{\mathbf{e}}_C^T$ have different directions and the sum results in a rank two matrix

5.3.1.2 Linear Error Model:

If the indirect MRAC structure or the predictor based MRAC structure is used we assume a parameterized plant dynamics which is linear in the parameters (compare Eq.(4.15) and Eq.(4.29)). In the following similar to [109] [110] [111] the predictor based approach is exemplarily used. As mentioned, integration over a moving time window as well as filtering can be used to obtain the algebraic error model of Eq.(5.97), which is linear in the unknown parameters.

Considering the following cost function

$$J\left(\widehat{\boldsymbol{\Theta}}_P^T\right) = \frac{1}{2}\bar{\mathbf{e}}_P^T\bar{\mathbf{e}}_P = \frac{1}{2}\left[\mathbf{B}_P\widehat{\boldsymbol{\Theta}}_P^T\bar{\boldsymbol{\omega}}_P - \bar{\boldsymbol{\upsilon}}\right]^T\left[\mathbf{B}_P\widehat{\boldsymbol{\Theta}}_P^T\bar{\boldsymbol{\omega}}_P - \bar{\boldsymbol{\upsilon}}\right], \tag{5.108}$$

by application of the gradient method the following update laws for parameter identification can be derived

$$\dot{\widehat{\boldsymbol{\Theta}}}_P = -\boldsymbol{\Gamma}_P\frac{\partial J\left(\widehat{\boldsymbol{\Theta}}_P^T\right)}{\partial\widehat{\boldsymbol{\Theta}}_P^T} = -\boldsymbol{\Gamma}_P\,\bar{\boldsymbol{\omega}}_P\left[\mathbf{B}_P\widehat{\boldsymbol{\Theta}}_P^T\bar{\boldsymbol{\omega}}_P - \bar{\boldsymbol{\upsilon}}\right]^T\mathbf{B}_P = -\boldsymbol{\Gamma}_P\,\bar{\boldsymbol{\omega}}_P\bar{\mathbf{e}}_P^T\mathbf{B}_P \tag{5.109}$$

Now the standard update laws from Eq.(4.38) can be altered by the additional term from Eq.(5.109)

$$\dot{\widehat{\boldsymbol{\Theta}}}_P = -\boldsymbol{\Gamma}_P(\boldsymbol{\omega}_P\mathbf{e}_P^T\mathbf{P} + \gamma_C\bar{\boldsymbol{\omega}}_P\bar{\mathbf{e}}_P^T)\mathbf{B}_P \tag{5.110}$$

Following the argumentation in [100] it can be shown that the closed loop system is globally stable and $\mathbf{e}_P$ and $\bar{\mathbf{e}}_P$ converge to zero asymptotically. This can be shown with the Lyapunov function candidate:

$$V = \frac{1}{2}\mathbf{e}_P^T\mathbf{P}\mathbf{e}_P + \frac{1}{2}\mathrm{Tr}\left[\widetilde{\widehat{\boldsymbol{\Theta}}}_P^T\boldsymbol{\Gamma}_P^{-1}\widetilde{\widehat{\boldsymbol{\Theta}}}_P\right] \tag{5.111}$$

The proof is also shown in Appendix D.

5.3.2 Concurrent Learning

The concurrent learning was introduced and evaluated in [112] [113] [160] [161] where input output linearization is used to cancel known nonlinearities in the system in advance. This makes sense as the desired reference dynamics is usually linear, but it is not necessary and for consistency, in the following the approach is presented in a more general way. The adaptation laws of MRAC use only instantaneous signals to update the parameters and this leads to a rank one limitation of the adaptation laws, as explained in Section 5.3.1. The idea of the proposed methods is to additionally use stored background data for the adaptation to overcome the rank one limitation and achieve faster convergence with global approximation of the system uncertainty. Hence, not only one point is used as it was done in the previous Section 5.3.1, where a rank two update could be achieved, but additional points are stored and used for adaptation to obtain higher ranks in the update matrix. In early publications the adaptation based on stored data was designed such that the current learning is not affected by it, and concurrent learning only takes place in directions perpendicular to current learning direction (in the nullspace of the current learning) [112] [113] [160] [161]. This idea however, is no longer pursued in recent publications [162] [163] [164].

The approach as it was presented in [112] [113] [160] [161] requires the knowledge of the state derivatives, and therefore a smoothing algorithm is used to obtain them from the measured states. Once a suitable data point $\mathbf{x}_{P,i}$ is selected the smoothing algorithm is initiated to obtain the derivative $\dot{\mathbf{x}}_{P,i}$. As mentioned before, if the state derivatives are available the system dynamics directly provides an algebraic equation that is either bilinear or linear in the parameters, dependent on the chosen approach.

Instead of directly using the state derivatives, it is also possible to use the integrated or filtered system dynamics, as shown previously. In the following a linear parameterization is assumed which leads to an algebraic constraint according to Eq.(5.96), where for a certain stored data point, denoted by index i, we have

$$\bar{\mathbf{v}}_i = \mathbf{B}_P \boldsymbol{\Theta}_P^{*T} \bar{\boldsymbol{\omega}}_{P,i} \tag{5.112}$$

This is equal to the algebraic equation considered in the previous section. This means, the adaptation law from Eq.(5.110) is valid for parameter estimation.

However, the key feature of the method is that multiple, sufficiently different data points are selected, stored, and used in the adaptation law to achieve a global estimation of the system uncertainty.

According to Eq.(5.109) a single data point can be taken into account by using gradient based minimization

$$\dot{\hat{\boldsymbol{\Theta}}}_{P,b,i} = -\boldsymbol{\Gamma}_P \bar{\boldsymbol{\omega}}_{P,i} \bar{\mathbf{e}}_{P,i}^T \mathbf{B}_P \tag{5.113}$$

where the subscript b denotes that this is the update based on recorded data from point i.

To include the effect of all stored data points n, a summation of $\dot{\hat{\boldsymbol{\Theta}}}_{P,b,i}$ is used and Lyapunov based update laws can be altered according to Eq.(5.110) to obtain

$$\dot{\hat{\boldsymbol{\Theta}}}_P = -\boldsymbol{\Gamma}_P \left(\boldsymbol{\omega}_P \mathbf{e}_P^T \mathbf{P} + \gamma_C \sum_1^n \bar{\boldsymbol{\omega}}_{P,i} \bar{\mathbf{e}}_{P,i}^T \right) \mathbf{B}_P \tag{5.114}$$

If there is enough excitation of the system and the right points are selected, then the sum over $\bar{\boldsymbol{\omega}}_{P,i} \bar{\mathbf{e}}_{P,i}^T$ will yield a matrix with full rank.

Of course, the approach only makes sense if the system contains uncertain nonlinearities which should be approximated in a global way, and if the approximation term for the nonlinearity provides enough freedom to allow for an approximation over the whole domain where data points have been recorded. In this perspective the approach is mainly suitable for application in conjunction with neural networks, and in [112] [113] [160] [161] the extension to general nonlinear-in-the-parameter neural networks is also shown. The remaining issues are governed by the questions: how should the data points be selected, and how many data points should be stored? This is of course a problem specific question, and the answer depends on the expected uncertainties.

5.3.3 Recursive Least-Square Modification

Instead of the gradient based modification, recursive least-square estimation with adaptive learning gain can be used for the parameter update, as suggested in [4] [115]. In the following the method is shown for linearly parameterized error models such as Eq.(5.102). The idea of the least-square method is to find the estimate $\hat{\boldsymbol{\Theta}}_P(t)$ that minimizes the square of all errors $\bar{\mathbf{e}}_P\left(\hat{\boldsymbol{\Theta}}_P\right) = \mathbf{B}_P \hat{\boldsymbol{\Theta}}_P^T(t) \bar{\boldsymbol{\omega}}_P(\tau) - \bar{\boldsymbol{\upsilon}}(\tau)$ over the time interval $0 < \tau < t$. To achieve this, define the integral cost functional

$$J\left(\hat{\boldsymbol{\Theta}}_P^T\right) = \frac{1}{2} \int_0^t \bar{\mathbf{e}}_P^T \bar{\mathbf{e}}_P \, d\tau = \frac{1}{2} \int_0^t \left[\mathbf{B}_P \hat{\boldsymbol{\Theta}}_P^T(t) \bar{\boldsymbol{\omega}}_P(\tau) - \bar{\boldsymbol{\upsilon}}(\tau)\right]^T \left[\mathbf{B}_P \hat{\boldsymbol{\Theta}}_P^T(t) \bar{\boldsymbol{\omega}}_P(\tau) - \bar{\boldsymbol{\upsilon}}(\tau)\right] d\tau. \tag{5.115}$$

The minimum of this cost function has to satisfy

$$\frac{\partial J(\hat{\boldsymbol{\Theta}}_P^T)}{\partial \hat{\boldsymbol{\Theta}}_P^T} = \int_0^t \bar{\boldsymbol{\omega}}_P(\tau) \bar{\boldsymbol{\omega}}_P^T(\tau) \, d\tau \hat{\boldsymbol{\Theta}}_P(t) \mathbf{B}_P^T \mathbf{B}_P - \int_0^t \bar{\boldsymbol{\omega}}_P(\tau) \bar{\boldsymbol{\upsilon}}^T(\tau) \, \mathbf{B}_P d\tau = \mathbf{0}. \tag{5.116}$$

Differentiating Eq.(5.116) with respect to time we obtain

$$\bar{\boldsymbol{\omega}}_P(t) \bar{\boldsymbol{\omega}}_P^T(t) \hat{\boldsymbol{\Theta}}_P(t) \mathbf{B}_P^T \mathbf{B}_P + \dot{\hat{\boldsymbol{\Theta}}}_P(t) \int_0^t \bar{\boldsymbol{\omega}}_P(\tau) \bar{\boldsymbol{\omega}}_P^T(\tau) \, d\tau \mathbf{B}_P^T \mathbf{B}_P - \bar{\boldsymbol{\omega}}_P(t) \bar{\boldsymbol{\upsilon}}^T(t) \mathbf{B}_P = \mathbf{0}. \tag{5.117}$$

By defining

$$\mathbf{R}^{-1} = \int_0^t \bar{\boldsymbol{\omega}}_P(\tau) \bar{\boldsymbol{\omega}}_P^T(\tau) \, d\tau > \mathbf{0}, \tag{5.118}$$

and applying it to Eq.(5.117) we get

$$\bar{\boldsymbol{\omega}}_P(t) \bar{\boldsymbol{\omega}}_P^T(t) \hat{\boldsymbol{\Theta}}_P(t) \mathbf{B}_P^T \mathbf{B}_P + \mathbf{R}^{-1} \dot{\hat{\boldsymbol{\Theta}}}_P(t) \mathbf{B}_P^T \mathbf{B}_P - \bar{\boldsymbol{\omega}}_P(t) \bar{\boldsymbol{\upsilon}}^T(t) \mathbf{B}_P = \mathbf{0}. \tag{5.119}$$

Furthermore the following identity holds

$$\frac{\mathrm{d}}{\mathrm{d}t}\mathbf{I} = \frac{\mathrm{d}}{\mathrm{d}t}\mathbf{R}^{-1}\mathbf{R} = \dot{\mathbf{R}}^{-1}\mathbf{R} + \mathbf{R}^{-1}\dot{\mathbf{R}} = \mathbf{0}. \tag{5.120}$$

By resolving Eq.(5.119) with respect to $\dot{\hat{\boldsymbol{\Theta}}}_P$ and Eq.(5.120) with respect to $\dot{\mathbf{R}}$ the update laws are obtained

$$\dot{\hat{\boldsymbol{\Theta}}}_P(t) = -\mathbf{R}\left[\bar{\boldsymbol{\omega}}_P \underbrace{\left(\bar{\boldsymbol{\omega}}_P^T\hat{\boldsymbol{\Theta}}_P\mathbf{B}_P^T - \bar{\boldsymbol{\upsilon}}^T\right)}_{\bar{\mathbf{e}}_P^T}\mathbf{B}_P^{l^T}\right] \tag{5.121}$$

$$\dot{\mathbf{R}} = -\mathbf{R}\dot{\mathbf{R}}^{-1}\mathbf{R} = -\mathbf{R}\bar{\boldsymbol{\omega}}_P\bar{\boldsymbol{\omega}}_P^T\mathbf{R}, \tag{5.122}$$

where the left pseudo-inverse $\mathbf{B}_P^l = (\mathbf{B}_P^T\mathbf{B}_P)^{-1}\mathbf{B}_P^T$ must exist.

$\mathbf{R}$ is the covariance matrix which is updated from a differential equation: Eq.(5.122). Because $\mathbf{R}$ is also the learning rate (adaptation gain) for the parameter update in Eq.(5.121), this constitutes an adaptation law with adaptive learning rate. From Eq.(5.122) it is clear that $\bar{\boldsymbol{\omega}}_P\bar{\boldsymbol{\omega}}_P^T$ is positive semi definite, and thus the covariance will converge to the origin in presence of persistent excitation. This is behavior is called covariance wind-up. On the one hand this characteristic leads to better and more robust estimation in the presence of measurement noise. On the other hand the reduction of the update gain will lead to problems if the system parameters are not constant but change over time. To circumvent the wind-up problem a forgetting factor in the update law for the covariance matrix can be used. But then boundedness of $\mathbf{R}$ is no longer guaranteed without additional modifications like bounding of the covariance matrix by means of the projection operator [88] or bounded-gain forgetting [4].

To guarantee signal boundedness and convergence of the tracking error, again, a combination of Eq.(5.121) and Eq.(5.122) with the Lyapunov based adaptation law in Eq.(4.38) can be used:

$$\dot{\hat{\boldsymbol{\Theta}}}_P = -\mathbf{R}\left[\boldsymbol{\omega}_P\mathbf{e}_P^T\mathbf{P}\mathbf{B}_P + \bar{\boldsymbol{\omega}}_P\bar{\mathbf{e}}_P^T\mathbf{B}_P^{l^T}\right] \tag{5.123}$$

$$\dot{\mathbf{R}} = -\mathbf{R}\dot{\mathbf{R}}^{-1}\mathbf{R} = -\mathbf{R}\bar{\boldsymbol{\omega}}_P\bar{\boldsymbol{\omega}}_P^T\mathbf{R} \tag{5.124}$$

It can be shown that the closed loop system is globally stable and $\mathbf{e}_P$ and $\bar{\mathbf{e}}_P$ converge to zero asymptotically. This can be established with the following Lyapunov function candidate:

$$\mathrm{V} = \frac{1}{2}\mathbf{e}_P^T\mathbf{P}\mathbf{e}_P + \frac{1}{2}\mathrm{Tr}\left[\tilde{\boldsymbol{\Theta}}_P^T\mathbf{R}^{-1}\tilde{\boldsymbol{\Theta}}_P\right] \tag{5.125}$$

To account for the mentioned covariance wind-up a forgetting factor can be added, and this yields

$$\dot{\mathbf{R}} = -\mathbf{R}\dot{\mathbf{R}}^{-1}\mathbf{R} = -\mathbf{R}\bar{\boldsymbol{\omega}}_P\bar{\boldsymbol{\omega}}_P^T\mathbf{R} + \beta\mathbf{R} \tag{5.126}$$

with $\beta > 0$. Larger β means better ability to follow time varying parameters, but it also implies a shorter averaging time, which means less robustness in the presence of measurement noise.

5.3.4 Short Period Example

In the following the recursive least square modification suggested in the previous Section 5.3.3 is applied to the predictor based approach used in Section 5.1.7.1. This means, following Eq.(5.123) and Eq.(5.124) the modified version of the update laws from Eq.(5.30) is given by

$$\begin{aligned}\dot{\hat{\boldsymbol{\theta}}}_P &= \begin{bmatrix}\dot{\hat{\boldsymbol{\theta}}}_y \\ \dot{\hat{\lambda}}\end{bmatrix} = -\mathbf{R}_{ma}\left[\boldsymbol{\omega}_P \mathbf{e}_P^T \mathbf{P}\mathbf{b}_{P,n_Z}^{+} + \gamma_C \bar{\boldsymbol{\omega}}_P\left(\bar{\boldsymbol{\omega}}_P^T \hat{\boldsymbol{\theta}}_P^T \mathbf{b}_{P,n_Z}^{+} - \bar{\boldsymbol{\upsilon}}^T\right)\mathbf{b}_{P,n_Z}^{+,l^T}\right] \\ \dot{\mathbf{R}}_{ma} &= -\mathbf{R}_{ma}[\bar{\boldsymbol{\omega}}_P \bar{\boldsymbol{\omega}}_P^T]_{ii}\mathbf{R}_{ma} + \beta[\mathbf{R}_{ma}]_{ii}.\end{aligned} \tag{5.127}$$

With $\bar{\boldsymbol{\omega}}_P^T = [\bar{\mathbf{y}}_P^+ \quad \bar{\eta}]$. The update law for the unmatched uncertainties from Eq.(5.63) is modified to

$$\begin{aligned}\dot{\hat{\boldsymbol{\theta}}}_{y,um} &= -\mathbf{R}_{um}\left[\mathbf{y}_P^+ \mathbf{e}_P^T \mathbf{P}\mathbf{b}_{P,um,n_Z}^{+} + \gamma_C \bar{\mathbf{y}}_P^+\left(\bar{\mathbf{y}}_P^{+^T}\hat{\boldsymbol{\theta}}_{y,um}^T \mathbf{b}_{P,n_Z,um}^{+} - \bar{\boldsymbol{\upsilon}}^T\right)\mathbf{b}_{P,um,n_Z}^{+,l^T}\right] \\ \dot{\mathbf{R}}_{um} &= -\mathbf{R}_{um}\left[\bar{\mathbf{y}}_P^+ \bar{\mathbf{y}}_P^{+^T}\right]_{ii}\mathbf{R}_{um} + \beta[\mathbf{R}_{um}]_{ii}\end{aligned} \tag{5.128}$$

To reduce the number of parameters the update laws for the covariance matrices $\mathbf{R}_{ma}$ and $\mathbf{R}_{um}$ are modified, such that only the diagonal elements are adjusted. The selection of the diagonal elements of a matrix is denoted by $[\bullet]_{ii}$. Additionally the parameter γ_C is introduced as weighting factor for the update base on the algebraic error.

In the following the filter approach is applied. Thus, from Eq.(5.100) and by taking into account that the modification for unmatched uncertainties form Section 5.1.4 is applied we obtain for $\bar{\boldsymbol{\upsilon}}$

$$\bar{\boldsymbol{\upsilon}} = -\left(\lambda_F(\mathbf{y}_P^+ - \bar{\mathbf{y}}_P^+) - \mathbf{A}_{P,n_Z}^{+}\bar{\mathbf{y}}_P^{+} - \mathbf{b}_r^+ \bar{\mathrm{r}} + \mathbf{b}_{P,n_Z,um}^{+}\hat{\boldsymbol{\theta}}_{y,um}\bar{\mathbf{y}}_P^{+}\right) \tag{5.129}$$

Compared to Eq.(5.100), here the system matrix $\mathbf{A}_{P,n_Z}^{+}$ is used instead of the ideal system matrix $\mathbf{A}_{M,n_Z}^{+}$ because the control input η contains the feedback of the baseline controller, whereat in Section 5.3.1 only an adaptive feedback signal was assumed.

The filtered signals are given by

$$\begin{aligned}\bar{\mathbf{y}}_P^+(s) &= \frac{\lambda_F}{s+\lambda_F}\mathbf{y}_P^+(s) \\ \bar{\eta}(s) &= \frac{\lambda_F}{s+\lambda_F}\eta(s) \\ \bar{r}\,(s) &= \frac{\lambda_F}{s+\lambda_F}r(s),\end{aligned} \tag{5.130}$$

and $\lambda_F = 1$ is selected for the following simulation results.

The adaptive controller is assembled by Eq.(5.26), Eq.(5.60), Eq.(5.61), Eq.(5.67), Eq.(5.29), Eq.(5.127), Eq.(5.128), Eq.(5.129) and (5.130).

The controller parameters, to which the same tuning and constraints as in Section 5.1.7.1 were applied, are the initial conditions for of the covariance matrices $\mathbf{R}_{ma}(0)$

and $\mathbf{R}_{um}(0)$, the forgetting factor β, and the error feedback gain k_e. To assure boundedness of $\mathbf{R}_{ma}$ and $\mathbf{R}_{um}$ projection is used to enforce the upper bounds given by the initial conditions, $\mathbf{R}_{ma}(0)$ and $\mathbf{R}_{um}(0)$. Together with a cost function value of J=0.465 the parameter values in Table 5.15 are obtained. Again, uncertainties in the dynamics of the integrated error $\mathbf{e}_I$ are not expected and the respective entries in $\mathbf{R}_{ma}(0)$ and $\mathbf{R}_{um}(0)$ are set to zero.

$\mathbf{R}_{ma}(0)$	$\mathbf{R}_{um}(0)$	β	γ_C	k_e
$\begin{bmatrix} 2.31 & 0 & 0 & 0 \\ 0 & 1.41 & 0 & 0 \\ 0 & 0 & 0 & 0 \\ 0 & 0 & 0 & 0.11 \end{bmatrix}$	$\begin{bmatrix} 2.38 & 0 & 0 \\ 0 & 0.75 & 0 \\ 0 & 0 & 0 \end{bmatrix}$	0.81	3.44	0.95

Table 5.15: Controller parameter

In the following only the time delay margin are calculated and shown in Table 5.16 and the robust performance is evaluated in Figure 5.73 - Figure 5.78. It is clear that a performance increase should not be expected, because the reduction of the learning rate in the presence of excitation will lead to slower parameter adjustment. From Figure 5.73 - Figure 5.78 it can be concluded that the performance deteriorates for the initial step input.

	1g CMD	2g CMD
TDM	0.30s	0.25s

Table 5.16: Time delay margins

From the time delay margins given in Table 5.16 no increase in robustness can be seen. However, the performance of the approach is still better than the baseline controller and form the theory a robustness increase w.r.t. measurement noise can be expected.

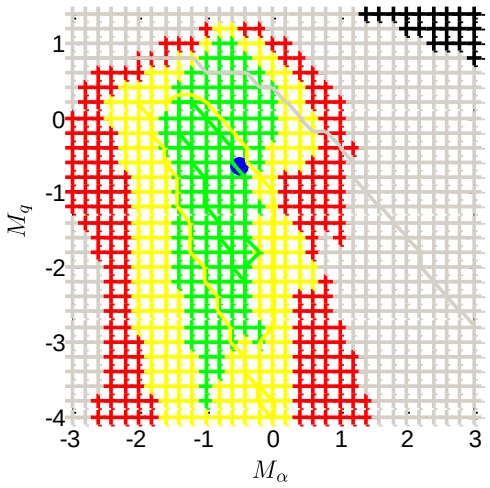

Figure 5.73: Robust perfomance w.r.t. M_α and M_q; $n_{Z,CMD}$=1

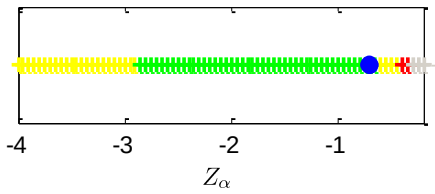

Figure 5.74: Robust perfomance w.r.t. Z_α; $n_{Z,CMD}$=1

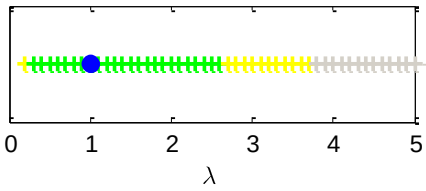

Figure 5.75: Robust perfomance w.r.t. λ $n_{Z,CMD}$=1

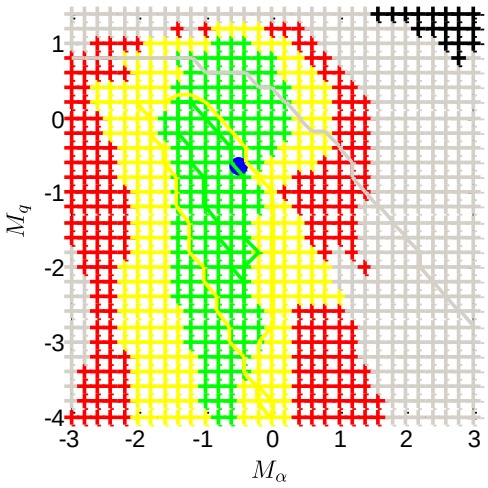

Figure 5.76: Robust perfomance w.r.t. M_α and M_q; $n_{Z,CMD}$=2

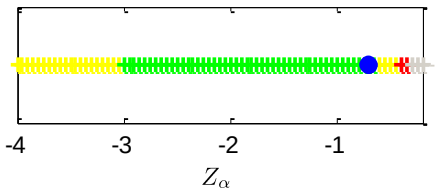

Figure 5.77: Robust perfomance w.r.t. Z_α; $n_{Z,CMD}$=2

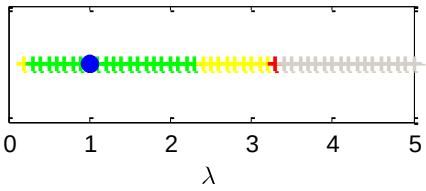

Figure 5.78: Robust perfomance w.r.t. λ $n_{Z,CMD}$=2

Chapter 6

$\mathcal{L}_1$ Adaptive Control

In recent years $\mathcal{L}_1$ adaptive control was suggested as advancement to standard MRAC and its benefits have been controversially discussed. In this chapter the basic theory is presented. Furthermore the similarities of applying a hedging signal to the reference model, used in model reference adaptive control to account for dynamic constraints in the input channel (see Section 5.1.1), and $\mathcal{L}_1$ adaptive control are discussed. For the sake of simplicity the approach is displayed for single input system according to [95] and [165], but the extension to MIMO systems is possible [23], [26], [166]. Successful applications of $\mathcal{L}_1$ adaptive control can be found in [25] [26] [167] [168] [169] [170] [171] [172] [173] [174].

In the previous section we could see that fast adaptation is desirable as it allows a fast compensation of uncertainties. Therefore, a fast adjustment of the parameters is necessary and hence a high adaptation gain must be used. We could also see in the previous section that without the hedging only small adaptation gains are possible, because large gains lead to oscillations in the parameters which then also occur in the input channel. These oscillations in the input channel are undesirable and with actuator and structural filter dynamics the high gain can easily lead to instability [86].

To solve this drawback the theory of $\mathcal{L}_1$ adaptive control was developed [95] [96] [97], with the objective to decouple robustness and adaptation, and thus decouple control from estimation. The key idea of $\mathcal{L}_1$ is to restrict the bandwidth of the control signal by using a low-pass filter in the input channel to prevent high frequencies from entering the system. But fast adjustment of the parameters is still desirable and therefore the influence of fast parameter changes has to be visible in the error signal. This led to special architectural choice of $\mathcal{L}_1$ adaptive control.

In the following it is shown how and why this special structure is used for $\mathcal{L}_1$ adaptive control [165]. As already mentioned, a low-pass filter is used in the input channel as shown in Figure 6.1, where the red dot indicates where the filter would have to be installed in the direct and in the predictor based structure.

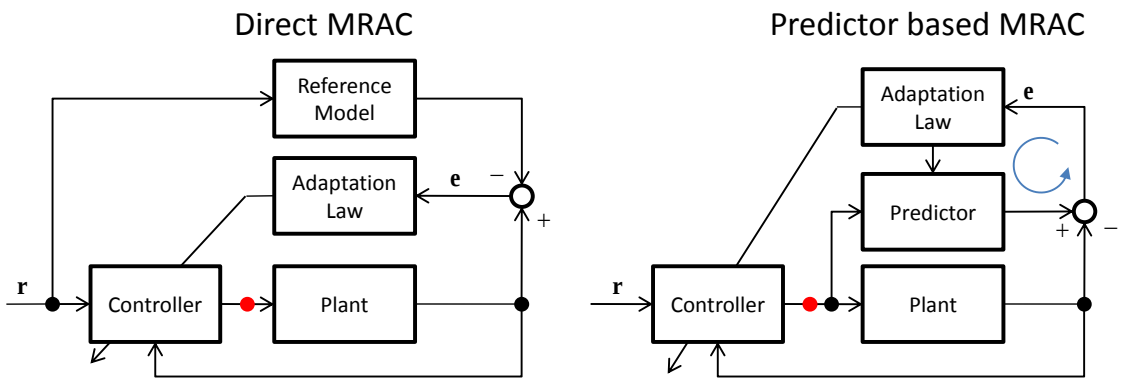

Figure 6.1: Effect of the lowpass filter on direct MRAC and predictor based MRAC

Assume we are using the direct approach and apply the low-pass filter in the input channel. It becomes clear, that the higher frequencies are filtered out from the command signals. Hence, the effect of fast parameter changes would not be visible in the error signal. Furthermore, with the additional filter dynamics the plant differs from the reference model and thus the reference model cannot be tracked for high frequency commands.

If we are using the predictor based MRAC, we can also implement a low-pass filter in the input channel to prevent corruptive frequencies from exciting the plant. In difference to the feedforward characteristic of the reference model the predictor uses the input signal $\mathbf{u}$ as well as the unfiltered estimated parameters. This can be seen from the predictor dynamics in Eq.(4.30):

$$\dot{\hat{\mathbf{x}}}_P = \mathbf{A}_M \hat{\mathbf{x}}_P + \mathbf{B}_P\left(\widehat{\boldsymbol{\Lambda}}\mathbf{u} - \boldsymbol{\Theta}_x \mathbf{x}_P - \boldsymbol{\Theta}_\varphi \boldsymbol{\varphi}(\mathbf{x}_P) - \boldsymbol{\Theta}_d\right). \tag{6.1}$$

Even if $\mathbf{u}$ is filtered, the high frequency content enters the predictor via the estimated parameters. Hence, the influence of fast parameter changes is still visible in the error which is used for adaptation. So information contained in the high frequency content is not filtered out but is still used for adaptation. This is the reason why the predictor based architecture is used for $\mathcal{L}_1$ adaptive control [95].

As mentioned before, the idea is to choose the adaptation gain as large as possible and shifting the design freedom towards the introduced filter. This filter has to be chosen appropriately to guarantee the stability of the adaptive system. Recently a similar approach was suggested where the design of the filter is based on H_∞ control design [175] [176].

The modification is much more complex than just the insertion of the filter, due to the fact that the input to the predictor is also filtered. Thus the predictor is not equal to the reference model as it was in Section 4.4 (see Eq.(4.34)), and the Small-Gain-Theorem has to be used to proof stability. The new architecture and the claims that are made within $\mathcal{L}_1$ adaptive control theory raised concerns in the adaptive control community

because some researchers think that the claims cannot be met. However, in the following it is shown that $\mathcal{L}_1$ adaptive control basically provides a method to account for dynamic constraints in the input channel of the plant, legitimatized by sound mathematical proofs.

In particular the similarities of applying a hedging signal to the reference model used in direct MRAC, to account for dynamic constraints in the input channel, and $\mathcal{L}_1$ adaptive control are discussed. It is shown that in the case where the control effectiveness is known, both approaches are exactly the same, where the contribution of the $\mathcal{L}_1$ theory is the mathematically correct framework that provides a stability poof/condition which has not been available for the hedging approach. In the case of unknown control effectiveness the two methods are slightly different and the $\mathcal{L}_1$ approach additionally adjusts the cutoff frequency of the low pass filter. This difference allows for the elegant stability proof given by $\mathcal{L}_1$ theory. At the end the two approaches are compared based on a simple short period model of a large transport aircraft by assessing the robust performance w.r.t. model uncertainties.

In general the approach is of course also possible with nonlinear regressors, however the notion in $\mathcal{L}_1$ adaptive control is, to achieve adaptation that is fast enough to make nonlinear regressors unnecessary [95]. To point out the main idea, in the following the approach is at first shown for a single input system with known high frequency gain and constant uncertainties. Then the approach for systems with unknown high frequency gain and time varying parameters is shown.

In the last section of this chapter $\mathcal{L}_1$ piecewise constant control is discussed and evaluated for the simple short period model. Even though this cannot be considered as an adaptive control approach it is presented in this chapter as the idea originated from $\mathcal{L}_1$ adaptive control.

6.1 Plant with Known High-Frequency Gain

Analogously to Eq.(4.29) the plant dynamics for a single input system are given by (matching condition holds)

$$\dot{\mathbf{x}}_P = \mathbf{A}_M \mathbf{x}_P + \mathbf{b}_P \left(u - \widehat{\boldsymbol{\theta}}_x^{*\,T} \mathbf{x}_P \right) \tag{6.2}$$

$\widehat{\boldsymbol{\theta}}_x^{*\,T} \in \mathbb{R}^{1\times n}$ is an unknown parameter vector and it is assumed that a bound on the system uncertainties is known such that $\widehat{\boldsymbol{\theta}}_x^{*\,T}$ belongs to a convex, compact set: $\widehat{\boldsymbol{\theta}}_x^{*\,T} \in \boldsymbol{\Omega}_\Theta$. Here no nonlinear and constant uncertainties and no uncertainties in the control effectiveness are assumed.

According to Eq.(4.30) the state predictor is given by

$$\dot{\hat{\mathbf{x}}}_P = \mathbf{A}_M \hat{\mathbf{x}}_P + \mathbf{b}_P \big(u - \widehat{\boldsymbol{\theta}}_x^{T} \mathbf{x}_P \big). \tag{6.3}$$

The error dynamics for the considered case is similar to Eq.(4.35):

$$\dot{\mathbf{e}}_P = \dot{\hat{\mathbf{x}}}_P - \dot{\mathbf{x}}_P = \mathbf{A}_M \mathbf{e}_P + \mathbf{b}_P \tilde{\boldsymbol{\theta}}_x^T \mathbf{x}_P. \tag{6.4}$$

The parameter update law from Lyapunov theory is also used for $\mathcal{L}_1$ adaptive control and is given by (see Eq.(4.38))

$$\dot{\hat{\boldsymbol{\theta}}}_x = \boldsymbol{\Gamma}_x \mathbf{x}_P \mathbf{e}_P^T \mathbf{P} \mathbf{b}_P. \tag{6.5}$$

6.1.1 Controller Structure

In Figure 6.2 the $\mathcal{L}_1$ structure is shown, where the difference to the predictor based MRAC is given by the stable, strictly-proper, linear low-pass filter $C(s)$, with DC gain of one, in the input channel of both, the plant and the predictor. For $C(s) = 1$ the $\mathcal{L}_1$ architecture obviously collapses to the predictor based MRAC.

According to Eq.(4.32) the MRAC control law is given by

$$u_{MRAC} = k_r r + \hat{\boldsymbol{\theta}}_x^T \mathbf{x}_P. \tag{6.6}$$

The $\mathcal{L}_1$ control law is given by a filtered version of the previous, which can be denoted in the Laplace domain by

$$u_{\mathcal{L}_1}(s) = C(s) u_{MRAC}(s) \tag{6.7}$$

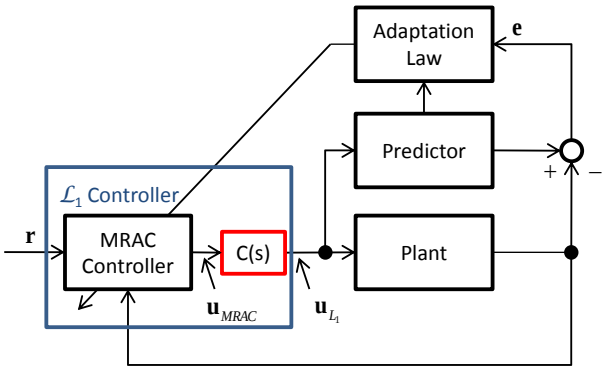

Figure 6.2: Basic $\mathcal{L}_1$ architecture

Instantly this newly introduced filter raises the question of how does it impact the stability. The problem is actually the same that was encountered by taking into account additional dynamics in the input channel and applying a hedging signal (see Section 5.1.1). Due to the additional dynamics of the filter the normal Lyapunov stability proof is not applicable. However, the theory of $\mathcal{L}_1$ provides a stability proof under compliance with additional requirements [95], which are given in Section 6.1.3.

Filter with Constant Cut-off Frequency

To be a low pass filter, $C(s)$ must be strictly proper, i.e. its numerator degree must be lower than the denominator degree. Additionally, as a prerequisite for overall system stability, $C(s)$ has to be stable, see Section 6.1.2. The general structure of the filter is the following

$$C(s) = \frac{\omega_C D(s)}{1+\omega_C D(s)}, \tag{6.8}$$

with $D(s)$ being any transfer function that leads to a strictly proper and stable $C(s)$ and a DC gain equal to one: $C(0) = 1$ To obtain a strictly proper $C(s)$ the relative degree of $D(s)$ must be greater than zero. The filter can be implemented as shown in Figure 6.3. For the considered case, where the control effectiveness is know, the low pass filter can of course be implemented in a simpler way. However, for the case where the control effectiveness is unknown this structure is necessary (see Section 6.2). Thus, for consistency the same structure is already used here.

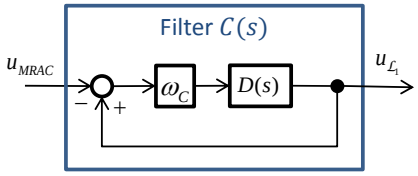

Figure 6.3: Filter with constant cut-off frequency

For example, a 1st order filter evolves from $D(s) = 1/s$. This yields $(s) = \frac{\omega_C}{s+\omega_C}$, where ω_C is the crossover frequency. From Eq.(6.6) the control law is given by

$$u_{\mathcal{L}_1}(s) = \frac{\omega_C}{s+\omega_C}\ u_{MRAC}(s). \tag{6.9}$$

Transforming Eq.(6.9) to the time domain we get

$$\dot{u}_{\mathcal{L}_1}(t) = \omega_C \left[u_{MRAC}(t) - u_{\mathcal{L}_1}(t)\right]. \tag{6.10}$$

For a 1st order filter, Figure 6.4 gives an overview of the entire $\mathcal{L}_1$ control architecture derived in this section.

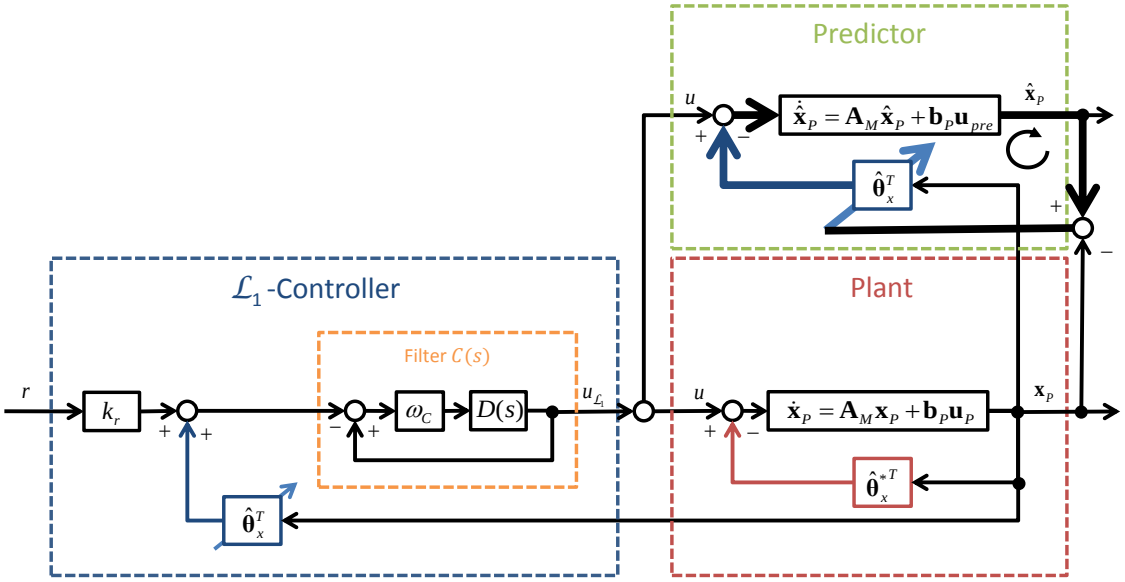

Figure 6.4: Complete $\mathcal{L}_1$ control architecture for known high frequency gain (on the basis of [165])

6.1.2 Ideal $\mathcal{L}_1$ Reference Model

With the optimal parameters $\widehat{\boldsymbol{\theta}}_x^*$ the ideal control law can be directly written for the in the form:

$$u_{MRAC,REF} = k_r r + \widehat{\boldsymbol{\theta}}_x^{*\,T}\mathbf{x}_{P,ref}. \tag{6.11}$$

With the ideal control law the MRAC reference model can be represented as a closed loop system consisting of the plant and the ideal input signal $u_{MRAC,REF}$. It was seen that for the predictor based MRAC structure the predictor in Eq.(6.3) becomes the reference model by inserting the control law given in Eq.(6.6):

$$\dot{\mathbf{x}}_M = \mathbf{A}_M\mathbf{x}_M + \underbrace{\mathbf{b}_P k_r}_{\mathbf{b}_M} r. \tag{6.12}$$

If the low-pass filter is introduced, this is not the case anymore. Actually the ideal reference model cannot be seen anymore, in the $\mathcal{L}_1$ structure. For the $\mathcal{L}_1$ architecture an ideal reference model can be derived by filtering the ideal control input given in Eq.(6.11)

$$u_{\mathcal{L}_1,REF}(s) = C(s)u_{MRAC,REF}(s). \tag{6.13}$$

Applying it to the plant results in the ideal $\mathcal{L}_1$-reference model:

$$\dot{\mathbf{x}}_{REF}(t) = \mathbf{A}_M\mathbf{x}_{REF}(t) + \mathbf{b}_P\left[u_{\mathcal{L}_1,REF}(t) - \widehat{\boldsymbol{\theta}}_x^{*\,T}\mathbf{x}_{REF}(t)\right] \tag{6.14}$$

$$u_{\mathcal{L}_1,REF}(s) = C(s)u_{MRAC,REF}(s) = C(s)\left\{k_r r(t) + \widehat{\boldsymbol{\theta}}_x^{*\,T}\mathbf{x}_{REF}(t)\right\}_s. \tag{6.15}$$

In the Laplace domain Eq.(6.14) can be denoted by

$$\mathbf{x}_{REF}(s) = (s\mathbf{I} - \mathbf{A}_M)^{-1}\mathbf{b}_P \left[u_{\mathcal{L}_1,REF}(s) - \widehat{\boldsymbol{\theta}}_x^{*\,T}\mathbf{x}_{REF}(s)\right] + (s\mathbf{I} - \mathbf{A}_M)^{-1}\,\mathbf{x}(0), \tag{6.16}$$

The initial condition of the plant states $\mathbf{x}(0)$ is taken into account for completeness as it has an effect on the signal bounds that will be derived. Inserting the control law from Eq.(6.15) into Eq.(6.16) yields

$$\begin{aligned}\mathbf{x}_{REF}(s) &= (s\mathbf{I} - \mathbf{A}_M)^{-1}\mathbf{b}_P \left[C(s)\left(k_r r(s) + \widehat{\boldsymbol{\theta}}_x^{*\,T}\mathbf{x}_{REF}(s)\right) - \widehat{\boldsymbol{\theta}}_x^{*\,T}\mathbf{x}_{REF}(s)\right] + (s\mathbf{I} - \mathbf{A}_M)^{-1}\,\mathbf{x}(0)\\ \mathbf{x}_{REF}(s) &= (s\mathbf{I} - \mathbf{A}_M)^{-1}\mathbf{b}_P \left[C(s)k_r r(s) + (C(s)-1)\widehat{\boldsymbol{\theta}}_x^{*\,T}\mathbf{x}_{REF}(s)\right] + (s\mathbf{I} - \mathbf{A}_M)^{-1}\,\mathbf{x}(0).\end{aligned} \tag{6.17}$$

By defining

$$\mathbf{H}(s) = (s\mathbf{I} - \mathbf{A}_M)^{-1}\mathbf{b}_P \tag{6.18}$$

$$\mathbf{G}(s) = \mathbf{H}(s)(C(s) - 1) \tag{6.19}$$

$$\mathbf{x}_{INI}(s) = (s\mathbf{I} - \mathbf{A}_M)^{-1}\,\mathbf{x}(0), \tag{6.20}$$

the reference model of Eq.(6.17) can be denoted by

$$\mathbf{x}_{REF}(s) = \mathbf{H}(s)C(s)k_r r(s) + \mathbf{G}(s)\widehat{\boldsymbol{\theta}}_x^{*\,T}\mathbf{x}_{REF}(s) + \mathbf{x}_{INI}(s). \tag{6.21}$$

Due to the low-pass filter the reference dynamics of $\mathbf{H}(s)$ (this is the MRAC reference model) can only be tracked for low frequencies, whereas for frequencies above the cut of frequency of $C(s)$ the influence of $\mathbf{G}(s)$ becomes visible. This means the $\mathcal{L}_1$ reference model is not a "clean" reference system, because the control objective is reduced by the filter. However, the filter can account for bandwidth restrictions in the input channel and therewith render the control objective feasible.

Because of the filter it is also not a-priori clear from a stable $\mathbf{A}_M$ whether the reference model is stable, even though the system from Eq.(6.14) and Eq.(6.15) is a linear feedback system as it only uses the constant ideal parameters. However, by using the small gain theorem a condition for Bounded-Input-Bounded-Output stability (BIBO stability, see definition in C.1.4) can be derived. BIBO stability means that if the input signal is element $\mathcal{L}_\infty$ (bounded) than the output signal is also element $\mathcal{L}_\infty$, and the $\mathcal{L}_\infty/\mathcal{L}_\infty$ -induced system norm is the $\mathcal{L}_1$-norm [95] [89]. This means for a system of the form $\mathbf{x}(s) = \mathbf{G}(s)\,\mathbf{u}(\mathbf{s})$, with $\mathbf{G}(s) \in R^{n\times m}$ and impulse response $\mathbf{g}(t)$ it holds that $\|\mathbf{x}(t)\|_{\mathcal{L}_\infty} \leq \|\mathbf{G}(s)\|_{\mathcal{L}_1}\,\|\mathbf{u}(t)\|_{\mathcal{L}_\infty}$. Here the notation $\|\boldsymbol{G}(s)\|_{\mathcal{L}_1} \coloneqq \|\mathbf{g}(t)\|_{\mathcal{L}_1}$ is used, and $\|\mathbf{g}(t)\|_{\mathcal{L}_1} = \max_{i=1,..,m}\left[\sum_{j=1}^{n}\left\|g_{ij}(s)\right\|_{\mathcal{L}_1}\right]$.

From the BIBO stability analysis it follows that the $\mathcal{L}_1$ ideal reference model is only stable, if the $\mathcal{L}_1$-criterion is fulfilled [95].

$$\bar{\theta}_x\|\mathbf{G}(s)\|_{\mathcal{L}_1} < 1, \tag{6.22}$$

where

$$\bar{\theta}_x = \max_{\widehat{\boldsymbol{\theta}}_x^* \in \boldsymbol{\Omega}_\Theta} \sum_{i=1}^{n} \left|\widehat{\boldsymbol{\theta}}_{x,i}^*\right|. \tag{6.23}$$

The derivation can be found in [95], but due to the importance it is revisited in the following.

With the $\mathcal{L}_\infty/\mathcal{L}_\infty$ induced system norm applied to Eq.(6.21), one can find an upper bound on the states of the reference model by

$$\|\mathbf{x}_{REF}\|_{\mathcal{L}_\infty} \leq \|k_r \mathbf{H}(s)C(s)\|_{\mathcal{L}_1} \|r\|_{\mathcal{L}_\infty} + \|\mathbf{G}(s)\|_{\mathcal{L}_1} \left\|\widehat{\boldsymbol{\theta}}_x^{*T} \mathbf{x}_{REF}\right\|_{\mathcal{L}_\infty} + \|\mathbf{x}_{INI}\|_{\mathcal{L}_\infty}. \tag{6.24}$$

To show BIBO-stability we need to resolve w.r.t. $\|\mathbf{x}_{REF}\|_{\mathcal{L}_\infty}$ and therefore we need to separate $\left\|\widehat{\boldsymbol{\theta}}_x^{*T} \mathbf{x}_{REF}\right\|_{\mathcal{L}_\infty}$, what can be achieved by the following estimate

$$\left\|\widehat{\boldsymbol{\theta}}_x^{*T} \mathbf{x}_{REF}\right\|_{\mathcal{L}_\infty} = \max_{\widehat{\boldsymbol{\theta}}_x^* \in \boldsymbol{\Omega}_\Theta} \sum_{i=1}^{n} \left|\widehat{\boldsymbol{\theta}}_{x,i}^*\right| \|\mathbf{x}_{REF}\|_{\mathcal{L}_\infty} = \bar{\theta}_x \|\mathbf{x}_{REF}\|_{\mathcal{L}_\infty} \tag{6.25}$$

Substituting Eq.(6.25) into Eq.(6.24) yields

$$\|\mathbf{x}_{REF}\|_{\mathcal{L}_\infty} \leq k_g \|\mathbf{H}(s)C(s)\|_{\mathcal{L}_1} \|r\|_{\mathcal{L}_\infty} + \bar{\theta}_x \|\mathbf{G}(s)\|_{\mathcal{L}_1} \|\mathbf{x}_{REF}\|_{\mathcal{L}_\infty} + \|\mathbf{x}_{INI}\|_{\mathcal{L}_\infty}, \tag{6.26}$$

And resolved with respect to $\|\mathbf{x}_{REF}\|_{\mathcal{L}_\infty}$ gives

$$\|\mathbf{x}_{REF}\|_{\mathcal{L}_\infty} \leq \frac{1}{1-\bar{\theta}_x \|\boldsymbol{G}(s)\|_{\mathcal{L}_1}} \left[k_r \|\mathbf{H}(s)C(s)\|_{\mathcal{L}_1} \|r\|_{\mathcal{L}_\infty} + \|\mathbf{x}_{INI}\|_{\mathcal{L}_\infty}\right]. \tag{6.27}$$

For $\mathbf{x}_{REF}$ to be bounded, $\|\mathbf{H}(s)C(s)\|_{\mathcal{L}_1}$ and $\|\mathbf{G}(s)\|_{\mathcal{L}_1}$ must exist, i.e. the transfer functions $\mathbf{G}(s) = (s\mathbf{I} - \mathbf{A}_M)^{-1}\mathbf{b}_P[1 - C(s)]$, $\mathbf{H}(s) = (s\mathbf{I} - \mathbf{A}_M)^{-1}\mathbf{b}_P$ must be stable. This is fulfilled, since $\mathbf{A}_M$ is Hurwitz and $C(s)$ is stable. Additionally, the denominator $1 - \bar{\theta}_x \|\mathbf{G}(s)\|_{\mathcal{L}_1}$ must not be zero, which is what the small gain theorem states and this leads to the $\mathcal{L}_1$-criterion in Eq.(6.22).

Thus, we obtained a condition for $C(s)$ such that the reference model, defining the reduced control objective, is stable. This is already one advantage of the $\mathcal{L}_1$ adaptive control framework: it provides a constraint on the uncertainty domain dependent on the bandwidth restrictions in the input channel. E.g. if we consider $C(s)$ to be the actuator dynamics we can draw a conclusion on the system uncertainties that can be theoretically tolerated without causing instability. Vice versa this means the larger the uncertainty $\widehat{\boldsymbol{\theta}}_x^{*T}$ can get, or the less knowledge about the compact set $\boldsymbol{\Omega}_\Theta$ is available, the larger the bandwidth of the input channel must be (higher ω_C).

This does not jet guarantee stability of the whole system. Furthermore, the reference model is not sufficient to introduce certain specification (overshoot, rise time, settling time, etc.). In the following sections, at first stability is show by application of the small gain theorem to the predictor dynamics, and then it is shown that performance bounds with respect to reference model can be established (depended on the adaptive gain) in order to fulfill the specifications.

6.1.3 Stability of the $\mathcal{L}_1$ Controller

For the following proof, according to [95], it is necessary to apply the projection operator to the adaptive law such that $\widehat{\boldsymbol{\theta}}_x$ is bounded to the assumed uncertainty set $\boldsymbol{\Omega}_\Theta$.

At first it is shown that the prediction error $\mathbf{e}_P(t)$ is bounded by the normal Lyapunov analysis and secondly it is shown that the predictor is stable.

6.1.3.1 Stability of the Error Dynamics

Here the error dynamics from Eq.(6.4) is considered:

$$\dot{\mathbf{e}}_P = \dot{\hat{\mathbf{x}}}_P - \dot{\mathbf{x}}_P = \mathbf{A}_M \mathbf{e}_P + \mathbf{b}_P \tilde{\boldsymbol{\theta}}_x^T \mathbf{x}_P. \tag{6.28}$$

Consider the Lyapunov function candidate

$$\mathrm{V} = \frac{1}{2} \mathbf{e}_P{}^T \mathbf{P} \mathbf{e}_P + \frac{1}{2} \tilde{\boldsymbol{\theta}}_x^T \boldsymbol{\Gamma}_x^{-1} \tilde{\boldsymbol{\theta}}_x. \tag{6.29}$$

It can be easily verified that with the update law from Eq.(6.5)

$$\dot{\mathrm{V}} \leq -\frac{1}{2} \mathbf{e}_P{}^T \mathbf{Q} \mathbf{e}_P. \tag{6.30}$$

If the initial error $\mathrm{e}_P(0) = 0$ and all elements of $\boldsymbol{\Gamma}_\mathrm{x}$ are equal to γ, then Eq.(6.29) implies that

$$\mathrm{V}(0) = \frac{1}{2}\frac{1}{\gamma} \tilde{\boldsymbol{\theta}}_x^T(0) \tilde{\boldsymbol{\theta}}_x(0) \geq \mathrm{V(t)} \geq \frac{1}{2} \mathbf{e}_P{}^T \mathbf{P} \mathbf{e}_P. \tag{6.31}$$

Since the projection operator ensures that $\widehat{\boldsymbol{\theta}}_x$ is bounded to $\boldsymbol{\Omega}_\Theta$

$$\frac{1}{2}\frac{1}{\gamma} \tilde{\boldsymbol{\theta}}_x^T(0) \tilde{\boldsymbol{\theta}}_x(0) \leq \frac{1}{2}\frac{1}{\gamma} 4 \max_{\widehat{\boldsymbol{\theta}}_x \in \boldsymbol{\Omega}_\Theta} \left\| \tilde{\boldsymbol{\theta}}_x \right\|_2^2 \leq 2\frac{\beta}{\gamma}, \tag{6.32}$$

where $\beta = \max_{\widehat{\boldsymbol{\theta}}_x \in \boldsymbol{\Omega}_\Theta} \left\| \tilde{\boldsymbol{\theta}}_x \right\|_2^2$. With Eq.(6.32) and the minimum eigenvalue $\underline{\lambda}(\mathbf{P})$ from $\mathbf{P}$, an upper bound on $\mathbf{e}_P$ is given from Eq.(6.31)

$$\|\mathbf{e}_P\|_2^2 \leq \frac{4\beta}{\underline{\lambda}(\mathbf{P})\gamma}. \tag{6.33}$$

This bound holds uniformly in time and with $\|\cdot\|_\infty \leq \|\cdot\|_2$ we get

$$\|\mathbf{e}_P\|_{\mathcal{L}_\infty} \leq \sqrt{\frac{4\beta}{\underline{\lambda}(\mathbf{P})\gamma}} \tag{6.34}$$

This ensures that $\|\mathbf{e}_P\|_{\mathcal{L}_\infty} = \max_{i=1,..,n} |\mathrm{e}_{P,i}| \leq \sqrt{\frac{4\beta}{\underline{\lambda}(\mathbf{P})\gamma}}$ and with the triangular relationship

$$\left| \|\hat{\mathbf{x}}_P\|_{\mathcal{L}_\infty} - \|\mathbf{x}_P\|_{\mathcal{L}_\infty} \right| \leq \sqrt{\frac{4\beta}{\underline{\lambda}(\mathbf{P})\gamma}} \tag{6.35}$$

we have

$$\|\mathbf{x}_P\|_{\mathcal{L}_\infty} \leq \|\hat{\mathbf{x}}_P\|_{\mathcal{L}_\infty} + \sqrt{\frac{4\beta}{\underline{\lambda}(\mathbf{P})\gamma}}. \tag{6.36}$$

6.1.3.2 Stability of the Predictor

Inserting the control law of Eq.(6.7) in the predictor dynamic of Eq.(6.3) we obtain

$$\dot{\hat{\mathbf{x}}}_P(t) = \mathbf{A}_M\hat{\mathbf{x}}_P(t) + \mathbf{b}_P\left(\{\mathrm{C}(s)u_{CMD}(s)\}_t - \widehat{\boldsymbol{\theta}}_x^T(t)\mathbf{x}_P(t)\right), \tag{6.37}$$

where $u_{CMD}(s) = u_{MRAC}(s)$. Adding and subtracting $\mathbf{b}_P k_r r$ yields

$$\dot{\hat{\mathbf{x}}}_P(t) = \mathbf{A}_M\hat{\mathbf{x}}_P(t) + \mathbf{b}_P\left(\{\mathrm{C}(s)u_{CMD}(s)\}_t \underbrace{-\widehat{\boldsymbol{\theta}}_x^T(t)\mathbf{x}_P(t) - \mathbf{b}_P k_r r(t)}_{-u_{CMD}} + \mathbf{b}_P k_r r(t)\right). \tag{6.38}$$

Or equally

$$\dot{\hat{\mathbf{x}}}_P(t) = \mathbf{A}_M\hat{\mathbf{x}}_P(t) + \mathbf{b}_P k_r r(t) + \mathbf{b}_P(\{(\mathrm{C}(s)-1)u_{CMD}(s)\}_t). \tag{6.39}$$

With the definitions of Eq.(6.18) and Eq.(6.19), and by inserting the control law form Eq.(6.6) into Eq.(6.39) we obtain in the frequency domain

$$\hat{\mathbf{x}}_P(s) = \mathbf{G}(s)\left\{\widehat{\boldsymbol{\theta}}_x^T(t)\hat{\mathbf{x}}_P(t)\right\}_s + \mathbf{G}(s)k_r r(s) + \mathbf{H}(s)k_r r(s) + \mathbf{x}_{ini}(s). \tag{6.40}$$

Thus the following bound holds

$$\|\hat{\mathbf{x}}_P\|_{\mathcal{L}_\infty} \leq \|\mathbf{G}(s)\|_{\mathcal{L}_1}\left\|\widehat{\boldsymbol{\theta}}_x^T\mathbf{x}_P\right\|_{\mathcal{L}_\infty} + \|\mathbf{G}(s)+\mathbf{H}(s)\|_{\mathcal{L}_1}\|k_r r\|_{\mathcal{L}_\infty} + \|\mathbf{x}_{INI}\|_{\mathcal{L}_\infty}. \tag{6.41}$$

Due to the projection operator it holds that

$$\left\|\widehat{\boldsymbol{\theta}}_x^T\mathbf{x}_P\right\|_{\mathcal{L}_\infty} = \max_{\widehat{\boldsymbol{\theta}}_x \in \boldsymbol{\Omega}_\Theta}\sum_{i=1}^{n}\left|\widehat{\boldsymbol{\theta}}_{x,i}\right|\|\mathbf{x}_P\|_{\mathcal{L}_\infty} = \bar{\theta}_x\|\mathbf{x}_P\|_{\mathcal{L}_\infty}. \tag{6.42}$$

Applying Eq.(6.42) and Eq.(6.36) to Eq.(6.41) gives

$$\|\hat{\mathbf{x}}_P(t)\|_{\mathcal{L}_\infty} \leq \|\mathbf{G}(s)\|_{\mathcal{L}_1}\bar{\theta}_x\left(\|\hat{\mathbf{x}}_P(t)\|_{\mathcal{L}_\infty} + \sqrt{\frac{4\beta}{\underline{\lambda}(\mathbf{P})\gamma}}\right) + \|\mathbf{G}(s)C(s)\|_{\mathcal{L}_1}\|k_r r(t)\|_{\mathcal{L}_\infty} + \|\mathbf{x}_{INI}\|_{\mathcal{L}_\infty}. \tag{6.43}$$

Resolved with respect to $\|\hat{\mathbf{x}}_P(t)\|_{\mathcal{L}_\infty}$ we obtain

$$\|\hat{\mathbf{x}}_P\|_{\mathcal{L}_\infty} \leq \frac{\left(\|\mathbf{G}(s)\|_{\mathcal{L}_1}\bar{\theta}_x\sqrt{\frac{4\beta}{\underline{\lambda}(\mathbf{P})\gamma}} + \|\mathbf{G}(s)C(s)\|_{\mathcal{L}_1}\|k_r r\|_{\mathcal{L}_\infty} + \|\mathbf{x}_{INI}\|_{\mathcal{L}_\infty}\right)}{1-\bar{\theta}_x\|\mathbf{G}(s)\|_{\mathcal{L}_1}}. \tag{6.44}$$

Since all terms in Eq.(6.44) are bounded, and for stability of the reference model it was already required in Eq.(6.20) that $\bar{\theta}_x\|\boldsymbol{G}(s)\|_{\mathcal{L}_1} < 1$, it follows that $\|\hat{\mathbf{x}}_P\|_{\mathcal{L}_\infty}$ is finite and thus $\hat{\mathbf{x}}_P(t)$ is uniformly bounded. From Eq.(6.35) it follows that $\|\mathbf{x}_P\|_{\mathcal{L}_\infty}$ exists and $\mathbf{x}_P(t)$ is uniformly bounded. Furthermore, it follows from the error dynamics that $\dot{\mathbf{e}}_P$ is bounded, and Barbalat's Lemma can be applied to show that $\lim_{t\to\infty}\mathbf{e}_P(t) = \mathbf{0}$.

It is furthermore possible to derive transient performance bounds as shown in [95]. These performance bounds have the following form:

$$\begin{aligned} \left\|\hat{\mathbf{x}}_P - \mathbf{x}_P\right\|_{\mathcal{L}_\infty} &\leq c_1 \\ \left\|\mathbf{x}_{REF} - \mathbf{x}_P\right\|_{\mathcal{L}_\infty} &\leq c_2 \\ \left\|u_{\mathcal{L}_1,REF} - u\right\|_{\mathcal{L}_\infty} &\leq c_3 \end{aligned} \tag{6.45}$$

where c_1, c_2, and c_3 are positive constants. It should be noted that these constants depend on the $\mathcal{L}_1$ norms of the systems transfer matrix, and therefore the bounds can be conservative for higher order systems.

In Section 6.2, the case of unknown control effectiveness is discussed. For unknown control effectiveness the approach is slightly different and thus the stability proof and the performance bounds are different, too.

6.1.4 Equivalence of Hedging and $\mathcal{L}_1$ adaptive control

In this section the equivalence of direct MRAC with hedging and $\mathcal{L}_1$ adaptive control for the case of known control effectiveness is shown.

Looking at the predictor dynamics of Eq.(6.39), we can see, that it can be equivalently written in a form where a hedging signal is present

$$\dot{\hat{\mathbf{x}}}_P(t) = \mathbf{A}_M\hat{\mathbf{x}}_P(t) + \underbrace{\mathbf{b}_P k_r}_{\mathbf{b}_M} r(t) + \mathbf{b}_P \underbrace{(\{(\mathrm{C}(s)-1)u_{CMD}(s)\}_t)}_{\Delta u}. \tag{6.46}$$

Comparing this with the reference model with hedging of Eq.(5.25) it is directly obvious that both approaches are mathematically equivalent. Thus, it is clear that both methods have the same properties and provide the same performance. This means, the only difference can be found in the structural implementation, what can be seen by comparing the $\mathcal{L}_1$ architecture shown in Figure 6.5 to the reference model with hedging of Figure 5.1, which is repeated for convenience in Figure 6.7.

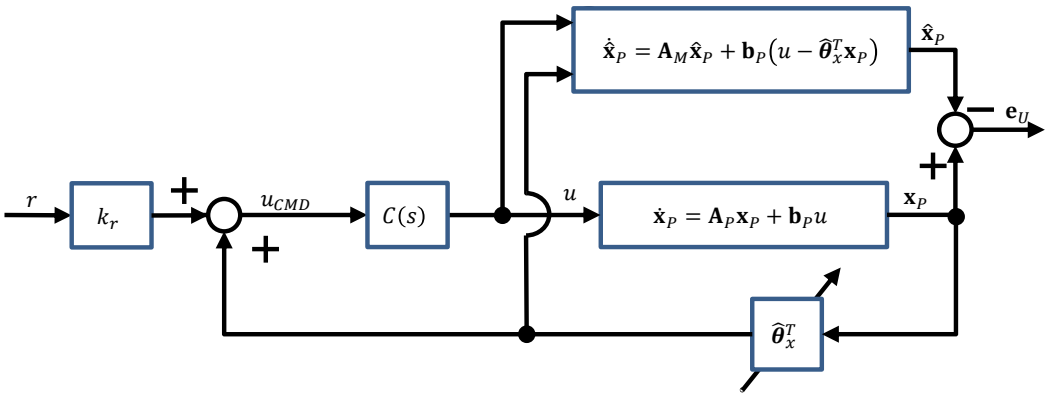

Figure 6.5: Architecture of $\mathcal{L}_1$ control

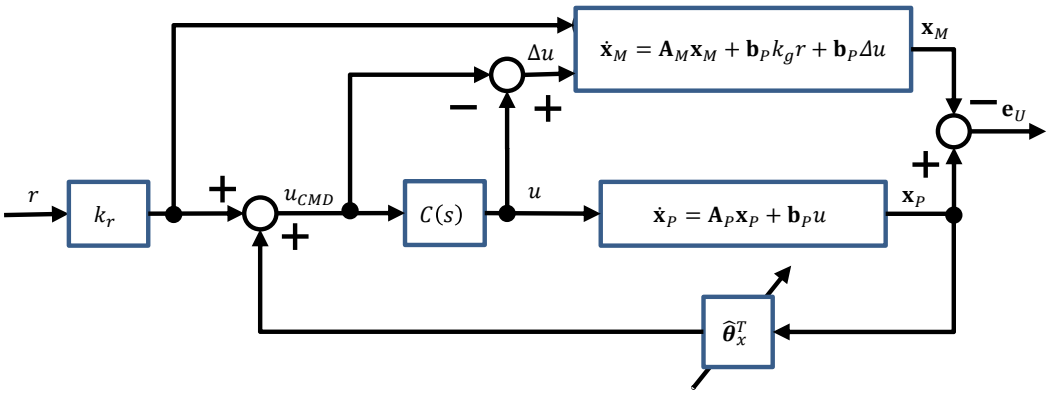

Figure 6.6: Repition of Figure 5.1: Architecture of direct MRAC with hedging

However, an important improvement is that the theory of $\mathcal{L}_1$ adaptive control provides a stability condition for the state predictor, and due to the mathematical equivalence, this also guarantees stability for the reference model modified by hedging. Hence, $\mathcal{L}_1$ adaptive control also provides the first stability proof/condition that justifies the application of a hedging signal to account for bandwidth limiting dynamics in the input channel. Additionally, all performance bounds presented in [95] are also valid for hedging if the control effectiveness is known. It has to be noted that in the case of unknown control effectiveness the hedging approach and $\mathcal{L}_1$ approach are not exactly the same. Thus, the stability condition and the performance bounds provided by the $\mathcal{L}_1$ theory cannot be easily transferred to the hedging approach as shown in the next section.

6.2 Plant with Unknown High-Frequency Gain

In the following the control effectiveness is assumed to be unknown. Furthermore the unknown parameters are assumed to be time varying, as this is allowed in the theory of $\mathcal{L}_1$ adaptive control, and stability can be shown if a certain bound on the rate of change can be given. That is, the plant dynamics are given by (matching condition holds)

$$\dot{\mathbf{x}}_P = \mathbf{A}_M\mathbf{x}_P + \mathbf{b}_P\left(\lambda u - \hat{\boldsymbol{\theta}}_x^{*\,T}(t)\mathbf{x}_P\right), \tag{6.47}$$

where $\lambda \in \mathbb{R}$ is the unknown, positive control effectiveness, and $\hat{\boldsymbol{\theta}}_x^{*\,T}(t) \in \mathbb{R}^{1\times n}$ is an unknown, time varying parameter vector. It is assumed that the following bounds on the uncertainties can be established: $\hat{\boldsymbol{\theta}}_x^{*\,T} \in \boldsymbol{\Omega}_\Theta$, and $\lambda \in [\lambda_{min}, \lambda_{max}]$ with λ_{max}, $\lambda_{min} > 0$.

According to Eq.(4.30) the state predictor is given by

$$\dot{\hat{\mathbf{x}}}_P = \mathbf{A}_M\hat{\mathbf{x}}_P + \mathbf{b}_P\left(\hat{\lambda}\mathrm{u} - \hat{\boldsymbol{\theta}}_x^T\mathbf{x}_P\right). \tag{6.48}$$

The error dynamics for the considered case yield, similar to Eq.(4.36),

$$\dot{\mathbf{e}}_P = \dot{\hat{\mathbf{x}}}_P - \dot{\mathbf{x}}_P = \mathbf{A}_M \mathbf{e}_P + \mathbf{b}_P\left(\tilde{\lambda}\mathbf{u} + \tilde{\boldsymbol{\theta}}_x^T \mathbf{x}_P\right). \tag{6.49}$$

The parameter update law from Lyapunov theory is also used for $\mathcal{L}_1$ adaptive control and is given by (see Eq.(4.38))

$$\begin{aligned} \dot{\hat{\boldsymbol{\theta}}}_x^T &= \boldsymbol{\Gamma}_x \mathbf{x}_P \cdot \mathbf{e}_P{}^T \mathbf{P}\mathbf{b}_P \\ \dot{\hat{\lambda}} &= -\gamma_\Lambda u \cdot \mathbf{e}_P{}^T \mathbf{P}\mathbf{b}_P \end{aligned}. \tag{6.50}$$

6.2.1 Controller Structure

As the control effectiveness is unknown the control law is chosen slightly different to the previous section. It still holds that similar to the previous section, the MRAC control signal is filtered by a low-pass filter, but now an adaptive cut-off frequency is used for the filter. The cut-off frequency of the filter will be dependent on the estimation of the control effectiveness $\hat{\lambda}$. The control law is given by

$$u_{\mathcal{L}_1}(s) = -k_f D(s)\left\{\hat{\lambda}(t) u_{\mathcal{L}_1}(t) - \widehat{\boldsymbol{\theta}}_x^T(\mathrm{t})\mathbf{x}_P(t) - k_r r(t)\right\}_s, \tag{6.51}$$

where $k_f > 0$ and $D(s)$ is a strictly proper transfer function. Or equivalently this control law can be denoted by

$$u_{\mathcal{L}_1}(s) = -k_f D(s)\left\{\hat{\lambda}(\mathrm{t})\left(u_{\mathcal{L}_1}(t) - \underbrace{\frac{1}{\hat{\lambda}(\mathrm{t})}\left(\widehat{\boldsymbol{\theta}}_x^T(t)\mathbf{x}_P(t) + k_r r(t)\right)}_{u_{MRAC}}\right)\right\}_s, \tag{6.52}$$

u_{MRAC} is the input, which is used for the predictor based MRAC (Eq.(4.32)):

$$u_{MRAC} = \frac{1}{\hat{\lambda}(t)}\left(\widehat{\boldsymbol{\theta}}_x^T(\mathrm{t})\boldsymbol{x}_P(t) + k_r r(t)\right). \tag{6.53}$$

Filter with Variable Cut-off Frequency

If $\hat{\lambda}$ would be constant and equal to the true value λ this would result in

$$\begin{aligned} u_{\mathcal{L}_1}(s) &= \frac{k_f \lambda D(s)}{1 + k_f \lambda D(s)}\left\{\frac{1}{\lambda}\left(\widehat{\boldsymbol{\theta}}_x^T(t)\mathbf{x}_P(t) + k_r r(t)\right)\right\}_s \\ &= C(s)\left\{\frac{1}{\lambda}\left(\widehat{\boldsymbol{\theta}}_x^T(t)\mathbf{x}_P(\mathrm{t}) + k_r r(t)\right)\right\}_s, \end{aligned} \tag{6.54}$$

where $C(s)$ is a stable low pass filter whose cut-off frequency depends on λ. This means Eq.(6.51) basically implements a low pass filter where the cut-off frequency is adjusted by the estimation of $\hat{\lambda}$. This also gets obvious in Figure 6.7 where the two different implementations of Eq.(6.51) and Eq.(6.52) are shown. It should be noted that Eq.(6.51) represents the implementation that is commonly suggested in literature.

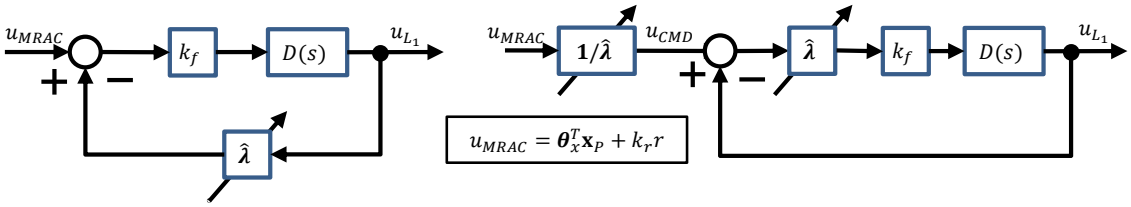

Figure 6.7: Different implementations of the adaptive filter

For example, a 1st order filter evolves from $D(s) = 1/s$ and yields for Eq.(6.52) in the time domain

$$\dot{u}_{\mathcal{L}_1}(t) = k_f \hat{\lambda}(t) \left[u_{MRAC}(t) - u_{\mathcal{L}_1}(t) \right] \tag{6.55}$$

where $k_f \hat{\lambda}(t) = \omega_c(t)$ can be interpreted as the time varying crossover frequency.

With Eq.(6.55) and Eq.(6.53) the control law for a filter with variable cut-off frequency is obtained. This is shown in Table 6.1, where in comparison the control law for a filter with fixed cut-off frequency, as used in the previous section, is shown. The similarity to the control law with constant low pass filter can be also seen by comparing Figure 6.8 with Figure 6.3.

$\omega_c(t) = k_f \hat{\lambda}(\mathrm{t})$	$\omega_c = \mathrm{const}$
$\dot{u}_{\mathcal{L}_1}(t) = \hat{\lambda}(\mathrm{t}) k_f \left[u_{MRAC}(t) - u_{\mathcal{L}_1}(t) \right]$	$\dot{u}_{\mathcal{L}_1}(t) = \omega_c \left[u_{MRAC}(t) - u_{\mathcal{L}_1}(t) \right]$

Table 6.1: $\mathcal{L}_1$ control law for 1st order filter with variable and fixed crossover frequency

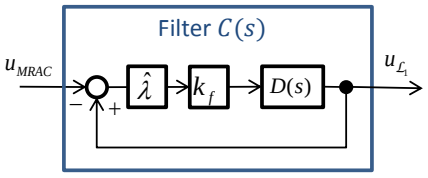

Figure 6.8: Filter with variable cut-off frequency

For a 1st order filter, Figure 6.9 gives an overview of the entire $\mathcal{L}_1$ control architecture for systems with unknown high frequency gain, where an adaptive cut-off frequency is used in the filter.

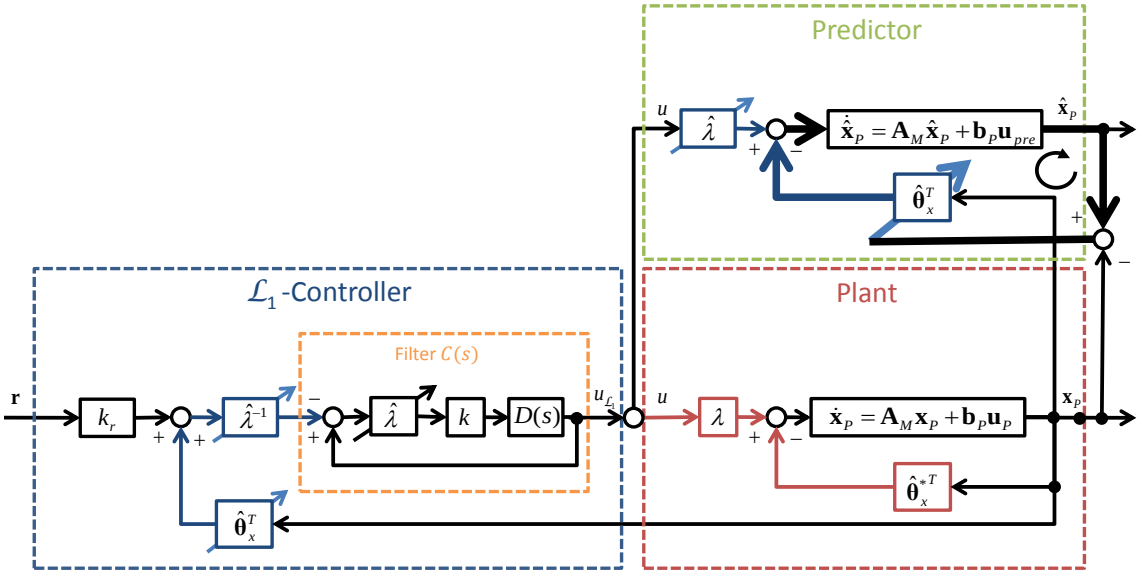

Figure 6.9: Complete $\mathcal{L}_1$ control architecture for unknown high frequency gain (on the basis of [165])

6.2.2 Ideal $\mathcal{L}_1$ Reference Model

Similar to the previous section the reference model is obtained by considering an ideal input to the plant that renders the plant equal to desired dynamics by using the ideal, non-adaptive MRAC control law.

$$u_{MRAC,REF}(t) = \frac{1}{\lambda}\left[k_r r(t) + \widehat{\boldsymbol{\theta}}_x^{*T}(t)\mathbf{x}_{REF}(t)\right]. \tag{6.56}$$

To obtain the ideal $\mathcal{L}_1$ reference model the same, ideal input is filtered

$$u_{\mathcal{L}_1,REF}(s) = C(s)u_{MRAC,REF}(s) = \frac{1}{\lambda}C(s)\left[k_r r(s) + \widehat{\boldsymbol{\theta}}_x^{*T}(s)\mathbf{x}_{REF}(s)\right], \tag{6.57}$$

and applied to the plant given by Eq.(6.47) we can obtain the ideal reference system

$$\mathbf{x}_{REF}(s) = \mathbf{G}(s)\left\{\widehat{\boldsymbol{\theta}}_x^{*T}(t)\mathbf{x}_{REF}(t)\right\}_s + \mathbf{H}(s)C(s)k_r r(s) + \mathbf{x}_{INI}(s). \tag{6.58}$$

Similar to the previous section the ideal reference dynamics is only stable, if the $\mathcal{L}_1$ criterion is fulfilled. This condition is derived next.

6.2.3 Stability of the $\mathcal{L}_1$ Controller

In the following the proof according to [95] is not completely revisited, but only the main steps and results are provided.

As previously it is necessary to apply the projection operator to the adaptive law such that $\widehat{\boldsymbol{\theta}}_x$ and $\hat{\lambda}$ are bounded to the assumed uncertainty sets: $\widehat{\boldsymbol{\theta}}_x \in \boldsymbol{\Omega}_\Theta$ and $\hat{\lambda} \in [\lambda_{min}, \lambda_{max}]$. At first it is shown that the prediction error $\mathbf{e}_P(t)$ is bounded by the normal Lyapunov analysis and secondly it is shown that the predictor is stable

6.2.3.1 Stability of the Error Dynamics

In [95] it is shown that with a Lyapunov function of the form

$$\mathrm{V} = \frac{1}{2}\mathbf{e}_P{}^T\mathbf{P}\mathbf{e}_P + \frac{1}{2}\tilde{\boldsymbol{\theta}}_x^T\,\boldsymbol{\Gamma}_x^{-\mathbf{1}}\tilde{\boldsymbol{\theta}}_x + \frac{1}{2}\gamma_\lambda^{-1}\tilde{\lambda}^2 \tag{6.59}$$

it can be verified that if the initial error $\mathrm{e}_P(0) = 0$ and all elements of $\boldsymbol{\Gamma}_\mathrm{x}$ and γ_λ are equal to γ the error is bounded by

$$\|\mathbf{e}_P\|_{\mathcal{L}_\infty} \leq \sqrt{\frac{4\beta}{\underline{\lambda}(\mathbf{P})\gamma}} \tag{6.60}$$

where β is now given by

$$\beta = \max_{\widehat{\boldsymbol{\theta}}_x^* \in \boldsymbol{\Omega}_\Theta} \left\|\widehat{\boldsymbol{\theta}}_x^*\right\|_2^2 + \frac{1}{4}(\lambda_{max} - \lambda_{min})^2 + \frac{\overline{\lambda}(\mathbf{P})}{\underline{\lambda}(\mathbf{Q})} + d_\theta \cdot \max_{\widehat{\boldsymbol{\theta}}_x^* \in \boldsymbol{\Omega}_\Theta} \left\|\widehat{\boldsymbol{\theta}}_x^*\right\|_2^2. \tag{6.61}$$

Here $\mathbf{Q}$ is again the solution of the Lyapunov Equation: $\mathbf{P}\mathbf{A}_M + \mathbf{A}_M^T\mathbf{P} = -\mathbf{Q}$. Now β also includes the limits for λ and an upper bound on the maximum rate of change of $\widehat{\boldsymbol{\theta}}_x^*$ given by $d_\theta \geq \left\|\dot{\widehat{\boldsymbol{\theta}}}_x^*(t)\right\|_2$. The bound on the rate of $\widehat{\boldsymbol{\theta}}_x^*$ is necessary as itwas assumed to be time varying.

6.2.3.2 Stability of the Closed Loop

In the previous section, where the control effectiveness was known, the stability of the closed loop was established by stability of the predictor. This could be also shown here, but due to the time varying $\hat{\lambda}$ the transfer functions of $\mathbf{H}(s)$ and $(C(s) - 1)$ cannot be multiplied in the frequency domain. This leads to a more conservative stability condition as we cannot take the $\mathcal{L}_1$-norm of $\|\mathbf{G}(s)\|_{\mathcal{L}_1}$, but instead need to take the norms of $\|\mathbf{H}(s)\|_{\mathcal{L}_1}$ and $\|(C(s) - 1)\|_{\mathcal{L}_1}$ separately. However, as shown in [95] boundedness of $\mathbf{x}_P$ w.r.t. $\mathbf{x}_{REF}$ can be shown in an elegant way, and in addition to proofing stability this also directly provides a performance bound. In particular the following bound can be derived

$$\|\mathbf{x}_{REF} - \mathbf{x}_P\|_{\mathcal{L}_\infty} \leq \frac{\|C(s)\|_{\mathcal{L}_1}}{1 - \|\mathbf{G}(s)\|_{\mathcal{L}_1}\overline{\theta}_x}\sqrt{\frac{4\beta}{\underline{\lambda}(\mathbf{P})\gamma}}. \tag{6.62}$$

6.2.4 Similarities of Hedging and $\mathcal{L}_1$ adaptive control

The choice of the low pass filter with adaptive cutoff frequency can be motivated by the elegant stability proof and the performance bounds that can be obtained. This is the key innovation of $\mathcal{L}_1$ adaptive control. It must be noted that in general a filter as shown in Figure 6.7 can also be accounted for by hedging, by just applying the control deficiency between filter input and output to the reference model dynamics. However, if the dynamics in the input channel are already fixed, as for example by an actuator,

the control law of Eq.(6.51) cannot be applied because the actuator dynamics cannot be adjusted by $\hat{\lambda}$ and thus the stability proof and the performance bounds do not hold anymore. Therefore, the results are of theoretical nature, but as already mentioned before, a more conservative stability condition can be derived for the case when the filter dynamics are not adjusted by $\hat{\lambda}$. Getting back to the currently considered problem where $\hat{\lambda}$ is time varying, we again use the control law of Eq.(6.7) and insert it in the predictor dynamic of Eq.(6.48) to obtain

$$\dot{\hat{\mathbf{x}}}_P(t) = \mathbf{A}_M\hat{\mathbf{x}}_P(t) + \mathbf{b}_P\big(\hat{\lambda}(t)\cdot\{\mathrm{C}(s)u_{CMD}(s)\}_t - \widehat{\boldsymbol{\theta}}_x^T(t)\mathbf{x}_P(t)\big), \tag{6.63}$$

where $u_{CMD}(s) = u_{MRAC}(s)$ defined by Eq.(6.54). Adding and subtracting $\mathbf{b}_P k_r r$ to Eq.(6.63) yields

$$\dot{\hat{\mathbf{x}}}_P(t) = \mathbf{A}_M\hat{\mathbf{x}}_P(t) + \mathbf{b}_P\left(\hat{\lambda}(t)\cdot\{\mathrm{C}(s)u_{CMD}(s)\}_t \underbrace{-\widehat{\boldsymbol{\theta}}_x^T(t)\mathbf{x}_P(t) - k_r r(t)}_{-\hat{\lambda}(t)u_{CMD}(t)} + k_r r(t)\right), \tag{6.64}$$

or equally

$$\dot{\hat{\mathbf{x}}}_P(t) = \mathbf{A}_M\hat{\mathbf{x}}_P(t) + \mathbf{b}_P k_r r(t) + \mathbf{b}_P\big(\hat{\lambda}(t)\cdot\{(\mathrm{C}(s)-1)u_{CMD}(s)\}_t\big). \tag{6.65}$$

With the definitions of Eq.(6.18) and Eq.(6.19), Eq.(6.65) can be denoted in the frequency domain by

$$\begin{aligned}\hat{\mathbf{x}}_P(s) &= \mathbf{H}(s)\big(\hat{\lambda}(s) * [(\mathrm{C}(s)-1)u_{CMD}(s)]\big) + \mathbf{H}(s)k_r r(s) + \mathbf{x}_{INI}(s)\\ \hat{\mathbf{x}}_P(s) &= \mathbf{H}(s)\left(\hat{\lambda}(s) * \left[(\mathrm{C}(s)-1)\left\{\frac{1}{\hat{\lambda}(t)}\big(\widehat{\boldsymbol{\theta}}_x^T(t)\mathbf{x}_P(t) + k_r r(t)\big)\right\}_s\right]\right) + \mathbf{H}(s)k_r r(s) + \mathbf{x}_{INI}(s)\end{aligned} \tag{6.66}$$

Here it is obvious, that if we want to obtain a norm bound on $\hat{\mathbf{x}}_\mathrm{P}$ it will become more conservative than the bound of the previous section, because the $\mathcal{L}_1$ norm of $\mathbf{H}(\mathrm{s})$ and $(\mathrm{C}(s)-1)$ must be taken separately, due to the time varying $\hat{\lambda}$. Appling the $\mathcal{L}_\infty$ norm to Eq.(6.66) we get

$$\begin{aligned}\|\hat{\mathbf{x}}_P\|_{\mathcal{L}_\infty} &\le \|\mathbf{H}(s)\|_{\mathcal{L}_1}\left\|\hat{\lambda}(s) * \left[(\mathrm{C}(s)-1)\left\{\frac{1}{\hat{\lambda}(t)}\big(\widehat{\boldsymbol{\theta}}_x^T(t)\mathbf{x}_P(t) + k_r r(t)\big)\right\}_s\right]\right\|_{\mathcal{L}_\infty} + \|\mathbf{H}(s)\|_{\mathcal{L}_1}\|k_r r\|_{\mathcal{L}_\infty} + \|\mathbf{x}_{INI}\|_{\mathcal{L}_\infty}\\ &\le \|\mathbf{H}(s)\|_{\mathcal{L}_1}\lambda_{max}\left\|(\mathrm{C}(s)-1)\left\{\frac{1}{\hat{\lambda}(t)}\big(\widehat{\boldsymbol{\theta}}_x^T(t)\mathbf{x}_P(t) + k_r r(t)\big)\right\}_s\right\|_{\mathcal{L}_\infty} + \|\mathbf{H}(s)\|_{\mathcal{L}_1}\|k_r r\|_{\mathcal{L}_\infty} + \|\mathbf{x}_{INI}\|_{\mathcal{L}_\infty}\\ &\le \|\mathbf{H}(s)\|_{\mathcal{L}_1}\lambda_{max}\|(\mathrm{C}(s)-1)\|_{\mathcal{L}_1}\left\|\frac{1}{\hat{\lambda}(t)}\big(\widehat{\boldsymbol{\theta}}_x^T(t)\mathbf{x}_P(t) + k_r r(t)\big)\right\|_{\mathcal{L}_\infty} + \|\mathbf{H}(s)\|_{\mathcal{L}_1}\|k_r r\|_{\mathcal{L}_\infty} + \|\mathbf{x}_{INI}\|_{\mathcal{L}_\infty}\end{aligned} \tag{6.67}$$

Hence, the following bound on $\hat{\mathbf{x}}_P$ can be obtained

$$\|\hat{\mathbf{x}}_P\|_{\mathcal{L}_\infty} \le \frac{\lambda_{max}}{\lambda_{min}}\|\mathbf{H}(s)\|_{\mathcal{L}_1}\|\mathrm{C}(s)-1\|_{\mathcal{L}_1}\left\|\widehat{\boldsymbol{\theta}}_x^T\mathbf{x}_P + k_r r\right\|_{\mathcal{L}_\infty} + \|\mathbf{H}(s)\|_{\mathcal{L}_1}\|k_r r\|_{\mathcal{L}_\infty} + \|\mathbf{x}_{INI}\|_{\mathcal{L}_\infty} \tag{6.68}$$

Using Eq.(6.42) and Eq.(6.60) we get

$$\begin{aligned}\|\hat{\mathbf{x}}_P\|_{\mathcal{L}_\infty} \le \frac{\lambda_{max}}{\lambda_{min}}\|\mathbf{H}(s)\|_{\mathcal{L}_1}\|C(s)-1\|_{\mathcal{L}_1}\bar{\theta}_x\left(\|\hat{\mathbf{x}}_P\|_{\mathcal{L}_\infty} + \sqrt{\frac{2\beta}{\underline{\lambda}(\mathbf{P})\gamma}}\right)\\ +\|\mathbf{H}(s)\|_{\mathcal{L}_1}\left(\frac{\lambda_{max}}{\lambda_{min}}\|C(s)-1\|_{\mathcal{L}_1}+1\right)\|k_r r\|_{\mathcal{L}_\infty} + \|\mathbf{x}_{INI}\|_{\mathcal{L}_\infty}.\end{aligned} \tag{6.69}$$

Resolved w.r.t. $\|\hat{\mathbf{x}}_P(t)\|_{\mathcal{L}_\infty}$ yields

$$\|\hat{\mathbf{x}}_P\|_{\mathcal{L}_\infty} \leq \frac{\frac{\lambda_{max}}{\lambda_{min}}\left(\|\mathbf{H}(s)\|_{\mathcal{L}_1}\|C(s)-1\|_{\mathcal{L}_1}\bar{\theta}_x\sqrt{\frac{2\beta}{\underline{\lambda}(\mathbf{P})\gamma}}+\|\mathbf{H}(s)\|_{\mathcal{L}_1}\left(\|C(s)-1\|_{\mathcal{L}_1}+1\right)\|k_r r\|_{\mathcal{L}_\infty}\right)}{1-\frac{\lambda_{max}}{\lambda_{min}}\|\mathbf{H}(s)\|_{\mathcal{L}_1}\|C(s)-1\|_{\mathcal{L}_1}\bar{\theta}_x} + \frac{\|\mathbf{x}_{INI}\|_{\mathcal{L}_\infty}}{1-\frac{\lambda_{max}}{\lambda_{min}}\|\mathbf{H}(s)\|_{\mathcal{L}_1}\|C(s)-1\|_{\mathcal{L}_1}\bar{\theta}_x} \tag{6.70}$$

Similar to Eq.(6.44) the stability condition is directly visible from the denominator and it is clear that the condition is more conservative.

6.3 Short Period Example

In the following the approach from Section 5.1.7.1 is extended by an additional filter in the input channel according to Eq.(6.51). Thus the control law is given by

$$\eta_{CMD,\mathcal{L}_1}(s) = -k_f D(s)\left\{\hat{\lambda}(\mathrm{t})\left(\eta_{CMD,\mathcal{L}_1}-\eta_{CMD}\right)\right\}_{\mathrm{s}} \tag{6.71}$$

$$\eta_{CMD} = \frac{1}{\hat{\lambda}}(\eta_{BL}+\eta_{AD}) \tag{6.72}$$

For the following results the simple choice of $D(s) = 1/s$ is made.

Irrespective of the control law, the rest of the adaptive controller is the same as in Section 5.1.7.1 and it is assembled by Eq.(6.71), Eq.(6.72), Eq.(5.60), Eq.(5.61), Eq.(5.67), Eq.(5.29), Eq.(5.30), and Eq.(5.63):

$$\eta_{AD} = \widehat{\boldsymbol{\theta}}_y^T\mathbf{y}_P^+ - \Delta\widehat{\boldsymbol{\theta}}_{y,M}^T\mathbf{y}_P^+ \tag{5.58}$$

$$\Delta\widehat{\boldsymbol{\theta}}_{y,M} = \begin{cases} \widehat{\boldsymbol{\theta}}_y & for \quad \widehat{\boldsymbol{\theta}}_{y,M,min}^* \leq \widehat{\boldsymbol{\theta}}_y \leq \widehat{\boldsymbol{\theta}}_{y,M,max}^* \\ \widehat{\boldsymbol{\theta}}_{y,M,max}^* & for \quad \widehat{\boldsymbol{\theta}}_y < \widehat{\boldsymbol{\theta}}_{y,M,max}^* \\ \widehat{\boldsymbol{\theta}}_{y,M,min}^* & for \quad \widehat{\boldsymbol{\theta}}_y > \widehat{\boldsymbol{\theta}}_{y,M,min}^* \end{cases} \tag{5.59}$$

$$\dot{\hat{\mathbf{x}}}_P^+ = \mathbf{A}_P^+\hat{\mathbf{x}}_P^+ + \mathbf{b}_P^+\eta_M + \mathbf{b}_r^+ r + \mathbf{b}_P^+\hat{\lambda}\,\Delta\eta - \mathbf{b}_P^+\Delta\widehat{\boldsymbol{\theta}}_{y,M}^T\mathbf{y}_P^+ - \mathbf{b}_{P,um}^+\widehat{\boldsymbol{\theta}}_{y,um}^T\mathbf{y}_P^+ - k_e\mathbf{e}_P$$

$$\hat{\mathbf{y}}_P^+ = \mathbf{C}_P^+\hat{\mathbf{x}}_P^+ + \mathbf{d}_P^+\eta_M \tag{5.65}$$

$$\eta_M = \mathbf{k}_y^T\hat{\mathbf{y}}_P^+ + k_r r$$

$$\Delta\eta(s) = (G_{act}(s)G_{fil}(s)G_{del}(s)-1)\cdot\eta_{CMD}(s) \tag{5.29}$$

$$\dot{\hat{\boldsymbol{\theta}}}_y = \boldsymbol{\Gamma}_y\mathbf{y}_P^+\cdot\mathbf{e}_P^T\mathbf{P}\mathbf{b}_{P,n_Z}^+ \qquad \dot{\hat{\lambda}} = -\Gamma_\Lambda\eta\cdot\mathbf{e}_P^T\mathbf{P}\mathbf{b}_{P,n_Z}^+ \tag{5.30}$$

$$\dot{\hat{\boldsymbol{\theta}}}_{y,um} = -\boldsymbol{\Gamma}_{y,um}\mathbf{y}_P^+\cdot\mathbf{e}_P^T\mathbf{P}\mathbf{b}_{P,n_Z,um}^+ \tag{5.61}$$

Furthermore the same tuning as used in Section 5.1.7.1 is applied, where k_f is an additional parameter for the optimization algorithm. This leads to an objective function

of $J = 0.163$ with the controller parameters ginven in Table 6.2. From the smaller objective function and the larger time delay margin (see Table 6.3) it seem that the additional filter improves the performance and simultaneously also shows better robust stability. However the performance improvement is not a general result as can be concluded from the performance assessment shown in Figure 6.10 - Figure 6.15. Especially for matched uncertainties a robust performance loss can be seen. Furthermore, compared to the results from Section 5.1.7.1 the performance seems to be less homogenous w.r.t. different step sizes.

It should be noted that the parameters are tuned for performance maximization, where $\mathcal{L}_1$ adaptive control was originally suggested to provide a trade-off between robustness and performance. This trade-off can be seen here. While the timed delay margin increases the performance w.r.t. matched uncertainties deteriorates.

$\boldsymbol{\Gamma}_y$	Γ_Λ	$\boldsymbol{\Gamma}_{y,um}$	k_e	k_f
$\begin{bmatrix} 492.8 & 0 & 0 \\ 0 & 2.45 & 0 \\ 0 & 0 & 0 \end{bmatrix}$	1.6	$\begin{bmatrix} 7.3 & 0 & 0 \\ 0 & 25.1 & 0 \\ 0 & 0 & 0 \end{bmatrix}$	4.2	127.6

Table 6.2: Controller parameter

	1g CMD	2g CMD
TDM	0.35	0.34

Table 6.3: Time delay margins

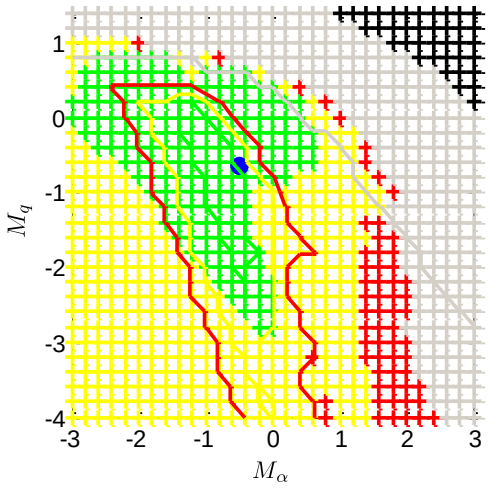

Figure 6.10: Robust perfomance w.r.t. M_α and M_q; $n_{z,CMD}$=1

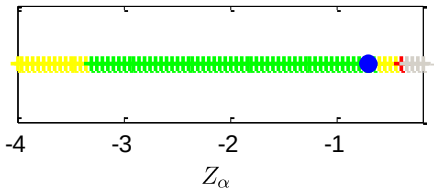

Figure 6.11: Robust perfomance w.r.t. Z_α; $n_{z,CMD}$=1

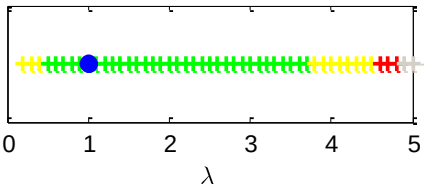

Figure 6.12: Robust perfomance w.r.t. λ $n_{z,CMD}$=1

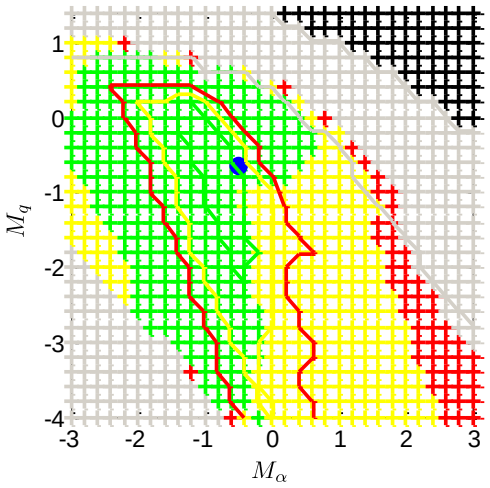

Figure 6.13: Robust perfomance w.r.t. M_α and M_q; $n_{z,CMD}$=2

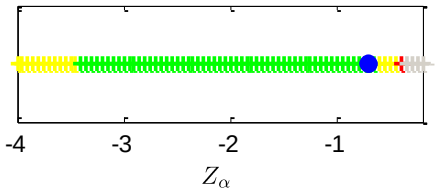

Figure 6.14: Robust perfomance w.r.t. Z_α; $n_{z,CMD}$=2

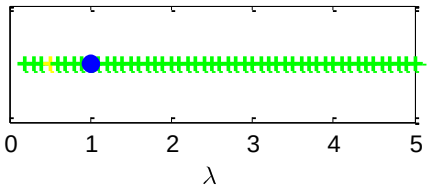

Figure 6.15: Robust perfomance w.r.t. λ $n_{z,CMD}$=2

6.4 $\mathcal{L}_1$ Piecewise Constant

The $\mathcal{L}_1$ piecewise constant control architecture was first introduced in [177] in the context of output-feedback. In the first section the theory according to [95] and [177] is presented. Here only the main assumptions and the equations necessary for implementation are presented, where the proofs can be found in [95]. The approach is called piecewise constant as it assumes a discrete control law. It is pointed out in the following that the $\mathcal{L}_1$ piecewise constant control law can be interpreted as a linear, dynamic control law. Whether it is linear time variant or invariant depends on how the controller and the predictor are implemented, because the predictor could run with a smaller sample time than the rest of the control law [95]. However, as this seems to provide no benefit in the following the time invariant implementation is considered. Thus, the control law is LTI and it is the authors opinion that the approach should not be referred to as adaptive control. The linear character of the control law was also pointed out and investigated in [178], Furthermore, in [179] the limiting behavior on the control architecture for infinite feedback gain was analyzed, and it was found that for the case of output feedback it is equivalent to a disturbance observer (DOB). The $\mathcal{L}_1$ piecewise constant structure is a type of model following control, where the proportional feedback gain for the error is determined by the desired dynamics and the sample time of the controller. This means the $\mathcal{L}_1$ piecewise constant approach provides a very easy design for the error feedback gain. However, as it is a linear control law also other design methods could result in the same controller. In difference to other design approaches, where the resulting dynamic controller is often treated as a black box, for the $\mathcal{L}_1$ piecewise constant controller the additionally introduced states have a physical meaning, as they are the states of the reference model. The application of a reference model is the only commonality of $\mathcal{L}_1$ piecewise constant and adaptive control. However, for $\mathcal{L}_1$ piecewise constant, the error is not intregrated to estimate parameters, but directly fed back to the plant input, where the multiplication of the error with a certain gain is considerd as an “estimation” of the plant disturbance in the theory of $\mathcal{L}_1$ piecewise constant. However this in no real estimation in the sense of adaptive control and therefore the word “estimation” is used in quotes.

For $\mathcal{L}_1$ piecewise constant control law, the available processor power of the controller is of special interest as, due to the design method, the feedback gain for the error is direcly dependet on the sample time. Thus, also the disturbance “estimation” is directly dependet on the sample time. From this it follows, that the sample time should be as small as possible, to achive good performance. However, to a certain extent, this holds for most control systems.

Recently the approach was applied to a multitude of control tasks in different aerospace applications, like the inner loop design of the NASA GTM [180] [38], control of the Boeing X-48B blended wing body [181], control of flexible aircraft [182] [183],

the design [184] and augmentation [185] of missile autopilots, as well as satellite orbit stabilization [186].

The piecewise constant algorithm can guarantee semi-global uniform performance bounds for the system's inputs and outputs. Furthermore it ensures uniform transient response in addition to steady state tracking [95]. The derivations and proofs of the control approach can be found in [95] and [187]. However, for the sake of easier understanding, the proofs are omitted in the following and only the assumptions and properties are mentioned.

6.4.1 Problem Formulation

Consider the following system dynamics:

$$\begin{aligned}\dot{\mathbf{x}}_P &= \mathbf{A}_M\mathbf{x}_P + \mathbf{B}_P\boldsymbol{\Lambda}\mathbf{u} + \mathbf{f}(t,\mathbf{x}_P,\mathbf{z}_P),\\ \dot{\mathbf{x}}_z &= \mathbf{g}(t,\mathbf{x}_z,\mathbf{x}_P),\\ \mathbf{y}_C &= \mathbf{C}_C\mathbf{x}_P\\ \mathbf{z}_P &= \mathbf{g}_{\mathrm{o}}(t,\mathbf{x}_z)\end{aligned} \tag{6.73}$$

where $\mathbf{x}_P \in \mathbb{R}^n$ is the measurable state vector of the system, with the initial condition assumed to be inside an arbitrary large known set: i.e. $\exists \rho_0 < \infty$: $\|\mathbf{x}_P(0)\|_\infty \leq \rho_0$. $\mathbf{u} \in \mathbb{R}^m$ is the control input ($m \leq n$), and $\mathbf{y}_C \in \mathbb{R}^m$ is the controlled output. $\mathbf{x}_z \in \mathbb{R}^l$ is the non-measurable state vector of the unmodeled, internal dynamics, and $\mathbf{z}_P \in \mathbb{R}^p$ is the output of the internal dynamics that affects the dynamics of $\mathbf{x}_P$. $\mathbf{A}_M \in \mathbb{R}^{n\times n}$ is a known Hurwitz matrix defining the desired dynamics for the closed-loop system, $\mathbf{B}_P \in \mathbb{R}^{n\times m}$ is a known constant matrix defining the matched input, with $(\mathbf{A}_M, \mathbf{B}_P)$ controllable. $\mathbf{C}_C \in \mathbb{R}^{m\times n}$ is a known constant matrix defining the controlled output, with $(\mathbf{A}_M, \mathbf{C}_C)$ observable. $\boldsymbol{\Lambda} \in \mathbb{R}^{m\times m}$ is the unknown, diagonal system input gain matrix (control effectiveness), which is assumed to be inside a known compact convex set $\boldsymbol{\Lambda} \in \boldsymbol{\Omega}_{\boldsymbol{\Lambda}} \subset \mathbb{R}^{m\times m}$. Furthermore, the sign of the control effectiveness $\mathrm{sgn}(\lambda_{ii})$ is assumed to be known, and the nominal system input gain matrix is equal to the identity matrix. The function $\mathbf{f}\colon \mathbb{R}\times\mathbb{R}^n\times\mathbb{R}^p \to \mathbb{R}^n$ is an unknown nonlinear mapping that reflects the system uncertainties in the dynamics of the measurable states. $\mathbf{g}\colon \mathbb{R}\times\mathbb{R}^l\times\mathbb{R}^n \to \mathbb{R}^l$ is an unknown nonlinear function defining the dynamics of the unmodeled internal states, and $\mathbf{g}_o\colon \mathbb{R}\times\mathbb{R}^l \to \mathbb{R}^p$ is an unknown nonlinear function defining the output of the unmodeled internal dynamics. The nonlinearities $\mathbf{f}$, $\mathbf{g}$, and $\mathbf{g}_o$ satisfy the standard assumptions for existence and uniqueness of solutions.

Assume the unmodeled internal dynamics to be BIBO stable both with respect to the initial conditions $\mathbf{x}_z(0)$ and the input $\mathbf{x}_P$, i.e. there exists $L_z, B_z > 0$ such that

$$\|\mathbf{z}_t\|_{\mathcal{L}_\infty} \leq L_z\|\mathbf{x}_P\|_{\mathcal{L}_\infty} + B_z \quad \forall t \geq 0. \tag{6.74}$$

The nonlinear uncertainty $\mathbf{f}(t,\mathbf{x}_P,\mathbf{z}_P)$ can be devided in a matched component and an unmatched component

$$\begin{aligned}\mathbf{f}(t,\mathbf{x}_P,\mathbf{z}_P) &= \mathbf{B}_P\mathbf{f}_1(t,\mathbf{x}_P,\mathbf{z}_P) + \mathbf{B}_{P,um}\mathbf{f}_2(t,\mathbf{x}_P,\mathbf{z}_P)\\ &= \underbrace{[\mathbf{B}_P \quad \mathbf{B}_{P,um}]}_{\mathbf{B}}\begin{bmatrix}\mathbf{f}_1(t,\mathbf{x}_P,\mathbf{z}_P)\\ \mathbf{f}_2(t,\mathbf{x}_P,\mathbf{z}_P)\end{bmatrix}.\end{aligned} \tag{6.75}$$

Consistent to Section 5.1.4, $\mathbf{B}_{P,um} \in \mathbb{R}^{n\times(n-m)}$ is a constant matrix defining the unmatched input space such that it spans the null space of $\mathbf{B}_P^T$. This means it holds that $\mathbf{B}_P^T\mathbf{B}_{P,um} = 0$, and $\mathbf{B} = [\mathbf{B}_P \quad \mathbf{B}_{P,um}]$. The function $\mathbf{f}_1\colon \mathbb{R}\times\mathbb{R}^n\times\mathbb{R}^p \to \mathbb{R}^m$ is an unknown nonlinear function contributing to the matched component of the uncertainty $\mathbf{f}(t,\mathbf{x}_P,\mathbf{z}_P)$, and the mapping $\mathbf{f}_2\colon \mathbb{R}\times\mathbb{R}^n\times\mathbb{R}^p \to \mathbb{R}^{(n-m)}$ is an unknown nonlinear function contributing to the unmatched component of the uncertainty $\mathbf{f}(t,\mathbf{x}_P,\mathbf{z}_P)$.

Let $\boldsymbol{X}_P \triangleq [\mathbf{x}_P^T,\mathbf{z}_P^T]^T$, and with a slight abuse of language let $\mathbf{f}_i(t,\boldsymbol{X}_P) \triangleq \mathbf{f}_i(t,\mathbf{x}_P,\mathbf{z}_P)$, with $i = 1,2$ to streamline the equations. Assume that $\mathbf{f}_1(t,\mathbf{0})$ and $\mathbf{f}_2(t,\mathbf{0})$ are bounded, i.e. there exists $B_{i0} > 0$ such that

$$\|\mathbf{f}_i(t,\mathbf{0})\|_\infty \le B_{i0} \quad \forall t \ge 0,\ i = 1,2. \tag{6.76}$$

We further assume a semi-global Lipschitz condition that holds uniformly in t:

$$\exists K_{i_\delta}\colon \|\mathbf{f}_i(t,\boldsymbol{X}_1) - \mathbf{f}_i(t,\boldsymbol{X}_2)\|_\infty \le K_{i_\delta}\|\boldsymbol{X}_1 - \boldsymbol{X}_2\|_\infty \quad \forall\|\boldsymbol{X}_j\|_\infty \le \delta \quad \forall\delta \ge 0\ ,\ i,j = 1,2. \tag{6.77}$$

Using (6.75) we can rewrite the system equations given in Eq.(6.73) by

$$\begin{aligned}\dot{\mathbf{x}}_P &= \mathbf{A}_M\mathbf{x}_P + \mathbf{B}_P\big(\boldsymbol{\Lambda}\mathbf{u} + \mathbf{f}_1(t,\mathbf{x}_P,\mathbf{z}_P)\big) + \mathbf{B}_{P,um}\mathbf{f}_2(t,\mathbf{x}_P,\mathbf{z}_P)\\ \mathbf{y}_C &= \mathbf{C}_C\mathbf{x}_P\\ \dot{\mathbf{x}}_z &= \mathbf{g}(t,\mathbf{x}_z,\mathbf{x}_P)\\ \mathbf{z}_P &= \mathbf{g}_0(t,\mathbf{x}_z)\end{aligned} \tag{6.78}$$

The control objective is to design a state feedback controller that guarantees the tracking of a desired output response. The desired system is defined by the reference dynamics in Eq.(4.2) and the output Equation $\mathbf{y}_C = \mathbf{C}_C\mathbf{x}_P$. In the frequency domain the desired transfer characteristics are

$$\mathbf{y}_C(s) = \mathbf{M}(s)\mathbf{r}(s) \tag{6.79}$$

$$\mathbf{M}(s) = \mathbf{C}_C(s\mathbf{I} - \mathbf{A}_M)^{-1}\mathbf{B}_P\mathbf{K}_r, \tag{6.80}$$

For the simple choice of $\mathbf{K}_r = -(\mathbf{C}_C\mathbf{A}_M^{-1}\mathbf{B}_P)^{-1}$, the diagonal elements of the desired transfer matrix $\mathbf{M}(s)$ have DC gain equal to one, while the off-diagonal elements have zero DC gain.

Next, let us define the following transfer matrices which will be applied in the following sections:

$$\mathbf{H}_{x,m}(s) = (s\mathbf{I} - \mathbf{A}_M)^{-1}\mathbf{B}_P \tag{6.81}$$

$$\mathbf{H}_{x,um}(s) = (s\mathbf{I} - \mathbf{A}_M)^{-1}\mathbf{B}_{P,um} \tag{6.82}$$

$$\mathbf{H}_m(s) = \mathbf{C}_C\,\mathbf{H}_{x,m}(s) = \mathbf{C}_C(s\mathbf{I} - \mathbf{A}_M)^{-1}\mathbf{B}_P \tag{6.83}$$

$$\mathbf{H}_{um}(s) = \mathbf{C}_C\,\mathbf{H}_{x,um}(s) = \mathbf{C}_C(s\mathbf{I} - \mathbf{A}_M)^{-1}\mathbf{B}_{P,um} \tag{6.84}$$

Having defined these transfer matrices, let us further assume that the transmission zeros of $\mathbf{H}_m(s)$ lie in the open left-half plane. This means, the iversion of $\mathbf{H}_m(s)$ is stable, and this property will be necessary to compensate for unmatched uncertainties.

6.4.2 $\mathcal{L}_1$ Piecewise Constant Control Architecture

6.4.2.1 Control Law

According to Eq.(6.78) the ideal control law to compensate the uncertainties would be

$$\mathbf{u} = -\boldsymbol{\Lambda}^{-1}\{\mathbf{f}_1(s,\mathbf{x}_P,\mathbf{z}_P) + \mathbf{H}_m^{-1}(s)\mathbf{H}_{um}(s)\mathbf{f}_2(s,\mathbf{x}_P,\mathbf{z}_P) - \mathbf{K}_r\mathbf{r}(s)\}_t. \tag{6.85}$$

However, for the approach with piecewise constant control law, there is no explicit online estimation of $\boldsymbol{\Lambda}$. Instead the identity matrix, i.e. the best a-priori available estimation of $\boldsymbol{\Lambda}$, replaces the system input gain matrix. As in the previous sections we can add a low pass filter $\mathbf{C}(s)$ in the input channel to account for bandwidth restrictions. So the actual control law is given by

$$\mathbf{u}(s) = -\mathbf{C}(s)\big(\widehat{\boldsymbol{\sigma}}_1(s) + \mathbf{H}_m^{-1}(s)\mathbf{H}_{um}(s)\widehat{\boldsymbol{\sigma}}_2(s) - \mathbf{K}_r\mathbf{r}(s)\big), \tag{6.86}$$

where $\widehat{\boldsymbol{\sigma}}_1(t) \in \mathbb{R}^m$ is the "estimate" of $\mathbf{f}_1(t,\mathbf{x}_P,\mathbf{z}_P)$, and $\widehat{\boldsymbol{\sigma}}_2(t) \in \mathbb{R}^{n-m}$ is the "estimate" of $\mathbf{f}_2(t,\mathbf{x}_P,\mathbf{z}_P)$. Here it is assumed that the uncertainties in the control effectiveness can also be compensated by $\widehat{\boldsymbol{\sigma}}_1(t)$ and $\widehat{\boldsymbol{\sigma}}_2(t)$, but it is obvious that the change in the feedforward channel, caused by the uncertain input gain $\boldsymbol{\Lambda}$, cannot be exactly compensated.

6.4.2.2 State Predictor

A state predictor, as presented in the MRAC chapter, depends on estimations of the control effectiveness, the matched, and unmatched uncertainties, but as already mentioned, there is no explicit online estimation of $\boldsymbol{\Lambda}$ and instead the identity matrix is used, resulting in the following predictor

$$\begin{aligned}\dot{\hat{\mathbf{x}}}_P &= \mathbf{A}_M\hat{\mathbf{x}}_P + \mathbf{B}_P(\mathbf{u} + \widehat{\boldsymbol{\sigma}}_1) + \mathbf{B}_{P,um}\widehat{\boldsymbol{\sigma}}_2\\ \hat{\mathbf{y}}_P &= \mathbf{C}_P\hat{\mathbf{x}}_P\end{aligned} \tag{6.87}$$

Inserting the control law from Eq.(6.86) into the predictor dynamics in Eq.(6.87) gives

$$\begin{aligned}\dot{\hat{\mathbf{x}}}_P(t) = \mathbf{A}_M\hat{\mathbf{x}}_P(t) + \mathbf{B}_P\{\mathbf{C}(s)\mathbf{K}_r\mathbf{r}(s)\}_t + \mathbf{B}_P\{-\mathbf{C}(s)\widehat{\boldsymbol{\sigma}}_1(s) + \widehat{\boldsymbol{\sigma}}_1(s)\}_t\\ -\big\{\mathbf{B}_P\mathbf{C}(s)\mathbf{H}_m^{-1}(s)\mathbf{H}_{um}(s)\widehat{\boldsymbol{\sigma}}_2(s) + \mathbf{B}_{P,um}\widehat{\boldsymbol{\sigma}}_2(s)\big\}_t\end{aligned} \tag{6.88}$$

where we can see, that for low frequencies ($\mathbf{C}(s) \approx \mathbf{I}$), the predictor dynamics is equal to a reference model.

6.4.2.3 Update Law

Here only the applied "update law" is shown, but the derivation, which also explains the idea behind, is shown in Appendix E. Defining the error by

$$\mathbf{e}_P = \hat{\mathbf{x}}_P - \mathbf{x}_P, \tag{6.89}$$

an appropriate discrete "update law" shall be defined as

$$\begin{aligned}\widehat{\boldsymbol{\sigma}}(t) = \begin{bmatrix}\widehat{\boldsymbol{\sigma}}_1(iT_s)\\ \widehat{\boldsymbol{\sigma}}_2(iT_s)\end{bmatrix} &= -\mathbf{B}^{-1}\,[\mathbf{A}_M^{-1}(e^{\mathbf{A}_M T_s}-\mathbf{I})]^{-1}\,e^{\mathbf{A}_M T_s}\,\mathbf{e}_P(iT_s)\\ &= -\mathbf{B}^{-1}\,\boldsymbol{\Phi}^{-1}(T_s)\;\boldsymbol{\mu}(iT_s), \qquad t\in[iT_s,(i+1)T_s[,\;\; i=0,1,2,\dots\end{aligned} \tag{6.90}$$

with

$$\boldsymbol{\Phi}(T_s) = \mathbf{A}_M^{-1}\left(e^{\mathbf{A}_M T_s}-\mathrm{I}\right) \tag{6.91}$$

$$\boldsymbol{\mu}(iT_s) = e^{\mathbf{A}_M T_s}\,\mathbf{e}(iT_s) \tag{6.92}$$

$$\mathbf{e}_P(t) = \hat{\mathbf{x}}_P(t) - \mathbf{x}_P(t) \tag{6.93}$$

Here T_s is the sample time of the controller. The "update law" is chosen such that the propagation of the error $\mathbf{e}_P$ over the interval $[iT_s,(i+1)T_s[$ is compensated by the input [95] [177]. It should be noted that according to Eq.(6.90) the "adaptation" of $\widehat{\boldsymbol{\sigma}}(t)$ is given by multiplying the error $\mathbf{e}_P$ with a constant gain matrix, which is dependent on the desired system dynamics $\mathbf{A}_M$, the input directions of the system $\mathbf{B}$, and the sample time T_s.

$$\begin{aligned}\widehat{\boldsymbol{\sigma}}(t) = \begin{bmatrix}\widehat{\boldsymbol{\sigma}}_1(iT_s)\\ \widehat{\boldsymbol{\sigma}}_2(iT_s)\end{bmatrix} &= -\underbrace{\mathbf{B}^{-1}\,[\mathbf{A}_M^{-1}(e^{\mathbf{A}_M T_s}-\mathbf{I})]^{-1}\,e^{\mathbf{A}_M T_s}}_{\mathbf{K}_e\,(\mathbf{A}_M,\mathbf{B},T_s)}\cdot\,\mathbf{e}_P(iT_s)\\ \widehat{\boldsymbol{\sigma}}(t) = \begin{bmatrix}\widehat{\boldsymbol{\sigma}}_1(iT_s)\\ \widehat{\boldsymbol{\sigma}}_2(iT_s)\end{bmatrix} &= \mathbf{K}_e\,(\mathbf{A}_M,\mathbf{B},T_s)\cdot\;\mathbf{e}_P(iT_s)\end{aligned} \tag{6.94}$$

It is also obvious that for $T_s\to 0\;\Rightarrow\;\mathbf{K}_e\to\infty$. Furthermore, from linearity of the control signal in Eq.(6.86) and linearity of the predictor Eq.(6.87), the complete control law is linear. As the system input is basically given by a low pass filtered, proportional feedback of the error the control law constitutes a special kind of model following control.

As mentioned, small sample times T_s will result in a large feedback gain $\mathbf{K}_e$, and usually high feedback gain poses a robustness problem as it reduces the gain and phase margin. However, this in not necessarily the case for the $\mathcal{L}_1$ piecewise constant architecture, because the gain is only effective in a certain frequency domain, which is achieved by the low pass filter. To see this consider that there are no unmatched uncertainties, then from Eq.(6.88) the predictor dynamics are

$$\dot{\hat{\mathbf{x}}}_P(t) = \mathbf{A}_M\hat{\mathbf{x}}_P(t) + \mathbf{B}_P\{\mathbf{C}(s)\mathbf{K}_r\mathbf{r}(s)\}_t + \mathbf{B}_P\{-\mathbf{C}(s)\widehat{\boldsymbol{\sigma}}_1(s) + \widehat{\boldsymbol{\sigma}}_1(s)\}_t. \tag{6.95}$$

It is obvious from Eq.(6.95) that the feedback of the command signal to the predictor has the same effect as a hedging signal. Hence, for large frequencies, which are beyond the bandwidth of the $\mathbf{C}(s)$, the predictor dynamics is adjusted such that it follows the plant. In difference, for low frequencies the predictor behaves like the

reference model. Hence, for large frequencies the effect of the feedback gain $\mathbf{K}_e$ is reduced, such that it does not harm the stability properties.

6.4.2.4 Closed-Loop System

The complete closed loop architecture according to Eq.(6.86), Eq.(6.87) and Eq.(6.90) is shown in Figure 6.16.

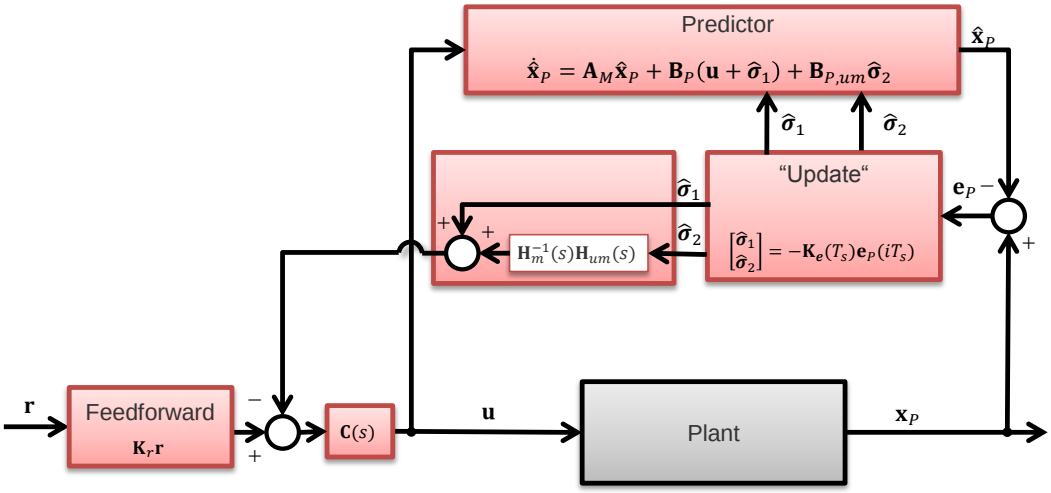

Figure 6.16: Block diagram of $\mathcal{L}_1$ piecewise constant

With the $\mathcal{L}_1$ piecewise constant controller the following bounds can be established [95]

$$\begin{aligned}
\|\mathbf{x}_P\|_{\mathcal{L}_\infty} &< \rho \;\; = \rho_r + \bar{\gamma}_1 \\
\|\mathbf{u}\|_{\mathcal{L}_\infty} &< \rho_u = \rho_{ur} + \gamma_2 \\
\|\mathbf{e}_P\|_{\mathcal{L}_\infty} &< \bar{\gamma}_0 \\
\|\mathbf{x}_{REF} - \mathbf{x}_P\|_{\mathcal{L}_\infty} &< \gamma_1 \;\le \bar{\gamma}_1 \\
\|\mathbf{u}_{REF} - \mathbf{u}\|_{\mathcal{L}_\infty} &< \gamma_2 \\
\|\mathbf{y}_{REF} - \mathbf{y}_P\|_{\mathcal{L}_\infty} &< \|\mathbf{C}_C\|_\infty \gamma_1
\end{aligned} \tag{6.96}$$

Thereby the variables $\mathbf{x}_{REF}$, $\mathbf{u}_{REF}$ and $\mathbf{y}_{REF}$ refer to an ideal reference system, while the various ρ's and γ's on the right hand side are positive constants. The bounds will not be derived in the following, as a detailed derivation can be found in [95] and [177].

To derive the bounds a sufficiently small sampling time $T_s > 0$ is required, which can be associated with the sampling rate of the available CPU. Furthermore the bounds are subject to the $\mathcal{L}_1$-norm condition

$$\|\mathbf{G}_m(s)\|_{\mathcal{L}_1} + \|\mathbf{G}_{um}(s)\|_{\mathcal{L}_1}\ell_0 < \frac{\rho_r - \rho_{in} - \|\mathbf{H}_{xm}(s)\mathbf{C}(s)\mathbf{K}_r\|_{\mathcal{L}_1}\|\mathbf{r}\|_{\mathcal{L}_\infty}}{L_{1\rho_r}\rho_r + B_0} \tag{6.97}$$

To be able to conduct the proofs of stability and derive performance bounds, the "choice" of the filter $\mathbf{C}(s)$ has to ensure that, for a given ρ_0, there exists a $\rho_r > \rho_{in}$

such that the $\mathcal{L}_1$-norm condition holds, with the definitions: $\|\mathbf{x}_P(0)\|_\infty \leq \rho_0$, $\rho_{in} = \rho_0 \|s(s\mathbf{I} - \mathbf{A}_M)^{-1}\|_{\mathcal{L}_1}$, and $\left\|\mathbf{x}_{\mathrm{ref}_\tau}\right\|_{\mathcal{L}_\infty} \leq \rho_r$. The condition and the stability proofs hold for nonlinear systems in the form of Eq.(6.73), but it should be noted, that if the plant is considered to be linear, then all linear analysis techniques can be applied.

6.5 Short-Period Example

In the following the $\mathcal{L}_1$ piecewise constant control law is applied to the short-period model with pitch-up nonlinearity.

However, the approach presented in the previous section is not directly applicable if a baseline PI control law is used, and in this case a slightly modified version has to be used which is presented subsequently.

In the case when a PI baseline control law is used, the estimate of the unmatched uncertainty is not fed to the actuating variables, as in Eq.(6.86) because $\mathbf{H}_m^{-1}\mathbf{H}_{um}$ contains integral behavior. However, an integrator is already implemented in the baseline controller and therefore it is sufficient to feed the unmatched part to the integrator of PI control law. Thus, the integral part of the PI controller is used to account for unmatched uncertainties.

6.5.1 Application

Control Law

As already mentioned the piecewise constant control law is now modified. The control signal from Eq.(6.86) is split up in matched part $\eta_{AD,1} = -C_1(s)\hat{\sigma}_1(s)$ and an unmatched part $\eta_{AD,2}(s) = -C_2(s)H_m^{-1}\mathbf{H}_{um}\hat{\boldsymbol{\sigma}}_2$, where the matched part from $\eta_{AD,1}$ is still fed to the actuation variable

$$\eta_{CMD} = \eta_{AD,1} + \eta_{BL} \tag{6.98}$$

$$\eta_{AD,1}(s) = -C_1(s)\hat{\sigma}_1(s). \tag{6.99}$$

However, the control signal $\eta_{AD,2}$ resulting from the unmatched part is now fed to the integrator of the PI controller

$$\eta_{AD,2}(s) = -C_2(s)H_m^{-1}\mathbf{H}_{um}\hat{\boldsymbol{\sigma}}_2, \tag{6.100}$$

where $C_1(s)$ and $C_2(s)$ are stable low-pass filters. The modification for $\eta_{AD,2}$ is necessary because if we would use $H_m(s)$ give by Eq.(6.83) we get for the considered problem

$$H_m(s) = \mathbf{c}_C^T(s\mathbb{I} - \mathbf{A}_M^+)^{-1}\mathbf{b}_P^+ \tag{6.101}$$

where $\mathbf{c}_C^T$ is the first row of $\mathbf{C}_P^+$ in Eq.(2.13), which gives the output of the desired tracking variable n_Z. As $\mathbf{A}_M^+$ is augmented by the integrator state e_I the open loop transfer function $H_m(s)$ contains a zero in the origin. This results in pole in the origin for $H_m^{-1}\mathbf{H}_{um}$, and thus the transfer function that feeds back the "error" $\hat{\boldsymbol{\sigma}}_2$ ($\hat{\boldsymbol{\sigma}} = \mathbf{K}_e\ \mathbf{e}_P$)

has integral behavior. However, the system already contains integral error feedback and therefore a second integral error feedback should not be added. Therefore $\eta_{AD,2}$ is directly fed to the integrator of the PI controller. Due to the different input point of $\eta_{AD,2}$, the transfer function $H_m(s)$ is also slightly different. For $H_m(s)$, $\mathbf{b}_r^+$ ($\mathbf{b}_r^{+T} = [0 \quad 0 \quad 1]^T$) is used instead of $\mathbf{b}_{P,n_Z}^+$, such that $H_m(s)$ gives the transfer characteristics from integrator input to tracking output n_Z:

$$H_m(s) = \mathbf{c}_C^T(s\mathbb{I} - \mathbf{A}_M^+)^{-1}\mathbf{b}_r^+ \tag{6.102}$$

$$\mathbf{H}_{um}(s) = \mathbf{c}_C^T(s\mathbb{I} - \mathbf{A}_M^+)^{-1}\mathbf{B}_{P,um}^+. \tag{6.103}$$

In terms of numerical values the transferfunctions are given by

$$H_m(s) = 0.03\frac{(\mathrm{s}+31.1)\,(\mathrm{s}+1)}{(\mathrm{s}+1.01)\,(\mathrm{s}^2 + 1.40\mathrm{s} + 0.98)} \tag{6.104}$$

$$\boldsymbol{H}_{um}(s) = \begin{bmatrix} -0.32\frac{(\mathrm{s}+1.66)(\mathrm{s}+0.006)}{(\mathrm{s}+1.01)(\mathrm{s}^2+1.40\mathrm{s}+0.98)} \\ -0.003\frac{(\mathrm{s}-24.83)(\mathrm{s}+15.26)}{(\mathrm{s}+1.01)(\mathrm{s}^2+1.40\mathrm{s}+0.98)} \end{bmatrix}^T. \tag{6.105}$$

The only design parameters for the adpative control law are given by the choice of the filters $C_1(s)$ and $C_2(s)$. In the following simple first order lag filters are used

$$C_1(s) = \frac{\omega_{\mathrm{c},1}}{\mathrm{s} + \omega_{\mathrm{c},1}} \tag{6.106}$$

$$C_2(s) = \frac{\omega_{\mathrm{c},2}}{\mathrm{s} + \omega_{\mathrm{c},2}}. \tag{6.107}$$

This means the design parameters of the control law are $\omega_{\mathrm{c},1}$ and $\omega_{\mathrm{c},2}$. However, it is of course also possible to use higher order filters.

State-Predictor

As the piecewise constant control law is modified this also has to be taken into account for the predictor. It was mentioned that the "estimate" of the unmatched uncertainty will be fed to the integrator of the PI controller. Therefore the piecewise constant control signal is split up into two parts. The first part, $\eta_{AD,1}$, is resulting from the matched uncertainties and is fed to the actuating variables, and the second part, $\eta_{AD,2}$, is resulting from the unmatched uncertainties and is fed to the Integrator. Under these consideration the predictor is given by

$$\begin{aligned} \dot{\hat{\mathbf{x}}}_P^+ &= \mathbf{A}_P^+\hat{\mathbf{x}}_P^+ + \mathbf{b}_P^+\eta_M + \mathbf{b}_P^+\left(\eta_{AD,1} + \hat{\sigma}_1\right) + \mathbf{B}_{P,um}^+\widehat{\boldsymbol{\sigma}}_2 + \mathbf{b}_r^+\eta_{AD,2} + \mathbf{b}_P^+\Delta\eta + k_e\mathbf{e}_P \\ \hat{\mathbf{y}}_P^+ &= \mathbf{C}_P^+\hat{\mathbf{x}}_P^+ + \mathbf{d}_P^+\eta_M \\ \eta_M &= \mathbf{k}_y^T\hat{\mathbf{y}}_P^+ + k_r r, \end{aligned} \tag{6.108}$$

Where

$$\Delta\eta(s) = (G_{act}(s)G_{fil}(s)G_{del}(s) - 1)\cdot\eta_{CMD}(s), \tag{6.109}$$

accounts for the control deficiency due to the dynamics in the input channel (see Eq.(2.6)-(2.8)). An additional error feedback according to Section 5.1.6 is used such that k_e is an additional tuning parameter.

$\mathbf{A}_P^+$, $\mathbf{b}_P^+$, and $\mathbf{b}_r^+$ are given by Eq.(2.13). As $\mathbf{B}_{P,um}^+$ spans the null-space of $\mathbf{b}_P^+$ we obtain

$$\mathbf{b}_P^+ = \begin{bmatrix} Z_\eta \\ M_\eta \\ 0 \end{bmatrix} = \begin{bmatrix} -0.02 \\ -1.35 \\ 0 \end{bmatrix} \quad \rightarrow \quad \mathbf{B}_{P,um}^+ = \begin{bmatrix} -1 & -0.008 \\ 0.019 & -0.008 \\ -0.008 & 1 \end{bmatrix}$$

$\mathcal{L}_1$ Piecewise Constant Feedback

The $\mathcal{L}_1$ piecewise constant error feedback from Eq.(6.94) is implemented and given by

$$\begin{bmatrix} \hat{\sigma}_1 \\ \hat{\boldsymbol{\sigma}}_2 \end{bmatrix} = -\mathbf{K}_{\boldsymbol{e}}(T_s) \cdot \mathbf{C}_P^+ \cdot \mathbf{e}_P, \tag{6.110}$$

where $\mathbf{e}_P = \hat{\mathbf{y}}_P^+ - \mathbf{y}_P^+$ is transformed to the original error states by $\mathbf{C}_P^+$. The gain $\mathbf{K}_{\boldsymbol{e}}(T_s)$ is only dependent on the sample time, and according to Eq.(6.90) it is given by

$$\mathbf{K}_{\boldsymbol{e}}(T_s) = -\mathbf{B}^{-1}\left[\mathbf{A}_M^{-1}\left(e^{\mathbf{A}_M T_s} - \mathbf{I}\right)\right]^{-1} e^{\mathbf{A}_M T_s}\, \mathbf{e}_P(iT_s). \tag{6.111}$$

The complete control architecture is shown in Figure 6.17.

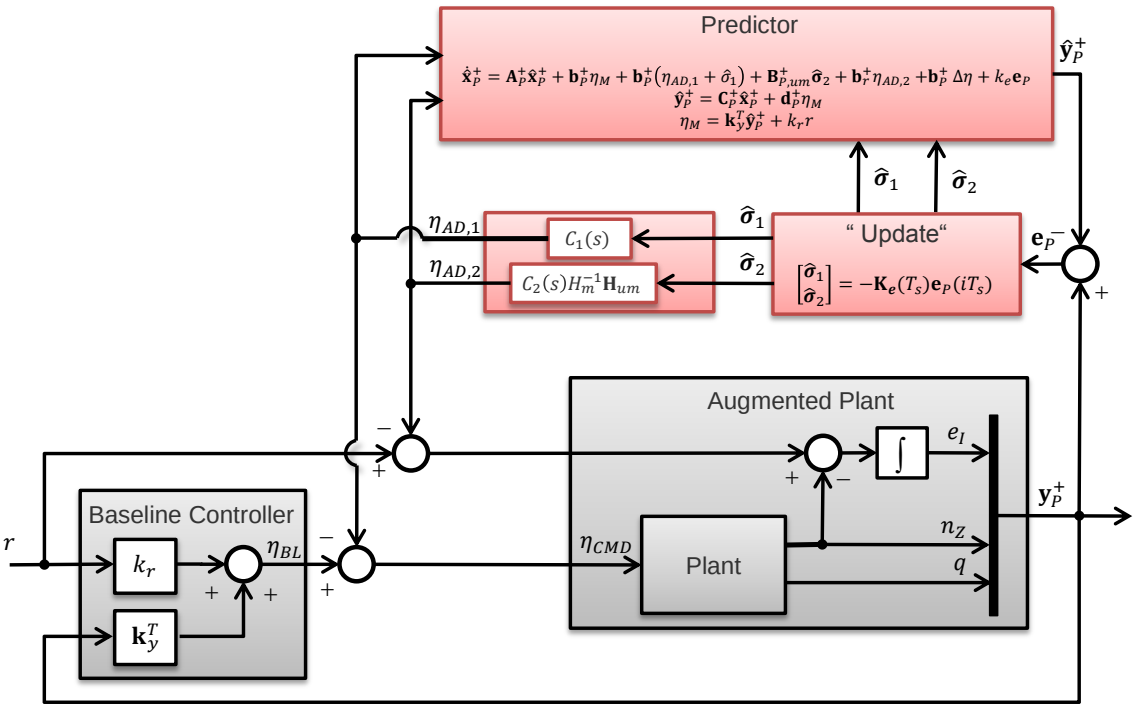

Figure 6.17: $\mathcal{L}_1$ Piecewise Constant with baseline PI controller

6.5.2 Evaluation

In the following the $\mathcal{L}_1$ piecewise constant control law, proposed in the previous section is evaluated and for all results a sample time of $T_s = 0.001$ seconds is used. At first the control law is applied to the pitch-up problem and in the following the robustness of the control law w.r.t. the design parameters is evaluated. The design parameters are the cut-off frequencies of the low-pass filters $\omega_{c,1}$ and $\omega_{c,2}$ from Eq.(6.106) and Eq.(6.107) and the error feed-back gain k_e in the predictor dynamics of Eq.(6.108). To assess the robustness, on the one hand classic metrics (e.g. gain and phase margin) are calculated, and on the other hand the robust performance w.r.t. parameteric uncertainties is evaluated based on simulations similar to the previous chapters.

6.5.2.1 Pitch-up nonlinearity

For the considered problem of the pitch-up nonlinearity the response for the $\mathcal{L}_1$ piecewise constant control law is shown in Figure 6.18, where $\omega_{c,1} = 100$, $\omega_{c,1} = 0.0001$ and $k_e = 0$. It can be seen, that in comparison to baseline control law the performance is increased and almost perfect following of the reference model is achieved. In Figure 6.19 the time history of the elevator command and rate is shown, and in Figure 6.20 the signals $\hat{\sigma}_1$ and $\hat{\boldsymbol{\sigma}}_2 = [\hat{\sigma}_{2,1} \quad \hat{\sigma}_{2,2}]^T$ are displayed.

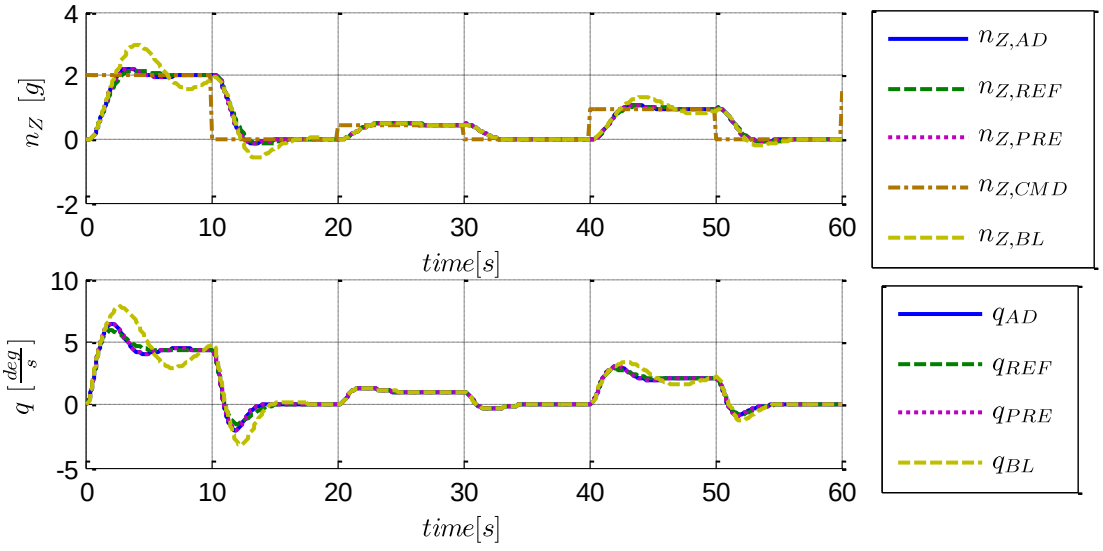

Figure 6.18: Response with $\mathcal{L}_1$ piecewise constant augmentaion

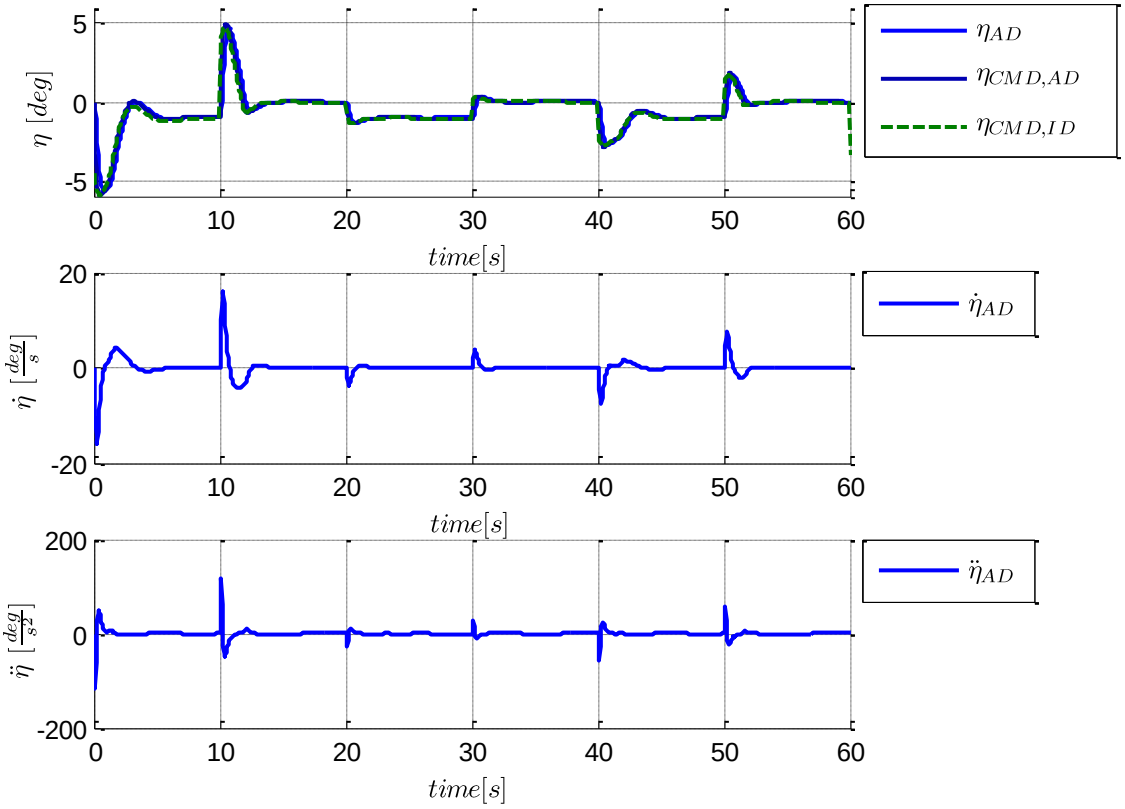

Figure 6.19: Elevator command and rate with $\mathcal{L}_1$ piecewise constant augmentation

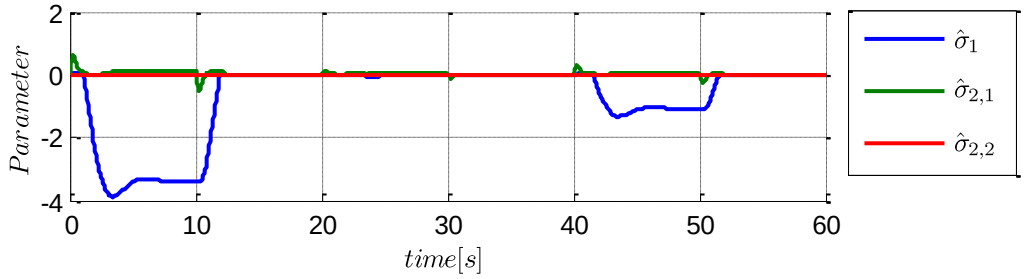

Figure 6.20: Parameter of the $\mathcal{L}_1$ piecewise constant controller

6.5.2.2 Assesment w.r.t $\omega_{c,1}$

At first the effect of the parameter $\omega_{c,1}$ is addressed, whereat $\omega_{c,2}$ and k_e are fixed with $\omega_{c,2} = 0.0001$ and $k_e = 0$.

Robust Stability

As already mentioned the $\mathcal{L}_1$ piecewise constant controller resembles a linear control law, therefore it is directly possible to calculate gain and phase margin for the closed loop.

In Table 6.4 the gain and phase margins for different cut-off frequencies $\omega_{c,1}$ of the lowpass filters are given. From Table 6.4 it becomes obvious that by increasing the cut-off frequency of the filters the gain and the phase margin of the controlled system are reduced. The reduced gain margin directly translates to a reduced robustness with repect to uncertainties in the input matrix $\mathbf{b}_P$ of the system.

$\omega_{c,1}$	0.01	0,1	1	10	50	100
GM [dB]	15.7	15.1	12.1	9.4	10.3	10.7
PM [deg]	69.8	64.8	46.7	44.2	47.8	48.6

Table 6.4: Gain and phase margins for the $\mathcal{L}_1$ piecewise constant controller for different cut-off frequencies $\omega_{c,1}$

In Figure 6.21 the Bode plots of the open loop piecewise constant controller controller are shown and in Figure 6.22 the Nyquist plots are shown. In both cases the graphs are given for the different cut-off frequencies of Table 6.4.

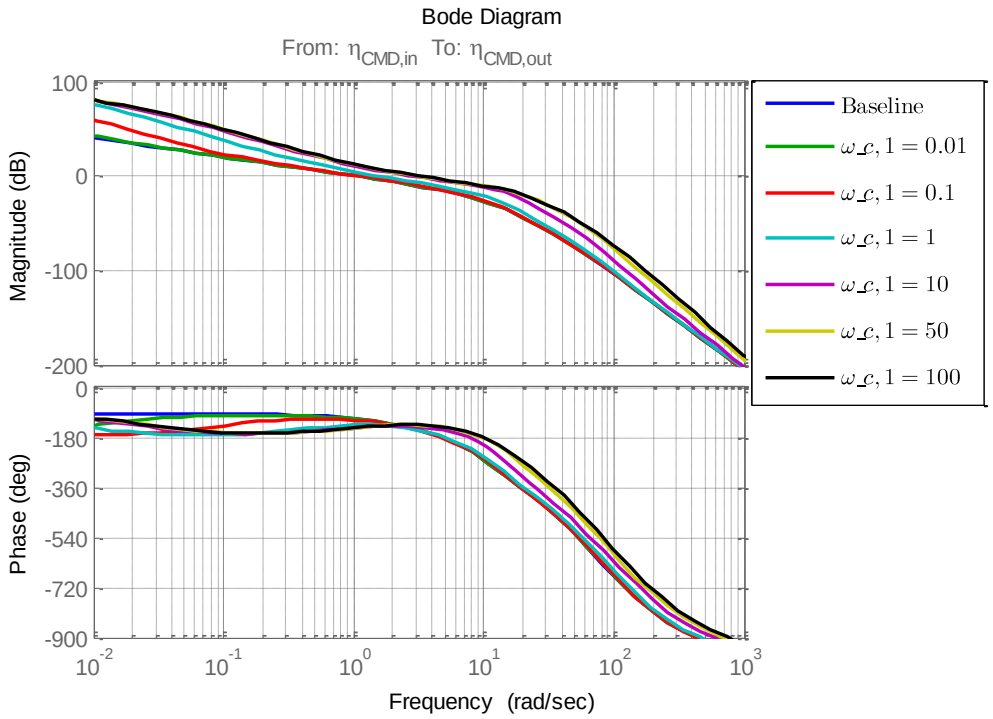

Figure 6.21: Bode plot of the $\mathcal{L}_1$ piecewise constant controller for different cut-off frequencies $\omega_{c,1}$

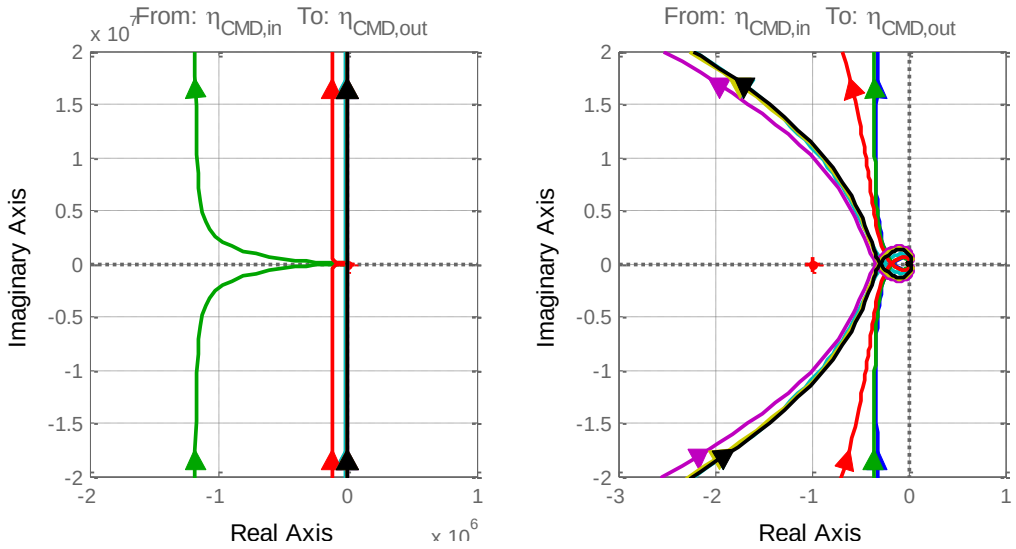

Figure 6.22: Nyquist plot of the $\mathcal{L}_1$ piecewise constant controller for different cut-off frequencies $\omega_{c,1}$

Robust Performance

In the following the robust performance of the $\mathcal{L}_1$ piecewise constant controller is investigated with respect to the baseline control law. Therefore, according to Section 3.1 the performance with respect to parameter uncertainties in the system dynamics is evaluated. At first simultaneous uncertainties in the coefficients M_α and M_q are assumed and in Figure 6.23 - Figure 6.28 the handling quality regions of $\mathcal{L}_1$ piecewise constant controller are shown for $\omega_{c,1} = [0.01 \quad 0.1 \quad 1 \quad 10 \quad 50 \quad 100]$, $\omega_{c,2} = 0.0001$, $k_e = 0$, where one can see that the robustness w.r.t. uncertainties in M_α and M_q increases with increasing filter bandwidth. Remember the contour lines refer to the baseline performance. Secondly, the robustness with respect to uncertainties in the coefficient Z_α is presented in Figure 6.29 - Figure 6.34. It can be seen that the robustness with respect to unmatched uncertainties is only affected in a negative way when $\omega_{c,1}$ is small. At last the robustness assessment w.r.t. uncertainty in the input gain λ is shown in Figure 6.35 - Figure 6.40 and it can be concluded that with increasing $\omega_{c,1}$ the robust performance in the presence of increasing λ is reduced. This is in accordance to the reduction of the gain margin given in Table 6.4.

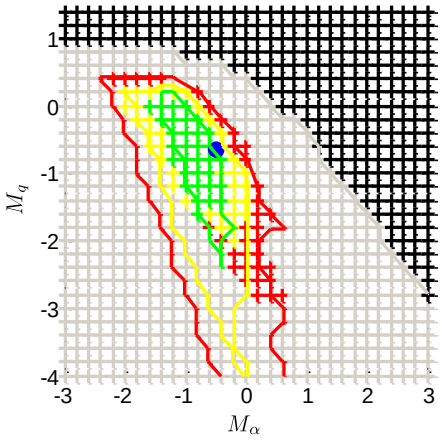

Figure 6.23: Robust perfomance w.r.t. M_α and M_q; $\omega_{c,1}$=0.01

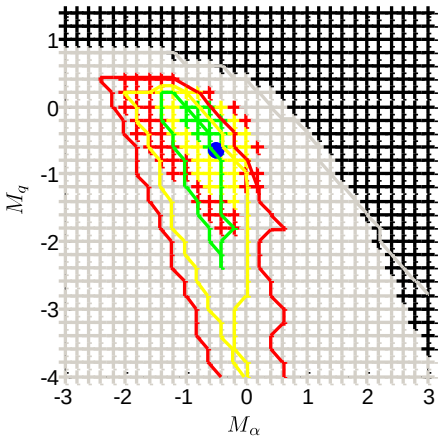

Figure 6.24: Robust perfomance w.r.t. M_α and M_q; $\omega_{c,1}$=1

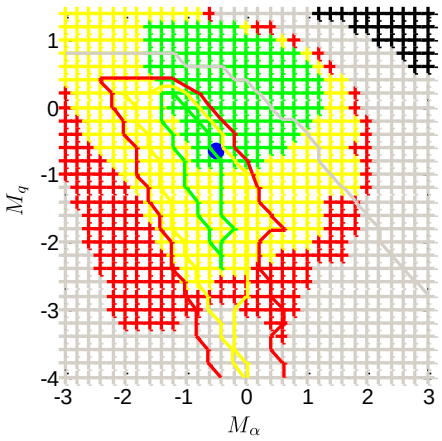

Figure 6.25: Robust perfomance w.r.t. M_α and M_q; $\omega_{c,1}$=50

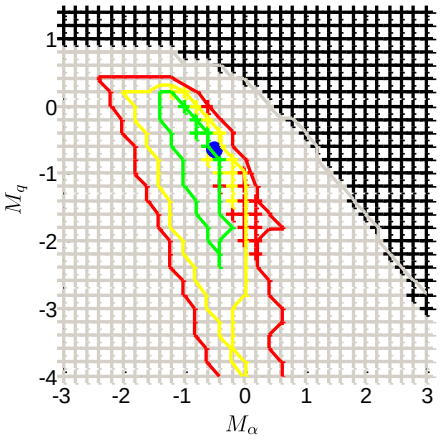

Figure 6.26: Robust perfomance w.r.t. M_α and M_q; $\omega_{c,1}$=0.1

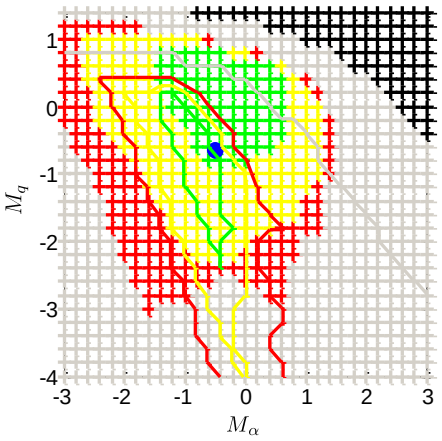

Figure 6.27: Robust perfomance w.r.t. M_α and M_q; $\omega_{c,1}$=10

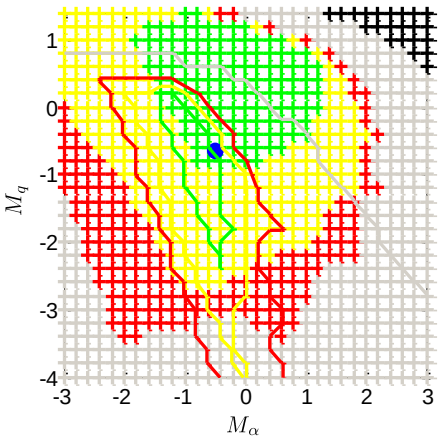

Figure 6.28: Robust perfomance w.r.t. M_α and M_q; $\omega_{c,1}$=100

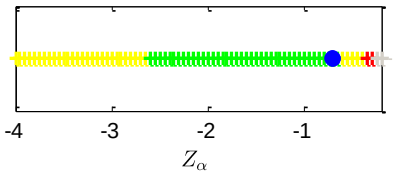

Figure 6.29: Robust perfomance w.r.t. Z_α; $\omega_{c,1}$=0.01

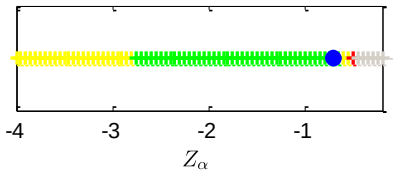

Figure 6.30: Robust perfomance w.r.t. Z_α; $\omega_{c,1}$=1

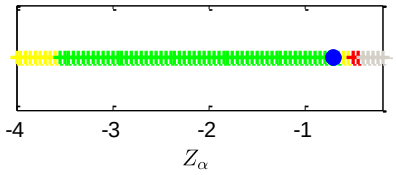

Figure 6.31: Robust perfomance w.r.t. Z_α; $\omega_{c,1}$=50

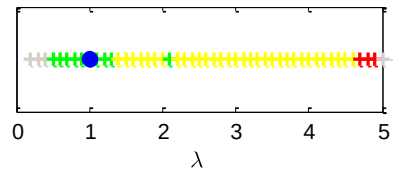

Figure 6.35: Robust perfomance w.r.t. λ $\omega_{c,1}$=0.01

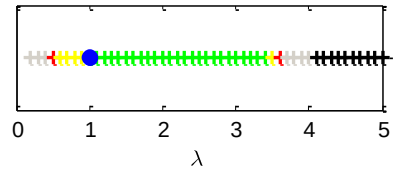

Figure 6.36: Robust perfomance w.r.t. λ $\omega_{c,1}$=1

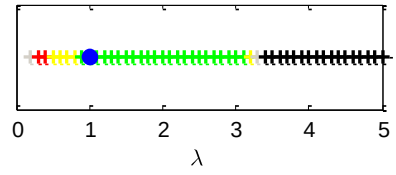

Figure 6.37: Robust perfomance w.r.t. λ $\omega_{c,1}$=50

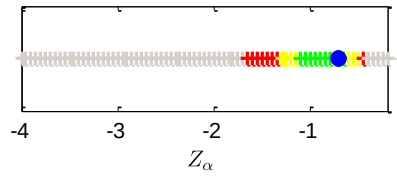

Figure 6.32: Robust perfomance w.r.t. Z_α; $\omega_{c,1}$=0.1

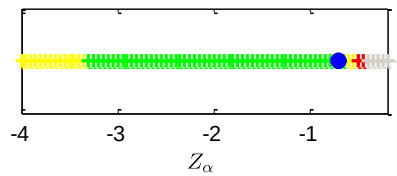

Figure 6.33: Robust perfomance w.r.t. Z_α; $\omega_{c,1}$=10

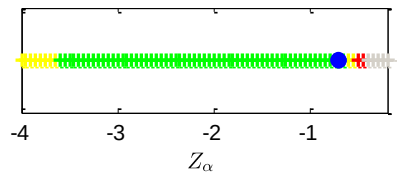

Figure 6.34: Robust perfomance w.r.t. Z_α; $\omega_{c,1}$=100

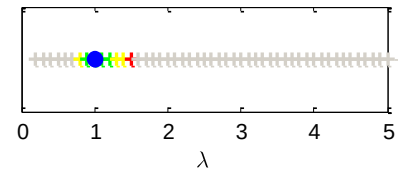

Figure 6.38: Robust perfomance w.r.t. λ $\omega_{c,1}$=0.1

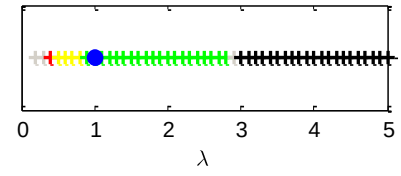

Figure 6.39: Robust perfomance w.r.t. λ $\omega_{c,1}$=10

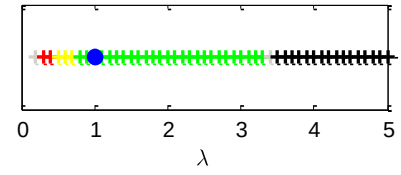

Figure 6.40: Robust perfomance w.r.t. λ $\omega_{c,1}$=100

6.5.2.3 Assesment w.r.t $\omega_{c,2}$

Here the effect of the parameter $\omega_{c,2}$ is investigated. Therefore $\omega_{c,1} = 100$ and $k_e = 0$ are fixed.

Robust Stability

In Table 6.5 the gain and phase margin of the closed loop are given for different filter frequencies $\omega_{c,2} = [0.01 \quad 0.1 \quad 1 \quad 5 \quad 10 \quad 20]$ and it can be seen that both, the gain and the phase margin are mentionable reduced with increasing $\omega_{c,2}$. In Figure 6.41 and Figure 6.42 the Bode and the Nyquist plots are shown, respectively.

$\omega_{c,2}$	0.01	0.1	1	5	10	20
GM [dB]	10.7	10.7	9.47	4.05	1.96	0.79
PM [deg]	48.6	48.1	43.8	34.3	31.9	30.8

Table 6.5: Gain and phase margins for the $\mathcal{L}_1$ piecewise constant controller for different cut-off frequencies $\omega_{c,2}$

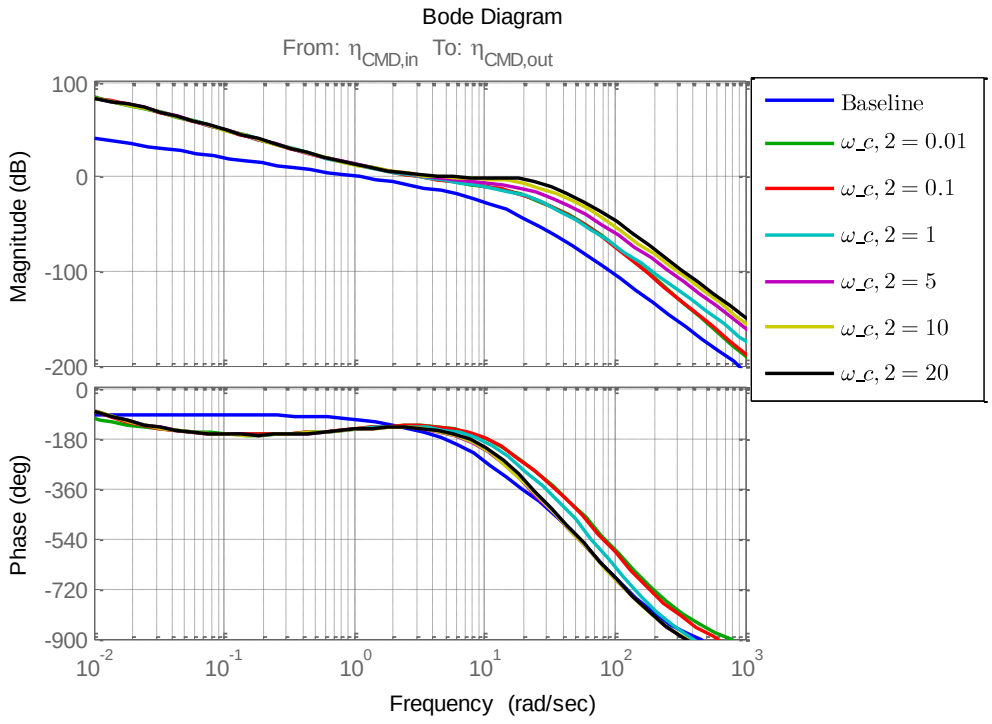

Figure 6.41:Bode plot of the $\mathcal{L}_1$ piecewise constant controller for different for different cut-off frequencies $\omega_{c,2}$

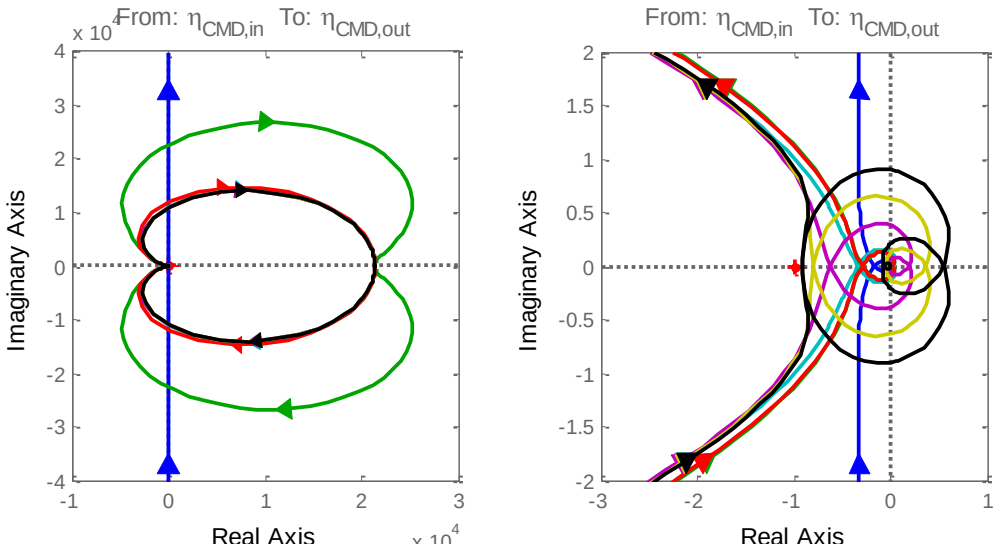

Figure 6.42: Nyquist plot of the $\mathcal{L}_1$ piecewise constant controller for different cut-off frequencies $\omega_{c,2}$

Robust Performance

The robust performance is evaluated in the same way as before for $\omega_{c,1}$, but now different values for $\omega_{c,2} = [0.01 \quad 0.1 \quad 1 \quad 5 \quad 10 \quad 20]$ are investigated. On the robustness w.r.t. matched uncertainties the impact of the parameter $\omega_{c,2}$ seems to be negligible as can be concluded from Figure 6.43 - Figure 6.48. But the feedback of $\eta_{ad,2}$, and thus $\omega_{c,2}$ affects the performance w.r.t. unmatched uncertainties. In Figure 6.49 - Figure 6.54 it can be seen that with increasing $\omega_{c,2}$ the robust performance increases at first, but then it deteriorates. In Figure 6.55 - Figure 6.60 it can be seen that the robustness w.r.t. changes in the input gain is largely affected by $\omega_{c,2}$, and it decreases as it was already predicted by the reduction of the gain margin. From this it can be concluded that for the considered problem, the feedback of $u_{ad,2}$ should not be used.

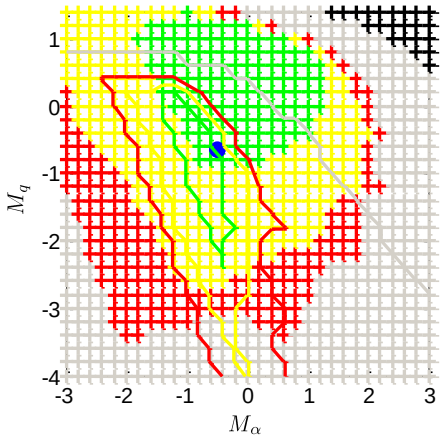

Figure 6.43: Robust perfomance w.r.t. M_α and M_q; $\omega_{c,z}$=0.01

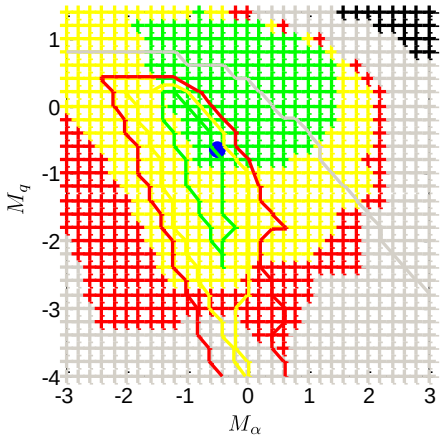

Figure 6.44: Robust perfomance w.r.t. M_α and M_q; $\omega_{c,z}$=1

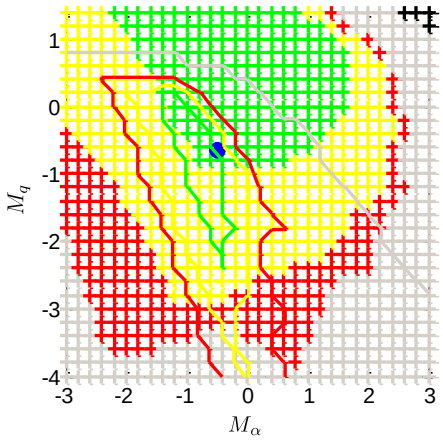

Figure 6.45: Robust perfomance w.r.t. M_α and M_q; $\omega_{c,z}$=10

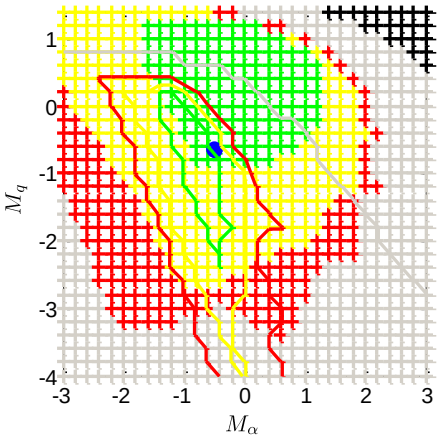

Figure 6.46: Robust perfomance w.r.t. M_α and M_q; $\omega_{c,z}$=0.1

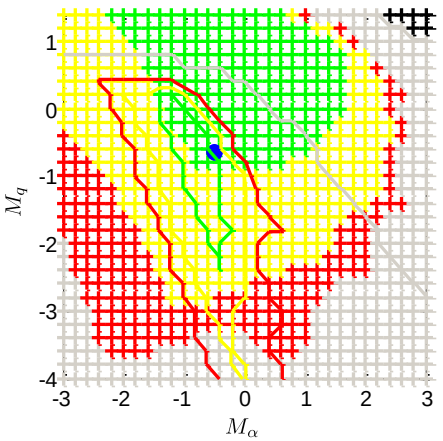

Figure 6.47: Robust perfomance w.r.t. M_α and M_q; $\omega_{c,z}$=5

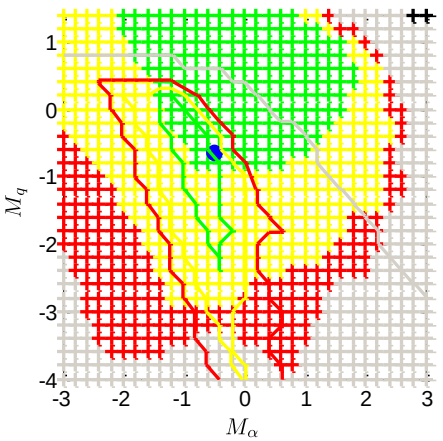

Figure 6.48: Robust perfomance w.r.t. M_α and M_q; $\omega_{c,z}$=20

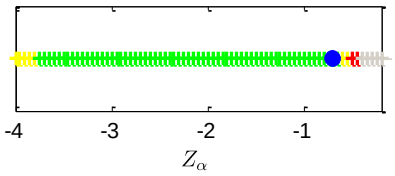

Figure 6.49: Robust perfomance w.r.t. Z_α; $\omega_{c,z}$=0.01

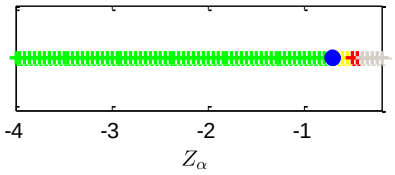

Figure 6.50: Robust perfomance w.r.t. Z_α; $\omega_{c,z}$=1

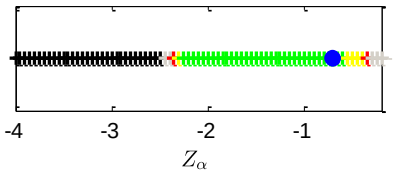

Figure 6.51: Robust perfomance w.r.t. Z_α; $\omega_{c,z}$=10

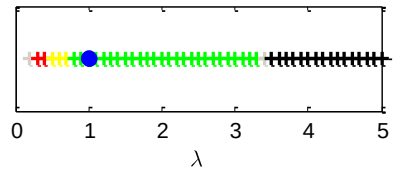

Figure 6.55: Robust perfomance w.r.t. λ $\omega_{c,z}$=0.01

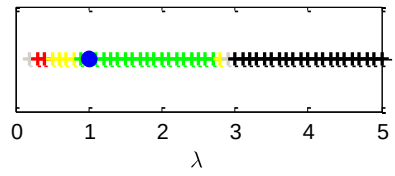

Figure 6.56: Robust perfomance w.r.t. λ $\omega_{c,z}$=1

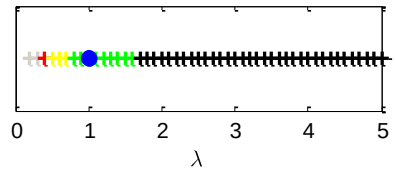

Figure 6.57: Robust perfomance w.r.t. λ $\omega_{c,z}$=10

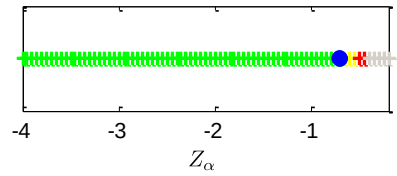

Figure 6.52: Robust perfomance w.r.t. Z_α; $\omega_{c,z}$=0.1

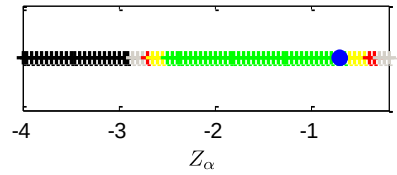

Figure 6.53: Robust perfomance w.r.t. Z_α; $\omega_{c,z}$=5

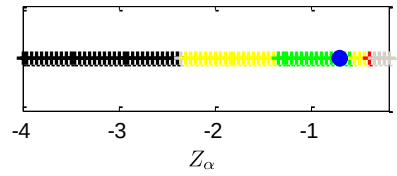

Figure 6.54: Robust perfomance w.r.t. Z_α; $\omega_{c,z}$=20

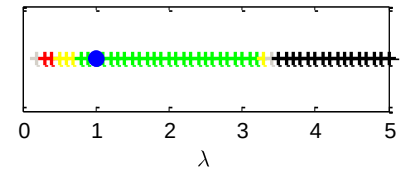

Figure 6.58: Robust perfomance w.r.t. λ $\omega_{c,z}$=0.1

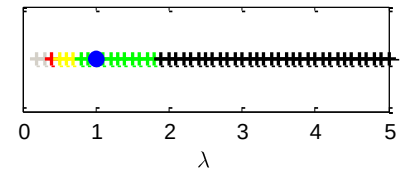

Figure 6.59: Robust perfomance w.r.t. λ $\omega_{c,z}$=5

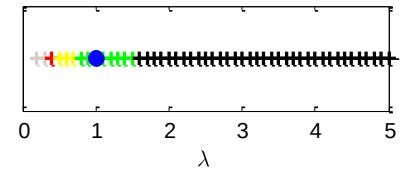

Figure 6.60: Robust perfomance w.r.t. λ $\omega_{c,z}$=20

6.5.2.4 Assesment w.r.t k_e

Finally the effect of the parameter k_e is addressed, where $\omega_{c,1} = 100$ and $\omega_{c,2} = 0.0001$ are fixed. As discussed in Chapter 5.1.6, with an error feedback to the predictor it takes the form of a Luenberger observer, and the feedback reduces the error in particular during transients as it drives the predictor towards the plant trajectory. This means, the amount of error feedback from the piecewise constant controller is reduced and the intended model following will be less aggressive.

Robust Stability

In Table 6.6 the effect of k_e on the gain and phase margin is shown and it can be seen that with increasing $k_e = [1 \quad 10 \quad 50 \quad 100 \quad 200 \quad 300]$ also the gain and phase margin are rising again. Furthermore in Figure 6.61 and Figure 6.62 the Bode and the Nyquist plots of the closed loop are shown.

k_e	1	10	50	100	200	300
GM [dB]	10.2	10.3	10.8	11.4	12.4	13.2
PM [deg]	48.4	48.8	50.4	52.4	55.9	59.1

Table 6.6: Gain and phase margins for the $\mathcal{L}_1$ piecewise constant controller for different error feedback gains k_e

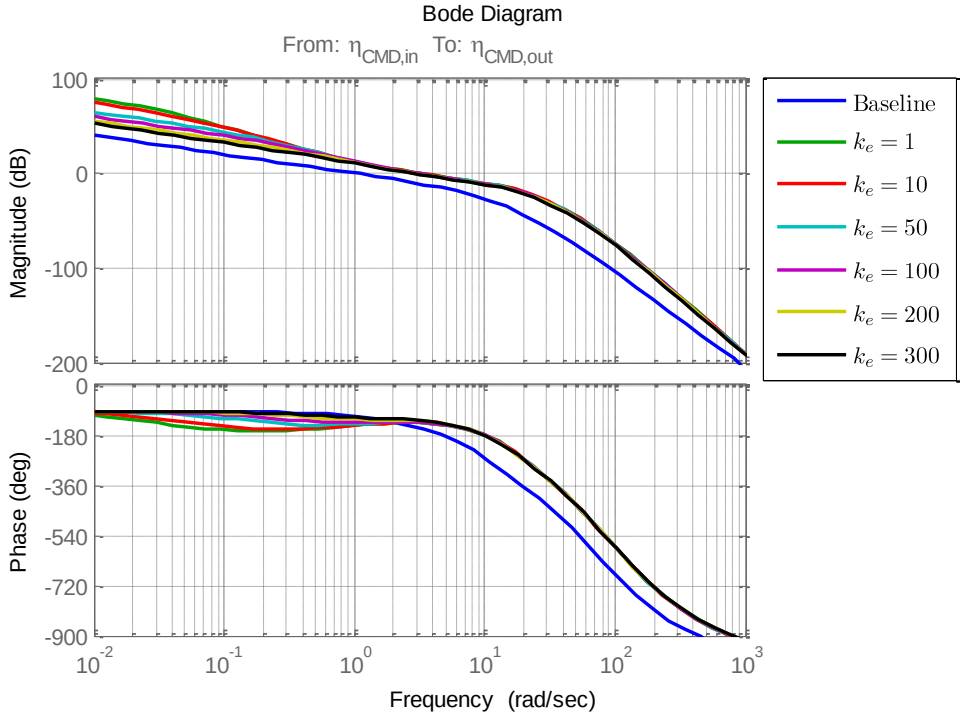

Figure 6.61: Bode plot of the $\mathcal{L}_1$ piecewise constant controller for different error feedback gains k_e

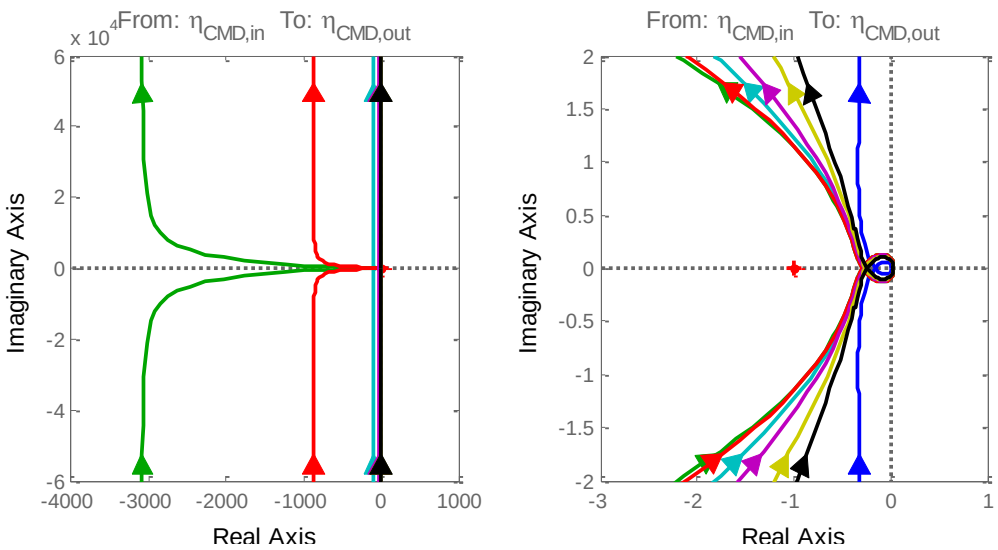

Figure 6.62: Nyquist plot of the $\mathcal{L}_1$ piecewise constant controller for different error feedback gains k_e

Robust Performance

Again the robust performance is addressed for $k_e = [1 \quad 10 \quad 50 \quad 100 \quad 300]$. And from Figure 6.63 - Figure 6.68 it seems that the robustness w.r.t. matched uncertainties is even further increased. For the unmatched uncertainties the performance remains constant as shown in Figure 6.69 - Figure 6.74. However, for uncertainties in the control effectives it can be clearly stated that the robustness is increased by introducing the error feedback and increasing k_e as shown in Figure 6.75 - Figure 6.80.

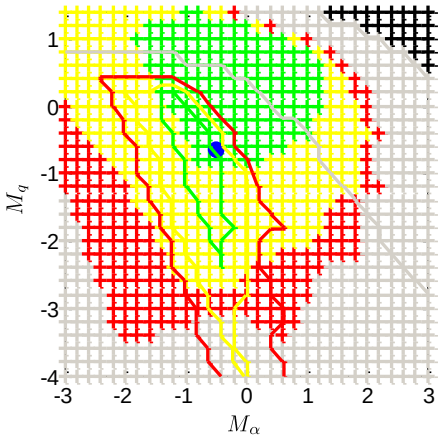

Figure 6.63: Robust perfomance w.r.t. M_α and M_q; k_e=1

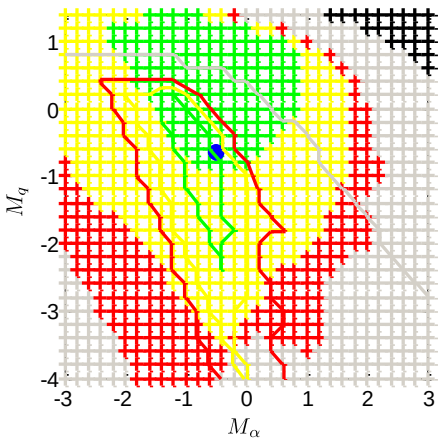

Figure 6.64: Robust perfomance w.r.t. M_α and M_q; k_e=50

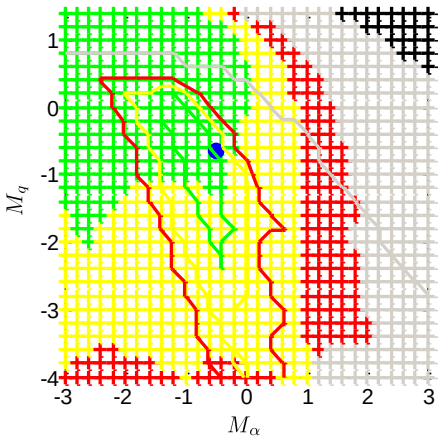

Figure 6.65: Robust perfomance w.r.t. M_α and M_q; k_e=200

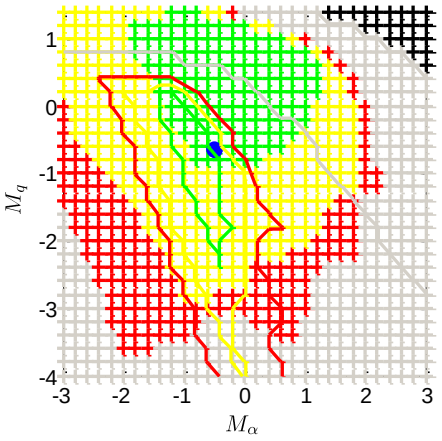

Figure 6.66: Robust perfomance w.r.t. M_α and M_q; k_e=10

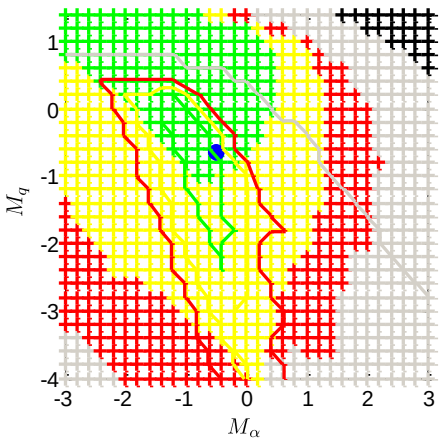

Figure 6.67: Robust perfomance w.r.t. M_α and M_q; k_e=100

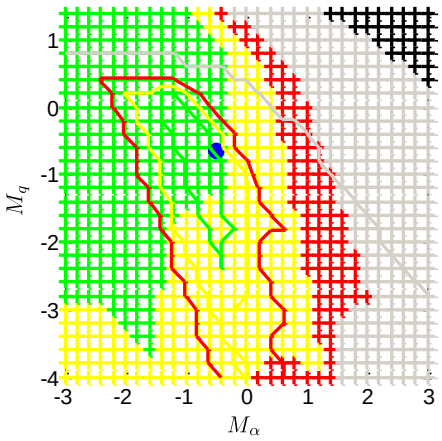

Figure 6.68: Robust perfomance w.r.t. M_α and M_q; k_e=300

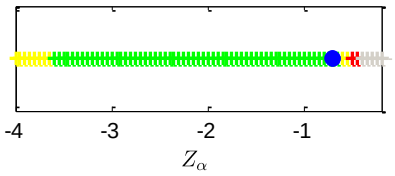

Figure 6.69: Robust perfomance w.r.t. Z_α; k_e=1

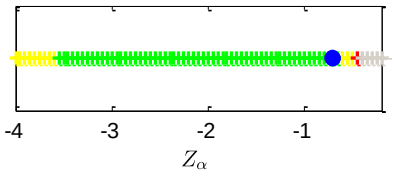

Figure 6.70: Robust perfomance w.r.t. Z_α; k_e=50

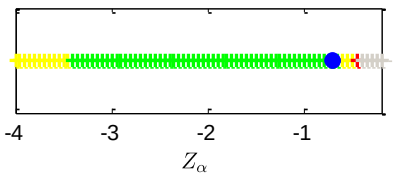

Figure 6.71: Robust perfomance w.r.t. Z_α; k_e=200

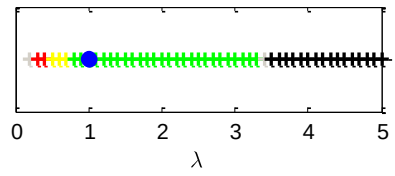

Figure 6.75: Robust perfomance w.r.t. λ k_e=1

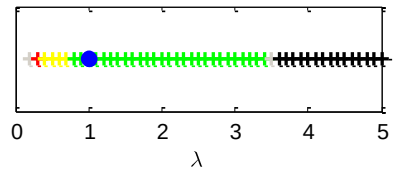

Figure 6.76: Robust perfomance w.r.t. λ k_e=50

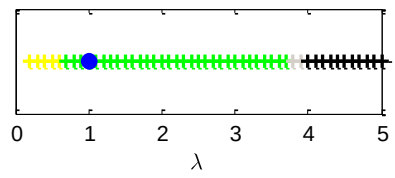

Figure 6.77: Robust perfomance w.r.t. λ k_e=200

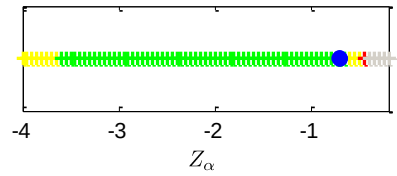

Figure 6.72: Robust perfomance w.r.t. Z_α; k_e=10

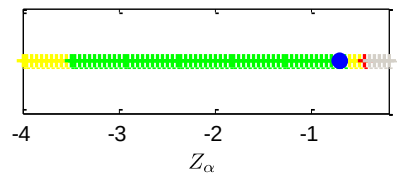

Figure 6.73: Robust perfomance w.r.t. Z_α; k_e=100

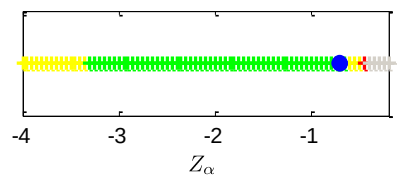

Figure 6.74: Robust perfomance w.r.t. Z_α; k_e=300

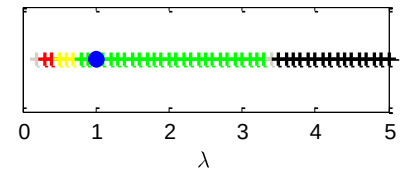

Figure 6.78: Robust perfomance w.r.t. λ k_e=10

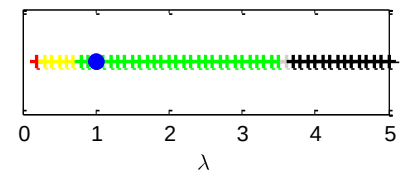

Figure 6.79: Robust perfomance w.r.t. λ k_e=100

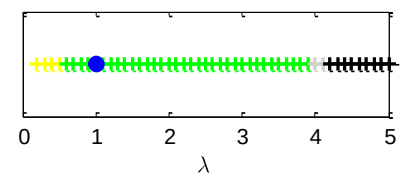

Figure 6.80: Robust perfomance w.r.t. λ k_e=300

Chapter 7

Application to Full Nonlinear Model

In the following different control methods are applied to the problem stated for the full nonlinear model described in Section 2.2. Remember that the problem formulation is different from the pitch-up problem, as now a loss of the calibrated airspeed measurement, which is used for gain scheduling of the baseline controller, is considered. This means, the augmenting control law has to adjust to slowly changing parameters, as the dynamics change with the variation of air speed. The baseline controller does not account for this anymore due to the loss of scheduling information. It is assumed that the scheduling parameter $V_{CAS,EST}$ is fixed to 320kts as stated in Section 2.2.3.

In the following at first the piecewise constant control law from Section 6.4 is applied as this provided very good results for the simple benchmark problem, while it is still a linear control law. But as it was already pointed out, for this problem formulation the augmenting control law has to adjust to slowly changing. Considering the slow dynamic changes, the MRAC approach also seems to be a suitable choice to solve the problem and it is applied in Section 7.2. Finally also an Extended Kalman Filter is investigated, which directly estimates the air speed, as this seems to be the most natural approach. Compared to the online adjustment of controller gains by MRAC the missing measurement is directly substituted. The approach and the results for the EKF are shown in Section 7.3.

7.1 $\mathcal{L}_1$ Piecewise Constant

For the following results the $\mathcal{L}_1$ piecewise constant approach from Section 6.4 is applied. The baseline control law is very similar to the baseline control law that was used for the pitch-up problem, in the sense that it is also a linear PI control law, where the load factor is the command variable. Therefore, the applied piecewise constant

control law is basically the same as the one in Section 6.5. This means, the elevator deflection is given by Eq.(6.98) and Eq.(6.99):

$$\begin{aligned} \eta &= \eta_{AD,1} + \eta_{BL} \\ \eta_{AD,1}(s) &= -C_1(s)\hat{\sigma}_1(s) \end{aligned} \tag{7.1}$$

The control signal $\eta_{AD,2}$ resulting from the unmatched part, which was given by Eq.(6.100), is not used here as in the previous assessment no improvement could be achieved.

The first challenge is to define a sufficient reference response by choosing the dynamics of the predictor. For the predictor the closed loop, linear short period approximation of the plant is used, again. This means the implemented predictor is equal to Eq.(6.108) without the unmatched term

$$\begin{aligned} \dot{\hat{\mathbf{x}}}_P^+ &= \mathbf{A}_P^+\hat{\mathbf{x}}_P^+ + \mathbf{b}_P^+\eta_M + \mathbf{b}_P^+\left(\eta_{AD,1} + \hat{\sigma}_1\right) + \mathbf{b}_P^+\Delta\eta + k_e\mathbf{e}_P \\ \hat{\mathbf{y}}_P^+ &= \mathbf{C}_P^+\hat{\mathbf{x}}_P^+ + \mathbf{d}_P^+\eta_M \\ \eta_M &= \mathbf{k}_y^T\hat{\mathbf{y}}_P^+ + k_r r, \end{aligned} \tag{7.2}$$

where the control deficiency

$$\Delta\eta = \eta - \eta_{CMD}, \tag{7.3}$$

is the difference between the commanded elevator deflection η_{CMD} and the realized deflection η, which is obtained from the actuator model given in Section 2.2.1.2. $\mathbf{k}_y^T = [k_{n_z} \quad k_q \quad k_{e_I}]$ and k_r are given by the baseline controller gains at $V_{CAS} = 320kts$.

The short period approximation ($\mathbf{A}_P^+, \mathbf{b}_P^+, \mathbf{C}_P^+, \mathbf{d}_P^+$) is obtained by linearizing the open loop plant. It is assumed that the gains of the baseline control law ($\mathbf{k}_y^T$, k_r) are fixed to the values associated with $V_{CAS,EST} = 320kts$. Therefore, for the linearization point, a steady state horizontal flight with $V_{CAS} = 320kts$ and $h = 30000ft$ is chosen. Hence, the desired reference response is given by the linearized, closed loop dynamics of the short period at $V_{CAS} = 320kts$. It should be noted that the height has basically no influence on the dynamics of the aircraft as long as $V_{CAS} = const.$

The parameters, that must be chosen for the piecewise constant control law are the filter constants $\omega_{c,1}$, and the error feedback gain k_e. These parameters were investigated in Section 6.5.2. The best results were obtained when $\omega_{c,1}$ is chosen large, which means that the filter $C_1(s)$ has basically no effect and $\hat{\sigma}_1(s)$ is directly fed to the input. Note that the input was still filtered by the structural filter. In particular, for the following results, it is chosen $\omega_{c,1} = 100$. The second parameter is the parameter k_e, which can "pull" the predictor towards the plant and thus reduce the aggressiveness of the control law. In the following $k_e = 300$ is used. The results of the handling quality assessment are shown in Figure 7.1. Comparing the results with the

ones from Section 3.2.2.2 it can be seen that over a large domain of the envelope the rise time and the rise time parameter improve. However, simultaneously the equivalent time delay that the pilot experiences gets larger and this leads to deteriorated handling qualities. Note that the rise time could be further improved by reducing the parameter k_e but this would lead to an even larger equivalent time delay. The reason therefore can be seen in Figure 7.2 and Figure 7.3, where the load factor and the pitch rate trajectories obtained for the piecewise constant control law are shown in comparison to the non-scheduled baseline controller. It is obvious that for small air speeds the rise time improves and the response seems to be more homogenous over the envelope. But as the piecewise constant control law does not change the feed forward gain the initial response can basically not be affected. It follows that a faster rise time requires a steeper slope of the response, and this directly leads to a larger equivalent time delay.

At the end it is difficult to judge from a step response whether a pilot will like or dislike the response because this can only be evaluated in real flight tests. However, the results clearly show that for the piecewise constant control law a trade of between rise time improvement and equivalent time delay deterioration must be faced.

MRAC should be able to tackle this issue, as it is capable of adjusting the feed forward gain. Therefore, the MRAC approach is applied in the following section.

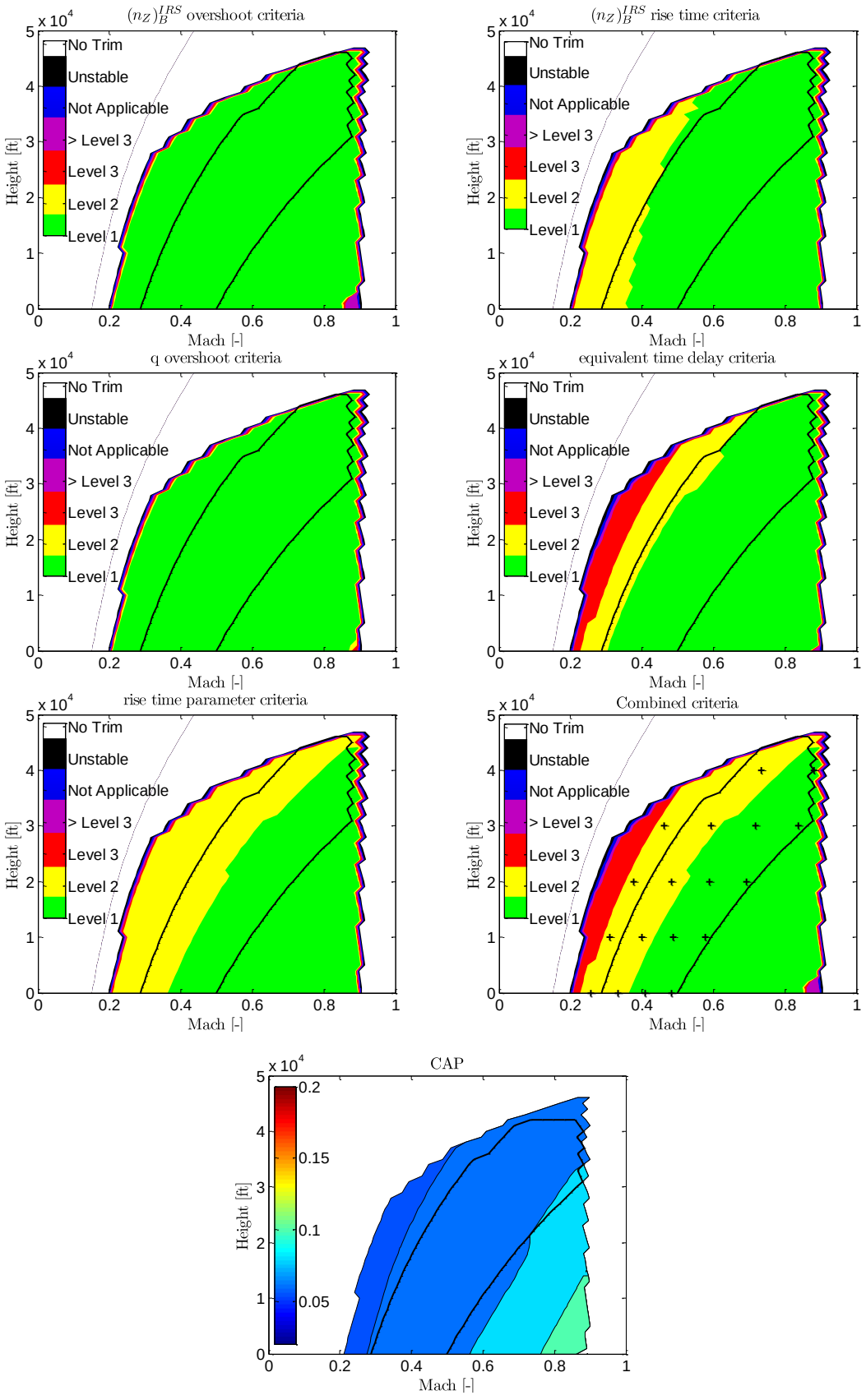

Figure 7.1: HQ assessment of the piecewise constant control law

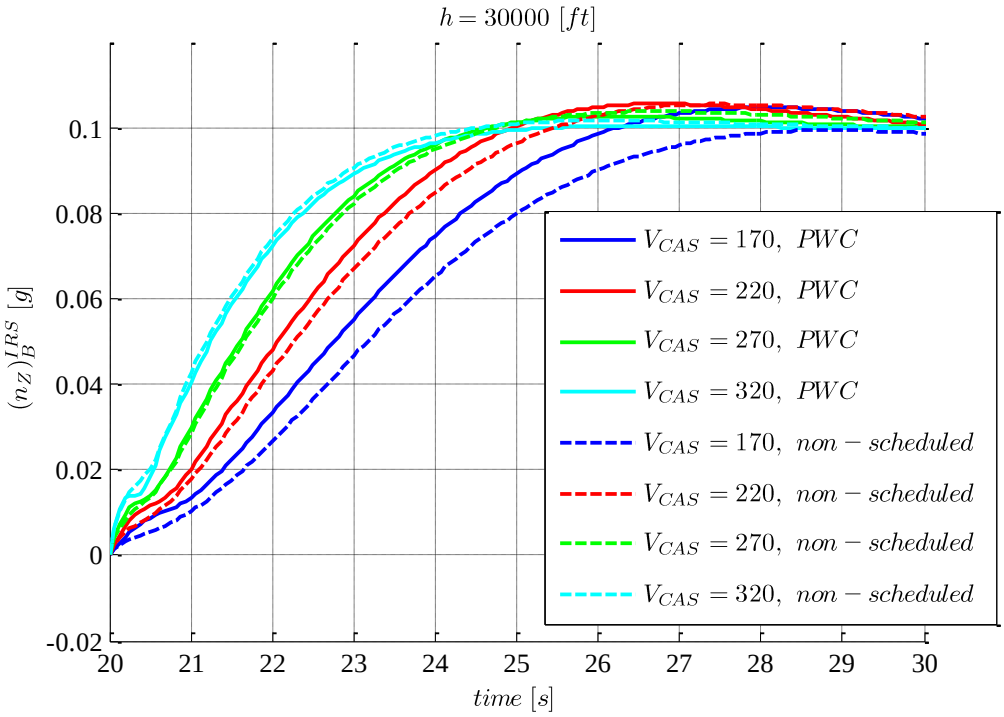

Figure 7.2: Load factor response of the piecewise constant control law

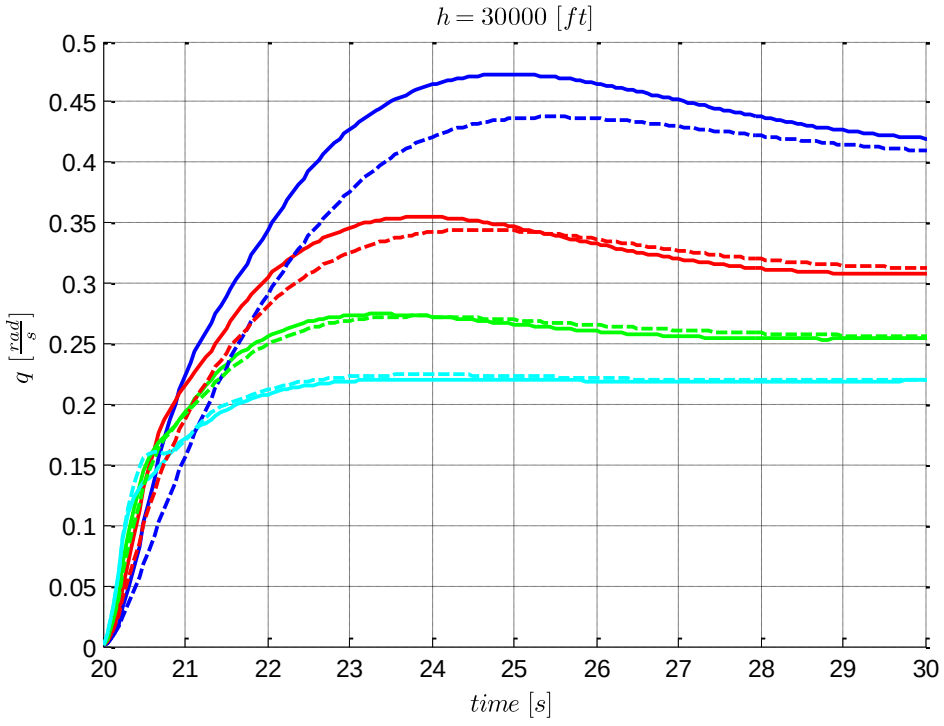

Figure 7.3: Pitch rate response of the piecewise constant control law

7.2 Predictor Based MRAC

In principle the predictor based approach from Section 4.4 is applied. Additionally some of the previously discussed modifications are applied. For the design of the adaptive controller it is assumed that only the short period dynamics have to be controlled. Furthermore, it is desired that the adaptive controller has the same feedback structure as the linear baseline controller. Hence, the design is based on the linearized plant dynamics for a steady state wings leveled flight. As we want to control the short period dynamics the phygoid dynamics is neglected in the following. This means the assumed plant, with integrator state, is the same as the one considered in Eq.(2.13), only without the nonlinearity

$$\begin{aligned} \dot{\mathbf{x}}_P^+ &= \mathbf{A}_P^+ \mathbf{x}_P^+ + \mathbf{b}_P^+ \eta + \mathbf{b}_r^+ r \\ \mathbf{y}_P^+ &= \mathbf{C}_P^+ \mathbf{x}_P^+ + \mathbf{d}_P^+, \end{aligned} \tag{7.4}$$

where $\mathbf{A}_P^+$, $\mathbf{b}_P^+$, $\mathbf{C}_P^+$, $\mathbf{d}_P^+$ are obtained by linearizing the plant at $V_{CAS} = 320kts$ and $h = 30000ft$.

Due to the same premises, the same adaptive control approach, which was already used for the simple short period model with pitch-up nonlinearity, is applied (compare Eq.(4.23) and Eq.(5.60)). In the following also the modifications suggested in Chapter 5 are applied.

With the baseline controller the commanded elevator deflection is given by

$$\eta_{CMD} = \frac{1}{\hat{\lambda}} \left(\eta_{AD,FB} + \eta_{BL} \right) \tag{7.5}$$

$$\eta_{AD,FB} = \widehat{\boldsymbol{\theta}}_y^T \mathbf{y}_P^+ - \Delta \widehat{\boldsymbol{\theta}}_{y,M}^T \hat{\mathbf{y}}_P^+, \tag{7.6}$$

where $\boldsymbol{\theta}_y^T = [\theta_{n_z} \quad \theta_q \quad \theta_{e_I}]$, and $\Delta\widehat{\boldsymbol{\theta}}_{y,M}$ is defined on the basis of Eq.(5.43)

$$\Delta \widehat{\boldsymbol{\theta}}_{y,M} = \begin{cases} \widehat{\boldsymbol{\theta}}_y & for \quad \widehat{\boldsymbol{\theta}}_{y,M,min}^* \le \widehat{\boldsymbol{\theta}}_y \le \widehat{\boldsymbol{\theta}}_{y,M,max}^* \\ \widehat{\boldsymbol{\theta}}_{y,M,max}^* & for \quad \widehat{\boldsymbol{\theta}}_y < \widehat{\boldsymbol{\theta}}_{y,M,max}^* \\ \widehat{\boldsymbol{\theta}}_{y,M,min}^* & for \quad \widehat{\boldsymbol{\theta}}_y > \widehat{\boldsymbol{\theta}}_{y,M,min}^* \end{cases} . \tag{7.7}$$

The hypercube within which no adaptive feedback is generated is defined by $\widehat{\boldsymbol{\theta}}_{y,M,max}^{*T} = [4 \quad 0.5 \quad 2]$ and $\widehat{\boldsymbol{\theta}}_{y,M,min}^{*T} = [0 \quad 0 \quad 0]$. These values are chosen to prohibit instability by applying to large feedback gains. The maximum gains which are necessary to obtain the same performance for low speeds, as for $V_{CAS} = 320kts$, would lead to instability, because the same performance cannot be achieved due to actuator limitations. Therefore, the modification assures that only the amount of additional gain can be applied which is necessary to achieve level 1 HQ.

The integrated error e_I is calculated from Eq.(2.24) by

$$e_I = \frac{1}{K_{Int}(V_{CAS,EST}=320kts)} \eta_{FB,Int}. \tag{7.8}$$

One particular challenge for this example is the choice of the reference model, as it must be suitable for the complete envelope. Of course it is desirable to have a homogenous response over the complete envelope, but for the MRAC state feedback approach the controller gains are adjusted with the objective to drive the error vector to zero and this is not generally possible in the presence of unmatched uncertainties. This problem could already be seen in Section 5.1.2, where a loss of robustness with respect to changes in the unmatched parameter Z_α of the short-period dynamics was observed. Therefore the solution suggested in Section 5.1.4 is used, where additionally the unmatched uncertainties are estimated and the reference model is adjusted based on these estimates to remain achievable. The predictor dynamics are given in similar from as in Eq.(5.58), but in difference to Eq.(5.58) the unmatched uncertainties are not only directly fed back. They are also used to calculate the ideal feedback gains, which have to be applied in order to maintain the poles of the predictor at the original position, even in presence of the input $\mathbf{b}_{P,um}^{+}\widehat{\boldsymbol{\theta}}_{y,um}^{T}\hat{\mathbf{y}}_{P}^{+}$. This means an additional term $\Delta\mathbf{k}_{um}^{T}(\widehat{\boldsymbol{\theta}}_{y,um}^{T})\hat{\mathbf{y}}_{P}^{+}$ is added to the command of the reference baseline controller η_M:

$$\begin{aligned}\dot{\hat{\mathbf{x}}}_{P}^{+} &= \mathbf{A}_{P}^{+}\hat{\mathbf{x}}_{P}^{+} + \mathbf{b}_{P}^{+}\eta_{M} + \mathbf{b}_{r}^{+}r + \mathbf{b}_{P}^{+}\,\hat{\lambda}\,\Delta\eta - \mathbf{b}_{P}^{+}\Delta\widehat{\boldsymbol{\theta}}_{y,M}^{T}\hat{\mathbf{y}}_{P}^{+} - \mathbf{b}_{P,um}^{+}\widehat{\boldsymbol{\theta}}_{y,um}^{T}\hat{\mathbf{y}}_{P}^{+} - k_{e}\mathbf{e}_{P}\\ \hat{\mathbf{y}}_{P}^{+} &= \mathbf{C}_{P}^{+}\hat{\mathbf{x}}_{P}^{+} + \mathbf{d}_{P}^{+}\eta_{M}\\ \eta_{M} &= \mathbf{k}_{y}^{T}\hat{\mathbf{y}}_{P}^{+} + k_{r}r + \Delta\mathbf{k}_{um}^{T}(\boldsymbol{\theta}_{x,um}^{T})\hat{\mathbf{y}}_{P}^{+}.\end{aligned} \tag{7.9}$$

$\Delta\eta$ is the deficiency between the commanded elevator deflection η_{CMD} and the realized deflection η which is obtained from the actuator model given in Section 2.2.1.2

$$\Delta\eta = \eta - \eta_{CMD}, \tag{7.10}$$

and $\mathbf{k}_{y}^{T} = [k_{n_Z} \quad k_q \quad k_{e_I}]$ and k_r are given by the baseline controller gains at $V_{CAS} = 320kts$.

The effect of the input $\mathbf{b}_{P,um}^{+}\widehat{\boldsymbol{\theta}}_{y,um}^{T}\hat{\mathbf{y}}_{P}^{+}$ on the predictor dynamics is given by

$$\mathbf{A}_{P,\theta_{um}}^{+} = \mathbf{A}_{P}^{+} - \mathbf{b}_{P,um}^{+}\widehat{\boldsymbol{\theta}}_{y,um}^{T}. \tag{7.11}$$

This matrix $\mathbf{A}_{P,\theta_{um}}^{+}$ can be transformed to the output domain by

$$\mathbf{A}_{P,\theta_{um},n_Z}^{+} = \mathbf{C}_{P}^{+}\mathbf{A}_{P,\theta_{um}}^{+}{\mathbf{C}_{P}^{+}}^{-1} = \begin{bmatrix} Z'_{n_Z} & Z'_{q} & 0\\ M'_{n_Z} & M'_{q} & M'_{e}\\ -1 & 0 & 0\end{bmatrix}. \tag{7.12}$$

Based on the matrix-parameters in Eq.(7.18)(7.12) we can calculate the feedback gains which are necessary to maintain the poles of the predictor at the same location as the poles of $\mathbf{A}_{M}^{+} = \mathbf{A}_{P}^{+} + \mathbf{b}_{P}^{+}\mathbf{k}_{y}^{T}\hat{\mathbf{y}}_{P}^{+}$. If the desired poles are specified by $\lambda_{1/2} = \sigma \pm \omega i$ and λ_3, than these feedback gains $\mathbf{k}_{um}^{T} = [k'_{n_Z} \quad k'_{q} \quad k'_{e_I}]$ can be calculated by

$$
\begin{aligned}
k'_{n_Z} &= \frac{1}{M_\eta Z'_q}\left(\omega^2 + \sigma^2 - 2\sigma Z'_\alpha + \sigma\lambda_3 + {Z'_\alpha}^2 - \lambda_3 Z'_\alpha + M'_{n_Z} Z'_q\right) \\
k'_q &= \frac{1}{M_\eta}\left(\lambda_3\omega^2 + 2\sigma - M'_q - Z'_\alpha\right) \\
k'_{e_I} &= \frac{1}{M_\eta Z'_q}\left(\lambda_3\omega^2 + \lambda_3\sigma^2 - M'_e Z'_q\right).
\end{aligned}
\tag{7.13}
$$

The increment $\Delta\mathbf{k}_{um}^T$ that is added in Eq.(7.9) is calculated from

$$
\Delta\mathbf{k}_{um}^T = \mathbf{k}_{um}^T - \mathbf{k}_y^T. \tag{7.14}
$$

As it was mentioned before the modification suggested in Section 5.1.3 is also applied. For the current example this is in particular important, because keeping the poles of the predictor at the same location in presence of unmatched uncertainties can require large feedback gain. By applying the modification from Section 5.1.3 the requirement on the desired response is reduced as a certain portion of the adaptive feedback gains is at first used to adjust the reference model, instead of the plant dynamics.

To improve the robustness the recursive least-square update modification from Section 5.3.3 is applied. A slightly modified, normalized version of the update laws of Section 5.3.4 is used (compare Eq.(5.127) and Eq.(5.128)), where additionally the parameters $\mathbf{\Gamma}_y$, $\mathbf{\Gamma}_{y,um}$, and γ_λ are introduced

$$
\begin{aligned}
\dot{\hat{\boldsymbol{\theta}}}_P &= \begin{bmatrix}\dot{\hat{\boldsymbol{\theta}}}_y \\ \dot{\hat{\lambda}}\end{bmatrix} = -\mathbf{R}_{ma}\begin{bmatrix}\mathbf{\Gamma}_y & \mathbf{0} \\ \mathbf{0} & \gamma_\lambda\end{bmatrix}\left[\boldsymbol{\omega}_{P,f}\mathbf{e}_{P,f}^T\mathbf{P}\mathbf{b}_{P,n_Z}^+ + \gamma_C\bar{\boldsymbol{\omega}}_{P,f}\left(\bar{\boldsymbol{\omega}}_{P,f}^T\hat{\boldsymbol{\theta}}_P^T\mathbf{b}_{P,n_Z}^+ - \bar{\boldsymbol{\upsilon}}^T\right)\mathbf{b}_{P,n_Z}^{+^r}\right] \\
\dot{\mathbf{R}}_{ma} &= -\mathbf{R}_{ma}\left[\bar{\boldsymbol{\omega}}_{P,f}\bar{\boldsymbol{\omega}}_{P,f}^T\right]_{ii}\mathbf{R}_{ma} + \beta[\mathbf{R}_{ma}]_{ii}.
\end{aligned}
\tag{7.15}
$$

with $\boldsymbol{\omega}_{P,f}^T = \begin{bmatrix}\mathbf{y}_{P,f}^+ & \eta_f\end{bmatrix}$. The update law for the unmatched uncertainties is modified to

$$
\begin{aligned}
\dot{\hat{\boldsymbol{\theta}}}_{y,um} &= -\mathbf{R}_{um}\mathbf{\Gamma}_{y,um}\left[\mathbf{y}_{P,f}^+\mathbf{e}_{P,f}^T\mathbf{P}\mathbf{b}_{P,um,n_Z}^+ + \gamma_C\bar{\mathbf{y}}_{P,f}^+\left(\bar{\mathbf{y}}_{P,f}^{+^T}\hat{\boldsymbol{\theta}}_{y,um}^T\mathbf{b}_{P,n_Z,um}^+ - \bar{\boldsymbol{\upsilon}}^T\right)\mathbf{b}_{P,um,n_Z}^{+^r}\right] \\
\dot{\mathbf{R}}_{um} &= -\mathbf{R}_{um}\left[\bar{\mathbf{y}}_{P,f}^+\bar{\mathbf{y}}_{P,f}^{+^T}\right]_{ii}\mathbf{R}_{um} + \beta[\mathbf{R}_{um}]_{ii}
\end{aligned}
\tag{7.16}
$$

The subscript f denotes that the respective signals are filter by the washout filter

$$
y_f = \frac{Ts}{Ts+1}y, \tag{7.17}
$$

where $T = 10s$ is used. This washout filter is applied to remove the steady state values and the effects of the phygoid mode.

The chosen values for the initial conditions of the covariance matrices $\mathbf{R}_{ma}(0)$ and $\mathbf{R}_{um}(0)$, the forgetting factor β, the weighting factor γ_C, and the filter parameter λ_F are given in Table 7.1. To assure boundedness of $\mathbf{R}_{ma}$ and $\mathbf{R}_{um}$ projection is used to enforce the upper bounds, which are defined by the initial conditions, $\mathbf{R}_{ma}(0)$ and $\mathbf{R}_{um}(0)$. The remaining controller parameters that have to be selected are given in Table 7.2. To prevent instability as a result of too large feedback gains the adaptive

parameter $\hat{\lambda}$ is bounded by projection. The limits for $\hat{\lambda}$ are given by $\hat{\lambda} \in [0.5; 1.1]$. The limits for the parameters $\widehat{\boldsymbol{\theta}}_y^T$ and $\widehat{\boldsymbol{\theta}}_{y,max}^T$ are obtained from worst case consideration, meaning they are determined from the maiximum possible change in the linearized system dynamics that can be cause by an airspeed reduction. From this consideration the limits enforced by projection are for $\widehat{\boldsymbol{\theta}}_y^T$ defined by $\widehat{\boldsymbol{\theta}}_{y,max}^T = [13 \quad 0.7 \quad 8]$ and $\widehat{\boldsymbol{\theta}}_{y,min}^T = [-0.1 \quad -0.1 \quad -0.1]$, and for $\widehat{\boldsymbol{\theta}}_{y,um}$ the limits are given by $\widehat{\boldsymbol{\theta}}_{y,um,max}^T = [1.3 \quad 0.1 \quad 0.3]$ and $\widehat{\boldsymbol{\theta}}_{y,um,min}^T = [-0.1 \quad -0.7 \quad -0.5]$.

$\mathbf{R}_{ma}(0)$	$\mathbf{R}_{um}(0)$	β	γ_C	λ_F
$\begin{bmatrix}1&0&0&0\\0&1&0&0\\0&0&1&0\\0&0&0&1\end{bmatrix}$	$\begin{bmatrix}1&0&0\\0&1&0\\0&0&1\end{bmatrix}$	0.02	0.01	1

Table 7.1: Parameters of the recursive least-square modification for full model

$\boldsymbol{\Gamma}_y$	Γ_Λ	$\boldsymbol{\Gamma}_{y,um}$	k_e
$\begin{bmatrix}270&0&0\\0&25&0\\0&0&40\end{bmatrix}$	5	$\begin{bmatrix}30&0&0\\0&7&0\\0&0&0\end{bmatrix}$	12

Table 7.2: Adaptive controller parameter for full model

Obviously the assessment of the MRAC controller cannot be performed in the same way as for the piecewise constant controller, due to time varying character of the adaptive system. The fact that the adaption of controller gains improves the response over time requires realistic assessment scenarios. Otherwise we would perform a worst case evaluation. As a reasonable evaluation scenario it is assumed that a maneuver is performed where the calibrated airspeed is reduced from 320kts to 200kts and the altitude from 30000ft to 5000ft as shown in Figure 7.4. The maneuver ends with a 0.1g step command at 1600s to assess the handling qualities.

We assume that the airspeed measurement is lost and the gains of the baseline control law cannot be scheduled anymore. They remain fixed for $\mathrm{V_{CAS}} = 320kts$. Due to the large changes in the flight envelope the response to pilot inputs changes and the handling qualities deteriorate. This was already discussed in Section 3.2.2 and is again shown in Figure 7.5 and Figure 7.6, where the load factor and pitch response to a 0.1g command at $\mathrm{V_{CAS}} = 200kts$ and $\mathrm{h} = 5000ft$ for the non-scheduled and the scheduled baseline control laws are shown. The associated parameter for the handling qualities are given in Table 7.3. Additionally the response of the adaptive controller after the given maneuver is assessed. Two different scenarios are

considered. On the one hand only the stated maneuver is performed by the autopilot (labeled: “w/o excitation”), and on the other hand an additional excitation in the form of low pass filtered white noise with zero mean and a standard deviation of 0.096g is added to the commanded load factor (labeled: “w/ excitation”). In Figure 7.5 and Figure 7.6 as well as in Table 7.3 it is illustrated that without excitation already a noticeable improvement in the rise time can be achieved. The response w/o excitation is almost close to the scheduled response. Although, the rise time parameter Δt is still only level 2, in Table 7.3 we can see that compared to the non-scheduled controller it is reduced by approximately half and is very close to the rise time parameter of the scheduled controller. In the case where an additional excitation is applied it can be seen that also the rise time parameter improves to level 1 so that according to the chosen parameters the overall performance is of level 1. In difference to the piecewise constant control law the time delay increases only slightly, but it is still level one. In Figure 7.5 and Figure 7.6 it can be seen that the response is even faster than the scheduled control law. This is because the reference dynamics, which the adaptive controller is trying to enforce, is the dynamics of the controlled aircraft at $\mathrm{V_{CAS}} = 320kts$. In Figure 7.7 and Figure 7.8 the evolution of the adaptive parameters is shown for the maneuver w/ and w/o excitation, respectively. It can be seen that w/o additional exaction the information in the measurements is still enough, that the estimate of the control effectiveness converges to its lower limit of $\hat{\lambda} = 0.5$. Though the other parameters do not converge, due to the lack of excitation, it could be seen that already a good response can be achieved. This is because $\hat{\lambda}$ is the most important parameter for the considered problem, and a value of 0.5 for $\hat{\lambda}$ doubles the gains of the baseline controller (see Eq.(7.5)). When additional excitation is added during the maneuver, it can be seen in Figure 7.8 that also the adaptive feedback gains and the estimation of the unmatched uncertainties converge closely to the true values.

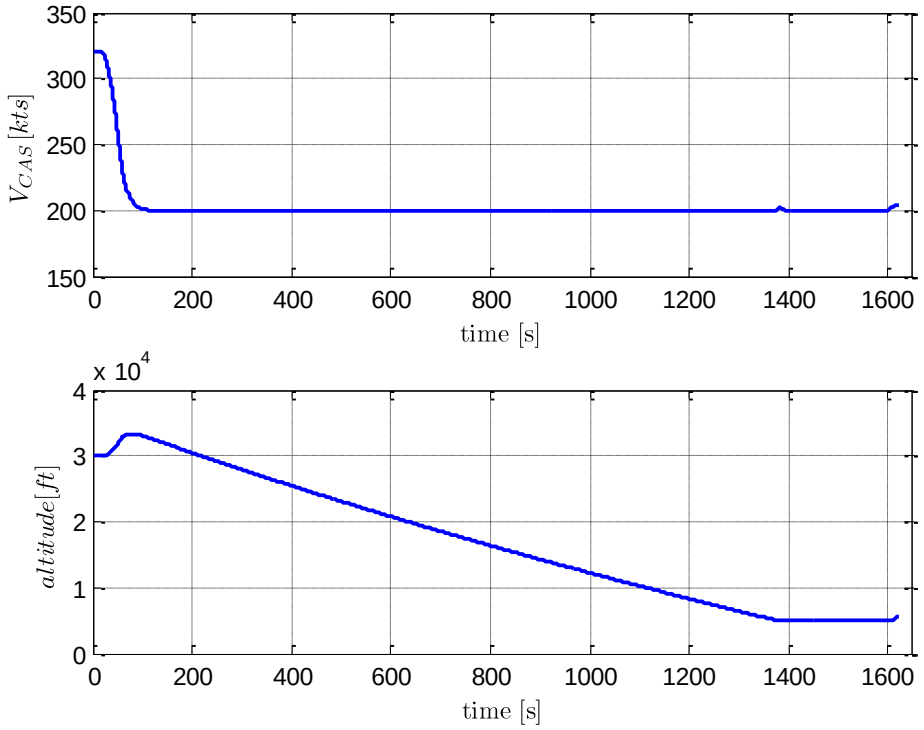

Figure 7.4: V_{CAS} and height trajectory for the example maneuver

	Overshoot		80% Rise time		Δt		t_1	
	Value	Level	Value	Level	Value	Level	Value	Level
Scheduled	4.75%	1	3.813	1	1.189	1	0.063	1
Fixed gain	9.47%	1	4.938	2	2.411	2	0.084	1
MRAC w/o excitation	3.95%	1	3.500	1	1.195	2	0.106	1
MRAC w/ excitation	1.45%	1	3.125	1	1.110	1	0.112	1

Table 7.3: HQ parameters for different controllers after maneuver

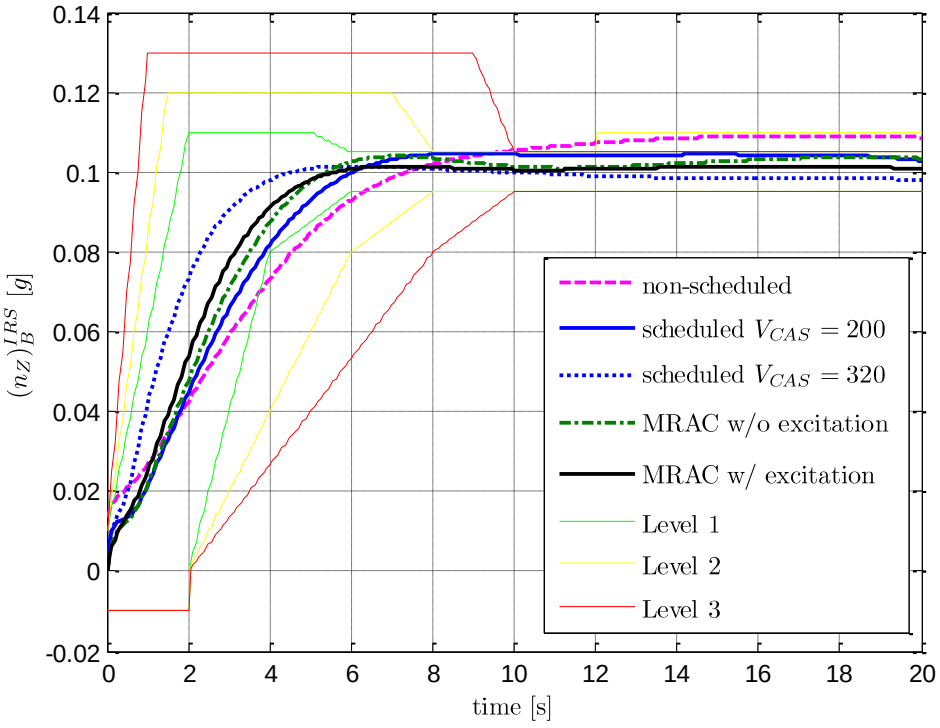

Figure 7.5: Comparison of load factor response after maneuver

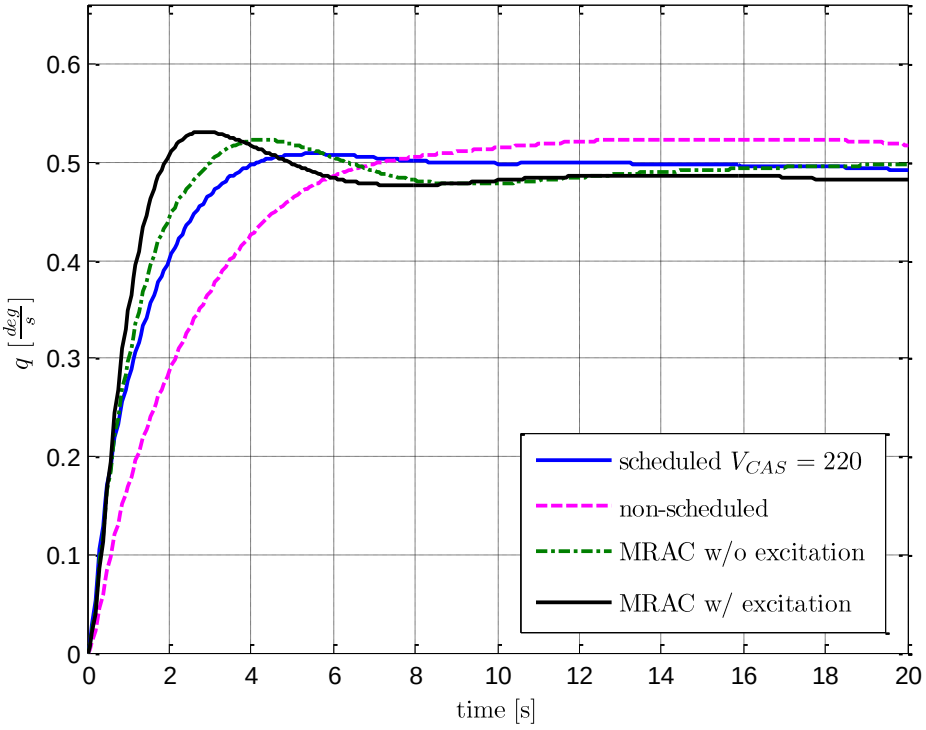

Figure 7.6: Comparison of pitch rate response after maneuver

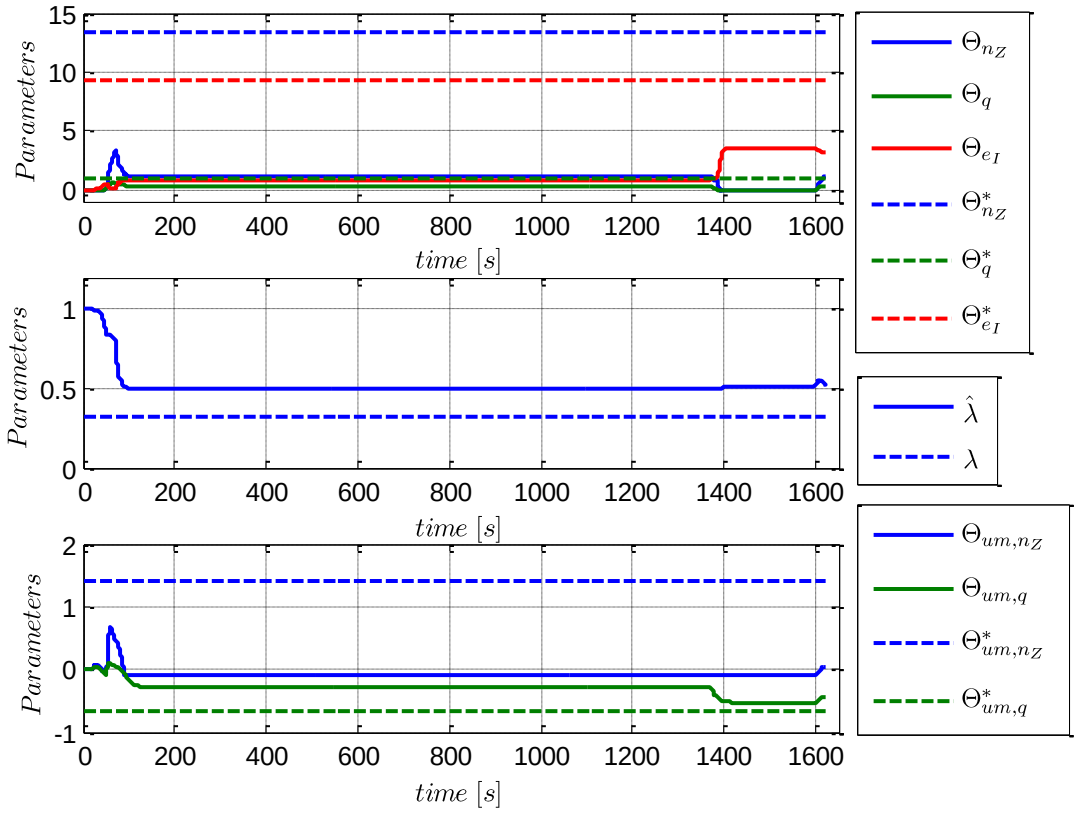

Figure 7.7: Evolution of adaptive parameters during maneuver without excitation

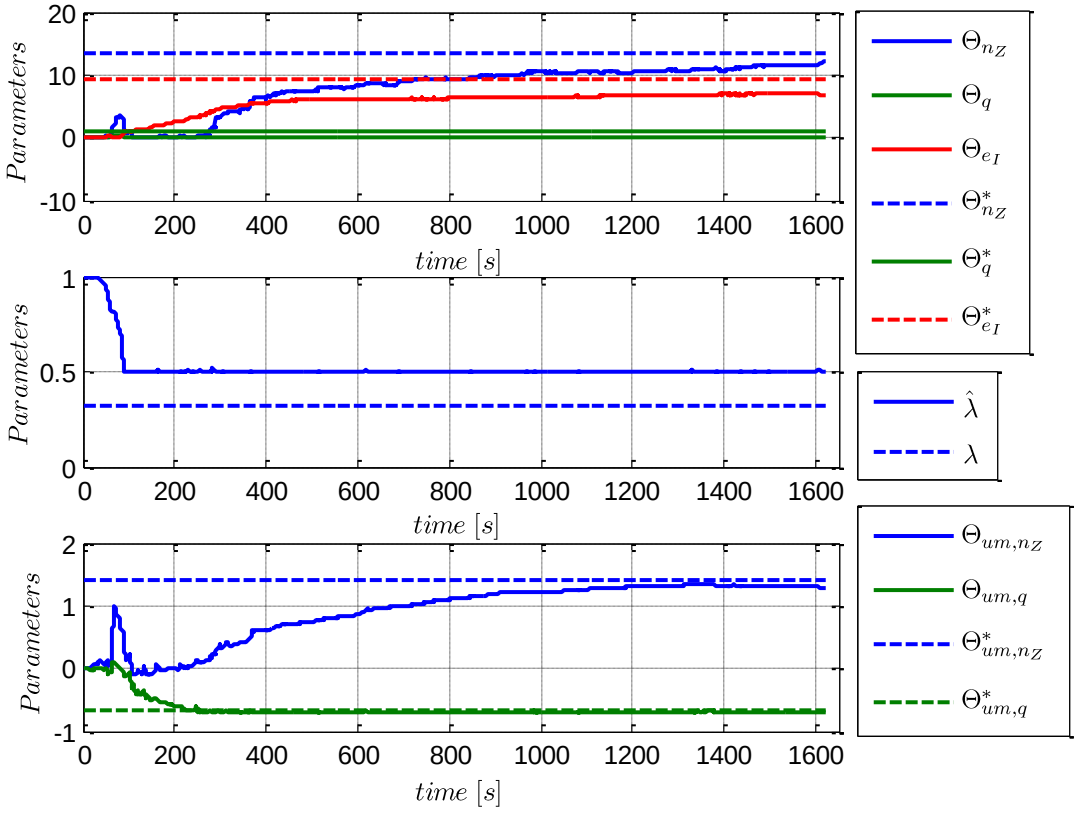

Figure 7.8: Evolution of adaptive parameters during maneuver with excitation

In Figure 7.10 a worst case assessment is shown to illustrate that the initial and transient response will not deteriorate in presence of the adaptive controller. This is important because the theory of MRAC provides no guarantees for the transient response. Therefore the handling qualities based on the initial response to a step command of 0.1g are evaluated. Again the flight envelope is gridded and the simulation starts from different trim points. The gains of the baseline controller are for all points set to the non-scheduled value of $\mathrm{V_{CAS}} = 320kts$. This means the adaptive controller had no prior time to adjust to the new dynamics. It can be seen in Figure 7.10 that the adaptive augmentation cannot improve the performance for the first step command, and it remains the same as the performance of the baseline controller shown in Figure 3.12. This however also shows that during the transient, where the parameters are adjusted, the adaptive augmentation does not deteriorate the response.

Finally the performance is evaluated after a sequence of large input commands which is shown in Figure 7.9. The assessment is again conducted for 0.1g command, which is applied at 130s.

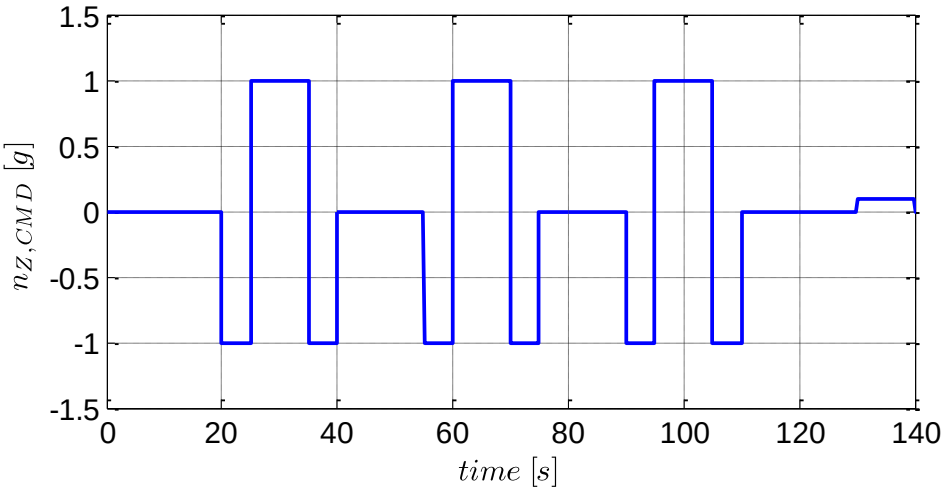

Figure 7.9: Input sequence of consecutive steps

Equally to the previous assessment, the evaluation is performed over the envelope starting from different trim conditions. The evaluation of the handling quality criteria's is shown in Figure 7.11: HQ assessment of the MRAC control law after consecutive step inputs. It can be seen that due to the large excitation the rise time criteria (based on $(n_Z)_B^{IRS}$ response) is now level 1 over the complete envelope. The rise time parameter criteria (based on q response), however is not level 1 over the complete envelope. Further, it should be noted that for low initial speeds, where it actually became level 1, the improvement is also promoted by an increase of the velocity

during the maneuver. However, if the numeric values are examined it could be seen that the rise time criteria improves over the complete envelope, even though this is not obvious in Figure 7.11: HQ assessment of the MRAC control law after consecutive step inputs. Hence, for low velocities the responsiveness improves, and this does not lead to a deterioration for the equivalent time delay, as it was seen for the piecewise constant control law. It can also be concluded that CAP becomes more homogenous. In Figure 7.12 and Figure 7.13 the response trajectories of $(n_Z)_B^{IRS}$ and q are shown for certain points, and in Figure 7.14 and Figure 7.15 the magnified trajectories for h=30000ft are displayed. Especially here it can be seen that a much more consistent load factor response is achieve for different flight speeds. Accordingly, the initial response of the pitch rate is more homogenous and the responsiveness for low speeds improves.

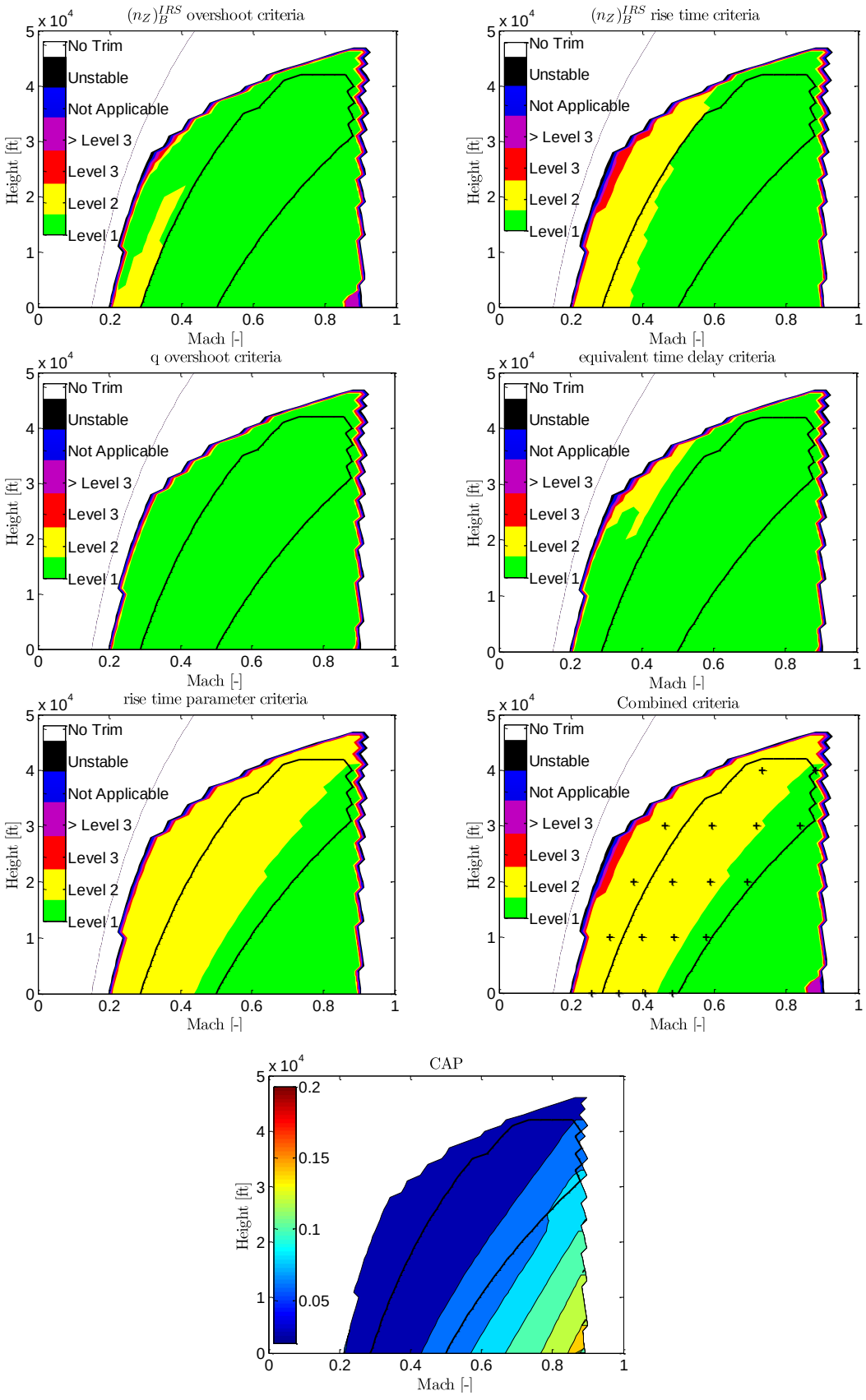

Figure 7.10: Worst case HQ assessment of the MRAC control law

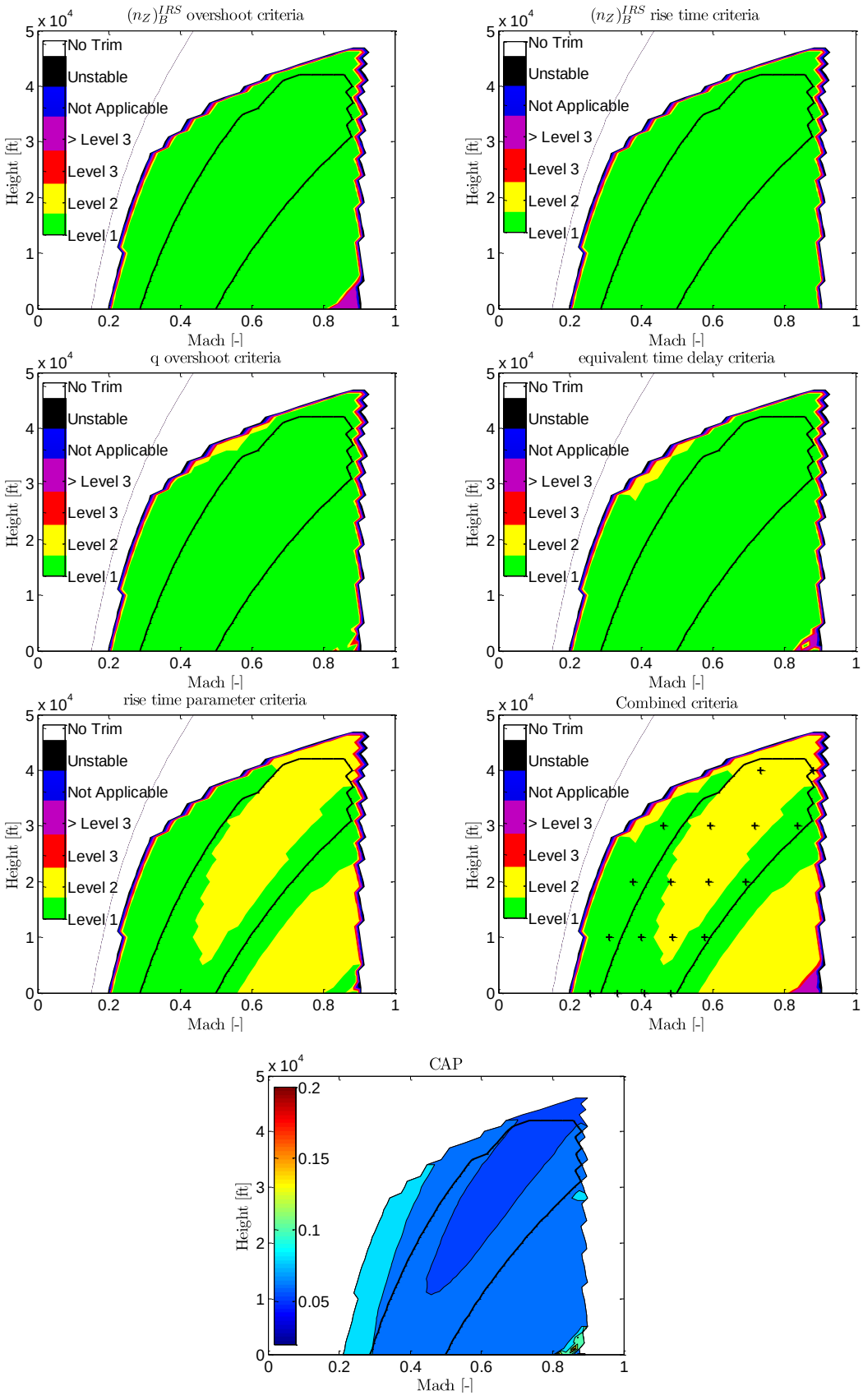

Figure 7.11: HQ assessment of the MRAC control law after consecutive step inputs

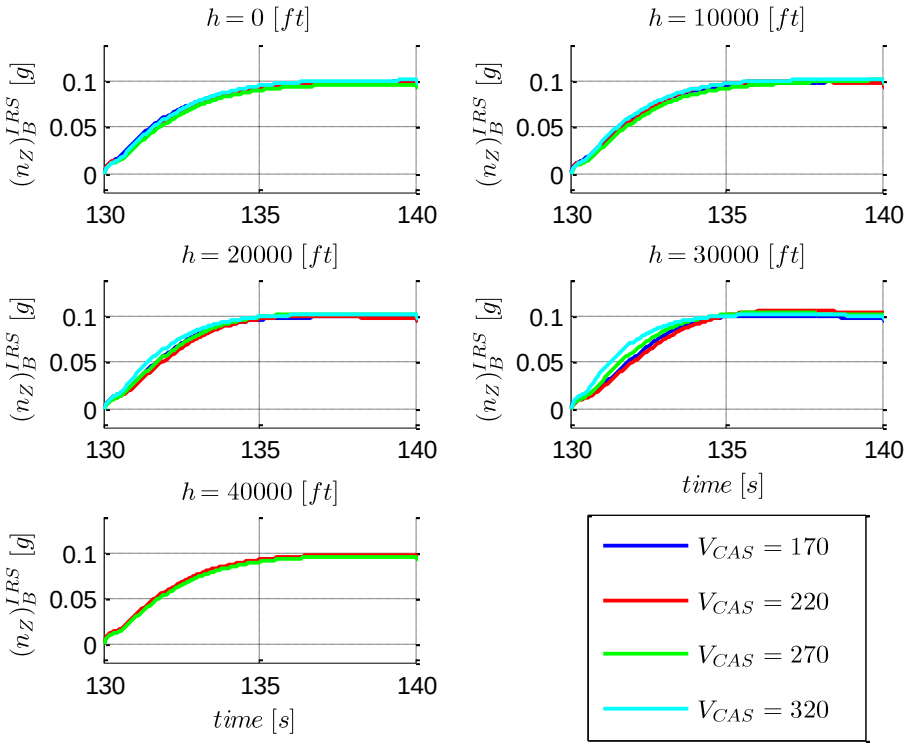

Figure 7.12: Load factor response of MRAC at different envelope points after consecutive step inputs

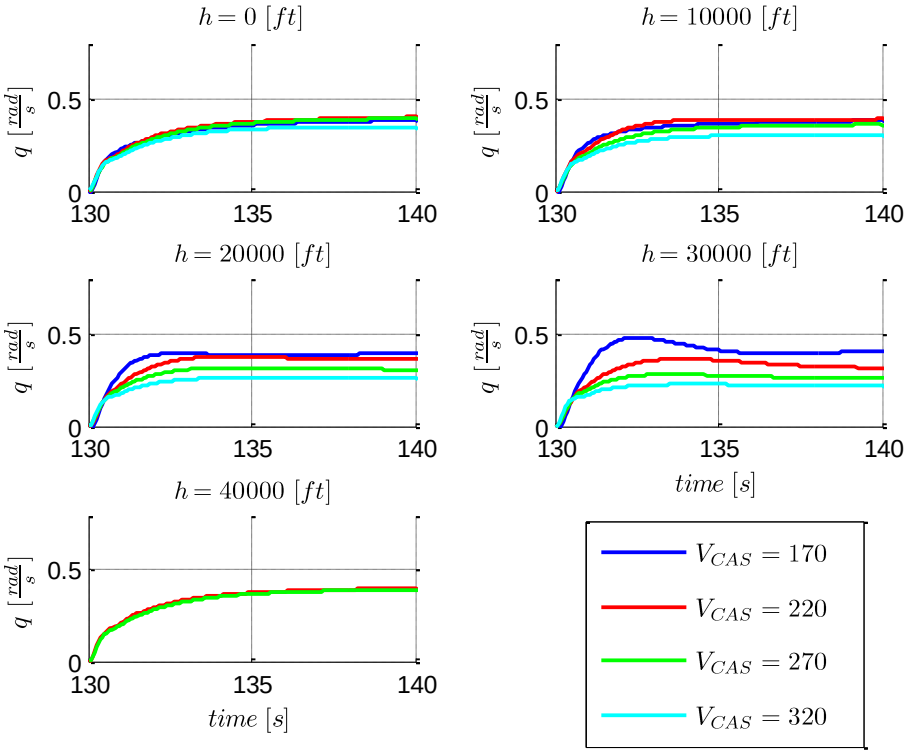

Figure 7.13: Pitch rate response of MRAC at different envelope points after consecutive step inputs

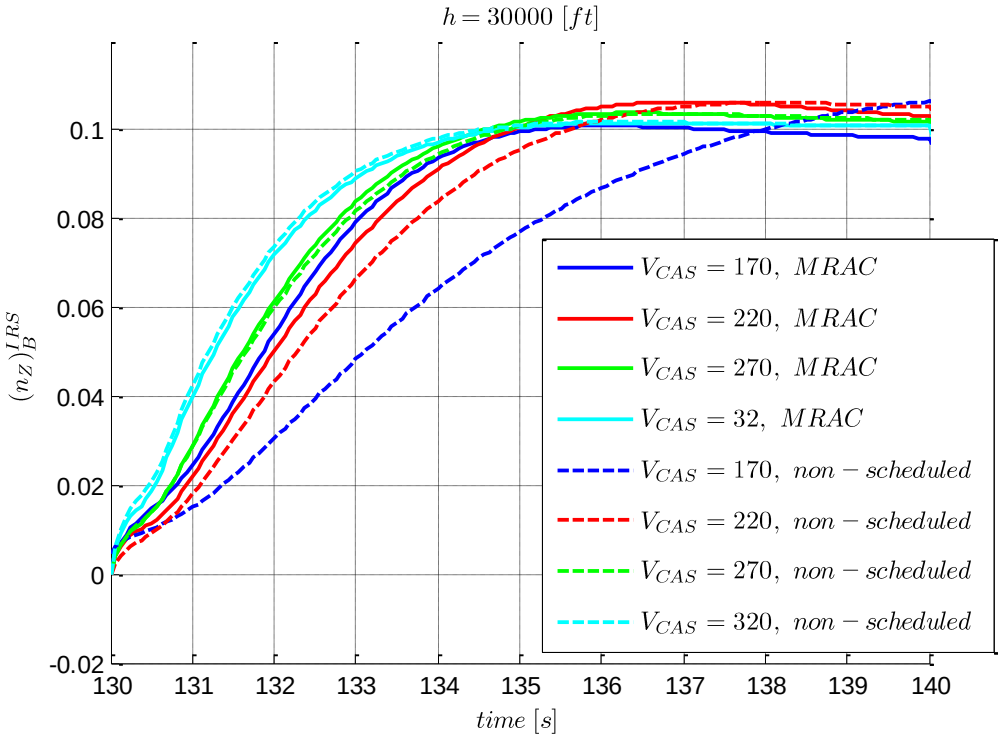

Figure 7.14: Load factor response of MRAC at h=30000ft after consecutive step inputs

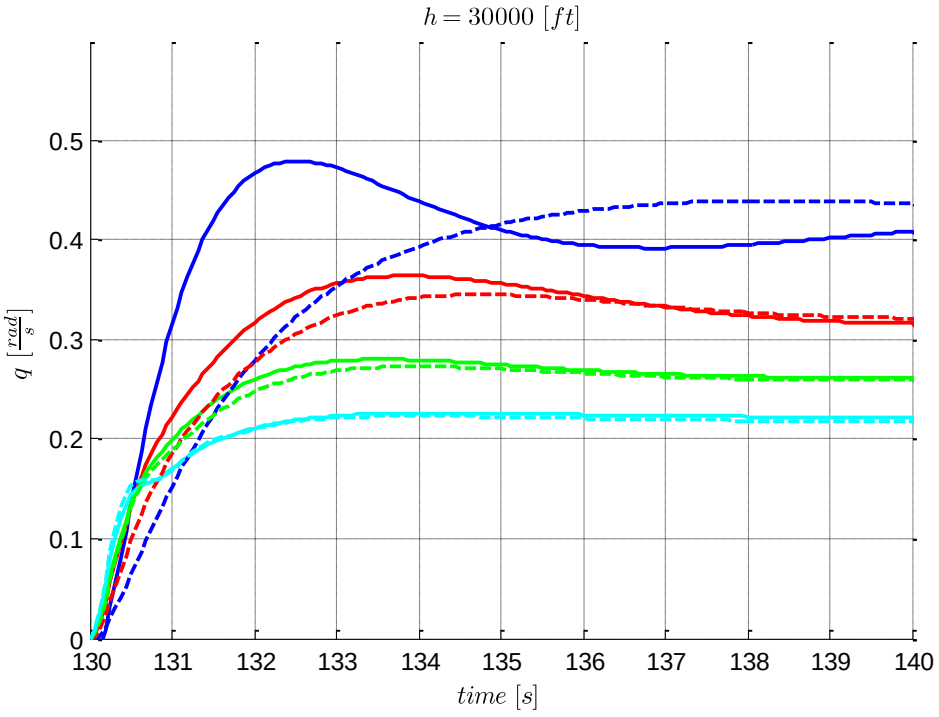

Figure 7.15: Pitch rate response of MRAC at h=30000ft after consecutive step inputs

7.3 Kalman Filter

In the previous section it was shown that an augmentation with an adaptive controller based on the MRAC approach can improve the response if the excitation of the system provides enough information. In the MRAC approach the controller gains are directly adjusted, however, as the considered problem results from a loss of the V_{CAS} measurement a quite intuitive way would be to directly estimate V_{CAS}, as it is the origin the problem. Therefore, in the following an Extended Kalman Filter (EKF) is suggested. The theory is not covered in the following but only the specific problem is presented. A theoretical introduction to Kalman filtering can for example be found in [188] [189] [158].The EKF will be based on the nonlinear system dynamics for the angle of attack and the airspeed [81]

$$\begin{aligned}\dot{\alpha} &= -\frac{L}{mV_{TAS}} - \frac{X_P \sin\alpha}{mV_{TAS}} + \frac{g}{V_{TAS}}\cos(\theta-\alpha) + q \\ \dot{V}_{TAS} &= -\frac{D}{m} + \frac{X_P \cos\alpha}{m} - g\sin(\theta-\alpha),\end{aligned} \tag{7.18}$$

where it is assumed that q and θ are measurable inputs. L is the lift force, D is the drag, and X_P is the propulsion force in direction of the x-axis of the b-frame. It is assumed that X_P is known (measurable). According to Eq.(2.17), L and D can be denoted by

$$\begin{aligned}L &= \rho \cdot V_{TAS}^2 \cdot S \cdot C_L \\ D &= \rho \cdot V_{TAS}^2 \cdot S \cdot C_D.\end{aligned} \tag{7.19}$$

So the dynamics can be written by

$$\begin{aligned}\dot{\alpha} &= -\frac{\rho \cdot V_{TAS} \cdot S}{2m} C_L - \frac{X_P \sin\alpha}{m \cdot V_{TAS}} + \frac{g}{V_{TAS}}\cos(\theta-\alpha) + q \\ \dot{V}_{TAS} &= -\frac{\rho \cdot V_{TAS}^2 \cdot S}{2m} C_D + \frac{X_P \cos\alpha}{m} - g\sin(\theta-\alpha),\end{aligned} \tag{7.20}$$

where the uncertain aerodynamic parameters are the lift coefficient C_L and the drag coefficient C_D, as they are nolinear functions of Ma and α (see Appendix B). The non-measurable states are the angle of attack α and the true airspeed V_{TAS}.

The available measurements are the accelerations at the center of gravity, and thus the measurement equations for the EKF are given by

$$\begin{aligned}(n_z)_B^{CG} &= \frac{\rho \cdot V_{TAS}^2 \cdot S}{2mg}(-C_L \cos\alpha - C_D \sin\alpha) \\ (n_x)_B^{CG} &= \frac{\rho \cdot V_{TAS}^2 \cdot S}{2mg}(C_L \sin\alpha - C_D \cos\alpha) + \frac{X_P}{mg}\end{aligned} \tag{7.21}$$

For the full nonlinear model C_L and C_D are dependent on the angle of attack and the Mach number. However, this aerodynamic model would lead to a larger number of

unknown parameters if it is used for the Kalman filter. Therefore, the following simplified aerodynamic model is used for the EKF

$$\begin{aligned} C_L &= C_{L0} + C_{L\alpha}\alpha \\ C_D &= C_{D0} + kC_L^2. \end{aligned} \tag{7.22}$$

The main uncertainties are in $C_{L\alpha}$ and k, because the uncertainties in C_{L0} and C_{D0} can be neglected. Hence, $C_{L\alpha}$ and k are the parameters which are estimated by the Kalman filter additionally to the states α and V_{TAS}. C_{L0} and C_{D0} are assumed to be constant, with $C_{L0} = 0.0154$ and $C_{D0} = 0.195$. Comparing the aerodynamic model used for the EKF with the aerodynamic model of the full nonlinear model, provided in Section 2.2 and Appendix B, the simplifications can be seen easily.

To model the uncertainties a first order Gauss Markov process [158] is assumed for $C_{L\alpha}$ and k

$$\begin{aligned} \dot{C}_{L\alpha} &= w_3 - \sigma_3 C_{L\alpha} \\ \dot{k} &= w_4 - \sigma_4 k, \end{aligned} \tag{7.23}$$

where w_3, w_4 is zero mean Gaussian white noise. $\sigma_3, \sigma_4 > 0$ are modeling parameters that limit the process variables, and the effect is similar as for the σ-modification applied in MRAC. By Eq.(7.23) the parameters $C_{L\alpha}$ and k are modeled as states of the system. Thus, the system equations for the observer of the EKF are given by replacing the real states in Eq.(7.20), Eq.(7.22), and Eq.(7.23) by the estimated states. This yields

$$\dot{\hat{\mathbf{z}}} = \begin{bmatrix} \dot{\hat{\alpha}} \\ \dot{\hat{V}}_{TAS} \\ \dot{\hat{C}}_{L\alpha} \\ \dot{\hat{k}} \end{bmatrix} = \begin{bmatrix} -\frac{\rho \cdot \hat{V}_{TAS} \cdot S}{2m}(C_{L0} + \hat{C}_{L\alpha}\hat{\alpha}) - \frac{X_P \sin\hat{\alpha}}{m \cdot \hat{V}_{TAS}} + \frac{g}{\hat{V}_{TAS}}\cos(\theta - \hat{\alpha}) + \mathrm{q} \\ -\frac{\rho \cdot \hat{V}_{TAS}^2 \cdot S}{2m}(C_{D0} + \hat{k}\hat{C}_L^2) + \frac{X_P \cos\hat{\alpha}}{m} - g\sin(\theta - \hat{\alpha}) \\ -\sigma_3 \hat{C}_{L\alpha} \\ -\sigma_4 \hat{k} \end{bmatrix} + \begin{bmatrix} w_1 \\ w_2 \\ w_3 \\ w_4 \end{bmatrix} = \mathbf{f}^*(\hat{\mathbf{z}}, u), \tag{7.24}$$

where "hat" denotes that these are estimated states. $\boldsymbol{w} = [w_1 \quad w_2 \quad w_3 \quad w_4]^T \sim (\mathbf{0}, \mathbf{Q})$ is the process noise, which is zero mean Gaussian white noise with covariance $\mathbf{Q}$.

The output-estimation equation is obtained from Eq.(7.21) and Eq.(7.22)

$$\hat{\mathbf{y}} = \begin{bmatrix} \hat{n}_Z \\ \hat{n}_x \end{bmatrix}_{\mathrm{B}}^{CG} = \begin{bmatrix} \frac{\rho \hat{V}_{TAS}^2 S}{2mg}\left(-(C_{L0} + \hat{C}_{L\alpha}\hat{\alpha})\cos\hat{\alpha} - (C_{D0} + k\hat{C}_L^2)\sin\hat{\alpha}\right) \\ \frac{\rho \hat{V}_{TAS}^2 S}{2mg}\left((C_{L0} + \hat{C}_{L\alpha}\hat{\alpha})\sin\hat{\alpha} - (C_{D0} + \hat{k}\hat{C}_L^2)\cos\hat{\alpha}\right) + \frac{X_P}{mg} \end{bmatrix} + \begin{bmatrix} \nu_1 \\ \nu_2 \end{bmatrix} = \mathbf{h}^*(\hat{\mathbf{z}}, u), \tag{7.25}$$

where $\boldsymbol{\nu} = [\nu_1 \quad \nu_2]^T \sim (\mathbf{0}, \mathbf{R})$ is the measurement noise, which is zero mean Gaussian white noise with covariance $\mathbf{R}$.

To implement the EKF a linearization of the system model Eq.(7.24) and the output equation Eq.(7.25) w.r.t. the system states, and the process and measurement noise must be obtained. The matrices obtained by this linearization are given in Eq.(7.26):

$$\mathbf{A}_{KF} = \frac{\partial \mathbf{f}^*}{\partial \hat{\mathbf{z}}} =$$

$$\begin{bmatrix} -\frac{\rho \hat{V}_{TAS} S}{2m}\frac{\partial \hat{C}_L}{\partial \hat{\alpha}} - \frac{X_P \cos\hat{\alpha}}{m\hat{V}_{TAS}} + \frac{g}{\hat{V}_{TAS}}\sin(\theta-\hat{\alpha}) & -\frac{\rho S}{2m}C_L - \frac{\rho \hat{V}_{TAS} S}{2m}\frac{\partial \hat{C}_L}{\partial \hat{V}_{TAS}} + \frac{X_P \sin\hat{\alpha}}{m\hat{V}_{TAS}^2} - \frac{g}{\hat{V}_{TAS}^2}\cos(\theta-\hat{\alpha}) & -\frac{\rho \hat{V}_{TAS} S}{2m}\hat{\alpha} & 0 \\ -\frac{\rho \hat{V}_{TAS}^2 S}{2m}\frac{\partial \hat{C}_D}{\partial \hat{\alpha}} - \frac{X_P \sin\hat{\alpha}}{m} + g\cos(\theta-\hat{\alpha}) & -\frac{\rho \hat{V}_{TAS} S}{m}\hat{C}_D - \frac{\rho \hat{V}_{TAS}^2 S}{2m}\frac{\partial \hat{C}_D}{\partial \hat{V}_{TAS}} & -\frac{\rho \hat{V}_{TAS}^2 S}{2m}2\hat{k}\hat{C}_L\hat{\alpha} & -\frac{\rho \hat{V}_{TAS}^2 S}{2m}\hat{C}_L^2 \\ 0 & 0 & -\sigma_3 & 0 \\ 0 & 0 & 0 & -\sigma_4 \end{bmatrix}$$

$$\mathbf{L}_{KF} = \frac{\partial \mathbf{f}^*}{\partial \mathbf{w}} =$$

$$\begin{bmatrix} 1 & 0 & 0 \\ 0 & \ddots & 0 \\ 0 & 0 & 1 \end{bmatrix}$$

(7.26)

$$\mathbf{C}_{KF} = \frac{\partial \mathbf{h}^*}{\partial \hat{\mathbf{z}}} =$$

$$\begin{bmatrix} \frac{\rho \hat{V}_{TAS}^2 S}{2mg}\left(\hat{C}_L\sin\hat{\alpha} - \hat{C}_D\cos\hat{\alpha} - \frac{\partial \hat{C}_L}{\partial \hat{\alpha}}\cos\hat{\alpha} - \frac{\partial \hat{C}_D}{\partial \hat{\alpha}}\sin\hat{\alpha}\right) & \frac{\rho \hat{V}_{TAS}^2 S}{2mg}\left(-\frac{\partial \hat{C}_L}{\partial \hat{V}_{TAS}}\cos\hat{\alpha} - \frac{\partial \hat{C}_D}{\partial \hat{V}_{TAS}}\sin\hat{\alpha}\right) + \frac{\rho \hat{V}_{TAS} S}{mg}\left(-\hat{C}_L\cos\hat{\alpha} - \hat{C}_D\sin\hat{\alpha}\right) & \frac{\rho \hat{V}_{TAS}^2 S}{2mg}\left(-\hat{\alpha}\cos\hat{\alpha} - 2\hat{k}\hat{C}_L\hat{\alpha}\sin\hat{\alpha}\right) & -\frac{\rho \hat{V}_{TAS}^2 S}{2mg}\hat{C}_L^2\sin\hat{\alpha} \\ \frac{\rho \hat{V}_{TAS}^2 S}{2mg}\left(\hat{C}_L\cos\hat{\alpha} + \hat{C}_D\sin\hat{\alpha} + \frac{\partial \hat{C}_L}{\partial \hat{\alpha}}\sin\hat{\alpha} - \frac{\partial \hat{C}_D}{\partial \hat{\alpha}}\cos\hat{\alpha}\right) & \frac{\rho \hat{V}_{TAS}^2 S}{2mg}\left(\frac{\partial \hat{C}_L}{\partial \hat{V}_{TAS}}\sin\hat{\alpha} - \frac{\partial \hat{C}_D}{\partial \hat{V}_{TAS}}\cos\hat{\alpha}\right) + \frac{\rho \hat{V}_{TAS} S}{mg}\left(\hat{C}_L\sin\hat{\alpha} - \hat{C}_D\cos\hat{\alpha}\right) & \frac{\rho \hat{V}_{TAS}^2 S}{2mg}\left(\hat{\alpha}\sin\hat{\alpha} - 2\hat{k}\hat{C}_L\hat{\alpha}\cos\hat{\alpha}\right) & -\frac{\rho \hat{V}_{TAS}^2 S}{2mg}\hat{C}_L^2\cos\hat{\alpha} \end{bmatrix}$$

$$\mathbf{M}_{KF} = \frac{\partial \boldsymbol{h}}{\partial \mathbf{v}} =$$

$$\begin{bmatrix} 1 & 0 & 0 \\ 0 & \ddots & 0 \\ 0 & 0 & 1 \end{bmatrix}$$

With the previous preparation a continuous time, EKF according to [188] can be implemented.

The observer is given by

$$\dot{\hat{\mathbf{z}}} = \boldsymbol{f}^*(\hat{\mathbf{z}}, \mathbf{u}) + \mathbf{K}_{KF}[\mathbf{y} - \hat{\mathbf{y}})]. \tag{7.27}$$

The Kalman gain is given by

$$\mathbf{K}_{KF} = \mathbf{P}\mathbf{C}_{KF}^T \widetilde{\mathbf{R}}^{-1}. \tag{7.28}$$

The covariance update is given by

$$\dot{\mathbf{P}} = \mathbf{A}_{KF}\mathbf{P} + \mathbf{P}\mathbf{A}_{KF}^T + \widetilde{\mathbf{Q}} - \mathbf{P}\mathbf{C}_{KF}^T \widetilde{\mathbf{R}}^{-1}\mathbf{C}_{KF}\mathbf{P}. \tag{7.29}$$

The design parameter of the system are the covariance matrices of the process noise $\widetilde{\mathbf{Q}}$ and of the measurement noise $\widetilde{\mathbf{R}}$, where $\widetilde{\mathbf{Q}} = \mathbf{L}_{KF}\mathbf{Q}\mathbf{L}_{KF}^T$ and $\widetilde{\mathbf{R}} = \mathbf{M}_{KF}\mathbf{R}\mathbf{M}_{KF}^T$. Furthermore an initial condition for the covariance $\mathbf{P}(0)$ must be chosen.

From the observer an estimation of α, V_{TAS}, $C_{L\alpha}$, and k is obtained. However, for the scheduling of the control law the calibrated airspeed V_{CAS} is needed. To calculate $\hat{V}_{CAS}$ from the estimate $\hat{V}_{TAS}$ the following equation for an inviscid, compressible flow is used

$$\hat{V}_{CAS} = a_0\sqrt{5}\sqrt{\left[\frac{p_s}{p_0}\left(\left[1 + 0.2\left(\frac{\hat{V}_{TAS}}{a_0}\right)^2\right]^{\frac{7}{2}} - 1\right) + 1\right]^{\frac{2}{7}} - 1}. \tag{7.30}$$

Hereby the subscript 0 denotes values at sea level based on the International Standard Atmosphere (ISA). a_0 is the speed of sound at sea level and p_0 is the static preassure at sea level. As p_s is the static pressure at the current altitude, and it must be either measured directly or calculated from a height measurement using the ISA model. Hence, either p_s can be measured or the altitude must be known to calculate p_s.

For evaluation, in the following a maneuver is performed by the autopilot, where the speed command is repeatedly decreasing and increasing. In Figure 7.16 the commanded speed profile is shown. The maneuver is performed at a constant height of 30000ft.

In the following three different scenarios are considered:

- 1) Simulation w/o additional excitation and w/o turbulence
- 2) Simulation w/ additional excitation and w/o turbulence
- 3) Simulation w/o additional excitation and w/ turbulence

For the second case the addition excitation is introduced by an added load factor command which is given by low pass filtered white noise with zero mean and a standard deviation of 0.096g (same as in Section 7.2). The wind velocity of the

turbulence in the third scenario is modeled by zero mean Gaussian white noise with variances $\sigma_x = 0.5\ kts$, $\sigma_y = 0.4\ kts$, and $\sigma_z = 0.1\ kts$ in the respective directions of the NED-frame. For the following simulation the initial conditions for the states α and V_{TAS} result from trim, where $\alpha(0) = 1.38\ deg$ and $V_{TAS}(0) = 254\frac{m}{s}$ ($\equiv V_{CAS}(0) = 320kts$). The initial conditions for the Kalman filter are given in Table 7.4, where for the states $\hat{\alpha}$ and $\hat{V}_{TAS}$ an offset to the real initial condition is assumed and for $\hat{C}_{L\alpha}(0)$ and $\hat{k}(0)$ reasonable assumptions are made. The design parameters for the EKF which are used in the following simulation are given in Table 7.5, where especially the covariance matrices of the process and measurement noise affect the estimation. It can be seen that the main emphasis is directed to the estimation of the parameters $\hat{V}_{TAS}$ and $\hat{C}_{L\alpha}$, as the respective values in the covariance matrices of the process noise $\widetilde{\mathbf{Q}}$ are chosen comparatively large. As the design parameters were obtained by manual tuning further room for improvement is given.

$\hat{\alpha}(0)$	$\hat{V}_{TAS}(0)$	$\hat{C}_{L\alpha}(0)$	$\hat{k}(0)$
0	$285\frac{m}{s}$ $\equiv \hat{V}_{CAS}(0) = 362kts$	2π	0.034

Table 7.4: Initial condition of the Kalman filter

$\widetilde{\mathbf{Q}}$	$\widetilde{\mathbf{R}}$	$\mathbf{P}(0)$	$\sigma_3 = \sigma_4$
$\begin{bmatrix} 0.0001 & 0 & 0 & 0 \\ 0 & 1000 & 0 & 0 \\ 0 & 0 & 2 & 0 \\ 0 & 0 & 0 & 0.001 \end{bmatrix}$	$\begin{bmatrix} 1 & 0 \\ 0 & 1 \end{bmatrix}$	$\begin{bmatrix} 0 & 0 & 0 & 0 \\ 0 & 0 & 0 & 0 \\ 0 & 0 & 0 & 0 \\ 0 & 0 & 0 & 0 \end{bmatrix}$	0.01

Table 7.5: Parameters of the Kalman filter

In Figure 7.16 and Figure 7.17 the results for the first case are shown, where in Figure 7.16 the estimation of the angle of attack and the calibrated airspeed is shown, and in Figure 7.17 the estimation of the uncertain aerodynamic parameters are displayed in from of their change w.r.t. the initial values: $\Delta\hat{C}_{L\alpha} = \hat{C}_{L\alpha}(t) - \hat{C}_{L\alpha}(0)$ and $\Delta\hat{k} = \hat{k}(t) - \hat{k}(0)$. For the angle of attack it is obvious that part of the initial offset is reduced very fast in the beginning, but especially for low speeds an offset remains. This offset is a result of the simple aerodynamic model, where C_{L0} was assumed to be constant, however in reality it is a function of Ma (see B.1.2). Moreover, it can be seen that even without additional excitation the airspeed estimation follows the real airspeed. Furthermore the initial offset of 42kts between V_{TAS} and $\hat{V}_{TAS}$ is reduced quite fast, and after 150s the difference does not exceed 6kts. For the second scenario, where

additional excitation in added is, the results are shown in Figure 7.18 and Figure 7.19. Disregarding the high frequency part for the angle of attack measurement, which is introduced by the excitation, it is obvious that the estimation shows the same characteristic as in the previous scenario, and an offset to the real value remains. For the estimation of $\hat{V}_{TAS}$, still approximately the same time is necessary to reduce the initial offset between V_{TAS} and $\hat{V}_{TAS}$. However, after the intial offset decayed, the estmation of $\hat{V}_{TAS}$ is much more accurate than in the previous example, and after 150s the error between V_{TAS} and $\hat{V}_{TAS}$ remains less than 3.2kts. The results for the third scenario, where turbulence is added to the simulation, are shown in Figure 7.20 and Figure 7.21. It can be seen that in the presence of this disturbance the states of the Kalman filter remain bounded. Furthermore, the estimation of the airspeed is basically still as good as for the case where no disturbances are present.

An evaluation based on the step response is not conducted here. If the estimation of the true air speed is correct and the calibrated air speed can be calculated correctly using the height, then using the estimated calibrated airspeed for scheduling the control law will yield level one performance. However, further evaluation for different scenarios (e.g. initial conditions, maneuvers) would be necessary, as it has to be guaranteed, that the performance cannot deteriorate compared to a robust controller with fixed gains. It should also be noted that further improvement for the EKF seems possible. This could for example be achieved by using a more realistic aerodynamic model, although this will introduce further complexity. Or, as already mentioned, more effort could be directed towards the choice of the EKF design parameters. Here a physically motivated choice of the covariance matrices of the process and measurement noise, based on the expected uncertainties and the sensor specification, seems promising.

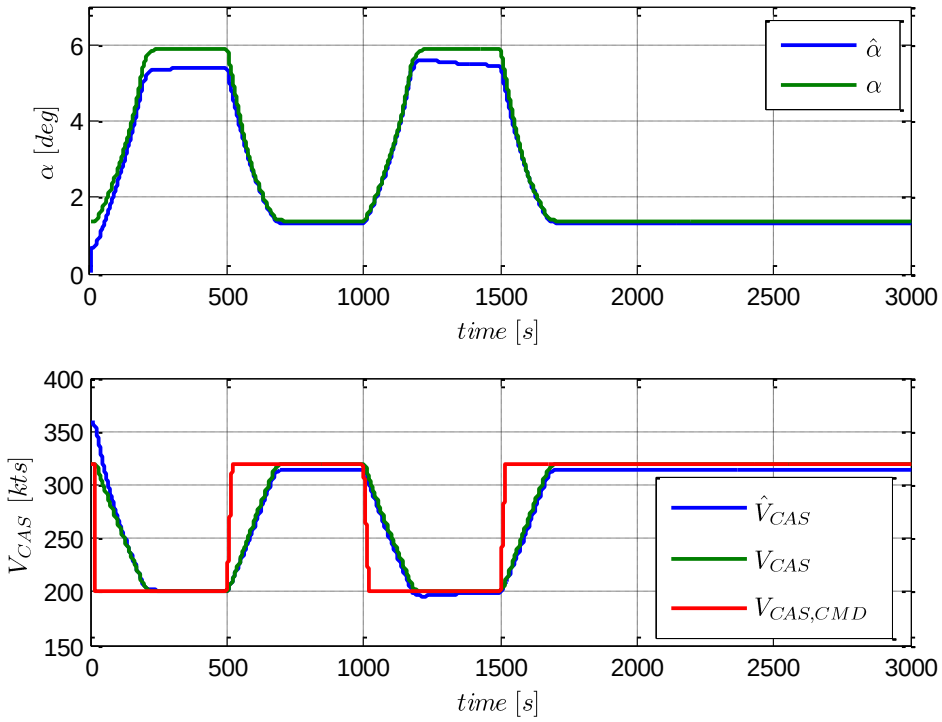

Figure 7.16: Estimated states w/o turbulence and w/o excitation

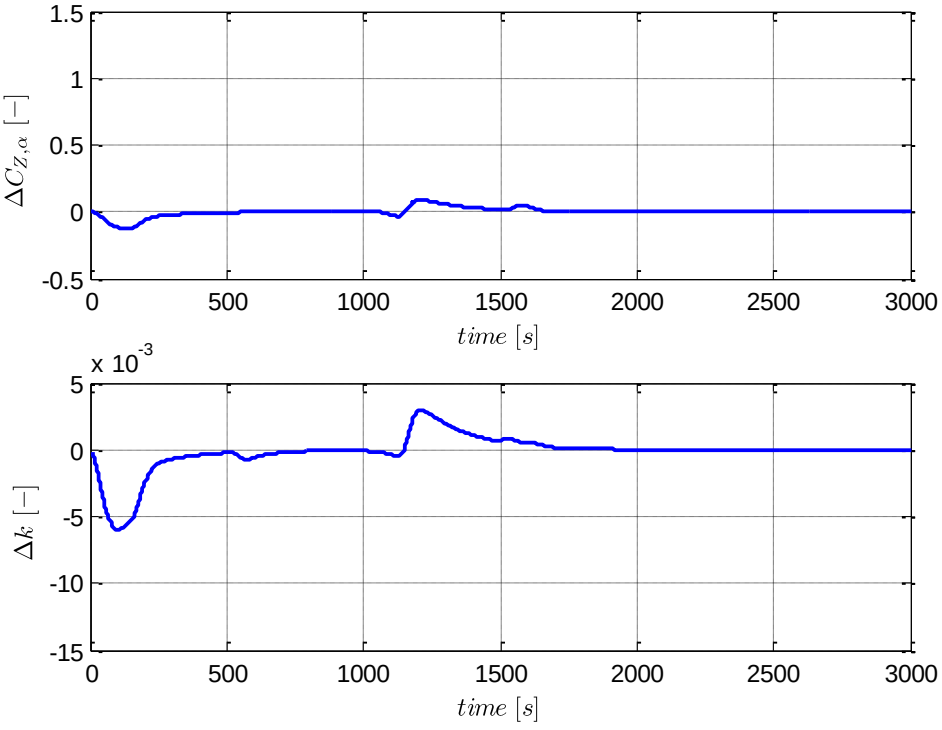

Figure 7.17: Estimated aerodynamic parameter w/o turbulence and w/o excitation

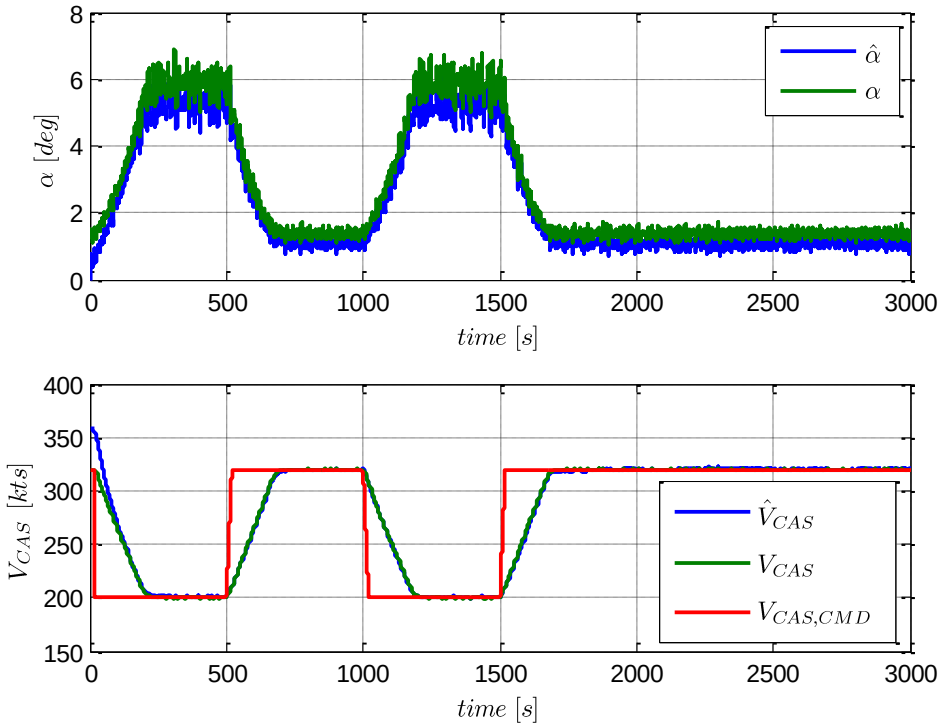

Figure 7.18: Estimated states w/o turbulence and w/ excitation

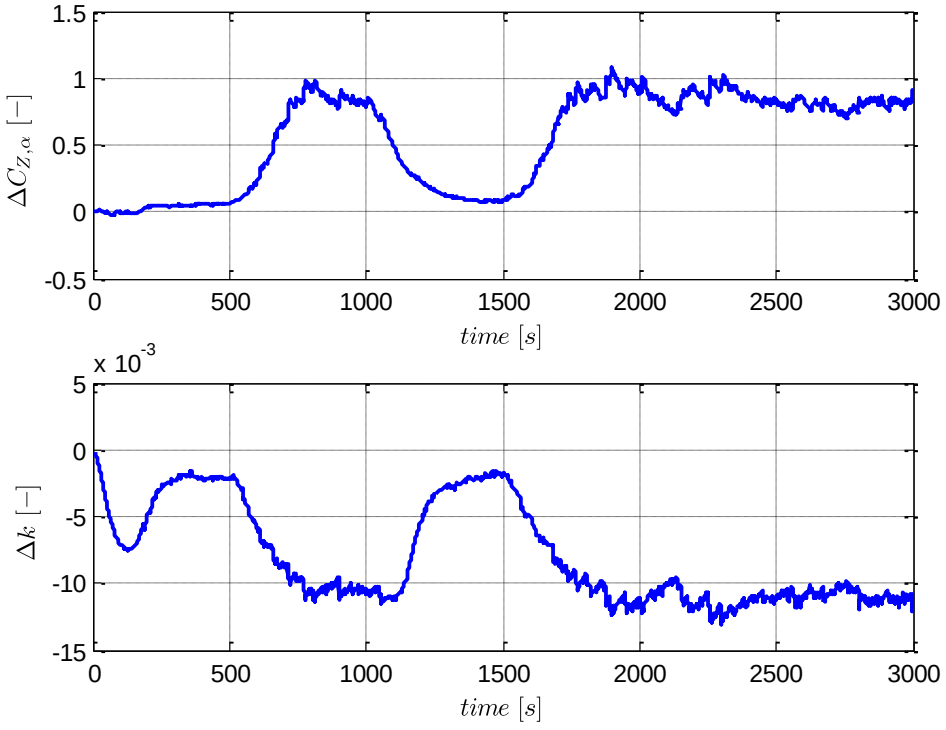

Figure 7.19: Estimated aerodynamic parameter w/o turbulence and w/ excitation

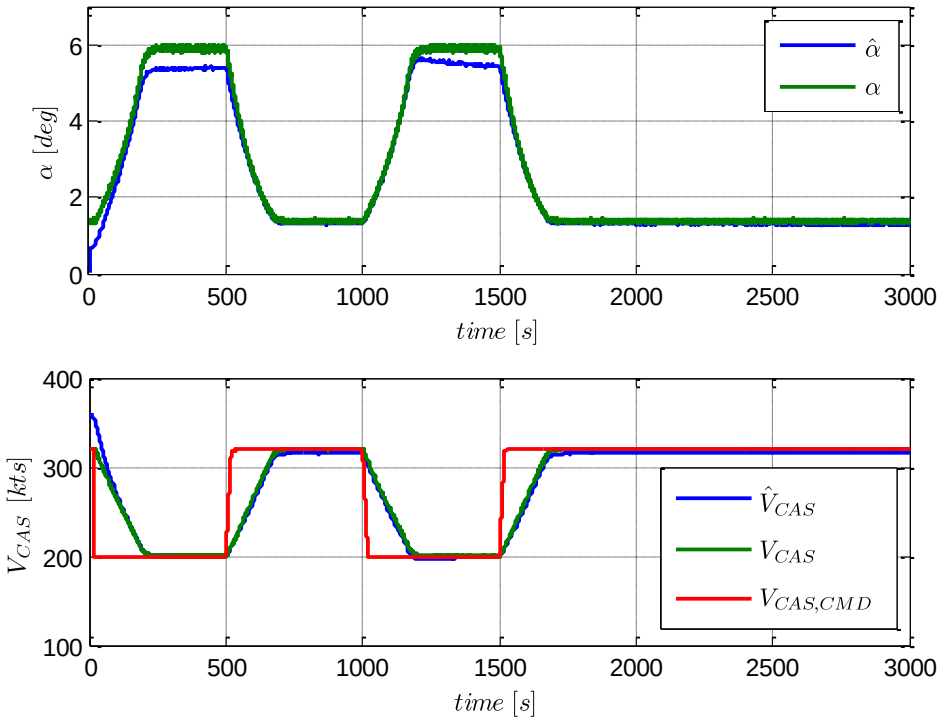

Figure 7.20: Estimated states w/ turbulence and w/o excitation

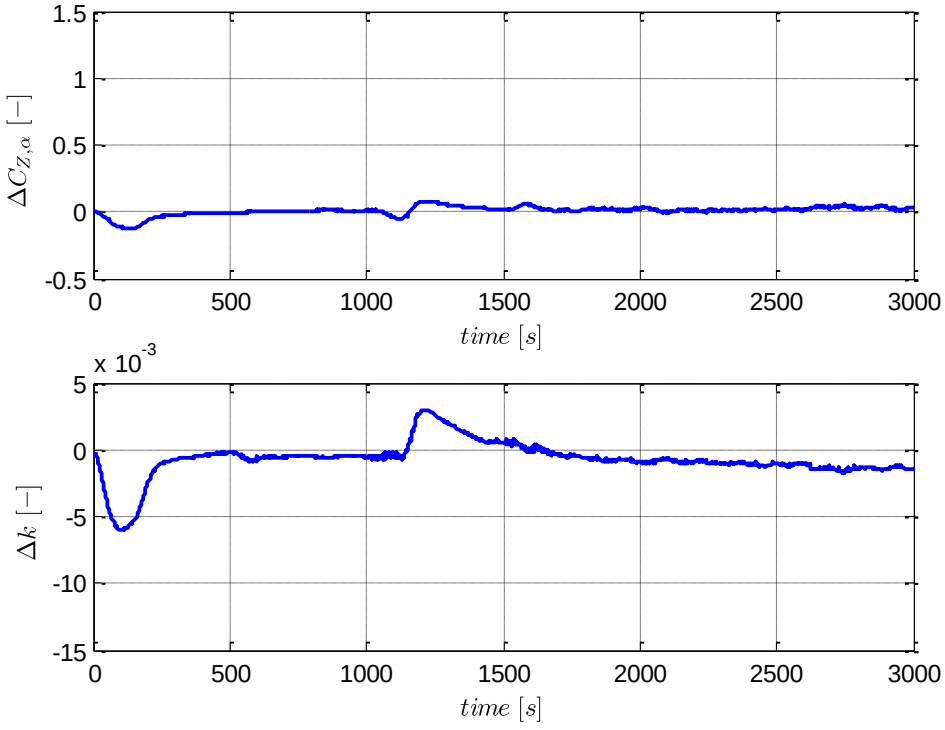

Figure 7.21: Estimated aerodynamic parameter w/ turbulence and w/o excitation

Chapter 8

Conclusions and Recommendations

8.1 Conclusions

The main contribution of this thesis was the presentation and comparison of different MRAC approaches and modification in a unified framework. From this, important conclusions can be drawn about what modifications are necessary to achieve robustness improvements compared to standard PI controllers. Here, two novel modifications of the reference model are also introduced, which are necessary to achieve the desired robust performance requirements in the presence of certain matched and unmatched parameter uncertainties. Furthermore, within the thesis it was possible to point out the similarities of hedging and $\mathcal{L}_1$ adaptive control. From a theoretical point of view it was shown that for the case where the control effectiveness is known, hedging applied for linear dynamic constraints and $\mathcal{L}_1$ adaptive control are mathematically equivalent. Thus, the theory of $\mathcal{L}_1$ adaptive control can be used to provide a stability proof for the modified reference model, which results from the application of a hedging signal. This also means that the same performance guarantees provided by $\mathcal{L}_1$ adaptive control hold. However, for the case were the control effectiveness is unknown, the $\mathcal{L}_1$ approach differs from MRAC with hedging because it is driven by the stability and performance proof and therefore applies a filter where the bandwidth is adjusted by the estimated control effectives. Although analytic performance bounds might not be available for MRAC, this does not mean that the approach provides worse performance. This could also be verified by a simulation example where both methods provide approximately the same robust performance.

For the pitch-up problem introduced in Section 2.1, at first MRAC was applied. Here it could be seen that in the presence of additional dynamics in the input channel like actuators or structural filters, the standard MRAC approach, even though it can improve the performance for a particular uncertainty, generally reduces the robust

performance. The main reason was the unmodeled dynamics from actuators, sensors and computational delay. However, it was shown that the bandwidth limitations and time delay in the input channel can either be addressed by modifying the reference model with a hedging signal or $\mathcal{L}_1$ adaptive control can be applied.

It was also seen that for the state feedback MRAC approach, the robust performance with respect to certain matched uncertainties, unmatched uncertainties and with respect to time delay can be reduced. While the loss of time delay margin is a well-known fact for MRAC and one needs to accept this tradeoff, solutions were suggested to overcome the loss of robustness regarding matched and unmatched uncertainties . These solutions are also based on a modification of the reference model. In particular, for matched uncertainties it was seen that in the presence of bandwidth limitations in the input channel (e.g. actuators or structural filters), the desired performance of the reference model can be too aggressive in certain cases. Therefore a modification of the adaptive control signal and the reference model is suggested, where the adaptive controller is not trying to compensate all system uncertainties. Instead, for a selected domain of matched uncertainties, the reference model is adjusted such that it follows the plant. For unmatched uncertainties, a very similar solution was suggested, whereby the unmatched uncertainties are estimated and this estimate is used to adjust the reference model in a way that the produced reference trajectories for the states remain achievable for the plant. In order that the reference trajectories are not only achievable but also maintain the desired characteristics, a simple, analytic, online pole placement for the reference model is suggested for the case of single input systems. Applying this modification makes the reference model an LTV system. Hence, stability can only be guaranteed by constraining the estimated unmatched uncertainties to a set that satisfies a stability condition for LTV systems. As the stability condition that was given in this thesis is only sufficient, further research could be directed toward finding less conservative conditions which are tailored to the specific application. Or the adjustment of the reference model needs to be much slower than the dynamics of the reference model, such that a time scale separation argument is valid.

Applying the suggested modification, the considered pitch-up problem could be solved satisfactorily by MRAC, while providing very good robust performance w.r.t. a general set of parametric uncertainties. But as already mentioned, a reduction of the time delay margin still has to be accepted. Applying certain robustness modifications, like σ-, e-, or optimal-modification, can improve the robust stability in terms of time delay margin. However, from the pitch-up simulation example it could be seen that these modifications concurrently reduce the performance of the adaptive controller, where for the considered problem the optimal-modification showed the best results. The application of additional update law modifications, which use additional information from an algebraic error equation, could achieve no improvement for the pitch-up problem. But for other problems, where long term learning is possible and desired, these modifications seem to be promising.

The recently suggested $\mathcal{L}_1$ piecewise constant control law was also tested for the pitch-up problem. Although the idea originates from $\mathcal{L}_1$ adaptive control, it was pointed out that in contrast with adaptive control methods, $\mathcal{L}_1$ piecewise constant control can be implemented as a linear control law. Therefore, linear assessment methods could be applied for the considered problem. Compared to MRAC, very view parameters have to be chosen, and for the problem considered, good results could also be achieved. This can be attributed to the proportional error feedback in $\mathcal{L}_1$ piecewise constant, whereas MRAC uses an integral feedback to update the controller gains. Considering the robust performance analysis of the benchmark problem, $\mathcal{L}_1$ piecewise constant control clearly improves the robustness, but compared to MRAC with the suggested modifications, it shows inferior results. Especially if enough excitation is given, MRAC clearly outperforms $\mathcal{L}_1$ piecewise constant when robust performance is considered. On the other hand, it must be noted that for the results achieved with $\mathcal{L}_1$ piecewise constant, the phase margin and time delay margin are only slightly reduced, while for MRAC a larger reduction of the time delay margin was seen.

In general it can be summarized that in the cases where fast varying uncertainties or nonlinearities, which are difficult to parameterize, are present, a model following approach like $\mathcal{L}_1$ piecewise constant with proportional error feedback seems to provide good results. Here $\mathcal{L}_1$ piecewise constant control provides some interesting novelties considering the choice of the feedback gains and the reference model design. Furthermore, due to the implementation of a reference model, the approach is physically motivated and easily traceable.

For the second problem stated, where the loss of scheduling with the calibrated airspeed was considered, different approaches are also applied. While it provided a good solution for the pitch-up problem, $\mathcal{L}_1$ piecewise constant shows some problems here, where slow changing dynamics are considered. The reason for this is that $\mathcal{L}_1$ piecewise constant only provides proportional error feedback, but the feed-forward gain is not adjusted, and although it can improve the rise time it simultaneously leads to a deterioration of the equivalent time delay.

Contrastingly for MRAC, the feed-forward gain or the control effectiveness are adjusted (dependent on the approach), and thus better performance can be achieved. However, a certain excitation of the system is necessary for the parameters/gains to converge. But even with only a small excitation, good results could be obtained and a more homogenous response is achieved. Moreover, a worst case analysis for the transient performance was conducted that showed that for the initial response, the adaptive controller does not deteriorate the performance of the baseline controller. However, the complete proof of compliance for the adaptive controller remains a challenge due to the time varying character, and a much more extensive evaluation would be necessary.

As the missing measurement for the scheduling is actually the calibrated airspeed, it also seems physically reasonable to estimate this state directly with an Extended Kalman filter. It could be seen that instead of the calibrated air speed, only the true airspeed can be estimated and the height has to be available as an additional measurement to calculate the calibrated airspeed. Further it must be noted that for the Kalman filter, the acceleration measured in the longitudinal direction is also used. If these additional measurements can be used, an excellent estimation of the calibrated airspeed could be obtained with the Kalman filter. Hence it seems to be a very good approach to account for the loss of the air speed measurement. It should also be noted that with the Kalman filter, the control signal is not augmented and the estimated airspeed is only used for scheduling in replacement of the measurement. As with MRAC, the same challenges have to be faced for the proof of compliance. Additionally, in contrast to MRAC, even under idealized assumptions, a stability proof for the closed loop is not known when the Kalman filter estimate is used to schedule the control law.

8.2 Recommendations

The results within this thesis are mainly of theoretical nature, because the evaluation of the adaptive controller is only simulation based. Although the assessment is representative in the sense that time domain criteria are used, which should theoretically guarantee good handling qualities, this cannot replace pilot in-the-loop assessments. The pilot himself is an adaptive system and therefore his interaction with the adaptive controller cannot be easily predicted. It is especially difficult to forecast how a pilot will perceive the time varying character of the adaptive controller and until today, research on this subject is very limited.

Although compared to the available literature, a quite extensive assessment of the adaptive control law was conducted, the requirements and uncertainties that are taken into account are limited to the most important ones in order to obtain a traceable comparison of different modifications. However, if an adaptive approach is intended for use on a real aircraft, the analysis need to be further extended, where especially non parametric uncertainties need to be included. It is suggested that for future research, statistically relevant uncertainties should be considered.

The statistical relevance of the expected uncertainties should already be taken into account for the tuning of the adaptive controller. In this thesis, the controller parameter design is driven only by the performance increase with respect to a particular uncertainty in combination with the constraint that the robust performance of the baseline controller should not deteriorate. However, if the probability distributions for the expected uncertainties are known, then they should be used to tune the adaptive controller in a way that is best fitted to the particular problem. In general, the parameter design for adaptive controllers is still an open question, as no

analytic methods are available to determine the controller parameters (e.g. adaptive learning rates) such that a certain performance and robustness is guaranteed. In this work, a genetic algorithm was used to optimize the controller parameter. Although very good results were achieved, the algorithm is time consuming as it is based on time domain simulation where a large number of parameters must be tested, and thus an analytic design method would still be preferable.

Due to the problem that no analytic metrics are available for adaptive controllers, the certification for vehicles operated in non-segregated airspace remains a challenge. The core of certification is to prove that the probability of a (catastrophic) failure, loss of the vehicle, or severe consequences to its passengers or the environment is below a certain threshold. For the flight control system, this means that during its operational life, the probability of a loss of function must be below a certain threshold. For conventional flight controllers, the computation of gain margin and phase margin has been considered to be an acceptable means of compliance to demonstrate the stability of the closed-loop dynamic behavior. For novel flight control strategies, it may be impossible or hard to follow the given compliance path. Hence, new certification and compliance strategies are required to prove that these systems feature at least an equivalent level of safety (ELOS) when compared to the classical process.

There have been many recent research results that address stability and performance characteristics of novel flight controllers, and they provide a good theoretical foundation. However, even though some of them seem to be very promising, until now none of the suggested metrics is accepted as a performance and robustness guarantee, which is certification relevant for real applications. Therefore future research should be directed towards the development of metrics that ensure an Equivalent Level of Safety (ELOS) when compared to the classical approach.

Past accidents and incidents proved in a dramatic manner that stabilizing a severely damaged aircraft is one challenge. Whereas past research demonstrated that this issue can successfully be addressed by adaptive control, the remaining but equally important challenge of predicting the remaining capabilities and envelope has been neglected. Flying out of the envelope where stabilization is possible makes any controller fail as a system may never be controlled beyond its physical limits (e.g. El Al Cargo LY 1862, Amsterdam 1992). Even more importantly, for UAVs less effort will be made for pilot training and no physical feedback is available to the pilot during flight. Hence, it is extremely difficult for the pilot to predict the flight envelope constraints in nominal as well as damage or failure scenarios. Additionally, in the absence of a human pilot, an autonomous onboard reaction is required under adverse conditions. Nowadays, envelope protection is a vital and well-established element of electronic flight control systems. However, envelope prediction is unavailable in flight control and protection is performed based on rigid limits determined during the development process based on nominal models and engineering data. Therefore, today's envelope protection may only protect the nominal envelope in case of vehicle integrity, but it

cannot adjust to degradations stemming from failure or damage, as no online prediction of the current capabilities of the vehicle is available. Furthermore, due to the reliance on model data (e.g. aerodynamics), classical envelope protections are often rather conservative. They limit the available maneuvering and performance capabilities to a subset with significant margins to the physical capabilities of the vehicle. Past research in envelope prediction demonstrated the basic possibilities, but with no prospect of being available for real-time applications currently. Thus, predicting a safe flight envelope under adverse conditions and utilizing it for the planning of safe continuation and return trajectories in real-time remains an open challenge.

Bibliography

[1] K. S. Narendra and A. M. Annaswamy, *Stable adaptative systems*,. Mineola, New York: Dover, 2005.

[2] P. A. Ioannou and J. Sun, *Robust adaptive control*,. Upper Saddle River, NJ: PTR Prentice-Hall, 1996.

[3] K. J. Åström and B. Wittenmark, *Adaptive control*, 2nd ed.,. Mineola, N.Y: Dover Publications, 2008.

[4] J.-J E. Slotine and Weiping Li, *Applied nonlinear control*,. Englewood Cliffs, N.J: Prentice Hall, 1991.

[5] H. Kaufman, I. Bar-Kana, and K. Sobel, *Direct adaptive control algorithms*, 2nd ed.,. New York: Springer, 1998.

[6] M. Krstić, I. Kanellakopoulos, and P. V. Kokotović, *Nonlinear and adaptive control design*,. New York: Wiley, 1995.

[7] P. C. Gregory, "Wright Air Development Center Technical Report: WADC TR 59-49," *Proceedings of the Self Adaptive Flight Control Systems*, pp. 1-3, 1959.

[8] K. J. Åström, "Adaptive control arround 1960," *IEEE Control Systems*, no. 3, pp. 44-49, 1996.

[9] B. Boskovich and R. E. Kaufmann, "Evolution of the Honeywell First-Generation Adaptive Autopilot and its Application to F-94, F-101, X-15, and X-20 Vehicles," *Journal of Aircraft*, no. 4, pp. 296-304, 1966.

[10] Staff of the Flight Research Center, *Experience with the X-15 adaptive flight control system*,. TN D-6208, Edwards, CA: NASA, Flight Research Center, 1971.

[11] D. R. Jenkins, *Hypersonics Before the Shuttle: A Concise History of the X-15 Research Airplane*,.: Monographs in Aerospace History Number 18, NASA Publication SP-2000-4518, 2000.

[12] Z. T. Dydek, A. M. Annaswamy, and E. Lavretsky, "Adaptive Control and the NASA X-15-3 Flight Revisited," *IEEE Control System Magazine*, vol. 30, no. 3, pp. 32-48, 2010.

[13] Z. T. Dydek, A. M. Annaswamy, and E. Lavretsky, "Adaptive Control and the NASA X-15 Program: A Concise History, Lessons Learned, and Provably Correct Design," *Proceedings of American Control Conference, Seattle, Washington, USA*, pp. 2957-2962, 2008.

[14] X-36 Tailless Fighter Agility Research Aircraft. [Online]. http://www.nasa.gov/centers/dryden/news/FactSheets/FS-065-DFRC.html

[15] J. S. Brinker and K. A. Wise, "Reconfigurable Flight Control of a Tailless Advanced Fighter Aircraft," *Proceedings of AIAA Guidance, Naviagtion and Control Conference, Boston, Massachusetts, USA*, 1998.

[16] K. A. Wise et al., "Direct adaptive reconfigurable flight control for a tailless advanced fighter aircraft," *International Journal of Robust and Nonlinear Control*, vol. 9, no. 14, pp. 999-1012, 1999.

[17] A. J. Calise, S. Lee, and M. Sharma, "Development of a reconfigurable flight control law for the X-36 tailless fighter aircraft," *Proceedings of AIAA Guidance, Naviagtion and Control Conference, Denver, Colorado, USA*, vol. 2000.

[18] J. Brinker and K. A. Wise, "Flight Testing of a Reconfigurable Flight Control Law on the X-36 Tailless Fighter Aircraft," *Proceedings of AIAA Guidance, Naviagtion and Control Conference, Denver, Colorado, USA*, vol. 2000.

[19] M. Sharma, "A neuro-adaptive autopilot design for guided munitions," Aeronautical Engineering, Dissertation 2001.

[20] M. Sharma, A. J. Calise, and J. Corban, "Application of an Adaptive Autopilot Design to a Family of Guided Munitions," *Proceedings of AIAA Guidance, Naviagtion and Control Conference, Denver, Colorado, USA*, 2000.

[21] M. Sharma, K. A. Wise, and E. Lavretsky, "Application and Flight Testing of an Adaptive Autopilot on Precision Guided Munitions," *Proceedings of AIAA Guidance, Naviagtion and Control Conference, Keystone, Colorado, USA*, 2006.

[22] K. A. Wise et al., "Adaptive Flight Control of a Sensor Guided Munitions," *Proceedings of AIAA Guidance, Naviagtion and Control Conference, San Francisco, California, USA*, 2005.

[23] K. A. Wise, E. Lavretsky, and N. Hovakimyan, "Verifiable Adaptive Control: UCAV and Aerial Refueling," *Proceedings of AIAA Guidance, Naviagtion and Control Conference, Honolulu, Hawaii, USA*, 2008.

[24] K. A. Wise and E. Lavretsky, "Robust and Adaptive Control of X-45A J-UCAS: A Design Trade Study," *18th IFAC World Congress, Milano, Italy*, 2011.

[25] V. V. Patel, C. Cao, N. Hovakimyan, K. A. Wise, and E. Lavretsky, "L_1 Adaptive Control for Tailless Unstable Aircraft in th Presence of Unknown Actuator Failures ," *Proceedings of AIAA Guidance, Naviagtion and Control Conference, Hilton Head, South Carolina, USA*, 2007.

[26] J. Wang, "Verifiable Adaptive Control Solutions for Flight Control Applications," Virginia Polytechnic Institute and State University, Blacksburg, VA, Dissertation 2009.

[27] C. Edwards, T. Lombaerts, and H. Smaili, *Fault Tolerant Flight Control*, Online-Ausg. ed.,. Berlin, Heidelberg: Springer-Verlag Berlin Heidelberg, 2010.

[28] T. J. J. Lombaerts, "Fault Tolerant Flight Control: A Physical Model Approach," Dissertation 2010.

[29] F-15B Intelligent Flight Control System. [Online]. http://www.nasa.gov/centers/dryden/news/FactSheets/FS-076-DFRC_prt.htm

[30] P. S. Williams-Hayes, *Flight Test Implementation of a Second Generation Intelligent Flight Control System*,. TM-2005-213669, Edwards, CA: NASA Dryden Flight Research Center, 2005.

[31] J.J Burken, P. Williams-Hayes, J. T. Kaneshige, and S. J. Stachowiak, "Adaptive Control Using Neural Network Augmentation for a Modified F-15 Aircraft," *14th Mediterranean Conference on Control and Automation, Ancona, Italy*, 2006.

[32] J. T. Bosworth and P. S. Williams-Hayes, Flight Test Results from the NF-15B Intelligent Flight Control System (IFCS) Project with Adaptation to a Simulated Stabilator Failure.

[33] Case Study: Rockwell Collins demonstrates damage tolerant flight controls and autonomous landing capabilities. [Online]. http://www.rockwellcollins.com/sitecore/content/Data/Success_Stories/DARPA_Damage_Tolerance.aspx

[34] V. Gavrilets, "Damage Tolerant Flight Control Systems for Unmanned Aircraft," *ICAS Conference, Gosier, Guadeloupe*, 2008.

[35] Integrated Resilient Aircraft Control. [Online]. http://www.nasa.gov/centers/dryden/research/FA-18_IRAC/index.html

[36] K. Krishnakumar, S. Vikien, and N. T. Nguyen, "Integrated Resilient Aircraft Control - Stability, Maneuverability, and Safe Landing in the Presence of Adverse Conditions," NASA Aeronautics Research Mission Directorate Aviation Safety, Technical Plan 2009.

[37] S. F. Campbell, J. T. Kaneshige, N. T. Nguyen, and K. S. Krishnakumar, "An Adaptive Control Simulation Study using Pilot Handling Qualities Evaluations," *Proceedings of AIAA Guidance, Naviagtion and Control Conference, Toronto, Canada, USA*, 2010.

[38] I. M. Gregory, E. Xargay, C. Cao, and N. Hovakimyan, "Flight Test of an L_1 Adaptive Controller on the NASA AirSTAR Flight Test Vehicle ," *Proceedings of AIAA Guidance, Naviagtion and Control Conference, Toronto, Canada, USA*, 2010.

[39] J. Guo and G. Tao, "A Multivariable MRAC Scheme Applied to the NASA GTM with Damage," *Proceedings of AIAA Guidance, Naviagtion and Control Conference, Toronto, Canada, USA*, 2010.

[40] J. Guo, S. Narkhede, and G. Tao, "An Adaptive LQ-Based Control Design with Parameter Projection Applied to the NASA GTM," *Proceedings of AIAA Guidance, Naviagtion and Control Conference, Toronto, Canada, USA*, 2010.

[41] Boskovic J. D., Knoebel N., and J. A. Jackson, "An Initial Study of Pilot-Adaptive Controller Interactions in Flight Control," *Proceedings of AIAA Guidance, Naviagtion and Control Conference, Toronto, Canada, USA*, 2010.

[42] L. G. Crespo, Matsutani M., J. Jang, T. E. Gibson, and A. M. Annaswamy, "Design and Verification of an Adaptive Controller for the Generic Transport Model," *Proceedings of AIAA Guidance, Naviagtion and Control Conference, Chicago, Illinois, USA*, 2009.

[43] Matsutani M., A. M. Annaswamy, and L. G. Crespo, "Application of a Novel Adaptive Reset Controller to the GTM," *Proceedings of AIAA Guidance, Naviagtion and Control Conference, Toronto, Canada*, 2010.

[44] Matsutani M., A. M. Annaswamy, and L. G. Crespo, "Adaptive Control in the Presence of Rate Saturation with Application to a Transport Aircraft Model," *Proceedings of AIAA Guidance, Naviagtion and Control Conference, Chicago, Illinois, USA*, 2009.

[45] L. G. Crespo, Matsutani M., and A. M. Annaswamy, "Design of a Model Reference Adaptive Controller for an Unmanned Air Vehicle," *Proceedings of AIAA Guidance, Naviagtion and Control Conference, Toronto, Canada, USA*, 2010.

[46] L. Ma and Y. Zhang, "Fault Detection and Diagnosis for GTM UAV with Dual Unscented Kalman Filter," *Proceedings of AIAA Guidance, Naviagtion and Control Conference, Toronto, Canada, USA*, 2010.

[47] R. Choe, E. Xargay, N. Hovakimyan, C. Cao, and I. M. Gregory, "L_1 Adaptive Control under Anomaly: Flying Qualities and Adverse Pilot Interaction ," *Proceedings of AIAA Guidance, Naviagtion and Control Conference, Toronto, Canada, USA*, 2010.

[48] T. Yucelen and A. J. Calise, "Derivative-Free Model Reference Adaptive Control of a Generic Transport Model," *Proceedings of AIAA Guidance, Naviagtion and Control Conference, Toronto, Canada, USA*, 2010.

[49] V. Stepanyan, S. Campbell, and K. Krishnakumar, "Adaptive Control of a Damaged Transport Aircraft Using M-MRAC," *Proceedings of AIAA Guidance, Naviagtion and Control Conference, Toronto, Canada, USA*, 2010.

[50] B. C. Coffer, J. B. Hoagg, and D. S. Bernstein, "Retrospective Cost Adaptive Control of the NASA GTM Model," *Proceedings of AIAA Guidance, Naviagtion and Control Conference, Toronto, Canada, USA*, 2010.

[51] I. Tuzcu and N. T. Nguyen, "Aeroelastic Modeling and Adaptive Control of GTM," *Proceedings of AIAA Guidance, Naviagtion and Control Conference, Toronto, Canada, USA*, 2010.

[52] E. Xargay et al., "L_1 Adaptive Flight Control System: Systematic Design and Verification and Validaiton of Control Metrics ," *Proceedings of AIAA Guidance, Naviagtion and Control Conference, Toronto, Canada, USA*, 2010.

[53] R. Gadient, J. Levin, and E. Lavretsky, "Comparison of Model Reference Adaptive Controller Designs Applied to the NASA Generic Transport Model," *Proceedings of AIAA Guidance, Naviagtion and Control Conference, Toronto, Canada, USA*, 2010.

[54] S.F Campbell and J.T Kaneshige, "A nonlinear dynamic inversion Predictor-Based Model Reference Adaptive Controller for a Generic Transport Model," *Proceedings of American Control Conference, Baltimore, Maryland, USA*, pp. 868-873, 2010.

[55] N. T. Nguyen and Ishihara A. K., "Robust Adaptive Optimal Control Modification with Large Adaptive Gain," *Proceedings of American Control Conference, St. Louis, Missouri, USA*, 2009.

[56] J. Guo, G. Tao, and Y. Liu, "A multivariable MRAC design for aircraft systems under failure and damage conditions," *Proceedings of American Control Conference, Portland, Oregon, USA*, pp. 600-605, 2011.

[57] T. Yucelen, N. Kim, A. J. Calise, and N. T. Nguyen, "Derivative-free output feedback adaptive control of an aeroelastic generic transport model," *Proceedings of AIAA Guidance, Naviagtion and Control Conference, Portland, Oregon, USA*, 2011.

[58] Y. Liu and L. G. Crespo, "Adaptive Control in the Presence of Actuator Failures," *Proceedings of AIAA Guidance, Naviagtion and Control Conference, Toronto, Canada, USA*, 2010.

[59] J.J Burken, N. T. Nguyen, and B. J. Griffin, "Adaptive Flight Control Design with Optimal Control Modification on an F-18 Aircraft Model," *AIAA Infotech@Aerospace Conference, Atlanta, Georgia, USA*, 2010.

[60] N. T. Nguyen, J.J Burken, and C. Hanson, "Optimal Control Modification Adaptive Law with Covariance Adaptive Gain Adjustment and Normalizat," *Proceedings of AIAA Guidance, Naviagtion and Control Conference, Portland, Oregon, USA*, 2011.

[61] N. T. Nguyen, "Optimal control modification for robust adaptive control with large adaptive gain," *Systems & Control Letters*, no. 61, pp. 485-494, 2012.

[62] C. Hanson, J. Schaefe, J.J Burken, M. Johnson, and N. T. Nguyen, "Handling Qualities Evaluations of Low Complexity Model Reference Adaptive Controllers for Reduced Pitch and Roll Damping Scenarios," *Proceedings of AIAA Guidance, Naviagtion and Control Conference, Portland, Oregon, USA*, 2011.

[63] K. A. Wise, E. Lavretsky, and N. Hovakimyan, "Adaptive Control of Flight: Theory, Application, and Open Problems," *Proceedings of American Control Conference, Minneapolis, Minnesota, USA*, 2006.

[64] V. Stepanyan, K. S. Krishnakumar, N. T. Nguyen, and L. van Eykeren, "Stability and Performance Metrics for Adaptive Flight Control," *Proceedings of AIAA Guidance, Naviagtion and Control Conference, Chicago, Illinois, USA*, 2009.

[65] M. S. Kimbrell, E. N. Johnson, G. V. Chowdhary, A. J. Calise, and R. Chandramohan, "A Process to Obtain Robustness Metrics for Adaptive Fligth Controllers," *Proceedings of AIAA Guidance, Naviagtion and Control Conference, Chicago, Illinois, USA*, 2009.

[66] A. M. Annaswamy, J. Jang, and E. Lavretsky, "Stability margins for adaptive controllers in the presence of time-delay," *Proceedings of AIAA Guidance, Naviagtion and Control Conference, Honolulu, Hawaii, USA*, 2008.

[67] Z. T. Dydek, H. Jain, J. Jang, and A. M. Annaswamy, "Theoretically Verifiable Stability Margins for an Adaptive Controller," *Proceedings of AIAA Guidance, Naviagtion and Control Conference, Keystone, Colorado, USA*, 2006.

[68] M. Schwager, H. Jain, A. M. Annaswamy, and E. Lavretsky, "Towards Verifiable Adaptive Flight Control For Safety Critical Applications," *Proceedings of AIAA Guidance, Naviagtion and Control Conference, San Francisco, California, USA*, 2005.

[69] N. T. Nguyen, Ishihara A. K., K. S. Krishnakumar, and M. Bakhtiari-Nejad, "Bounded Linear Stability Analysis - A Time Delay Margin Estimation Approach for Adaptive Control," *Proceedings of AIAA Guidance, Naviagtion and Control Conference, Chicago, Illinois, USA*, 2009.

[70] N. T. Nguyen and Boskovic J. D., "Bounded Linear Stability Margin Analysis of Nonlinear Hybrid Adaptive Control," *Proceedings of American Control Conference, Seattle, Washington, USA*, 2008.

[71] P. Seiler, A. Dorobantu, and G. Balas, "Robustness Analysis of an L_1 Adaptive Controller ," *Proceedings of AIAA Guidance, Naviagtion and Control Conference, Toronto, Canada, USA*, 2010.

[72] A. Dorobantu, P. Seiler, and G. Balas, "Nonlinear Analysis of Adaptive Flight Control Laws," *Proceedings of AIAA Guidance, Naviagtion and Control Conference, Toronto, Canada, USA*, 2010.

[73] A. K. Ishihara, S. Ben-Menahem, and N. T. Nguyen, "Time Delay Margin Computation via the Razumikhin Method for an Adaptive Control System," *Proceedings of AIAA Guidance, Naviagtion and Control Conference, Chicago, Illinois, USA*, 2009.

[74] L. G. Crespo, Matsutani M., and A. M. Annaswamy, "Verification and Tuning of an Adaptive Controller for an Unmanned Air Vehicle," *Proceedings of AIAA Guidance, Naviagtion and Control Conference, Toronto, Canada, USA*, 2010.

[75] Bong-J Yang, T. Yucelen, Jong-Y Shin, and A. J. Calise, "An LMI-based Analysis for Adaptive Flight Control with Unmodeled Input Dynamics," *Proceedings of AIAA Guidance, Naviagtion and Control Conference, Toronto, Canada, USA*, 2010.

[76] Boskovic J. D. and Knoebel N., "A Comparison Study of Several Adaptive Control Strategies for Resilent Flight Control," *Proceedings of AIAA Guidance, Naviagtion and Control Conference, Chicago, Illinois, USA*, 2009.

[77] T. Bierling, Höcht L., F. Holzapfel, R. Maier, and A. Wildschek, "Comparative Analysis of MRAC Architectures in a Unified Framework," *Proceedings of AIAA Guidance, Naviagtion and Control Conference, Toronto, Canada*, 2010.

[78] T. Bierling, L. Höcht, C. Merkl, F. Holzapfel, and R. Maier, "Similarities of Hedging and L1 Adaptive Control," *CEAS EuroGNC, Delft, Netherlands*, 2013.

[79] T. Bierling, M. Mühlegg, F. Holzapfel, and R. Maier, "Reference Model Modification for Robust Performance Conservation of Model Reference Adaptive Controllers," *Proceedings of AIAA Guidance, Naviagtion and Control Conference, Boston, Massachusetts, USA*, 2013.

[80] B. Etkin and L. D. Reid, *Dynamics of flight*, 3rd ed.,. New York: Wiley, 1996.

[81] B. L. Stevens and F. L. Lewis, *Aircraft control and simulation*, 2nd ed.,. Hoboken, NJ: John Wiley, 2003.

[82] R. Brockhaus, W. Alles, and R. Luckner, *Flugregelung*, 3rd ed.,. Berlin: Springer Berlin, 2010.

[83] J. Hodgkinson, *Aircraft handling qualities*,. Oxford: Blackwell, 1998.

[84] I. Kitsios et al., "Experimental Validation of a Metrics Driven L_1 Adaptive Control in the Presence of General Unmodeled Dynamics ," *Proceedings of AIAA Guidance, Naviagtion and Control Conference, Chicago, Illinois, USA*, 2009.

[85] Q. Sang and G. Tao, "Gain Margins of Adaptive Control Systems," *IEEE Transactions on Automatic Control*, no. 1, pp. 104-115, 2010.

[86] C. Cao et al., "Are Phase and Time-delay Margins Always Adversly Affected by High Gain," *Proceedings of AIAA Guidance, Naviagtion and Control Conference, Keystone, Colorado, USA*, 2006.

[87] G. Tao, *Adaptive control design and analysis*,. New York: IEEE Press, 2004.

[88] P. A. Ioannou and B. Fidan, *Adaptive control tutorial*,. Philadelphia, PA: Society for Industrial and Applied Mathematics, 2006.

[89] H. K. Khalil, *Nonlinear systems*, 2nd ed.,. Upper Saddle River, NJ: Prentice Hall, 1996.

[90] A. Isidori, *Nonlinear control systems*, 3rd ed.,. Berlin: Springer, 1995.

[91] Durante M. A. and K. S. Narendra, "Combined Direct and Indirect Approach to Adaptive Control," *IEEE Transactions on Automatic Control*, no. 10, pp. 1071-1075, 1989.

[92] E. Lavretsky, "Combined/Composite Model Reference Adaptive Control," *Proceedings of AIAA Guidance, Naviagtion and Control Conference, Chicago, Illinois, USA*, 2009.

[93] E. Lavretsky, R. Gadient, and I. M. Gregory, "Predictor-Based Model Reference Adaptive Control," *Proceedings of American Control Conference, St. Louis, Missouri*, 2009.

[94] E. Lavretsky, R. Gadient, and I. M. Gregory, "Predictor-Based Model Reference Adaptive Control," *Journal of Guidance, Control, and Dynamics*, no. 4, pp. 1195-1201, 2010.

[95] N. Hovakimyan and C. Cao, *L_1 adaptive control theory* ,. Philadelphia, Pa: SIAM, 2010.

[96] C. Cao and N. Hovakimyan, "Design and analysis of a novel L_1 adaptive control architecture, Part I: Guaranteed transient performance ," *Proceedings of American Control Conference, Minneapolis, Minnesota, USA*, pp. 3397-3402, 2006.

[97] C. Cao and N. Hovakimyan, "Design and Analysis of a Novel L_1 Adaptive Controller, Part II: Guaranteed Transient Performance," American Control Conference ," *Proceedings of American Control Conference, Minneapolis, Minnesota, USA*, pp. 3403-3408, 2006.

[98] C. Cao and N. Hovakimyan, "Guaranteed Transient Performance with L_1 Adaptive Controller for Systems with Unknown Time-varying Parameters and Bounded Disturbances: Part I ," *Proceedings of American Control Conference, New York City, New York, USA*, pp. 3925-3930, 2007.

[99] C. Cao and N. Hovakimyan, "Stability Margins of L_1 Adaptive Controller: Part II ," *Proceedings of American Control Conference, New York City, New York, USA*, pp. 3931-3936, 2007.

[100] C. Cao and N. Hovakimyan, "Design and Analysis of a Novel L_1 Adaptive Control Architecture With Guaranteed Transient Performance ," *IEEE Transactions on Automatic Control*, no. 53, pp. 586-591, 2008.

[101] B. S. Kim and A. J. Calise, "Nonlinear Flight Control Using Neural Networks," *Journal of Guidance, Control, and Dynamics*, vol. 1997, no. 20, pp. 26-33.

[102] R. Rysdyk and A. J. Calise, "Fault tolerant flight control via adaptive neural network augmentation," *Proceedings of AIAA Guidance, Naviagtion and Control Conference, New Orleans, Lousiana, USA*, 1998.

[103] F. L. Lewis, S. Jagannathan, and A. Yeşildirek, *Neural network control of robot manipulators and nonlinear systems,*. London: Taylor & Francis, 1999.

[104] F. Holzapfel, "Nichtlineare adaptive Regelung eines unbemannten Fluggeräts," Technische Universität München, München, Dissertation 2004.

[105] A. M. Annaswamy, F. P. Skantze, and Ai-P Loh, "Adaptive Control of Continous Time Systems with Convex/Concave Parameterization," *Automatica*, no. 34, pp. 33-49, 1998.

[106] F. P. Skantze, A. Kojić, A. P. Loh, and A. M. Annaswamy, "Adaptive estimation of discrete-timesystems with nonlinear parameterization," *Automatica*, no. 36, pp. 1879-1887, 2000.

[107] M. Netto, A. M. Annaswamy, S. Mammar, and Glaser S., "A New Adaptive Control Algorithm for Systems with Multilinear Parameterization," *Proceedings of American Control Conference, Minneapolis, Minnesota, USA*, 2006.

[108] E. Lavretsky, A. M. Annaswamy, Z. T. Dydek, and W. Vega-Brown, "On the Computation of Stability Margins for Adaptive Controllers using Linear System Tools," *Proceedings of AIAA Guidance, Naviagtion and Control Conference, Chicago, Illinois, USA*, 2009.

[109] K. Y. Volyanskyy, A. J. Calise, and Bong-J Yang, "A Novel Q-Modification Term for Adaptive Control," *Proceedings of American Control Conference, Minneapolis, Minnesota, USA*, 2006.

[110] K. Y. Volyanskyy, W. M. Haddad, and A. J. Calise, "A New Neuroadaptive Control Architecture for Nonlinear Uncertain Dynamical Systems: Beyond σ- and e- Modifications," *IEEE Transactions on Neural Networks*, 2009.

[111] T. Yucelen, A. J. Calise, W. M. Haddad, and K. Y. Volyanskyy, "A Comparison of a New Neuroadaptive Controller Architecture with the σ- and e- Modification Architectures," *Proceedings of AIAA Guidance, Naviagtion and Control Conference, Chicago, Illinois, USA*, 2009.

[112] E. N. Johnson and S.-M Oh, "Adaptive Control Using Combined Online and Background Learning Neural Network," *Proceedings of AIAA Guidance, Naviagtion and Control Conference, Providence, Rhode Island*, 2004.

[113] G. V. Chowdhary and E. N. Johnson, "Adaptive Neural Network Flight Control Using both Current and Recorded Data," *Proceedings of AIAA Guidance, Naviagtion and Control Conference, Hilton Head, South Carolina, USA*, 2007.

[114] G. V. Chowdhary, "Concurrent Learning for Convergence in Adaptive Control Without Persistency on Excitation," Georgia Institute of Technology, Atlanta, GA, Dissertation 2010.

[115] N. T. Nguyen, K. S. Krishnakumar, and J. Kaneshige, "Flight Dynamics and Hybrid Adaptive Control of Damaged Aircraft," *Journal of Guidance, Control, and Dynamics*, no. 3, pp. 751-764, 2008.

[116] N. T. Nguyen, M. Bakhtiari-Nejad, and Y. Huang, "Hybrid Adaptive Flight Control with Bounded Linear Stability Analysis," *Proceedings of AIAA Guidance, Naviagtion and Control Conference, Hilton Head, South Carolina, USA*, 2007.

[117] T. Yucelen and A. J. Calise, "A Kalman Filter Optimization Approach to Direct Adaptive Control," *Proceedings of AIAA Guidance, Naviagtion and Control Conference, Chicago, Illinois, USA*, 2009.

[118] J. Schumann, P. Gupta, and S. Nelson, "On Verification and Validation of Neural Network Based Controllers," *Proc. International Conference on Engineering Applications of Neural Networks, Malaga, Spain*, 2003.

[119] F. Peter, M. Leitão, and F. Holzapfel, "Adaptive Augmentation of a New Baseline Control Architecture for Tail-Controlled Missiles Using a Nonlinear Reference Model," *Proceedings of AIAA Guidance, Naviagtion and Control Conference, Minneapolis, Minnesota*, 2012.

[120] M. Leitão, F. Peter, and F. Holzapfel, "Adaptive Augmentation of a Fighter Aircraft Autopilot Using a Nonlinear Reference Model," *Proceedings of the EuroGNC, 2nd CEAS Specialist Conference, Delft, Netherlands*, 2013.

[121] F. Holzapfel, F. Schuck, L. Höcht, and G. Sachs, "Flight Dynamics Aspects of Path Control," *Proceedings of AIAA Guidance, Naviagtion and Control Conference, Hilton Head, South Carolina, USA*, 2007.

[122] F. Holzapfel, F. Schuck, L. Höcht, F. Kurth, and G. Sachs, "Non-Linear High Bandwidth Control of UAVs for Autonomous Mission Capability," *45th AIAA Aerospace Sciences Meeting, Reno, Nevada, USA*, 2007.

[123] S. Lorenz, "Adaptive nichtlineare Regelung zur automatisierten Flugbereichserweiterung für den Technologiedemonstrator Artis," Technische Universität Carolo-Wilhelmina zu Braunschweig, Braunschweig, Dissertation 2010.

[124] S. P. Karason and A. M. Annaswamy, "Adaptive Control in the Presences of Input Constraints," *IEEE Transactions on Automatic Control*, no. 11, pp. 2325-2330, 1994.

[125] M. Schwager, A. M. Annaswamy, and E. Lavretsky, "Adaptation-Based Reconfiguration in the Presence of Actuator Failures and Saturations," *Proceedings of American Control Conference, Portland, Oregon, USA*, pp. 2640-2645, 2005.

[126] E. N. Johnson, "Limited Authority Adaptive Flilght Control," Georgia Institute of Technology, Atlanta, GA, Dissertation 2000.

[127] E. N. Johnson, A. J. Calise, and H. A. El-Shirbiny, "Feedback linearization with neural network augmentation applied to X-33 attitude control," *Proceedings of AIAA Guidance, Naviagtion and Control Conference, Denver, Colorado, USA*, 2000.

[128] Tea-G Lee and Uk-Y Huh, "An Error Feedback Model Based Adaptive Controller for Nonlinear Systems," *IEEE Symposium on Industrial Electronics*, 1997.

[129] V. Stepanyan and K. Krishnakumar, "Input and Output Performance of M-MRAC in the Presence for Bounded Disturbances," *Proceedings of AIAA Guidance, Naviagtion and Control Conference, Toronto, Canada, USA*, 2010.

[130] E. Lavretsky, "Reference Dynamics Modification in Adaptive Controllers for Improved Transient Performance," *Proceedings of AIAA Guidance, Naviagtion and Control Conference, Portland, Oregon, USA*, 2011.

[131] S. Boyd and Sastry S. S., "Necessary and sufficient conditions for parameter convergence in adaptive control," *Automatica*, vol. 22, no. 6, pp. 629-639, 1986.

[132] R. M. Sanner and J.-J E. Slotine, "Gaussian Networks for Direct Adaptive Control," *IEEE Transactions on Neural Networks*, no. 6, pp. 837-863, 1992.

[133] Y. Shin, "Neural Network Based Adaptive Control for Nonlinear Dynamic Regimes," Georgia Institute of Technology, Atlanta, GA, Dissertation 2005.

[134] L. Sonneveldt, "Adaptive backstepping flight control for modern fighter aircraft," Dissertation 2010.

[135] E. R. van Oort, "Adaptive backstepping control and safety analysis for modern fighter aircraft," Dissertation 2011.

[136] R. Rysdyk and A. J. Calise, "Robust nonlinear adaptive flight control for consistent handling qualities," *IEEE Transactions on Control Systems Technology*, vol. 13, no. 6, pp. 896-910, 2005.

[137] R. Monopoli, "Adaptive control for systems with hard saturation," *IEEE Conference on Decision, Houston, Texas, USA*, pp. 841-843, 1975.

[138] A. M. Annaswamy and Jo-Ey Wong, "Adaptive control in the presence of saturation non-linearity," *International Journal of Adaptive Control and Signal Processing*, vol. 11, no. 1, pp. 3-19, 1997.

[139] L. G. Crespo, M. Matsutani, Jang J., T. Gibson, and A. Annaswamy, "Design and Verification of an Adaptive Controller for the Generic Transport Model," *AIAA Guidance, Navigation and Control Conference*, 2009.

[140] Matsutani M., A. M. Annaswamy, and L. G. Crespo, "Adaptive Control in the Presence of Rate Saturation with Application to a Transport Aircraft Model," *Proceedings of AIAA Guidance, Naviagtion and Control Conference, Toronto, Canada*, 2010.

[141] T. S. VanZwieten, M. J. Balas, and J. H. VanZwieten, "Adaptive Output Tracking and Disturbance Rejection with Saturation Constraints," *Proceedings of AIAA Guidance, Naviagtion and Control Conference, Honolulu, Hawaii, USA*, 2008.

[142] D. Li, N. Hovakimyan, and C. Cao, "L_1 Adaptive Controller in the Presence of Input Saturation ," *Proceedings of AIAA Guidance, Naviagtion and Control Conference, Chicago, Illinois, USA*, 2009.

[143] K. Y. Volyanskyy, W. M. Haddad, and J. M. Bailey, "Neuroadaptive Output Feedback Control for Nonlinear Nonnegative Dynamical Systems with Actuator Amplitude and Integral Constraints," *Proceedings of American Control Conference, St. Louis, Missouri*, 2009.

[144] B. Braun, "Untersuchung und Implementierung adaptiver Regelungsmethoden für Systeme mit gesättigtem Eingang," Technische Universität München, München, Semesterarbeit 2007.

[145] D. Li, V. V. Patel, C. Cao, N. Hovakimyan, and K. Wise, "Optimization of the Time-Delay Margin of L_1 Adaptive Controller via the Design of the Underlying Filter ," *Proceedings of AIAA Guidance, Naviagtion and Control Conference, Hilton Head, South Carolina, USA*, 2007.

[146] V. Stepanyan and K. Krishnakumar, "MRAC Revisited: Guaranteed Performance with Reference Model Modificaiton," *Proceedings of American Control Conference, Baltimore, Maryland, USA*, pp. 93-98, 2010.

[147] V. Stepanyan and K. Krishnakumar, "M-MRAC for Nonlinear Systems with Bounded Disturbances," *50th IEEE Conference on Decision and Control and European Control Conference, Orlando, Florida*, 2011.

[148] T. E. Gibson and A. M. Annaswamy, "Improved Transient Response in Adaptive Control Using Projection Algorithms and Closed Loop Reference Models," *Proceedings of AIAA Guidance, Naviagtion and Control Conference, Minneapolis, Minnesota*, 2012.

[149] C. Rohrs, L. Valavani, M. Athans, and G. Stein, "Robustness of continuous-time adaptive control algorithms in the presence of unmodeled dynamics," *IEEE Transactions on Automatic Control*, vol. 30, no. 9, pp. 881-889, 1985.

[150] K. J. Åström, "Analysis of Rohrs counterexamples to adaptive control," *IEEE Conference on Decision and Control, San Antonio, Texas, USA*, vol. 22, pp. 982-987, 1983.

[151] B. D. O. Anderson, "Failuers of Adaptive Control Theory and their Resolution," *Communications in Informatio and Systems*, vol. 5, no. 1, pp. 1-20, 2005.

[152] A. J. Calise, T. Yucelen, J. A. Muse, and Bong-J Yang, "A Loop Recovery Method for Adaptive Control," *Proceedings of AIAA Guidance, Naviagtion and Control Conference, Chicago, Illinois, USA*, 2009.

[153] Yucelen T. and Calise A. J. Kim K., "K-Modification based H_2 Adaptive Control ," *Proceedings of AIAA Guidance, Naviagtion and Control Conference, Toronto, Canada, USA*, 2010.

[154] T. E. Gibson, Matsutani M., A. M. Annaswamy, and L. G. Crespo, "Integral Algorithm Monitors for Adaptive Systems," *AAC/TM*, 2010.

[155] P. A. Ioannou and K. Tsakalis, "A Robust Direct Adaptive Controller," *IEEE Transactions on Automatic Control*, vol. 31, no. 11, pp. 1033-1043, 1986.

[156] K. S. Narendra and A. M. Annaswamy, "A New Adaptive Law for Robust Adaptive Control without Persistent Excitation," *IEEE Transactions on Automatic Control*, vol. 21, no. 2, 134-145.

[157] N. T. Nguyen, K. Krishnakumar, and Boskovic J., "An Optimal Control Modification to Model-Reference Adaptive Control for Fast Adaptation," *Proceedings of AIAA Guidance, Naviagtion and Control Conference, Honolulu, Hawaii, USA*, 2008.

[158] A. Gelb, *Applied optimal estimation*,. Cambridge, Mass.: M.I.T. Press, 1974.

[159] K. Y. Volyanskyy, W. M. Haddad, and A. J. Calise, "A New Neuroadaptive Control Architecture for Nonlinear Uncertain Dynamical Systems: Beyond σ- and e-Modification," *47th IEEE Conference on Decision and Control, Cancun, Mexico*, 2008.

[160] G. V. Chowdhary and E. N. Johnson, "Theory and Flight Test Validation of a Long Term Learning Adaptive Flight Controller," *Proceedings of AIAA Guidance, Naviagtion and Control Conference, Honolulu, Hawaii, USA*, 2008.

[161] G. V. Chowdhary and E. N. Johnson, "Flight Test Validation of a Neural Network based Long Term Learning Adaptive Flight Controller," *Proceedings of AIAA Guidance, Naviagtion and Control Conference, Chicago, Illinois, USA*, 2009.

[162] H. Kingravi, G. V. Chowdhary, P. Vela, and E. N. Johnson, "Reproducing Kernel Hilbert Space Approach for the Online Update of Radial Bases in Neuro-Adaptive Control," *IEEE Transactions on Neural Networks and Learning Systems*, vol. 36, no. 7, pp. 1130-1141, 2012.

[163] G. V. Chowdhary, T. Yucelen, M. Mühlegg, and E. N. Johnson, "Concurrent Learning Adaptive Control of Linear Systems with Exponentially Convergent bounds," *Wiley International Journal of Adaptive Control and Signal Processing*, vol. DOI: 10.1002/acs.2297, 2012.

[164] M. Mühlegg, G. V. Chowdhary, and E. N. Johnson, "Concurrent Learning Adaptive Control of Linear Systems with Noisy Measurements," *CEAS EuroGNC, Delft, Netherlands*, 2013.

[165] M. Filippi, "L_1 Adaptive Control and Model-Reference Adaptive Control: General Investigation and Flight Controller Implementation ," Technische Universität München, München, Diplomarbeit 2009.

[166] E. Xargay and N. Hovakimyan, "L_1 Adaptive Controller for Multi–Input Multi–Output Systems in the Presence of Nonlinear Unmatched Uncertainties ," *Proceedings of American Control Conference, Baltimore, Maryland, USA*, pp. 874-879, 2010.

[167] V. Dobrokhodov et al., "Flight validation of metrics driven L_1 adaptive control ," *Proceedings of AIAA Guidance, Naviagtion and Control Conference, Honolulu, Hawaii, USA*, 2008.

[168] I. M. Gregory, C. Cao, V. V. Patel, and N. Hovakimyan, "Adaptive control laws for flexible semi-span wind tunnel model of high-aspect ratio flying wing," *Proceedings of AIAA Guidance, Naviagtion and Control Conference, Hilton Head, South Carolina, USA*, 2007.

[169] I. Kaminer et al., "Coordinated path following for time-critical missions of multiple UAVs via L_1 adaptive output feedback controllers ," *Proceedings of AIAA Guidance, Naviagtion and Control Conference, Hilton Head, South Carolina, USA*, 2007.

[170] E. Kharisov, I. M. Gregory, C. Cao, and N. Hovakimyan, "L_1 adaptive control for flexible space launch vehicle and proposed plan for flight validation ," *Proceedings of AIAA Guidance, Naviagtion and Control Conference, Honolulu, Hawaii, USA*, 2008.

[171] Y. Lei, C. Cao, E. M. Cliff, N. Hovakimyan, and J. Kurdila, "Design of an L_1 adaptive controller for air-breathing hypersonic vehicle model in the presence of unmodeled dynamics ," *Proceedings of AIAA Guidance, Naviagtion and Control Conference, Hilton Head, South Carolina, USA*, 2007.

[172] E. Xargay, N. Hovakimyan, and C. Cao, "L_1 Adaptive Output-Feedback Controller for Non-Strictly-Positive-Real Reference Systems: Missile Longitudinal Autopilot Design ," *Journal of Guidance, Control, and Dynamics*, vol. 32, no. 9, pp. 717-726, 2009.

[173] E. Xargay, N. Hovakimyan, and C. Cao, "Benchmark problems of adaptive control revisited by L_1 adaptive control ," *17th Mediterranean Conference on Control and Automation,Thessaloniki, Greece*, pp. 31-36, 2009.

[174] C. Cao, N. Hovakimyan, and E. Lavretsky, "Application of L_1 adaptive controller to wing rock ," *Proceedings of AIAA Guidance, Naviagtion and Control Conference, Keystone, Colorado, USA*, 2006.

[175] J. A. Muse, "An H_∞ Minimization Approach for Adaptive Control ," Georgia Institute of Technology, Atlanta, GA, Dissertation 2010.

[176] J. Muse and A. Calise, "H_∞ neural network adaptive control ," *Proceedings of American Control Conference, Baltimore, Maryland, USA*, pp. 4925-4930, 2010.

[177] M. Geiser, "L_1 Adaptive Control of High Agility UAV with a Large Number of Control Devices ," Technische Universität München, München, 2010.

[178] A. Petterson, K. J. Åström, A. Robertsson, and R. Johansson, "Augmenting L_1 adaptive control of piecewise constant type to a fighter aircraft. Performance and robustness evaluation for rapid maneuvering ," *Proceedings of AIAA Guidance, Naviagtion and Control Conference, Minneapolis, Minnesota*, 2012.

[179] E. Kharisov, K. K. K. Kim, X. Wang, and N. Hovakimyan, "Limiting Behavior of L_1 Adaptive Controllers ," *Proceedings of AIAA Guidance, Naviagtion and Control Conference, Minneapolis, Minnesota*, 2012.

[180] I. M. Gregory, C. Cao, E. Xargay, N. Hovakimyan, and X. Zou, "L_1 Adaptive Control Design for NASA AirSTAR Flight Test Vehicle ," *Proceedings of AIAA Guidance, Naviagtion and Control Conference, Chicago, Illinois, USA*, 2009.

[181] Tyler J. Leman, *L1 Adaptive Control Augmentation System for the X-48B Aircraft*. Urbana, IL: Master Thesis, University of Illinois at Urbana-Champaign, 2009.

[182] G. Avanzini et al., "L_1 Adaptive Control of Flexible Aircraft: Preliminary Results ," *Proceedings of AIAA Guidance, Naviagtion and Control Conference, San Francisco, California, USA*.

[183] J. Che, I. M. Gregory, and C. Cao, "Integrated Flight/Structural Mode Control for Very Flexible Aircraft Using L_1 Adaptive Output Feedback Controller ," *Proceedings of AIAA Guidance, Naviagtion and Control Conference, Minneapolis, Minnesota*, 2012.

[184] D. Erdos, T. Shima, E. Kharisov, and N. Hovakimyan, "L_1 Adaptive Control Integrated Missile Autopilot and Guidance ," *Proceedings of AIAA Guidance, Naviagtion and Control Conference, Minneapolis, Minnesota*, 2012.

[185] F. Peter, F. Holzapfel, E. Xargay, and N. Hovakimyan, "L_1 Adaptive Augmentation of a Missile Autopilot ," *Proceedings of AIAA Guidance, Naviagtion and Control Conference, Minneapolis, Minnesota*, 2012.

[186] A. Elahidoost, J. Cooper, C. Cao, and K. Pham, "Satellite Orbit Stabilization Using L_1 Adaptive Control ," *Proceedings of AIAA Guidance, Naviagtion and Control Conference, Minneapolis, Minnesota*, 2012.

[187] C. Cao and N. Hovakimyan, "L_1 Adaptive Output-Feedback Controller for Non-Strictly-Positive-Real Reference Systems: Missile Longitudinal Autopilot Design ," *Journal of Guidance, Control, and Dynamics*, vol. 32, no. 3, 2009.

[188] Dan Simon, *Optimal state estimation*,. Hoboken, N.J: Wiley-Interscience, 2006.

[189] Jan Wendel, *Integrierte Navigationssysteme*, 2nd ed.,. München: Oldenbourg, R, 2010.

[190] Kemin Zhou, John Comstock Doyle, and K. Glover, *Robust and optimal control*,. Upper Saddle River, N.J: Prentice Hall, 1996.

Appendix A

Frequency Domain Analysis

In Figure A.1 the bode plots of the plant transfer functions from the input η_{CMD} to the filtered outputs $n_{Z,fil}$ and q_{fil} are shown. Furthermore, for feedback of the filtered outputs $n_{Z,fil}$ and q_{fil} the root locus plots are shown in Figure A.2 and Figure A.3, and the Nichols plots are shown in Figure A.4 and Figure A.5.

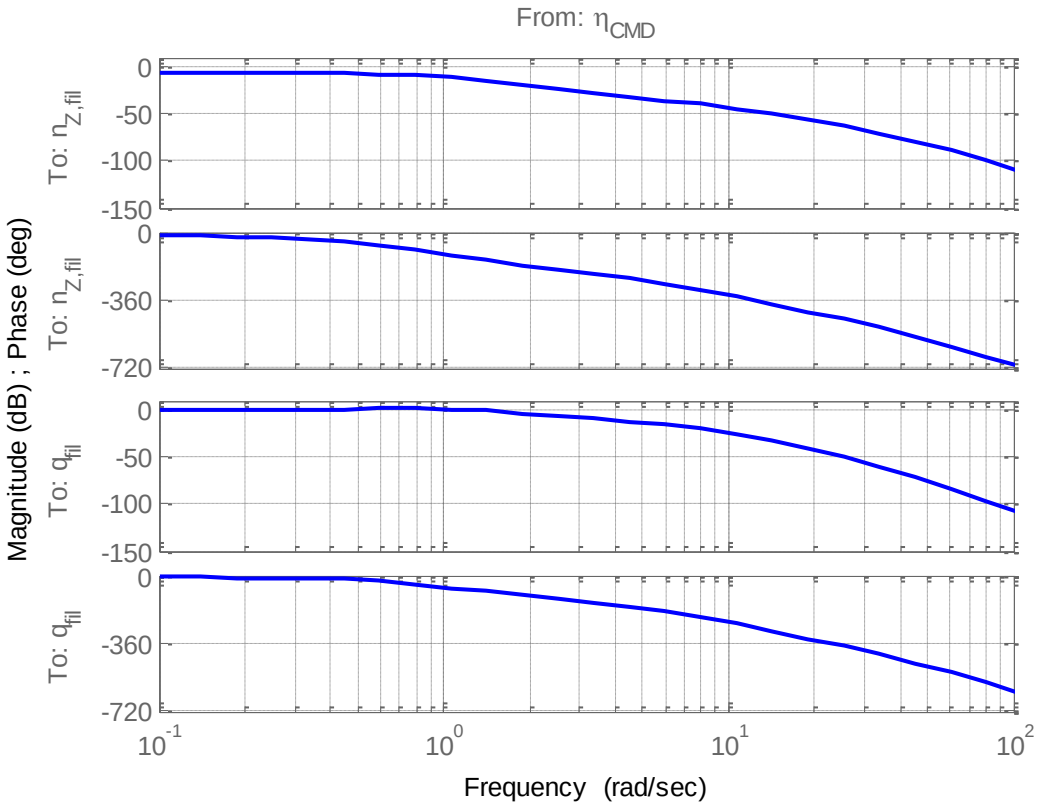

Figure A.1: Open loop bode plot of elevator transfer functions

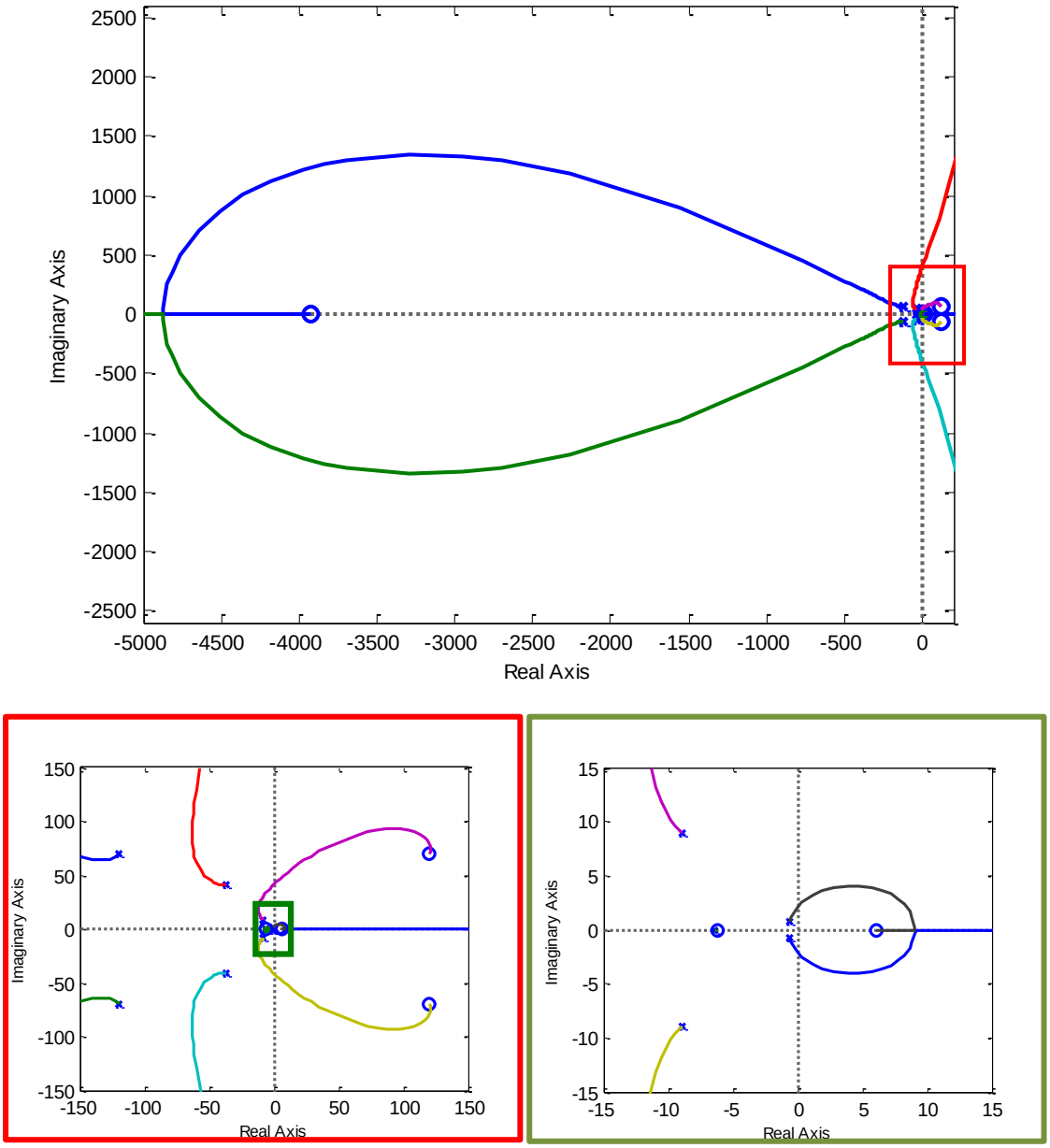

Figure A.2: Root locus from $n_{Z,fil}$ to η_{CMD}

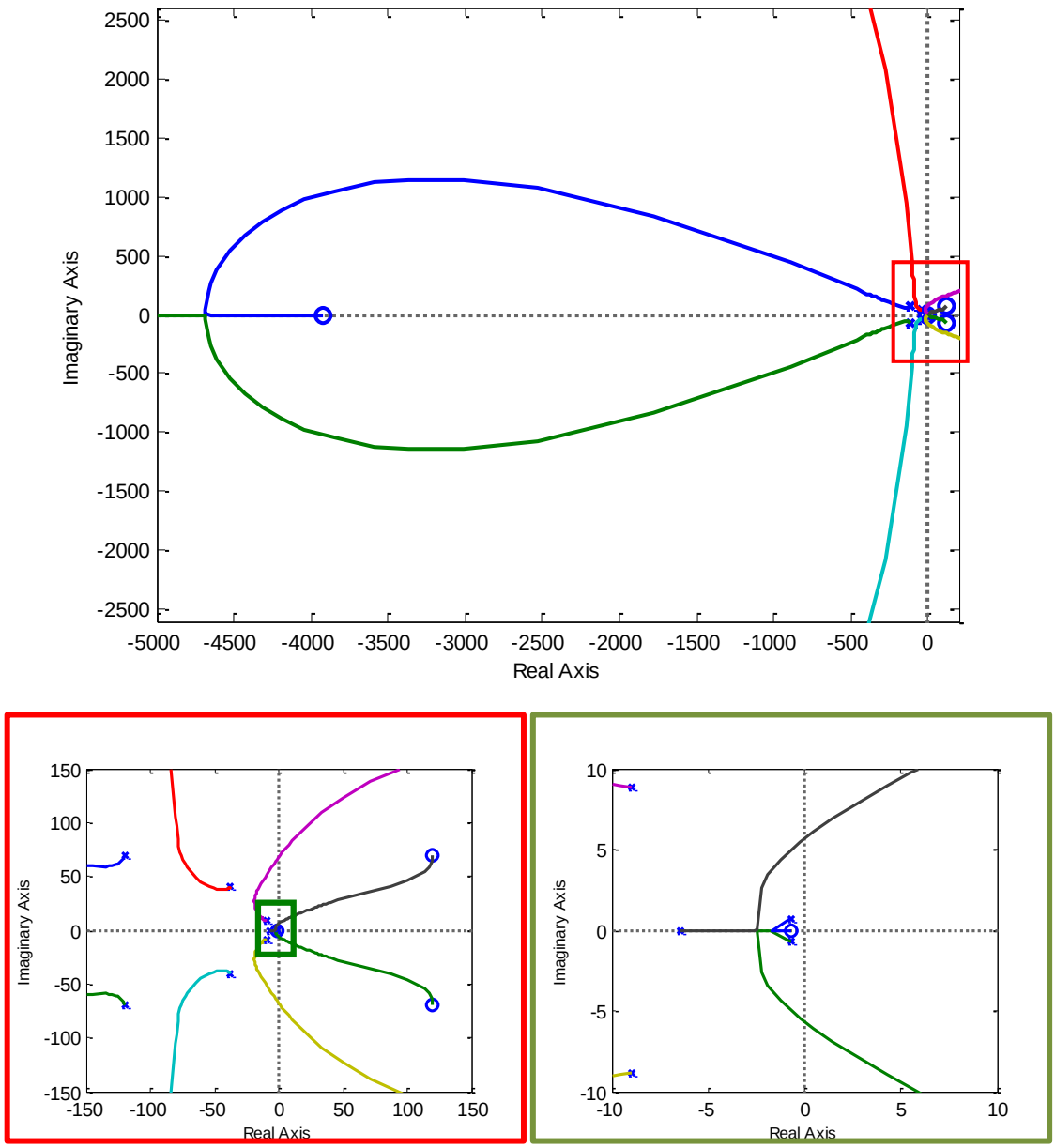

Figure A.3: Root locus from q_{fll} to η_{CMD}

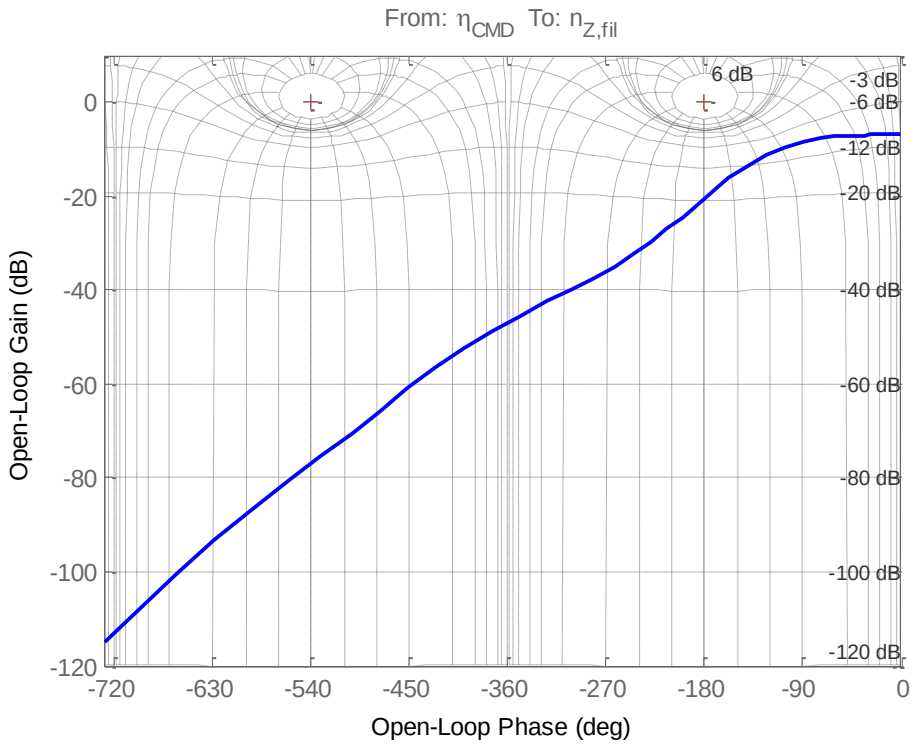

Figure A.4: Nichols plot from η_{CMD} to $n_{Z,fil}$

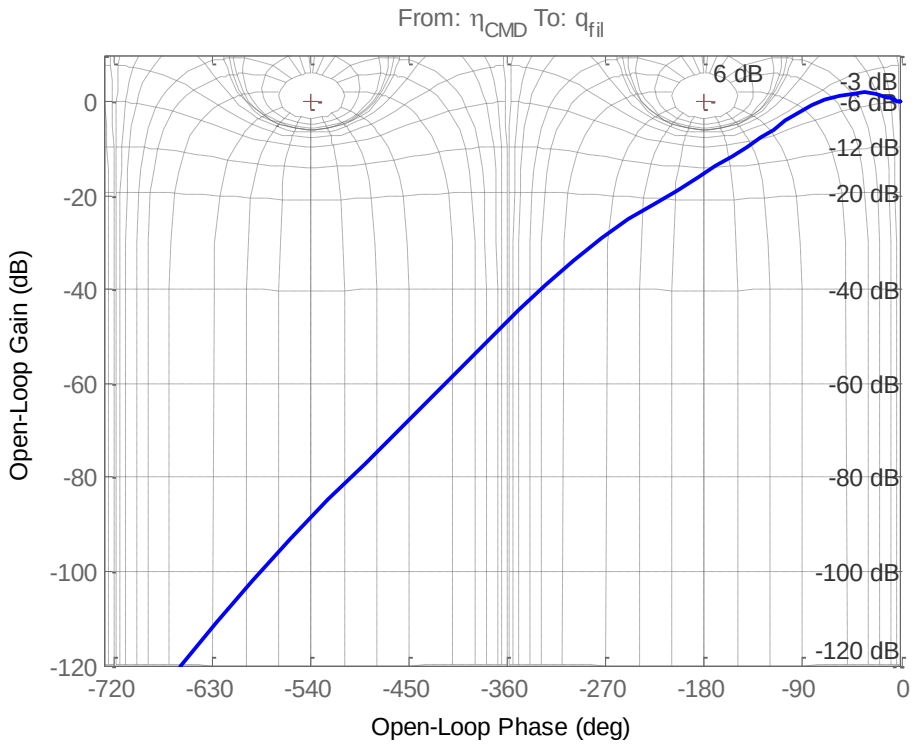

Figure A.5: Nichols plot from η_{CMD} to $q_{Z,fil}$

Appendix B

Aerodynamic Coefficients

B.1 Force Coefficients

B.1.1 Drag Coefficient C_D

The drag coefficient is dependent on α and Ma:

$$C_D(\alpha, Ma) = C_{D,0} + k \cdot C_L^2 \tag{B.1}$$

The characteristic of $C_D(\alpha, Ma)$ is shown in Figure B.1.

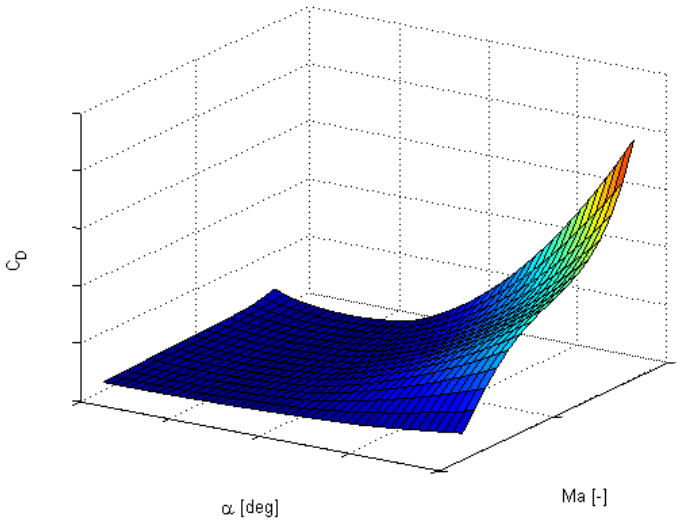

Figure B.1: Drag coefficient $C_D(\alpha,Ma)$

B.1.2 Lift Coefficient C_L

The lift coefficient is dependent on α and Ma:

$$C_L(\alpha, Ma) = C_{L,V} + C_{L,H} \tag{B.2}$$

The characteristic of $C_L(\alpha, Ma)$ is shown in Figure B.2.

$$C_{L,V} = C_{L0,V}(Ma) + C_{L\alpha,V}(Ma) \cdot \alpha \tag{B.3}$$

$C_{L,H}$ is the lift contribution of the horizontal tail and given by:

$$C_{L,H} = \frac{S_H}{S} C_{L\alpha_H,H}(Ma)\alpha_H \tag{B.4}$$

α_H is the angle of attack at the horizontal tail:

$$\alpha_H = \alpha - e + \eta + 1{,}3 \cdot q_B \cdot \frac{l_H}{V_k} \tag{B.5}$$

Where l_H is the distance between 25% of wing chord and 25% of tail chord. V_k is the Euclidian norm of the kinematic velocity, and e is the induced angle of attack/downwash.

$$e = \frac{e_0(Ma)}{57{,}3} + \varepsilon_\alpha(Ma)\alpha \tag{B.6}$$

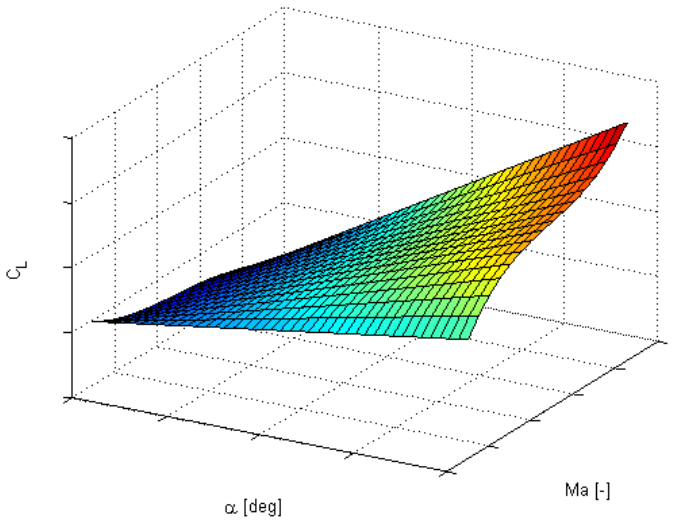

Figure B.2: Lift coefficient $C_L(\alpha,Ma)$

B.1.3 Side Force Coefficient C_Y

The side force coefficient is dependent on the aerodynamics angles, α and β, the roll and picht rate, p_B and r_B, and the rudder deflection ζ.

$$C_Y(\alpha, \beta, p_B, r_B, \delta_r) = C_{Y\beta}(\alpha) \cdot \beta + C_{Yp}(\alpha) \cdot \frac{l}{V_k} p_B + C_{Yr}(\alpha) \cdot \frac{l}{V_k} r_B + C_{Y\delta_r}(\alpha) \cdot \zeta \quad \text{(B.7)}$$

where l is the length of the reference wing chord. The characteristic of $C_Y(\alpha, \beta, p_B, r_B, \zeta)$ is shown in Figure B.3

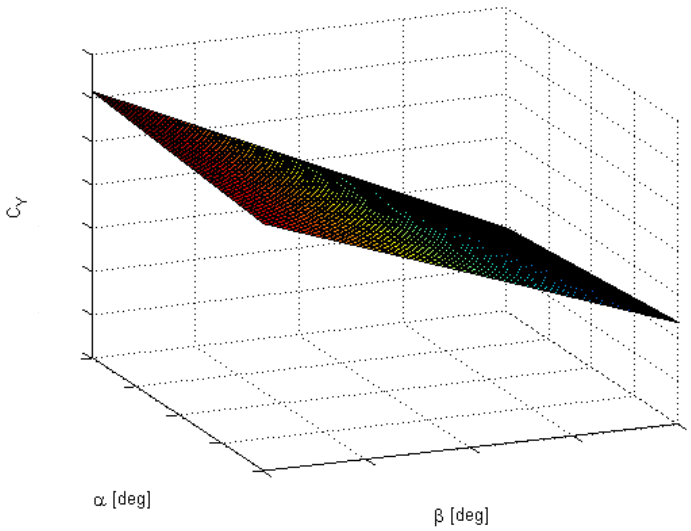

Figure B.3: Side force coefficient $C_Y(\alpha,\beta)$

B.2 Moment Coefficients

B.2.1 Pitch Moment Coefficient C_m

The pitch moment coefficient is dependent on α and Ma:

$$C_{m,aero}(\alpha, Ma) = C_{m0} - v_h \left(C_{Z\alpha_{H,H}}(Ma)(\alpha - e) \right) \quad \text{(B.8)}$$

with $v_h = \frac{S \cdot l}{S_h \cdot l_h}$. The characteristic of $C_{m,aero}(\alpha, Ma)$ is shown in Figure B.4.

The moment coefficinet that describes the pitch moment induced by agular rates is modeled by

$$\boldsymbol{C}_{m,\omega}(q) \cdot \boldsymbol{\omega}_B^{OB} = [0 \quad C_{mq} \quad 0] \cdot [p \quad q \quad r]_B^T. \quad \text{(B.9)}$$

The coefficient that models the pitch moment resulting from control surface deflections is given by

$$\boldsymbol{C}_{m,\delta}(\eta, Ma) \cdot \boldsymbol{\delta} = [0 \quad C_{m\eta}(Ma) \quad 0] \cdot [\xi \quad \eta \quad \zeta]^T \quad \text{(B.10)}$$

$C_{m\eta}(Ma)$ is shown in Figure B.5.

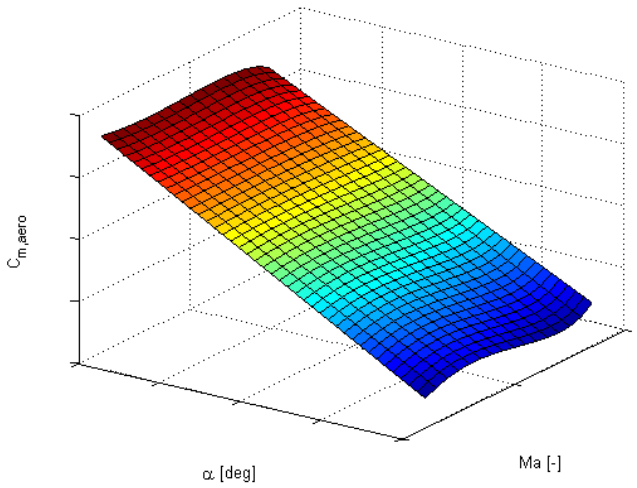

Figure B.4: Pitch momemt coefficient $C_{m,aero}(\alpha,Ma)$

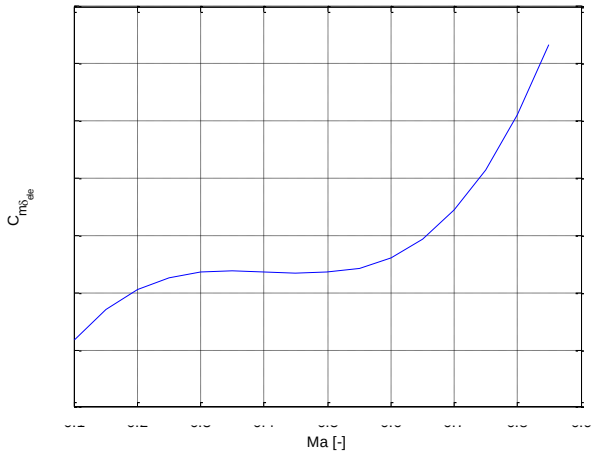

Figure B.5: $C_{m\eta}(Ma)$

B.2.2 Roll Moment Coefficient C_l

The roll moment coefficient is dependent on α and β:

$$C_{l,aero}(\beta,\alpha) = C_{l\beta}(\alpha)\cdot\beta \tag{B.11}$$

The characteristic of $C_{l,aero}(\beta,\alpha)$ is shown in Figure B.6.

The moment coefficinet that describes the roll moment induced by agular rates is modeled by

$$\boldsymbol{C}_{l,\omega}(p,r,\alpha)\cdot\boldsymbol{\omega}_B^{OB} = [C_{lp}(\alpha) \quad 0 \quad C_{lr}(\alpha)]\cdot[p \quad q \quad r]_B^T. \tag{B.12}$$

The coefficient that models the roll moment resulting from control surface deflections is given by

$$\boldsymbol{C}_{l,\delta}(\xi,\zeta,\alpha)\cdot\boldsymbol{\delta}=[C_{l\xi}\quad 0\quad C_{l\eta}(\alpha)]\cdot[\xi\quad\eta\quad\zeta]^T \tag{B.13}$$

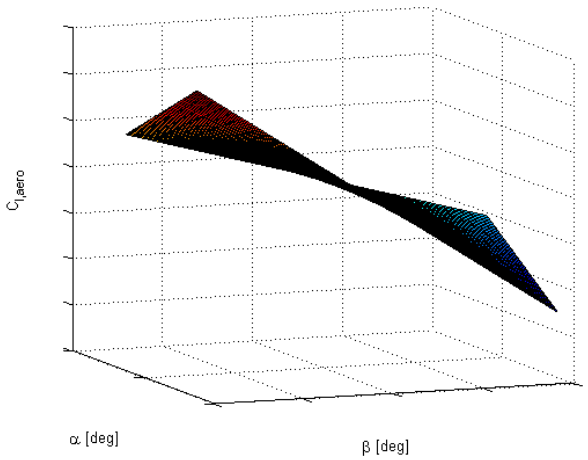

Figure B.6: Roll momemt coefficient $C_{l,aero}(\alpha,\beta)$

B.2.3 Yaw Moment Coefficient C_N

The yaw moment coefficient is dependent on α and β:

$$C_{n,aero}(\beta,\alpha)=C_{n\beta}(\alpha)\cdot\beta \tag{B.14}$$

The characteristic of $C_{n,aero}(\beta,\alpha)$ is shown in Figure B.7.

The moment coefficinet that describes the yaw moment induced by agular rates is modeled by

$$\boldsymbol{C}_{n,\omega}(p,\alpha)\cdot\boldsymbol{\omega}_B^{OB}=[C_{np}(\alpha)\quad 0\quad 0]\cdot[p\quad q\quad r]_B^T \tag{B.15}$$

The coefficient that models the yaw moment resulting from control surface deflections is given by

$$\boldsymbol{C}_{n,\delta}(\zeta,\alpha)\cdot\boldsymbol{\delta}=[0\quad 0\quad C_{n\zeta}(\alpha)]\cdot[\xi\quad\eta\quad\zeta]^T \tag{B.16}$$

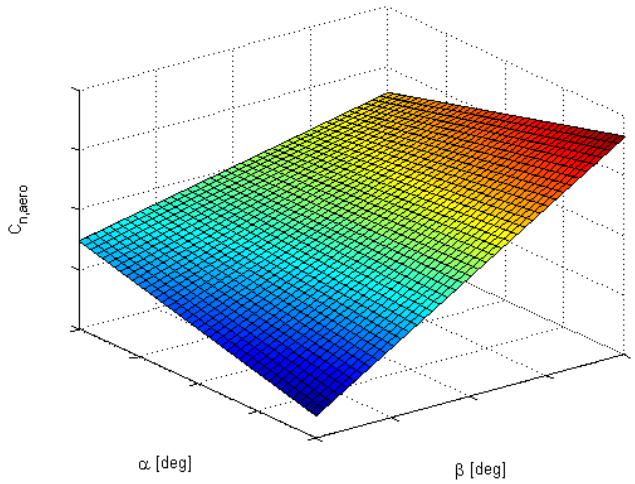

Figure B.7: Yaw momemt coefficient $C_{n,aero}(\alpha,\beta)$

Appendix C

Mathematical Definitions

C.1 Norms

The following definitions for norms and $\mathcal{L}$-stability can also be found in [89] and [95].

C.1.1 Vector Norms

In the scope of this thesis the n-dimensional Euclidean Space denoted $\mathbb{R}^n$ will be used predominantly. The Euclidean Space is a normed linear vector space, where the inner product of two vectors is defined.

In general the p-norm with $p \in [1, \infty[$ of a vector is defined by

$$\|\mathbf{x}\|_p = (|x_1|^p + \ldots + |x_n|^p)^{1/p} \tag{C.1}$$

and

$$\|\mathbf{x}\|_\infty = \max_i |x_i| \tag{C.2}$$

For the Euclidean Space the following properties are satisfied

(1) $\|\mathbf{x}\| > 0 \quad \forall\, \mathbf{x} \in \mathbb{R}^n$, with $\|\mathbf{x}\| = 0$ if and only if $\mathbf{x} = \mathbf{0}$
(2) $\|\mathbf{x} + \mathbf{y}\| \leq \|\mathbf{x}\| + \|\mathbf{y}\| \quad \forall\, \mathbf{x}, \mathbf{y} \in \mathbb{R}^n$
(3) $\|c \cdot \mathbf{x}\| = |c| \cdot \|\mathbf{x}\| \quad \forall\, c \in \mathbb{R}$ and $\mathbf{x} \in \mathbb{R}^n$

In general p-norms can be used equivalently. They are equivalent in the sense that for two different norms $\|\cdot\|_a$ and $\|\cdot\|_b$ there exist positive constants c_1 and c_2 such that

$$c_1 \cdot \|\mathbf{x}\|_a \leq \|\mathbf{x}\|_a \leq c_2 \cdot \|\mathbf{x}\|_a. \tag{C.3}$$

If no subscript is used, in the course of the thesis, $\|\cdot\|$ can be any p-norm

C.1.2 Matrix Norms

For a matrix $\mathbf{A} \in \mathbb{R}^{m \times n}$ two different kinds of norms exist: direct norms and induced norms.

C.1.2.1 Direct Matrix Norms

Direct norms are similar to vector norms and provide a "length" of the matrix by summation over all elements

$$\|\mathbf{A}\|_p = \left(\sum_{i=1}^{m} \sum_{j=1}^{n} |a_{ij}|^p \right)^{1/\mathrm{p}}, \tag{C.4}$$

with $p \in [1, \infty]$.

The most commonly used case is the Frobenius norm for $p = 2$

$$\|\mathbf{A}\|_2 = \|\mathbf{A}\|_F = \sqrt{\left(\sum_{i=1}^{m} \sum_{j=1}^{n} |a_{ij}|^2 \right)} = \sqrt{\mathrm{tr}[\mathbf{A}^H \mathbf{A}]}, \tag{C.5}$$

where $\mathbf{A}^H$ is the conjugate complex of $\mathbf{A}$, and the trace operator $\mathrm{tr}[\bullet]$ is defined for a square matrix $\mathbf{B} \in \mathbb{R}^{n \times n}$ by the sum over its diagonal elements:

$$\mathrm{tr}[\mathbf{B}] = \sum_{i=1}^{n} b_{ii}\,. \tag{C.6}$$

C.1.2.2 Induced Matrix Norms

If $\mathbf{A}$ is considered to be an operator that performs a mapping $\mathbf{A}: \mathbb{R}^n \to \mathbb{R}^m$ between two vector spaces

$$\mathbf{y} = \mathbf{A}\mathbf{x}, \tag{C.7}$$

then the induce matrix norm relates the length of an element in the definition range $\mathbb{R}^n$ to its length in the image range $\mathbb{R}^m$. The induced matrix norm is defined by

$$\|\mathbf{A}\|_{p,i} = \sup_{\mathbf{x} \neq \mathbf{0}} \frac{\|\mathbf{A}\mathbf{x}\|_p}{\|\mathbf{x}\|_p} = \max_{\|\mathbf{x}\|_p = 1} \|\mathbf{A}\mathbf{x}\|_p\,. \tag{C.8}$$

C.1.3 $\mathcal{L}$-Spaces and Norms

In general the $\mathcal{L}_\mathrm{p}$-space is defined as the space of all piece-wise continuous signals $\mathbf{x}(t): [0, \infty) \to \mathbb{R}^n$ such that it holds

$$\|\mathbf{x}\|_{\mathcal{L}_p} = \left(\int_0^\infty \|\mathbf{x}(t)\|^p dt\right)^{\frac{1}{p}} < \infty \quad \text{for } p \in [0,\infty[, \tag{C.9}$$

and

$$\|\mathbf{x}\|_{\mathcal{L}_\infty} = \sup_{t\geq 0}\|\mathbf{x}(t)\| < \infty, \tag{C.10}$$

where $\|\mathbf{x}(t)\|$ can be any vector norm.

$\mathcal{L}$-norms are used to calculate input-output gains, and show input-output stability of systems [190]. As signals on the time interval $t \in [0,\infty)$ are considered the class of signals, which can satisfy Eq.(C.9), to be $\in \mathcal{L}_p$, is largely restricted. To allow a larger class of signals an extended space $\mathcal{L}_{p,e}$ can be defined by

$$\mathcal{L}_{p,e} = \{\mathbf{x}|\mathbf{x}_\tau \in \mathcal{L}_p \forall \tau \geq 0\}, \tag{C.11}$$

where $\mathbf{x}_\tau$ is the truncated signal

$$\mathbf{x}_\tau(t) = \begin{cases}\mathbf{x}(t), & 0 \leq t \leq \tau \\ 0, & t > \tau\end{cases}. \tag{C.12}$$

C.1.4 $\mathcal{L}$-Stability

If we consider the following input-output relation

$$\mathbf{y} = \mathbf{G}\mathbf{u}, \tag{C.13}$$

where $\mathbf{G}$ is an operator that maps the input $\mathbf{u} \in \mathbb{R}^m$ to the output $\mathbf{y} \in \mathbb{R}^k$ then input-output stability can be defined by:

Definition C.1: *The mapping* $\mathbf{G}$: $\mathcal{L}^m \to \mathcal{L}^k$ *is* $\mathcal{L}$*-stable if there exists a class* $\mathcal{K}$ *function* α, *defined on* $[0,\infty)$, *and a nonnegative constant* β *such that*

$$\|\mathbf{G}\mathbf{u}\|_{\mathcal{L}} \leq \alpha(\|\mathbf{u}\|_{\mathcal{L}}) + \beta$$

for all $\mathbf{u} \in \mathcal{L}^m$. *It is finite-gain* $\mathcal{L}$*-stable if there exist nonnegative constants* γ *and* β *such that*

$$\|\mathbf{G}\mathbf{u}\|_{\mathcal{L}} \leq \gamma\|\mathbf{u}\|_{\mathcal{L}} + \beta$$

for all $\mathbf{u} \in \mathcal{L}^m$.

Bounded-Input Bounded-Output stability of system (C.13) is given if Definition B.1 holds for the $\mathcal{L}_\infty$*-norm.* Δ

Definition C.2: *A continuous function* $\alpha: [0,a) \longrightarrow [0,\infty)$ *belongs to class* $\mathcal{K}$ *if it is strictly increasing and* $\alpha(0) = 0$. Δ

C.2 Stability Concepts

According to [1], the following stability concepts are used for system of the form

$$\dot{\mathbf{x}} = \mathbf{f}(\mathbf{x}, t). \tag{C.14}$$

With the equilibrium at the origin $\mathbf{f}(\mathbf{0}, t) = \mathbf{0}\ \forall\ t > t_0$ and with the initial condition $\mathbf{x}(t = 0) = \mathbf{x}_0$.

Definition C.3: *The equilibrium state* $\mathbf{x} = \mathbf{0}$ *of the system is said to be stable if for every* $\varepsilon > 0$ *and* $t_0 > 0$, *there exists a* $\delta(\varepsilon, t_0) > 0$ *such that* $\|\mathbf{x}_0\| < \delta$ *implies that* $\|\mathbf{x}(t, \mathbf{x}_0, t_0)\| < \varepsilon\ \forall\ t > t_0$. *This is shown in Figure C.1.* Δ

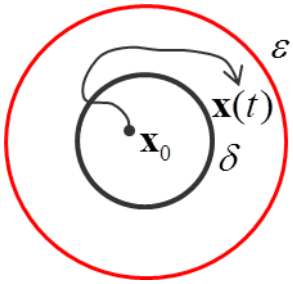

Figure C.1: General stability definition

Definition C.4: *The equilibrium state* $\mathbf{x} = \mathbf{0}$ *of the system is said to be attractive if for some* $\rho > 0$ *and every* η *and* $t_0 > 0$, *there exists a number* $T(\eta, \mathbf{x}_0, t_0)$ *such that* $\|\mathbf{x}_0\| < \rho$ *implies that* $\|\mathbf{x}(t, \mathbf{x}_0, t_0)\| < \eta\ \forall\ t > t_0 + T$. *The concept of an attractive equilibrium is displayed in Figure C.2.* Δ

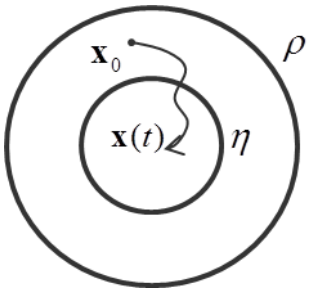

Figure C.2: Asymptotic stability

Definition C.5: *The equilibrium state* $\mathbf{x} = \mathbf{0}$ *of the system is said to be asymptotically stable if it is both, stable and attractive.* Δ

Definition C.6: *The equilibrium state* $\mathbf{x} = \mathbf{0}$ *of the system is said to be uniformly stable if in Definition 1,* δ *is independent of* t_0. Δ

Definition C.7: *The equilibrium state* $\mathbf{x} = \mathbf{0}$ *of the system is uniformly asymptotically stable (u.a.s) if it is uniformly stable and for some* ε_1 *and every* ε_2*, there exists* $T(\varepsilon_1, \varepsilon_2) > 0$ *such that if* $\|\mathbf{x}_0\| < \varepsilon_1$*, then* $\|\mathbf{x}(t, \mathbf{x}_0, t_0)\| < \varepsilon_2 \; \forall \; t > t_0 + T$. Δ

Definition C.8: *The equilibrium state* $\mathbf{x} = \mathbf{0}$ *of the system is exponentially stable if there exist constants* $a > 0$ *and* $b > 0$ *such that* $\|\mathbf{x}(t, \mathbf{x}_0, t_0)\| < a \cdot \mathbf{x}_0 \cdot e^{-b(t-t_0)} \; \forall \; t > t_0 + T$*, for all* t_0 *in a certain neighborhood* B *of the origin*. Δ

Lyapunov's Theoreme for autonomous systems (according to [89]**):**

Consider the autonomous system

$$\dot{\mathbf{x}} = \mathbf{f}(\mathbf{x}). \tag{C.15}$$

Let $\mathbf{x} = \mathbf{0}$ *be an equilibrium point of Eq.(C.15) and* $D \subset \mathbb{R}^n$ *be a domain containing* $\mathbf{x} = \mathbf{0}$*. Let* $\mathrm{V} = D \to \mathbb{R}$ *be a continuously differentiable function such that*

$$\mathrm{V}(\mathbf{0}) = 0 \text{ and } \mathrm{V}(\mathbf{x}) > \mathbf{0} \text{ in } D \setminus \{\mathbf{0}\} \tag{C.16}$$

Then $\mathbf{x} = \mathbf{0}$ *is stable if*

$$\dot{\mathrm{V}} \leq 0 \;\; \text{in } D \tag{C.17}$$

Moreover, $\mathbf{x} = \mathbf{0}$ *is asymptotically stable if*

$$\dot{\mathrm{V}} < 0 \;\; \text{in } D \setminus \{\mathbf{0}\} \tag{C.18}$$

Results in (C.17) and (C.18) hold globally (globally stable, globally asymptotic stable), if $D = \mathbb{R}^n$ *and* $\lim_{\|\mathbf{x}\| \to \infty} \mathrm{V}(\mathbf{x}) = \infty$ *(*V *is radially unbounded).* Δ

Barbalat's Lemma (according to [89]**):**

Let $\Phi: \mathbb{R} \to \mathbb{R}$ *be a uniformly continuous function on* $[\mathbf{0}, \infty)$*. Suppose that* $\lim_{t \to \infty} \int_0^t \Phi(\tau) \, d\tau = \infty$ *exists and is finite. Then,*

$$\Phi(\tau) \to 0 \;\; \text{as} \;\; t \to \infty$$

Δ

Appendix D

Stability Proofs

D.1 Direct MRAC

Starting from the Lyapunov function candidate given in Eq.(4.9)

$$\mathrm{V} = \tfrac{1}{2}\mathbf{e}_C^T\mathbf{P}\mathbf{e}_C + \tfrac{1}{2}\mathrm{Tr}\left[\widetilde{\boldsymbol{\Theta}}_x^T\boldsymbol{\Gamma}_x^{-1}\widetilde{\boldsymbol{\Theta}}_x\boldsymbol{\Lambda}\right] + \tfrac{1}{2}\mathrm{Tr}\left[\widetilde{\boldsymbol{\Theta}}_\varphi^T\boldsymbol{\Gamma}_\varphi^{-1}\widetilde{\boldsymbol{\Theta}}_\varphi\boldsymbol{\Lambda}\right] + \tfrac{1}{2}\mathrm{Tr}\left[\gamma_d^{-1}\widetilde{\boldsymbol{\theta}}_d\widetilde{\boldsymbol{\theta}}_d^T\boldsymbol{\Lambda}\right] + \tfrac{1}{2}\mathrm{Tr}\left[\widetilde{\boldsymbol{\Theta}}_r\boldsymbol{\Gamma}_r^{-1}\widetilde{\boldsymbol{\Theta}}_r^T\boldsymbol{\Lambda}\right], \quad \text{(D.1)}$$

if we take the derivative with respect to time we obtain

$$\dot{\mathrm{V}} = \dot{\mathbf{e}}_C^T\mathbf{P}\mathbf{e}_C + \mathrm{Tr}\left[\widetilde{\boldsymbol{\Theta}}_x^T\boldsymbol{\Gamma}_x^{-1}\dot{\widetilde{\boldsymbol{\Theta}}}_x\boldsymbol{\Lambda}\right] + \mathrm{Tr}\left[\widetilde{\boldsymbol{\Theta}}_\varphi^T\boldsymbol{\Gamma}_\varphi^{-1}\dot{\widetilde{\boldsymbol{\Theta}}}_\varphi\boldsymbol{\Lambda}\right] + \mathrm{Tr}\left[\gamma_d^{-1}\widetilde{\boldsymbol{\theta}}_d\dot{\widetilde{\boldsymbol{\theta}}}_d^T\boldsymbol{\Lambda}\right] + \mathrm{Tr}\left[\widetilde{\boldsymbol{\Theta}}_r\boldsymbol{\Gamma}_r^{-1}\dot{\widetilde{\boldsymbol{\Theta}}}_r^T\boldsymbol{\Lambda}\right]. \quad \text{(D.2)}$$

Inserting the error dynamics from Eq.(4.8) yields

$$\begin{aligned}\dot{\mathrm{V}} = \frac{1}{2}\mathbf{e}_C^T\underbrace{\left(\mathbf{P}\mathbf{A}_M + \mathbf{A}_M^T\mathbf{P}\right)}_{-\mathbf{Q}}\mathbf{e}_C + \mathbf{e}_C^T\mathbf{P}\mathbf{B}_P\boldsymbol{\Lambda}\left(\widetilde{\boldsymbol{\Theta}}_x^T\mathbf{x}_P + \widetilde{\boldsymbol{\Theta}}_\varphi^T\boldsymbol{\varphi}(\mathbf{x}_P) + \widetilde{\boldsymbol{\theta}}_d + \widetilde{\boldsymbol{\Theta}}_r\mathbf{r}\right)\\ +\mathrm{Tr}\left[\widetilde{\boldsymbol{\Theta}}_x^T\boldsymbol{\Gamma}_x^{-1}\dot{\widetilde{\boldsymbol{\Theta}}}_x\boldsymbol{\Lambda}\right] + \mathrm{Tr}\left[\widetilde{\boldsymbol{\Theta}}_\varphi^T\boldsymbol{\Gamma}_\varphi^{-1}\dot{\widetilde{\boldsymbol{\Theta}}}_\varphi\boldsymbol{\Lambda}\right] + \mathrm{Tr}\left[\gamma_d^{-1}\widetilde{\boldsymbol{\theta}}_d\dot{\widetilde{\boldsymbol{\theta}}}_d^T\boldsymbol{\Lambda}\right] + \mathrm{Tr}\left[\widetilde{\boldsymbol{\Theta}}_r\boldsymbol{\Gamma}_r^{-1}\dot{\widetilde{\boldsymbol{\Theta}}}_r^T\boldsymbol{\Lambda}\right].\end{aligned} \quad \text{(D.3)}$$

$\mathbf{P} \in \mathbb{R}^{n\times n}$ is the symmetric positive definite solution of the Lyapunov equation

$$\mathbf{P}\mathbf{A}_M + \mathbf{A}_M^T\mathbf{P} = -\mathbf{Q}, \quad \text{(D.4)}$$

where $\mathbf{Q} \in \mathbb{R}^{n\times n}$ is a symmetric positive definite matrix and a design parameter for the adaptive controller.

By applying the trace identity $\mathbf{a}^T\mathbf{b} = \mathrm{Tr}[\mathbf{b}\mathbf{a}^T]$ we can rewrite the following terms

$$\begin{aligned}\mathbf{e}_C^T\mathbf{P}\mathbf{B}_P\boldsymbol{\Lambda}\cdot\widetilde{\boldsymbol{\Theta}}_x^T\mathbf{x}_P &= \mathrm{Tr}\left[\widetilde{\boldsymbol{\Theta}}_x^T\mathbf{x}_P\cdot\mathbf{e}_C^T\mathbf{P}\mathbf{B}_P\boldsymbol{\Lambda}\right]\\ \mathbf{e}_C^T\mathbf{P}\mathbf{B}_P\boldsymbol{\Lambda}\cdot\widetilde{\boldsymbol{\Theta}}_\varphi^T\boldsymbol{\varphi}(\mathbf{x}) &= \mathrm{Tr}\left[\widetilde{\boldsymbol{\Theta}}_\varphi^T\boldsymbol{\varphi}(\mathbf{x}_P)\cdot\mathbf{e}_C^T\mathbf{P}\mathbf{B}_P\boldsymbol{\Lambda}\right]\\ \mathbf{e}_C^T\mathbf{P}\mathbf{B}_P\boldsymbol{\Lambda}\cdot\widetilde{\boldsymbol{\theta}}_d &= \mathrm{Tr}\left[\widetilde{\boldsymbol{\theta}}_d\cdot\mathbf{e}_C^T\mathbf{P}\mathbf{B}_P\boldsymbol{\Lambda}\right]\\ \mathbf{e}_C^T\mathbf{P}\mathbf{B}_P\boldsymbol{\Lambda}\cdot\widetilde{\boldsymbol{\Theta}}_r\mathbf{r} &= \mathrm{Tr}\left[\widetilde{\boldsymbol{\Theta}}_r\mathbf{r}\cdot\mathbf{e}_C^T\mathbf{P}\mathbf{B}_P\boldsymbol{\Lambda}\right]\end{aligned} \quad \text{(D.5)}$$

Using these results we can collect terms in Eq.(D.3)

$$\begin{aligned}\dot{\mathrm{V}} = -\frac{1}{2}\mathbf{e}_C^T\mathbf{Q}\mathbf{e}_C\\ +\mathrm{Tr}\left[\widetilde{\boldsymbol{\Theta}}_x^T\left(\boldsymbol{\Gamma}_x^{-1}\dot{\widetilde{\boldsymbol{\Theta}}}_x + \mathbf{x}_P\cdot\mathbf{e}_C^T\mathbf{P}\mathbf{B}_P\right)\boldsymbol{\Lambda}\right]\\ +\mathrm{Tr}\left[\widetilde{\boldsymbol{\Theta}}_\varphi^T\left(\boldsymbol{\Gamma}_\varphi^{-1}\dot{\widetilde{\boldsymbol{\Theta}}}_\varphi + \boldsymbol{\varphi}(\mathbf{x}_P)\cdot\mathbf{e}_C^T\mathbf{P}\mathbf{B}_P\right)\boldsymbol{\Lambda}\right]\end{aligned} \quad \text{(D.6)}$$

$$+\mathrm{Tr}\left[\tilde{\boldsymbol{\theta}}_d\left(\gamma_d^{-1}\dot{\tilde{\boldsymbol{\theta}}}_d^T+\mathbf{e}_C^T\mathbf{P}\mathbf{B}_P\right)\boldsymbol{\Lambda}\right]$$
$$+\mathrm{Tr}\left[\tilde{\boldsymbol{\Theta}}_r\left(\boldsymbol{\Gamma}_r^{-1}\dot{\tilde{\boldsymbol{\Theta}}}_r^T+\mathbf{r}\cdot\mathbf{e}_C^T\mathbf{P}\mathbf{B}_P\right)\boldsymbol{\Lambda}\right]$$

Obviously, if we now choose the following update laws

$$\begin{aligned}\dot{\tilde{\boldsymbol{\Theta}}}_x &= -\boldsymbol{\Gamma}_x\mathbf{x}_P\cdot\mathbf{e}_C^T\mathbf{P}\mathbf{B}_P\\ \dot{\tilde{\boldsymbol{\Theta}}}_\varphi &= \boldsymbol{\Gamma}_\varphi\boldsymbol{\varphi}(\mathbf{x}_P)\cdot\mathbf{e}_C^T\mathbf{P}\mathbf{B}_P\\ \dot{\tilde{\boldsymbol{\theta}}}_d^T &= -\gamma_{dd}\cdot\mathbf{e}_C^T\mathbf{P}\mathbf{B}_P\\ \dot{\tilde{\boldsymbol{\Theta}}}_r^T &= -\boldsymbol{\Gamma}_r\mathbf{r}\cdot\mathbf{e}_C^T\mathbf{P}\mathbf{B}_P\end{aligned}, \tag{D.7}$$

the sign indefinite terms are canled and the time derivative of the Lyapunov function becomes negative semidefinite:

$$\dot{\mathrm{V}}=-\frac{1}{2}\mathbf{e}_C^T\mathbf{Q}\mathbf{e}_C. \tag{D.8}$$

Lyapunov's Theorem, given in Section C.2, ensures boundedness of the states $\mathbf{e}_C$, $\tilde{\boldsymbol{\Theta}}_x$ $\tilde{\boldsymbol{\Theta}}_\varphi$, $\tilde{\boldsymbol{\Theta}}_d$, and $\tilde{\boldsymbol{\Theta}}_r$ for the closed loop adaptive system. As $\mathbf{e}_C$ is bounded it follows from boundedness of the reference model that $\mathbf{x}_P=\mathbf{x}_M+\mathbf{e}_C$ is bounded. For the controller implementation we are actually not interested in the parameter errors $\tilde{\boldsymbol{\Theta}}$, but in the estimated parameters $\boldsymbol{\Theta}$. As $\tilde{\boldsymbol{\Theta}}=\boldsymbol{\Theta}-\boldsymbol{\Theta}^*$, and the ideal parameters $\boldsymbol{\Theta}^*$ are assumed to be constant the adaptation laws for the parameters are given by Eq.(4.10):

$$\begin{aligned}\dot{\boldsymbol{\Theta}}_x &= -\boldsymbol{\Gamma}_x\mathbf{x}_P\cdot\mathbf{e}_C^T\mathbf{P}\mathbf{B}_P\\ \dot{\boldsymbol{\Theta}}_\varphi &= \boldsymbol{\Gamma}_\varphi\boldsymbol{\varphi}(\mathbf{x}_P)\cdot\mathbf{e}_C^T\mathbf{P}\mathbf{B}_P\\ \dot{\boldsymbol{\theta}}_d^T &= -\gamma_{dd}\cdot\mathbf{e}_C^T\mathbf{P}\mathbf{B}_P\\ \dot{\boldsymbol{\Theta}}_r^T &= -\boldsymbol{\Gamma}_r\mathbf{r}\cdot\mathbf{e}_C^T\mathbf{P}\mathbf{B}_P\end{aligned}. \tag{D.9}$$

Additionally, from boundedness of the system states ($\mathbf{e}_C$, $\tilde{\boldsymbol{\Theta}}_x, \tilde{\boldsymbol{\Theta}}_\varphi, \tilde{\boldsymbol{\theta}}_d, \text{and } \tilde{\boldsymbol{\Theta}}_r \in \mathcal{L}_\infty$), the existence of the integral

$$\int_{t_0}^{\infty}\dot{\mathrm{V}}(\tau)d\tau=\mathrm{V}(\infty)-\mathrm{V}(t_0)<\infty \tag{D.10}$$

follows, and thus the error $\mathbf{e}_C$ is square integrable, that is $\mathbf{e}_C\in\mathcal{L}_2$:

$$\int_{t_0}^{\infty}\mathbf{e}_C^T(\tau)\mathbf{Q}\mathbf{e}_C(\tau)\,d\tau<\infty \tag{D.11}$$

If the reference command $\mathbf{r}$ is bounded ($\mathbf{r}\in\mathcal{L}_\infty$), then from the boundedness of $\mathbf{e}_C, \tilde{\boldsymbol{\Theta}}_x, \tilde{\boldsymbol{\Theta}}_\varphi, \tilde{\boldsymbol{\theta}}_d, \tilde{\boldsymbol{\Theta}}_r$ and the error dynamics in Eq.(4.8) it follows that $\dot{\mathbf{e}}_C$ is bounded. With $\dot{\mathbf{e}}_C\in\mathcal{L}_\infty$, Barbalat's Lemma (see Section C.2) can be applied, and it can be shown that

$$\lim_{t\to\infty}\mathbf{e}_C(t)=\lim_{t\to\infty}(\mathbf{x}_P-\mathbf{x}_M)=\mathbf{0}.$$

D.2 Indirect MRAC

D.2.1 Calculation of Controller Gains

We start by using the Lyapunov function candidate

$$\mathrm{V} = \tfrac{1}{2}\mathbf{e}_I^T\mathbf{P}\mathbf{e}_I + \tfrac{1}{2}\mathrm{Tr}\left[\widetilde{\mathbf{A}}_P\boldsymbol{\Gamma}_A^{-1}\widetilde{\mathbf{A}}_P^T\right] + \tfrac{1}{2}\mathrm{Tr}\left[\widetilde{\boldsymbol{\Lambda}}\boldsymbol{\Gamma}_\Lambda^{-1}\widetilde{\boldsymbol{\Lambda}}^T\right] + \tfrac{1}{2}\mathrm{Tr}\left[\widetilde{\boldsymbol{\Theta}}_f\boldsymbol{\Gamma}_f^{-1}\widetilde{\boldsymbol{\Theta}}_f^T\right] + \tfrac{1}{2}\mathrm{Tr}\left[\gamma_d^{-1}\tilde{\mathbf{d}}\tilde{\mathbf{d}}^T\right], \tag{D.12}$$

Taking the time derivative of the Lyapunov function candidate and inserting the identification error dynamics of Eq.(4.16) we obtain

$$\begin{aligned}\dot{\mathrm{V}} = \frac{1}{2}\mathbf{e}_I^T\underbrace{\left(\mathbf{P}\mathbf{A}_M + \mathbf{A}_M^T\mathbf{P}\right)}_{-\mathbf{Q}}\mathbf{e} + \mathbf{e}_I^T\mathbf{P}\left(\widetilde{\mathbf{A}}_P\mathbf{x}_P + \mathbf{B}_P\widetilde{\boldsymbol{\Lambda}}\mathbf{u} + \widetilde{\boldsymbol{\Theta}}_f\boldsymbol{\varphi}(\mathbf{x}_P) + \tilde{\mathbf{d}}\right)\\ +\mathrm{Tr}\left[\widetilde{\mathbf{A}}_P\boldsymbol{\Gamma}_A^{-1}\dot{\widetilde{\mathbf{A}}}_P^T\right] + \mathrm{Tr}\left[\widetilde{\boldsymbol{\Lambda}}\boldsymbol{\Gamma}_\Lambda^{-1}\dot{\widetilde{\boldsymbol{\Lambda}}}^T\right] + \mathrm{Tr}\left[\widetilde{\boldsymbol{\Theta}}_f\boldsymbol{\Gamma}_f^{-1}\dot{\widetilde{\boldsymbol{\Theta}}}_f^T\right] + \mathrm{Tr}\left[\gamma_d^{-1}\tilde{\mathbf{d}}\dot{\tilde{\mathbf{d}}}^T\right].\end{aligned} \tag{D.13}$$

Again the trace identity $\mathbf{a}^T\mathbf{b} = \mathrm{Tr}[\mathbf{b}\mathbf{a}^T]$ has to be applied

$$\begin{aligned}\dot{\mathrm{V}} = -\frac{1}{2}\mathbf{e}_I^T\mathbf{Q}\mathbf{e}_I\\ +\mathrm{Tr}\left[\widetilde{\mathbf{A}}_P\mathbf{x}_P\mathbf{e}_I^T\mathbf{P} + \widetilde{\mathbf{A}}_P\boldsymbol{\Gamma}_A^{-1}\dot{\widetilde{\mathbf{A}}}_P^T\right]\\ +\mathrm{Tr}\left[\widetilde{\boldsymbol{\Lambda}}\mathbf{u}\mathbf{e}_I^T\mathbf{P}\mathbf{B}_P + \widetilde{\boldsymbol{\Lambda}}\boldsymbol{\Gamma}_\Lambda^{-1}\dot{\widetilde{\boldsymbol{\Lambda}}}^T\right]\\ +\mathrm{Tr}\left[\widetilde{\boldsymbol{\Theta}}_f\boldsymbol{\varphi}(\mathbf{x}_P)\mathbf{e}_I^T\mathbf{P} + \widetilde{\boldsymbol{\Theta}}_f\boldsymbol{\Gamma}_f^{-1}\dot{\widetilde{\boldsymbol{\Theta}}}_f^T\right]\\ +\mathrm{Tr}\left[\tilde{\mathbf{d}}\mathbf{e}_I^T\mathbf{P} + \gamma_d^{-1}\tilde{\mathbf{d}}\dot{\tilde{\mathbf{d}}}^T\right]\end{aligned} \tag{D.14}$$

By choosing the following adaptation laws

$$\begin{aligned}\dot{\widetilde{\mathbf{A}}}_P^T &= -\boldsymbol{\Gamma}_A\mathbf{x}_P\cdot\mathbf{e}_I^T\mathbf{P}\\ \dot{\widetilde{\boldsymbol{\Lambda}}}^T &= -\boldsymbol{\Gamma}_\Lambda\mathbf{u}\cdot\mathbf{e}_I^T\mathbf{P}\mathbf{B}_P\\ \dot{\widetilde{\boldsymbol{\Theta}}}_f^T &= -\boldsymbol{\Gamma}_f\boldsymbol{\varphi}(\mathbf{x}_P)\cdot\mathbf{e}_I^T\mathbf{P}\\ \dot{\tilde{\mathbf{d}}}^T &= -\gamma_d\mathbf{e}_I^T\mathbf{P}\end{aligned} \quad\Leftrightarrow\quad \begin{aligned}\dot{\widehat{\mathbf{A}}}_P^T &= -\boldsymbol{\Gamma}_A\mathbf{x}_P\cdot\mathbf{e}_I^T\mathbf{P}\\ \dot{\widehat{\boldsymbol{\Lambda}}}^T &= -\boldsymbol{\Gamma}_\Lambda\mathbf{u}\cdot\mathbf{e}_I^T\mathbf{P}\mathbf{B}_P\\ \dot{\widehat{\boldsymbol{\Theta}}}_f^T &= -\boldsymbol{\Gamma}_f\boldsymbol{\varphi}(\mathbf{x}_P)\cdot\mathbf{e}_I^T\mathbf{P}\\ \dot{\hat{\mathbf{d}}}^T &= -\gamma_d\mathbf{e}_I^T\mathbf{P}\end{aligned}, \tag{D.15}$$

the Lyapunov function is rendered negative semi definite. Hence, stable parameter estimation is guaranteed by Lyapunov's Theorem (see Section C.2). This means the states $\mathbf{e}_I$, $\widetilde{\mathbf{A}}_P$, $\widetilde{\boldsymbol{\Lambda}}$, $\widetilde{\boldsymbol{\Theta}}_f$, and $\tilde{\mathbf{d}}$ are bounded.

Inserting the control law of Eq.(4.19) in the identification model of Eq.(4.14) we immediately obtain

$$\dot{\hat{\mathbf{x}}}_P = \mathbf{A}_M\hat{\mathbf{x}}_P + \mathbf{B}_M\,\mathbf{r}. \tag{D.16}$$

Choosing $\hat{\mathbf{x}}_P(t_0) = \mathbf{x}_M(t_0)$, it follows that $\hat{\mathbf{x}}_P(t) = \mathbf{x}_M(t)\ \forall\ t \geq t_0$, and hence the predictor dynamics are equal to the dynamics of the reference model. This also means that for a stable reference model $\hat{\mathbf{x}}_P$ is bounded. As $\mathbf{e}_I$ is bounded, $\mathbf{x}_P = \hat{\mathbf{x}}_P - \mathbf{e}_I$ is bounded. Furthermore, by application of Barbalat's Lemma (see Section C.2) it can be shown that

$$\lim_{t\to\infty}\mathbf{e}_I(t) = \lim_{t\to\infty}(\hat{\mathbf{x}}_P - \mathbf{x}_P) = \mathbf{0}.$$

D.2.2 Update of Controller Gains

To proof stability for the adaptation laws choose the Lyapunov function candidate from Eq.(4.24)

$$\begin{aligned} \mathrm{V} = \frac{1}{2}\mathbf{e}_I^T\mathbf{P}\mathbf{e}_I + \frac{1}{2}\mathrm{Tr}\left[\widetilde{\boldsymbol{\Theta}}_x^T\boldsymbol{\Gamma}_x^{-1}\widetilde{\boldsymbol{\Theta}}_x\boldsymbol{\Lambda}\right] + \frac{1}{2}\mathrm{Tr}\left[\widetilde{\boldsymbol{\Theta}}_\varphi^T\boldsymbol{\Gamma}_\varphi^{-1}\widetilde{\boldsymbol{\Theta}}_\varphi\boldsymbol{\Lambda}\right] + \frac{1}{2}\mathrm{Tr}\left[\gamma_{dd}^{-1}\widetilde{\boldsymbol{\theta}}_d\widetilde{\boldsymbol{\theta}}_d^T\boldsymbol{\Lambda}\right] + \frac{1}{2}\mathrm{Tr}\left[\widetilde{\boldsymbol{\Theta}}_r\boldsymbol{\Gamma}_r^{-1}\widetilde{\boldsymbol{\Theta}}_r^T\boldsymbol{\Lambda}\right] \\ + \tfrac{1}{2}\mathrm{Tr}\left[\widetilde{\mathbf{A}}_P\boldsymbol{\Gamma}_A^{-1}\widetilde{\mathbf{A}}_P^T\right] + \tfrac{1}{2}\mathrm{Tr}\left[\widetilde{\boldsymbol{\Theta}}_f\boldsymbol{\Gamma}_f^{-1}\widetilde{\boldsymbol{\Theta}}_f^T\right]\tfrac{1}{2}\mathrm{Tr}\left[\gamma_{di}^{-1}\tilde{\mathbf{d}}\tilde{\mathbf{d}}^T\right] + \tfrac{1}{2}\mathrm{Tr}\left[\widetilde{\boldsymbol{\Lambda}}\boldsymbol{\Gamma}_\Lambda^{-1}\widetilde{\boldsymbol{\Lambda}}^T\right], \end{aligned} \tag{D.17}$$

Taking the time derivative we obtain

$$\begin{aligned} \dot{\mathrm{V}} = \frac{1}{2}\mathbf{e}_I^T\underbrace{\left(\mathbf{P}\mathbf{A}_M + \mathbf{A}_M^T\mathbf{P}\right)}_{-\mathbf{Q}}\mathbf{e}_I + \mathbf{e}_I^T\mathbf{P}\left(\widetilde{\mathbf{A}}_P\mathbf{x}_P + \mathbf{B}_P\widetilde{\boldsymbol{\Lambda}}\mathbf{u} + \widetilde{\boldsymbol{\Theta}}_f\boldsymbol{\varphi}(\mathbf{x}_P) + \tilde{\mathbf{d}}\right) \\ + \mathrm{Tr}\left[\widetilde{\boldsymbol{\Theta}}_x^T\boldsymbol{\Gamma}_x^{-1}\dot{\widetilde{\boldsymbol{\Theta}}}_x\boldsymbol{\Lambda}\right] + \mathrm{Tr}\left[\widetilde{\boldsymbol{\Theta}}_\varphi^T\boldsymbol{\Gamma}_\varphi^{-1}\dot{\widetilde{\boldsymbol{\Theta}}}_\varphi\boldsymbol{\Lambda}\right] + \mathrm{Tr}\left[\gamma_{dd}^{-1}\widetilde{\boldsymbol{\theta}}_d\dot{\widetilde{\boldsymbol{\theta}}}_d^T\boldsymbol{\Lambda}\right] + \mathrm{Tr}\left[\widetilde{\boldsymbol{\Theta}}_r\boldsymbol{\Gamma}_r^{-1}\dot{\widetilde{\boldsymbol{\Theta}}}_r^T\boldsymbol{\Lambda}\right] \\ + \mathrm{Tr}\left[\widetilde{\mathbf{A}}_P\boldsymbol{\Gamma}_A^{-1}\dot{\widetilde{\mathbf{A}}}_P^T\right] + \mathrm{Tr}\left[\widetilde{\boldsymbol{\Theta}}_f\boldsymbol{\Gamma}_f^{-1}\dot{\widetilde{\boldsymbol{\Theta}}}_f^T\right] + \mathrm{Tr}\left[\gamma_{di}^{-1}\tilde{\mathbf{d}}\dot{\tilde{\mathbf{d}}}^T\right] + \mathrm{Tr}\left[\widetilde{\boldsymbol{\Lambda}}\boldsymbol{\Gamma}_\Lambda^{-1}\dot{\widetilde{\boldsymbol{\Lambda}}}^T\right]. \end{aligned} \tag{D.18}$$

Inserting the adaptation laws from Eq.(4.26) and Eq.(4.27) leads t

$$\begin{aligned} \dot{\mathrm{V}} = -\frac{1}{2}\mathbf{e}_I^T\mathbf{Q}\mathbf{e}_I + \mathbf{Tr}\left[\left(\widetilde{\mathbf{A}}_P\mathbf{x}_P + \mathbf{B}_P\widetilde{\boldsymbol{\Lambda}}\mathbf{u} + \widetilde{\boldsymbol{\Theta}}_f\boldsymbol{\varphi}(\mathbf{x}_P) + \tilde{\mathbf{d}}\right)\mathbf{e}^T\mathbf{P}\right] \\ -\mathrm{Tr}\left[\widetilde{\boldsymbol{\Theta}}_x^T\gamma_\varepsilon\boldsymbol{\varepsilon}_x^T\mathbf{B}_P\boldsymbol{\Lambda}\right] - \mathrm{Tr}\left[\widetilde{\boldsymbol{\Theta}}_\varphi^T\gamma_\varepsilon\boldsymbol{\varepsilon}_\varphi^T\mathbf{B}_P\boldsymbol{\Lambda}\right] - \mathrm{Tr}\left[\widetilde{\boldsymbol{\theta}}_d\gamma_\varepsilon\boldsymbol{\varepsilon}_d^T\mathbf{B}_P\boldsymbol{\Lambda}\right] - \mathrm{Tr}\left[\widetilde{\boldsymbol{\Theta}}_r\gamma_\varepsilon\boldsymbol{\varepsilon}_r^T\mathbf{B}_P\boldsymbol{\Lambda}\right] \\ -\mathrm{Tr}\left[\widetilde{\mathbf{A}}_P(\mathbf{x}_P\mathbf{e}^T\mathbf{P} + \gamma_\varepsilon\boldsymbol{\varepsilon}_x^T)\right] - \mathrm{Tr}\left[\widetilde{\boldsymbol{\Theta}}_f\left(\boldsymbol{\varphi}(\mathbf{x}_P)\mathbf{e}^T\mathbf{P} + \gamma_\varepsilon\boldsymbol{\varepsilon}_\varphi^T\right)\right] - \mathrm{Tr}\left[\tilde{\mathbf{d}}(\mathbf{e}^T\mathbf{P} + \gamma_\varepsilon\boldsymbol{\varepsilon}_d^T)\right] \\ -\mathrm{Tr}\left[\widetilde{\boldsymbol{\Lambda}}\left(\mathbf{u}\mathbf{e}_\mathbf{I}^T\mathbf{P} + \boldsymbol{\Theta}_x^T\gamma_\varepsilon\boldsymbol{\varepsilon}_x^T + \gamma_\varepsilon\boldsymbol{\Theta}_\varphi^T\boldsymbol{\varepsilon}_\varphi^T + \gamma_\varepsilon\boldsymbol{\theta}_d\boldsymbol{\varepsilon}_d^T + \boldsymbol{\Theta}_r\gamma_\varepsilon\boldsymbol{\varepsilon}_r^T\right)\mathbf{B}_P\right]. \end{aligned} \tag{D.19}$$

Collecting same ε's we obtain

$$\begin{aligned} \dot{\mathrm{V}} = -\frac{1}{2}\mathbf{e}_I^T\mathbf{Q}\mathbf{e}_I \\ -\mathrm{Tr}\left[\left(\mathbf{B}_P\boldsymbol{\Lambda}\widetilde{\boldsymbol{\Theta}}_x^T + \mathbf{B}_P\widetilde{\boldsymbol{\Lambda}}\boldsymbol{\Theta}_x^T + \widetilde{\mathbf{A}}_P\right)\gamma_\varepsilon\boldsymbol{\varepsilon}_x^T\right] \\ -\mathrm{Tr}\left[\left(\mathbf{B}_P\boldsymbol{\Lambda}\widetilde{\boldsymbol{\Theta}}_\varphi^T + \mathbf{B}_P\widetilde{\boldsymbol{\Lambda}}\boldsymbol{\Theta}_\varphi^T + \widetilde{\boldsymbol{\Theta}}_f\right)\gamma_\varepsilon\boldsymbol{\varepsilon}_\varphi^T\right] \\ -\mathrm{Tr}\left[\left(\mathbf{B}_P\boldsymbol{\Lambda}\widetilde{\boldsymbol{\theta}}_d + \mathbf{B}_P\widetilde{\boldsymbol{\Lambda}}\boldsymbol{\theta}_d + \tilde{\mathbf{d}}\right)\gamma_\varepsilon\boldsymbol{\varepsilon}_d^T\right] \\ -\mathrm{Tr}\left[\left(\mathbf{B}_P\boldsymbol{\Lambda}\widetilde{\boldsymbol{\Theta}}_r + \mathbf{B}_P\widetilde{\boldsymbol{\Lambda}}\boldsymbol{\Theta}_r\right)\gamma_\varepsilon\boldsymbol{\varepsilon}_r^T\right]. \end{aligned} \tag{D.20}$$

By canceling same terms in Eq.(D.20) we get

$$\begin{aligned} \dot{\mathrm{V}} = -\frac{1}{2}\mathbf{e}_I^T\mathbf{Q}\mathbf{e}_I \\ -\mathrm{Tr}\left[\left(\mathbf{B}_P\boldsymbol{\Lambda}\boldsymbol{\Theta}_x^{*T} + \mathbf{B}_P\widehat{\boldsymbol{\Lambda}}\boldsymbol{\Theta}_x^T + \widetilde{\mathbf{A}}_P\right)\gamma_\varepsilon\boldsymbol{\varepsilon}_x^T\right] \\ -\mathrm{Tr}\left[\left(\mathbf{B}_P\boldsymbol{\Lambda}\boldsymbol{\Theta}_\varphi^{*T} + \mathbf{B}_P\widehat{\boldsymbol{\Lambda}}\boldsymbol{\Theta}_\varphi^T + \widetilde{\boldsymbol{\Theta}}_f\right)\gamma_\varepsilon\boldsymbol{\varepsilon}_\varphi^T\right] \\ -\mathrm{Tr}\left[\left(\mathbf{B}_P\boldsymbol{\Lambda}\boldsymbol{\theta}_d^* + \mathbf{B}_P\widehat{\boldsymbol{\Lambda}}\boldsymbol{\theta}_d + \tilde{\mathbf{d}}\right)\gamma_\varepsilon\boldsymbol{\varepsilon}_d^T\right] \\ -\mathrm{Tr}\left[\left(\mathbf{B}_P\boldsymbol{\Lambda}\boldsymbol{\Theta}_r^* + \mathbf{B}_P\widehat{\boldsymbol{\Lambda}}\boldsymbol{\Theta}_r\right)\gamma_\varepsilon\boldsymbol{\varepsilon}_r^T\right]. \end{aligned} \tag{D.21}$$

For the ideal plant and controller parameters Eq.(4.25) takes the from

$$\begin{aligned} \mathbf{0} = \mathbf{A}_P + \mathbf{B}_P\boldsymbol{\Lambda}\boldsymbol{\Theta}_x^{*T} - \mathbf{A}_M \quad &\Leftrightarrow \quad -\mathbf{B}_P\boldsymbol{\Lambda}\boldsymbol{\Theta}_x^{*T} = \mathbf{A}_P - \mathbf{A}_M \\ \mathbf{0} = \mathbf{B}_P\boldsymbol{\Lambda}\boldsymbol{\Theta}_\varphi^{*T} + \boldsymbol{\Theta}_f \quad &\Leftrightarrow \quad -\mathbf{B}_P\boldsymbol{\Lambda}\boldsymbol{\Theta}_\varphi^{*T} = \boldsymbol{\Theta}_f \\ \mathbf{0} = \mathbf{B}_P\boldsymbol{\Lambda}\boldsymbol{\theta}_d^* + \mathbf{d} \quad &\Leftrightarrow \quad -\mathbf{B}_P\boldsymbol{\Lambda}\boldsymbol{\theta}_d^* = \mathbf{d} \\ \mathbf{0} = -\mathbf{B}_P\boldsymbol{\Lambda}\boldsymbol{\Theta}_r^* + \mathbf{B}_M \quad &\Leftrightarrow \quad \mathbf{B}_P\boldsymbol{\Lambda}\boldsymbol{\Theta}_r^* = \mathbf{B}_M \end{aligned} \tag{D.22}$$

Inserting these results in Eq.(D.21) yields

$$\begin{aligned}\dot{\mathrm{V}} = &-\frac{1}{2}\mathbf{e}_I^T\mathbf{Q}\mathbf{e}_I \\ &-\mathrm{Tr}\left[\left(\mathbf{B}_P\widehat{\mathbf{\Lambda}}\mathbf{\Theta}_x^T + \mathbf{A}_P - \mathbf{A}_M + \widehat{\mathbf{A}}_P - \mathbf{A}_P\right)\gamma_\varepsilon\boldsymbol{\varepsilon}_x^T\right] \\ &-\mathrm{Tr}\left[\left(\mathbf{B}_P\widehat{\mathbf{\Lambda}}\mathbf{\Theta}_\varphi^T + \mathbf{\Theta}_f + \widehat{\mathbf{\Theta}}_f - \mathbf{\Theta}_f\right)\gamma_\varepsilon\boldsymbol{\varepsilon}_\varphi^T\right] \\ &-\mathrm{Tr}\left[\left(\mathbf{B}_P\widehat{\mathbf{\Lambda}}\boldsymbol{\theta}_d + \mathbf{d} + \hat{\mathbf{d}} - \mathbf{d}\right)\gamma_\varepsilon\boldsymbol{\varepsilon}_d^T\right] \\ &-\mathrm{Tr}\left[\left(\mathbf{B}_P\widehat{\mathbf{\Lambda}}\mathbf{\Theta}_r - \mathbf{B}_M\right)\gamma_\varepsilon\boldsymbol{\varepsilon}_r^T\right].\end{aligned} \tag{D.23}$$

Simplified, Eq.(D.23) can be written by

$$\begin{aligned}\dot{\mathrm{V}} = &-\frac{1}{2}\mathbf{e}_I^T\mathbf{Q}\mathbf{e}_I \\ &-\mathrm{Tr}\left[\underbrace{\left(\widehat{\mathbf{A}}_P - \mathbf{A}_M + \mathbf{B}_P\widehat{\mathbf{\Lambda}}\mathbf{\Theta}_x^T\right)}_{\boldsymbol{\varepsilon}_x}\gamma_\varepsilon\boldsymbol{\varepsilon}_x^T\right] \\ &-\mathrm{Tr}\left[\underbrace{\left(\widehat{\mathbf{\Theta}}_f + \mathbf{B}_P\widehat{\mathbf{\Lambda}}\mathbf{\Theta}_\varphi^T\right)}_{\boldsymbol{\varepsilon}_\varphi}\gamma_\varepsilon\boldsymbol{\varepsilon}_\varphi^T\right] \\ &-\mathrm{Tr}\left[\underbrace{\left(\hat{\mathbf{d}} + \mathbf{B}_P\widehat{\mathbf{\Lambda}}\boldsymbol{\theta}_d\right)}_{\boldsymbol{\varepsilon}_d}\gamma_\varepsilon\boldsymbol{\varepsilon}_d^T\right] \\ &-\mathrm{Tr}\left[\underbrace{\left(-\mathbf{B}_M + \mathbf{B}_P\widehat{\mathbf{\Lambda}}\mathbf{\Theta}_r\right)}_{\boldsymbol{\varepsilon}_r}\gamma_\varepsilon\boldsymbol{\varepsilon}_r^T\right].\end{aligned} \tag{D.24}$$

Hence, $\dot{\mathrm{V}}$ reduces to

$$\dot{\mathrm{V}} = -\frac{1}{2}\mathbf{e}_I^T\mathbf{Q}\mathbf{e}_I - \gamma_\varepsilon\mathrm{Tr}[\boldsymbol{\varepsilon}_x\boldsymbol{\varepsilon}_x^T] - \gamma_\varepsilon\mathrm{Tr}\left[\boldsymbol{\varepsilon}_\varphi\boldsymbol{\varepsilon}_\varphi^T\right] - \gamma_\varepsilon\mathrm{Tr}[\boldsymbol{\varepsilon}_d\boldsymbol{\varepsilon}_d^T] - \gamma_\varepsilon\mathrm{Tr}[\boldsymbol{\varepsilon}_r\boldsymbol{\varepsilon}_r^T] \leq 0 \tag{D.25}$$

Thus the time derivative of the Lyapunov function is negative semi definite. As the Lyapunov function is a dependent on the states $\mathbf{e}_I$, $\widetilde{\mathbf{\Theta}}_x$, $\widetilde{\mathbf{\Theta}}_\varphi$, $\widetilde{\boldsymbol{\theta}}_d$, $\widetilde{\mathbf{\Theta}}_r$, $\widetilde{\mathbf{A}}_P$, $\widetilde{\mathbf{\Theta}}_f$, $\tilde{\mathbf{d}}$ and $\widetilde{\mathbf{\Lambda}}$, the identification error as well as the plant parameters and the controller parameters are guaranteed to be bounded by Lyapunov's Theorem (see Section C.2).

From boundedness of the system states the existence of

$$\int_{t_0}^{\infty}\dot{\mathrm{V}}(\tau)d\tau = \mathrm{V}(\infty) - \mathrm{V}(t_0) < \infty \tag{D.26}$$

follows. Hence, the errors $\mathbf{e}_I$, $\boldsymbol{\varepsilon}_x$, $\boldsymbol{\varepsilon}_\varphi$, $\boldsymbol{\varepsilon}_d$, and $\boldsymbol{\varepsilon}_r$ are square integrable ($\in \mathcal{L}_2$) and bounded ($\in \mathcal{L}_\infty$):

$$\begin{aligned}\int_{t_0}^{\infty}\big(&\mathbf{e}_I^T(\tau)\mathbf{Q}\mathbf{e}_I(\tau) - \gamma_\varepsilon\mathrm{Tr}[\boldsymbol{\varepsilon}_x(\tau)\boldsymbol{\varepsilon}_x^T(\tau)] - \gamma_\varepsilon\mathrm{Tr}\left[\boldsymbol{\varepsilon}_\varphi(\tau)\boldsymbol{\varepsilon}_\varphi^T(\tau)\right] - \gamma_\varepsilon\mathrm{Tr}[\boldsymbol{\varepsilon}_d(\tau)\boldsymbol{\varepsilon}_d^T(\tau)] \\ &- \gamma_\varepsilon\mathrm{Tr}\left[\boldsymbol{\varepsilon}_r(\tau)\boldsymbol{\varepsilon}_r^{T(\tau)}\right]\big)\,d\tau < \infty\end{aligned} \tag{D.27}$$

Furthermore, from the time derivatives of the closed loop estimation errors are bounded

$$\begin{aligned}
\frac{d}{dt}\boldsymbol{\varepsilon}_x &= \frac{d}{dt}\left[\widehat{\mathbf{A}}_P + \mathbf{B}_P\widehat{\boldsymbol{\Lambda}}\boldsymbol{\Theta}_x^T - \mathbf{A}_M\right] &&\in \mathcal{L}_\infty \\
\frac{d}{dt}\boldsymbol{\varepsilon}_\varphi &= \frac{d}{dt}\left[\mathbf{B}_P\widehat{\boldsymbol{\Lambda}}\boldsymbol{\Theta}_\varphi^T + \widehat{\boldsymbol{\Theta}}_f\right]\boldsymbol{\varphi}(\mathbf{x}_P) &&\in \mathcal{L}_\infty \\
\frac{d}{dt}\boldsymbol{\varepsilon}_d &= \frac{d}{dt}\left[\mathbf{B}_P\widehat{\boldsymbol{\Lambda}}\boldsymbol{\theta}_d + \hat{\mathbf{d}}\right] &&\in \mathcal{L}_\infty \\
\frac{d}{dt}\boldsymbol{\varepsilon}_r &= \frac{d}{dt}\left[\mathbf{B}_P\widehat{\boldsymbol{\Lambda}}\boldsymbol{\Theta}_r + \mathbf{B}_M\right] &&\in \mathcal{L}_\infty
\end{aligned} \tag{D.28}$$

Thus, if the matching condition holds, it follows from Barbalat's Lemma that

$$\lim_{t\to\infty}\boldsymbol{\varepsilon}_x = \lim_{t\to\infty}\boldsymbol{\varepsilon}_\varphi = \lim_{t\to\infty}\boldsymbol{\varepsilon}_d = \lim_{t\to\infty}\boldsymbol{\varepsilon}_r = 0$$

However, boundedness of $\mathbf{x}_P$, $\hat{\mathbf{x}}_P$ and $\mathbf{u}$ has not jet been established. Therfore, recall the dynamics of the identification model from Eq.(4.14) and insert the control law from Eq.(4.23)

$$\begin{aligned}
\dot{\hat{\mathbf{x}}}_P &= \mathbf{A}_M\hat{\mathbf{x}}_P + \underbrace{\left(\left[\widehat{\mathbf{A}}_P - \mathbf{A}_M\right] + \mathbf{B}_P\widehat{\boldsymbol{\Lambda}}\boldsymbol{\Theta}_x\right)}_{\boldsymbol{\varepsilon}_x}\mathbf{x}_P + \underbrace{\left(\widehat{\boldsymbol{\Theta}}_f + \mathbf{B}_P\widehat{\boldsymbol{\Lambda}}\boldsymbol{\Theta}_\varphi\right)}_{\boldsymbol{\varepsilon}_\varphi}\boldsymbol{\varphi}(\mathbf{x}_P) + \underbrace{\hat{\mathbf{d}} + \mathbf{B}_P\widehat{\boldsymbol{\Lambda}}\boldsymbol{\theta}_d}_{\boldsymbol{\varepsilon}_d} + \underbrace{\mathbf{B}_P\widehat{\boldsymbol{\Lambda}}\boldsymbol{\Theta}_r}_{\boldsymbol{\varepsilon}_r+\mathbf{B}_M}\mathbf{r} \\
&= \mathbf{A}_M\hat{\mathbf{x}}_P + \mathbf{B}_M\,\mathbf{r} + \boldsymbol{\varepsilon}_x\mathbf{x}_P + \boldsymbol{\varepsilon}_\varphi\boldsymbol{\varphi}(\mathbf{x}_P) + \boldsymbol{\varepsilon}_d + \boldsymbol{\varepsilon}_r\mathbf{r}
\end{aligned} \tag{D.29}$$

From Lemma 2.2 in [1] and with $\boldsymbol{\varepsilon}_x \in \mathcal{L}_2$ and $\boldsymbol{\varepsilon}_\varphi$, $\boldsymbol{\varepsilon}_d$, $\boldsymbol{\varepsilon}_r$, $\mathbf{r}$, and $\boldsymbol{\varphi}(\mathbf{x}_P) \in \mathcal{L}_\infty$ it follows that $\hat{\mathbf{x}}_P$ is bounded. Furthermore, from boundedness of $\mathbf{e}_I$ it follows that $\mathbf{x}_P$ is bounded. Boundedness of $\dot{\mathbf{e}}_I$ can be concluded from the error dynamics in Eq.(4.16), and thus it follows from Barbalat's Lemma (see Section C.2) that

$$\lim_{t\to\infty}\mathbf{e}_I\,(t) = \lim_{t\to\infty}(\hat{\mathbf{x}}_P - \mathbf{x}_P) = \mathbf{0}$$

D.3 Gradient Based Modification

Starting from the Lyapunov function candidate given in Eq.(5.111)

$$V = \frac{1}{2}\mathbf{e}_P^T\mathbf{P}\mathbf{e}_P + \frac{1}{2}\mathrm{Tr}\left[\widetilde{\boldsymbol{\Theta}}_P^T\boldsymbol{\Gamma}_P^{-1}\widetilde{\boldsymbol{\Theta}}_P\right] \tag{D.30}$$

if we take the derivative with respect to time we obtain

$$\dot{\mathrm{V}} = \dot{\mathbf{e}}_P^T\mathbf{P}\mathbf{e}_P + \mathrm{Tr}\left[\widetilde{\boldsymbol{\Theta}}_P^T\boldsymbol{\Gamma}_P^{-1}\dot{\widetilde{\boldsymbol{\Theta}}}_P\boldsymbol{\Lambda}\right]. \tag{D.31}$$

Inserting the error dynamics from Eq.(4.36) yields

$$\dot{\mathrm{V}} = \frac{1}{2}\mathbf{e}_P^T\underbrace{\left(\mathbf{P}\mathbf{A}_M + \mathbf{A}_M^T\mathbf{P}\right)}_{-\mathbf{Q}}\mathbf{e}_P + \mathbf{e}_P^T\mathbf{P}\mathbf{B}_P\widetilde{\boldsymbol{\Theta}}_P^T\boldsymbol{\omega}_P + \mathrm{Tr}\left[\widetilde{\boldsymbol{\Theta}}_P^T\boldsymbol{\Gamma}_P^{-1}\dot{\widetilde{\boldsymbol{\Theta}}}_P\right]. \tag{D.32}$$

By applying the trace identity $\mathbf{a}^T\mathbf{b} = \mathrm{Tr}[\mathbf{b}\mathbf{a}^T]$ we can rewrite the following terms

$$\mathbf{e}_P^T\mathbf{P}\mathbf{B}_P\cdot\widetilde{\boldsymbol{\Theta}}_P^T\boldsymbol{\omega}_P = \mathrm{Tr}\left[\widetilde{\boldsymbol{\Theta}}_P^T\boldsymbol{\omega}_P\cdot\mathbf{e}_P^T\mathbf{P}\mathbf{B}_P\right] \tag{D.33}$$

Using this result we rewrite Eq.(D.32)

$$\dot{\mathrm{V}} = -\frac{1}{2}\mathbf{e}_P^T\mathbf{Q}\mathbf{e}_P + \mathrm{Tr}\left[\widetilde{\boldsymbol{\Theta}}_P^T\left(\boldsymbol{\Gamma}_P^{-1}\dot{\widetilde{\boldsymbol{\Theta}}}_P + \boldsymbol{\omega}_P\cdot\mathbf{e}_P^T\mathbf{P}\mathbf{B}_P\right)\right] \tag{D.34}$$

Inserting the update law from Eq.(5.110)

$$\dot{\hat{\boldsymbol{\Theta}}}_P = \dot{\widetilde{\boldsymbol{\Theta}}}_P = -\boldsymbol{\Gamma}_P(\boldsymbol{\omega}_P \mathbf{e}_P^T \mathbf{P} + \gamma_C \bar{\boldsymbol{\omega}}_P \bar{\mathbf{e}}_P^T)\mathbf{B}_P \tag{D.35}$$

in Eq. we obtain

$$\dot{\mathrm{V}} = -\frac{1}{2}\mathbf{e}_P^T \mathbf{Q}\mathbf{e}_P + \mathrm{Tr}\left[-\widetilde{\boldsymbol{\Theta}}_P^T \gamma_C \bar{\boldsymbol{\omega}}_P \bar{\mathbf{e}}_P^T \mathbf{B}_P\right] \tag{D.36}$$

The trace identity is in general not invariant with respect to permutation, but it is invariant under cyclic permutation: $\mathrm{Tr}[\mathrm{ABCD}] = \mathrm{Tr}[\mathrm{BCDA}] = \mathrm{Tr}[\mathrm{CDAB}] = \mathrm{Tr}[\mathrm{DABC}]$. Hence we can rewrite Eq.(D.36)

$$\begin{aligned}\dot{\mathrm{V}} &= -\frac{1}{2}\mathbf{e}_P^T \mathbf{Q}\mathbf{e}_P + \gamma_C \mathrm{Tr}\left[-\underbrace{\mathbf{B}_P \widetilde{\boldsymbol{\Theta}}_P^T \bar{\boldsymbol{\omega}}_P}_{\bar{\mathbf{e}}_P} \bar{\mathbf{e}}_P^T\right] \\ &= -\frac{1}{2}\mathbf{e}_P^T \mathbf{Q}\mathbf{e}_P + \gamma_C \bar{\mathbf{e}}_P^T \bar{\mathbf{e}}_P\end{aligned} \tag{D.37}$$

From Lyapunov's Theorem, given in Section C.2, it follows that $\mathbf{e}_P, \bar{\mathbf{e}}_P, \widetilde{\widetilde{\boldsymbol{\Theta}}}_P \in \mathcal{L}_\infty$. Furthermore, from boundedness of the system states the existence of the integral

$$\int_{t_0}^{\infty} \dot{\mathrm{V}}(\tau) d\tau = \mathrm{V}(\infty) - \mathrm{V}(t_0) < \infty \tag{D.38}$$

follows, and thus the errors $\mathbf{e}_C$ and $\bar{\mathbf{e}}_P$ are square integrable, that is $\mathbf{e}_C$ and $\bar{\mathbf{e}}_P \in \mathcal{L}_2$:

$$\int_{t_0}^{\infty} \mathbf{e}_C^T(\tau)\mathbf{Q}\mathbf{e}_C(\tau)\, d\tau + \int_{t_0}^{\infty} \gamma_C \bar{\mathbf{e}}_P^T(\tau)\bar{\mathbf{e}}_P(\tau)\, d\tau < \infty \tag{D.39}$$

From the boundedness of systems states it follows from the error dynamics that $\dot{\mathbf{e}}_P \in \mathcal{L}_\infty$ and by application of Barbalat's Lemma it can be shown that the error converges to zero asymptotically

$$\lim_{t\to\infty} \mathbf{e}_P(t) = \lim_{t\to\infty}(\hat{\mathbf{x}}_P - \mathbf{x}_P) = \mathbf{0}.$$

To show that also $\bar{\mathbf{e}}_P$ converges to zero we need to show that $\dot{\bar{\mathbf{e}}}_P$ is bounded in order to apply Barbalat's Lemma. Taking the time derivative of $\bar{\boldsymbol{\varepsilon}}$ from Eq.(5.97) we get

$$\dot{\bar{\mathbf{e}}}_P(\boldsymbol{\Theta}) = \mathbf{B}_P\left(\dot{\hat{\boldsymbol{\Theta}}}_P^T \bar{\boldsymbol{\omega}}_P + \hat{\boldsymbol{\Theta}}_P^T \dot{\bar{\boldsymbol{\omega}}}_P\right) - \dot{\bar{\boldsymbol{\upsilon}}}. \tag{D.40}$$

How to obtain the time derivative of $\bar{\boldsymbol{\omega}}$ and $\bar{\mathbf{y}}$ is in following exemplarily shown for the integral approach. Thus from Eq.(5.93) and Eq. the derivative are given by

$$\dot{\bar{\boldsymbol{\omega}}}_P = \boldsymbol{\omega}_P(t) - \boldsymbol{\omega}_P(t - t_d) \tag{D.41}$$

$$\dot{\bar{\boldsymbol{\upsilon}}} = \mathbf{B}_P \hat{\boldsymbol{\Theta}}_P^{*\,T}\left(\boldsymbol{\omega}_P(t) - \boldsymbol{\omega}_P(t - t_d)\right), \tag{D.42}$$

Inserting the derivatives in Eq.(D.40) gives

$$\dot{\bar{\mathbf{e}}}_P(\boldsymbol{\Theta}) = \mathbf{B}_P\left(\dot{\hat{\boldsymbol{\Theta}}}_P^T \bar{\boldsymbol{\omega}}_P + \hat{\boldsymbol{\Theta}}_P^T\left(\boldsymbol{\omega}_P(t) - \boldsymbol{\omega}_P(t - t_d)\right)\right) - \mathbf{B}_P \hat{\boldsymbol{\Theta}}_P^{*\,T}\left(\boldsymbol{\omega}_P(t) - \boldsymbol{\omega}_P(t - t_d)\right) \tag{D.43}$$

From the control law it follows that $\mathbf{u} \in \mathcal{L}_\infty$. Now since $\boldsymbol{\omega}_P = \begin{bmatrix}\mathbf{x}_\mathbf{P}^T & \boldsymbol{\varphi}(\mathbf{x}_\mathbf{P})^T & 1 & \mathbf{u}^T\end{bmatrix}^T$ is bounded it follows from the update law that $\dot{\widehat{\boldsymbol{\Theta}}}_P^T \in \mathcal{L}_\infty$. That is, $\dot{\bar{\mathbf{e}}}_P \in \mathcal{L}_\infty$, and thus Barbalat's Lemma can be applied and the error converges to zero asymptotically

$$\lim_{t\to\infty} \bar{\mathbf{e}}_P\,(t) = \mathbf{0}.$$

D.4 Recursive Least-Square Modification

Starting from the Lyapunov function candidate given in Eq.(5.125)

$$\mathrm{V} = \frac{1}{2}\mathbf{e}_P^T\mathbf{P}\mathbf{e}_P + \frac{1}{2}\mathrm{Tr}\left[\widetilde{\boldsymbol{\Theta}}_P^T\mathbf{R}^{-1}\widetilde{\boldsymbol{\Theta}}_P\right] \tag{D.44}$$

if we take the derivative with respect to time we obtain

$$\dot{\mathrm{V}} = \dot{\mathbf{e}}_P^T\mathbf{P}\mathbf{e}_P + \mathrm{Tr}\left[\widetilde{\widehat{\boldsymbol{\Theta}}}_P^T\mathbf{R}^{-1}\dot{\widetilde{\widehat{\boldsymbol{\Theta}}}}_P\right] + \frac{1}{2}\mathrm{Tr}\left[\widetilde{\widehat{\boldsymbol{\Theta}}}_P^T\left(\frac{\mathrm{d}}{\mathrm{dt}}\mathbf{R}^{-1}\right)\widetilde{\widehat{\boldsymbol{\Theta}}}_P\right]. \tag{D.45}$$

Inserting the error dynamics from Eq.(4.36) yields

$$\dot{\mathrm{V}} = \frac{1}{2}\mathbf{e}_P^T\underbrace{\left(\mathbf{P}\mathbf{A}_M + \mathbf{A}_M^T\mathbf{P}\right)}_{-\mathbf{Q}}\mathbf{e}_P + \mathbf{e}_P^T\mathbf{P}\mathbf{B}_P\widetilde{\widehat{\boldsymbol{\Theta}}}_P^T\boldsymbol{\omega}_P + \mathrm{Tr}\left[\widetilde{\widehat{\boldsymbol{\Theta}}}_P^T\mathbf{R}^{-1}\dot{\widetilde{\widehat{\boldsymbol{\Theta}}}}_P\right] + \frac{1}{2}\mathrm{Tr}\left[\widetilde{\widehat{\boldsymbol{\Theta}}}_P^T\left(\frac{\mathrm{d}}{\mathrm{dt}}\mathbf{R}^{-1}\right)\widetilde{\widehat{\boldsymbol{\Theta}}}_P\right]. \tag{D.46}$$

By applying the trace identity $\mathbf{a}^T\mathbf{b} = \mathrm{Tr}[\mathbf{b}\mathbf{a}^T]$ we can rewrite the following terms

$$\mathbf{e}_P^T\mathbf{P}\mathbf{B}_P \cdot \widetilde{\widehat{\boldsymbol{\Theta}}}_P^T\boldsymbol{\omega}_P = \mathrm{Tr}\left[\widetilde{\widehat{\boldsymbol{\Theta}}}_P^T\boldsymbol{\omega}_P \cdot \mathbf{e}_P^T\mathbf{P}\mathbf{B}_P\right] \tag{D.47}$$

Using this result we rewrite Eq.(D.46)

$$\dot{\mathrm{V}} = -\frac{1}{2}\mathbf{e}_P^T\mathbf{Q}\mathbf{e}_P + \mathrm{Tr}\left[\widetilde{\widehat{\boldsymbol{\Theta}}}_P^T\left(\mathbf{R}^{-1}\dot{\widetilde{\widehat{\boldsymbol{\Theta}}}}_P + \boldsymbol{\omega}_P \cdot \mathbf{e}_P^T\mathbf{P}\mathbf{B}_P\right)\right] + \frac{1}{2}\mathrm{Tr}\left[\widetilde{\widehat{\boldsymbol{\Theta}}}_P^T\left(\frac{\mathrm{d}}{\mathrm{dt}}\mathbf{R}^{-1}\right)\widetilde{\widehat{\boldsymbol{\Theta}}}_P\right] \tag{D.48}$$

Inserting the update law from Eq.(5.123) and Eq.(5.124)

$$\dot{\widehat{\boldsymbol{\Theta}}}_P = -\mathbf{R}\left[\boldsymbol{\omega}_P\mathbf{e}_P^T\mathbf{P}\mathbf{B}_P + \bar{\boldsymbol{\omega}}_P\bar{\mathbf{e}}_P^T\mathbf{B}_P^{l^T}\right] \tag{D.49}$$

$$\dot{\mathbf{R}} = -\mathbf{R}\dot{\mathbf{R}^{-1}}\mathbf{R} = -\mathbf{R}\bar{\boldsymbol{\omega}}_P\bar{\boldsymbol{\omega}}_P^T\mathbf{R} \tag{D.50}$$

In Eq.(D.48) gives

$$\dot{\mathrm{V}} = -\frac{1}{2}\mathbf{e}_P^T\mathbf{Q}\mathbf{e}_P + \mathrm{Tr}\left[-\widetilde{\widehat{\boldsymbol{\Theta}}}_P^T\bar{\boldsymbol{\omega}}_P\bar{\mathbf{e}}_P^T\mathbf{B}_P^{l^T}\right] + \frac{1}{2}\mathrm{Tr}\left[\widetilde{\widehat{\boldsymbol{\Theta}}}_P^T\bar{\boldsymbol{\omega}}_P\bar{\boldsymbol{\omega}}_P^T\widetilde{\widehat{\boldsymbol{\Theta}}}_P\right] \tag{D.51}$$

With the definition of $\bar{\mathbf{e}}_P^T$ from Eq.(5.97)

$$\begin{aligned}
\dot{\mathrm{V}} &= -\frac{1}{2}\mathbf{e}_P^T\mathbf{Q}\mathbf{e}_P + \mathrm{Tr}\left[-\widetilde{\widehat{\boldsymbol{\Theta}}}_P^T\bar{\boldsymbol{\omega}}_P\underbrace{\left(\mathbf{B}_\boldsymbol{P}\widehat{\boldsymbol{\Theta}}_\boldsymbol{P}^\boldsymbol{T}\,\bar{\boldsymbol{\omega}}_P - \mathbf{B}_\boldsymbol{P}\widehat{\boldsymbol{\Theta}}_\boldsymbol{P}^{*\,\boldsymbol{T}}\bar{\boldsymbol{\omega}}_\boldsymbol{P}\right)^T}_{\bar{\mathbf{e}}_P^T}\mathbf{B}_P^{l^T}\right] + \frac{1}{2}\mathrm{Tr}\left[\widetilde{\widehat{\boldsymbol{\Theta}}}_P^T\bar{\boldsymbol{\omega}}_P\bar{\boldsymbol{\omega}}_P^T\widetilde{\widehat{\boldsymbol{\Theta}}}_P\right] \\
&= -\frac{1}{2}\mathbf{e}_P^T\mathbf{Q}\mathbf{e}_P + \mathrm{Tr}\left[-\widetilde{\widehat{\boldsymbol{\Theta}}}_P^T\bar{\boldsymbol{\omega}}_P\bar{\boldsymbol{\omega}}_\boldsymbol{P}^T\underbrace{\left(\widehat{\boldsymbol{\Theta}}_\boldsymbol{P} - \widehat{\boldsymbol{\Theta}}_\boldsymbol{P}^*\right)}_{\widetilde{\widehat{\boldsymbol{\Theta}}}_P}\underbrace{\mathbf{B}_\boldsymbol{P}^T\mathbf{B}_P^{l^T}}_{\mathbf{I}}\right] + \frac{1}{2}\mathrm{Tr}\left[\widetilde{\widehat{\boldsymbol{\Theta}}}_P^T\bar{\boldsymbol{\omega}}_P\bar{\boldsymbol{\omega}}_P^T\widetilde{\widehat{\boldsymbol{\Theta}}}_P\right] \\
&= -\frac{1}{2}\mathbf{e}_P^T\mathbf{Q}\mathbf{e}_P - \mathrm{Tr}\left[\widetilde{\widehat{\boldsymbol{\Theta}}}_P^T\bar{\boldsymbol{\omega}}_P\bar{\boldsymbol{\omega}}_\boldsymbol{P}^T\widetilde{\widehat{\boldsymbol{\Theta}}}_P\right] + \frac{1}{2}\mathrm{Tr}\left[\widetilde{\widehat{\boldsymbol{\Theta}}}_P^T\bar{\boldsymbol{\omega}}_P\bar{\boldsymbol{\omega}}_P^T\widetilde{\widehat{\boldsymbol{\Theta}}}_P\right] \\
&= -\frac{1}{2}\mathbf{e}_P^T\mathbf{Q}\mathbf{e}_P - \frac{1}{2}\mathrm{Tr}\left[\widetilde{\widehat{\boldsymbol{\Theta}}}_P^T\bar{\boldsymbol{\omega}}_P\bar{\boldsymbol{\omega}}_\boldsymbol{P}^T\widetilde{\widehat{\boldsymbol{\Theta}}}_P\right]
\end{aligned} \tag{D.52}$$

$$= -\frac{1}{2}\mathbf{e}_P^T\mathbf{Q}\mathbf{e}_P - \frac{1}{2}\bar{\boldsymbol{\omega}}_{\boldsymbol{P}}^T\tilde{\tilde{\boldsymbol{\Theta}}}_P\tilde{\tilde{\boldsymbol{\Theta}}}_P^T\bar{\boldsymbol{\omega}}_P \leq 0$$

From Lyapunov's Theorem, given in Section C.2, it follows that $\mathbf{e}_P$, $\bar{\mathbf{e}}_P$, $\hat{\boldsymbol{\Theta}}_P$, and $\mathbf{R}$ $\epsilon\, \mathcal{L}_\infty$. Furthermore, from boundedness of the system states the existence of the integral

$$\int_{t_0}^{\infty} \dot{\mathrm{V}}\,(\tau)d\tau = \mathrm{V}(\infty) - \mathrm{V}(t_0) < \infty \tag{D.53}$$

follows, and thus the errors $\mathbf{e}_C$ and $\bar{\mathbf{e}}_P$ are square integrable, that is $\mathbf{e}_C$ and $\bar{\mathbf{e}}_P$ $\epsilon\, \mathcal{L}_2$:

$$\begin{aligned}
&\int_{t_0}^{\infty} \mathbf{e}_C^T(\tau)\mathbf{Q}\mathbf{e}_C(\tau)\,d\tau + \int_{t_0}^{\infty} \bar{\boldsymbol{\omega}}_{\boldsymbol{P}}^T(\tau)\tilde{\tilde{\boldsymbol{\Theta}}}_P(\tau)\tilde{\tilde{\boldsymbol{\Theta}}}_P^T(\tau)\bar{\boldsymbol{\omega}}_P(\tau)\,d\tau < \infty \\
\Rightarrow &\int_{t_0}^{\infty} \mathbf{e}_C^T(\tau)\mathbf{Q}\mathbf{e}_C(\tau)\,d\tau + \int_{t_0}^{\infty} \underbrace{\bar{\boldsymbol{\omega}}_{\boldsymbol{P}}^T(\tau)\tilde{\tilde{\boldsymbol{\Theta}}}_P(\tau)\mathbf{B}_{\boldsymbol{P}}^T}_{\bar{\mathbf{e}}_P^T}\underbrace{\mathbf{B}_{\boldsymbol{P}}\tilde{\tilde{\boldsymbol{\Theta}}}_P^T(\tau)\bar{\boldsymbol{\omega}}_P(\tau)}_{\bar{\mathbf{e}}_P}\,d\tau < \infty \\
&\int_{t_0}^{\infty} \mathbf{e}_C^T(\tau)\mathbf{Q}\mathbf{e}_C(\tau)\,d\tau + \int_{t_0}^{\infty} \bar{\mathbf{e}}_P^T\bar{\mathbf{e}}_P\,d\tau < \infty
\end{aligned} \tag{D.54}$$

From the boundedness of systems states, it follows from the error dynamics that $\dot{\mathbf{e}}_P$ $\epsilon\, \mathcal{L}_\infty$ and by application of Barbalat's Lemma it can be shown that the error converges to zero asymptotically

$$\lim_{t\to\infty} \mathbf{e}_P\,(t) = \lim_{t\to\infty}(\hat{\mathbf{x}}_P - \mathbf{x}_P) = \mathbf{0}.$$

To show that also $\bar{\mathbf{e}}_P$ converges to zero we need to show that $\dot{\bar{\mathbf{e}}}_P$ is bounded. This was already shown in the previous Section D.3 and is not repeated here.

Appendix E

Piecewise Constant Update Law

The error dynamics can be derived from Eq.(6.87) and Eq.(6.87) :

$$\begin{aligned}\dot{\mathbf{e}}_P(t) &= \dot{\hat{\mathbf{x}}}_P(t) - \dot{\mathbf{x}}_P(t), \quad \mathbf{e}_P(0) = \mathbf{0} \\ &= \mathbf{A}_M \mathbf{e}_P(t) + \mathbf{B}_P\big((\mathbf{I}-\boldsymbol{\Lambda})\mathbf{u}(t) + \hat{\boldsymbol{\sigma}}_1(t) - \mathbf{f}_1(t)\big) + \mathbf{B}_{P,um}\big(\hat{\boldsymbol{\sigma}}_2(t) - \mathbf{f}_2(t)\big)\end{aligned} \tag{E.1}$$

Using the sample time T_S and the fact that $\hat{\boldsymbol{\sigma}}_1(t)$ and $\hat{\boldsymbol{\sigma}}_2(t)$ are constant one sample interval $t \in [iT_S, (i+1)T_S[$ for $i = 0, 1, 2, \ldots$ we can write Eq.(E.1) in a discrete way

$$\begin{aligned}\mathbf{e}_P(iT_S + t) = e^{\mathbf{A}_M t}\,\mathbf{e}_P(iT_S) &+ \int_{iT_S}^{iT_S+t} \mathbf{e}^{\mathbf{A}_M(iT_S+t-\xi)}\,\Big(\mathbf{B}_P\hat{\boldsymbol{\sigma}}_1(iT_S) + \mathbf{B}_{P,um}\hat{\boldsymbol{\sigma}}_2(iT_S)\Big)\,d\xi \\ &- \int_{iT_S}^{iT_S+t} \mathbf{e}^{\mathbf{A}_M(iT_S+t-\xi)}\,\Big(\mathbf{B}_P\big((\boldsymbol{\Lambda}-\mathbf{I})\mathbf{u}(\xi) + \mathbf{f}_1(\xi)\big) + \mathbf{B}_{P,um}\mathbf{f}_2(\xi)\Big)\,d\xi\end{aligned} \tag{E.2}$$

With $\mathbf{B} = [\mathbf{B}_P \quad \mathbf{B}_{P,um}]$ the error at the next time step $t = (i+1)T_S$ can be denoted by

$$\begin{aligned}\mathbf{e}_P\big((i+1)T_S\big) = e^{\mathbf{A}_M T_S}\,\mathbf{e}_P(iT_S) &+ \int_0^{T_S} \mathbf{e}^{\mathbf{A}_M(T_S-\xi)}\,\mathbf{B}\begin{bmatrix}\hat{\boldsymbol{\sigma}}_1(iT_S)\\ \hat{\boldsymbol{\sigma}}_2(iT_S)\end{bmatrix}d\xi \\ &- \int_0^{T_S} \mathbf{e}^{\mathbf{A}_M(T_S-\xi)}\,\Big(\mathbf{B}_P\big((\boldsymbol{\Lambda}-\mathbf{I})\mathbf{u}(\xi) + \mathbf{f}_1(\xi)\big) + \mathbf{B}_{P,um}\mathbf{f}_2(\xi)\Big)\,d\xi\end{aligned} \tag{E.3}$$

With the definitions

$$\begin{aligned}\hat{\boldsymbol{\sigma}} &= \begin{bmatrix}\hat{\boldsymbol{\sigma}}_1(iT_S)\\ \hat{\boldsymbol{\sigma}}_2(iT_S)\end{bmatrix} \\ \boldsymbol{\Delta}\big((i+1)T_S\big) &= \int_0^{T_S} \mathbf{e}^{\mathbf{A}_M(T_S-\xi)}\,\Big(\mathbf{B}_P\big((\boldsymbol{\Lambda}-\mathbf{I})\mathbf{u}(\xi) + \mathbf{f}_1(\xi)\big) + \mathbf{B}_{P,um}\mathbf{f}_2(\xi)\Big)\,d\xi\end{aligned} \tag{E.4}$$

We can write Eq.(E.3) as

$$\mathbf{e}_P\big((i+1)T_S\big) = e^{\mathbf{A}_M T_S}\,\mathbf{e}_P(iT_S) + \int_0^{T_S} \mathbf{e}^{\mathbf{A}_M(T_S-\xi)}\,\mathbf{B}\hat{\boldsymbol{\sigma}}(iT_S)d\xi - \boldsymbol{\Delta}\big((i+1)T_S\big) \tag{E.5}$$

The idea is now to calculate $\hat{\boldsymbol{\sigma}}(iT_S)$ such that it compensates for the propagation of the prediction error $\mathbf{e}_P(iT_S)$ over T_S.That means we are choosing $\hat{\boldsymbol{\sigma}}(iT_S)$ such that the first two terms in Eq.(E.5) cancel. However, the uncertainties $\boldsymbol{\Delta}$, stemming form $\boldsymbol{\Lambda}$, $\mathbf{f}_1$, and $\mathbf{f}_2$ still will introduce an error at $\mathbf{e}_P\big((i+1)T_S\big)$. Hence it is desired that

$$e^{\mathbf{A}_M T_s}\,\mathbf{e}_P(iT_s) + \int_0^{T_s} e^{\mathbf{A}_M(T_s-\xi)}\;\mathbf{B}\hat{\boldsymbol{\sigma}}(iT_s)d\xi = \mathbf{0} \tag{E.6}$$

It follows that

$$\begin{aligned} e^{\mathbf{A}_M T_s}\,\mathbf{e}_P(iT_s) &= -\int_0^{T_s} e^{\mathbf{A}_M(T_s-\xi)}\;\mathbf{B}\hat{\boldsymbol{\sigma}}(iT_s)d\xi \\ &= -\left[-\mathbf{A}_M^{-1}e^{\mathbf{A}_M(T_s-\xi)}\mathbf{B}\,\hat{\boldsymbol{\sigma}}(iT_s)\right]_0^{T_s} \\ &= -\mathbf{A}_M^{-1}(e^{\mathbf{A}_M T_s}-\mathbf{I})\mathbf{B}\,\hat{\boldsymbol{\sigma}}(iT_s) \end{aligned} \tag{E.7}$$

Resolving w.r.t. to $\hat{\boldsymbol{\sigma}}$ we obtain

$$\begin{aligned} \hat{\boldsymbol{\sigma}}(t) = \begin{bmatrix}\hat{\boldsymbol{\sigma}}_1(iT_s)\\ \hat{\boldsymbol{\sigma}}_2(iT_s)\end{bmatrix} &= -\mathbf{B}^{-1}\,[\mathbf{A}_M^{-1}(e^{\mathbf{A}_M T_s}-\mathbf{I})]^{-1}\,e^{\mathbf{A}_M T_s}\,\mathbf{e}_P(iT_s) \\ &= -\mathbf{B}^{-1}\,\boldsymbol{\Phi}^{-1}(T_s)\;\boldsymbol{\mu}(iT_s), \qquad t\in[iT_s,(i+1)T_s[,\;\; i=0,1,2,\ldots \end{aligned} \tag{E.8}$$

with

$$\boldsymbol{\Phi}(T_s) = \mathbf{A}_M^{-1}(e^{\mathbf{A}_M T_s}-\mathrm{I}) \tag{E.9}$$

$$\boldsymbol{\mu}(iT_s) = e^{\mathbf{A}_M T_s}\,\mathbf{e}(iT_s) \tag{E.10}$$

$$\mathbf{e}_P(t) = \hat{\mathbf{x}}_P(t) - \mathbf{x}_P(t) \tag{E.11}$$

In this way $\mathbf{e}_P\big((i+1)T_s\big)$ only consists of the error that has culminated within T_s due to the uncertainties and an error in the estimation of the system input gain matrix, i.e.

$$\mathbf{e}_P\big((i+1)T_s\big) = \boldsymbol{\Delta}\big((i+1)T_s\big). \tag{E.12}$$